Radiation Chemistry

Volume II. Gases, Solids, Organic Liquids

An international conference

sponsored by

Argonne National Laboratory

Argonne, Ill.

Aug. 12-15, 1968

Edwin J. Hart

Conference Chairman

ADVANCES IN CHEMISTRY SERIES 82

AMERICAN CHEMICAL SOCIETY

WASHINGTON, D. C. 1968

Publication Date: January 1, 1968 | doi: 10.1021/ba-1968-0082.fw001

Publication Date: January 1, 1968 | doi: 10.1021/ba-1968-0082.fw001

Library of Congress Catalog Card 68-55363

PRINTED IN THE UNITED STATES OF AMERICA

Advances in Chemistry Series

Robert F. Gould, *Editor*

Advisory Board

AMERICAN CHEMICAL SOCIETY PUBLICATIONS

Publication Date: January 1, 1968 | doi: 10.1021/ba-1968-0082.fw001

Publication Date: January 1, 1968 | doi: 10.1021/ba-1968-0082.fw001

FOREWORD

ADVANCES IN CHEMISTRY SERIES was founded in 1949 by the American Chemical Society as an outlet for symposia and collections of data in special areas of topical interest that could not be accommodated in the Society's journals. It provides a medium for symposia that would otherwise be fragmented, their papers distributed among several journals or not published at all. Papers are refereed critically according to ACS editorial standards and receive the careful attention and processing characteristic of ACS publications. Papers published in ADVANCES IN CHEMISTRY SERIES are original contributions not published elsewhere in whole or major part and include reports of research as well as reviews since symposia may embrace both types of presentation.

PREFACE

Exceptional strides are now being made in radiation chemistry although growth has been gradual. This long induction period dates back to the discovery of radioactivity and the development of x-ray tubes. Radium salts, the first radiation sources, were supplanted in the third and fourth decades of this century by x-rays. During this period, pioneering scientists such as Fricke, Lind, Mundt, Risse, and their collaborators laid the foundations of radiation-induced gaseous and aqueous reactions. From these modest beginnings research in this field gradually gathered momentum in the fifth decade by the use of Van de Graaff and cyclotron accelerators and in the sixth through the availability of powerful ^{60}Co γ-ray sources. Finally in the seventh decade the results of basic research exploded into prominence through the use of electron pulse accelerators. In this decade, we are reaping the benefits of these new developments by drawing attention to the applications of radiation chemistry. Since the 1930s the number of active workers in this field has multiplied a hundredfold, and research has expanded from a few universities and national laboratories to research centers the world over.

The early workers established phenomena connected with the qualitative, and later with the quantitative changes taking place during irradiation. Products and some intermediate species were identified in gases and in aqueous solutions, and work progressed in three areas: dosimetry, radical and ionic yields, and relative rate constants. From these results, speculations regarding the mechanism of energy loss, of free radical and ion pair formation and distribution, were mathematically formulated and tested by the developing specialty of diffusion kinetics.

More recently, assisted by photochemistry, spectroscopy in its varied forms, chromatography, computers, and applied electronics, radiation chemistry is assaulting many of the problems associated with the properties of transient species at an unprecedented rate. Commonplace, already, is the study of intermediates lasting only milli- and micro-seconds. A rapidly developing subdivision is on the horizon—that of nanosecond and picosecond chemistry. Knowledge of the nature and rates of these reactions has been of inestimable aid in untangling reaction mechanisms in chemistry and biology. For example, the discovery of the hydrated electron and the determination of its rate constants has aided the interpretation of reactions in aqueous media. Recent studies on solvated and

Publication Date: January 1, 1968 | doi: 10.1021/ba-1968-0082.pr001

In Radiation Chemistry; Hart, E.;
Advances in Chemistry; American Chemical Society: Washington, DC, 1968.

trapped electrons in liquids and solids assist materially in explaining phenomena in these media. Similarly, the identification of singlet and triplet states in the radiolysis of gases and organic liquids provides data crucial for understanding these complex systems.

The papers reported in these two volumes constitute about two-thirds of those presented at the Argonne National Laboratory-sponsored International Conference on Radiation Chemistry, to which 200 prominent scientists and students from 21 countries and 81 universities and institutes were invited. This conference was in celebration of Argonne National Laboratory's participation in a decade of pulse radiolysis. All phases of radiation chemistry, from the theoretical to the fundamental changes taking place in complex molecules, were included. A special session on dosimetry was planned for Dr. Hugo Fricke on August 15, his 76th birthday, to honor him for his many contributions to radiation chemistry over the past 40 years. The conference papers are assembled in these two volumes: one, largely on aqueous solutions, consists of the survey and original papers given in the aqueous, biological, and dosimetry sessions; the other, largely organic, deals with similar groups of papers on gases, liquids, and solids. The broad scope and interest in these papers reflects the influence and applications of radiation chemistry in most branches of chemistry today.

Argonne, Ill.
July 1968

EDWIN J. HART

Publication Date: January 1, 1968 | doi: 10.1021/ba-1968-0082.pr001

ESR of Radiation Damage in Inorganic Solids

M. C. R. SYMONS

The University, Leicester, England

The way in which electron spin resonance can be applied to the problem of identification of species formed on exposure of inorganic materials to high energy radiation is outlined. Recent results for a wide range of inorganic radicals formed in this way are collated and discussed. Radicals are classified as σ or π depending upon their electronic structure, and the problem of spin-polarization in π-radicals is discussed in some depth. Among the more recently discovered radicals mentioned are SH, S_2^-, Se_2^-, PH_2, CS_2^-, FOO, ClOO, BH_3^-, CO_3^{3-}, $C_2H_2^-$, and $S_2N_2^+$. The structure of a center originally described as F^{2-} formed in beryllium oxide is discussed in terms of the unit Be_2F^{2+}. Assignments are viewed critically, and in some instances alternative identifications are offered.

The primary aim of this review is to supplement three earlier discussions of the magnetic properties of inorganic radicals (*9*, *19*, *83*).

Irradiation of diamagnetic solids commonly results in the formation of one or more paramagnetic "centers" because the initial act is electron ejection. If the ejected electron can be trapped in some manner at a distance from the parent molecule or ion and if the residual cation becomes sufficiently modified to prevent hole-migration, then these initially trapped products, which must necessarily be paramagnetic, can generally be detected by ESR.

Now that a large number of such centers have been identified, the study of new centers is often quite straightforward. Apart from electrons trapped at holes in the solid, such as anion vacancies (for brevity, these will be referred to simply as "trapped electrons"), the centers are usually molecular in nature, having properties that are largely those of a small molecule or ion, with relatively minor perturbations by the environment.

In Radiation Chemistry; Hart, E.;
Advances in Chemistry; American Chemical Society: Washington, DC, 1968.

For systems with orbitally degenerate ground states, such as S_2^- (*see Some Diatomic Radicals*), there is often a large "crystal field" splitting of the levels. Sometimes there is a minor hyperfine coupling to adjacent ions; interesting recent examples being the H-center in alkali halides which consists of Hal_2^- units weakly coupled to two flanking halide ions lying along the molecular axis (*1*), and ^{23}Na hyperfine coupling in the spectra of CS_2^- (*13*) and N_2^- (*48*). The ENDOR technique should prove to be particularly powerful for studying such weak interactions.

However, if the magnetic center is part of a polymeric system such as the silicates or borates, then its properties may be considerably distorted compared with expectation for the corresponding small molecule. This field has been recently reviewed (*19, 83*) and will not be elaborated here.

The great power of the ESR technique is that the hyperfine- and, to a less extent, the *g*-tensors give quite intimate structural detail, leading to estimates of spin-density in *s*- and *p*-orbitals on one or more of the atoms in the center. It is convenient to classify radicals as σ or π (*82*), the major distinction being that in the former there is a real contribution from an atomic *s*-orbital of at least one of the atoms, this giving rise to an appreciable isotropic hyperfine coupling if the nucleus involved is magnetic. For π-radicals there is usually a small residual isotropic coupling which appears to stem largely from spin-polarization of the valence electrons, especially those involved in σ-bonding (*57*). This also gives useful structural information and the magnitude of this coupling can be an important aid in identification. One way of proceeding will be outlined later.

It has proved convenient to classify centers other than trapped electrons as monatomic, diatomic, triatomic, tetra-atomic and penta-atomic (*9*), these classes being expanded to include more complex species having similar basic structures. Thus, the radicals R_2NO and $(SO_3)_2NO^{2-}$ were classed with the corresponding simple AB_3 tetra-atomic radicals.

A selection of the basic radicals discussed at length in References *9, 19,* and *83* are given in Table I. In this review we examine a range of more recently studied radicals and conclude with a brief discussion of the mechanisms of damage in the solids under consideration.

Spin Polarization in π-Radicals

Despite the complexity of the theory underlying the appearance of contact hyperfine coupling in π-radicals, it seems that, for many radicals, the results are sufficiently simple as to provide a useful guide in identification and in structural analysis (*57*).

Publication Date: January 1, 1968 | doi: 10.1021/ba-1968-0082.ch001

Our basic approach is to consider, as with σ-radicals, the apparent spin-density in the highest filled atomic *s*-orbital of the atom concerned. It has proved convenient to invoke the U^X-value which is related to the familiar Q^X-value (*65*) by dividing by the appropriate A^X-value for the atom (X) concerned and multiplying by 100 to give the value as a percentage.

These Q- or U-values can be broken down into terms for the polarization of σ-bonding, lone-pair and core electrons, but we find that the equation

$$100a^X/A^X = \rho_X U^X + \Sigma \rho_Y U^X_{YX} \qquad (1)$$

adequately accommodates a wide range of results for organic and inorganic radicals (*57*). Here a^X is the experimental isotropic hyperfine coupling in gauss, A^X is the atomic value for the highest filled *s*-orbital, ρ_X and ρ_Y are spin-densities on X, the nucleus concerned, and on Y, any adjacent nucleus having significant spin-density.

Table I. Some of the Simple Radicals Recently Detected and Studied by ESR Spectroscopy

Atoms and Monatomic Ions	H, N, Cl, Ag
Diatomic Radicals	OH, N_2^-, F_2^-, Cl_2^-, FCl^-, XeF, KrF
Triatomic Radicals	CO_2^-, CS_2^-, NO_2, NO_2^{2-}, O_3^-, SO_2^-, SeO_2^-, NF_2, PF_2, FOO, ClOO
Tetra-atomic Radicals	BH_3^-, CH_3, NH_3^+, SiH_3, CO_3^-, NO_3, NO_3^{2-}, CF_3, PO_3^{2-}, SO_3^-, ClO_3, SeO_3^-, AsO_3^{2-}, HPO_2^-
Penta-atomic Radicals	PF_4, SF_4^+, $As(OH)_4$, PO_4^{2-}, SO_4^-

We find that in cases where ρ_X is known unambigously, U^X is remarkably constant, being about 3.9% for all radicals. There is a real trend to smaller values as the number of σ-bonds to X decreases and values as low as 2.2% have been obtained (*see* Table II). However, on going from molecules to atoms there is a dramatic fall to about 0.2%, and this has been taken to mean that the major contribution comes from polarization of bonding or lone-pair electrons, thus justifying the use of Equation 1.

The "adjacent atom" terms, U^X_{YX}, can also be obtained directly for a few radicals such as NO_3, where the unpaired electron is confined entirely to an orbital on the oxygen atoms. This term is found to depend markedly upon the hybridization of the σ-orbitals involved, but otherwise seems to be relatively insensitive to changes in the structure of the radicals studied.

Publication Date: January 1, 1968 | doi: 10.1021/ba-1968-0082.ch001

Table II. Values of U^A and U^A_{BA} for Selected Atoms and Radicals

	Species	*Nucleus A, (ρ^A)*	U^A_{BA}[a]		U^A
Atoms	N	^{14}N (1)			0.22
	O	^{17}O (1)			0.20
	F	^{19}F			0.21
	P	^{31}P (1)			0.18
Average					0.20 ± 0.02
Diatomic Radicals	NO	^{14}N (0.8)	−2.0	(0.5)	2.2
	N_2^-	^{14}N (0.5)	−2.0	(0.5)	2.5
Average					2.35
Triatomic Radicals	NH_2	^{14}N (1)			2.3
		^{1}H (0)	−4.7	(1)	
	$NH(SO_3)^-$	^{14}N (1)			2.4
	$N(SO_3)_2^{2-}$	^{14}N (1)			2.4
	NF_2	^{14}N (0.8)	−1.0	(0.33)	3.7
		^{19}F (0.1)	−0.4	(0.1)	4.9
Average (central atom)					2.9
Tetra-atomic Radicals	CH_3	^{13}C (1)			3.4
		^{1}H (0)	−4.5	(1)	
	NH_3^+	^{14}N (1)			3.6
		^{1}H (0)	−4.9	(1)	
	$(SO_3)_2NO$	^{14}N (0.6)	−1.0	(0.33)	4.8
		^{17}O (0.4)	−0.7	(0.2)	4.1
	CO_3^-	^{13}C (0)	−1.0	(0.33)	
	NO_3	^{14}N (0)	−1.0	(0.33)	
Average (central atom)					3.9
Penta-atomic Radicals	PO_4^{2-}	^{31}P (0)	−0.7	(0.25)	

For atoms the hyperfine splitting has been divided by the number of unpaired electrons.
[a] The number in parenthesis gives the fractional *s*-character used for obtaining U^A_{BA}.

We feel that a sufficient number of results have now been accommodated to permit the application of Equation 1 to the calculation of spin-densities or to help the task of identifying unknown centers. Some results are gathered together in Table II.

Some Diatomic Radicals

·OH and ·SH. The hydroxyl radical, though well established through studies of electric-dipole transitions in the gas-phase, has proven most elusive in the liquid and solid states.

This is because of the strong coupling between the electron spin and its orbital angular momentum about the molecular axis. For an ESR

Publication Date: January 1, 1968 | doi: 10.1021/ba-1968-0082.ch001

signal to be readily detected in condensed phases an interaction with the medium is required to quench the angular momentum. Hence, rare-gas matrices are unsatisfactory, but strongly polar media such as ice or salt hydrates ought to be suitable, and strong resonance signals are indeed obtained from these materials after exposure to high energy radiation.

Interpretation of the resulting spectra has not been an easy task. For ice this is probably because the spectra of single crystals for most orientations arise from radicals in many magnetically non-equivalent sites. These spectra are dominated by an apparently almost isotropic doublet close to the free-spin *g*-value and separated by about 40 gauss (*12*). However, the earlier discussion of U-values shows that the isotropic hyperfine coupling to the OH radical proton ought to be about −25 gauss rather than the +40 gauss suggested. Also, it was hard to understand why the result should differ so greatly from the value of −27 gauss obtained for gas-phase radicals (*76*), and why the purely dipolar coupling was apparently too small for unit spin-density (*81*).

Further study (*21*) has shown that a broad, low-field feature, previously assigned to other radical species, is really an integral part of the spectrum. Two full analyses of the single crystal data (*22, 36*) together with a re-interpretation of the spectra of various irradiated salt hydrates along the same lines (*53*) have revealed many details of the way in which the hydroxyl radical interacts with the environment, although there remain several obscurities (*22*).

Basically, it seems that one of the four hydrogens surrounding a given oxygen atom in ice is displaced, with a consequent relaxation of the oxygen probably towards the remaining three protons. It is the two hydrogen-bonded protons that are responsible for quenching the orbital angular momentum and their presence is confirmed by the appearance of a small triplet splitting on the main lines for certain orientations.

The hyperfine tensor (Table III) is now far closer to that expected, but the anisotropy is still less than that for gas-phase radicals or that calculated using simple theory (*22*). This may be because of a residual movement or libration and it is hoped that studies at 4.2°K. will shed further light on this.

It would be interesting to compare these results with those for the HS radical, and recently spectra have been described which are said to relate to this radical (*52, 55*). Hadley et al. (*55*) irradiated frozen aqueous hydrogen sulfide with ultraviolet light and obtained a powder spectrum which was reasonably well fitted by the parameters of Table III. This analysis was supported by the results from deuterated samples. Gunning *et al.* (*52*) obtained spectra from both H_2S and D_2S after irradiation of the solids, which are quite similar in appearance (Table III).

Publication Date: January 1, 1968 | doi: 10.1021/ba-1968-0082.ch001

Table III. Magnetic Parameters

Lattice	*g-values*		
	g_x	g_y	g_z
OH ice	2.005 ± 0.002	2.009 ± 0.001	2.06 ± 0.01
ice	2.005 ± 0.001	2.009 ± 0.005	2.0585 ± 0.002
$CaSO_4 \cdot 2H_2O$	2.0028	2.0028	2.1108
$LiSO_4 \cdot H_2O$	2.0065	2.0065	2.0667
SH H_2S	2.003	2.024	2.061
aqueous H_2S	(2.000	2.025	2.039)

[a] Calculated (*21*) from Radford's gas phase data (*76*).

Table IV. Magnetic Parameters

Radical	*Medium*	*Nucleus*	*g-tensor*		
			g_{xx}	g_{yy}	g_{zz}
	NaCl	^{17}O	1.9483	1.9436	2.4529
	KCl		1.9512	1.9551	2.4360
O_2^-	KBr		1.9268	1.9314	2.5203
	KI		1.9370	1.9420	2.4859
	RbCl		1.9836	1.9846	2.2947
	RbI		1.9674	1.9695	2.3774
	NaI	^{33}S	1.9942	2.0178	2.2303
	KCl		0.9484	0.9500	3.4303
S_2^-	KBr		0.8388	0.8434	3.5037
	KI		1.6254	1.6369	3.0629
	RbI		1.2895	1.2968	3.3595
Se_2^-	NaI	^{77}Se	1.8148	1.9042	2.8015
	KI		0.7698	0.7824	3.7079
	NaI	^{77}Se ^{33}S	1.9004	1.9575	2.6064
SSe^-	KI	^{77}Se ^{33}S	0.9532	0.9681	3.6290

[a] The data in References 70, 71 and 60 were given in Mc/s. They have not been converted into gauss because of insufficient information.

The presence of a radical having an isotropic hyperfine coupling to a single proton in the 7 to 10 gauss region and an anisotropic *g*-tensor seems to be indicated, but several features of the results, especially on annealing, are puzzling.

Given that these spectra have been correctly analyzed, it is difficult to see how they could relate to the SH radical. The *g*-tensor is close to that for ·OH radicals, but for ·SH in H_2S one would expect a far larger

Publication Date: January 1, 1968 | doi: 10.1021/ba-1968-0082.ch001

for OH and (possibly) SH

Hyperfine coupling constants (gauss)			
A_x	A_y	A_z	*Ref.*
−26 ± 4	−44 ± 2	0 ± 6	*22*
−26 ± 3	−43.7 ± 0.05	±5 ± 5	*36*
−32.5	−43	±3.3	*53, 54*
−24	−46	±4	*53*
−42.6 ± 0.3	−42.6 ± 0.3	+5.0 ± 0.3	[a]
−35.6	−49.6	+5.2	[b]
7	7	7	*52*
9.5	9.5	9.5	*55*

[b] Calculated (*21*) from Radford's gas phase value (*76*) of $A_{iso} = -26.7 \pm 0.2$ and using the method of McConnell and Strathdee (*66*).

for O_2^-, S_2^-, Se_2^-, and SSe^-

Hyperfine tensor (Mc/s)[a]			
a_{xx}	a_{yy}	a_{zz}	*Ref.*
189.3	0 ± 10	55.1	
181.3	0 ± 10	71.1	
184.3	0 ± 10	64.2	*60*
201.6			
193.7			
[b]	[b]	[b]	
[b]	[b]	137 ± 2	
[b]	[b]	145 ± 2	
64 ± 5	[b]	93 ± 3	
[b]	[b]	105 ± 5	
320 ± 10	<30	265 ± 10	*70, 71*
70 ± 10	45 ± 15	740 ± 5	
450 ± 10	30	145 ± 25	
[b]	[b]	[b]	
120 ± 5	<20	750 ± 5	
<20	<60	140 ± 5	

[b] Results not obtainable from the spectra.

variation in *g*. Also, it is hard to see why the proton coupling should be so small. Firstly, it should be strongly anisotropic, since any rotation capable of averaging the hyperfine anisotropy ought also to average the *g*-tensor, but, in fact, three different *g*-values are rather strongly indicated. Also, the U-value analysis of a range of radicals (*8*) strongly supports the contention that a_{iso} (H) ought to be in the region of −25 gauss. [Compare CH_3 (−24 gauss), NH_3^+ (−24 gauss), NH_2 (−25 gauss) and OH

(−27 gauss)]. The value assigned to PH_2 of (−)18 gauss is less (*26*), but the spectra were poorly resolved so this is only approximate. The coupling of ±8 gauss for SiH_3 is indeed very small, but this almost certainly arises because the radical is pyramidal (*see Some Tetra-atomic Radicals*).

It seems far more likely that radicals such as HS_2 or HS_x are responsible for these spectra. Some support for this stems from the fact that "polymeric" sulfur radicals were identified by their ESR spectra after annealing under various conditions (*52, 55, 77*).

Some confusion has arisen because of the result for HS radicals in the gas-phase. The proton hyperfine coupling of about 5 gauss (*67*) has been taken by both groups to be the Fermi contact value, whereas, in fact, it does not relate directly to the contact term.

O_2^-, S_2^-, Se_2^- and Related Species. Results for these radicals are given in Table IV. Although S_2^- and Se_2^- could well be important products of radiation damage of many materials, they were, in fact, formed by direct doping of alkali halide melts with the vapor of the elements. Their ESR spectra (*70, 71*) are of great interest, since the *g*-values are quite similar to the values of 4 and 0 which would be expected had there been no quenching of the orbital angular momentum.

If one uses the standard, highly simplified, procedure for deducing the total spin-density (*9*), the values which are obtained are so close to unity that they lend very strong support not only to the calculated value of $<r^{-3}>$ but also to the basic approach of neglecting overlap effects (which can be supported on other grounds although many authors contend that overlap ought to be taken into account) and neglecting orbital expansion or contraction. That the calculated $<r^{-3}>$ values are reasonable can also be gauged by the good agreement with the values obtained from atomic beam experiments (*58*).

Some AB σ-Radicals. In a previous review (*19*) we showed how the fluorine hyperfine parameters (*17, 23, 43, 44, 47*) for various XF^- σ-radicals (V_K centers) depend upon the electronegativity of the other halogen atoms (X). Revised values for the parameters (*79*) have led us to present the data again (*see* Figure 1 and Table V). Also included are results assigned to KrF and XeF, although direct comparison is difficult because it is not clear what measure of electron-attracting power one needs to use.

It is clear that there is a drift of spin-density away from fluorine as the electron-attracting power of X falls. This is because of the antibonding nature of the unpaired electron. Also, there is an increase in the *s*-character of the X-orbital as the electron-attracting power of X falls. This probably arises partly because of a greater direct admixture of the atomic *s*-orbital into the σ^*-level and partly from a greater spin

Publication Date: January 1, 1968 | doi: 10.1021/ba-1968-0082.ch001

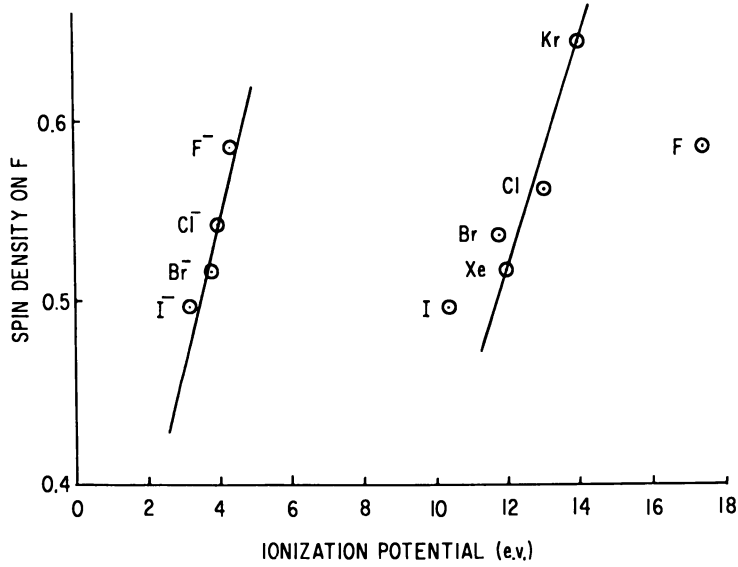

Figure 1. Dependence of the spin-density on fluorine in XF σ-radicals as a function of the ionization potential of X

polarization of the nearest filled σ-level which will have a relatively large contribution from the *s*-orbital of the least electronegative atom.

It is interesting to consider the parameters for a radical (*16*) thought to be FO^{2-} in the light of these trends. The data, which are included in Table V certainly accord, qualitatively, with expectation for this radical. However, the total spin-density on fluorine is very low indeed, being less than that in FOO. Because the sign of $A_\perp$ is unknown, there are two possible sets for the ^{17}O parameters (Table V). If set (i) is taken, then about 84% of the electron is accounted for, but the *p/s* ratio of about 60 is far larger than one would predict by comparison with the V_K centers. Set (ii) gives an acceptable *p/s* ratio, but the net spin-density is only 58%. It is not possible to predict a value for the spin-density on fluorine from the curves of Figure 1, but in view of the very small spread of values recorded there, the very different value for the radical described as FO^{2-} is hard to understand. Possibly, the unit is better pictured as an O^- ion strongly perturbed by an adjacent F^-. The ^{17}O parameters remain curious, however, and it may well be that the FO^{2-} formulation is oversimplified.

Some Triatomic Radicals

NH_2, PH_2 and SH_2. The radical NH_2 has been studied in a variety of matrices and pertinent results are summarized in Table VI. The

Publication Date: January 1, 1968 | doi: 10.1021/ba-1968-0082.ch001

Table V. Magnetic Parameters for

Radical	Nucleus	Medium	g-tensor g_1	g_2	g_3
F_2^-	^{19}F	KF	2.0020	2.0218	2.0218
Cl_2^-	^{35}Cl	KCl	2.0012	2.0426	2.0426
Br_2^-	^{81}Br	KBr	1.9833	2.169	2.169
I_2^-	^{127}I	KI	1.913	2.34	2.34
FCl^-	^{19}F	KCl	2.0018	2.030	2.030
	^{35}Cl				
FBr^-	^{19}F	KCl	1.9891	2.125	2.125
	^{81}Br				
FI^-	^{19}F	KCl	1.9363	2.26	2.26
	^{127}I				
XeF	^{19}F	XeF_4	1.9740	2.126	2.126
KrF	^{19}F	KrF_4	2.000	2.068	2.068
ICl^-	^{127}I	KCl	1.86	2.39	2.39
	^{35}Cl				
FO^{2-}	^{17}O	CaF_2	2.0016	2.0458	2.0458
	^{19}F				

[a] $a_{||}$ and $a_{\perp}$ for ^{17}O and ^{19}F positive and [b] $a_{||}$ positive and $a_{\perp}$ negative.

results for γ-irradiated aqueous ammonia are clearly anomalous, and relate in our view to the parallel features of the rigidly held radical, whereas the remainder relate to rotating NH_2 or have been analyzed to give the true isotropic data. Unfortunately, the spectra in ice are not well enough resolved to warrant detailed analysis. Even so, there seems to be a definite upward trend in the isotropic hyperfine coupling to ^{14}N as the hydrogen-bonding power of the medium is increased.

Changes in a_{iso} with medium are commonly detected, but arise generally because of changes in the distribution of the electron in a delocalized molecular orbital. This can hardly be the case for NH_2, and we suggest two possible alternative causes (*39*). Both relate to the fact that the upward trend in a_{iso} (^{14}N) is towards the value of 18 gauss found for NH_3^+ in various matrices. Since this represents the limit of very strong hydrogen bonding to the NH_2 lone-pair, it is reasonable that weaker bonding should also increase a_{iso}. It is tempting to assign one third of the coupling (6 gauss) for NH_3^+ to each N–H bond and hence to interpret the gradual rise purely in terms of increasing polarization of the lone-pair electrons. The alternative extreme would be to assign the whole increase to the change in *s–p* hybridization of the N–H orbitals as the bond angle opens from 103° for NH_2 to 120° for NH_3^+. This would have no overall

Publication Date: January 1, 1968 | doi: 10.1021/ba-1968-0082.ch001

some Hal_2^- and Related σ-Radicals

Hyperfine tensor (gauss)					
$B_{\|\|}$	$B_\perp$	A_{iso}	a_s^2	a_p^2	*Ref.*
634	−317	274	0.016	0.586	*79*
61.2	−30.6	39.9	0.024	0.582	*79*
288	−144	162	0.019	0.586	*79*
240	−120	147	0.020	0.563	*79*
608	−304	198	0.011	0.562	*79*
73.6	−36.8	52.5	0.032	0.700	
582	−291	153	0.009	0.538	*79*
354	−177	247	0.030	0.720	
538	−269	98	0.006	0.498	*79*
300	−150	261	0.035	0.703	
558	−279	388	0.022	0.516	*43, 79*
696	−348	564	0.033	0.644	*44, 79*
74	−37	348	0.048	0.175	*50*
40	−20	27	0.016	0.40	
56.3	−28.2	48.2	0.03	0.54[a]	
or	or	or	or	or	
83.0	−41.5	21.5	0.013	0.80[b]	*16*
25.8	−12.9	27.9	0.0016	0.026[a]	
or	or	or	or	or	
45.8	−22.9	7.9	0.0005	0.042[b]	

effect on a_{iso} (^{14}N) if polarization of the "lone-pair" remained unchanged on bonding since the total 2*s*-electron density remains distributed between the σ-bonds and the lone-pair. If, however, polarization of the lone-pair is considerably enhanced on bonding, the combined trend could be as observed. This is reasonable since the outward attenuation of the lone-pair is expected to increase as θ increases.

[To test this, we have studied the effect of a wide range of solvents upon the ^{14}N isotropic hyperfine coupling for pyrazine anions and cations (*39*). Here the bond-angle is only able to change slightly on protonation so that changes in a_{iso} must be caused by changes in polarization of the lone-pair electrons provided the π-electron distribution is unaffected. In fact, the changes are very small, showing, we feel, that the dominating effect for NH_2 is associated with the change in bond angle.]

Recently the radical PH_2 has been obtained by radiolysis of PH_3 in rare-gas matrices, but unfortunately the lines are broad and partially hidden beneath more intense features assigned to phosphorus atoms. Thus, the results (*26*) in Table VI have to be treated with some reserve.

As they stand, the results show that the U-value for ^{31}P (2.2) is essentially identical with that for ^{14}N in NH_2, but that the coupling to the protons is appreciably reduced.

Publication Date: January 1, 1968 | doi: 10.1021/ba-1968-0082.ch001

Table VI. Magnetic Parameters

		^{14}N, ^{15}N, ^{31}P, or ^{33}S Hyperfine Coupling constants (gauss)			
	Medium	B_{xx}	B_{yy}	B_{zz}	A_{iso}
NH_2	Argon				10.3
	NH_3				15.0
	aqueous NH_3 (5%)				31.0
	aqueous NH_3 (50%)				18.0
	Argon				10.7
	Argon				10.4
	Krypton				10.7
	Xenon				10.8
	KNH_2/NH_3				16.7
$^{15}NH_2$	KNH_2SO_3	34.9	−16.6	−18.3	18.61
PH_2	Krypton				80.0
SH_2^-	H_2S				60 ± 2
	KCl				

Two groups have recently claimed to have prepared the radical H_2S^-, which has two electrons more than NH_2 or PH_2 (*14, 56*). One group prepared their radical by photolysis of alkali halide crystals doped with HS^- ions. At 20°K. only trapped hydrogen atoms were detected, but after annealing at 110°K. for a few seconds and recooling, spectra assigned to S^- and H_2S^- were obtained. The results for the latter species, summarized in Table VI, show indeed that one sulfur and two equivalent protons are present. Since the protons remain magnetically equivalent for all orientations, the molecule was taken to be linear.

The species prepared by depositing alkali metal atoms and a stream of H_2S gas upon a rotating cold-finger (*14*) gave a rather poorly resolved spectrum which was interpreted in terms of the data in Table VI.

In our view, neither of these radicals has the magnetic properties to be expected for H_2S^-. The only radical bearing any resemblance to this species that has been unambiguously identified by ESR is PF_4 (*8, 68*). The unpaired electron is bound in a molecular orbital closely related to the lowest σ^*-orbital of the tetrahedral molecule, which distorts to reduce the antibonding character. Hence, there is a large *s*-character associated with the central atom. The lowest lying vacant orbital for H_2S is probably also σ^* in character. Hence, the radical H_2S^- is expected to have a very large isotropic proton hyperfine coupling, the situation being similar to that envisaged for deeply trapped hydrogen atoms (*6*) in—*e.g.*, a halide salt. In fact, HCl^- is closely related to H_2S^-, but nevertheless trapped H

Publication Date: January 1, 1968 | doi: 10.1021/ba-1968-0082.ch001

for NH_2, PH_2, and SH_2^-

^1H Hyperfine Coupling constants (gauss)					
B_{xx}	B_{yy}	B_{zz}	A_{iso}	g_{av}	*Ref.*
			−23.9	2.00481	*20*
			−24.5		*75*
			−24.5		*75*
			−23.0		*3*
			−24.8		*32*
			−23.9	2.0038	*25*
			−23.95	2.0036	
			−24.0	2.003	
			−25.2		*24*
−4.0	+1.8	+2.3	−27.4		*69*
			18.0	2.0087	*28*
			7.7 ± 0.3	$g_{\parallel} = 2.0023$; $g_{\perp} = 2.0164$	*14*
−9.1	+4.5	+4.5	−24.2	$g_{\parallel} = 1.9865$; $g_{\perp} = 2.2055$	*56*

atoms have ESR spectra close to that of the gas-phase atoms. We would not expect to find a major contribution from sulfur 3*d* orbitals, but if the electron was primarily a *d*-electron, the *g*-value should be less than the free-spin, whereas in these species there are large positive deviations.

For these and other reasons it seems improbable that H_2S^- is a correct formulation for either of these radicals. Possible alternatives include H_2S^+, isoelectronic with PH_2, and species such as $H_2S_2^-$, $H_2S_2^+$, or more complex polysulfide radicals. The radical H_2S^+ is a possible candidate for the species in alkali halide crystals (*56*), which apparently contains only one sulfur atom, except that some restricted rotational motion would need to be invoked to explain the equivalence of the two protons. Rotation within the molecular plane would achieve this, and would also account for the form and magnitude of the anisotropic proton coupling. The ^{33}S tensor is also accommodated reasonably well, as also is the positive *g*-shift. However, the very large value for Δg is more difficult to reconcile with this formulation.

That the species formed by reaction between H_2S and alkali metal atoms could be more complex than originally envisaged (*14*) is supported by the observation of secondary "polymeric" sulfur radicals on annealing.

CS_2^-, PF_2, and Related Species. The former has not yet been detected as a product of irradiation, but has been unambiguously identified as the initial product in the reaction between alkali metal atoms and

Publication Date: January 1, 1968 | doi: 10.1021/ba-1968-0082.ch001

carbon disulfide. Its magnetic properties, summarized in Table VI, are quite in accord with expectation for this radical, which is isostructural with CO_2^- and NO_2. It is noteworthy that the calculated spin-densities on carbon are almost the same for CO_2^- and CS_2^-, whereas because of the lower electronegativity of sulfur relative to that of oxygen one would have expected a lower spin-density on carbon in CS_2^- than in CO_2^-. However, the p/s ratio for carbon is increased because of the greater bond angle in CS_2^- which offsets this trend. This situation is also found for AB_3 radicals, and is discussed later in detail.

The radical PF_2, isostructural with the stable NF_2, has been made by electron bombardment of solid SF_6 containing about 1% of PF_3 and has also been detected in γ-irradiated NH_4PF_6 (*15*).

Only the isotropic ^{19}F and ^{31}P hyperfine coupling constants were obtained and hence it is difficult to draw any firm conclusions about the structure of this π-radical. The parameters are quite similar to those for NF_2 except if one assumes that, as with NF_2, the spin-density is almost 100% on the central atom, the U-value for ^{31}P is lower than that for ^{14}N. This probably means that the bond angle for PF_2 is less than that for NF_2.

The radicals S_3^- and Se_3^-, which are isostructural with PF_2, have been detected in alkali halides doped with sulfur or selenium, the identification being based upon the appearance of two different ^{33}S or ^{77}Se coupling constants (Table VII). Because of sign ambiguity in the tensor, two sets of data result. However, we favor set (ii) because we expect the spin-density on the central atom to be less than that on the corresponding oxy-radicals SO_2^- and SeO_2^-.

Table VII. Magnetic Parameters

			g-tensor		
Radical	*Matrix*	*Nucleus*	g_{xx}	g_{yy}	g_{zz}
CS_2^-	CS_2	^{13}C	2.0079	1.9661	1.9993
CO_2^-	$NaHCO_2$	^{13}C	2.0032	1.9975	2.0014
PF_2	ND_4PF_6	^{31}P		$g_{iso} = 2.0108$	
		^{19}F			
NF_2	Ne	^{14}N	2.0011	2.0079	2.0042
		^{19}F			
S_3^-	KCl	^{33}S	2.0499	2.0319	2.0026 [a]
		^{33}S [c]			[b]
Se_3^-	KCl	^{77}Se	2.2205	2.1545	1.9885 [a]
		^{77}Se [c]			[b]
SO_2^-	KCl	^{33}S	2.0110	2.0071	2.0025

[a] a_{xx} + ve.
[b] a_{xx} − ve.

Publication Date: January 1, 1968 | doi: 10.1021/ba-1968-0082.ch001

The Radicals FOO and ClOO. It has recently been proposed that a radical containing one chlorine atom, previously thought to be the monoxide, ClO (*4*), is more likely to be the peroxide, ClOO (*38*). The radical is readily formed on photolysis of chlorine dioxide in γ-irradiated $KClO_4$ at room temperature and also from rigid solutions of chlorine dioxide in sulfuric acid at 77°K. However, photolysis of ClO_2 in a chlorate lattice does not result in the formation of this species. If the radical is indeed ClOO, this can be understood since chlorate is an extremely efficient oxygen atom acceptor, which would favor formation of ClO rather than ClOO. Also, many details of the ESR spectra are readily accommodated if ClOO is the correct formulation but very hard to understand if the species is ClO.

The properties of this radical are similar to those of the stable fluorine analogue, FOO, and they are compared in Table VIII. In general, the radical ABO will be more stable than BAO when the electronegativity of A is greater than that of B. Hence, FO_2 is not detected in solutions containing FOO, but ClO_2 is more stable than ClOO. Our results (*38*) show that ClOO isomerizes to ClO_2 in $KClO_4$ at room temperature.

Another example of a peroxy-oxyradical is O_3SOO^-, which is formed on photolysis or radiolysis of potassium persulfate crystals (*10*). It seems probable that peroxy radicals of this type, including XOO, OXOO, O_2XOO, and O_3XOO, ought to be considered as possible species in radiation-damage studies of oxy-salts.

The Radical Be_2F^{2+}. The detection of a widely spaced doublet having extra hyperfine splitting for each component in X-irradiated BeO

for CS_2^-, PF_2, and Related Radicals

Hyperfine tensor (gauss)

a_{xx}	a_{yy}	a_{zz}	a_s^2	$a_{P_z}^2$	$a_{P_x}^2$	*p/s*	*Ref.*
73.1	67.0	121.6	0.077	0.560	0.06	7.3	13
155.8	150.8	195.1	0.15	0.50	0.08	3.3	*74*
	$a_{iso} = 36$		0.01				*15*
	$a_{iso} = 60.5$		0.004				
49 ± 0.5	0 ± 1.0	0 ± 1.0	0.03	0.94			*61*
212 ± 2.0	−16.9 ± 1.0	−16.9 ± 1.0	0.004	0.14			
−10	−2	+52	0.013	0.69			*37*
+1	0	+19	0.007	0.21			
−1	0	+19	0.006	0.23			
−48	−59	+247	0.010	0.74			*37*
+17	0	+72	0.006	0.16			
−17	0	+72	0.004	0.20			
−7.1	−8.6	+52.5	0.013	0.71			*37*

[c] outermost atoms.

Publication Date: January 1, 1968 | doi: 10.1021/ba-1968-0082.ch001

Table VIII. Magnetic Parameters for FOO and ClOO

		A tensor (^{35}Cl or ^{19}F) in gauss			*g-tensor*			
Radical	*Medium*	a_{11}	a_{22}	a_{33}	g_{11}	g_{22}	g_{33}	*Ref.*
ClOO	H_2SO_4	[a]	[a]	15.3	[a]	[a]	2.0115	*38*
	$KClO_4$	(−)5.3	(+)7.2	(−)14.9	1.9983	2.0017	2.0130	*38*
FOO	Argon	(∓)50	(∓)14.0	(±)103	2.0008	2.0022	2.0080	*2*

[a] These values were not obtained.

powder led to the postulate (*73*) that an unpaired electron was trapped in the 3*s* level of a substitutional fluoride ion. The structure of this center has been discussed in terms of bonding to neighboring beryllium cations (*19, 83*) which led to the idea that the large isotropic coupling to fluorine involved the 2*s*-rather than the 3*s*-orbital. The model postulated involved an unpaired electron in a σ^*-orbital between fluoride and one of the three equivalent beryllium ions adjacent thereto. This orbital closely resembles that for the unpaired electron in nitrogen centers in diamond (*18, 49*), and the electron should have a high density on the beryllium 2*s* orbital and a low density on fluorine. A rapid fluctuation between the three beryllium ions would then give the required equivalence.

Many features of this model have been confirmed by a recent study of fluoride-doped single crystals of beryllium oxide (*42*). The basic unit is Be_2F^{2+} rather than BeF and hopping then occurs between the three possible states involving the three beryllium ions. However, the normal model for such a hopping process was incompatible with the temperature dependence, and a model involving quantum mechanical coupling between the three states was devised to account for the behavior (*42*).

Some Tetra-atomic Radicals

BH_3^-, SiH_3, and Related Species. The radical BH_3^- has been identified as one of the products in potassium tetrahydridoborate, after γ-irradiation at 77°K. (*84*). The results, given in Table IX, show that the proton coupling is somewhat lower than that for the isoelectronic radicals CH_3 and NH_3^+, but that the U-value for boron is very close to those for ^{13}C and ^{14}N. There is a steady trend to lower g_{av} values on going from NH_3^+ to BH_3^- (Table IX).

That the proton hyperfine coupling for SiH_3 radicals was much smaller ($\sim \pm 8$ gauss) has been known for some time (*29*) and it was surmised that this was because the radical could well be pyramidal with a positive coupling (*80*). The detection of a large ^{29}Si hyperfine coupling has confirmed this postulate (*27*). This trend from planar CH_3 to pyramidal SiH_3 follows the decrease in bond angle on going from NH_3 to PH_3.

Publication Date: January 1, 1968 | doi: 10.1021/ba-1968-0082.ch001

The Radicals NO_3^{2-}, CO_3^{3-}, and Related Species. The radical NO_3^{2-}, identified originally in irradiated nitrates and nitrate-doped alkali halides (*33, 59*), has now been prepared in nitrate-doped calcite (*40*). Its properties are interesting in that its bond angle, as deduced from the ^{14}N hyperfine tensor (*7*) (115°), is almost midway between that for the planar radical (120°) and the strongly pyramidal isostructural radicals such as PO_3^{2-} ($\sim$ 110°).

The detection of CO_3^{3-} in irradiated calcite (*40, 64*) enables us to draw some conclusions regarding the overall factors which control the degree of bending in these 25-electron radicals. The situation we envisage is depicted in Figure 2 in which the difference in electronegativity between the central and outer atoms is plotted against total spin-density on the central atom. There is a steady decrease in the p/s ratio on going from NO_3^{2-} (7.8) to CO_3^{3-} (5.25) and CF_3 ($\sim$ 3) as the spin-density on the central atom rises.

It seems that there is a greater tendency for the first row radicals to be planar, possibly for steric reasons, and it is particularly those radicals with intermediate bond angles that are sensitive to changes in electronegativity. The increase in 2*s*-character on the central atom leads to an increase in its effective electronegativity and hence to a fall in the spin-density thereon. The result for the isoelectronic radical CF_3 has been included in Figure 2. The p/s ratio for carbon in this radical must be close to three and so it has the same shape as the second and third row radicals. We conclude that, when a series of radicals have shapes which are intermediate between the normal extremes, an increase in the electronegativity difference between the outer and central atoms will lead to an increased bending and to a decrease in the normal growth of the spin-density on the central atom.

$C_2N_2^-$, $S_2N_2^+$, and Related Species. The radical $C_2N_2^-$ is thought to bear a structural resemblance to the cyanogen molecule, and is related to the V_K centers in being the simplest hole-center in cyanide salts (*78*). It is formed on exposure of alkali metal cyanides or cyanide-doped halides to γ-radiation and analysis of the ESR spectrum strongly supports a *trans*-bent structure.

This is a 19-electron radical and can be contrasted with the radical N_4^-, a 21-electron radical, which is thought to have a distorted square-planar structure, with all the nitrogen atoms equivalent (*81*). Another center, with four equivalent sulfur atoms, has recently been described, although details are not given (*37*). A square-planar structure again seems possible and it would be of interest to discover the nature of the orbital of the unpaired electron. Certainly the factors which determine the most stable geometry of these tetra-atomic radicals are a matter of some interest.

Publication Date: January 1, 1968 | doi: 10.1021/ba-1968-0082.ch001

Table IX. Magnetic Parameters

Radical	Matrix	Nucleus	Anisotropic Hyperfine tensor (gauss) A_1	A_2	A_3
BH_3^-	KBH_4	^{11}B ^{1}H			
CH_3	CH_3I CH_4 Krypton	^{13}C ^{1}H			
NH_3^+	NH_4ClO_4	^{14}N ^{1}H			
SiH_3	Krypton	^{29}Si ^{1}H		46–52	

Some 31 Electron Penta-atomic Radicals

Although radicals such as PO_4^{2-} or SO_4^- have often been reported, many aspects of their structure remain obscure. Some time ago it was suggested that the unpaired electron would be expected to be in a t_1 orbital in the undistorted tetrahedral radicals, which is purely non-bonding on oxygen (*80*). All the species to which this structure has been assigned have markedly asymmetric *g*-tensors with near axial symmetry, but the nature of the distortions which cause this deviation from symmetry remain obscure.

Perhaps the most characteristic feature is the small, nearly isotropic hyperfine coupling to the central atom, which corresponds to a U-value in the range 0.6 to 0.8. This fits in well with the proposed correlation between U-values and σ-bond hybridization (*57*), but the results recently assigned to ClO_4 do not (*72*). The species under consideration is formed by exposure of $KClO_4$ crystals to γ-rays at 77°K. and is lost irreversibly on warming to above 100°K. The magnetic properties are given together with those assigned to PO_4^{2-} and SO_4^- in Table X and it can be seen that both the total 3*s*-character and the p/s ratio are larger than expected. Furthermore, the form of the *g*-tensor is quite different from that for the other radicals. Whilst these differences may well be a consequence of a different form of distortion preferred by ClO_4, it seems possible that the species involved is not the normal ClO_4. However, its identity then poses a problem, since most of the "normal" monochlorine radicals are known. One alternative which bears scrutiny is the peroxy-radical O_2ClOO. The orbital of the unpaired electron would be considerably delocalized on to the peroxy-oxygens, but nevertheless the basic structure should be closely related to that of the σ-radical ClO_3 (*5*).

Publication Date: January 1, 1968 | doi: 10.1021/ba-1968-0082.ch001

for BH_3^-, CH_3, NH_3^+, and SiH_3

A_{iso}	g_{av}	a_B^2	U^X	*Ref.*
(+)24	2.0013	0.033	3.3	*84*
(−)16.5		0.033		*84*
(+)41	2.0026	0.037	3.7	*27, 31,*
(−)23.0		0.045		*and 46*
(+)19.5	2.0035	0.036	3.6	*30*
(−)25.9		0.051		
200–300	2.006	0.2		*27*
−8.1		0.016		

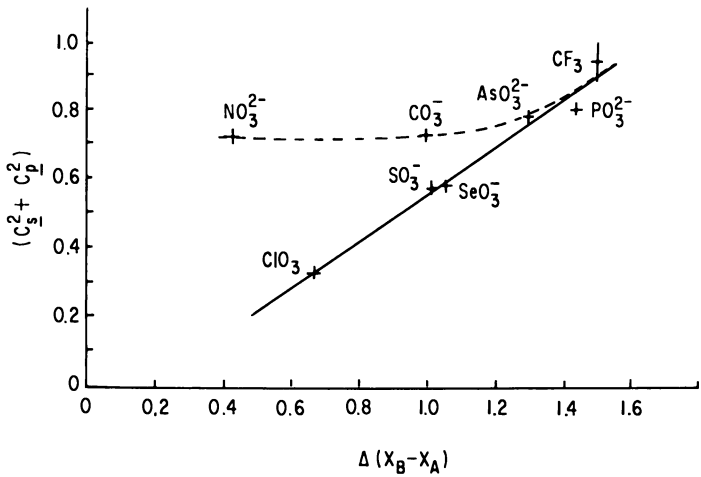

Figure 2. Dependence of the spin-density on A for certain AB_3 radicals as a function of the difference in the electronegativities of A and B $\Delta(\chi_B - \chi_A)$

One curious feature of the results is the appearance of two rather similar radicals: it seems that further studies are needed before firm conclusions about their structure can be drawn.

Another class of radical which seems to be readily formed on radiolysis consists of transition-metal XO_4 analogues such as VO_4^{2-} and WO_4^-. Again, however, the results are not clear-cut. The radical WO_4^- is not itself detected in irradiated tungstates, but rather a two-tungsten center is found which could be the WO_4^-–WO_4^{2-} (*62*) analog of the V_K centers.

Table X. Magnetic Parameters

Radical	Medium	Nucleus	g-tensor g_{xx}	g_{yy}	g_{zz}
PO_4^{2-}	Calcite	^{31}P	2.0072	2.0033	2.0122
SO_4^-	$K_2S_2O_8$	^{33}S	2.0047	2.0034	2.0142
ClO_4	$KClO_4$	a) ^{35}Cl	2.0024	2.0548	2.0553
		b) ^{35}Cl	2.005	2.036	2.038
VO_4^{2-}	$CaMoO_4$	^{51}V		$g_{av} = 2.023$	
(WO_4^-–WO_4^{2-})	$CaWO_4$	^{183}W	2.0013	2.0064	2.0352

Radicals having rather similar properties (Table X) containing one vanadium atom are formed on exposure of molybdates doped with vanadate to γ-rays (*41*). We have also prepared radicals which could well be NbO_4^{2-} and MoO_4^-.

The difficulty with the formulation XO_4–XO_4^- can be understood if one envisages its formation from the peroxide O_3XOOXO_3 by adding an extra electron. While this could possibly be accommodated in the O–O σ^*-orbital, it is far more likely to go into one of the π-d metal orbitals, probably with an equal distribution between the two metal atoms. The magnetic properties of the two-tungsten center in calcium tungstate do not accord with either of these formulations, so it may be that the center is better described as WO_4^-, there being a fortuitously rapid electron transfer between two tungstates having identical environments.

If it is accepted that the vanadium species is indeed VO_4^{2-}, then the way in which the vanadium atom acquires an isotropic hyperfine coupling, remains obscure. The latter is almost three times larger than would be predicted from the U-value of PO_4^{2-}, but is much smaller than the "normal" value of about 100 gauss resulting from spin polarization of inner s-electrons by an unpaired $3d$-electron.

Some Conclusions and Aspects of Mechanism

Despite the rapid rise in understanding the factors involved, the task of interpreting ESR spectra remains formidable in many cases, especially when only powder spectra are available. In that case, the use of two frequencies (say X- and Q-band) can be a great help in unravelling the difference between hyperfine and g-features, as can the use of different isotopes. Extracting the hyperfine and g-tensors from single-crystal spectra is more satisfactory than the use of powders, and gives, of course, directions, which cannot be deduced from powders. However, pitfalls again abound and we strongly recommend the parallel study of powders, which will give an overall guide to the sort of results to be expected from the crystal.

Publication Date: January 1, 1968 | doi: 10.1021/ba-1968-0082.ch001

for Some XO_4 Radicals

Hyperfine tensor (gauss)					
A_{xx}	A_{yy}	A_{zz}	a_s^2	a_p^2	*Ref.*
18.76	20.06	18.61	0.0053	0.004	*63*
ca 4	*ca* 4	*ca* 4	*ca* 0.004		*11*
	$A_{iso} = 57$		0.034		*72*
69	71	83	0.044	0.09	
	$A_{iso} = 19.5$				*41*
9.5	10.5	9.0			*41*

Magnetic "centers" are frequently normal "molecules" unless they are part of a polymeric network, but their characteristic spectra may be greatly modified by minor interaction with their environment, which can nevertheless give rise to extra features.

The characteristic magnetic properties of a particular radical may be so greatly modified by various possible modes of restricted rotation that, unless this is appreciated, the spectrum may be assigned to a new radical. The results for the fluorine center in BeO comprise an interesting variation on this theme.

The task of identification may be aided by the following general points—

(1) If a given nuclear hyperfine coupling tensor on analysis shows that there is a large atomic *s*-character in the orbital, then this atom is probably a "central" atom in a σ-radical.

(2) If the hyperfine coupling clearly indicates *p*-character (or *d*-character) only, then it is either a central or "ligand" atom in a π-radical. The "ligand" atoms in σ-radicals may show a large or small percentage of *s*-character depending upon the *s*-contribution to the σ-orbital and the dominating mechanism of delocalization. This has been discussed in detail elsewhere (*19*).

Attempts to prepare simple electron-deficient species by γ-irradiation of suitable solids may be frustrated by their tendency to bond, weakly, or strongly, to neighboring molecules. Thus, our attempts to prepare the CN radical from cyanide ions have always been frustrated by the formation of $C_2N_2^-$ radicals.

Another way in which the spectra of trapped radicals can be greatly modified is by spin-spin coupling to neighboring radicals. Radical pairs may be formed in relatively low abundance, in which case weak satellite lines may be found at high gain, which can be confused with traces of secondary radicals, or with features from molecules containing low-abundant isotopes. For example, the features assigned to $N_2O_2^+$ in irradiated sodium nitroprusside crystals (*34*) were in fact a property of pairs of the highly-abundant "parent" radicals (*51*).

Publication Date: January 1, 1968 | doi: 10.1021/ba-1968-0082.ch001

Sometimes the mechanism of damage is such that these pairs dominate the spectra, in which case the basic pattern will be that of a triplet-state radical.

We conclude with a brief survey of some of the mechanistic features which emerge from these studies. After ejection, electrons will be rapidly trapped, not necessarily at the deepest traps available, but rather at the most abundant, which are deep enough to lead to a stationary state for the electron at the temperature involved. Then the residual "hole" must be sufficiently immobile to prevent migration and recombination.

The situation can be exemplified by considering our results for calcite doped with nitrate ions. Exposure to γ-rays at 77°K. gives CO_3^- and NO_3 as hole-centers, and CO_3^{3-} and NO_3^{2-} as electron-excess centers. The radical NO_3 readily gains electrons from neighboring carbonate ions which are relatively "mobile" because of electron-transfer, but which presumably distort sufficiently at low temperature to act as traps. On annealing these centers decay, as does the CO_3^{3-} center which is stabilized with respect to electron-transfer by its pyramidal distortion. The NO_3^{2-} center is stable to above 150°K. because there is now no tendency for electron-transfer and charge-neutrality is achieved. Similarly, phosphate-doped calcite gives the hole-center on exposure to high energy radiation, which is again remarkably stable because of charge neutrality (*63*).

Often these centers are "fixed" or stabilized by chemical reaction rather than by simple distortion, and if protons are present in hole-centers it often comprises proton loss to the medium (*83*). Alternatively, holes and electrons may re-combine but the resulting excited parent molecule may decompose before dropping to the ground-state, in which case the decomposition resembles a photolysis.

The pair-wise trapping of radicals is probably a more common occurrence than was originally appreciated, though it remains difficult to predict when it is likely to be sufficiently specific to do more than broaden ESR lines. That solid-state photolysis might be expected to give pairs of radicals has long been appreciated, a clear-cut example of this being the photolysis of potassium persulfate crystals (*10*). However, high energy radiation may also give rise to such pair-trapping, the pairs being either a minor product (*51*), or occasionally almost the sole radical product (*35*). At least in certain cases it seems probable that when this happens it is the result of normal bond homolysis (*35*), although mechanisms involving further reactions of initially formed neighboring holes and electron-excess centers can be envisaged (*83*).

Acknowledgments

Thanks are offered to D. Tinling and to R. Eachus for considerable assistance in preparing this review.

Literature Cited

(1) Adams, R. J., Catton, R. C., Harrison, L. G., *J. Chem. Phys.* **45,** 4023 (1966).
(2) Adrian, F. J., *J. Chem. Phys.* **46,** 1543 (1967).
(3) Al-Naimy, B. S., Moorthy, P. N., Weiss, J. J., *J. Phys. Chem.* **70,** 3654 (1966).
(4) Atkins, P. W., Brivati, J. A., Keen, N., Symons, M. C. R., Trevalion, P. A., *J. Chem. Soc.* **1962,** 4785.
(5) *Ibid.*, **1962,** 4785.
(6) Atkins, P. W., Keen, N., Symons, M. C. R., Wardale, H. W., *J. Chem. Soc.* **1963,** 5594.
(7) Atkins, P. W., Symons, M. C. R., *J. Chem. Soc.* **1962,** 4794.
(8) *Ibid.*, **1964,** 4364.
(9) Atkins, P. W., Symons, M. C. R., "The Structure of Inorganic Radicals," Elsevier, Amsterdam, 1967.
(10) Barnes, S. B., Symons, M. C. R., *J. Chem. Soc., A.* **1966,** 66.
(11) Barnes, S. B., Symons, M. C. R. (unpublished results).
(12) Baum, L. H., Fluornoy, J. W., Siegel, S., Skolnik, S., *J. Chem. Phys.* **32,** 1249 (1960).
(13) Bennett, J. E., Mile, B., Thomas, A., *Trans. Faraday Soc.* **63,** 262 (1967).
(14) Bennett, J. E., Mile, B., Thomas, A., *Chem. Comm.* **1966,** 182.
(15) Bernstein, H. J., Morton, J. R., Wan, J. K. S., *Can. J. Chem.* **44,** 1957 (1966).
(16) Bill, H., Lacroix, R., *J. de Physique Suppl.* **28,** C4-138 (1967).
(17) Boesman, E., Schoemaker, D., *J. Chem. Phys.* **37,** 671 (1962).
(18) Bower, H. J., Symons, M. C. R., *Nature* **210,** 1037 (1966).
(19) Bower, H. J., Symons, M. C. R., Tinling, D. J. A., "Radical Ions," Chapt. 10, E. Kaiser, L. Kevan, eds., Wiley Interscience, New York, 1967.
(20) Bowers, V. A., Cochran, E. L., Foner, S. N., Jen, C. K., *Phys. Rev. Letters* **1,** 91 (1958).
(21) Brivati, J. A., Symons, M. C. R., Tinling, D. J. A., Wardale, H. W., Williams, D. O., *Chem. Comm.* **1,** 402 (1965).
(22) Brivati, J. A., Symons, M. C. R., Tinling, D. J. A., Wardale, H. W., Williams, D. O., *Trans. Faraday Soc.* **63,** 2112 (1967).
(23) Castner, T. A., Kanzig, W., *J. Phys. Chem. Solids* **3,** 178 (1957).
(24) Catterall, R. (unpublished results).
(25) Charles, S. W., Fischer, P. H. H., McDowell, C. A., *J. Chem. Phys.* **46,** 2162 (1967).
(26) Christiansen, J. J., Gordy, W., Morehouse, R. L., *J. Chem. Phys.* **45,** 1747 (1966).
(27) *Ibid.*, **45,** 1751 (1966).
(28) *Ibid.*, **45,** 1747 (1966).
(29) Cochran, E. L., *4th Intern. Symp. on Free Radicals, Washington* (1959).
(30) Cole, T., *J. Chem. Phys.* **35,** 1169 (1961).
(31) Cole, T., Davidson, N. R., McConnell, H. M., Pritchard, H. O., *Mol. Phys.* **1,** 406 (1958).
(32) Coope, J. A. R., Farmer, J. B., Gardner, C. L., McDowell, C. A., *J. Chem. Phys.* **42,** 2628 (1965).
(33) Cunningham, J., *5th Intern. Symp. on Free Radicals,* Uppsala (1961).
(34) Danon, J., Muniz, R. P. A., *Mol. Phys.* **9,** 599 (1965).
(35) Davis, A., Golden, J. H., McRae, J. A., Symons, M. C. R., *Chem. Comm.* **1967,** 398.
(36) Dibdin, G. H., *Trans. Faraday Soc.* **63,** 2098 (1967).
(37) Dischler, Raeuber, A., Schneider, J., *Phys. Stat. Solidi* **13,** 141 (1966).
(38) Eachus, R. S., Edwards, P. R., Subramanian, S., Symons, M. C. R., *Chem. Comm.* **1967,** 1036.

(39) Eachus, R. S., Symons, M. C. R. (unpublished results).
(40) Eachus, R. S., Symons, M. C. R., *J. Chem. Soc. A*, **1968**, 790.
(41) Edwards, P. R., Subramanian, S., Symons, M. C. R. (unpublished results).
(42) Estle, T. L., Reinberg, A. R., *Phys. Rev.* **160**, 263 (1967).
(43) Falconer, W. E., Morton, J. A., *Proc. Chem. Soc.* **1963**, 95.
(44) Falconer, W. E., Morton, J. R., Streng, A. G., *J. Chem. Phys.* **41**, 902 (1964).
(45) Fessenden, R. W., Schuler, R. H., *J. Chem. Phys.* **45**, 1845 (1966).
(46) *Ibid.*, **39**, 2147 (1963).
(47) Gabriel, J. R., Wilkins, J. W., *Phys. Rev.* **132**, 1950 (1963).
(48) Gelerinter, E., Silsbee, R. H., *J. Chem. Phys.* **45**, 1703 (1966).
(49) Gelles, I. L., Lasher, G. J., Smith, W. V., Sorokin, P. P., *Phys. Rev.* **115**, 1546 (1959).
(50) Goldberg, L. S., Meistrich, M. L., *Solid State Comm.* **4**, 469 (1966).
(51) Goodman, B. A., McNeil, A. C., Raynor, J. B., Symons, M. C. R., *J. Chem. Soc.* **1966**, 1547.
(52) Gunning, H. E., Stiles, D. A., Strausz, O. P., Tyerman, W. J. R., *Can. J. Chem.* **44**, 2149 (1966).
(53) Gunter, T. E., *J. Chem. Phys.* **46**, 3818 (1967).
(54) Gunter, T. E., Jeffries, C. D., University of California Radiation Laboratory, **11387S**, 8 (1964).
(55) Hadley, S. G., Volman, D. H., Wolstenholme, J., *J. Phys. Chem.* **71**, 1798 (1967).
(56) Hausmann, A., *Z. Phys.* **192**, 313 (1966).
(57) Hunter, T. F., Symons, M. C. R., *J. Chem. Soc., A* **1967**, 1770.
(58) Jaccarino, V., King, J. G., *Phys. Rev.* **84**, 852 (1951).
(59) Jaccard, C., *Phys. Rev.* **124**, 60 (1961).
(60) Kanzig, W., Shuey, R. T., Zeller, H. R., *J. de Physique, Suppl.* **28**, C4-81 (1967).
(61) Kasai, P. H., Whipple, E. B., *Mol. Phys.* **9**, 497 (1965).
(62) Livingston, R., Zeldes, H., *J. Chem. Phys.* **34**, 247 (1961).
(63) Marshall, S. A., Serway, R. A., *J. Chem. Phys.* **45**, 4098 (1966).
(64) *Ibid.*, **46**, 1949 (1967).
(65) McConnell, H., *J. Chem. Phys.* **24**, 764 (1959).
(66) McConnell, H. M., Strathdee, J., *Mol. Phys.* **2**, 129 (1959).
(67) McDonald, C. C., *J. Chem. Phys.* **39**, 2587 (1963).
(68) Morton, J. R., *Can. J. Phys.* **41**, 706 (1963).
(69) Morton, J. R., Smith, D. R., *Can. J. Chem.* **44**, 1951 (1966).
(70) Morton, J. R., Vanotti, L. E., *Phys. Rev.* **161**, 282 (1967).
(71) Morton, J. R., Vanotti, L. E., *Phys. Letters* **24A**, 520 (1967).
(72) Morton, J. R., *J. Chem. Phys.* **45**, 1800 (1966).
(73) Novak, L., Sroubek, Z., Zdansky, K., *Phys. Status Solidi* **6**, 173 (1964).
(74) Ovenall, D. W., Whiffen, D. H., *Mol. Phys.* **4**, 135 (1961).
(75) Pshezhetskii, S. Ya., Tupikov, V. I., *Russ. J. Phys. Chem.* **38**, 1364 (1964).
(76) Radford, H. E., *Phys. Rev.* **126**, 1035 (1962).
(77) Radford, H. E., Rice, F. O., *J. Chem. Phys.* **33**, 774 (1960).
(78) Root, K. D. J., Symons, M. C. R., *J. Chem. Soc., A*, **1968**, 21.
(79) Schoemaker, D., *Phys. Rev.* **149**, 693 (1966).
(80) Symons, M. C. R., ADVAN. CHEM. SER. **36**, 76 (1962).
(81) Symons, M. C. R., *J. Chem. Soc.* **1963**, 570.
(82) *Ibid.*, **1965**, 2276.
(83) Symons, M. C. R., "Radiation Research 1966," North-Holland Publishing Co., Amsterdam, 1967.
(84) Symons, M. C. R., Wardale, H., *Chem. Comm.* **1967**, 758.

RECEIVED January 30, 1968.

Electron-Scavenging Processes in the Radiolysis of Hydrocarbon Solutions

JOHN M. WARMAN, K.-D. ASMUS, and ROBERT H. SCHULER

Radiation Research Laboratories, Mellon Institute, Carnegie-Mellon University, Pittsburgh, Pa. 15213

Publication Date: January 1, 1968 | doi: 10.1021/ba-1968-0082.ch002

The current state of knowledge of electron-scavenging processes in liquid hydrocarbons is summarized. Interpretation of data is critically discussed in the light of the possible complicating factors. The relation

$$G(S^-) = G_{f1} + \frac{G_{g1}\{\alpha_s[S]\}^{1/2}}{1 + \{\alpha_s[S]\}^{1/2}}$$

is found to describe the concentration dependence of electron scavenging in a number of cases. Using this relation it is shown that a detailed treatment of the scavenging kinetics in competitive situations is possible. Secondary reactions involving negative ions are postulated to explain anomalies found in the available data. For nitrous oxide solutions the high nitrogen yields observed can be quantitatively explained by secondary ionic reactions with the nitrous oxide.

Radiation chemists have been aware for about 15 years that the presence of dilute solutes in liquid hydrocarbons can change the course of radiation chemical reactions by other than the normally expected secondary radical reactions. For example, Manion and Burton (*40*) in early work on the radiolysis of benzene–cyclohexane solutions, drew attention to the possibility of energy transfer from solvent to solute. Furthermore, it is known that in hydrocarbon solvents certain solutes are capable of capturing electrons, thus interfering with the normal ion-recombination process (*14, 20, 65, 72*). Though ionic products can be observed readily in hydrocarbon glasses [*e.g.*, (*19, 21*)] demonstration of effects which can be specifically ascribed to electron capture in the liquid state has been elusive until recently. Reaction of positive ions prior to neutralization can play an important role as demonstrated recently by studies on

In Radiation Chemistry; Hart, E.;
Advances in Chemistry; American Chemical Society: Washington, DC, 1968.

the production of HD from ND_3 solutions (*10, 71*) and on the formation of propane from cyclopropane (*3*).

In one of the first attempts to probe electron scavenging in hydrocarbon solutions, Williams and Hamill (*72*) studied the production of alkyl radicals from the dissociation of solute alkyl halides and found appreciable yields ($G \sim 3$) which they attributed largely to dissociative electron capture by the halide. Although current work indicates that this interpretation is for the most part correct, significant difficulty exists in distinguishing between chemistry which results from electron scavenging and that which results from hydrogen atom attack on the solute. Because of this and additional difficulties related to other possible modes of energy transfer, even the yields of hydrogen atoms from the radiolysis of particular hydrocarbons have been questionable. For example, the hydrogen atom yield, $G(H)$, in such a commonly studied material as cyclohexane has been suggested to be anywhere from quite small to about 3. At the moment, the yield indicated from various experiments seems to point to a value of about 1.5, but interpretation of available results is still far from being completely straightforward.

The interest and attention of radiation chemists have recently been redirected to electron-scavenging processes in liquid hydrocarbons by the finding of Scholes and Simic (*63*) that high nitrogen yields [$G(N_2) \sim 3.8$ at $0.1M$ N_2O] are formed in the radiolysis of solutions of nitrous oxide. The formation of nitrogen from nitrous oxide solutions in the gaseous and aqueous phases has been shown to result specifically from electron capture by the nitrous oxide. It seems likely therefore, as suggested by Scholes and Simic, that the observed nitrogen results from the reaction of electrons with nitrous oxide before recombination occurs with the positive ion. This conclusion is supported by the finding that the addition of a second electron scavenger such as CCl_4 or SF_6 competes with the N_2O and reduces the nitrogen yield. These observations, together with the other information reviewed here, leave little doubt at present that electron scavenging can be of considerable importance and must be properly considered in studies of the radiation chemistry of hydrocarbon solutions. However, as will be seen, the detailed interpretation of results is still not completely satisfactory, and the subject is currently in an active state of development. It is hoped that this summary may provide a firmer foundation for considering the possible complicating factors in electron-scavenging studies.

General Considerations

In liquid hydrocarbon radiolysis, analogies are frequently drawn from gas-phase studies, particularly in regard to ionic processes. We

Publication Date: January 1, 1968 | doi: 10.1021/ba-1968-0082.ch002

begin, therefore, with a general description of the physical differences existing between the two phases and the ways in which these differences can affect ion recombination and electron capture. Attention is focused on processes occurring with low LET radiations since essentially all experimental studies on electron scavenging have used ^{60}Co γ-rays.

Upon irradiating the gas phase, a uniform distribution of electrons and positive ions results, and ion yields can be readily determined by applying an electric field and measuring the saturation ion current. For most hydrocarbons, the yield of ions, G_i, is *ca.* 4 (*42*). For liquid hydrocarbons the yield of ions which ultimately become uniformly distributed throughout the solutions is found, from conductivity experiments, to be only *ca.* 0.1 (*1, 15, 16, 30, 62*). These ions are frequently referred to as free ions, and their yield will be designated here as G_{fi}. Since the primary excitation processes in radiation chemistry are not considered to depend to a large extent on the density of the medium, the low yield of these free ions indicates that only a few percent of the electrons initially formed ultimately become thermalized at a distance from the positive ion where they can escape its coulombic force field. The majority of electrons are recaptured by the parent positive ion (geminate recombination) at least qualitatively along the lines of the model originally suggested by Samuel and Magee (*59*) although this model has been somewhat modified in a recent treatment (*43*) which indicates that there is no explicit electron energy below which geminate recombination always occurs. Since the yield of products attributed to electron scavenging is considerably greater than the yield of free ions, it must be assumed that the majority of electrons which react are those which would otherwise undergo geminate recombination. For this to occur, the reaction time must be longer than the 10^{-13} sec. given by the original geminate recombination arguments (which would provide little opportunity for reaction with solutes) and is probably more of the magnitude of 10^{-11} sec. suggested by Burton, Dillon, and Rein (*9*).

In the one experimental study on electron scavenging carried out with high LET radiations Burns and Reed (*8*) have examined the yields of N_2 and H_2 produced from nitrous oxide–cyclohexane solutions by 2 Mev. helium ions (LET $\sim$ 20 e.v./A.). At particular N_2O concentrations they find significantly lower N_2 yields and smaller decreases in the H_2 than observed in the γ-ray experiments (at 0.1*M* N_2O $G(N_2) = 0.6$ in experiments with helium ions *vs.* 3.8 for those with γ-rays; $\Delta G(H_2) = 0.2$ *vs.* 2.3). Here reaction between the electron and a positive ion other than its original partner apparently becomes significant, and the electron-scavenging process cannot compete as efficiently as at low LET's.

While the nature of the electrons produced in liquids may not differ significantly from those produced in the gas phase, the chemistry and

Publication Date: January 1, 1968 | doi: 10.1021/ba-1968-0082.ch002

kinetics of reactions involving such electrons may be considerably changed owing to their much shorter lifetimes. In particular, it is expected that the ordinary laws of homogeneous kinetics will not apply. As a corollary, effects which interfere chemically before the occurrence of ion recombination will be extremely difficult to saturate, and chemical approaches to the measurement of ion-pair yields will give only lower limits to these values. In recent years considerable attention has been given to attempts to obtain, both theoretically and empirically, the expected kinetic behavior. A considerable portion of the present summary is devoted to this topic.

Whether the electrons are "free" or not, their ultimate fate in the absence of an electron scavenger will be recombination with a positive ion.

$$e^- + RH^+ \rightarrow RH^* \quad (1)$$

Owing to the close packing of molecules in the liquid phase, the energetics and mechanism of ion recombination may differ considerably from those in the gas phase. In the latter case all of the potential energy arising from the spatial separation of the ions is recovered in the recombination process as kinetic energy of the colliding ions. The energy released on recombination is therefore equal to the ionization potential. In the liquid phase, however, the kinetic energy gained by the electron as it drifts toward the positive ion is continually dissipated by collision with neutral molecules. The total energy so dissipated will be approximately equal to the potential energy of the ion pair when the electron has approached the positive ion to a distance of one molecular diameter and can no longer collide with other molecules. This is given in units of electron volts by $14.4/\epsilon d_M$ when d_M is in angstroms. The recombination energy, R_E, will therefore be less than the gas-phase ionization potential by this amount which for $\epsilon = 2$ and $d_M = 5$ is 1.5 e.v. Since ionization potentials are of the order of 10 e.v. for hydrocarbons, the recombination energy will still be considerably greater than bond energies ($\sim$4 e.v.), and dissociation of the excited neutral product of Reaction 1 is a possible subsequent step to recombination.

$$RH^* \rightarrow \text{products} \quad (2)$$

Although both atomic and molecular hydrogen are likely products of Reaction 2, it is not necessary that hydrogen be formed with unit efficiency. In the gas phase the yield of hydrogen resulting from electron-ion recombination is considerably less than the ion yield (*32, 73*). This raises a question about the validity of an assumption sometimes made: that the reduction in the hydrogen yield which occurs in the liquid phase as a result of the addition of an electron scavenger can be taken as a direct measurement of the number of scavenged electrons.

Publication Date: January 1, 1968 | doi: 10.1021/ba-1968-0082.ch002

When an electron scavenger is present, electrons may be captured before recombination. Electron capture must initially result in the formation of a molecular anion with internal energy equal to the sum of the electron affinity of XY and the kinetic energy of the incident electron.

$$e^- + XY \rightarrow XY^{*-} \quad (3)$$

Since the ion XY^{*-} contains sufficient energy for the reverse of Reaction 3 to occur, the electron will eventually be emitted

$$XY^{*-} \rightarrow XY + e^- \quad (4)$$

unless there is some mechanism whereby the excited anion can be stabilized. The lifetime for electron emission can be as short as 10^{-11} sec. (*39*) for a simple molecule or as long as 10^{-4} sec. (*35*) for a more complex molecule such as SF_6. For permanent electron capture, de-excitation or reaction of XY^{*-} must, therefore, occur in a time less than or comparable with that for emission. Negative-ion formation can be rendered irreversible either by collisional deactivation or by dissociation of XY^{*-}.

Removal of some of the internal energy of the XY^{*-} ion on collision with a neutral molecule has been invoked to explain the pressure dependence of the electron capture cross sections of O_2 (*13*), NO (*22*), and N_2O (*68*) in the gas phase.

$$XY^{*-} + M \rightarrow XY^- + M^* \quad (5)$$

In the oxygen system at approximately 50 mm. pressure (collision frequency $\sim 10^9$ sec.$^{-1}$) half of the O_2^{*-} ions are stabilized before emission can take place (*13*). In the condensed phase, therefore, deactivation should compete to the exclusion of electron emission. The much higher probability of collisional deactivation in liquids may explain why compounds such as CO_2 and CH_3Cl, for which attachment is very inefficient in the gas phase, are often effective electron scavengers in liquid systems. One must be wary, therefore, of using even relative gas-phase electron attachment coefficients in liquid-phase studies. For molecules with very small electron affinities (< 0.1 e.v.) the reversibility of Reaction 3 may have to be considered even after the excitation energy of the negative ion has been removed by collision.

For certain molecules, such as the alkyl halides, the XY^{*-} ion will be formed in an excited state above the dissociation asymptote of the ion. Dissociation will then occur in a time of the order of 10^{-12} sec.

$$XY^{*-} \rightarrow X + Y^- \quad (6)$$

In the gas phase, where the collision frequencies normally encountered are 10^9 to 10^{10} sec.$^{-1}$, dissociation would be expected to be favored over collisional deactivation. In the liquid phase, however, if the ion XY^- has energy levels below the dissociation asymptote, stabilization could occur,

Publication Date: January 1, 1968 | doi: 10.1021/ba-1968-0082.ch002

giving the molecular anion before dissociation occurs. Evidence (discussed later) would suggest that this is the case for methyl chloride in solution.

The conversion of electrons to negative ions by adding an electron scavenger profoundly affects solvent decomposition. This has been attributed to a decrease in the energy available for excitation of the neutral product RH on recombination, which thereby decreases the probability of its dissociation. Two sources of this reduction are apparent; first, the recombination energy will be decreased by an amount equal to the electron affinity involved, and second, the energy released can be taken up at least in part by the other neutral product.

$$RH^+ + XY^- \rightarrow (RH + XY)^* \qquad (7)$$

The yields of hydrogen, cyclohexene, and bicyclohexyl decrease markedly on adding CO_2 or SF_6 to cyclohexane (*56*, *57*), and these decreases can be qualitatively accounted for in this way. The energy taken up by XY in Reaction 7 may result in formation of products derived from the solute.

$$(RH + XY)^* \rightarrow RH + X + Y \qquad (7a)$$

For example, when perfluorocyclohexane is used as an electron scavenger high yields of c-$C_6F_{11}H$ are observed (*58*). Since the formation of c-C_6F_{11} radicals by dissociative electron capture is prohibitively endothermic and cannot occur directly, c-$C_6F_{11}H$ must result from the formation of c-C_6F_{11} radicals by some process such as Reaction 7a. The possibility discussed above that molecular anions may be formed in alkyl halide solutions does not conflict with the large radical yields observed since the radicals could be formed after recombination.

Factors Complicating the Specificity of Electron Scavenging

In many studies to date, where the solute is expected to have electron-scavenging properties, specific electron scavenging has frequently been assumed with little experimental work directed toward this assumption. Optimally, solutes should be used whose reactions with species other than the electron are known to occur to an insignificant extent or, if such reactions occur, where sufficient information is available to account for these reactions. This condition, though apparently obvious, often seems forgotten. Thus, the yields of nitrogen from nitrous oxide solutions are used to check theoretical predictions and to measure the electron-scavenging ability of second solutes, despite the anomalously high nitrogen yields from this system. Possible complicating effects caused by the reactions of positive and negative ions, hydrogen atoms, hydrocarbon radicals, and electronically excited molecules should all be considered.

Publication Date: January 1, 1968 | doi: 10.1021/ba-1968-0082.ch002

Hydrogen Atoms. It is difficult in many cases to distinguish between chemistry which results from electron capture and that which results from hydrogen atom attack on the solute. Thus, in the methyl iodide system (discussed later) methyl radicals appear to be produced by both Reactions 8 and 9,

$$e^- + CH_3I \rightarrow CH_3\cdot + I^- \quad (8)$$

$$H\cdot + CH_3I \rightarrow CH_3\cdot + HI \quad (9)$$

and without some prior knowledge the contributions from each would be extremely difficult to disentangle.

The olefins, and in particular ethylene where the ethyl radical formed by hydrogen atom addition

$$H\cdot + C_2H_4 \rightarrow C_2H_5\cdot \quad (10)$$

can be readily examined (*25, 38*), suggest themselves as appropriate reagents for H atoms. The data in Table I show that ethylene does not appreciably effect the methyl radical yield from either methyl chloride or bromide solutions or the nitrogen yield from N_2O solutions (*69*). Similarly tetramethylethylene does not affect the radical yields from either methyl- or ethyl bromide. These olefins cannot, therefore, be interfering with electron scavenging in these cases. Conversely, product formation from these solutes does not appear to be caused by hydrogen atom attack. It is, of course, possible that the second solute is considerably more reactive towards hydrogen atoms than is the olefin. This possibility can be eliminated by noting (Table I) that the presence of the various electron scavengers produces only a small decrease in the ethyl radical yield and that this decrease is similar for all the solutes except methyl iodide. From measurements at lower ethylene concentrations it is found for the above-mentioned solutes that the fractional reduction in ethyl radical yield depends solely on the concentration of electron scavenger and not upon the ratio of the two solute concentrations—a fact which indicates that competition of the two solutes for hydrogen atoms is unimportant. The observed decrease can be reasonably attributed to a reduction in the yield of hydrogen atoms resulting from changes of the ion-recombination process.

For methyl iodide–ethylene solutions in cyclohexane the ethyl radical yields are very low (*69*), showing that hydrogen atoms react competitively with these solutes (with $k_9/k_{10} \sim 5$).

Positive Ions. A potential complicating factor, which is difficult to eliminate, is the reaction of positive ions. Arguments against such reactions cannot be based simply on a consideration of the relative ionization potentials of the solvent and solute. Thus, ND_3 and C_2H_5OD, whose ionization potentials are somewhat higher than cyclohexane's,

Publication Date: January 1, 1968 | doi: 10.1021/ba-1968-0082.ch002

Table I. Product Yields from Cyclohexane Solutions Containing Ethylene and an Electron Scavenger

Scavenger	$\frac{G(P)_o}{G(P)_{C_2H_4}}$ [a]	$\frac{G(C_2H_5)_S}{G(C_2H_5)_o}$ [b]
N_2O	1.02	0.82
SF_6	—	0.82
CH_3Cl	0.97	0.92
CH_3Br	1.10	0.64
CH_3Br [c]	1.02	—
C_2H_5Br [c]	1.01	—
CH_3I	0.90	0.20
CO_2	—	0.88

[a] Product yields from solutions 0.1*M* in each solute relative to solutions containing only electron scavenger (N_2 in the case of N_2O solutions, alkyl radicals in the case of alkyl halides).
[b] Ethyl radical yield from solutions 0.1*M* in each solute relative to a solution containing only ethylene.
[c] 0.1*M* tetramethylethylene used instead of ethylene in these cases.

Publication Date: January 1, 1968 | doi: 10.1021/ba-1968-0082.ch002

react with positive ions *via* proton transfer (*7, 10, 71*). An obvious test of the positive ion-scavenging ability of a solute might be made by studying the effect of that solute on the yield of HD from ND_3 or C_2H_5OD solutions. However, such a test may be ambiguous since the presence of an electron scavenger may prevent the formation of D atoms from ion recombination rather than by a competitive reaction for positive ions. For cyclopropane solutions the products arising from positive-ion scavenging are formed before recombination (*3*), and the ambiguity discussed above will therefore not be possible. Where competition for positive ions does not occur, the scavenging efficiency of cyclopropane is increased by adding an electron scavenger (*3, 54, 55*). This increased efficiency is ascribed to an increase in the ion lifetime owing to the formation of the less mobile negative ions. The effects of various electron scavengers on the product yield from cyclopropane–cyclohexane solutions is illustrated in Table II (*55*). For N_2O, SF_6, CH_3Cl, CH_3Br, and CCl_4 the concentration required to produce a given increase in product yield agrees with estimates of their electron scavenging abilities. This indicates strongly that positive ions are not reacting with these solutes. For the alkyl iodides, however, competition for the positive ions does occur, as shown by a reduction in the product yield.

A specific test has been carried out (*69*) in the case of methyl chloride where an attempt to use cyclopropane to compete for a possible positive-ion contribution to the normally obtained methyl radical yield shows no effect (Table III). For systems where the electrons have been converted to negative ions, positive-ion reactions occur with a markedly

increased efficiency, and it becomes doubly important to consider this problem.

Hydrocarbon Radicals. Secondary reactions of radicals can complicate the interpretation of electron scavenging experiments. Thus, methyl radicals produced from the methyl halides will, in the absence of a radical scavenger, react with the solute to give methane.

$$CH_3\cdot + RH \rightarrow CH_4 + R\cdot \qquad (11)$$

At the normal dose rates used in radiolysis this abstraction reaction is not quantitative (*37*) owing to competing radical-radical reactions, so that the methane produced is not a true measure of the radical yield. For example, for methyl chloride solutions the methane observed in the absence of radical scavengers is only 75% of the methyl radical detected with iodine. For methyl iodide the methyl iodide is itself a radical scavenger

$$R\cdot + CH_3I \rightarrow RI + CH_3\cdot \qquad (12)$$

and gives rise to additional methane *via* a short chain (*65*) involving Reactions 11 and 12. A dose-rate dependent methane yield of the order of 17, which is many times the radical yield found in scavenging experiments, is observed in this case. Fortunately, only very low concentrations of iodine are usually necessary to completely suppress such secondary radical reactions (*37*).

Publication Date: January 1, 1968 | doi: 10.1021/ba-1968-0082.ch002

Table II. Effect of Electron Scavengers on Positive Ion Scavenging by Cyclopropane in Cyclohexane

Scavenger	*G(Product)*[a]
—	0.31
CH_3Cl	0.55
SF_6	0.76
N_2O	0.68
CH_3Br	0.68
CCl_4	0.67
CH_3I	0.1

[a] Total ^{14}C product from 0.01*M* cyclopropane-^{14}C in the presence of 0.01*M* solute. *G*(Product) approaches the limit ~ 0.85 at high electron scavenger concentrations.

Table III. Effect of Cyclopropane on the Methyl Radical Yield from Methyl Chloride Solutions in Cyclohexane[a]

[*Cyclopropane*]	*G*(CH_3)
0	0.81
0.08	0.80
0.40	0.81

[a] 0.01*M* CH_3Cl in cyclohexane.

Reactions of radicals which cannot be interfered with present another possible difficulty. For example the radiolysis of methyl iodide solutions produces appreciable methane which cannot be scavenged by iodine despite the fact that the thermal methyl radicals present readily react with the iodine (*20, 65*). At 0.1*M* CH_3I a $G(CH_4)_{unscavengeable} = 0.6$ is observed (*65*). This could be produced by the abstraction of hydrogen by hot methyl radicals or, as suggested by Hamill (*53*) and by Holroyd (*26*), more likely by a diffusion-controlled recombination of the products of Reaction 9.

$$H\cdot + CH_3I \rightarrow [CH_3\cdot + HI] \rightarrow CH_4 + I\cdot \qquad (13)$$

Such a mechanism has, of course, no relevance for electron capture and will therefore affect only the hydrogen atom component of the yield. This was tested for methyl chloride and methyl bromide (*69*) where, as argued above, reactions of hydrogen atoms do not appear to contribute to the yield. For 0.1*M* solutions containing $10^{-3}M$ I_2 as scavenger the methane yields were small (0.03 and 0.05). For deuterium iodide solutions this consideration seems quite important since at high concentrations the observed value of $G(HD)$ is considerably larger than expected (*46, 47*). This implies a yield of HD from the DI *via* some process which does not involve thermal hydrogen atoms.

Excited Species. One of the processes most difficult to eliminate as the source of a particular product is the transfer of electronic excitation energy to a solute molecule. Dissociation of alkyl halides to form alkyl radicals readily occurs photolytically, and energy transfer might well be advanced to explain the radiolysis results. However, in recent studies (*2*) in these laboratories, it has been found that when 0.1*M* solutions of perfluoroazomethane and perfluoroacetone in cyclohexane are irradiated, neither nitrogen nor carbon monoxide are formed. These products are formed efficiently on photolysis of these compounds. It might be argued from this that energy is not available in a form which is transferable to produce dissociation of the solutes. Holroyd (*27*) has, however, recently found appreciable nitrogen yields in the 1470-A. photolysis of N_2O solutions in cyclohexane, which he has explained in terms of energy transfer. He suggested that significant energy transfer also occurs in the radiolysis. Hentz and Knight (*24*) and Yoshida and Sato (*74*) have taken the opposite tack and argued that localization of energy in scintillator solutions in aliphatic hydrocarbons, which has conventionally been thought to represent an energy transfer process, actually results from trapping of the electron by the scintillator molecule. Considerable attention should be given to the difficult problem of distinguishing between electron capture and energy transfer.

Publication Date: January 1, 1968 | doi: 10.1021/ba-1968-0082.ch002

Negative Ion-Molecule Reactions. Complications caused by reaction of negative ions are in a category different from those caused by positive ions since they must necessarily be secondary to the electron-scavenging process itself. Two examples of the probable importance of negative-ion reactions are (1) a reaction with N_2O to produce additional nitrogen from nitrous oxide solutions, and (2) electron transfer from one solute to a second which complicates competitive studies. Both examples are discussed at length later. At present there is no definite evidence that negative ions can undergo ion-molecule reactions with solvent hydrocarbons.

Concentration Dependence of Electron Scavenging in Single Solute Systems

Solutes which react with electrons fall into two categories: those for which a product resulting from electron capture by the solute may be studied directly—*e.g.*, nitrous oxide where nitrogen can be observed; and those such as SF_6, for which studies must be carried out either by examining an effect on the decomposition of the solvent or by competition with a solute of the first category. The first type of study is more attractive since the involvement of the solute can be measured down to low concentrations providing that sufficiently sensitive methods are available. The number of solutes which have been found to lead to a suitably measurable product arising specifically from electron scavenging is, however, at present somewhat limited. Studies on the formation of benzyl radical from benzyl chloride (*23*), hydrogen-containing derivatives from the perfluorocycloalkanes (*58*), and, as indicated above, recent work on the production of alkyl radicals from alkyl chloride and bromides (*69*) indicate these systems to be reasonably promising. In the latter case studies have been carried out over the concentration range 10^{-4} to $0.5M$, from which certain empirical generalizations concerning the concentration dependence have been derived (*see below*).

A large decrease in hydrogen yield is a general effect of electron scavenging. Where products from the solute cannot be examined and where other complications can be eliminated this effect can prove useful in determining the relative solute reactivities. However, since one measures a difference in hydrogen yields, meaningful measurements are restricted to relatively high concentrations; hence, studies of this type cannot be used rigorously to test mechanistic details.

Studies to date on the effects of electron scavengers on the yields of high molecular weight products of solvent decomposition indicate that the effect of a given solute is specific to the solute used (*56*, *57*, *58*).

Publication Date: January 1, 1968 | doi: 10.1021/ba-1968-0082.ch002

The potential use of these products to examine the reactivities of solutes does not, therefore, look particularly promising.

Kinetics of Electron Scavenging. If a single characteristic lifetime, $\tau = 1/k_1$, could be ascribed to the geminate recombination process

$$[RH^+ + e^-] \xrightarrow{k_1} RH^* \qquad (14)$$

it would be expected that the yield of a product, P, formed on electron capture

$$e^- + S \rightarrow S^- \rightarrow P \qquad (15)$$

would be determined by simple competition considerations and depend upon solute concentration according to I.

$$G(P) = \frac{G_i}{1 + \frac{1}{\tau k_s[S]}} \qquad (I)$$

Since, however, the lifetime for geminate recombination depends upon the thermalization distance, a spectrum of lifetimes reflecting the initial electron energy spectrum will exist. No single characteristic lifetime can be assigned to the recombination process, and the dependence of product yield on solute concentration is not expected to obey Equation I. The experimentally observed dependence, in fact, deviates considerably from this relationship. This is illustrated in Figure 1 (*69*) for the methyl radical yield observed from methyl chloride solutions. The product yield in the low scavenging efficiency region increases much less rapidly than with the first power of the concentration, and even at the highest concentrations there is no indication that saturation has been reached.

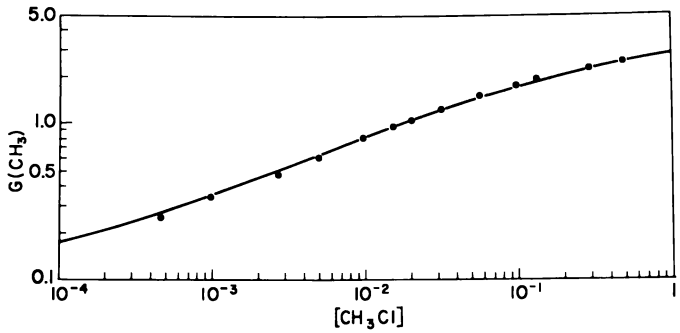

Figure 1. Dependence of methyl radical yield from solutions of methyl chloride in cyclohexane on the solute concentration. Solid curve given by Equation IV with $G_{fi} = 0.09$, $G_{gi} = 3.9$, *and* $\alpha_s = 5.6$

There have been several attempts (*7, 17, 18, 31, 60*) to derive a theoretical expression which would describe the solute concentration dependence of ion scavenging. In each case an assumption is made regarding the distribution of ion pair separations. The probability of reaction with a solute molecule as the electron returns to the parent positive ion is then considered. At this point the principal problem is to decide on the appropriate method for integrating this reaction probability. The functional dependence of the scavenging efficiency upon solute concentration is not given explicitly in the treatments of Freeman *et al.*, Buchanan and Williams, or Sato *et al.* but can only be obtained by a numerical integration specific for each case. The approach of Hummel (*31*) is more useful because it allows the concentration term to be brought outside of the integral determining the probability of reaction between an ion and the solute. At low concentrations this treatment predicts a dependence of the yield of scavenged ions, G_s, on solute concentration, [S], of the form

$$G_s = G_{fi} + K\{k_s[S]\}^{1/2} \qquad \text{(II)}$$

where K is a constant involving the appropriate integrals over the spatial parameters and k_s is the rate constant for electron capture.

The product yield from positive-ion scavenging studies has been known for some time to be approximately proportional to the square root of the solute concentration, and recently it has been found to be well described by an empirical expression identical in form to Equation II over the concentration range 10^{-4} to $10^{-2}M$ (product yields 0.13 to 0.30) (*54*)—*i.e.*,

$$G(P) = G_{fi} + \{\alpha_s[S]\}^{1/2} \qquad \text{(III)}$$

A limiting yield of ~ 0.1 was found at low concentrations in agreement with the value of G_{fi} determined by conductivity experiments. The quantity α_s in Equation III can be identified with the quantity K^2k_s from Hummel's expression, Equation II, and here it is called the reactivity since (according to this interpretation) it is proportional to the rate constant for reaction of electrons with the solute. Because the yield of ions formed is limited, a deviation from Equation III must necessarily occur at high scavenger concentrations. Equation III describes the data reasonably well for electron scavenging by the alkyl halides for concentrations below $10^{-3}M$ (with $G_{fi} = 0.09$). However, for electron scavenging, since the reaction rate is considerably greater, deviations from Equation III occur at much lower concentrations than for positive-ion scavenging.

By analogy with the limiting linear concentration dependence predicted by Equation I for low concentrations, the square-root dependence of Equation III suggested that an expression of the form of Equation IV

Publication Date: January 1, 1968 | doi: 10.1021/ba-1968-0082.ch002

might describe the electron scavenging results over a wider concentration range.

$$G(\mathrm{P}) = G_{\mathrm{fi}} + \frac{G_{\mathrm{gi}}}{1 + \frac{1}{\{\alpha_s[\mathrm{S}]\}^{1/2}}} \qquad \text{(IV)}$$

Here G_{gi} is the yield of ion pairs which undergo geminate recombination. Rearrangement to the linear form gives

$$\frac{1}{G(\mathrm{P}) - G_{\mathrm{fi}}} = \frac{1}{G_{\mathrm{gi}}} + \frac{1}{G_{\mathrm{gi}}\alpha_s^{1/2}} \cdot \frac{1}{[\mathrm{S}]^{1/2}} \qquad \text{(V)}$$

Alkyl Chlorides and Alkyl Bromides. The predicted linearity of a plot of $\frac{1}{G(\mathrm{P}) - G_{\mathrm{fi}}}$ *vs.* $\frac{1}{[\mathrm{S}]^{1/2}}$ was tested using the yields of methyl radicals formed from methyl chloride and methyl bromide and ethyl radicals from ethyl bromide solutions in cyclohexane (*69*). Figure 2 shows good linearity in each case. While there is at the moment no theoretical basis for Equation IV (at least at high concentrations), it unquestionably describes the data in great detail. Within the error of the extrapolation (± 0.1) a common intercept is observed for the three solutes and corresponds to $G_{\mathrm{gi}} = 3.9$. Because of the coincidence of the extrapolated values and the similarity of G_{gi} to that predicted for the electron yield from gas-phase W values it is suggested with some confidence that this represents the total yield of electrons which undergo geminate recombination. The values of α_s obtained from the slopes in Figure 2 are 15.8, 7.8, and 5.6 for MeBr, EtBr, and MeCl respectively. Since α_s is directly proportional to the rate constant for electron capture, k_s, the ratios of the above reactivities are equal to the ratios of the rate constants—*i.e.*, $k_{\mathrm{CH_3Br}}:k_{\mathrm{C_2H_5Br}}:k_{\mathrm{CH_3Cl}} = 1:0.49:0.35$. The reciprocals of the α values are of some interest since they represent the concentration at which half of the electrons are scavenged (0.063*M*, 0.129*M*, and 0.180*M* for MeBr, EtBr, and MeCl respectively). The decrease in reactivity in going from methyl to ethyl bromide is even more dramatic for the chlorides, where preliminary results indicate that ethyl chloride is *ca.* a factor of 10 less reactive than methyl chloride (*i.e.*, $\alpha_{\mathrm{C_2H_5Cl}} \sim 0.6$).

Benzyl Chloride. Hagemann and Schwarz (*23*) in pulse radiolysis studies have measured the benzyl radical (Bz) yield from solutions of benzyl chloride in cyclohexane. They find a dependence qualitatively similar to that given in Figure 1, and their data can be superimposed on this figure by multiplying the benzyl chloride concentrations by a factor of 3. Because of the larger scatter involved, extrapolating a plot of $G(\mathrm{Bz})^{-1}$ *vs.* $[\mathrm{BzCl}]^{-1/2}$ is relatively meaningless. However, if one assumes that the proper extrapolation limit corresponds to the value of G_{gi} observed here, the reactivity of benzyl chloride is found to be $\alpha_{\mathrm{BzCl}} \simeq 15$.

Publication Date: January 1, 1968 | doi: 10.1021/ba-1968-0082.ch002

The same workers find that N_2O depresses the benzyl radical yield, and from this depression they have concluded that benzyl chloride is more reactive toward electrons than N_2O (for which $\alpha \sim 16$, *see below*) by a factor of ~ 1.6. However, in view of the possible complicating effects of secondary ionic reactions discussed below the two solutes probably have more nearly equal reactivities as is also indicated by the above reactivity estimate.

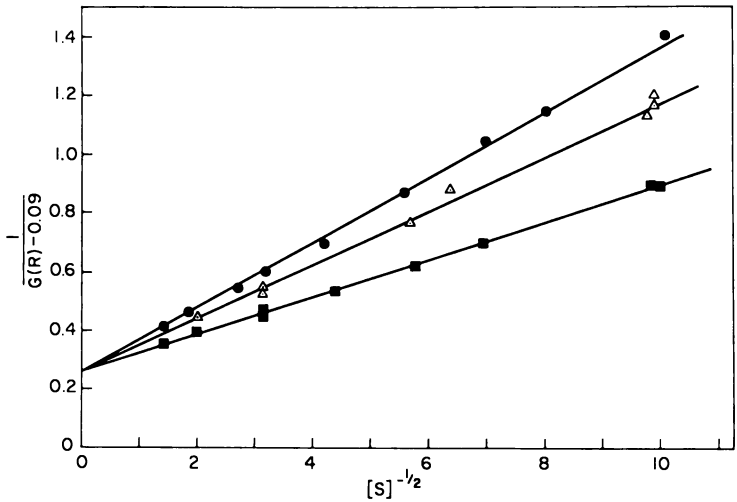

Figure 2. Plot of alkyl radical yields from CH_3Cl (●), C_2H_5Br (△), and CH_3Br (■) solutions in cyclohexane according to Equation V. Common intercept corresponds to $G_{gi} = 3.9$

Perfluorocycloalkanes. Sagert (*58*) has measured the yields of $C_6F_{11}H$ from solutions of perfluorocyclohexane in cyclohexane over the concentration range 0.02–0.3*M* and Fallgatter and Hanrahan (*12*) over the range 1–99% in each solute. At the lower concentrations electron scavenging by the perfluorocyclohexane seems to be involved in the formation of at least a major fraction of this product. Sagert's data can be reasonably well fitted to Equation IV with (from the *G* of 2.0 observed at 0.04*M* perfluorocyclohexane) $\alpha_{C_6F_{12}} \sim 25$. This solute thus appears to be one of the most reactive of those for which direct information is available. Extrapolating the highest value observed (3.4 at 0.3*M*) to infinite solute concentration (*via* Equation IV) gives a limit of ~ 4.4. Within the errors involved this limit is the same as the value of G_{gi} reported for the alkyl halides. The data of Fallgatter and Hanrahan are not amenable to the above treatment because of the high concentrations used and the resulting unknown contribution from direct effects.

Publication Date: January 1, 1968 | doi: 10.1021/ba-1968-0082.ch002

Alkyl Iodides. The various studies carried out on the alkyl iodides (*20, 65, 72*) all point to an important contribution from dissociative electron capture. The yield of alkyl radicals is large [$G(CH_3) = 2.9$ at $0.1M$ CH_3I] (*69*) and has a dependence similar to that given by Equation IV with however an extrapolated limit ~ 5. From data on competitive scavenging with ethylene (Table I) it can be shown that hydrogen atoms attack the methyl iodide according to Reaction 9 at a rate about five times that for addition to ethylene. Taking the rate constant of the latter process as 300 times the rate constant for hydrogen abstraction from the solvent (*38, 65*), Reaction 9 should occur with a 50% efficiency at $0.007M$ and be 95% complete at $0.1M$. From the hydrogen atom yield measured in ethylene-scavenging experiments (*25*), a contribution to the methyl radical yield ~ 1.0 is therefore indicated at this concentration. Unfortunately the argument is further complicated by the existence of an appreciable yield of unscavengeable methane as noted earlier. Adding this yield of unscavengeable methane (0.6) to that of the observable methyl radicals (2.9) gives a total of 3.5 which, after subtracting the hydrogen atom contribution, results in a yield of methyl radicals which can be attributed to electron scavenging of 2.5 (at $0.1M$). Since the unscavengeable methane has not been measured at other concentrations, its concentration dependence is unknown. However, the reactivity of methyl iodide ($\alpha_{CH_3I} \sim 13$) has been estimated from the decrease produced in the ethyl radical yield from ethyl bromide solutions (*69*). This value gives a calculated yield from Equation IV of 2.2 in approximate agreement with the net yield of 2.5 given above. From competition studies the reactivity of ethyl iodide has been estimated to be only slightly less than that for methyl iodide. Since the electron affinity of the iodine atom is considerably higher than the C-I bond strength in the alkyl iodides (by ~ 0.7 e.v.) it is not surprising that dissociative capture appears to be a relatively efficient process.

One further comment can be made. The hydrogen yield observed for cyclohexane solutions $0.1M$ in CH_3I is ~ 2.5 (*65*). This is lower (by 0.8) than the yield observed at similar concentrations of other electron scavengers (Figure 3). The total $G(H_2) + G(CH_3) + G(CH_4)_{\text{unscavengeable}}$ equals 6.0 which can be compared with the slightly lower totals indicated in Table IV for methyl chloride solutions. Thus, while studies of the effect of methyl iodide on the positive-ion reactions of cyclopropane indicate that the methyl iodide does undergo positive-ion reactions, these reactions do not seem to make more than a relatively minor contribution (possibly ~ 0.4) to the products under discussion.

Hydrogen Halides. In an initial study of solutions of HI in cyclohexane the hydrogen yield was greater than that from the pure solvent

Publication Date: January 1, 1968 | doi: 10.1021/ba-1968-0082.ch002

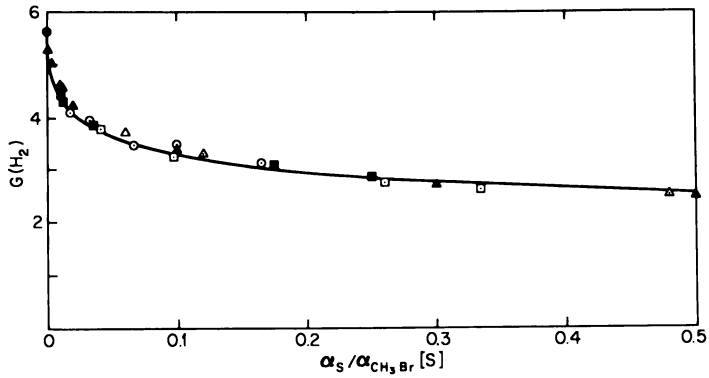

Figure 3. Dependence of the hydrogen yield on concentration of electron scavenger: ⊙, CH_3Cl; △, SF_6; □, CH_3Br; ▲, N_2O; and ■, CO_2. Concentrations of SF_6, CH_3Cl, N_2O and CO_2 have been normalized by factors of α_s/α_{CH_3Br} (1.2, 0.35, 1.0, and 0.5 respectively) as described in the text. Solid curve is given by Equation VIII

Table IV. Yields of Hydrogen and Methyl Radicals from Solutions of Methyl Chloride in Cyclohexane

$[CH_3Cl]$, M	$G(CH_3)$	$G(H_2)$	$\frac{G(H_2)_0 - G(H_2)_{CH_3Cl}}{G(CH_3)}$
0	—	5.62	—
0.10	1.70	3.95	0.98
0.30	2.25	3.49	0.95
0.50	2.49	3.14	1.00

by about a G of 1.5 at 0.1M (*65*). Since the yield should not have changed if the only effect of the HI was to scavenge hydrogen atoms, some form of energy localization in the HI was implicated. Isotope experiments have since been carried out in an attempt to distinguish the source of the hydrogen. This system is, however, fraught with difficulties since HI readily exchanges with any acidic hydrogen present. To avoid this experimental problem, Nash and Hamill carried out the somewhat novel experiment of irradiating HI in perdeuterocyclohexane (*45*). At high concentrations appreciable yields of H_2 were observed [$G(H_2) = 2.2$ at 0.07M HI] in addition to the HD which was expected. The H_2 presumably comes from the scavenging of hydrogen atoms produced from the solute, and a yield of dissociation of the HI of ~ 2 at 0.1M HI is implied. The yields of hydrogen from perdeuterocyclohexane are considerably lower than for normal cyclohexane, so that one can only roughly estimate the reactivity $\alpha_{HI} \sim$ 10–20 from the observed yield of H_2 in this

Publication Date: January 1, 1968 | doi: 10.1021/ba-1968-0082.ch002

system. In studies in these laboratories it was found possible to study DI solutions if the hydrocarbon samples are carefully dried and the reaction system is pretreated with DI (*46, 47*). Work with TI has also been undertaken and has some advantages at low concentrations. These studies were carried out in *n*-hexane so that the system could be examined at lower temperatures. Since the rate constant for hydrogen-atom scavenging by HI is known (*48*) relative to that for abstraction from the solvent, one can readily obtain the D atom yield which corresponds to the observed D_2. One can also estimate the decrease in the H_2 yield expected from the scavenging of H atoms by the DI and show that an additional decrease occurs which is similar to that observed for a number of other solutes not expected to react with H atoms. Two barriers to a comprehensive interpretation of this system exist. First, some of the deuterium atoms may abstract hydrogen from the solute in a hot process and therefore always appear as HD. Second, some further difficulty is apparent since the total yield of hydrogen increases appreciably (by $\sim G = 1$ at $0.05M$), this increase being reflected in the yield of HD + D_2 remaining after correcting for the H atom contribution. A simple electron-capture mechanism does not, therefore, seem to explain the details of the data, and a contribution from positive-ion reactions may be involved. Interpreting $G(D_2)$ as representing $G(S^-)$ gives $\alpha_{DI} \sim 16$ in *n*-hexane. At −78°C., where the total hydrogen yield is $\sim 10\%$ lower, the D_2 yields, after correcting for the scavenging efficiency of DI, are similar to the values observed at room temperature. Hence, the temperature coefficient for α is very small.

DCl solutions in cyclohexane have recently been studied (*44, 52*). Data similar to those from DI solutions have been obtained but can be more easily interpreted, at least in the low concentration region, since DCl is a relatively poor hydrogen-atom scavenger. Here too, however, the total hydrogen yield increases upon adding DCl [as noted earlier (*11, 29*)]. Allowing for a contribution of this excess to the HD yield, a value of $\alpha_{DCl} \sim 10$ can be estimated.

No data have been reported for solutions of DBr alone. However, one result reported in a study of the competition with N_2O (*44*) indicates that it too is very reactive towards electrons.

Following the original work of Scholes and Simic, many workers have studied the production of N_2 from nitrous oxide solutions. It is now generally agreed that the results cannot be interpreted solely in terms of electron capture. Because of this and because of the general interest in this system, this solute is treated in a separate section after the concentration dependence of secondary ionic reactions is discussed.

Publication Date: January 1, 1968 | doi: 10.1021/ba-1968-0082.ch002

Effect of Solutes on the Hydrogen Yields

The marked decrease in $G(H_2)$ found on adding solutes with positive electron affinities to liquid hydrocarbons was suggested more than 10 years ago (*65*) to result, at least in part, from electron capture by these solutes with subsequent interference in the normal ion-recombination process. Since then this effect has been found to be characteristic of electron scavenging for a large variety of solutes. Providing that the electron scavenger does not react with hydrogen atoms, the concentration dependence of the decrease in $G(H_2)$ is qualitatively the same in all cases, with a maximum $\Delta G(H_2) \sim 3$ being observed [*e.g.*, see Figure 3 (*2*)]. As for the product yields from electron scavengers, there is no indication that this effect is saturated even at the highest concentrations used. The stoichiometry involved may be generally described by the scheme

$$e^- + RH^+ \rightarrow RH^* \rightarrow f' \cdot H_2 \qquad (16)$$

$$e^- + S \rightarrow S^- \qquad (17)$$

$$S^- + RH^+ \rightarrow (RH + S)^* \rightarrow f'' \cdot H_2 \qquad (18)$$

where $f = f' - f''$ represents the difference in the efficiency of formation of H_2 from Reactions 16 and 18. If a measurable product, P, is formed from the solute with unit efficiency either as a result of Reaction 17 or 18, f can be determined from

$$f = \frac{G(H_2)_o - G(H_2)_s}{G(P)} \qquad (VI)$$

The yields of CH_3 radicals from CH_3Cl–cyclohexane solutions together with the corresponding hydrogen yields are shown in Table IV. In the last column, the quantity $[(G(H_2)_o - G(H_2)_{CH_3Cl})/G(CH_3)]$ is evaluated and is close to unity at all concentrations. If one assumes that no more than one molecule of H_2 can be produced by Reaction 16, then f'' must be close to zero. Conversely, the concern expressed earlier, that f' might be considerably smaller than 1, does not seem to be borne out by experimental observations for cyclohexane.

Combining Equations IV and VI gives for the general case

$$G(H_2)_S = G(H_2)_o - f\left(G_{fi} + \frac{G_{gi}\{\alpha_s[S]\}^{1/2}}{1 + \{\alpha_s[S]\}^{1/2}}\right) \qquad (VII)$$

Taking $f = 1$ and substituting $G_{fi} = 0.09$, $G_{gi} = 3.9$ and $G(H_2)_o =$ the observed yield of 5.62 gives, for the specific case of cyclohexane

$$G(H_2)_S = 5.53 - \frac{3.9\{\alpha_s[S]\}^{1/2}}{1 + \{\alpha_s[S]\}^{1/2}} \qquad (VIII)$$

In Radiation Chemistry; Hart, E.;
Advances in Chemistry; American Chemical Society: Washington, DC, 1968.

Since α_s is the only unknown in Equation VIII, this expression can be used to determine, from the decrease in hydrogen yield, the reactivity of the solute. In Figure 3 the solid line was calculated using Equation VIII and a value for α_s equal to that for CH_3Br (*i.e.*, $15.8M^{-1}$). The concentrations of the other solutes in the figure have been normalized by a factor α_s/α_{CH_3Br} which was taken to be, for CH_3Cl, SF_6, N_2O, and CO_2, respectively, 0.35, 1.2, 1.0, and 0.5. The first is the ratio obtained from CH_3 production measurements for the individual solutes, and the second is that obtained from competition studies (*see below* and Figure 4). The values for N_2O and CO_2 were taken to give the best data fit. When the concentrations are normalized this way, the H_2 yields for all five solutes fall on the calculated curve quite well (Figure 3). The conclusion from this that $\alpha_{N_2O} \approx \alpha_{CH_3Br}$ is of particular interest and will be discussed later.

Publication Date: January 1, 1968 | doi: 10.1021/ba-1968-0082.ch002

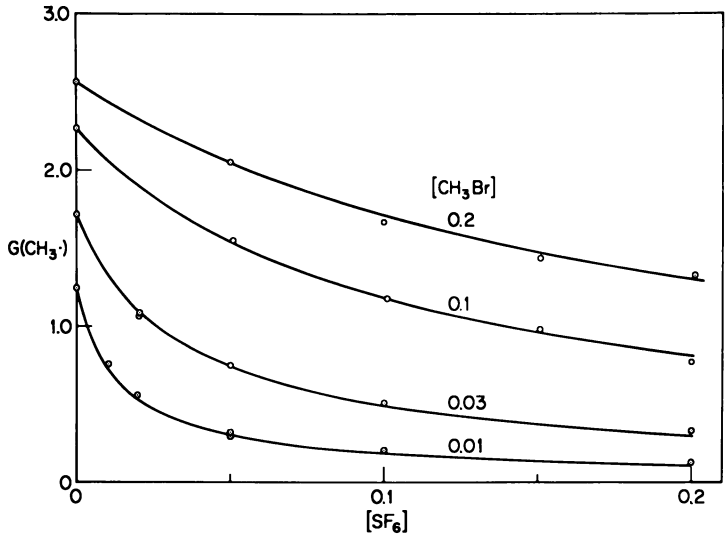

Figure 4. Dependence of methyl radical yield on SF_6 concentration for solutions 0.2-, 0.1-, 0.03-, and 0.01M in CH_3Br. Solid curves are given by Equation X with $G_{fi} = 0.09$, $G_{gi} = 3.9$, $\alpha_{CH_3Br} = 15.8$, and $\alpha_{SF_6} = 19.0$

The use of H_2 yields to determine reactivities, while of obvious use for solutes which give no measurable product, cannot give highly accurate values. At low concentrations the measurements are limited by the ability to measure yield differences accurately, and at high concentrations the decrease in $G(H_2)$ is so gradual that slight errors in measuring $G(H_2)$ values will be greatly magnified. For cyclohexane the concentration region most likely to give the least error in α_s is that where the observed

yield of hydrogen is between 5.0 and 3.5. This corresponds to values of $\alpha_s[S]$ of between 0.1 and 2.

Other workers have studied the effect of N_2O on the hydrogen yield (*50, 57, 61, 66*), and the form of the results in all cases is very similar to that given in Figure 3. A fair number of other studies have been carried out where the workers wished to examine the effect of electron scavenging on hydrogen production. Some authors have attempted to interpret the results in terms of a simple competition between the solvent and solute such as is described by Equation I. As implied by the agreement with Equation VIII indicated here, and as pointed out by Klots, Raef, and Johnsen (*36*), significant departures from Equation I exist. SO_2 was examined in the early study mentioned above and found to be about one-fourth as reactive as CH_3Br (*65*). In terms of the present treatment this gives $\alpha_{SO_2} \sim 4$. More recently, substances such as perfluorocyclobutane (*50, 51, 58*), perfluorocyclohexane (*58*), and CO_2 (*2, 44, 56, 60*) have been examined. Interpreting the data on the basis of Equation VIII gives from these studies $\alpha_{C_4F_8} \sim 16$, $\alpha_{C_6F_{12}} \sim 15$, and $\alpha_{CO_2} \sim 10$.

Competitive Scavenging

For many solutes such as SF_6 no easily measurable product is formed on electron capture. A method often used to estimate the reactivity of such compounds is to study their effect as a second solute on the product yield, P, from a measurable electron scavenging process.

$$e + S_1 \xrightarrow{k_{S_1}} P \tag{19}$$

$$e + S_2 \xrightarrow{k_{S_2}} Q \tag{20}$$

If competition for the electrons occurs solely between Reactions 19 and 20, k_{S_2}/k_{S_1} can be deduced from the decrease in the yield of P upon adding S_2. Sherman (*66*) has used this approach to estimate the rate constants relative to N_2O for many solutes from a study of the nitrogen yield decrease.

Because of the unusual kinetics of electron scavenging, assumptions are generally made to determine k_{S_2}/k_{S_1} in this type of study. The most usual assumption is that the yield of scavenged electrons does not change when the second solute is added. However, this is clearly not the case. Hagemann and Schwarz (*23*) have used a graphical method to take into account the increase in the yield of scavenged electrons when a second solute is added. An algebraic approach is obviously more general, and Equation IV, which describes the results for single solute systems from

Publication Date: January 1, 1968 | doi: 10.1021/ba-1968-0082.ch002

10^{-4} to 0.5*M*, can be used to derive an expression for two solute systems without any further assumptions. Thus, for the two solutes S_1 and S_2 the total solute effectivity is given by $\alpha_1[S_1] + \alpha_2[S_2]$ and from this the total yield of electrons scavenged by Equation IX.

$$G(\text{total scavenging}) = G_{fi} + G_{gi} \cdot \frac{\{\alpha_1[S_1] + \alpha_2[S_2]\}^{1/2}}{1 + \{\alpha_1[S_1] + \alpha_2[S_2]\}^{1/2}} \qquad \text{(IX)}$$

This equation is readily tested where products from both S_1 and S_2 can be measured. The total yields of CH_3 and C_2H_5 radicals formed from solutions of methyl bromide + ethyl bromide and methyl chloride + ethyl bromide (*69*) are shown in the next to the last columns of Tables V and VI. These totals agree well with the values given in the last column, calculated using Equation IX and α_s values derived from the single solute systems.

If there is no secondary interaction of the solutes, a fraction $\frac{\alpha_1[S_1]}{\alpha_1[S_1] + \alpha_2[S_2]}$ of the total electrons scavenged is expected to react with S_1 to form P. The yield of P in the presence of S_2 will then be given by

$$G(P)_{S_2} = \left[G_{fi} + G_{gi} \frac{\{\alpha_1[S_1] + \alpha_2[S_2]\}^{1/2}}{1 + \{\alpha_1[S_1] + \alpha_2[S_2]\}^{1/2}} \right] \frac{\alpha_1[S_1]}{\alpha_1[S_1] + \alpha_2[S_2]} \qquad \text{(X)}$$

From an analogous expression for the yield of product Q in the presence of S_1 one can readily obtain the usual equation for the relative yields of products from two reactants in a competitive situation.

$$\frac{G(P)_{S_2}}{G(Q)_{S_1}} = \frac{\alpha_1[S_1]}{\alpha_2[S_2]} \qquad \text{(XI)}$$

From this it should be possible to determine the relative reactivities of two solutes, where both have measurable products, without knowing the over-all concentration dependence and even in the presence of interference from additional solutes.

Table V. Radical Yields from Competitive Studies Between Methyl and Ethyl Bromides in Cyclohexane

		$G(CH_3)$		$G(C_2H_5)$		$\frac{G(C_2H_5)}{[C_2H_5Br]} \cdot \frac{G(CH_3)}{[CH_3Br]}$	$G(CH_3 + C_2H_5)$	
$[CH_3Br]$	$[C_2H_5Br]$	*Obs.*	*Calc.*	*Obs.*	*Calc.*		*Obs.*	*Calc.*
0.099	0.501	0.70	0.81	2.09	2.00	0.59	2.79	2.81
0.102	0.211	1.23	1.28	1.43	1.31	0.56	2.66	2.59
0.100	0.100	1.55	1.65	0.89	0.81	0.57	2.44	2.46
0.102	0.0290	1.95	2.05	0.36	0.28	0.65	2.31	2.33
0.0097	0.0098	0.91	0.90	0.51	0.45	0.55	1.42	1.35

Publication Date: January 1, 1968 | doi: 10.1021/ba-1968-0082.ch002

Since all parameters required for evaluating these equations are available for mixed alkyl halide systems from measurements on the individual solutes, the validity of the equations can be critically tested. The individual $CH_3\cdot$ and $C_2H_5\cdot$ yields expected from methyl bromide–ethyl bromide mixtures calculated on this basis are given in Table V. The agreement is reasonable with however the ethyl yields being slightly greater and the methyl yields slightly less than predicted. The ratio $\frac{G(C_2H_5)/[C_2H_5Br]}{G(CH_3)/[CH_3Br]}$ ~ 0.57 is slightly greater than $\alpha_{C_2H_5Br}/\alpha_{CH_3Br} = 0.49$. At this juncture one could easily assume that the minor discrepancy noted is caused by an inaccuracy in determining the ratio of the reactivities by intercomparing the individual absolute α's from the single solute measurements and that a value for this ratio of 0.57 would fit the data better. This point and the data from the methyl chloride–ethyl bromide system will be discussed later.

The decrease of methyl radical yield on adding SF_6 to CH_3Br–cyclohexane solutions illustrates the use of the above expression where Q cannot be measured directly. The observed dependence on SF_6 concentration is given in Figure 4 for several CH_3Br concentrations. Since α_{CH_3Br} is known from the single solute experiments, the only adjustable parameter is α_{SF_6}. The curves of Figure 4 were calculated using a value of $\alpha_{SF_6} = 19$ and are in excellent agreement with experiment at all CH_3Br concentrations. This gives 1.2 for the reactivity ratio $\alpha_{SF_6}/\alpha_{CH_3Br}$.

Let us digress to discuss certain problems which arise in handling data from competitive experiments. Since G_{fi} is small compared with the total yield of electrons scavenged in the region where competitive studies are usually carried out, it is convenient here to approximate Equation X by

$$G(P)_{S_2} = G_i \frac{\{\alpha_1[S_1] + \alpha_2[S_2]\}^{1/2}}{1 + \{\alpha_1[S_1] + \alpha_2[S_2]\}^{1/2}} \cdot \frac{\alpha_1[S_1]}{\alpha_1[S_1] + \alpha_2[S_2]} \qquad \text{(XII)}$$

where G_i is the total ion pair yield (*i.e.*, $= G_{fi} + G_{gi} = 4.0$ for cyclohexane). Using this expression, the ratio of the yield of P in the absence of S_2, $G(P)_o$, to that in the presence of S_2 is given by

$$\frac{G(P)_o}{G(P)_{S_2}} = \left(1 + \frac{\alpha_2[S_2]}{\alpha_1[S_1]}\right) \cdot \frac{1 + \dfrac{1}{\{\alpha_1[S_1] + \alpha_2[S_2]\}^{1/2}}}{1 + \dfrac{1}{\{\alpha_1[S_1]\}^{1/2}}} \qquad \text{(XIII)}$$

$$= \left(1 + \frac{\alpha_2[S_2]}{\alpha_1[S_1]}\right)^{1/2} \cdot \frac{\{\alpha_1[S_1] + \alpha_2[S_2]\}^{1/2} + 1}{1 + \{\alpha_1[S_1]\}^{1/2}} \qquad \text{(XIIIa)}$$

The limiting cases are for $\alpha_1[S_1] >> 1$

$$\frac{G(P)_o}{G(P)_{S_2}} = \left(1 + \frac{\alpha_2[S_2]}{\alpha_1[S_1]}\right) \qquad \text{(XIV)}$$

and for $\alpha_1[S_1] \cong \alpha_2[S_2] << 1$

$$\frac{G(P)_o}{G(P)_{S_2}} = \left(1 + \frac{\alpha_2[S_2]}{\alpha_1[S_1]}\right)^{1/2} \qquad \text{(XV)}$$

The first limiting case corresponds to that where complete electron scavenging occurs. Assuming that adding a second solute does not change the total yield of scavenged electrons is tantamount to assuming complete scavenging. These assumptions are in turn implied where, as commonly done, the reactivity ratios have been determined from Equation XIV. Complete scavenging is not, of course, of practical concern since it does not occur even at the highest concentrations. Values of α_2/α_1 determined from slopes of plots of $G(P)_o/G(P)_{S_2}$ *vs.* $[S_2]/[S_1]$ will therefore be lower than the true value, the discrepancy increasing with decreasing solute concentration. This is shown by the results from the CH_3Br–SF_6 mixed system, where the slopes of $G(CH_3)_o/G(CH_3)_{SF_6}$ *vs.* $[SF_6]/[CH_3Br]$ are 0.61, 0.74, 0.85, and 1.00 (instead of the limiting value of 1.2 above) for CH_3Br concentrations of 0.01-, 0.03-, 0.1-, and 0.2*M* respectively. Because of this, the reactivities relative to N_2O given by Sherman (*66*), which were obtained at N_2O concentrations of $5 \times 10^{-3}M$, will all be low by about a factor of 2.

The second limiting case gives too high a value for α_2/α_1. For competition between two reactive solutes both present at $10^{-2}M$, $\alpha_1[S_1] \sim \alpha_2[S_2] \sim 0.2$, and the second term on the right of Equation XIIIa (which does not depend strongly on the exact value of α_s) is ~ 1.12. For these conditions Equation XIIIa may be rewritten to give

$$\left(\frac{G(P)_o}{G(P)_{S_2}}\right)^2 = 1.25 + 1.25\,\frac{\alpha_1}{\alpha_2} \cdot \frac{[S_1]}{[S_2]} \qquad \text{(XVI)}$$

Thus, for equally reactive solutes a plot of $(G(P)_o/G(P)_S)^2$ *vs.* $[S_1]/[S_2]$ will have at $[S_2] = 0.01M$ an apparent slope ~ 1.5 times that given by Equation XV. Hentz and Knight (*24*) have performed very interesting studies of the effect of various electron scavengers on the luminescence of *p*-terphenyl (PTP) and 2,5-diphenyl-1,3,4-oxadiazole (PPD) solutions in cyclohexane. They concluded that light emission occurs upon the neutralization of charged forms of the scintillator. They obtained relative reactivities from competitive studies using an expression equivalent to XV which they derived from the low concentration square-root dependence. Including the term for yield fall-off from this square-root dependence (as done in Equation XIIIa) will reduce their quoted relative reactivities by about the factor of 1.5 given above. This can partly

Publication Date: January 1, 1968 | doi: 10.1021/ba-1968-0082.ch002

explain one of the anomalies they noted: that $\alpha_{PPD}/\alpha_{N_2O}$ is 2.9 when measured by the effect of PPD on the N_2 yield from N_2O solutions but only 1.4 when measured by the effect of N_2O on the emission from PPD. The effect appears doubly, directly in the first case and inversely in the second, so that a ratio of $\sim$ 2.0 would agree with both observations. Such a treatment introduces other difficulties into the data—*e.g.*, ethyl bromide appears to be less reactive than N_2O in measurements on N_2O solutions, while it quenches PPD luminescence more efficiently than N_2O.

We now return to the data on the methyl chloride–ethyl bromide system (*69*) and the first of the problems implicating secondary reactions of negative ions. In this system the total yield is predicted well by Equation IX using α_s values from the single solute systems. The individual methyl and ethyl radical yields, however, deviate considerably from the calculated values (bracketed values in Table VI) and are well outside the possible limits of the reactivity values and possible experimental errors. The ethyl radical yields are generally much greater and the methyl radical yields much less than the calculated values. In particular, the ratios of the quantity $\frac{G(C_2H_5)}{[C_2H_5Br]} \Big/ \frac{G(CH_3)}{[CH_3Cl]}$ are considerably greater than the value $\alpha_{CH_3Cl}/\alpha_{C_2H_5Br} = 1.40$ and vary between the individual experiments. The ethyl bromide appears to be more effective and the methyl chloride less effective than expected, and secondary reactions of some sort are implied. Since the increase in $G(C_2H_5)$ is complemented by a corresponding decrease in $G(CH_3)$ and since the total yields are as they should be, ionic reactions of the type

$$Cl^- + C_2H_5Br \rightarrow C_2H_5\cdot + BrCl^- \qquad (21)$$

can be ruled out. Electron transfer between an initially formed and stabilized methyl chloride anion appears to be a likely source of the nonideality in this system

$$CH_3Cl^- + C_2H_5Br \rightarrow CH_3Cl + [C_2H_5Br^-] \rightarrow C_2H_5\cdot + Br^- \qquad (22)$$

Obviously the possibility of reactions such as 22 occurring presents a serious problem in determining rate constant ratios from competitive studies.

To take into account such competitions, a solute interaction term must be added to Equation X. In general terms this may be described by the function $f([S_1],[S_2])$ and gives

$$G^*(P)_{S_2} = G(P)_{S_2} \cdot f([S_1],[S_2]) \qquad \text{XVII}$$

Here $G(P)_{S_2}$ is defined by Equation X, and $G^*(P)_{S_2}$ is the yield in the nonideal case. One must now attempt to define the nature of $f([S_1],[S_2])$.

Publication Date: January 1, 1968 | doi: 10.1021/ba-1968-0082.ch002

For the ideal case this will of course be unity. Where electron transfer can be considered to proceed in one direction—*i.e.*,

$$S_1^- + S_2 \rightarrow S_1 + S_2^- \qquad (23)$$

an approximate description can be derived. The capture of electrons can be assumed to result in the formation of a negative ion–positive ion spatial distribution similar to the original electron-positive ion distribution. The lifetime of the majority of negative ions will therefore be governed by the rate of recombination with the positive ions in much the same way as that of the electrons and will, if recombination occurs in the track, be very short. Early pulse radiolysis experiments (*34, 64*) indicated that few negative ions escape from the track and that recombination takes place on a time scale shorter than the time resolution involved in these experiments (microseconds). Recently, Thomas *et al.* (*67*) extended the time scale for observation of negative ions into the nanosecond region and found a yield $\sim$ 1 of negative ions from a solution of 0.1*M* diphenyl in cyclohexane. These negative ions decay with a period $\sim$ 50 nsec.

Table VI. Radical Yields from Competitive Studies Between Methyl Chloride and Ethyl Bromide in Cyclohexane

		$G(CH_3)$		$G(C_2H_5)$		$\frac{G(C_2H_5)}{[C_2H_5Br]} \frac{G(CH_3)}{[CH_3Cl]}$		$G(CH_3 + C_2H_5)$	
$[CH_3Cl]$	$[C_2H_5Br]$	*Obs.*	*Calc.*	*Obs.*	*Calc.*	*Obs.*	*Calc.*	*Obs.*	*Calc.*
0.203	0.101	1.00	(1.35) 0.97	1.29	(0.95) 1.33	2.6	2.7	2.29	2.30
0.102	0.104	0.63	(0.88) 0.63	1.50	(1.26) 1.51	2.3	2.3	2.13	2.14
0.0485	0.103	0.34	(0.51) 0.37	1.71	(1.51) 1.65	2.4	2.2	2.05	2.02
0.0209	0.103	0.18	(0.25) 0.18	1.68	(1.70) 1.75	1.9	2.0	1.86	1.95
0.201	0.202	0.68	(1.02) 0.66	1.77	(1.43) 1.79	2.6	2.7	2.45	2.45
0.103	0.202	0.38	(0.63) 0.41	1.92	(1.72) 1.94	2.6	2.5	2.30	2.35
0.103	0.491	0.17	(0.35) 0.19	2.47	(2.31) 2.47	3.0	2.8	2.64	2.66
0.100	0.048	0.93	(1.17) 0.92	1.03	(0.78) 1.03	2.3	2.3	1.96	1.95
0.107	0.0103	1.40	(1.56) 1.39	0.37	(0.22) 0.39	2.6	2.8	1.77	1.78
0.0098	0.0100	0.38	(0.45) 0.40	0.72	(0.65) 0.70	1.9	1.7	1.11	1.10

Publication Date: January 1, 1968 | doi: 10.1021/ba-1968-0082.ch002

The concentration dependence for the secondary reactions of negative ions in the above situation will be to a first approximation of the same form as that for electron scavenging—*i.e.*,

$$G(\text{secondary reaction of } S_1^-) = \frac{G(P)_{S_2}}{1 + \frac{1}{\{\beta_2[S_2]\}^{1/2}}} \qquad \text{(XIX)}$$

where β_2 is a constant describing the reactivity of S_2 toward the negative ion formed from S_1. This yield, which should normally appear as product P (from S_1), is therefore converted to product Q (from S_2).

$$G^*(P)_{S_2} = G(P)_{S_2} - \frac{G(P)_{S_2}}{1 + \frac{1}{\{\beta_2[S_2]\}^{1/2}}}$$

$$= G(P)_{S_2}\left(\frac{1}{1 + \{\beta_2[S_2]\}^{1/2}}\right) \qquad \text{(XX)}$$

The interaction term is in brackets, and for this case is independent of $[S_1]$. In the methyl chloride–ethyl bromide system such an independence is found—*e.g.*, for the four runs at ethyl bromide concentration of 0.1*M*, ratios observed for $G(P)_{S_2\,obs}/G(P)_{S_2\,calc}$ $(= f([S_1],[S_2])_{exp})$ are 0.74, 0.76, 0.67, and 0.72. From a ratio of 0.72 at 0.1*M* C_2H_5Br, β is evaluated as 1.51 (assuming of course the form of $f([S_1],[S_2])$). From this the individual yields may be calculated for the other experiments and are the unbracketed values in Table VI. The available data are well described by Equation XX. Using Equation XX and an analogous expression for $G^*(Q)_{S_1}$ one can show that where electron transfer occurs from S_1 to S_2

$$\frac{G^*(Q)_{S_1}}{G^*(P)_{S_2}} = \frac{\alpha_2[S_2]}{\alpha_1[S_1]} + \left(1 + \frac{\alpha_2[S_2]}{\alpha_1[S_1]}\right)\{\beta_2[S_2]\}^{1/2} \qquad \text{(XXI)}$$

Where β is not zero, the ratio $\dfrac{G^*(Q)_{S_1}/[S_2]}{G^*(P)_{S_2}/[S_1]}$ is not equal to α_2/α_1 and will depend on several factors including the relative concentrations of S_1 and S_2. Some of the apparently wild variations of the experimental values of this ratio in Table VI are completely explained by Equation XXI. At this point one may recall the slight discrepancy in the respective values of 0.49 for $\alpha_{C_2H_5Br}/\alpha_{CH_3Br}$ and the somewhat higher values ($\sim$ 0.57) given in Column 7 of Table V. If this difference is real, it can be accounted for by a value of $\beta_{C_2H_5Br} \sim 0.02$.

The original aim in undertaking this treatment of competitive kinetics was to simplify the process of obtaining consistent values for rate constant ratios. The main conclusion reached, however, is that where the reactivity of a solute cannot be determined from the single solute

Publication Date: January 1, 1968 | doi: 10.1021/ba-1968-0082.ch002

system then the use of competitive methods should be treated with great caution. Thus, for the SF_6–methyl bromide system discussed above the data can be fitted very well with $\alpha_{SF_6}/\alpha_{CH_3Br} = 1.2$ if one assumes that $f([SF_6],[CH_3Br])$ is unity. However, they could also be fitted by assuming a small interaction term. With $\beta = 0.025$ $f([CH_3Br],[SF_6]) = 0.95$ at $0.1M$, and best fit is obtained for $\alpha_{SF_6}/\alpha_{CH_3Br} = 1.1$. The observation that the decreases in hydrogen from these two solutes overlap when the concentration of SF_6 is normalized by a factor of 1.2, though this method is rather insensitive, indicates that the value obtained in the competitive studies is very nearly correct.

Publication Date: January 1, 1968 | doi: 10.1021/ba-1968-0082.ch002

Nitrous Oxide

Among electron scavengers nitrous oxide has received more attention than any other solute, probably because of its apparently specific electron-scavenging properties and the comparative ease with which the nitrogen formed can be measured. Twelve different groups (*2, 4, 5, 11, 24, 27, 41, 50, 57, 61, 63, 66*) have either made measurements bearing directly on this system or have used it as a reference point in competition studies. Most measurements have been made on cyclohexane solutions where, while agreeing qualitatively as to the form of the concentration dependence, there is an unfortunate lack of agreement as to the exact value of the N_2 yield at any particular N_2O concentration. Part of the variation between the different studies undoubtedly arises from inaccurate knowledge of the solute concentration where reaction vessels with relatively large vapor volumes were used. Most recent workers have attempted to correct for partition between the liquid and vapor phases by taking into account the solubility coefficients under the conditions of their experiments. Measurements of $G(N_2)$ have been made in these laboratories (*2*) on samples contained in cells with only a small vapor volume ($\sim$ 15%), and the values are given in the second column of Table VII.

Despite the large number of investigations there is still considerable uncertainty as to the over-all mechanism of nitrogen formation. The difficulty in interpreting the results arises from the fact that the observed yields of nitrogen are considerably greater than the expected total yield of electrons [values as high as $G(N_2) = 6.8$ having been obtained for a $0.3M$ solution in liquid ethane (*4*)]. Hydrogen atom reactions cannot contribute significantly to these high yields since N_2O and C_2H_4 have little mutual effect on the C_2H_5 and N_2 yields, respectively (Table I). This agrees with the observation of Sato *et al.* (*61*) that cyclohexene does not decrease the yield of N_2 from cyclohexane–N_2O solutions. The increase caused by N_2O in the yield of products owing to positive-ion scavenging

by cyclopropane (Table II) agrees with its electron-scavenging properties and argues strongly against the reaction of positive ions with N_2O. Hydrocarbon free radicals can be dismissed as a possible source of N_2 by the combined findings of Sagert (*57*), Asmus *et al.* (*2*), and Charlesby *et al.* (*5*). Thus, N_2O does not decrease the yields of cyclohexene or bicyclohexyl from cyclohexane, and in solutions containing both iodine and N_2O the yield of N_2 is unaffected by the presence of sufficient iodine to scavenge the radicals, while radical attack of the iodine is increased rather than decreased.

Table VII. Observed and Calculated Nitrogen Yields from Nitrous Oxide–Cyclohexane Solutions

$[N_2O]$, mM	*Observed* $G(N_2)$	*Calculated*[a] $G(S^-)$	$G(N_2)/G(S^-)$ [b]	$G(N_2)/G(S^-)$ [c]
0.80	0.56	0.49	1.14	1.13
2.7	0.96	0.78	1.23	1.22
9.5	1.74	1.22	1.43	1.35
19.0	2.25	1.52	1.48	1.44
95.0	3.77	2.29	1.65	1.63
285	4.99	2.78	1.79	1.75
475	5.48	2.99	1.83	1.79

[a] Calculated from Equation IV with $G_{fi} = 0.09$, $G_{si} = 3.9$, and $\alpha_{N_2O} = 16$.
[b] From Columns 2 and 3.
[c] Calculated from Equation XXII with $\beta = 30$.

Figure 3 shows that for cyclohexane–N_2O solutions the decrease in hydrogen yield closely follows that for CH_3Br solutions; the reactivities of these two solutes towards electrons would therefore appear to be similar. The yield of electrons scavenged by N_2O, $G(S^-)$, based on Equation IV with α_{N_2O} taken as equal to that for methyl bromide (*i.e.*, $16M^{-1}$) are given in Table VII, Column 3. The experimental values are considerably higher than those calculated indicating, as now generally recognized, that more than one N_2 is formed per electron captured. The explanations most frequently proposed to explain this involve secondary reactions of the negative ion formed on electron capture by N_2O. The nature of the ion produced on electron capture is therefore of some importance. The presently accepted value of 1.67 e.v. for the N-O bond energy (*33*) in N_2O when taken together with the electron affinity of the oxygen atom 1.46 e.v. (*6*) makes the dissociative capture of thermal electrons by N_2O

$$e^- + N_2O \rightarrow N_2 + O^- \qquad (24)$$

Publication Date: January 1, 1968 | doi: 10.1021/ba-1968-0082.ch002

$\sim$ 0.2 e.v. endothermic. Electron capture by N_2O in the gas phase has been found to be a pseudo-three-body process (*49, 68*) indicating the formation of the molecular anion.

$$e^- + N_2O \xrightarrow{M} N_2O^- \qquad (25)$$

N_2O^- is therefore most likely to be the initial negative ion formed in liquid hydrocarbons. If a minimum electron affinity for N_2O of 0.1 e.v. is assumed, then dissociation of the ion into N_2 and O^- has an activation energy of at least 0.3 e.v., and the lifetime with respect to dissociation must be greater than 10^{-7} sec. [A lifetime of 10^{-3} to 10^{-4} sec. has been estimated from gas-phase studies (*28*)]. This minimum lifetime is considerably longer than that for geminate recombination of ion pairs in liquid hydrocarbons (*67*). Therefore, in the absence of further reactions, the negative ion undergoing recombination in nitrous oxide solutions will be N_2O^-, and nitrogen formation must occur after recombination, presumably with the formation of only one molecule of nitrogen. For gaseous N_2O-hydrocarbon systems the nitrogen yield has been found to increase with increasing total pressure (*70*) in accord with a reaction scheme involving the following secondary reactions of N_2O^-:

$$N_2O^- + N_2O \rightarrow N_2 + N_2O_2^{*-} \qquad (26)$$

$$N_2O_2^{*-} \rightarrow NO + NO^- \qquad (26a)$$

$$N_2O_2^{*-} \xrightarrow{M} N_2O_2^- \xrightarrow{RH^+} N_2 + \text{products} \qquad (26b)$$

In the liquid phase, secondary reactions of N_2O^- would be expected to proceed exclusively by Reactions 26 and 26b which, where they occur, will result in the formation of two molecules of nitrogen per electron captured. Owing to the competition between Reaction 26 and the recombination of N_2O^- with positive ions the yield of nitrogen in the liquid systems should at low concentration approach a limit equal to the yield of scavenged electrons and at high concentration a limit twice that yield. This is at least approximately true (Column 4, Table VII). An argument identical to that used to derive the relationship for electron transfer in two solute systems can be used here to derive an approximate expression for the scavenging efficiency of N_2O towards N_2O^- and from this the nitrogen yield in the intermediate region. The multiplying factor for the above reaction scheme is then given by

$$\frac{G(N_2)}{G(S^-)} = 1 + \frac{\{\beta_{N_2O}[N_2O]\}^{1/2}}{1 + \{\beta_{N_2O}[N_2O]\}^{1/2}} \qquad (XXII)$$

Publication Date: January 1, 1968 | doi: 10.1021/ba-1968-0082.ch002

where β_{N_2O} is the reactivity of N_2O toward N_2O^- ions relative to their recombination. The values of $G(N_2)/G(S^-)$ (Table VII, Column 5) were calculated from Equation XXII taking $\beta_{N_2O} = 30$ and agree well with the values found. The value of β seems close to the limit expected for negative ion reactions but is within reason for a reactive solute. The agreement observed shows that N_2 yields from nitrous oxide solutions can be quantitatively described by assuming a secondary reaction of the N_2O^- ion with N_2O. It is therefore unnecessary to invoke energy transfer from excited hydrocarbon molecules, as recently suggested by Holroyd (*27*), to explain the results. While a combination of the two explanations cannot be ruled out, on the basis of energy transfer alone it would be necessary that the yield of excited molecules be nearer 3 than the value of 1.2 proposed.

Many workers have studied the competition between N_2O and other solutes and have found many cases where the second solute appears to have a reactivity comparable with that of N_2O. Because of the possible participation of excited species in nitrogen formation and the possibility of secondary reactions of the N_2O^- ion with the second solute, determining relative solute reactivities by studying the reduction in $G(N_2)$ from nitrous oxide solutions should be treated with considerable caution. However, the qualitative argument that a considerable decrease ($> 50\%$) in $G(N_2)$ upon adding a second solute is indicative of electron capture by that solute should still be valid. Conversely, the lack of an effect on the nitrogen yield, as for CF_4 and C_2F_6 (*50*), probably properly argues that little or no electron scavenging occurs for these solutes.

Literature Cited

(1) Allen, A. O., Hummel, A., *Discussions Faraday Soc.* **36,** 95 (1963).
(2) Asmus, K.-D., Warman, J. M., Schuler, R. H., to be published.
(3) Ausloos, P., Scala, A. A., Lias, S. G., *J. Am. Chem. Soc.* **88,** 1583, 5701 (1966).
(4) Bakale, G., Gillis, H. A., private communication.
(5) Blackburn, R., Charlesby, A., *Nature* **210,** 1036 (1966).
(6) Branscomb, L. M., Burch, D. S., Smith, S. J., Geltman, S., *Phys. Rev.* **111,** 504 (1958).
(7) Buchanan, J. W., Williams, F., *J. Chem. Phys.* **44,** 4377 (1966).
(8) Burns, W. G., Reed, C. R. V., private communication.
(9) Burton, M., Dillon, M., Rein, R., *J. Chem. Phys.* **41,** 2228 (1964).
(10) Busler, W. R., Martin, D. H., Williams, F., *Discussions Faraday Soc.* **36,** 102 (1963).
(11) Dyne, P. J., *Can. J. Chem.* **43,** 1080 (1965).
(12) Fallgatter, M. B., Hanrahan, R. J., "Abstracts of Papers," 154th Meeting, ACS, Sept. 1967.
(13) Fessenden, R. W., Warman, J. M., ADVAN. CHEM. SER. **82,** 222 (1968).
(14) Forrestal, L. J., Hamill, W. H., *J. Am. Chem. Soc.* **83,** 1535 (1961).
(15) Freeman, G. R., *J. Chem. Phys.* **38,** 1022 (1963).
(16) Freeman, G. R., Fayadh, J. M., *J. Chem. Phys.* **43,** 86 (1965).

(17) Freeman, G. R., *J. Chem. Phys.* **43,** 93 (1965).
(18) *Ibid.*, **46,** 2822 (1967).
(19) Gallivan, J. B., Hamill, W. H., *J. Chem. Phys.* **44,** 1279 (1966).
(20) Geissler, P. R., Willard, J. E., *J. Am. Chem. Soc.* **84,** 4627 (1962).
(21) Guarino, J. P., Hamill, W. H., *J. Am. Chem. Soc.* **86,** 777 (1964).
(22) Gunton, R. C., Shaw, T. M., *Phys. Rev.* **140A,** 748 (1965).
(23) Hagemann, R. J., Schwarz, H. A., *J. Phys. Chem.* **71,** 2694 (1967).
(24) Hentz, R. R., Knight, R. J., *J. Phys. Chem.*, to be published.
(25) Holroyd, R. A., *J. Phys. Chem.* **70,** 1341 (1966).
(26) Holroyd, R. A., Klein, G. W., *Int. J. Appl. Rad. Isotopes* **15,** 633 (1964).
(27) Holroyd, R. A., ADVAN. CHEM. SER. **82,** 488 (1968).
(28) Holtslander, W. J., Freeman, G. R., *Can. J. Chem.* **45,** 1661 (1967).
(29) Horner, P. J., Swallow, A. J., *J. Phys. Chem.* **65,** 953 (1961).
(30) Hummel, A., Allen, A. O., Watson, Jr., F. H., *J. Chem. Phys.* **44,** 3431 (1966).
(31) Hummel, A., in press.
(32) Johnson, G. R. A., Warman, J. M., *Trans. Faraday Soc.* **61,** 1709 (1965).
(33) Kaufmann, F., *J. Chem. Phys.* **46,** 2449 (1967).
(34) Keene, J. P., Land, E. J., Swallow, A. J., *J. Am. Chem. Soc.* **87,** 5284 (1965).
(35) Klots, C. E., *J. Chem. Phys.* **46,** 1197 (1967).
(36) Klots, C. E., Raef, Y., Johnsen, R. H., *J. Phys. Chem.* **68,** 2040 (1964).
(37) Kuntz, R. R., Schuler, R. H., *J. Phys. Chem.* **67,** 1004 (1963).
(38) McCrumb, J. L., Schuler, R. H., *J. Phys. Chem.* **71,** 1953 (1967).
(39) McDaniel, E. W., "Collision Phenomena in Ionized Gases," p. 385, Wiley, New York, 1964.
(40) Manion, J. B., Burton, M., *J. Phys. Chem.* **56,** 560 (1952).
(41) Meissner, G., Henglein, A., *Ber. Bunsenges. physik. Chem.* **69,** 264 (1965).
(42) Meisels, G. G., *J. Chem. Phys.* **41,** 51 (1964).
(43) Mozumder, A., Magee, J. L., *J. Chem. Phys.* **47,** 939 (1967).
(44) Munday, C. S., Richards, J. T., Scholes, G., Simic, M., "The Chemistry of Ionization and Excitation," G. R. A. Johnson and G. Scholes, eds., p. 151, Taylor and Francis, London, 1967.
(45) Nash, J. R., Hamill, W. H., *J. Phys. Chem.* **66,** 1097 (1962).
(46) Perner, D., "The Chemistry of Ionization and Excitation," G. R. A. Johnson and G. Scholes, eds., p. 168, Taylor and Francis, London, 1967.
(47) Perner, D., Schuler, R. H., to be published.
(48) Perner, D., Schuler, R. H., *J. Phys. Chem.* **70,** 317 (1966).
(49) Phelps, A. V., private communication.
(50) Rajbenbach, L. A., *J. Am. Chem. Soc.* **88,** 4275 (1966).
(51) Rajbenbach, L. A., Kaldor, U., *J. Chem. Phys.* **47,** 242 (1967).
(52) Richards, J. T., Scholes, G., *Chem. Commun.* **24,** 1261 (1967).
(53) Roberts, J., Hamill, W. H., *J. Phys. Chem.* **67,** 2446 (1963).
(54) Rzad, S. J., Schuler, R. H., *J. Phys. Chem.* **72,** 228 (1968).
(55) Rzad, S. J., Schuler, R. H., to be published.
(56) Sagert, N. H., *Can. J. Chem.* **46,** 336 (1968).
(57) Sagert, N. H., Blair, A. S., *Can. J. Chem.* **45,** 1351 (1967).
(58) Sagert, N. H., *Can. J. Chem.*, **46,** 95 (1968).
(59) Samuel, A. H., Magee, J. L., *J. Chem. Phys.* **21,** 1080 (1953); see Appendix.
(60) Sato, S., Terao, T., Kono, M., Shida, S., *Bull. Chem. Soc. Japan* **40,** 1818 (1967).
(61) Sato, S., Yugeta, R., Shinsaka, K., Terao, T., *Bull. Chem. Soc. Japan* **39,** 156 (1966).
(62) Schmidt, W. F., Abstracts 3rd International Congress Radiation Research, Cortina, Italy, June 1966.

(63) Scholes, G., Simic, M., *Nature* **202,** 895 (1964).
(64) Scholes, G., Simic, M., Adams, G. E., Boag, J. W., Michael, B. D., *Nature* **204,** 1187 (1964).
(65) Schuler, R. H., *J. Phys. Chem.* **61,** 1472 (1957).
(66) Sherman, W. V., *J. Chem. Soc.* **A,** 599 (1966).
(67) Thomas, J. K., Johnson, K., Klippert, T., Lowers, R., to be published.
(68) Warman, J. M., Fessenden, R. W., *J. Chem. Phys.*, in press.
(69) Warman, J. M., Asmus, K.-D., Schuler, R. H., to be published.
(70) Warman, J. M., to be published.
(71) Williams, F., *J. Am. Chem. Soc.* **86,** 3954 (1964).
(72) Williams, Jr., R. R., Hamill, W. H., *Radiation Res.* **1,** 158 (1954).
(73) Woodward, T. W., Back, R. A., *Can. J. Chem.* **41,** 1463 (1963).
(74) Yoshida, T., Sato, S., *Bull. Chem. Soc. Japan* **40,** 2216 (1967).

RECEIVED January 31, 1968. Supported in part by the U. S. Atomic Energy Commission.

3

Pulse Radiolysis Studies of Some Reactive States of Aromatic Molecules in Solution

LEON M. DORFMAN, NORMAN E. SHANK and SHIGEYOSHI ARAI

The Ohio State University, Columbus, Ohio 43210

Publication Date: January 1, 1968 | doi: 10.1021/ba-1968-0082.ch003

Reactive states of aromatic molecules in solution may be observed directly by the pulse radiolysis method. Extensive investigations of both aromatic molecule ions (particularly the radical anions) and electronically excited states have provided new information about not only the radiation chemical processes but also the general kinetic behavior of these reactive intermediates. Absolute rate constants have been determined for many elementary processes such as energy transfer and electron and proton transfer reactions.

The application of pulse radiolysis to radiation chemistry has contributed significantly to the solution of several central problems in this field over the past eight years. During this time, this fast reaction method has also developed as a generalized, versatile technique, of broad usefulness in many diverse areas of chemical kinetics in both the liquid and gas phase. One such area, to which this review is directed, concerns the kinetics of reactive states of aromatic molecules in solution. A good deal of new and important information has been developed about the kinetics of the chemical and physical reactions of aromatic molecules in both their ionic states and electronically excited states.

The study of ionic states of aromatic molecules has dealt largely with the radical anions of these molecules in polar liquids, and more recently to a lesser extent with aromatic cations. The study of electronically excited states has been concerned principally with the triplet state in both non-polar and polar liquids, and to a lesser extent with the singlet state. The direct observation of these reactive species has provided some understanding of fundamental phenomena in radiation chemistry such as the extent of charge separation in polar liquids and the persistence of this charge separation into the chemical stage of events, the mode of formation and yield of both ionic and electronically excited

In Radiation Chemistry; Hart, E.;
Advances in Chemistry; American Chemical Society: Washington, DC, 1968.

species, energy transfer and charge transfer processes, and so on. It is convenient, for purposes of this review, to consider separately the reactions of ionic states and the reactions of electronically excited states. It will be seen, however, that there are overlapping phenomena. In most of these investigations the identities of the reactive states is based directly on the optical absorption spectra of the species, which have already been established by other methods. The identity of the reactive transient is therefore not a matter of complex speculation for most cases, but is reliably known at the outset.

Aromatic Molecule Ions

In irradiated polar liquids containing aromatic compounds in solution, the aromatic radical anions are formed by attachment of solvated electrons:

$$e^-_{sol} + \text{Arene} = \text{Arene}^- \quad (1)$$

The general occurrence of electron solvation in irradiated polar organic liquids such as the alcohols (*1, 29, 32, 33*), ethers (*10*) and amines (*13*) has been established in pulse radiolysis studies. The anion formed in Reaction 1 is identified from the optical absorption spectrum previously known from studies of alkali metal solutions (*9, 14, 15*) in which the anions are relatively stable. Figure 1 shows the spectra of the diphenylide, anthracenide, and *p*-terphenylide anions (*4*) in ethyl alcohol. In general, the maxima and the shoulders of the observed bands correspond very closely with previously reported spectra. It is on the basis of this correlation, along with the observation that the solvated electron is the precursor, that the species are identified as the radical anions. The aromatic compounds were used in the early pulse radiolysis work as electron scavengers in determining the extinction coefficient (*29, 32*) of the solvated electron. Most of the investigations of the kinetics of the radical anions were carried out in the aliphatic alcohols as solvents.

The formation reaction, 1, is very rapid. Absolute rate constants for electron attachment to four aromatic compounds in ethyl alcohol (*4*) are shown in Table I. These rate constants increase in order of increasing electron affinities of the aromatic molecule, but it should be noted that such a correlation may be fortuitous. The magnitude of the rate constants is equal to or near that of a diffusion controlled reaction, and a correlation with molecular size is also seen for this set of reactants.

The decay of the radical anion may occur in several different processes (*3, 4, 7, 8, 32*), depending upon the system and the experimental conditions. At sufficiently high concentration of the radical anion (and of the corresponding alcohol counter-ion formed in the primary processes) a rapid combination reaction of the anion with the counter-ion

Publication Date: January 1, 1968 | doi: 10.1021/ba-1968-0082.ch003

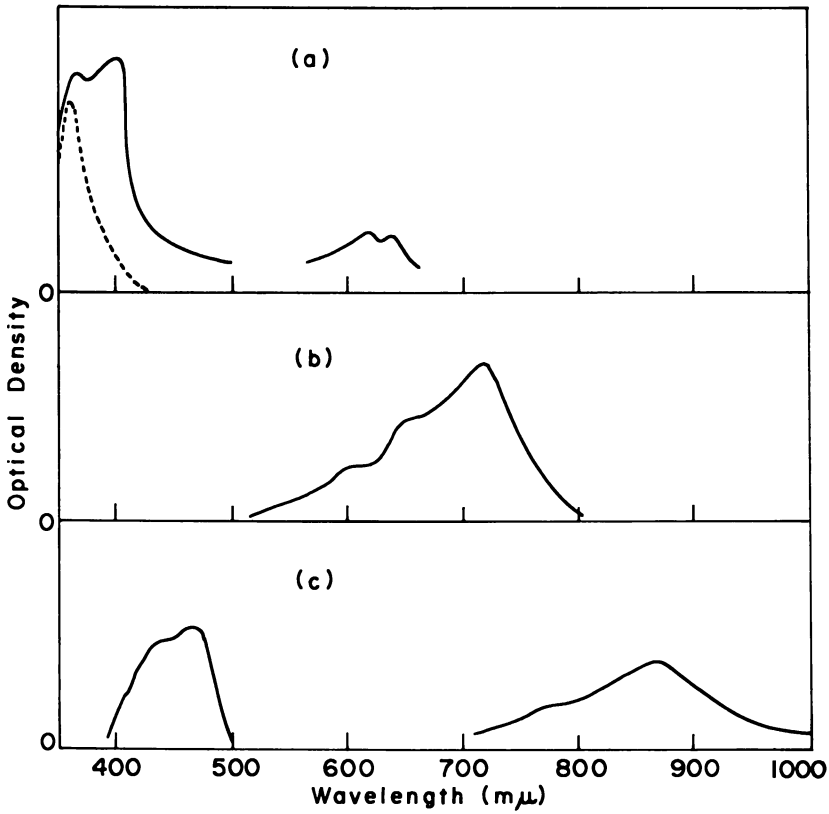

Figure 1. Absorption spectra of aromatic anions in ethyl alcohol, formed by electron attachment in pulse radiolysis. (a) Diphenyl in ethyl alcohol. The solid curve was obtained during the pulse. The dashed curve was obtained after a delay of 12 μsec. and is thought to be the adduct radical $C_{12}H_{11}$. (b) Anthracene in ethyl alcohol. This band of the anthracenide ion was observed spectrophotometrically at about 0.2 μsec. after the pulse. (c) p-Terphenylide ion in solutions of p-terphenyl in ethyl alcohol. Spectra are taken from Reference 4

Table I. Rate Constants for the Formation of Radical Anions by Electron Attachment in Ethyl Alcohol at 25°C.

Reaction	$k_1(M^{-1}\ sec.^{-1})$
e_{sol}^- + diphenyl	$(4.3 \pm 0.7) \times 10^9$
e_{sol}^- + naphthalene	$(5.4 \pm 0.5) \times 10^9$
e_{sol}^- + *p*-terphenyl	$(7.2 \pm 0.6) \times 10^9$
e_{sol}^- + naphthacene	$(10.2 \pm 0.8) \times 10^9$

may occur, as will be discussed. At very low concentration ($< 10^{-6}M$ for most of the radical anions studied) the ion combination reaction becomes relatively improbable and the intrinsic lifetime of the radical anion is determined by other processes. For example, in protonic polar liquids such as the lower aliphatic alcohols, the natural lifetime of most of the radical anions studied is determined by a proton transfer reaction from the alcohol:

$$\text{Arene}^- + \text{ROH} = \text{AreneH}\cdot + \text{RO}^- \qquad (2)$$

Absolute rate constants (*4*) for this protonation reaction (in units of M^{-1} sec.$^{-1}$) are given in Table II for four aliphatic alcohols. These protonation rate constants show a good correlation (*4*) with the relative acidity of the alcohols (*18, 26*), which is to be expected if the protonation involves the hydroxyl proton, and which may therefore be taken as an indication of the nature of Reaction 2. It is, however, clear that in changing the alcohol the solvent as well as the "reactant" is being changed and that the correlation is therefore not completely straightforward.

Table II. Proton Transfer Rate Constants for the Decay of Radical Anions in Aliphatic Alcohols at 25°C. The Rate Constant is in Units of M^{-1} sec.$^{-1}$

	Diphenyl	*Anthracene*	*Terphenyl*
Methyl Alcohol	$(6.9 \pm 1.2) \times 10^4$	$(8.1 \pm 2.0) \times 10^4$	$(4 \pm 1) \times 10^2$
Ethyl Alcohol	$(2.6 \pm 0.23) \times 10^4$	$(2.3 \pm 0.23) \times 10^4$	$(2 \pm 0.6) \times 10^2$
Propyl Alcohol	$(3.2 \pm 0.3) \times 10^4$	$(2.4 \pm 0.38) \times 10^4$	—
Isopropyl Alcohol	$(5.5 \pm 1.1) \times 10^3$	$(3.6 \pm 0.6) \times 10^3$	—

Table III. Protonation Rate Constants for Some Aromatic Radical Anions in Isopropyl Alcohol at 25°C.

Anion	$k_2(M^{-1}\ sec.^{-1})$
Naphthalene	$(4.4 \pm 0.8) \times 10^4$
Phenanthrene	$(2.6 \pm 0.4) \times 10^4$
o-Terphenyl	$(1.4 \pm 0.5) \times 10^4$
m-Terphenyl	$(1.1 \pm 0.4) \times 10^4$
Diphenyl	$(5.5 \pm 1.1) \times 10^3$
Anthracene	$(3.6 \pm 0.6) \times 10^3$
p-Terphenyl	$\leqslant 10^2$

The protonic character of the alcohols is not the only important parameter which determines the magnitude of k_2. There is a variation of at least two orders of magnitude in k_2, for a given alcohol, for the radical anions investigated. Table III shows the values of the protonation rate constants in isopropyl alcohol for seven different aromatic radical anions.

Publication Date: January 1, 1968 | doi: 10.1021/ba-1968-0082.ch003

The reaction of *p*-terphenylide anion in isopropyl alcohol is too slow to be reliably measured (because of impurity effects) by this method.

In view of the "low" values for these bimolecular rate constants, the activation energies (*8*) for several reactions were determined. For the anthracenide and diphenylide anions in both methyl alcohol and ethyl alcohol the activation energies for Reaction 2 are between 2 and 3 kcal./mole, and hence the pre-exponential factors in the form of the Arrhenius expression for the rate constants are approximately $3 \times 10^6 M^{-1}$ sec.$^{-1}$ at 25°C. The activation energies for anthracenide and diphenylide anions in isopropyl alcohol are approximately 6 kcal./mole, and the pre-exponential factor approximately $3 \times 10^8 M^{-1}$ sec.$^{-1}$. For the naphthalenide anion in isopropyl alcohol, the activation energy is 3.4 kcal./mole and the pre-exponential factor $1.3 \times 10^7 M^{-1}$ sec.$^{-1}$. The main reason for the "low" values of k_2 is thus not to be found in a high activation energy, but rather in the low pre-exponential factor. The low pre-exponential factor may reflect the entropy effect related to the reorientation of the liquid structure, in polar solvents, around the anion in the formation of the activated complex prior to the proton transfer. The effect of liquid reorganization should be greatest, as is the case, for the solvents with the largest dielectric constant. This effect is rather less for isopropyl alcohol for which the dielectric constant is somewhat lower than for methyl alcohol or ethyl alcohol. The activation energy for isopropyl alcohol, in accord with its lower acidity (*4*), is somewhat higher, as may be seen from the foregoing values.

As has been mentioned, the radical anion will also undergo a concurrent decay by reaction with the counter-ion at sufficiently high concentration:

$$\text{Arene}^- + \text{ROH}_2^+ = \text{AreneH}\cdot + \text{ROH} \qquad (3)$$

The counter-ion is here represented in the form of the alkyloxonium ion. Absolute rate constants for Reaction 3 have been determined (*4*) for the diphenylide, anthracenide, and *p*-terphenylide anions in ethyl alcohol. These are shown in Table IV.

The product of Reaction 3 is apparently the neutral hydrogen adduct free radical which shows the same absorption band as the product of

Table IV. Rate Constants for the Reaction of Aromatic Radical Anions with the Counter-Ion in Ethyl Alcohol at 25°C.

Radical Anion	k_3 (M^{-1} *sec.*$^{-1}$)
Diphenylide	$(3.3 \pm 0.5) \times 10^{10}$
Anthracenide	$(3.7 \pm 0.6) \times 10^{10}$
p-Terphenylide	$(1.9 \pm 0.3) \times 10^{10}$

Publication Date: January 1, 1968 | doi: 10.1021/ba-1968-0082.ch003

Reaction 2. The hydrogen adduct free radical formed in Reactions 2 and 3 decays in accord with a second-order rate law (probably the radical-radical reaction) at concentrations in excess of $10^{-6}M$, indicating that hydrogen abstraction from the solvent by the radical is a very slow process.

An interesting difference in the mechanism of the neutralization step, which will be discussed later, may be seen in the case of a non-polar, aprotic solvent such as cyclohexane. In that case the neutralization of the radical anion leads to a neutral electronically excited state of the aromatic molecule, an electron having been transferred. In the alcohols, a proton is transferred, giving a neutral free radical as the product (Reaction 3).

Finally, the last of the four types of anion reaction under investigation in our laboratory, and the one most extensively studied, is the transfer of an electron from one radical anion to a different aromatic compound in solution:

$$\text{Arene}_1^- + \text{Arene}_2 = \text{Arene}_1 + \text{Arene}_2^- \qquad (4)$$

It is apparent that if a two component solute system is made up in the alcohols such that $k_1[\text{Arene}_1] >> k_1[\text{Arene}_2]$, then Arene_1^- would be formed preferentially in the electron attachment process. The decay of Arene_1^- to form Arene_2^- and the formation of Arene_2^- could then be observed simultaneously for those pairs which do not exhibit an extensive spectral overlap. Concurrent with the decay of Arene_1^- in the electron transfer is its decay in the protonation reaction, (Reaction 2). In those cases for which the equilibrium is not overwhelmingly on the side of the acceptor anion, the back reaction also occurs. Absolute rate constants have been determined (*3*, *7*) for 12 donor-acceptor pairs. These rate constants, among which are two determined as back reaction constants, are shown in Table V. Of these 14 rate constants, seven or eight appear to be diffusion controlled. Those which have a lower value exhibit either a small or negative (as for the two back reaction constants) difference in the reduction potential of the donor-acceptor pair. The data have been applied (*3*) as a test of the theory of Marcus (*21*, *22*) for homogeneous electron transfer rates. Self-consistent values are obtained if a reasonable value of about 5 A. is used for the encounter radii in calculating the reorganization parameter of the theory, and the expected dependence upon the free energy of activation (calculated from the reduction potential differences and the dielectric properties of the liquid) is found. This test of the theory is discussed in another chapter (*3*) in this volume.

In a recent report (*2*), data are given for the electron transfer involving aromatic ketones such as acetophenone, benzophenone and fluorenone

Publication Date: January 1, 1968 | doi: 10.1021/ba-1968-0082.ch003

as both acceptor molecules and donor anions, in ethyl alcohol and water. The other molecules of the transferring pairs are nitrous oxide, oxygen, and acetone. Rate constants range from 10^9 to $10^{10} M^{-1}$ sec.$^{-1}$.

Table V. Electron Transfer Rate Constants for Aromatic Molecules in Isopropyl Alcohol at 25°C.[a]

Donor Radical Anion	*Acceptor Molecule*	*Rate Constant* (M^{-1} *sec.*$^{-1}$)
Anthracenide [b]	pyrene	$(2.1 \pm 0.9) \times 10^7$
9,10-Dimethylanthracenide [b]	pyrene	$(3.7 \pm 1.7) \times 10^7$
Diphenylide	naphthalene	$(2.6 \pm 0.8) \times 10^8$
Diphenylide	phenanthrene	$(6 \pm 3) \times 10^8$
Pyrenide	9,10-dimethylanthracene	$(1.3 \pm 0.3) \times 10^9$
Pyrenide	anthracene	$(1.8 \pm 0.3) \times 10^9$
m-Terphenylide	*p*-terphenyl	$(2.3 \pm 0.4) \times 10^9$
Diphenylide	*p*-terphenyl	$(3.2 \pm 0.7) \times 10^9$
Diphenylide	pyrene	$(5.0 \pm 1.8) \times 10^9$
Diphenylide	anthracene	$(6.4 \pm 2.0) \times 10^9$
p-Terphenylide	pyrene	$(3.6 \pm 1.1) \times 10^9$
p-Terphenylide	anthracene	$(5.5 \pm 0.9) \times 10^9$
m-Terphenylide	pyrene	$(3.5 \pm 1.2) \times 10^9$
o-Terphenylide	pyrene	$(4.0 \pm 1.8) \times 10^9$

[a] All these data are from References 3 and 7.
[b] Determined as back reaction constants.

Attempts to observe the aromatic cations in solution have only recently been made. There is a good deal of evidence (*17, 31*) of aromatic cation formation from work in low temperature glasses where the ions appear to be stable. Their identification from the spectra alone is, in most cases, a difficult matter because of the great similarity between the absorption spectra of the anions and cations. In the glasses, the identification is based, for the most part, on the premise of electron attachment to the solvent, generally a chlorinated compound, rather than to the aromatic solute. Further evidence is provided from scavenger effects.

Some evidence, in pulse radiolysis, has been obtained (*6, 35*) for the formation of the cation of diphenyl, *p*-terphenyl, anthracene, and *trans*-stilbene in dichloroethane and other chlorinated solvents, and for the *p*-terphenyl cation in chloroform (*6*). Some of these cation spectra are shown in Figure 2. The diphenyl solution shows absorption band at 690 mμ and 380 mμ. The diphenylide anion bands in the alcohols and in ethers are at 630 mμ and 405 mμ, so that the cation bands seem to be distinguishable. Anthracene in dichloroethane shows a band at 430 mμ,

Publication Date: January 1, 1968 | doi: 10.1021/ba-1968-0082.ch003

where the anion in ethyl alcohol does not absorb as well as a band at 730 mμ, where the anion does absorb. *p*-Terphenyl in both dichloroethane and chloroform shows bands at 960 mμ and 420 mμ, the former being quite different from the anion spectrum. All of these transient absorptions are unaffected by oxygen which completely eliminates the anion bands in ethyl alcohol. Aniline or diphenylamine, on the other hand, shows a scavenging effect upon these bands, while the anion bands in ethyl alcohol are unaffected by these amines (*6*). The lifetimes of these species in the pure solvent are on the order of a few μsec. and show complex decay kinetics.

Publication Date: January 1, 1968 | doi: 10.1021/ba-1968-0082.ch003

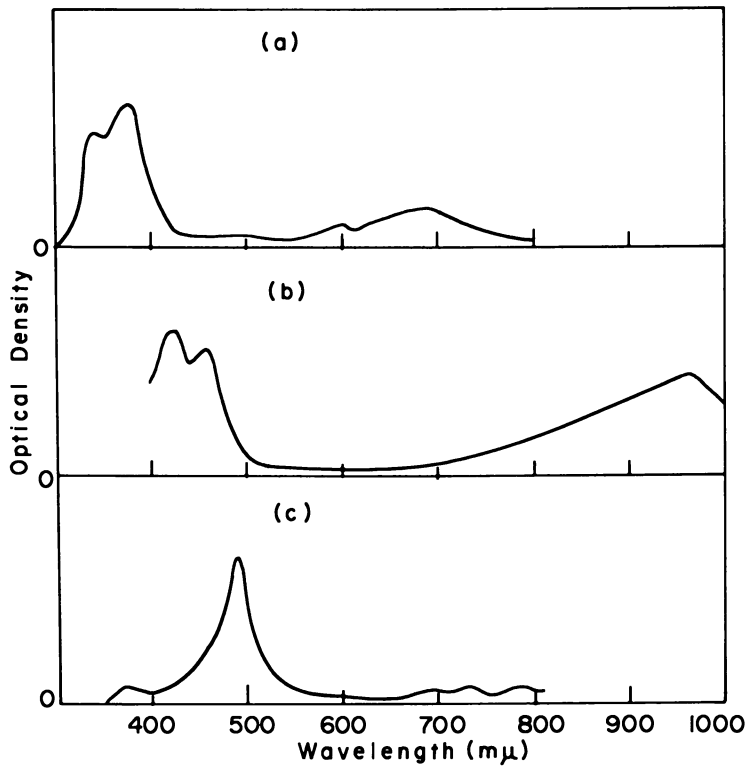

Figure 2. Absorption spectra of aromatic cations in chlorinated alkane solvents, formed in pulse radiolysis. (a) Diphenyl in 1,2-dichloroethane. The spectrum was obtained 2 μsec. after the electron pulse. (b) p-*Terphenyl in 1,2-dichloroethane. The spectrum was obtained 4 μsec. after the electron pulse. The band at 420 mμ may contain a small contribution from a long-lived species produced by the radiolysis. (c)* trans-*Stilbene in 1,2-dichloroethane, in 1,1,2-trichloroethane, and in 1,1,2,2-tetrachloroethane. Spectrum was obtained 1 μsec. after the electron pulse*

Aromatic Electronic States

Some of the early pulse radiolysis investigations were successful in identifying aromatic triplet states as reactive intermediates in irradiated systems. For many aromatic molecules, the lowest triplet state is readily identifiable from the absorption spectrum corresponding to the triplet-triplet transition. Such spectra had previously been reported in extensive investigations in organic glasses (*23*) and in the flash photolysis of liquids (*28*). In a few cases the molar extinction coefficients are known (*20, 28*), although with low accuracy, since the uncertainty is generally ±50% or greater. The first excited singlet state of aromatic molecules may be identified from the fluorescence emission bands (*11*).

There are several probable modes of formation of the triplet states of aromatic molecules in irradiated solutions. They may be formed in some of the same processes which occur in photoexcitation, such as by inter-system crossing from the singlet manifold. The triplet may be formed directly from the ground state singlet by direct electron impact excitation by low energy electrons in which case electron exchange excitation may occur. The probability of electron impact with the solute is not negligible for subexcitation electrons, and this process may play a significant role.

The primary processes, for the most part, however, involve ionization and electronic excitation of the solvent S, following which there may be a variety of reactions leading to the aromatic triplet. As yet, only a few rate constants have been determined for individual reactions, in contrast with the less complex case of the aromatic radical anions in polar liquids. The reactions which may occur are:

$$S + e^- = {}^1S + e^- \quad (5)$$

$$S + e^- = {}^3S + e^- \quad (6)$$

$$S + e^- = S^+ + 2e^- \quad (7)$$

followed by neutralization to form electronically excited states

$$S^+ + e^- = S^* \quad (8)$$

In addition, electron attachment of slow electrons may occur for certain solvents:

$$S + e^- = S^- \quad (9)$$

The excited solute molecules may then be formed by energy transfer:

$$^1S + \text{Arene} = S + {}^1\text{Arene} \quad (10)$$

$$^3S + \text{Arene} = S + {}^3\text{Arene} \quad (11)$$

where the superscript indicates the multiplicity, and the singlet arene

Publication Date: January 1, 1968 | doi: 10.1021/ba-1968-0082.ch003

designated is the excited singlet. Since intersystem crossing may occur for both the solvent and the solute, the solvent singlet may be a possible precursor of the solute triplet:

$$^1S = {}^3S \tag{12}$$

$$^1\text{Arene} = {}^3\text{Arene} \tag{13}$$

As has been pointed out in the first section, electron attachment to the solute to form the radical anion, as in Reaction 1, may occur readily in polar solvents. This will occur in non-polar solvents as well, if the concentration of the solute is sufficiently high to scavenge the free electron. The anion may be a precursor of the triplet state, which may be formed in a neutralization reaction such as:

$$\text{Arene}^- + S^+ = {}^3\text{Arene} + S \tag{14}$$

where the cation may be the solvent or other species, perhaps the aromatic cation. An analogous process could involve the aromatic cation and the solvent anion. Subexcitation electrons may lead directly to electronically excited states of the solute:

$$\text{Arene} + e_s^- = \text{Arene}^* \tag{15}$$

with either the triplet or excited singlet being formed. Some of these processes, such as Reaction 8, may not occur homogeneously throughout the solution, but may involve geminate pairs. Experimental evidence has been found for several of the foregoing processes.

In 1961, McCollum and Wilson (*25*) recorded the absorption spectra of the triplet states of anthracene, phenanthrene, naphthalene, and 9-acetylanthracene in paraffin oil irradiated with a pulse of electrons. The yield of anthracene triplet was estimated to be 0.5 molecule/100 e.v. The decay rate of the triplet in both paraffin oil and benzene was found to be several times faster than when photo-initiated in these systems. This is apparently due to the high concentration of radiation-produced quenchers, such as free radicals, and does not correspond to a single fundamental decay process of the triplet. In a subsequent study (*24*) the yields of both singlet and triplet states of anthracene and naphthalene in irradiated paraffin oil were measured. The ratio of the yields was compared with the inter-system crossing efficiency in photochemical systems, and found to be equivalent. From this observation it was concluded that the aromatic triplet in the irradiated system was formed largely through inter-system crossing, Reaction 13, and that processes such as Reactions 11, 14, and 15 are not important in their systems. It should be noted, however, that there is a very large uncertainty in the triplet yield, and such a precise conclusion may not be warranted.

Publication Date: January 1, 1968 | doi: 10.1021/ba-1968-0082.ch003

An observation of the triplet state of anthracene in benzene (*27*) is of special interest in that, in addition to the absorption spectrum of the triplet, a delayed fluorescence emission from the singlet at 4300 A. was recorded. The intensity of fluorescence, which was approximately proportional to the square of the triplet concentration at all times, was attributed to triplet-triplet quenching:

$$^3\text{Anthracene} + {}^3\text{Anthracene} = {}^1\text{Anthracene} + \text{Anthracene} \qquad (16)$$

The overall decay of the triplet may include some quenching by free radicals. The yield of anthracene triplet was estimated to be 0.7 molecule/100 e.v.

Publication Date: January 1, 1968 | doi: 10.1021/ba-1968-0082.ch003

Absolute rate constants have been determined for aromatic triplet formation in acetone solutions of several aromatic compounds (*5, 30*). The formation curves were observed directly for anthracene and naphthalene triplet (*5*) and for diphenyl triplet. These rate curves were found to fit a first order rate law, and were interpreted as a bimolecular energy transfer process from a state of the solvent molecule which is probably the triplet, that is, by Reaction 11. These rate constants, as well as the triplet yields, are listed in Table VI. The rate constants for anthracene and naphthalene triplet formation appear to correspond to diffusion controlled rate constants. Two further points are of interest, which are in contrast with observations in other systems which will be discussed. In acetone, most of the yield of aromatic triplet (at concentrations of the aromatic compound of $5 \times 10^{-3}M$ or lower) is formed in diffusional processes such as collisional energy transfer. Any "fast" formation appears

Table VI. Bimolecular Rate Constants and Radiation Chemical Yields for the Formation of Aromatic Triplets in Acetone at 25°C.

Solute	*k* (M^{-1} *sec.*$^{-1}$)	*G Value (molecules/100 e.v.)*
Anthracene	$(6.2 \pm 0.6) \times 10^9$	1.1 ± 0.7
1,2-Benzanthracene	—	1.9 ± 1.0
Naphthalene	$(4.5 \pm 0.9) \times 10^9$	< 3
Diphenyl	$\sim 5 \times 10^8$	—

to be small or negligible. Furthermore, the radical ion, observed separately, exhibits a very different decay rate from that of triplet formation, so that reactions such as 14 appear to be unimportant in this system. The half-life of the acetone state which is the precursor of the aromatic triplet was found to be > 5 μsec. If this is indeed the triplet state it is of interest to compare this value with the published lifetime (*16*) of 200 μsec. for the acetone triplet in the gas phase.

Pulse radiolysis of solutions of naphthalene and benzophenone (*12*) in various non-polar and polar liquids has shown the following. The naphthalene triplet was observed in benzene and in cyclohexane, and was not detected in ether, tetrahydrofuran, or methanol. The benzophenone triplet was observed in benzene, but appeared to have a small or negligible yield in cyclohexane and in tetrahydrofuran.

Some very interesting and important observations of the kinetics of formation of aromatic triplet states in cyclohexane have been reported by Hunt and Thomas (*19*) and more recently by Thomas (*34*) for naphthalene and anthracene in solution. The triplet yield (*19*), which increases with increasing solute concentration, was found to be as high as 4 molecules/100 e.v. for naphthalene in cyclohexane. The formation kinetics were observed with nanosecond detection equipment. It was found that there were two distinct rate processes. Approximately 70% of the triplet is formed in a "fast" process which is complete within less than 1 nsec. after the pulse at solute concentrations as low as $10^{-3}M$. This fast formation cannot therefore be accounted for by homogeneous diffusional reactions of molecular species involving encounter radii of molecular dimensions. Thus, it would seem that Reaction 10 followed by 13 is eliminated as the mechanism of fast triplet formation unless the cross section for Reaction 10 is unusually large. Moreover, direct observation of the fluorescence indicates that the singlet lifetime is greater than the half-time for fast triplet formation, so that the aromatic singlet is not the precursor. Reaction 11 would also appear to be eliminated as the mode of formation of the fast triplet, as would Reaction 14 which, as will be seen, seems to account for the "slow" triplet. Reaction 15 would be complete in a much shorter time than 1 nsec., but would be expected to account for only a very low yield.

The more recent work (*34*) seems to indicate that the "slow" triplet, accounting for the remainder, is formed from the aromatic radical anion, perhaps in reactions such as 14. This interpretation is consistent with the observation that the rate of decay of the anion corresponds to the rate of formation of the triplet, and that both species are eliminated by adding N_2O.

In pure benzene (*34*), an absorption band with maximum at 520 mμ is observed, which is suggested to be the absorption of the singlet in the transition $^1B_{2u}$–$^1E_{1u}$.

Current work in our laboratory (*30*) in two-component aromatic solute systems has indicated the feasibility of determining accurate rate constants for triplet-triplet energy transfer between aromatic donor-acceptor pairs by methods analogous to those used in our electron transfer investigations. Similarly, an attempt is being made to determine rate

Publication Date: January 1, 1968 | doi: 10.1021/ba-1968-0082.ch003

constants for singlet-singlet transfer from nanosecond observations of the fluorescence intensity.

Acknowledgment

Most of our own work discussed in this review was supported by the U. S. Atomic Energy Commission. More recently the program has also benefited from some support from the Petroleum Research Fund of the American Chemical Society under a Type C Grant. One of us (N. E. S.) is grateful for Fellowship support under the N.D.E.A.

Literature Cited

(1) Adams, G. E., Baxendale, J. H., Boag, J. W., *Proc. Roy. Soc. (London)* **A277**, 549 (1964).
(2) Adams, G. E., Michael, B. D., Richards, J. T., *Nature* **215**, 1248 (1967).
(3) Arai, S., Dorfman, L. M., ADVAN. CHEM. SER. **82**, 378 (1968).
(4) Arai, S., Dorfman, L. M., *J. Chem. Phys.* **41**, 2190 (1964).
(5) Arai, S., Dorfman, L. M., *J. Phys. Chem.* **69**, 2239 (1965).
(6) Arai, S., Firestone, R. F. (private communication).
(7) Arai, S., Grev, D. A., Dorfman, L. M., *J. Chem. Phys.* **46**, 2572 (1967).
(8) Arai, S., Tremba, E. L., Brandon, J. R., Dorfman, L. M., *Can. J. Chem.* **45**, 1119 (1967).
(9) Balk, P., Hoijtink, G. J., Schreurs, J. W. H., *Rec. Trav. Chim.* **76**, 813 (1957).
(10) Baxendale, J. H., Fielden, E. M., Keene, J. P., *Science* **148**, 637 (1965).
(11) Berlman, I. B., "Handbook of Fluorescence Spectra of Aromatic Molecules," Academic Press, New York, 1965.
(12) Dainton, F. S., Kemp, T. J., Salmon, G. A., Keene, J. P., *Nature* **203**, 1050 (1964).
(13) Dalton, L. R., Dye, J. L., Fielden, E. M., Hart, E. J., *J. Phys. Chem.* **70**, 3358 (1966).
(14) De Boer, E., Weissman, S. I., *Rec. Trav. Chim.* **76**, 824 (1957).
(15) Gill, D., Jagur-Grodzinski, J., Szwarc, M., *Trans. Faraday Soc.* **60**, 1424 (1964).
(16) Groh, H. J., Jr., Luckey, G. W., Noyes, W. A., Jr., *J. Chem. Phys.* **21**, 115 (1953).
(17) Guarino, J. P., Hamill, W. H., *J. Am. Chem. Soc.* **86**, 777 (1964).
(18) Hine, J., Hine, M., *J. Am. Chem. Soc.* **74**, 5266 (1952).
(19) Hunt, J. W., Thomas, J. K., *J. Chem. Phys.* **46**, 2954 (1967).
(20) Keller, R. A., Hadley, S. G., *J. Chem. Phys.* **42**, 2382 (1965).
(21) Marcus, R. A., *J. Chem. Phys.* **24**, 966 (1956).
(22) *Ibid.*, **43**, 2654 (1965).
(23) McClure, D. S., *J. Chem. Phys.* **19**, 670 (1951).
(24) McCollum, J. D., Nevitt, T. D., *U. S. Tech. Report* **ASD-TDR-63-616** (1963).
(25) McCollum, J. D., Wilson, W. A., *U. S. Tech. Report* **ASD-61-170** (1961).
(26) Murto, J., *Ann. Acad. Sci. Fennicae*, **Ser. A II**, 117 (1962).
(27) Nosworthy, J. M., Keene, J. P., *Proc. Chem. Soc.* **1964**, 114.
(28) Porter, G., Windsor, M. W., *Proc. Royal Soc.* **A 245**, 238 (1958).
(29) Sauer, M. C., Jr., Arai, S., Dorfman, L. M., *J. Chem. Phys.* **42**, 708 (1965).
(30) Shank, N. E., Dorfman, L. M. (unpublished results).

(31) Shida, T., Hamill, W. H., *J. Chem. Phys.* **44**, 2375 (1966).
(32) Taub, I. A., Harter, D. A., Sauer, M. C., Jr., Dorfman, L. M., *J. Chem. Phys.* **41**, 979 (1964).
(33) Taub, I. A., Sauer, M. C., Jr., Dorfman, L. M., *Discussions Faraday Soc.* **36**, 206 (1963).
(34) Thomas, J. K., *Preprints, ACS, Division of Petroleum Chemistry*, **13**, D18 (1968).
(35) Ueda, H., Dorfman, L. M. (unpublished results).

RECEIVED January 22, 1968.

Thermal Electron Attachment Studies by the Pulse-Sampling Technique

W. E. WENTWORTH and JOE C. STEELHAMMER
University of Houston, Houston, Tex. 77004

Publication Date: January 1, 1968 | doi: 10.1021/ba-1968-0082.ch004

Both dissociative and nondissociative thermal electron attachment processes have been studied utilizing the pulse-sampling technique. From these studies the following molecular parameters may be derived: molecular electron affinities, rate constants for dissociative and nondissociative thermal electron attachment, electron affinities of radicals, bond dissociation energies, and activation energies for electron attachment, detachment, and dissociation. Although this mode of electron attachment differs from that in electron swarm and beam studies, the results appear to be in agreement and are quite complementary in elucidating negative ion formation and reaction.

Over the past six years workers in our laboratory have studied and measured thermal electron attachment (TEA) to molecules by pulse sampling (*28*). This is a simple technique, capable of yielding precise and unique data—*e.g.*, molecular electron affinities, bond dissociation energies, electron affinities of radicals, kinetic information on electron attachment at thermal energies and subsequent negative ion reactions, etc. Some of this information cannot be obtained by any other known method. Electron attachment mechanisms as revealed by this technique were reviewed recently (*22*). However, the emphasis was on analytical applications, particularly the concentration and temperature dependence of the electron capture detector. The general purpose of this review is to discuss thoroughly thermal electron attachment mechanisms with particular emphasis on the molecular parameters that can be obtained from the TEA data associated with each mechanism. The TEA mechanisms, in addition to the kinetic and molecular parameters, should be valuable to radiation chemistry involving negative ions in the gas phase. The kinetic model for the pulse-sampling technique is reviewed

In Radiation Chemistry; Hart, E.;
Advances in Chemistry; American Chemical Society: Washington, DC, 1968.

with all its supporting evidence. In addition an exact mathematical evaluation of the electron capture coefficient in terms of the rate constants as a function of temperature is presented for each of the proposed mechanisms. The information obtained from electron beam and swarm methods is complementary to that from TEA studies, and the importance of the combined use of both sources in understanding electron attachment mechanisms is discussed.

Experimental

Thermal electron attachment studies in our laboratory utilize the so-called electron capture detector which is commonly used as a selective detector for gas chromatography. Our measurements are also carried out in conjunction with a gas chromatograph for reasons pointed out later. The electronic circuitry for the pulse mode of operation is identical to that originally proposed by Lovelock *et al.* (*14, 15*). The electron capture cell, employing tritium as a radiative β-source, has been modified slightly for practical reasons (*22*); however, the basic electrode geometry is parallel plate, as first proposed (*14, 15*).

The pulse-sampling technique was so named since the free electrons in the cell at any time are sampled by applying a periodic pulse of short duration and low potential. The free electrons are produced by the (tritium) β-ray interaction with the argon-moderating gas mixture at $\approx$ 1 atm. The moderating gas removes the excess energy which the electron possesses shortly after it is produced by ionization. Presumably the electrons attain a thermal distribution rapidly in a mixture of argon + 10% methane (*1*) during the relatively long field-free period between pulses. As the potentially electron-attaching compound leaves the gas chromatographic column and enters the electron capture cell, a decrease in the free electron concentration is monitored through the periodic pulse sampling. From the concentration dependence of this response (decrease) the electron capture coefficient for a compound can be evaluated.

The most commonly used carrier has been the argon + 10% methane mixture. Pulse widths of 0.3 μsec. with a field-free interval of 1000 μsec. are generally used with such a gas mixture (*22, 28*). These conditions can be varied by using a variable pulse generator so that rate constants associated with the production and loss of electrons in the cell can be evaluated.

To carry out the thermal electron attachment studies in conjunction with a gas chromatograph, the physical measurements must be made on a flowing, dynamic system. Under these conditions the precision is subject to additional variables that must be controlled above those encountered in a static system. Off-hand one may question whether any advan-

Publication Date: January 1, 1968 | doi: 10.1021/ba-1968-0082.ch004

tages can overcome the many complicating features of a flowing system. However, upon examining values of electron capture coefficients for a variety of compounds, a variation on the order of 10^6–10^7 will be noted. Hence, measurements on weakly capturing species can be seriously affected by minute traces of a highly capturing species. For example, if the impurity had a capture coefficient 10^6 greater than the compound being studied, an impurity of $1:10^6$ or 1 p.p.m. would result in a 100% error. Even 0.1 p.p.m. would cause an error of 10%. This is an extreme example, but it emphasizes the importance and value of the gas chromatograph. By using capillary columns, small but highly pure samples can be obtained by gas chromatography. By using a flowing rather than static system impurities owing to contaminants or failure to degas completely are minimized since a continuous flow of pure carrier gas is maintained (*12*).

Kinetic Model

A general kinetic model has been presented (*23*) which appears to be consistent with the data presently accumulated on some 100 compounds. The electron attachment steps and negative ion dissociation reactions are as follows:

$$e^- + AB \underset{k_{-1}}{\overset{k_1}{\rightleftharpoons}} AB^- \qquad \text{(I)}$$

$$e^- + AB \xrightarrow{k_{12}} A\cdot + B^- \qquad \text{(II)}$$

$$AB^- \xrightarrow{k_2} A\cdot + B^- \qquad \text{(III)}$$

$$\rightarrow A^- + B\cdot \qquad \text{(IV)}$$

[It has been pointed out that the proposed mechanisms are special cases of the more general mechanism involving an excited negative ion AB^-. The more general case can be reduced to the proposed mechanisms under the conditions of our experiment as shown later.] [The k_{12} dissociative mechanism, Reaction II, is considered to be spontaneous in the sense that the intermediate negative ion formed, AB^-, has a short lifetime of the order of vibration (10^{-12} sec.).] In addition the reaction steps for the production of electrons and neutralization and radical reaction steps for e^-, AB^-, and B^- or A^- must be included. The conditions under which the studies are carried out have been described in detail (*22*, *28*). Under these conditions one may assume steady state of the negative species and derive the following expression for the response of the electron capture cell as a function of concentration.

$$Ka = \frac{b - [e^-]}{[e^-]} \quad (1)$$

where $[e^-]$ and b are the concentrations of electrons with and without the capturing species present, respectively; a is the concentration of the capturing species, and K is the electron capture coefficient. The electron capture coefficient for the general case involving Reactions I-IV can be expressed in terms of the rate constants

$$K = \frac{1}{k_N + k_R}\left[k_{12} + \frac{k_1(k_2 + k_{N1} + k_{R1})}{(k_{-1} + k_2 + k_{N1} + k_{R1})}\right] \quad (2)$$

where $k_N + k_R$ is the sum of pseudo-first-order rate constants for e^- neutralization and radical reactions. $k_{N1} + k_{R1}$ are the analogous constants for AB^-.

The first term in Equation 2 corresponds to the dissociative step, Reaction II. This mechanism can be considered completely independent of the second term in Equation 2, or it can be derived from the second term by letting k_2 become extremely large. Then k_1 would become analogous to k_{12}. The derivation used is arbitrary. We used k_{12} to differentiate from the process which involves a stable negative ion intermediate which has a measurable lifetime.

The supporting evidence for the proposed kinetic model should start with evidence for a thermal or near thermal distribution for the electrons during the field-free period between pulses. In the original paper which presented the kinetic model (*28*) the time required to cool a 10-e.v. electron to an energy of 10% above the average thermal energy was estimated as 0.076 μsec. This calculation used the fractional energy loss per collision arising from elastic collisions, yet it is negligible compared with the reaction time under field-free conditions (on the order of 1000 μsec). Furthermore, recent studies, using drift velocity measurements in methane (*1*) give a substantial contribution from inelastic collisions, and the fractional energy loss per collision is some three orders of magnitude higher than that from only elastic collisions. With this estimate the time for electron thermalization would be considerably reduced from the above 0.076-μsec. estimate.

To interpret the electron attachment occurring at thermal energies, one must be concerned with the effect of the short 0.3-μsec., 30-volt pulse. Both the energy of the electrons during the pulse and the contribution of the reactions occurring during the pulse to the total reaction must be considered. From the drift velocity in Ar + 10% methane the average energy of the electrons has been estimated as slightly above the average thermal energy (*28*). For most reactions this small difference is probably not of great consequence. Furthermore, a comparison of the short pulse duration of 0.3 μsec. with the long pulse periods ~1000 μsec. suggests

Publication Date: January 1, 1968 | doi: 10.1021/ba-1968-0082.ch004

that the contribution during the pulse would be small. Actually a comparison with the time to attain steady-state conditions would be more valid. This has been done experimentally for a few compounds (*28*), and the time was found to be ≈500–1000 μsec.

The best evidence for assuming thermal energies comes from three different experimental studies. In the first the electron attachment to anthracene was measured with varying pulse potentials from 10–80 volts with no change in response (*28*). This suggests that the reaction during the pulse is a negligible contribution, or the electron energy is only slightly altered during the pulse. The second experiment compared electron attachment of chlorobenzene with azulene as a function of voltage and methane concentration (*28*). Chlorobenzene has a maximum cross section for electron attachment (≈0.86 e.v.), whereas azulene would be expected to have its maximum at lower energies. A higher relative response of chlorobenzene to azulene is obtained when shorter pulse intervals and lower concentrations of methane are used. At long pulse intervals (≈1000 μsec.) and high methane concentration (≈10%) the relative responses approach a limiting low value, suggesting that thermal distribution is attained under these conditions. The third experiment was completed just recently (*6*). As shown later, for some compounds the pulse-sampling technique can be used to determine the rate constant for thermal electron attachment. This has been done recently for SF_6 and perfluoromethylcyclohexane, for which there are some reliable thermal electron attachment rate constants from microwave studies (*16*). The agreement between the two studies is remarkably good: our experimental value for SF_6 was 2.41×10^{-7} cc./molecule-sec. compared with the literature value of 3.1×10^{-7} cc./molecule-sec. (*16*). Errors for both studies are on the order of 15–25%, so the agreement is well within the experimental error. As Mahan and Young point out the cross section for electron attachment to SF_6 decreases rapidly with increasing electron energy, and the maximum cross section would be expected at thermal energies. A large rate constant for electron attachment then suggests that a distribution of lower energy is attained. Because of the agreement between our work (*6*) and that of Mahan and Young (*16*), the distributions in both cases are probably thermal.

The greatest support for the actual mechanistic steps rests in the concentration dependence of the response (Equation 1) and more importantly the temperature dependence of the electron capture coefficient. The temperature dependence of the capture coefficient, as it pertains to the various mechanisms associated with Reactions I–IV, are discussed below, and agreement with experiment is strong supporting evidence for the kinetic model. The interpretation of the temperature dependence in terms of molecular parameters, such as molecular electron affinities or

Publication Date: January 1, 1968 | doi: 10.1021/ba-1968-0082.ch004

bond dissociation energies, and comparison with other experimental estimates of these parameters are considered later. Again, agreement between the experimental estimates of the parameters is strong support for the kinetic model. The only direct, absolute value that can be compared with the model is the thermal electron attachment rate constant to SF_6 and perfluoromethylcyclohexane, which serves to support the kinetic model and the assumption of a thermal electron distribution.

Thermal Electron Attachment Mechanisms

Many criteria could be used to classify electron attachment mechanisms or processes, especially if one considers the details of the potential energy curve of the negative molecular ion relative to that for the neutral molecule. However, we have chosen to classify the attachment mechanisms in the more conventional manner with respect to the actual species encountered in the reaction steps. Hence, Reactions I-IV are completely general for our system, and the resulting expression for the capture coefficient (Equation 2) is likewise general. When certain rate constants predominate or are zero (no reaction), the expression for K can take on various forms. Based on these assumptions and the various forms for K, we have classified the TEA mechanisms into four categories (discussed later).

In the subsequent discussion we assume that $(k_N + k_R)$ and $(k_{N1} + k_{R1})$ are temperature independent. Certainly the highly exothermic neutralization reactions are essentially temperature independent. They also probably predominate in the sum, and there is some experimental evidence to support this (23). If the electron or negative ion-radical reactions are temperature dependent, they are probably too small to contribute to the sum. Only if they were temperature independent would they contribute significantly, and the sum would then be temperature independent. Since these sums are assumed to be temperature independent, we will designate them by $k_D = (k_N + k_R)$ and $k_L = (k_{N1} + k_{R1})$.

The general form for the temperature dependence of the second term for K is

$$K = \frac{T^{-3/2}A_1 e^{-E_1^*/RT}(A_2 e^{-E_2^*/RT} + k_L)}{k_D(A_{-1}e^{-E_{-1}^*/RT} + A_2 e^{-E_2^*/RT} + k_L)} \qquad (3)$$

where E_n^* and A_n are the activation energy and frequency factor, respectively. Arrhenius expressions have been assumed for each of the rate constants with a $T^{-3/2}$ pre-exponential temperature dependence for k_1. This has been inserted to agree with the equibrium expression for electron attachment-detachment. Consistent with this equilibrium expression, ln $KT^{3/2}$ *vs.* $1/T$ is conventionally plotted. The $T^{3/2}$ term is actually

Publication Date: January 1, 1968 | doi: 10.1021/ba-1968-0082.ch004

appropriate only when k_{-1} is predominant in the denominator, but for comparison, ln $KT^{3/2}$ is plotted for all mechanisms. The essential reactions corresponding to each mechanism are Reactions I-IV (22).

Mechanism I: Stable Negative Ion Formation. When $k_2 = 0$ and $k_{12} = 0$,

$$K = \frac{k_1 k_L}{k_D(k_{-1} + k_L)} \tag{4}$$

[Since our statements with respect to the kinetic model are not general, one should consider $e^- + AB \underset{k_{-1}'}{\overset{k_1'}{\rightleftharpoons}} (AB^-)^* \underset{z_{-1}(m)}{\overset{z(m)}{\rightleftharpoons}} AB^-$ where $z(m)$ and $z_{-1}(m)$ represent the rate of stabilization and detachment, respectively. The "effective" forward rate constant would therefore be $k_1 = k'_1 \frac{(z(m))}{z(m) + k_{-1}'}$ and for the reverse $k_{-1} = z_{-1}(m) \frac{(k_{-1}')}{z(m) + k_{-1}'}$. If the pressure is sufficiently high, $z(m) >> k_{-1}$ as the case in the electron capture cell, then $k_1 = k_1'$. The k_{-1} represented in the kinetic model is not the same as the autoionization rate measured in recent beam experiments (9) but is modified by the ratio $\frac{z_{-1}(m)}{z(m)}$ $\left(i.e., k_{-1} = k_{-1}' \frac{z_{-1}(m)}{z(m)}\right)$.]

The second term in Equation 2 can acquire three forms depending upon the relative magnitudes of k_{-1}, k_2, and k_L. If k_2 is zero or extremely small, we have the mechanism involving only Reaction I, which results in the formation of a stable negative ion. Two different temperature dependencies can be observed corresponding to:

High Temperature

$$k_{-1} > k_L > k_2 = 0$$

$$K = \frac{k_L k_1}{k_D k_{-1}} \tag{5}$$

Low Temperature

$$k_L > k_{-1} > k_2 = 0$$

$$K = \frac{k_1}{k_D} \tag{6}$$

According to the principle of microscopic reversibility k_1/k_{-1} can be equated to the equilibrium constant for Reaction I, which in turn can be expressed in terms of the electron affinity through the statistical thermodynamic expression for an ideal gas (24).

$$K = \frac{k_L}{k_D} \frac{A}{T^{3/2}} e^{+EA/RT} \tag{7}$$

The partition function for the negative ion and neutral molecule have been cancelled except for the statistical weight of 2. Comparing Equation 7 with Equation 3 under these approximations, $A = A_1/A_{-1}$ and $EA = -(E_{-1} - E_1)$. A is a constant which can be evaluated from fundamental constants and the mass of the electron. As a result of the form of Equation 7, ln $KT^{3/2}$ *vs.* $1/T$ is plotted, and the positive slope gives the molecular

Publication Date: January 1, 1968 | doi: 10.1021/ba-1968-0082.ch004

electron affinity. If the neutral molecules have a strain which differs from that for the negative ion, the partition functions would not cancel. This would be especially true if there were a change in configuration associated with the electron attachment process. The subsequent error introduced in calculating the *EA* assuming cancellation of partition functions is difficult to estimate, but it should not exceed 0.5 kcal.

From Equation 6 the rate of electron attachment at thermal energies, k_1, can be evaluated. k_D can be evaluated by measuring the electron concentration as a function of pulse period (*28*). Frequently k_1 is relatively temperature independent, and this type of mechanism is characterized by a larger positive slope at higher temperatures, followed by a zero or slightly negative slope at lower temperatures. Several examples of this type of temperature dependence have been published (*25*, *28*) in which $E_1^* \approx 0$.

In some cases where there is a considerable amount of strain in the molecule which is released upon formation of the negative ion, E_1^* can be larger. Figure 1 shows a series of curves with a fixed electron affinity, but varying E_1^*, with 2,4,6-trimethylacetophenone as a typical example.

Mechanism II: Dissociative Electron Attachment. The dissociative mechanism leading directly to $A + B^-$ can be considered from the first term in Equation 2 where

$$K = \frac{k_{12}}{k_D} \tag{8}$$

If the temperature dependence of k_{12} is taken as the Arrhenius equation, a simple ln K *vs.* $1/T$ will be linear with a single negative slope. A ln $KT^{3/2}$ *vs.* $1/T$ is also linear, and several examples of this type have been published (*23*).

An equation analogous to 8 is obtained if $k_2 >> (k_{-1} + k_L)$ and $K = k_1/k_D$. However, this expression for K is identical to Equation 6 where k_L was the predominant rate constant and AB^- is formed. To differentiate between these processes, the k_{12} term has been adopted for the dissociative mechanism.

Mechanisms III and IV: Dissociative Attachment Preceded by Negative Molecular Ion Intermediate. When k_2 it not zero, the second term in Equation 2 can take on three possible expressions which could be observed in different temperature regions where K can have three

High Temperature	*Intermediate Temperature*	*Low Temperature*
$k_{-1} > k_2 > k_L$	$k_{-1} > k_L > k_2$	$k_L > k_{-1} > k_2$
$K = \frac{1}{k_D}\frac{k_1 k_2}{k_{-1}}$	$K = \frac{k_L}{k_D}\frac{k_1}{k_{-1}}$	$K = \frac{k_1}{k_D}$ (9)

expressions. [Consideration of an excited negative ion intermediate in the

Publication Date: January 1, 1968 | doi: 10.1021/ba-1968-0082.ch004

general mechanisms would have similar consequences as described previously, with the additional consideration of an excited intermediate prior to dissociation.]

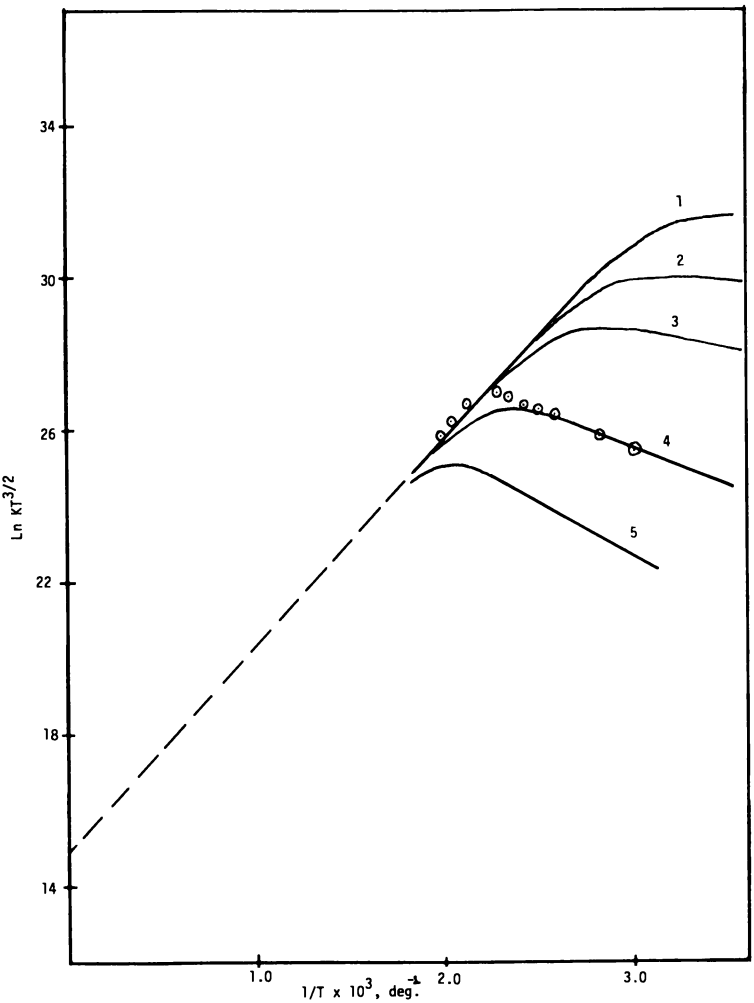

Figure 1. Temperature dependence for Mechanism I with E_1^* *variable;* EA = *10.9 kcal.,* E_1^* = *(1) −1; (2) 0; (3) 1; (4) 3.1; (5) 5 kcal. Circles represent data for 2,4,6-trimethylacetophenone*

The intermediate and low temperature expressions are identical to the two regions of Mechanism I. The high temperature region is associated with a negative slope of a ln $KT^{3/2}$ *vs.* $1/T$ plot. Mechanisms III and IV then take on the appearance of Figure 2, where all three linear regions

Publication Date: January 1, 1968 | doi: 10.1021/ba-1968-0082.ch004

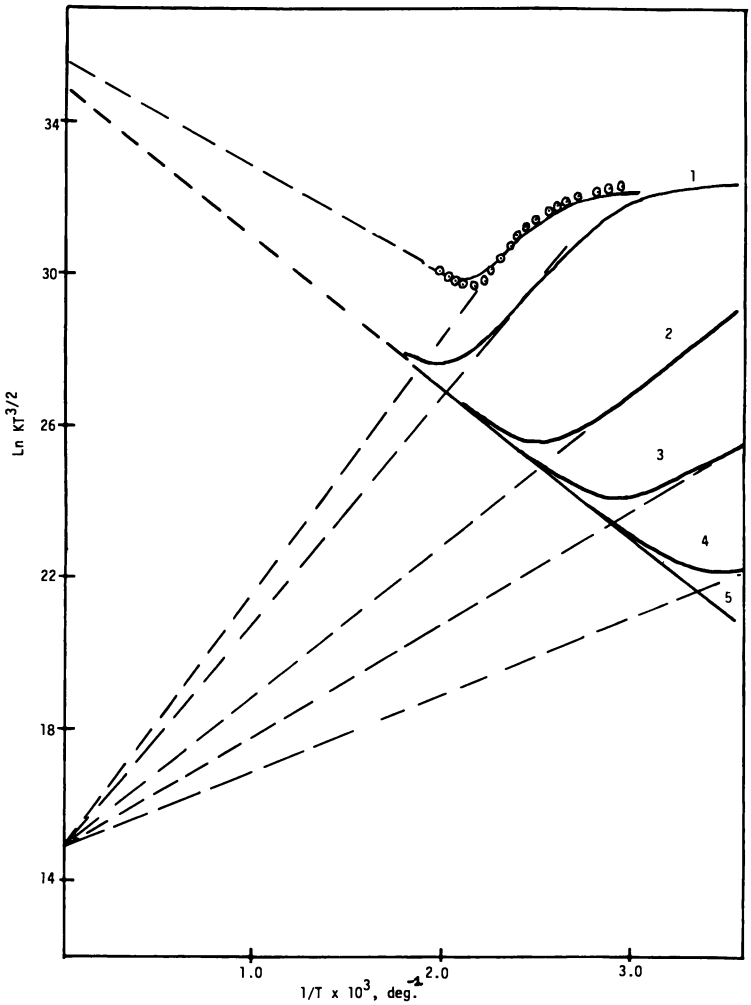

Figure 2. Temperature dependence for Mechanisms III and IV. $(E_2^* - EA) = 4.4$ kcal.; $E_1^* = 1.4$ kcal.; EA = (1) 12; (2) 8; (3) 6; (4) 4; (5) 0 kcal. Circles represent data for 3-chloroacetophenone; solid line through the data for the parameters: $E_2^* = 17.8$ kcal., EA = 13.4 kcal., $E_1^* = 1.4$ kcal.

may be observed. In Figure 2 electron affinity is varied, and $(E_2^* - EA)$ is held constant and $E_1^* = 0$. Deviations from linearity in the transition between linear regions should be noted. Using data over a temperature span which appears to be linear could lead to serious errors in the slopes. The family of curves in Figures 1–3 shows how good the approximations are that lead to the linear regions and shows the limitations of using only

the data in the "linear" regions. In some cases the "linear" region is almost nonexistent.

The specific example given is 3-chloroacetophenone. Figure 3 shows a series of curves varying E_2^*, holding EA constant and $E_1^* = 0$. Again the range of linearity should be noted.

Mechanisms III and IV cannot be differentiated kinetically. However, in Mechanism IV the activation energy (E^*) at high temperatures is equal to the change in internal energy (ΔE). This is important since

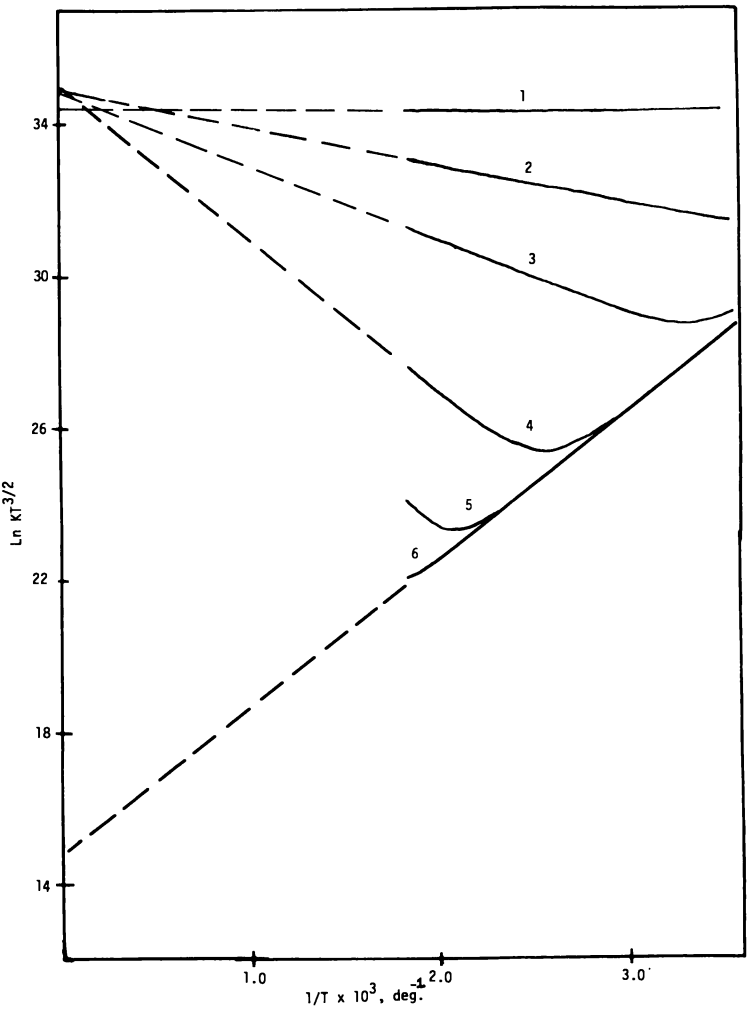

Figure 3. Temperature dependence for Mechanisms III and IV. EA = 7.7 kcal.; $E_1^* = 0$; E_2^* = (1) 6.4; (2) 8.4; (3) 10.4; (4) 14.4; (5) 18.4; (6) 22.4 kcal.

Publication Date: January 1, 1968 | doi: 10.1021/ba-1968-0082.ch004

the electron affinity of the radical or the bond dissociation energy can be determined from E^* providing the other quantity is known. Mechanisms III and IV can also be distinguished precisely on the basis of their potential energy curves. Mechanism IV involves only a single negative ion potential energy curve, whereas Mechanism III involves two negative ion potential energy curves leading to two different negative ions upon dissociation (*22*).

The various mechanisms are summarized in Figure 4. Representative two-dimensional potential energy curves are drawn to illustrate the reaction paths along with the typical temperature dependence of the capture coefficient for that case. The molecular parameters which can be derived from each mechanism and the relationship with the temperature dependence are given. Classes of compounds which have been investigated and clearly fit one of these mechanisms are also given.

Publication Date: January 1, 1968 | doi: 10.1021/ba-1968-0082.ch004

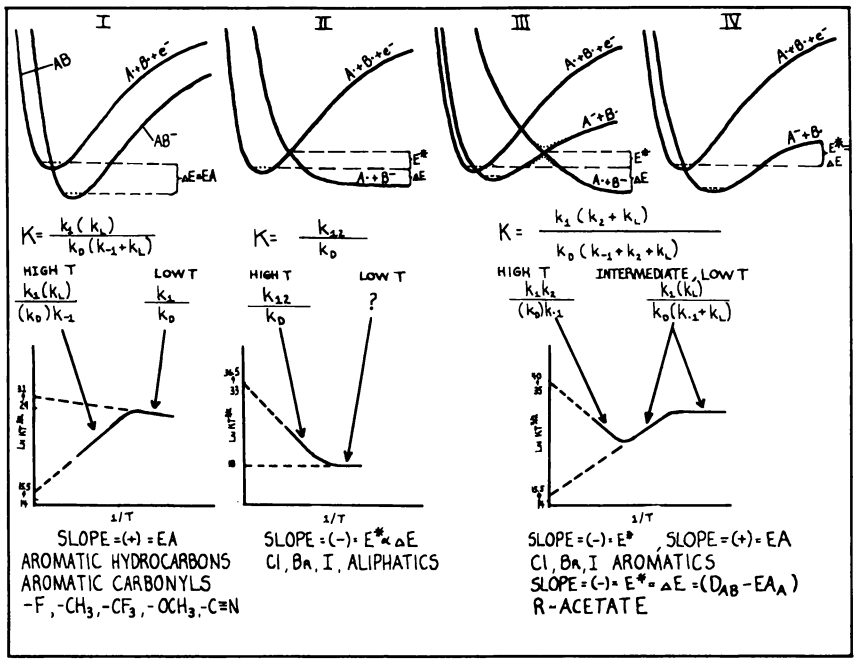

Figure 4. Representative potential energy curves and temperature dependence for the various TEA mechanisms

The distinction between Mechanism III and IV is quite clear in terms of potential energy diagrams. Actually Mechanisms I, II, IV are very similar since they involve a single negative ion potential energy curve and differ only in the depth of the curve and the relative energy

of the dissociative products (bond dissociation energy minus electron affinity of the radical). As discussed below, an empirical two-dimensional potential energy curve for the negative molecular ion has been proposed which should satisfy all three cases equally. On this basis one could reclassify the mechanisms and include all three into one category. However, phenomenologically they are distinct in that one leads to dissociation of the negative molecular ion whereas the other gives a stable negative ion.

The potential energy curves in Figure 4, being two dimensional, are approximations or cross sections of the actual multidimensional potential surface, which is necessary to represent a polyatomic molecule. For some polyatomics the two-dimensional representation may be satisfactory if the configurational change from the neutral molecule to the negative ion is principally the lengthening of a specific bond—*e.g.*, aliphatic halogens. On the other hand, there are other molecules where this is not a reasonable approximation—*e.g.*, polynuclear aromatics.

Publication Date: January 1, 1968 | doi: 10.1021/ba-1968-0082.ch004

Molecular Electron Affinities

According to Mechanism I the temperature dependence of k_1/k_{-1}, which is observed at higher temperatures, should yield the electron affinity of the molecule. The three- and four-ring polycyclic aromatic hydrocarbons were the first compounds investigated by the pulse-sampling technique, and these follow Mechanism I (*24, 28*). Since then, several of the five-ring compounds have been investigated (*2*). In general the electron affinities of the polycyclic aromatic hydrocarbons (alternate) compare well with every available estimate of relative or absolute values of electron affinities—namely, polarographic half-wave reduction potentials (*24*), frequency of lowest energy electronic absorption band (*2, 3*), are theoretical estimates (*2, 3, 24*). More recently a good correlation with electron attachment in solution by Chandhuri *et al.* (*5*) gives further support to the interpretation. Some aromatic aldehydes and ketones have also been reported recently (*25*). Again a reasonably good correlation with polarographic half-wave reduction potentials was observed.

The electron affinities of numerous F, Cl, $-CH_3$, $-CF_3$, $-OCH_3$, $-C\equiv N$ substituted aromatic hydrocarbons and aromatic aldehydes and ketones have been determined (*4*). For the most part the TEA occurred by Mechanism I. However, the chlorine derivatives can dissociate at higher temperatures according to Mechanism III. The *EA* can be evaluated from the temperature dependence in the intermediate temperature region.

Hückel calculations of the electron affinities of these substituted compounds have been carried out. The heteroatom inductive and resonance parameters, h_i and k_i, have been established for the previously mentioned substituents, and were determined by a procedure different from normal. The Hückel calculations were made on the difference in electron affinity from the parent compound, and the parameters were adjusted to agree with the experimental change in electron affinity. In general, Hückel calculations have severe limitations; however, when the calculations are made only on the ΔEA, the inaccuracy of the Hückel estimate of the aromatic framework is minimized. As a result good agreement was obtained between the Hückel estimates and the experimental ΔEA.

Publication Date: January 1, 1968 | doi: 10.1021/ba-1968-0082.ch004

Thermal Electron Attachment Rate Constants

According to Mechanism I, the electron capture coefficient in the low temperature region is given by k_1/k_D. Since k_D can be evaluated by measuring electron production as a function of time (*28*), k_1 can be evaluated readily, generally with a precision *ca.* ±15% with this technique. The accuracy or absolute error in k_1 is difficult to estimate since it depends on the validity of the kinetic model and a thermal distribution for electrons. Hence, the independent determination for the thermal electron attachment rate constant to SF_6 and perfluoromethylcyclohexane (*16*) is welcome. The agreement for SF_6 where $k_1 = 2.41 \times 10^{-7}$ cc./molecule-sec. compared with the literature value (*16*) of 3.1×10^{-7} cc./molecule-sec. itself is remarkable, and the data for perfluoromethylcyclohexane where $k_1 = 7.98 \times 10^{-8}$ cc./molecule-sec. compare even more favorably with the literature values (*16*) of 9.8×10^{-8} cc./molecule-sec. This excellent agreement not only gives support to the model but also justifies using the pulse-sampling technique to obtain thermal electron attachment rate constants. Of course this would be restricted to molecules which have a relatively large electron affinity so that the approximation $k_L >> k_{-1}$ will be valid.

The pulse-sampling technique is quite simple both in principle and practice. The temperature dependence of the rate constant can be evaluated readily. For the two compounds investigated in detail, perfluoromethylcyclohexane had an Arrhenius activation energy of 1.7 kcal., whereas the value for SF_6 was 0.9 kcal.

In previous publications (*25, 28*) data in this low temperature region have been reported for the polycyclic aromatic hydrocarbons and some aromatic aldehydes. The k_1 values can be evaluated from this data at lower temperatures; however, they are subject to more error than the

values given previously for SF_6 and perfluoromethylcyclohexane. If accurate values are desired, it is necessary to determine k_D at the same time under identical experimental conditions. This was not done in the earlier studies (*25, 28*) since the primary interest was the electron affinities of the molecules. This necessitates only precise relative electron capture coefficients since the electron affinities are determined from the slope of a ln $KT^{3/2}$ *vs.* $1/T$ plot.

Electron Attachment to Strained Molecules

A few compounds have been investigated which show an apparent activation energy for electron attachment to form a stable negative ion (*26*). According to the classification in Figure 4 they would fit Mechanism I, except that the slope at low temperatures is negative in contrast to the generally observed zero slope.

2,4,6-Trimethylacetophenone was synthesized, and the results can be compared with acetophenone whose *EA* has been determined precisely (*25*). The methyl substituents in the 2,6-positions result in considerable steric hindrance to the $-\overset{\overset{O}{\|}}{C}-CH_3$ group, causing the carbonyl group to rotate out of the plane of the ring. This conclusion is based principally on the observed shift in carbonyl stretching frequency relative to other aromatic ketones. To acquire the necessary stability of the negative molecular ion, the carbonyl group must be planar or nearly planar with the ring. Therefore, an activation energy associated with this torsional motion to a near-planar configuration would be expected before electron attachment could occur. An experimental activation energy of 3.1 kcal./mole is observed, which appears reasonable in comparison with other known strain energies. The experimental *EA* of 2,4,6-trimethylacetophenone is considerably larger than that of acetophenone. Considering the strain in the molecule one might not have anticipated this result. However, this can be rationalized logically if the strain in the molecule exceeds that of the negative ion. Thus, the internal energy of the neutral molecule is increased more than that of the negative ion, and the change in energy, $\Delta E = EA$, is increased.

Cyclooctatetraene and azulene have also been investigated, and each displays a negative slope at lower temperatures. Cyclooctatetraene is non-planar, whereas its negative ion is thought to be planar (*18*). This change in configuration is consistent with our observation of an activation energy for electron attachment. The structure of the negative ion of azulene has not been determined; however, the EPR spectra suggest a change in structure from the neutral molecule (*19*).

Publication Date: January 1, 1968 | doi: 10.1021/ba-1968-0082.ch004

Dissociative TEA to Aliphatic Halides

The aliphatic halides have been investigated extensively, and the conclusions from the early work are important (*23*). A paper on more recent work will be submitted shortly (*27*).

Aliphatic halides in general follow Mechanism II (Figure 4) (*23*). The temperature dependence shows a single linear region, except for a few compounds which have low capture coefficients at lower temperatures. In these cases, the capture coefficient appears to become constant. No great significance is placed on this result since it is thought to be simply a breakdown of the basic kinetic model. At these extremely low capture coefficients the concentration of the capturing species must be increased to the point where it competes with the 10% methane. At this point the molecule may enter into other reactions, such as positive ion formation. This uncertain interpretation is indicated by a question mark in Figure 4. Only two of the 14 aliphatic halides show this result, and in all cases ln $KT^{3/2}$ is around 18–20.

The unique result observed for the aliphatic halides is the linear relationship between the activation energy and the ΔE, which is equal to the bond dissociation energy minus the electron affinity of the dissociating halide. Equally amazing is the fact that chloro, bromo, and iodo compounds seem to fit the same linear relationship. In general one might expect the activation energy to be lower if the reaction were more exothermic. However, one would not necessarily expect a unit slope in such a relationship. The data are plotted in Figure 5.

This simple but unique result suggests that there must be some correspondingly unique or consistent relationship between the potential energy function for the negative ion of the aliphatic halides in relation to the neutral molecule. Since the reaction proceeds along the carbon-halogen internuclear separation, it was thought that a two dimensional approximation of the potential energy surface along this coordinate might be a satisfactory approximation. There are numerous empirical two-dimensional potential energy functions which have been proposed for diatomic molecules (*21*). One of the best known is the Morse potential, considered to be generally satisfactory for a three-parameter function. It is of the following form when referenced to the dissociated species as zero energy.

$$U(\mathrm{AB}) = -2D^{\circ}_{\mathrm{AB}}e^{-\beta(r-r_0)} + D^{\circ}_{\mathrm{AB}}e^{-2\beta(r-r_0)} \qquad (10)$$

Other three-parameter functions can be used, and the same relationship between E^* and ΔE can be derived—*e.g.*, Varshni's second potential function, which is a modified Morse potential (*21*) and Linnett's mixed exponential and inverse power of the internuclear distance (*12*).

In Radiation Chemistry; Hart, E.;
Advances in Chemistry; American Chemical Society: Washington, DC, 1968.

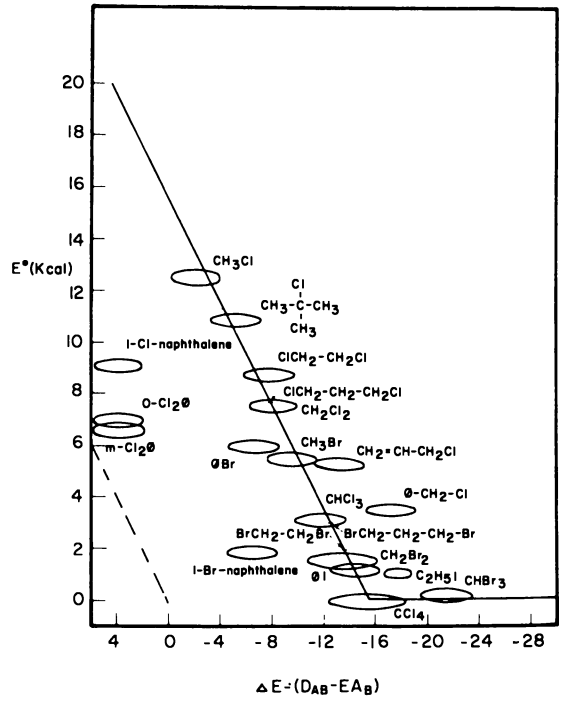

Figure 5. Correlation of E* *with* ΔE

The following two-dimensional potential energy function for the negative molecular ion is proposed.

$$U(AB^-) = -2kD^\circ_{AB}e^{-\beta(r-r_0)} + D^\circ_{AB}e^{-2\beta(r-r_0)} - EA_B \qquad (11)$$

where the dissociation leads to A + B^-. There are many arguments in favor of Equation 11 (*27*), but only a few will be mentioned. First, only a single new parameter, k, is introduced. This is all that should be necessary to equate to the single parameter, I, of the linear relationship between E^* and ΔE.

$$E^* = I + (D^\circ_{AB} - EA_B) \qquad (12)$$

Second, the repulsive term in the negative ion is set equal to that for the neutral molecule since the repulsion probably arises primarily from the core electrons and the positive nuclei. The added electrons in the negative ion should not greatly alter the repulsion. Linnett (*12*) has shown that the repulsive term for diatomic positive ions is the same as that for the neutral molecule. The deviation he observed for three diatomics was only 6%. Third, the constant, β, appearing in the exponential term in the negative ion is set equal to that for the neutral molecule. This is

Publication Date: January 1, 1968 | doi: 10.1021/ba-1968-0082.ch004

also supported by Linnett's calculations (*12*). He used a different potential function; however, his n in the attractive term (e^{-nr}) and the m in the respulsive term (r^{-m}) are approximately equal for the lowest energy state of the neutral molecule and positive ion.

The activation energy for TEA is interpreted as the intersection of the negative ion potential energy curve with that of the neutral molecule above the zero point level of the neutral molecule. Solving Equations 10 and 11 for the intersection, one obtains

$$E^* = \frac{[4D^\circ_{AB}k(1-k) - EA_B]}{4D^\circ_{AB}(1-k)^2} EA_B + (D_{AB} - EA_B) \qquad (13)$$

Equation 13 can be equated readily to Equation 12, from which k can be expressed in terms of I.

$$k = \tfrac{1}{2} - \frac{I - \frac{EA_B}{D^\circ_{AB}{}^{1/2}}[D^\circ_{AB} - (EA_B - I)]^{1/2}}{2(EA_B - I)} \qquad (14)$$

Thus, a negative ion potential energy curve has been found (substitution of Equation 14 into Equation 11), which is consistent with the linear relationship between E^* and ΔE.

The potential energy curves for the chlorinated methane series are shown in Figure 6. The intersection must occur at the same magnitude on such a graph to be consistent with the observed unit slope in Equation 12. The shallow minimum in the negative ion potential energy curves increases from CH_3Cl to CCl_4. This bond dissociation energy for the negative molecular ion can be shown to equal $k^2D^\circ_{AB}$. This shallow minimum is of no consequence to the electron attachment process since the process passes through (or near) the intersection of the potential energy curves which is well above the energy of the products A + B^-—*i.e.*, the AB^- would have a lifetime only on the order of the vibrational frequency, and the process can be considered simply dissociative. However, the shallow minimum would be of consequence in the recombination of R + Cl^- giving RCl^-. This would be important in radiation chemistry, for example. In a recent article (*11*) the existence of CH_3Br^- was necessary to explain the product from a γ-induced reaction of H atoms with CH_3Br. The potential energy curve for CH_3Br^- has a shallow minimum similar to the chloromethanes in Figure 6.

Dissociative TEA to Aromatic Chloro and Bromo Derivatives

The linear relationship shown in Figure 5 applies only to aliphatic halides. Except for iodobenzene, the aromatic halides fall below the aliphatics—*i.e.*, for the same ΔE the E^* is generally less for an aromatic

Publication Date: January 1, 1968 | doi: 10.1021/ba-1968-0082.ch004

halide in contrast to the aliphatic halides. This has been explained by postulating an intermediate negative molecular ion for the aromatic halides (*21*) and has been confirmed with a unique type of electron beam measurement, in which the SF_6^- peak is monitored in a mixture of SF_6 and another compound. New SF_6^- peaks occur at energies above the usually observed peak near zero energy. This is explained by the formation of a temporary negative ion state of the compound, followed by autoionization to give thermal electrons. The thermal electrons are then scavenged by the SF_6 to give SF_6^-. The energy of the new peaks will then correspond to the vertical electron affinity of the molecule. Stable negative ion intermediates are postulated for benzene, toluene, fluorobenzene, *o*-cholorotoluene, chlorobenzene, bromobenzene, *o*-bromotoluene and *o*-dichlorobenzene (*8*).

Publication Date: January 1, 1968 | doi: 10.1021/ba-1968-0082.ch004

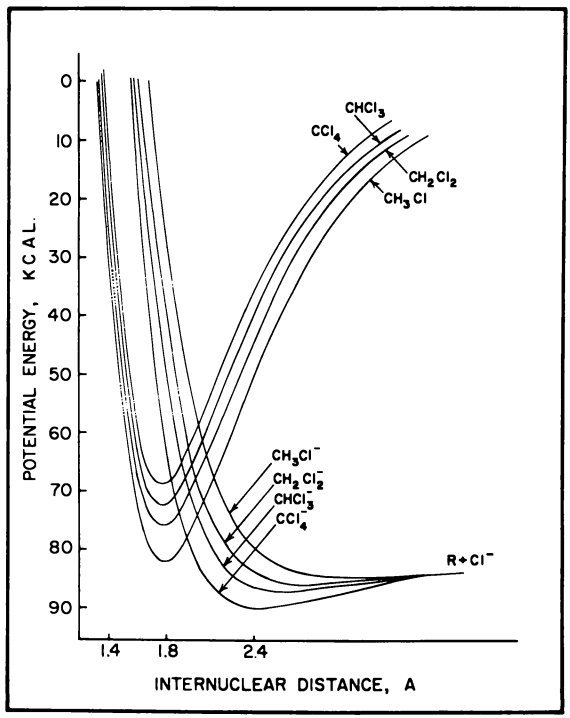

Figure 6. Potential energy curves for TEA for chloromethanes

Potential energy curves for the negative molecular ion have been described qualitatively to explain the correspondingly lower activation energy for the aromatic halide (*23*). This can be put on a more quantitative basis if one assumes the general form of Equation 11 to represent

the potential energy curve of the stable negative ion intermediate. The details of this work will be submitted shortly (29). The results of this study will be summarized at this time, and some representative results will be given. k can be evaluated from either the EA of the molecule, the vertical EA (obtainable from electron beam studies), or the activation energy. Both the EA and the activation energy may be determined from TEA measurements according to Mechanism III, providing the high and intermediate temperature regions are observed. The EA of the organic radical must also be known. k for the dissociative curve leading to the halide negative ion is calculated from Equation 14.

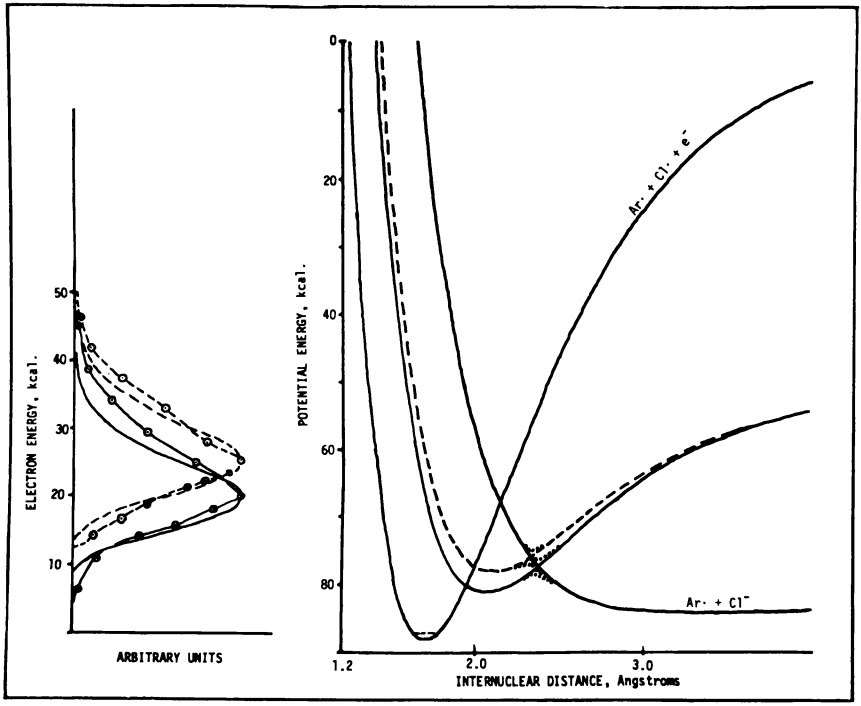

Figure 7. Potential energy curves for TEA to chlorobenzene (——) and o-chlorotoluene (– – –). Circles represent experimental curve of Cl^- current as a function of electron energy. $Ar = \phi$ or ϕCH_3. (. . . .) represents curves with "non-crossing rule" applied

Electron beam studies in addition to swarm methods have been reported on several aromatic halides (7). These results were used to calculate the potential energy curves for 10 of them. The results for chlorobenzene, chlorotoluene, bromobenzene, and bromotoluene are shown in Figures 7 and 8. The vertical EA was used to calculate k for

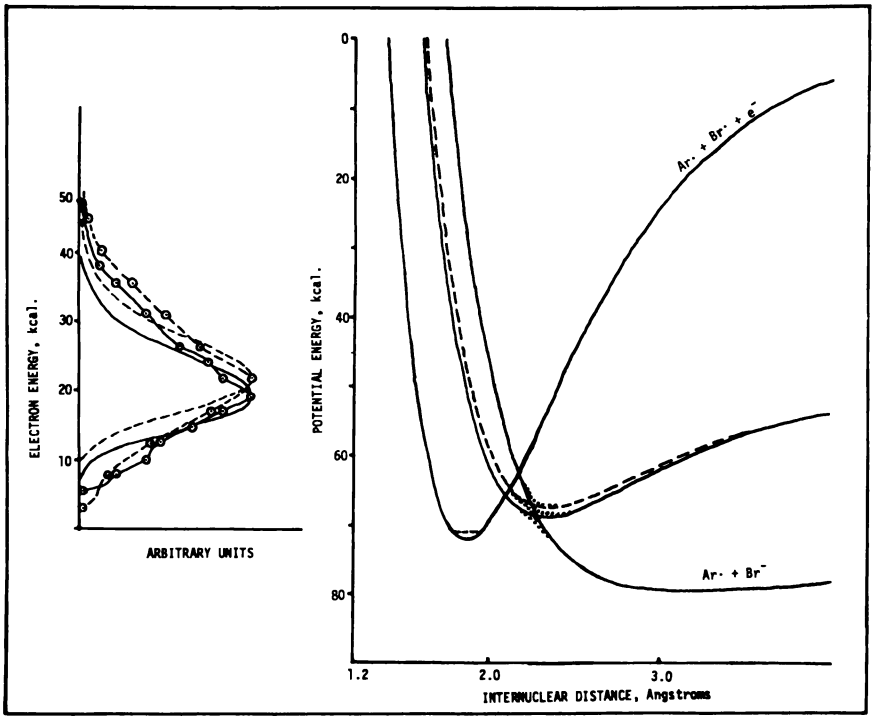

Figure 8. Potential energy curves for TEA to bromobenzene (——) and o-bromotoluene (– – –). Circles represent experimental curve of Br^- current as function of electron energy. Ar = ϕ or ϕCH_3. (. . . .) represents curves with "non-crossing rule" applied

the intermediate stable negative ion potential energy curve. The activation energy can be calculated from the intersection of the potential energy curves. Also the expected distribution of the relative electron capture cross section as a function of electron energy for the vertical process can be calculated from the probability distribution (harmonic oscillator approximation) for the zero point vibrational level. Both of these can be compared with the experimental results. In all cases the calculated activation energies agreed within 1 kcal./mole with the experimental values. The distributions of relative electron capture cross section also agree well (Figures 7 and 8). The distribution is drawn to the left of the potential energy diagram with the requisite electron energy (abscissa) coincident with the necessary change in the potential energy for the electron capture process to occur.

One surprising difference between the chloro and bromo derivatives shown is the position of the activation energy in terms of the intersections of the potential energy curves. In chlorobenzene and chlorotoluene the

Publication Date: January 1, 1968 | doi: 10.1021/ba-1968-0082.ch004

activation energy corresponds to the intersection of the two negative ion potential energy curves, in good agreement with the experimental values of 9.2 ± 0.6 and 10.3 ± 1.1 kcal./mole, respectively. On the other hand, the activation energy for bromobenzene and bromotoluene corresponds to the intersection of the intermediate negative ion potential energy curve with that of the neutral molecule, again in good agreement with the experimental values of 5.9 ± 0.3 and 6.3 ± 0.3, respectively. On this basis the molecular negative ion for bromobenzene and *o*-bromotoluene should be quite short lived with respect to dissociation.

If the two negative ion potential energy curves have the same symmetry, these curves will not cross as shown in Figures 4, 7, and 8. If this "non-crossing rule" does apply to the two curves, they would split (Figures 4, 7, and 8). This splitting would not affect the interpretation of the electron beam experiments, but it may affect the energy considerations and mechanisms shown in Figure 4.

Publication Date: January 1, 1968 | doi: 10.1021/ba-1968-0082.ch004

Dissociative TEA to Some Organic Acetates

The TEA to three acetate derivatives have been investigated: acetic anhydride, benzyl acetate, ethyl acetate (*30*). In all cases a negative slope in a ln $KT^{3/2}$ *vs.* $1/T$ graph was observed at higher temperatures which we associate with a dissociative step. For the three molecules included in the study, dissociative TEA leading to the acetate negative ion would be the most favored thermodynamically. The acetate radical is reported to have an electron affinity of 3.3 e.v. (*20*), which should far exceed the electron affinity of other possible radicals.

For all three molecules at lower temperatures the ln $KT^{3/2}$ *vs.* $1/T$ graph deviated from the linear region at higher temperatures. For benzyl and ethyl acetate the lower temperature data actually showed a positive slope, suggestive of Mechanism III or IV. Acetic anhydride showed a deviation from the high temperature linear region, but not a definite positive slope. Since only one radical is expected to have a significant electron affinity for these molecules, it is difficult to visualize how more than one negative molecular ion potential energy curve could be involved. For example, the electron affinity of the benzyl radical is 20.8 (*9*) kcal. and that of the ethyl radical 27.2 kcal. (*17*). From this and the agreement between E^* and $(D_{AB} - EA_A)$, the TEA process is assumed to proceed by Mechanism IV.

Since E^* is related to $(D_{AB} - EA_A) = \Delta E$ in Mechanism IV, the TEA activation energy can be used to evaluate D_{AB} or EA_A providing the other parameter is known. For the acetates we have estimates of both D_{AB} and EA_A, and the agreement between E^* and ΔE can be tested. With the experimental E^* and D_{AB} the electron affinity was

calculated and compared with the electron impact estimate (*20*). The weighted average from the three compounds was 3.36 ± 0.05 e.v. which agrees remarkably well with the electron impact estimate of 3.3 e.v.

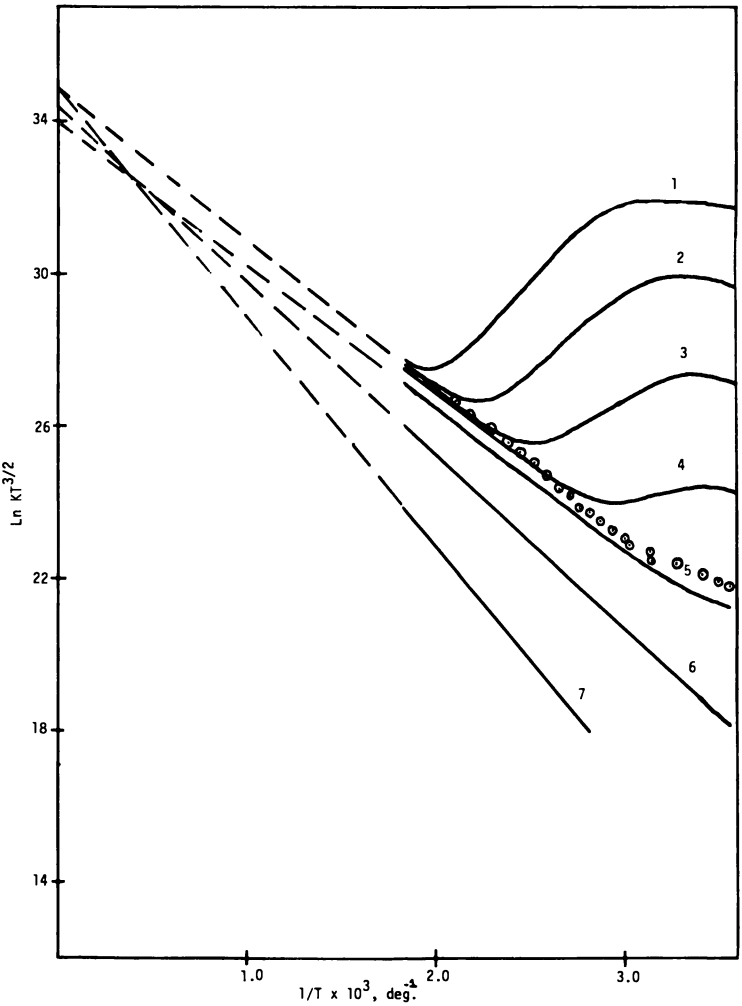

Figure 9. Temperature dependence for Mechanism IV. (E_2^* − EA) = *7.82 kcal.*; EA = *(1) 12; (2) 10; (3) 8; (4) 6; (5) 4; (6) 2; (7) 0. Circles represent experimental data for acetic anhydride*

The data for acetic anhydride in the graph of ln $KT^{3/2}$ *vs.* $1/T$ does not appear to agree with Mechanism IV. However, upon closer examination of the general Equation 3, the data are consistent with this

mechanism. In the previous discussion of the mechanisms three approximations were made which resulted in distinct linear regions in the graph. However, under certain conditions these regions unfortunately are not this distinct. A family of curves was generated using Equation 3 in conjunction with the proposed empirical negative ion potential energy curve, Equation 11. The electron affinity of the acetate radical was held constant, and k was varied to give molecular electron energies ranging from 0 to 12 kcal. The activation energies E_1^*, E_{-1}^*, E_2^* for each of these molecular electron affinities were then evaluated from the negative molecular ion potential energy curve relative to the neutral molecule potential energy curve. The family of curves is shown in Figure 9. Three distinct linear regions are observed when the molecular electron affinity is large and E_1^* is small. However, as k decreases and the electron affinity correspondingly decreases, E_1^* becomes larger, and the region of positive slope becomes smaller. Furthermore, the positive slope cannot be used to calculate the molecular electron affinity precisely—*e.g.*, $EA =$ 6 kcal. in Figure 9. The dashed lines of positive slope correspond to the electron affinity divided by R, the gas constant. Eventually at lower k values E_1^* exceeds E_2^*, and the process converts from Mechanism IV to Mechanism II. For the curves intermediate to these mechanisms, the intercept is lower since k_{-1} and k_2 both contribute to the denominator in Equation 2. Again, it should be emphasized that Equation 3 should be used rigorously to represent the electron capture coefficient as a function of temperature. The approximate expressions which can be derived from this general equation may be useful in evaluating the molecular parameters; however, caution should be exercised. The approximate expressions are useful for a qualitative assignment of the mechanism.

The actual experimental data for acetic anhydride are indicated by circles in Figure 9. The curve for $EA = 4.0$ kcal. would fit the experimental data if it were displaced along the ln $KT^{3/2}$ axis by 0.15 units. This could be accomplished by adjusting A_1 in Equation 3.

Publication Date: January 1, 1968 | doi: 10.1021/ba-1968-0082.ch004

Summary

The following molecular parameters can be derived from TEA measurements:

(1) Molecular electron affinity (EA) from Mechanisms I, III, or IV. Range: 0.8 e.v. $> EA >$ 0.1 e.v. using ^{3}H foil; maximum temp. 225°C. 1.1 e.v. $> EA >$ 0.1 e.v. using ^{63}Ni; maximum temp. 400°C.

(2) Rate constant for thermal electron attachment (k_1 or k_{12}) from Mechanism I at low temperatures and high electron affinity; Mechanism II for dissociative rate constant.

(3) Electron affinity of radicals (EA_A) from Mechanism IV if bond dissociation energy is known.

(4) Bond dissociation energy (D_{AB}) from Mechanism IV if electron affinity of the radical is known; also for aliphatic Cl, Br, I compounds from empirical relationship between E^* and ΔE.

(5) Activation energy for electron attachment (E_1^*) from Mechanism I, III, or IV.

(6) Activation energy for electron detachment (E_{-1}^*) from Mechanism I, III, or IV if E_1^* and EA can be determined.

(7) Activation energy for dissociation (E_2^*) from Mechanism III or IV if EA can be determined.

Acknowledgments

The authors express their appreciation to the Robert A. Welch Foundation for the financial support of this work.

Literature Cited

(1) Bain, I. C., Cottrell, T. L., *Proc. Roy. Soc.* **1964,** 218.
(2) Becker, R. S., Chen, E., *J. Chem. Phys.* **45,** 2403 (1966).
(3) Becker, R. S., Wentworth, W. E., *J. Am. Chem. Soc.* **85,** 2210 (1963).
(4) Becker, R. S., Wentworth, W. E., Wang, L., in preparation.
(5) Chandhuri, J., Jagur-Grodzinski, J., Szwarc, M., *J. Phys. Chem.* **71,** 3063 (1967).
(6) Chen, E., George, R., Wentworth, W. E., *J. Chem. Phys.*, in press.
(7) Christophorou, L. G., Compton, R. N., Hurst, G. S., Reinhardt, P. W., *J. Chem. Phys.* **45,** 536 (1966).
(8) Compton, R. N., Christophorou, L. G., Huebner, R. H., *Phys. Letters* **23,** 656 (1966).
(9) Compton, R. N., Christophorou, L. G., Hurst, G. S., Reinhardt, P. W., *J. Chem. Phys.* **45,** 4634 (1966).
(10) Gaines, A. F., Page, F. M., *Trans. Faraday Soc.* **59,** 1266 (1963).
(11) Johnson, G. R. A., Simic, M., *J. Phys. Chem.* **71,** 2775 (1967).
(12) Linnett, J. W., *Trans. Faraday Soc.* **36,** 1123 (1940).
(13) Loeb, L., "Basic Processes of Gaseous Electronics," University of California Press, Los Angeles, 1955.
(14) Lovelock, J. E., *Nature* **189,** 729 (1961).
(15) Lovelock, J. E., Gregory, N. L., "Gas Chromatography," N. Brenner, ed., p. 219, Academic Press, New York, 1962.
(16) Mahan, B. H., Young, C. E., *J. Chem. Phys.* **44,** 2192 (1966).
(17) Page, F. M., *Symp. Combust., 8th, 1962,* p. 160.
(18) Strauss, H. L., Katz, T. J., Fraenkel, G. F., *J. Am. Chem. Soc.* **85,** 2360 (1963).
(19) Streitweizer, A., "Molecular Orbital Theory for Organic Chemists," Wiley, New York, 1961.
(20) Tsuda, S., Hamill, W. H., *Advan. Mass Spectrometry* **III,** 247-257 (1966).
(21) Varshni, P. V., *Rev. Mod. Phys.* **29,** 664 (1957).
(22) Wentworth, W. E., Chen, E., *J. Gas Chromatog.* **5,** 170 (1967).
(23) Wentworth, W. E., Becker, R. S., Tung, R., *J. Phys. Chem.* **71,** 1652 (1967).
(24) Wentworth, W. E., Becker, R. S., *J. Am. Chem. Soc.* **84,** 4263 (1961).
(25) Wentworth, W. E., Chen, E., *J. Phys. Chem.* **71,** 1929 (1967).

(26) Wentworth, W. E., Ristau, W., *J. Phys. Chem.*, submitted.
(27) Wentworth, W. E., Keith, H., George, R., in preparation.
(28) Wentworth, W. E., Chen, E., Lovelock, J. E., *J. Phys. Chem.* **70**, 445 (1966).
(29) Wentworth, W. E., Steelhammer, J., in preparation.
(30) Wentworth, W. E., Chen, E., Steelhammer, J., *J. Phys. Chem.* **72**, 2671 (1968).

RECEIVED January 29, 1968.

The Radiolysis of Methane in a Wide-Range Radiolysis Source

P. S. RUDOLPH

Chemistry Division, Oak Ridge National Laboratory,
Oak Ridge, Tenn. 37830

Publication Date: January 1, 1968 | doi: 10.1021/ba-1968-0082.ch005

The radiolysis of methane was studied in a new type of three-stage wide-range radiolysis source attached to a research mass spectrometer. This source gave direct evidence of the various ionic and non-ionic reactive primary species, and by applying an electric field, it gave evidence of their relative roles in producing stable products. Under experimental conditions that minimized subsequent reactions of reactive stable products (i.e., *flow, low pressure, and localized ionization) it was found that the abundance of the unsaturated hydrocarbons produced in the radiolysis of methane was about three times the abundance of the saturated hydrocarbons. Threshold energy curves were determined which give valuable information as to the precursors of the various products. G values for the various products were calculated, and reaction mechanisms are postulated.*

The radiolysis of methane has been studied in many laboratories since methane was first irradiated at Louvain (*41*) over 40 years ago. From the beginning, reports on methane radiolysis have been fraught with disagreement. Mund and Koch (*41*) observed a slight pressure decrease in their α-radiolysis experiment, whereas Lind and Bardwell (*27*) in a similar experiment in the same year reported no pressure change.

The current discrepancies in the literature are more profound. They relate to the final stable products, especially the unsaturated hydrocarbon products, the radiolytic yields of final products, and the relative importance of ions and neutral species in the mechanisms leading to final products.

In Radiation Chemistry; Hart, E.;
Advances in Chemistry; American Chemical Society: Washington, DC, 1968.

There is universal agreement that ionizing radiations produce many highly reactive primary species, as typified by the following general notations for CH_4.

$CH_4 \overset{\sim\sim}{\longrightarrow} CH_4^+ + e$	Ionization	(I)
$CH_4 \overset{\sim\sim}{\longrightarrow} CH_n^{\pm} + (4-n)H_p \pm e$	Dissociative ionization ($n \leqq 3$)	(IIa)
$\overset{\sim\sim}{\longrightarrow} \cdot CH_n + (4-n)H_p^{\pm} \pm e$		(IIb)
$\overset{\sim\sim}{\longrightarrow} CH_n^{\pm} + (4-n)H_p^{\mp}$		(IIc)
$CH_4 \overset{\sim\sim}{\longrightarrow} \cdot CH_n + (4-n)H_p$	Dissociation ($n \leqq 3$)	(III)
$CH_4 \overset{\sim\sim}{\longrightarrow} CH_4^*$	Excitation	(IV)

The hydrogen products, H_p, in Reactions II and III may be H_2 and/or H; however, in Reactions IIb and IIc H_2 cannot be negative, and only one of the hydrogen species is charged.

The subsequent reactions of the primary reactive species are not as universally agreed upon. Several workers using various sources of radiant energy [—*e.g.*, vacuum-ultraviolet photons (up to 11.8 e.v.) (*28*), low energy electrons (15 to 100 e.v.) (*30*), and high energy electrons (2 Mev.) and ^{60}Co γ-rays (*31*)], conclude that the radiolysis of methane proceeds by a free-radical and/or excited-molecule (*28*) mechanism. Conversely, others (*25, 32*) using high energy electrons and x-rays (*32*) present evidence that the reaction proceeds *via* an ion-molecule mechanism. Still others, using γ-rays from fission products (*49*), ^{60}Co γ-rays and ultraviolet photons (*5, 6, 7, 16*) and photoionization (*48*) conclude that both ions and free-radicals are involved in the radiolytic mechanism of methane.

The production of unsaturated hydrocarbons as final products in methane radiolysis is also controversial. The results of numerous workers (*10, 11, 18, 20, 21, 25, 30, 31, 40, 42, 48, 49*), who have reported unsaturated hydrocarbon products from the radiolysis of pure methane, show no general agreement as to the products or their yields.

The majority of researchers who have irradiated "methane" added higher hydrocarbons, inorganic radical scavengers, and/or rare gases to the system to elucidate the mechanism. Thus, they were studying a mixture of gases and not methane alone. Even those who did not use additives but used static systems at high pressure (in the atmospheric range) soon after initiating the radiolysis were studying mixtures, owing to the buildup of higher hydrocarbons. These procedures led to numerous contradictions in the literature.

Some workers (*5, 6, 7, 16, 31, 44, 49*) using additives find unsaturated products. On this basis Johnsen (*44*) concludes that C_2H_4 is produced in the radiolysis of pure CH_4 by an ion-molecule reaction but that it is

Publication Date: January 1, 1968 | doi: 10.1021/ba-1968-0082.ch005

consumed by H· atom attack and is thus not a final product. He also states (*23, 44*) that C_2H_2 is not a product from the radiolysis of methane, contrary to Hummel's conclusion (*20*). In a later work Hummel (*21*) again reported C_2H_2 but in lesser quantities than expected from his early work (*20*).

We designed a novel three-compartment source (wide-range radiolysis source) for our research mass spectrometer, which was first used to study the radiolysis of methane. The present technique, employing flow, low pressure, localized ionization, and electric fields appears to be a straightforward approach to the problem, and we hoped that this technique would resolve some of the above discrepancies. Our objectives were to: (a) determine the percent abundance of the various reactive primary species—ionic and neutral; (b) ascertain the percent abundance of stable products under conditions that would minimize subsequent reactions of reactive stable products; (c) calculate *G* values for these products; (d) measure the relative contribution of ion-molecule reactions to the formation of stable products; (e) obtain the threshold energies and yield curves for such products to assign their precursors; and (f) postulate, from the above information and pressure studies, a mechanism for the production of the radiolytic products from methane.

Publication Date: January 1, 1968 | doi: 10.1021/ba-1968-0082.ch005

Experimental

The wide-range radiolysis source shown schematically in Figure 1 consisted of three separate stainless steel compartments (A, B, C) in series, each with its own electron beam (designated hereafter as EB—*e.g.*, EB-B means electrons beam in Compartment B). The energy and intensity of each EB emitted from a thoria-iridium filament could be varied independently by a versatile emission regulator (*22*) to suit the particular phase of the problem under study. The EB's were magnetically collimated to ensure localized ionization, and their intensities were usually about 10 μA.

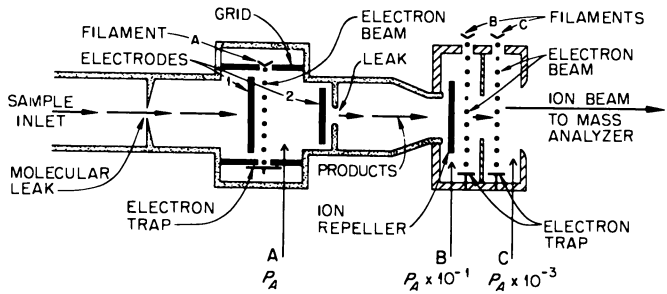

Figure 1. Schematic of the three-compartment mass spectrometer (wide-range radiolysis) source for studying gaseous systems

Compartment A contained two electrodes for applying an electric field during irradiation. Both the polarity on, and field strength between the electrodes were variable. EB-A was only 1 mm. from Electrode 1, so that when this electrode was negatively biased, at least 96% of the positive ions formed in EB-A at a methane pressure of 0.1 torr were collected (*40*).

A more detailed sketch of the electric-field radiation cell, Compartment A, is shown in Figure 2. The dual electron-beam section, Compartments B and C, has been described elsewhere (*34, 39*).

The three-compartment source was attached to the analyzer tube of a 6-inch radius 60° sector magnetic deflection mass spectrometer. Differential pumping was used between the source and analyzer regions. The ion detector was a 14-stage electron multiplier coupled to both a vibrating-reed electrometer and a pulse counter (*38*). The electrometer was connected to a strip-chart recorder and the counter to a printer. This arrangement allowed any range of e/m to be scanned or a given peak to be monitored.

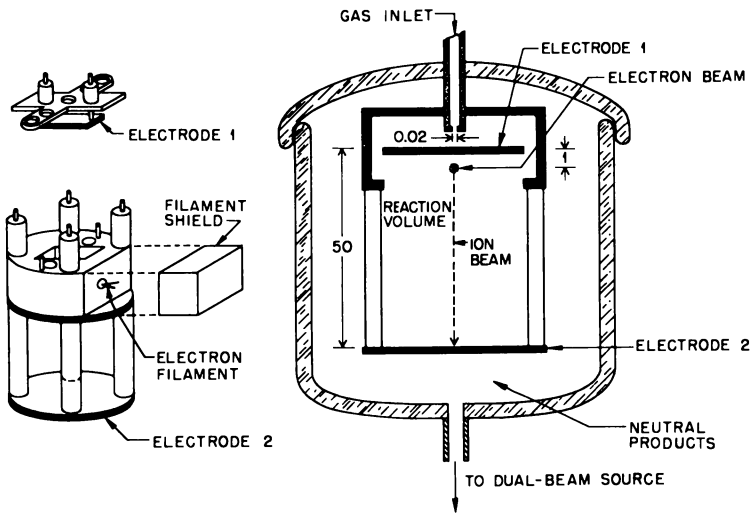

Figure 2. Detailed sketch of the electric-field compartment or radiation cell (Compartment A) of the wide-range radiolysis source. All dimensions are in millimeters

The pressure in each compartment was determined as previously described (*33*) using Ar as a standard. In addition, the pressures in Compartments B and C were determined by the ionization gage and the ion-molecule reaction methods (*33*) using the CH_5^+ ion (*25, 46*) and the $C_2H_5^+$ ion (*25, 43*) from CH_4. Results from all three methods agreed within 10%.

Research grade methane, without further purification, was used throughout these studies. A mass spectrometric analysis of the methane

showed that the abundance of the principal impurity, ethane, was less than 0.015%.

In all experiments, steady-state conditions were established (usually less than 5 minutes were required) before data were taken. Since the *modus operandi* of the wide-range radiolysis source was varied as different phases of the problem were investigated, the specific experimental techniques will be discussed individually in conjunction with the corresponding results.

Results and Discussion

Percent Abundance of Primary Species. The abundance of primary ionic species resulting from ionization (Reaction I) and dissociative ionization (Reaction II) of CH_4 were determined by standard mass spectrometric techniques (*38, 39*). Only EB-C was used at an electron energy of 100 e.v. and a pressure in Compartment C of 6×10^{-6} torr. The results are given in Table I. The mass spectra for positive and negative ions were calculated from the data in Table I and are compared with the results of previous workers (*3, 4, 36*) in Table II. The agreement for positive ions is satisfactory except for very low values of e/m; H^+ is considerably lower than reported (*3, 4*), and H_2^+ is higher than the API (*4*) value. We can not explain these discrepancies (*39*). The otherwise good agreement leads us to believe that the equipment was working satisfactorily. It is interesting to note, however, that our values for positive ions of $e/m \leqq 14$, except H^+, are intermediate values. The agreement between these and previous (*36*) negative-ion mass spectra are satisfactory considering the different sources used. However, owing to their low abundance (Table I), negative ions are not considered further.

Table I. Percent Abundance of Initial Products Produced by Methane Irradiation at 6×10^{-6} torr with 100 e.v. Electrons

Positive Ions		*Neutral Species*		*Negative Ions*	
Ion	*Primary Products, %*	*Neutral*	*Primary Products, %*	*Ion*	*Primary Products, % ($\times 10^{-5}$)*
H^+	0.47	·H	28.2	H^-	82
H_2^+	0.24	H_2	9.41		
C^+	0.59	·C	0.001	C^-	8.4
CH^+	1.65	·CH	1.18	CH^-	6.6
CH_2^+	3.29	$\cdot CH_2$	2.35	CH_2^-	2.5
CH_3^+	17.7	$\cdot CH_3$	14.1	CH_3^-	0.09
CH_4^+	21.2				
	45		55		0.001

Publication Date: January 1, 1968 | doi: 10.1021/ba-1968-0082.ch005

Table II. Mass Spectra for Positive and Negative Ionization of Methane by 100 e.v. Electrons

Ion	*Positive Ion Relative Abundance*			*Ion*	*Negative Ion Relative Abundance*	
	This Study	*Ref.* 3	*Ref.* 4[a]		*This Study*[b]	*Ref.* 36
CH_4^+	100	100	100			
CH_3^+	83.3	86.7	85.9	CH_3^-	1.1	0.8
CH_2^+	15.5	14.0	16.1	CH_2^-	29.8	25.4
CH^+	7.80	6.67	8.09	CH^-	78.8	85.6
C^+	2.78	2.67	2.80	C^-	100	100
H_2^+	1.13	1.33	0.21			
H^+	2.21	7.33	3.36			

[a] 70 e.v. electrons.
[b] For comparison, H^- was omitted in this tabulation since it was not reported in Ref. 36.

To determine the abundance of neutral species, methane at 6×10^{-6} torr was irradiated in Compartment B by EB-B with 100 e.v. electrons. Positive ions thus formed were collected by applying a negative potential on the ion repeller, while the neutral species diffused into C. EB-C, adjusted to an electron energy below the ionization potential of CH_4 (*i.e.*, $<$ 13.0 e.v.), ionized neutral species except for H· and H_2. For these species the electron energy of EB-C was raised to about 16 e.v. Runs were then made with the energy of EB-B approximately zero, all other conditions being identical. The difference in intensity of a given ion was taken to be the intensity of the neutral species produced by the 100 e.v. electrons in B by Reactions II and III. The cross sections for the production of primary neutral species were reported previously (39).

The results of these studies are given in Table I. The percent of all primary products is about equal for positive ions and neutral species (45% and 55%, respectively). Thus, it appears that any mechanism for producing stable products from the radiolysis of methane must include positive ions and neutral species.

Percent Abundance of Stable Products. The production and identification of stable products were accomplished by using Compartments A and C. Methane was radiolyzed with the intensity of EB-A sufficient to give about 1% decomposition with 100 e.v. electrons at a pressure of 10^{-2} torr in Compartment A. With Electrode 1 positive, the positive ions and neutral species produced in EB-A reacted as they diffused through the methane. We assume that only stable neutral products reached Compartment C where they were ionized by EB-C and analyzed by standard mass spectrometric techniques. The products and their percent abundances are given in Table III.

Publication Date: January 1, 1968 | doi: 10.1021/ba-1968-0082.ch005

Unsaturated hydrocarbons (HC) account for about 25% of total products compared with 8% for saturated HC (Table III). This result agrees with Cahill *et al.* (*11*), who used a single, very short and very high intensity pulse of high energy electrons in a static system. All previous workers found that saturated HC, especially C_2H_6, predominate. However, results obtained in flow systems or where an attempt was made to remove products by condensation (*20, 30, 32, 48*) showed appreciably larger yields of unsaturated HC than results in static systems, although, still *in toto* showing the saturated HC yield greater than the unsaturated HC yield. This situation would imply that unsaturated HC are products of the radiolysis of CH_4 but subsequently react with CH_4 or other products to yield saturated HC.

Our apparatus, which was designed to minimize the subsequent reactions of reactive unsaturated HC by using flow, relatively low pressure (10^{-2} torr), and localized ionization gave results in agreement with the trends discussed above. On the basis of such evidence, we believe that any mechanism for the radiolysis of CH_4 must include reaction steps leading to unsaturated HC products.

Radiolytic Yield of Final Products. The G values (molecules per 100 e.v. absorbed) were determined using both EB-A and EB-C at 100 e.v. The $-G(CH_4)$ was obtained from the percent decomposition of

Table III. Products Formed by the Irradiation of Methane (~ 1% Decomposition) at 1×10^{-2} torr with 100 e.v. Electrons

Product	*Percent Abundance*	*Fraction of Product Produced by Positive Ion-Molecule Reactions*[a]	G *Molecules per 100 e.v.*	*Slope of log-log Plot of Intensity* vs. *Pressure*[b]
H_2	66.3	0.23	6.9	1.0
C_2H_2	6.53	0.27	0.7	1.5
C_2H_4	15.5	0.41	1.6	1.4[c]
C_2H_6	5.50	0.45	0.6	1.6
C_3H_6	2.19	0.44	0.2	1.3
C_3H_8	2.09	0.67	0.2	1.3
C_4H_8	1.34	0.54	0.1	1.7
C_4H_{10}	0.59	0.55	0.06	1.1
CH_4 (All reactions)			−7.8	
CH_4 (Less positive ion-molecule reactions)			−5.5	

[a] Remainder of product is produced by other reactions which include electron-molecule, radical-molecule, radical-radical, etc.
[b] Pressure varied from (0.7 to 4.1) $\times 10^{-2}$ torr and 150 e.v. electrons used. Plots of all products were linear (*cf.* Ref. *c*).
[c] Least-squares value, assuming curvature of C_2H_4 plot is caused by scatter.

CH_4, the number of 100 e.v. electrons absorbed, and the residence time (35 sec.) of CH_4 in Compartment A. The energy absorption was calculated from the decrease in trap current of EB-A upon introducing the sample. On the basis of this decrease, we assumed that all secondary and scattered electrons were absorbed in the gas. This assumption leads to a maximum value for the energy absorbed. The G values of the products were calculated relative to the $-G(CH_4)$ and a material balance. These results are given in Table III. In Table IV, these yields are compared with those previously reported. The present values for $-G(CH_4)$ and $G(H_2)$ agree well with the average value of the other investigators. As mentioned, the present values are higher for the unsaturated HC and lower for the saturated HC.

Contribution of Ion-Molecule Reactions to Final Products. The variation of the abundance of products with polarity on Electrode 1 (other conditions were the same as for stable products) was studied. A positive potential on Electrode 1 (field positive) enhanced positive ion-molecule reactions, whereas, a negative potential on Electrode 1 (field negative) removed the positive ions from the reaction field. Thus, the difference in intensity of products under these conditions was a measure of the relative role of opsitive ion-molecule reactions.

To ascertain the optimum electric field strengths, the variation in abundance of the products was studied as a function of potential. Typical results for C_2H_6 as a function of the potential on Electrode 1 are shown in Figure 3. The fall in the curve above +10 volts may be caused by the decrease of products formed by neutralization of ions in the gas phase

Table IV. G Values for Products

H_2	C_2H_2	C_2H_4	C_2H_6	C_3H_6	C_3H_8
6.4		0.13	2.1	0	0.26
5.7		0.05	2.1		0.14
	0.038	0.46	1.2	0.089	0.24
5.6	⩾0.3	⩾0.3	2.0	0	0.35
14.6	0.37	1.05	1.26	0.20	0.17
5.7			1.2		0.41
4.7		0	1.9		0.34
5.51			2.18		
4.91			2.15		0.84
6.7		0.1	1.2		<0.1
	0.5	0.7	0.7		
5.4		0.034	2.0		0.27
					This
6.9	0.7	1.6	0.6	0.2	0.2

[a] Converted from M/N using $W = 29.4$ e.v./ion pair (Ref. 8).

Publication Date: January 1, 1968 | doi: 10.1021/ba-1968-0082.ch005

and/or a decrease in the number of excited states produced by secondary electrons.

Throughout the remainder of this phase of the study Electrode 1 was kept at −30 or +10 volts with respect to Electrode 2. Photographs of two typical scans (for H_2 and C_4H_{10}) are shown in Figure 4. "Radiation On" signifies that the potential on EB-A was changed from zero to 100 volts, "Field Negative" and "Field Positive" indicates the potential on Electrode 1 was −30 and +10 volts, respectively, with respect to Electrode 2.

The fraction of products produced by positive ion-molecule reactions was determined from the differences in intensities, and the results are given in Table III. These are minimum values since they are based on the assumption that all primary positive ions are collected at −30 volts. No attempt was made to determine the amount of product resulting from primary negative ions. The low percent abundance (Table I) suggests that the contribution from negative ions is small.

Despite the apparent straightforwardness of the present techniques for determining the contribution of positive ion-molecule reactions, there is some doubt as to whether the fractions shown in Table III are as accurate as reported since they are minimum values. Charge neutralization of ions at the electrodes may give free radicals which could enhance certain products. If this is true, this contribution is not nearly as pronounced as the effect of ion-molecule reactions which decrease $-G(CH_4)$ from 7.8 with the field positive to 5.5 with the field negative.

Produced by Methane Radiolysis

C_4H_8	C_4H_{10}	$-CH_4$	*Radiation*	*Ref.*
	0.19		γ	*49*
	0.04	7.6	e(2 Mev.)	*25*
0.12	0.06		e(2.8 Mev.)	*18*
	0.23		e(4 Mev.)	*20*
Trace	Trace		Photoionization[a]	*48*
	0.23	7.5	α(Rn)[a]	*27*
	0	6.8	α(Rn)[a]	*19*
			γ(^{60}Co)	*5*
		7.90	Fission fragments	*17*
	<0.1	8.0	e(2 Mev.), γ(^{60}Co)	*31*
			e(1.6 Mev.), pulsed	*11*
	0.034	8.2	Calculated[a]	*32*
study				
0.1	0.06	7.8	e(100 e.v.)	

Publication Date: January 1, 1968 | doi: 10.1021/ba-1968-0082.ch005

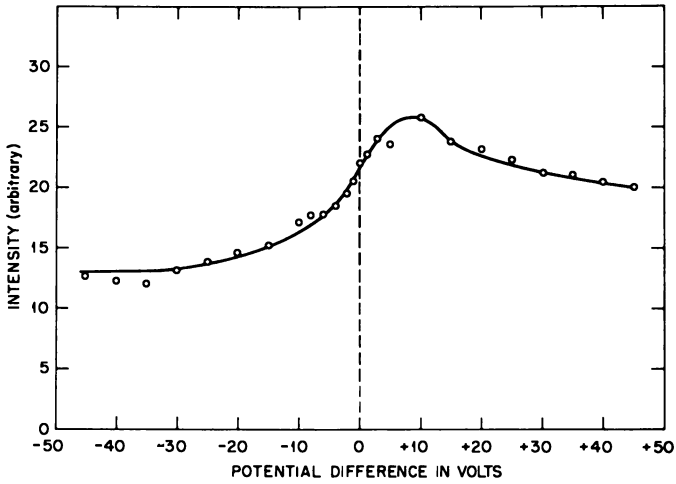

Figure 3. Abundance of ethane, produced by the radiolysis of CH_4 at 10^{-2} torr, as a function of polarity on and potential between Electrodes 1 and 2 in the radiation cell

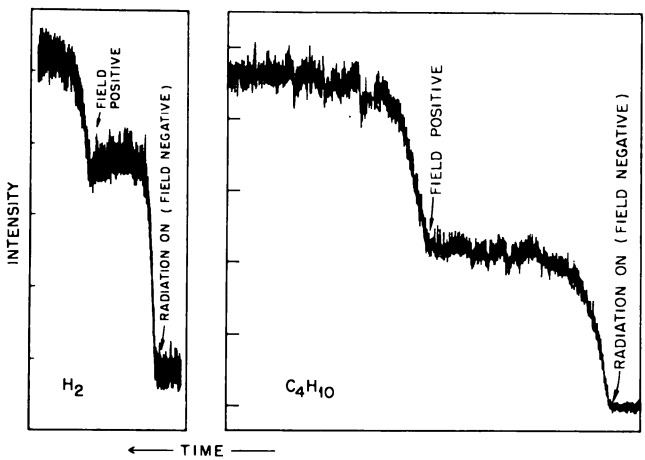

Figure 4. Effect of electric field in the radiation cell on the production of H_2 and C_4H_{10} from methane radiolysis at 10^{-2} torr. "Radiation On" indicates a potential of 100 e.v. applied to the electron beam in the radiation cell. "Field Negative" and "Field Positive" indicate that Electrode 1 was at a potential of −30 or + 10 volts with respect to Electrode 2

Publication Date: January 1, 1968 | doi: 10.1021/ba-1968-0082.ch005

Threshold Energies for Stable Products. "Threshold energy" is defined as the minimum energy of EB-A needed to produce a given product. Threshold energies were determined by varying the energy of EB-A from 0–20 e.v. and monitoring the intensity of the products by standard mass spectrometric techniques using Compartment C as the ion source. Owing to the low abundance of products in the 0–10 e.v. range, the values obtained were uncertain and thus are not reported. Above 17 e.v. the abundance of products was so large that it was impossible to identify structure in the yield curves; hence, these data are not reported either.

A summary of the relationship of the threshold energies, or breaks in the yield curves, of products to the energies of possible precursors, over the range 10–17 e.v., is given in Table V. Two of the eight experimental yield curves (those for C_2H_4 and C_3H_6) are shown in Figure 5. Since data above 17 e.v. could not be interpreted, the contribution of such probable precursors as CH^+ and C^+ to final products is unknown. Furthermore, the dissociation of CH_4 into $\cdot CH_3$ and $\cdot CH_2$ plus $\cdot H$ can occur below 10 e.v. (*24*), but these radicals formed at or near the dissociation energy of CH_4 cannot be of major importance owing to the low abundance of products below 10 e.v.; of course, such radicals formed at higher energies may contribute significantly to products.

The data in Table V show that C_2H_6 has CH_4^+, CH_3^+, and $\cdot H$ as possible precursors, whereas, C_3H_8 is probably formed from CH_4^{+*}, CH_3^+, $\cdot H$, and CH_2^+. This agrees with the conclusions of Lampe (*25*) that C_2H_6 and C_3H_8 are formed simultaneously and not consecutively. Our

Table V. Correlation of Threshold Energies at Which Products are Observed with the Energies Necessary to Produce Probable Primary Precursors From Methane Irradiation

	Energy (volts) at which Probable Primary Precursors are Observed				
Product	CH_4^*	CH_4^+	CH_4^{+*}	CH_3^+	CH_2^+
H_2		12.9		14.2	15.4
C_2H_2		12.9			15.4
C_2H_4		12.9		14.2	15.4
C_2H_6		12.9		14.4	
C_3H_6	11.8				15.4
C_3H_8			13.7	14.4	15.8
C_4H_8		12.9			
C_4H_{10}		12.9		14.2	15.4
Appearance Potential from CH_4	11.8[a]	13.0[b]	13.6[b]	14.3[c]	15.6[c]
		12.7[d]		14.3[d]	15.2[d]

[a] Excitation Potential (Refs. 9, *26*).
[b] Determined by electron impact (Ref. *35*).
[c] Ref. *13*.
[d] Determined by photoionization (Ref. *12*).

Publication Date: January 1, 1968 | doi: 10.1021/ba-1968-0082.ch005

data for C_2H_4 and C_4H_{10}, since they have common precursors, are inconclusive with regard to Lampe's (25) further conclusion that these HC are also formed simultaneously.

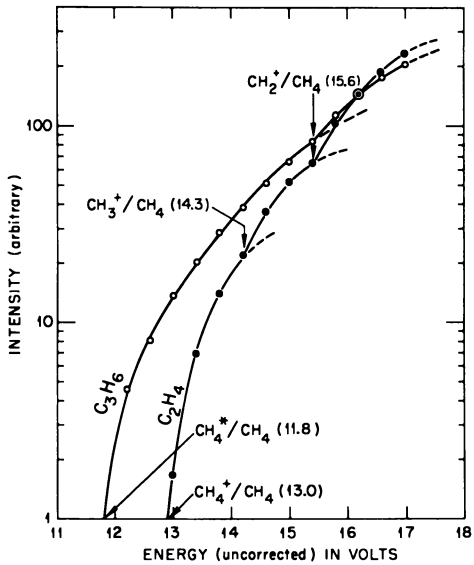

Figure 5. Threshold energy and yield curves for C_2H_4 and C_3H_6. Values in parentheses are literature values for the appearance of the respective reactive species from CH_4

Table V shows CH_4^{+*} appearing at 13.7 e.v. as a precursor for C_3H_8. Since CH_4 dissociates into $\cdot CH + 3H\cdot$ at 13.6 e.v. (*24*), these radicals may also be precursors for C_3H_8.

Variation of Intensity of Products with Pressure. The abundance of the neutral CH_3 and C_2H_5 radicals, produced by the radiolysis of methane, was studied using Compartments B and C as discussed earlier, except that the methane pressure was varied. The results are shown in Figure 6. The slopes of the logarithmic plots are almost equal to 1 and 2 for $\cdot CH_3$ and $\cdot C_2H_5$, respectively, suggesting first and second order CH_4 concentration dependence. This corroborates the conclusion (Table I) that $\cdot CH_3$ is a primary product. The slope of 2 for $\cdot C_2H_5$ is not as conclusive over the entire pressure range since the least-squares line (assuming second-order dependence) lies considerably below the standard deviation of the experimental points at the two lowest pressures. The low count rates at these low pressures make these points less reliable. Never-

Publication Date: January 1, 1968 | doi: 10.1021/ba-1968-0082.ch005

theless, one must consider the possibility that the experimental data are reliable and that there is a change in mechanism near 10^{-2} torr. If this is true, the order of reaction is less than 2 below this pressure. Above 10^{-2} torr the slope of 2 would indicate a second-order radical-molecule reaction.

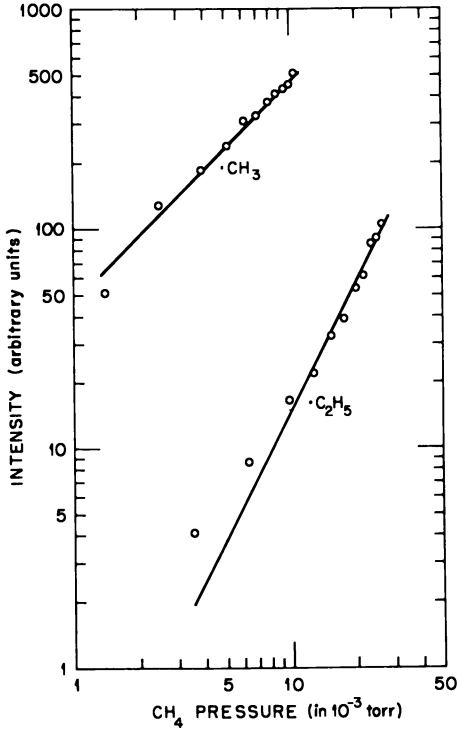

Figure 6. Abundance of the CH_3 and C_2H_5 radicals produced by the radiolysis of methane with 100 e.v. electrons as a function of methane pressure

Preliminary experiments, extending the pressure studies to final products, were performed. Methane was radiolyzed in Compartment A by 150 e.v. electrons in a positive field. The sample pressure was varied from (0.7 to 4.1) $\times$ 10^{-2} torr, and the intensities of the resulting final stable products were monitored as usual.

The slopes of the logarithmic plots of these data (intensity *vs.* pressure) were determined (Table III) and vary from 1.0 for H_2 to 1.7 for C_4H_8. Thus, the slopes give no simple order of reaction for final products as they do for free radicals and ions. This would indicate that the

Publication Date: January 1, 1968 | doi: 10.1021/ba-1968-0082.ch005

mechanism for the formation of stable products is very complicated and not simply a series of consecutive reactions.

Reaction Mechanisms for Stable Products. HYDROGEN FORMATION. Molecular hydrogen may result from the dissociative ionization (Reaction II) or dissociation (Reaction III) of CH_4 as a primary product. At low pressures (10^{-6} torr range) where ion-molecule and radical-molecule reactions are repressed all H_2 appears to be primary. The data in Table I shows that the summation of H_2 and H_2^+ equals 9.65% of the primary products. The summation of other probable fragments—CH_2^+, CH^+, $2(C^+)$, $\cdot CH_2$, $\cdot CH$, and $2(\cdot C)$—also totals 9.65%.

At higher pressures secondary and higher order reactions must also be considered as a source of H_2. Some well established (*1, 25, 43, 45, 46, 47, 48*) ion-molecule reactions which yield H_2 and which are in agreement with probable precursors (Table V) are:

$$CH_3^+ + CH_4 \rightarrow C_2H_5^+ + H_2 \quad (1)$$

$$CH_2^+ + CH_4 \rightarrow C_2H_3^+ + H_2 + H\cdot \quad (2)$$

$$CH^+ + CH_4 \rightarrow C_2H_2^+ + H_2 + H\cdot \quad (3)$$

$$CH_4^+ + CH_4 \rightarrow CH_5^+ + \cdot CH_3 \quad (4a)$$

$$CH_5^+ + e \rightarrow \cdot CH_5^* \quad (4b)$$

$$\cdot CH_5^* \rightarrow \cdot CH_3 + H_2 \quad (4c)$$

Non-ionic reactions can also give rise to H_2 (*16, 28, 30, 48*). Some possible reactions are:

$$H\cdot + H\cdot + M \rightarrow H_2 + M \quad (5)$$

$$CH_4 \overset{\wedge\wedge}{\longrightarrow} \cdot CH_2^* + H_2 \quad (6)$$

$$CH_4 \overset{\wedge\wedge}{\longrightarrow} \cdot CH + H_2 + H\cdot \quad (7)$$

Reaction 5 is quite probable since 28% of all primary species is $H\cdot$. Subsequent reactions of $\cdot CH_2^*$ also lead to H_2 (*30*). Since 66% (Table III) of the observed stable products is H_2, it must be formed by many different primary and subsequent reactions, both ionic and non-ionic.

ACETYLENE FORMATION. About 27% of the C_2H_2 is produced by ion-molecule reactions (Table III), and the ionic species involved are CH_4^+ and CH_2^+ (Table V). The predominant ion-molecule reaction of the parent ion is Reaction 4a. Recent studies (*1, 14*) show that the secondary ions—CH_5^+, $C_2H_5^+$ and $C_2H_4^+$—are unreactive toward CH_4. However, CH_5^+ does dissociate in the sequence Reaction 4b + 4c. Thus, a possible sequence involving CH_4^+ is Reaction 4a followed (*48*) by

$$\cdot CH_3 + \cdot CH_3 \rightarrow C_2H_6^* \quad (8a)$$

$$C_2H_6^* \rightarrow C_2H_2 + 2\,H_2 \quad (8b)$$

Other possible paths involving parent ion are

$$CH_4^+ + CH_4 \rightarrow C_2H_6^+ + H_2 \quad (9a)$$

$$C_2H_6^+ + e \rightarrow C_2H_6^* \quad (9b)$$

followed by Reaction 8b, and

$$CH_4^+ + CH_4 \rightarrow C_2H_4^+ + 2\,H_2 \quad (10a)$$

$$C_2H_4^+ + e \rightarrow C_2H_4^* \quad (10b)$$

$$C_2H_4^* \rightarrow C_2H_2 + H_2 \quad (10c)$$

A possible mechanism involving CH_2^+ is

$$CH_2^+ + CH_4 \rightarrow C_2H_6^+ \quad (11)$$

followed by Reactions 9b and 8b.

There is general agreement (*28, 29, 30, 48*) that the non-ionic mechanism for C_2H_2 involves the following steps, with minor variations. Reaction 6 followed by

$$CH_2^* + CH_4 \rightarrow C_2H_6^* \quad (12)$$

which dissociates as in Reaction 8b to yield C_2H_2.

ETHYLENE FORMATION. The breaks in the threshold energy curve for C_2H_4 (*see* Figure 5 and Table V) indicate that C_2H_4 is produced at the same energies as CH_4^+, CH_3^+, and CH_2^+, and ion-molecule reactions account for about 41% of the C_2H_4 (Table III). Ausloos (*5*), on the other hand, concludes that C_2H_4 is not formed by an ionic mechanism. The parent ion, CH_4^+, can contribute to C_2H_4 by Reactions 4a directly and the sequence: 4a + 4b + 4c to produce $\cdot CH_3$ which reacts by Reaction 8a followed by

$$C_2H_6^* \rightarrow C_2H_4 + H_2 \quad (13)$$

The CH_4^+ ion can also contribute *via* Reactions 9a, 9b, and 13, as well as 10a and 10b followed by

$$C_2H_4^* + M \rightarrow C_2H_4 + M \quad (14)$$

Previous workers (*16, 20, 48*) have reported ion-molecule reactions involving CH_3^+. The sequence of reactions (*20, 48*) is Reaction 1 followed by

$$C_2H_5^+ + e \rightarrow \cdot C_2H_5^* \quad (15a)$$

$$\cdot C_2H_5^* \rightarrow C_2H_4 + H\cdot \quad (15b)$$

and/or, Reaction 1 followed (*16*) by

$$C_2H_5^+ \rightarrow C_2H_4 + H^+ \quad (15c)$$

Publication Date: January 1, 1968 | doi: 10.1021/ba-1968-0082.ch005

Of these workers, only one (*16*) has reported CH_2^+ as a precursor for C_2H_4. A reaction mechanism is

$$CH_2^+ + CH_4 \rightarrow C_2H_4^+ + H_2 \quad (16)$$

followed by Reactions 10b and 14.

Several workers (*20, 28, 30*) have postulated the free radical "insertion" Reaction 12 followed by 13. Other possible free radical reactions are Reaction 8a followed by 13, and

$$\cdot CH_2 + \cdot CH_2 + M \rightarrow C_2H_4 + M \quad (17)$$

as well as

$$\cdot CH + CH_4 \rightarrow \cdot C_2H_5^* \quad (18)$$

followed by Reaction 15b.

ETHANE FORMATION. Our results (Table III) indicate that 45% of the C_2H_6 is produced by ion-molecule reactions. Threshold energy measurements (Table V) show that the ions involved are CH_4^+ and CH_3^+. Parent ion can contribute to C_2H_6 by Reactions 4a and 8a followed by

$$C_2H_6^* + M \rightarrow C_2H_6 + M \quad (19)$$

and, by the sequence: 9a, 9b, and 19.

Although the major ion-molecule reaction of CH_3^+ with CH_4 is Reaction 1, the intermediate complex $C_2H_7^+$ has been reported (*1, 14*). Thus, we postulate that C_2H_6 can be formed, as previously reported (*20*), by

$$CH_3^+ + CH_4 \rightarrow C_2H_7^{+*} \quad (20)$$

$$C_2H_7^{+*} + M \rightarrow C_2H_7^+ + M \quad (21a)$$

$$C_2H_7^+ + e \rightarrow C_2H_6 + H \quad (21b)$$

The free radicals, $\cdot CH_3$ and $\cdot CH_2$, formed by various non-ionic processes can react by Reactions 8a and 19 as well as 12 and 19 to yield the remaining 55% of the C_2H_6.

PROPYLENE FORMATION. It has been reported (*20*) that no C_3H_6 was observed as a radiolysis product of pure CH_4. We, however, observe about 2.2% of this product, 44% of which is produced by ion-molecule reactions (Table III). The only precursor ion we observe is CH_2^+; however, excited methane molecule is also a precursor (Figure 5 and Table V).

The most probable ion-molecule mechanism appears to be Reaction 2 followed by

$$C_2H_3^+ + CH_4 \rightarrow C_3H_6 + H^+ \quad (22)$$

The most likely paths for the CH_4^* precursor, representing the same overall reaction, are

$$CH_4^* + CH_4 \rightarrow C_2H_6^* + H_2 \quad (23a)$$

Publication Date: January 1, 1968 | doi: 10.1021/ba-1968-0082.ch005

$$C_2H_6^* + CH_4 \rightarrow C_3H_6 + 2\,H_2 \quad (23b)$$

and/or

$$CH_4^* + CH_4 \rightarrow C_2H_4^* + 2\,H_2 \quad (23c)$$

$$C_2H_4^* + CH_4 \rightarrow C_3H_6 + H_2 \quad (23d)$$

In addition to the excited molecule, free radicals can contribute to C_3H_6 (*20, 30*) by

$$\cdot CH_2 + C_2H_4 \rightarrow C_3H_6 \quad (24)$$

and

$$\cdot H + C_2H_2 \rightarrow \cdot C_2H_3 \quad (25a)$$

$$\cdot C_2H_3 + \cdot CH_3 \rightarrow C_3H_6 \quad (25b)$$

These reactions can account for the low yields of C_2H_2 and C_2H_4 in static systems; C_3H_6 would also be depleted under these conditions if it is a precursor for C_4H_{10} (*20*).

PROPANE FORMATION. Previous workers who report mechanisms for the formation of C_3H_8 (*20, 28, 30, 44*) invoke neutral-neutral reactions. From our results (Table III) these reactions account for only one-third of the C_3H_8 while two-thirds are caused by reactions involving CH_4^{+*}, CH_3^+, and CH_2^+ (Table V). Recent work (*2, 15, 37, 45, 47*) in simple HC systems has demonstrated that the contribution of excited states of reactant ions to ion-molecule reactions cannot be neglected. Similar considerations are true for radical-radical and radical-molecule reactions (*16*). We postulate the following ion-molecule reaction involving CH_4^{+*}.

$$CH_4^{+*} + CH_4 \rightarrow C_2H_5^+ + H_2 + H\cdot \quad (26a)$$

$$C_2H_5^+ + \cdot CH_3 \rightarrow C_3H_8^{+*} \quad (26b)$$

$$C_3H_8^{+*} + M \rightarrow C_3H_8 + M^+ \quad (26c)$$

If the above series of reactions produces C_3H_8 then CH_3^+ can react by Reactions 26b and 26c to give the same product.

The CH_2^+ ion can react by Reaction 2, followed by the following sequence.

$$C_2H_3^+ + CH_4 \rightarrow C_3H_5^+ + H_2 \quad (27a)$$

$$C_3H_5^+ + CH_4 \rightarrow C_4H_9^+ \quad (27b)$$

$$C_4H_9^+ + e \rightarrow C_3H_8 + \cdot CH \quad (27c)$$

Evidence for Reaction 27a and 27b has been presented previously (*1, 14*).

Numerous non-ionic reactions leading to C_3H_8 have been postulated by others (*20, 28, 30, 44*).

BUTENE FORMATION. Parent ion appears to be the only ionic precursor for C_4H_8. Several mechanisms for producing C_2H_4 and $C_2H_4^*$ from CH_4^+ were given above. These may be combined as:

$$C_2H_4^* + C_2H_4 \rightarrow C_4H_8^* \quad (28a)$$

Publication Date: January 1, 1968 | doi: 10.1021/ba-1968-0082.ch005

$$C_4H_8^* + M \rightarrow C_4H_8 + M \quad (28b)$$

BUTANE FORMATION. Threshold energy data (Table V) show that C_4H_{10} has the same three ionic precursors as C_2H_4 and two of the precursors of C_2H_6. Hummel (*20*) has suggested that C_4H_{10} is formed mainly from C_2H_4. This information lends credence to the following mechanisms. Reactions leading to the following reactants have been discussed above.

$$C_2H_4^* + C_2H_6 \rightarrow C_4H_{10}^* \quad (29a)$$

$$C_4H_{10}^* + M \rightarrow C_4H_{10} + M \quad (29b)$$

and/or

$$C_2H_6^* + C_2H_4 \rightarrow C_4H_{10}^* \quad (30)$$

followed by Reaction 29b.

Conclusions

The wide-range radiolysis source gives direct evidence of the relative role of ion-molecule reactions, initial stable products, the radiolytic yield, and the ionic precursors of these products by using flow, low pressure, localized ionization, and electric fields.

Although this study of the radiolysis of methane was exploratory, it illustrated the usefulness of the wide-range radiolysis source, and our results contribute to the understanding of the radiolytic process which has been so controversial. Further development of the apparatus and techniques are contemplated, and the methane system will be studied further and in more detail.

Acknowledgment

The author acknowledges his indebtedness to his former co-worker, C. E. Melton, with whom much of the source design and data collection and interpretation were done. The author also thanks R. Baldock, for his encouragement of and interest and help in this work.

This paper is dedicated to the memory of S. C. Lind (1879-1965) whose active interest in radiochemistry (the name he preferred for what is now termed radiation chemistry) spanned over half a century and to my precepter, Harry Essex, who was the first to use an electric-field technique in studies of reactions initiated by ionizing radiations.

Literature Cited

(1) Abramson, F. P., Futrell, J. H., *J. Chem. Phys.* **45**, 1925 (1966).
(2) Abramson, F. P., Futrell, J. H., *J. Chem. Phys.* **46**, 3264 (1967).
(3) Adamczyk, B., Boerboom, A. J. H., Schram, B. L., Kistemaker, J., *J. Chem. Phys.* **44**, 4640 (1966).

(4) American Petroleum Institute Research Project 44, "Catalog of Mass Spectral Data" (Carnegie Institute of Technology, Pittsburgh, Pa.) Serial No. 1.
(5) Ausloos, P., Gorden, R., Jr., Lias, S. G., *J. Chem. Phys.* **40,** 1854 (1964).
(6) Ausloos, P. J., Lias, S. G., *J. Chem. Phys.* **38,** 2207 (1963).
(7) Ausloos, P., Lias, S. G., Gorden, R., Jr., *J. Chem. Phys.* **39,** 3341 (1963).
(8) Bortner, T. E., Hurst, G. S., *Phys. Rev.* **93,** 1236 (1954).
(9) Bowman, C. R., Miller, W. D., *J. Chem. Phys.* **42,** 681 (1965).
(10) Cahill, R. W., Glass, R. A., *Radiation Res.* **31,** 652 (1967).
(11) Cahill, R. W., Seeler, A. K., Glass, R. A., *J. Phys. Chem.* **71,** 4564 (1967).
(12) Dibeler, V. H., Krauss, M., Reese, R. M., Harllee, F. N., *J. Chem. Phys.* **42,** 3791 (1965).
(13) Field, F. H., Franklin, J. L., "Electron Impact Phenomena," pp. 248, 249, Academic Press, New York, 1957.
(14) Field, F. H., Munson, M. S. B., *J. Am. Chem. Soc.* **87,** 3289 (1965).
(15) Giardini-Guidoni, A., Friedman, L., *J. Chem. Phys.* **45,** 937 (1966).
(16) Gorden, R., Jr., Ausloos, P., *J. Chem. Phys.* **46,** 4823 (1967).
(17) Hall, G. R., *Chem. Ind.* **46,** 1890 (1964).
(18) Hauser, W. P., *J. Phys. Chem.* **68,** 1576 (1964).
(19) Honig, R. E., Sheppard, C. W., *J. Phys. Chem.* **50,** 119 (1946).
(20) Hummel, R. W., *Discussions Faraday Soc.* **36,** 75 (1963).
(21) Hummel, R. W., *J. Phys. Chem.* **70,** 2685 (1966).
(22) Hutchison, D. A., Wolff, J. R., *Rev. Sci. Instr.* **25,** 1083 (1954).
(23) Johnsen, R. H., *J. Phys. Chem.* **69,** 3218 (1965).
(24) Laidler, K. J., Casey, E. J., *J. Chem. Phys.* **17,** 1087 (1949).
(25) Lampe, F. W., *J. Am. Chem. Soc.* **79,** 1055 (1957).
(26) Lassettre, E. N., Francis, S. A., *J. Chem. Phys.* **40,** 1208 (1964).
(27) Lind, S. C., Bardwell, D. C., *Science* **62,** 422 (1925).
(28) Magee, E. M., *J. Chem. Phys.* **39,** 855 (1963).
(29) Mahan, B. H., Mandal, R., *J. Chem. Phys.* **37,** 207 (1962).
(30) Manton, J. E., Tickner, A. W., *Can. J. Chem.* **38,** 858 (1960).
(31) Maurin, J., *J. Chim. Phys.* **59,** 15 (1962).
(32) Meisels, G. G., Hamill, W. H., Williams, R. R., Jr., *J. Phys. Chem.* **61,** 1456 (1957).
(33) Melton, C. E., "Mass Spectra of Organic Ions," F. W. McLafferty, ed., pp. 78-80, Academic Press, New York, 1963.
(34) Melton, C. E., *J. Sci. Instr.* **43,** 927 (1966).
(35) Melton, C. E., Hamill, W. H., *J. Chem. Phys.* **41,** 546 (1964).
(36) Melton, C. E., Rudolph, P. S., *J. Chem. Phys.* **31,** 1485 (1959).
(37) *Ibid.*, **32,** 1128 (1960).
(38) Melton, C. E., Rudolph, P. S., *Naturwiss.* **54,** 297 (1967).
(39) Melton, C. E., Rudolph, P. S., *J. Chem. Phys.* **47,** 1771 (1967).
(40) Melton, C. E., Rudolph, P. S., unpublished data.
(41) Mund, W., Koch, W., *Bull. Soc. Chim. Belges* **34,** 121 (1925).
(42) Rudolph, P. S., Melton, C. E., *J. Phys. Chem.* **71,** 4572 (1967).
(43) Schissler, D. O., Stevenson, D. P., *J. Chem. Phys.* **24,** 926 (1956).
(44) Sieck, L. W., Johnsen, R. H., *J. Phys. Chem.* **67,** 2281 (1963).
(45) Szabo, I., *U.S.A.F. Doc.* **AD 647941** (1966).
(46) Tal'roze, V. L., Lyubimova, A. K., *Dokl. Akad. Nauk. SSSR,* **86,** 909 (1952).
(47) von Koch, H., *Arkiv Fysik* **28,** 529 (1965).
(48) Walker, D. C., Back, R. A., *J. Chem. Phys.* **38,** 1526 (1963).
(49) Yang, K., Manno, P. J., *J. Am. Chem. Soc.* **81,** 3507 (1959).

RECEIVED December 26, 1967. Research supported by the U. S. Atomic Energy Commission under contract with Union Carbide Corp.

6

The X-Radiolysis of Perfluorocyclobutane and Mixtures of Perfluorocyclobutane and Methane in the Gas Phase

EDGAR HECKEL[1] and ROBERT J. HANRAHAN

University of Florida, Gainesville, Fla. 32601

Publication Date: January 1, 1968 | doi: 10.1021/ba-1968-0082.ch006

The x-radiolysis of perfluorocyclobutane in the gas phase consists of a combination of fragmentation and telomerization processes. More than 10 products were noted with chain lengths from C_5 to C_{14}, as well as C_2F_4, C_3F_6, C_3F_8, and a white polymer. Even-carbon exceeded odd-carbon products by two-fold. The radiolysis was not affected by added N_2O, but all heavier fluorocarbon products were eliminated by added O_2. With added CH_4 no products having more than five carbon atoms were found. It is postulated that the radiolysis of perfluorocyclobutane proceeds along three major paths: direct decomposition, giving two molecules of tetrafluoroethylene; a process giving perfluorocyclobutyl radicals plus fluorine atoms; and a process giving C_1 and C_3 species. The radicals then initiate a short chain polymerization of tetrafluoroethylene.

Perfluorocyclobutane differs from its hydrocarbon analog in many physical and chemical properties. It is more easily formed and more stable thermodynamically than cyclobutane (*17*). The thermal decomposition of perfluorocyclobutane proceeds by a direct unimolecular process to give two molecules of tetrafluoroethylene, although other processes contribute to some extent (*2*, *12*). Although Doepker and Ausloos have recently described the radiation chemistry of cyclobutane (*3*), the perfluorocarbon has received only slight attention. Fallgatter and Hanrahan (*5*) qualitatively studied the γ-radiolysis of liquid F-cyclobutane [F- is

[1] Present address: Chemistry Department, East Carolina University, Greenville, N. C. 27834.

In Radiation Chemistry; Hart, E.;
Advances in Chemistry; American Chemical Society: Washington, DC, 1968.

used as an abbreviation for perfluoro] and found F-ethylene, F-cyclopropane, and C_5, C_6, and C_7 perfluorocarbons, as well as fluoroform, which presumably arose from an impurity. Rajbenbach (*19*) published a brief account of the effect of fluorocarbons, including F-cyclobutane, on the hydrogen yield from hydrocarbons. The mass spectral cracking pattern of F-cyclobutane has also been published (*14*).

This paper describes a study of the gas-phase x-radiolysis of pure perfluorocyclobutane, including the effects of added N_2O and O_2 on the reaction. Mixtures of methane and F-cyclobutane were also examined over a broad composition range. The latter experiments were intended to shed light on the radiolysis mechanism of pure perfluorocyclobutane as well as to provide information on the radiolytic behavior of gas-phase fluorocarbon–hydrocarbon mixtures. Related studies on liquid phase mixtures of cyclohexane and F-cyclohexane are currently in progress in this laboratory.

Publication Date: January 1, 1968 | doi: 10.1021/ba-1968-0082.ch006

Experimental

Sample Preparation and Irradiation. The F-cyclobutane used in these studies was obtained from Air Products and Chemicals, Inc. and contained only small amounts of impurities; it was repurified using preparative gas chromatography. The column was 2.5 meters long, 3/8 inches in diameter, packed with silica gel of 60-200 mesh (W. H. Curtin), and was connected between the storage tank of F-cyclobutane and the vacuum line. After the column was evacuated to high vacuum over several hours, the F-cyclobutane was released cautiously from the tank. At the arrival of the first traces of gas, the pressure in the vacuum line increased. The first portion of the repurified gas was discarded. The main fraction of F-cyclobutane did not contain any impurities which could be detected by gas chromatography.

The methane used was Phillips Research Grade (99.68%) and contained ethane, ethylene, propane, nitrogen, and carbon dioxide. Repurification was simliar to the method described above. However, molecular sieve 13 × was used as the stationary phase. The purified methane contained only nitrogen and much less of the original ethane.

Nickel-plated copper vessels were used in all radiolysis experiments. The vessels were made from copper tubing, 1.5 inches in diameter. The bottom was a 1-mm. thick copper sheet which was silver soldered to the approximately 10-cm. high vessel. A Hoke brass valve with Teflon seat and phosphorus bronze bellows was attached to the top of the vessel by a 1/4-inch Swagelock fitting. Each vessel and all parts of the valves were nickel plated.

The radiation source was a General Electric laboratory model Maxitron 300 x-ray unit. The machine was operated at 300 kv. and 20 ma. in all experiments. The radiation vessel hung vertically, inverted so that its bottom was as close as possible to the window of the x-ray tube. Thus, the vessel partially shielded its valve from the x-ray beam. The bottom

of the vessel served also as a filter for the weak component in the x-radiation. All experiments were carried out at 30 ± 3°C.

To save time and cost of operating the x-ray machine, we used a special technique to prepare larger amounts of reaction products for microcombustion analysis. A 1-liter round-bottomed flask was provided with two stainless steel electrodes opposite each other and with a Fischer-Porter Teflon plug needle valve. The vessel was filled with 10 to 50 torr of gas, and an electrical discharge between the electrodes produced good yields of the same kind of products obtained by radiolysis. The discharge was generated by a small Tesla coil of the type used to check the pressure in a vacuum line. To duplicate the chromatograph patterns characteristic of the x-ray work, it was necessary to use the lowest setting of the Tesla coil which would maintain the discharge.

Sample Analysis. Qualitative and quantitative analyses of the radiolysis products of perfluorocyclobutane and mixtures of perfluorocyclobutane and methane were made using a combination of gas-liquid chromatography, mass spectrometry, and microcombustion analysis. These techniques, described in detail elsewhere (*8*), are based on the use of a specially constructed dual column, dual detector gas chromatograph with a vacuum input manifold. All products except hydrogen fluoride were analyzed in the "duplex" gas chromatograph. Hydrogen was separated from methane and traces of air on a 4.4-meter column of molecular sieve 5 A.; detection was by thermal conductivity. All other products were analyzed using a temperature-programmed unit (2.1°C. per minute, 15 minutes after injection) which had a flame ionization detector; the column used was silica gel (60–200 mesh).

A special approach was necessary to calibrate the flame ionization detector for the various radiolysis products (*8*) since standard samples of most higher fluorocarbons cannot be obtained. By means of a stream-splitting valve on the duplex gas chromatograph about half of the column effluent was diverted into a modified Miller-Winefordner (*15*) chromatographic-type microcombustion apparatus. Here all organic compounds are converted to CO_2 (and H_2O, if hydrogen is present). The combustion products are analyzed with a thermistor detector. This unit was calibrated on an absolute basis in terms of gram-atoms of carbon per unit chart area (1 sq. cm. of chart = 1.75×10^{-7} mole of carbon). After the molecular formula of each product was found by mass spectrometric analysis, the number of moles of compound in each chromatograph peak could be determined, and the sensitivity of the flame ionization detector could be calculated. A relatively large product yield, produced by several hours of x-irradiation (or by about 20 minutes of Tesla coil discharge) was necessary to obtain sufficient signal on the microcombustion unit. Radiolysis times of 15 to 150 minutes were used in other experiments.

Hydrogen fluoride was determined by a conventional analytical procedure. Using basically the qualitative test for fluoride ion as described by Feigel (*7*), 5 ml. of a solution containing zirconium chloride, alizarin sulfonate, and hydrochloric acid were introduced into the irradiation vessel through its valve. The valve was shut, and after shaking vigorously, an aliquot was placed in a 1-cm. borosilicate glass cuvette to measure the absorbance of the solution at 5200 A. This method is sensitive but not very reliable because the absorbance is time dependent.

Publication Date: January 1, 1968 | doi: 10.1021/ba-1968-0082.ch006

Successful detection of HF as a radiolysis product apparently depends on using metal radiolysis vessels since no HF could be found in an experiment using a glass vessel.

Dosimetry. The dose rate from the x-ray source was measured by using the hydrogen yield ($G_{H_2} = 1.3$) of the ethylene dosimeter (9). Using a 104.5-cc. vessel filled with 50 torr ethylene, we found a dose rate of 4.80×10^{20} e.v./gram-hour.

Energy absorption in F-cyclobutane and in methane–F-cyclobutane mixtures was calculated relative to the ethylene result. Since the vessels were nickel-plated copper, the radiation effects were mainly caused by secondary electrons ejected from the vessel walls. Dose rates in the gases were calculated using the Bragg-Gray principle and Bethe's formula for the electronic stopping power S_e. (Since the more complicated equation for electrons and the much simpler one for heavy charged particles give equivalent results for electrons in the range 50–200 Kev., the latter was actually used in the calculations.) Therefore, the relative stopping power per electron in two different materials, designated ζ_e, is given by

$$\zeta_e = S_{e1}/S_{e2} \tag{1}$$

where

$$S_e = \ln(2M_o c^2\beta^2/\bar{I}) - \ln(1 - \beta^2) - \beta^2 \tag{2}$$

In this expression β is the velocity of the electrons divided by the velocity of light, and $\bar{I}$ is the average excitation potential of the material. Equation 2 differs from the complete Bethe equation in that a combination of constant factors multiplying the logarithmic term, which would cancel in Equation 1, has been omitted. The $\bar{I}$ of a compound can be calculated from values of its atomic constituents by the approximate formula:

$$\ln(\bar{I}) = \Sigma_i[N_i Z_i \ln(\bar{I}_i)]/N_i Z_i \tag{3}$$

where N is the number of atoms of a given kind per formula unit, and the summation is over the various kinds of elements present (i) (9). Values of S_e are given for methane, ethylene, and F-cyclobutane in Table I. Values of $\bar{I}$ were found to be 40.8 e.v. for methane, 51.6 e.v. for ethylene, and 102.4 e.v. for F-cyclobutane.

For two different gases the ratio of the energy absorbed E (e.v./gram) is given by

$$\frac{E_1}{E_2} = \frac{N_1 S_{e1}}{N_2 S_{e2}}$$

where N_1 and N_2 are the number of electrons/gram for each gas, and S_{e1} and S_{e2} are the respective values of stopping power per electron. (To the extent that the Bragg-Gray principle applies, the energy absorption on a per gram basis is independent of the pressure.)

Publication Date: January 1, 1968 | doi: 10.1021/ba-1968-0082.ch006

Table I shows that electron stopping powers vary moderately over the energy range appropriate for secondary electrons from a 300 kv. x-ray set (we use the range 50–200 kv.). However, the ratio of stopping powers for any pair of gases varies by only about 2% for the energy range indicated. Accordingly, calculations were made using an average value of the ratio of S_r for each gas to S_e for the ethylene dosimeter. On this basis the measured absorbed dose rate of 4.80×10^{20} e.v./gram-hour in ethylene corresponded to an absorbed dose rate of 3.73×10^{20} e.v./gram-hour in F-cyclobutane and 5.40×10^{20} e.v./gram-hour in methane. For mixtures of methane and F-cyclobutane it was assumed that each gas

Table I. Stopping Power per Electron as a Function of Secondary Electron Energy

Energy, Kev.	β	*Methane*	*Ethylene*	*F-cyclobutane*
50	0.4128	8.34	8.12	7.42
100	0.5483	8.96	8.70	8.05
200	0.6954	9.55	9.32	8.62

absorbed energy independently in proportion to the mass of that gas present. The total pressure in these experiments was held constant at 150 torr.

Results

Product Identification. Several experiments were performed at a relatively high total x-ray dose (*ca.* 1×10^{21} e.v./gram, or about two hours of irradiation) to identify radiolysis products from pure F-cyclobutane. During the chromatographic analysis of each sample, five or six peaks were collected in U-traps and analyzed with a Bendix mass spectrometer. Owing to the small amount of material available, the samples were allowed to leak directly into the ion source *via* a needle valve; a conventional reservoir-gold leak system was not used. The assignments made for the molecular formulas of the various chromatograph peaks are listed in Table I.

Consideration of the peaks eluting before the parent F-cyclobutane, identification of C_2F_4 and C_3F_8 was straightforward since each gave a mass spectrum in good agreement with those tabulated by Majer (*14*). Perfluoromethane was not detected. Since its response in the flame detector was 1/1000 that of other fluorocarbons, it may be present despite our failure to detect it.

The molecular formula of C_3F_6 was definitely established from its mass spectrum, but there is some uncertainty about its structure. The

Publication Date: January 1, 1968 | doi: 10.1021/ba-1968-0082.ch006

mass spectrum was not identical to that of either F-propylene (*14*) or F-cyclopropane (*5*). The difficulty was probably caused by contamination of the sample with the parent F-cyclobutane, which eluted immediately afterwards. The compound is tentatively identified as F-cyclopropane, based on its elution position.

The olefin F-cyclobutene, which would be derived from the parent compound by loss of F_2, definitely is not produced. A standard sample of F-cyclobutene eluted between the peaks identified as C_5F_{12} and C_6F_{14}, where no radiolysis product appeared. Since the parent F-cyclobutane tailed badly on the silica gel column used, the presence of other possible C_4 fluorocarbons such as *n*-C_4F_8 or *n*-C_4F_{10} could have been masked.

Identification of the higher products through C_{10} is contingent upon the peculiarities of fluorocarbon mass spectra, which have been reviewed by Majer (*14*). One problem is the fact that saturated fluorocarbons generally do not give the parent ion. An ion with one fluorine atom less than the parent usually does occur but is usually only 1 or 2% of the base peak. As a result, molecular weight verification usually rests on interpreting a few small peaks at considerably higher masses than the main peaks of the spectrum. A doubt often exists as to whether these peaks might arise from impurities in the sample or from machine background. On the other hand, perfluoro-olefins usually do show a substantial parent ion peak, as well as other peaks near the parent mass. Since these features do not occur in any of our higher radiolysis products, we conclude that none of them are olefins. Instead, the several C_nF_{2n} products are believed to contain a C_4 ring, and the compound $C_{10}F_{18}$ must contain two rings. All products above C_5F_{12} showed a strong m/e 100 peak in their spectrum, consistent with the presence of a cyclobutane ring (*14*).

For products listed as C_{12}, C_{13}, and C_{14} it appeared that the column failed to resolve compounds of the same chain length. The mass spectra indicated that each of these peaks contained a mixture of substances.

Product Yields. Yields of all products from pure F-cyclobutane were measured as a function of the radiation dose. *G* values listed in Table II are taken from the slopes of the resulting graphs. All products below C_{12} gave linear plots; the heavier products are probably also linear with dose, but experimental error was greater for these compounds. At the higher temperatures and longer elution times necssary for the C_{12}, C_{13}, and C_{14} products, the peaks became broader, and the chromatograph background increased. In view of the fact that a white, Teflon-like polymer formed during radiolysis, higher products were probably formed but were not detected. The *G*-values given in Table II correspond to a total consumption rate of F-cyclobutane of 3.0 molecules per 100 e.v. Owing to the

Publication Date: January 1, 1968 | doi: 10.1021/ba-1968-0082.ch006

Table II. Products and Their Yields from X-ray Irradiated F-cyclobutane at 150 torr

Product	G *Value*
C_2F_4	0.13
C_3F_8	0.008
C_3F_6	0.005
C_5F_{12}	0.065
C_6F_{12}	0.091
C_7F_{14}	0.077
C_8F_{16}	0.21
C_9F_{18}	0.13
C_9F_{20}	0.007
$C_{10}F_{20}$ $C_{10}F_{18}$	0.12
C_{12}	0.18
C_{13}	0.17
C_{14}	0.12

production of polymer, this must be taken as a lower limit of the actual radiation sensitivity of F-cyclobutane.

Effect of Sample Pressure. The effect of F-cyclobutane pressure was investigated over 50–300 torr. No change in product *G*-values was found —*i.e.*, total product yields increased in direct proportion to the number of grams of F-cyclobutane irradiated. This implies both that the reactions involved are not appreciably pressure dependent in the range studied and also that the Bragg-Gray conditions are adequately met over this range. (The occurrence of equal but opposite trends from these two causes, which would cancel, appears unlikely.)

Effects of Added Scavengers. Several additives were used to obtain more information about the reaction mechanism. Adding 5% nitrous oxide had no measurable effect on product yields. However, with 5% added oxygen or ethylene, all products listed in Table II except C_2F_4 were eliminated, and new but unidentified products were formed. These results strongly suggest that the final products from pure F-cyclobutane arise from a free radical sequence.

Methane–F-cyclobutane Mixtures. Studies were performed on various mixtures of methane and F-cyclobutane with compositions between 3 and 97% methane. Products were also measured for pure methane. Results of these experiments are shown in Figures 1 and 2. Products from pure methane—namely hydrogen, ethane, ethylene, and propane—were found at all intermediate concentrations, although yields were depressed below "ideal mixture" lines. The radiolytic behavior of the F-cyclobutane, however, was drastically modified. All perfluorocarbon products beyond the parent F-cyclobutane were completely eliminated, even with 3%

Publication Date: January 1, 1968 | doi: 10.1021/ba-1968-0082.ch006

added methane. The fragmentation products—C_2F_4, C_3F_8, and C_3F_6—were enhanced in yield, maximizing between 30 and 50% added methane. HF was found in substantial amounts. The only other "cross-product" measured was tentatively identified as CH_3—CF=CF_2; its yield maximized at about 40% methane.

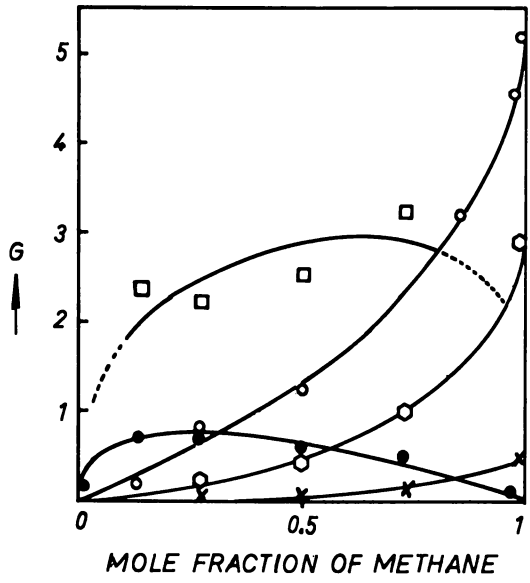

Figure 1. G values of the main products formed in the radiolysis of c-C_4F_8–CH_4 mixtures. □ *HF;* ○ H_2; ⬡ C_2H_6 × C_3H_8; ● C_2F_4

Other products which might be expected were probably masked by the F-cyclobutane peak. In particular, c-C_4F_7H may be masked in this way since it would be anticipated as a product from work on mixtures of cyclohexane and F-cyclohexane (*6*). One product peak was in fact observed on the tail of F-cyclobutane, but it was never separated sufficiently to analyze. Since this product appeared to maximize at high methane content, it may be c-$C_4F_7CH_3$ which also would be expected, at least in small yields (*6*).

Discussion

Pure F-cyclobutane. The general aspects of the radiolysis results are consistent with other studies of perfluorocarbon systems (*1*, *4*, *5*, *10*, *11*, *13*, *22*). Common features include considerable fragmentation of both C—C and C—F bonds, yielding diverse products, low yields for individual products, but a moderate over-all decomposition yield, absence

Publication Date: January 1, 1968 | doi: 10.1021/ba-1968-0082.ch006

of an olefin product derived from the parent by loss of F_2, and a mechanism involving free radical precursors for most products.

Several observations suggest that some type of chain polymerization is involved in the radiolysis of F-cyclobutane, especially since a white polymeric material was observed on the walls of radiolysis vessels and since measured G values do not decline appreciably with increasing chain length. The experiments with added methane suggest that the primary yield of tetrafluoroethylene may be appreciably greater than the net yield of 0.13 which is observed from pure F-cyclobutane. Furthermore, there appears to be a genetic relationship between several of the radiolysis products, based on the addition of successive C_2F_4 groupings. Accordingly we suggest a branching primary process followed by a sequence of competing free radical steps in which radicals may add to F-ethylene or react with one another. Because of the results obtained with N_2O, O_2, and C_2H_4 scavengers, it is assumed that all secondary processes are of the free radical type. In the following reaction sequence, F within the cyclobutane ring designates perfluoro.

Primary Processes

(5a)

$$\xrightarrow{\sim\sim} 2CF_2{=}CF_2 \qquad (5b)$$

$$\xrightarrow{\sim\sim} CF_3\cdot + CF_2{=}CF{-}CF_2\cdot \qquad (5c)$$

Chain Propagation

$$F\cdot + C_2F_4 \rightarrow C_2F_5\cdot \qquad (6)$$

$$C_2F_5\cdot + C_2F_4 \rightarrow C_4F_9\cdot \qquad (7)$$

$$C_4F_9\cdot + C_2F_4 \rightarrow C_6F_{13}\cdot \qquad (8)$$

etc.

$$CF_3\cdot + C_2F_4 \rightarrow C_3F_7\cdot \qquad (9)$$

$$C_3F_7 + C_2F_4 \rightarrow C_5F_{11}\cdot \qquad (10)$$

etc.

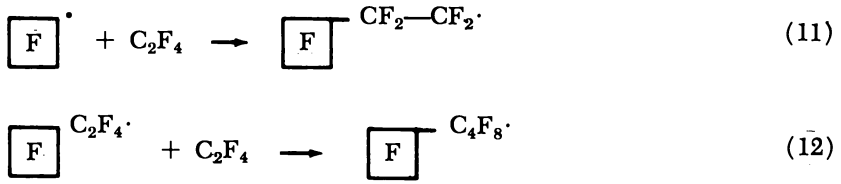

etc.

Chain Termination

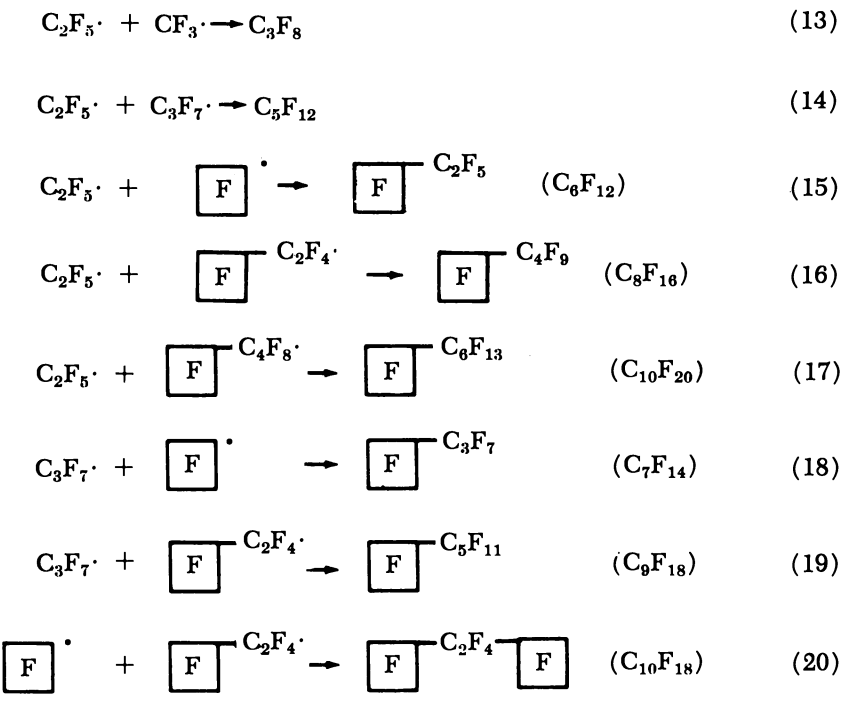

This reaction scheme gives a reasonable account of the formulas of the products and suggests structures for many of them. The radical-radical combination reactions are chosen because they lead to observed products. Other steps could be written, and presumably all possible combination steps occur to some extent, depending on the rates of formation of precursors, on the relative rate constants for the possible reaction channels disposing of each species, and on the concentration of the second species involved in each bimolecular step. Additional products are certainly formed. All major peaks beyond C_7 were double or triple, and

Publication Date: January 1, 1968 | doi: 10.1021/ba-1968-0082.ch006

intervening peaks too small to measure were seen. Furthermore, products beyond C_{14} must be formed since polymer was observed. Radical-radical disproportionation steps are omitted from the mechanism because there is experimental evidence that such processes do not occur in perfluorocarbon systems (*18*).

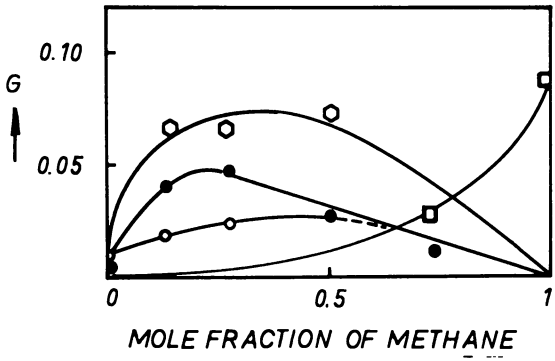

Figure 2. G values of the minor products formed in the radiolysis of c-C_4F_8–CH_4 mixtures. □ C_2H_4; ⬡ $CH_3C_2F_3$; ○ C_3F_8; ● C_3F_6

The postulated primary chemical steps can be examined in the light of the mass spectroscopic fragmentation pattern of F-cyclobutane (*14*), which shows $C_2F_4^+$ as the parent peak (abundance 100 arbitrary units). A 1–3 split is also favorable; $C_3F_5^+$ has an intensity of 87 units, and CF_3^+, 25 units. These data are consistent with Steps 5b and 5c. Rupture of a C—F bond (Reaction 5a) must be more important in the radiolysis mechanism than indicated by the low abundance of 0.1 unit for the $C_4F_7^+$ ion in the mass spectrum. However, this anomaly occurs not only in other fluorocarbon systems (*1, 5, 10, 11, 22*) but in most hydrocarbon systems studied to date. The intensities of CF_2^+ and CF^+ are also substantial in the mass spectrum, being 13 and 54 units respectively. These results, and the fact that CF_2 has often been found under pyrolytic conditions (*2, 12*), suggest the possibility that difluorocarbene plays a role in the mechanism, perhaps leading to a portion of the odd-carbon products. We have no evidence on this point, however.

Another process which should be considered is ring opening by fluorine atom attack (Reaction 21).

$$F\cdot + \boxed{F} \longrightarrow CF_3CF_2CF_2CF_2\cdot \qquad (21)$$

This reaction would not lead to a unique product since *n*-butyl radicals

Publication Date: January 1, 1968 | doi: 10.1021/ba-1968-0082.ch006

can be produced in other ways (*cf.* Reaction 7). However, Reaction 21 may be an additional source of these radicals. Reaction 21 is favored thermodynamically since the C—F bond strength exceeds the C—C bond strength in fluorocarbons by about 30 kcal./mole (*17*).

There are interesting parallels between the products obtained in this study and in the xenon-sensitized photolysis of F-cyclobutane, reported by Miller and Dacey (*16*). Products identified included CF_4, C_2F_6, C_3F_8, C_3F_6, and c-C_3F_6, as well as considerable amounts of higher molecular weight fluorocarbons thought to be C_8 compounds, but not positively identified. Although the authors considered a mechanism involving decomposition of excited F-cyclobutane an give F-ethylene, they discarded it in favor of a scheme involving abstraction of two fluorine atoms to give XeF_2 and excited F-cyclobutene.

The present data are broadly similar to earlier radiolysis results on liquid F-cyclobutane by Fallgatter and Hanrahan (*5*), who found C_2, C_3, C_5, C_6, and C_8 compounds. Higher products were not detected. Since the earlier work involved liquid rather than gaseous F-cyclobutane and since the radiolysis samples studied at that time were known to be slightly contaminated with hydrogen-containing materials, a detailed comparison with the present work is not warranted.

Methane–F-cyclobutane Mixtures. The present data on the radiolysis of methane–F-cyclobutane mixtures can be compared with several earlier studies. Rajbenbach (*19*, *20*) measured H_2 yields and competition between fluorocarbon and N_2O as electron scavengers in liquid-phase systems containing F-cyclobutane (or other fluorocarbons) in *n*-hexane and cyclohexane. A marked decrease in the hydrogen yield was demonstrated and attributed to nondissociative electron capture by the fluorocarbon. Fallgatter and Hanrahan (*6*) studied the full range of liquid mixtures of cyclohexane and F-cyclohexane from 0–100% fluorocarbon and measured several product yields as a function of dose. They found a large yield of c-$C_6F_{11}H$ ($G = 3.5$) and an increase in dicyclohexyl at intermediate concentrations, as well as confirming the drop in the hydrogen yield. It was pointed out that production of c-$C_6F_{11}H$ appears to rule out nondissociative electron capture as the main explanation of the effect on the hydrogen yield. Sagert (*21*) made detailed studies of more dilute solutions (0.3*M* or less) of F-cyclobutane, F-cyclohexane, and F-methylcyclohexane in cyclohexane and also noted extensive conversion of C—F to C—H bonds. He also interpreted this as evidence that processes other than nondissociative electron capture must be taking place.

Fallgatter and Hanrahan (*6*) noticed that the radiolysis products from their fluorocarbon–hydrocarbon mixtures resemble the pure hydrocarbon results rather than the products from the pure fluorocarbon. A similar generalization appears to be valid for the present experiments.

Publication Date: January 1, 1968 | doi: 10.1021/ba-1968-0082.ch006

For CH_4–c-C_4F_8 mixtures, H_2, C_2H_4, C_2H_6, and C_3H_8 all appear at intermediate concentrations, although their yields are depressed below ideal mixture lines, while all fluorocarbon products except C_2 and C_3 compounds are eliminated. However, a more detailed comparison of this work with the earlier studies shows a major difference in that efficient hydrogen scavenging at low concentrations of fluorocarbon was not observed. Whereas 0.2*M* added c-C_4F_8 decreased the hydrogen yield from liquid cyclohexane by 50% according to Rajbenbach (*19*), it required about 25 mole % F-cyclobutane to decrease the H_2 yield from gaseous methane by the same amount. These contrasting results may be caused by a larger role for ionic processes in the production of H_2 from gaseous methane than from liquid cyclohexane (*23*).

A marked regularity was found between the decrease in the hydrogen yield and the decreases in the yield of hydrocarbon products in the experiments depicted in Figures 2 and 3. In the absence of complications, stoichiometry indicates that:

$$\Delta G(H_2) = \Delta G(C_2H_6) + 2\Delta G(C_3H_8) + 2\Delta G(C_2H_4) \qquad (22)$$

The data given in Table III show that this regularity does occur. This result casts some doubt on the results of the HF analysis, also indicated in Figure 1. If protection of methane occurs by a physical process, then the simultaneous, coupled decrease in the yields of H_2 and hydrocarbons can be understood. If the scavenging is chemical and yields HF as a product, then a fate must be found for the methyl radicals or other species which are precursors of the missing hydrocarbon yields.

Table III. Decrease of the Yields of Hydrogen, Ethane, Propane, and Ethylene in Gaseous Mixtures of Methane and F-cyclobutane

CH_4,	ΔG		Δ2G		
mole fraction	H_2	C_2H_6	C_3H_8	C_2H_4	$\Delta\Sigma G(RH)$
0.95	1.00	0.65	0.20	0.10	0.95
0.90	1.20	0.85	0.30	0.08	1.23
0.80	1.45	1.05	0.40	0.05	1.50
0.70	1.50	1.10	0.45	0.03	1.58
0.60	1.40	1.05	0.45	0.02	1.52

Most aspects of the radiolysis results are consistent with the interpretation that F-cyclobutane protects methane while methane simultaneously protects F-cyclobutane, particularly as regards free radical fragmentation. Molecular fragmentation to give C_2F_4 clearly persists in the mixtures, along with some processes of low yield giving C_3 products. These protection effects can probably be explained in terms of ionic rather than free radical processes. As noted above, the radiolysis of methane is usually

Publication Date: January 1, 1968 | doi: 10.1021/ba-1968-0082.ch006

considered to proceed largely along ionic lines. Although we believe that final products from F-cyclobutane are formed in free radical steps, the primary physical processes indicated by the wavy arrows in Reactions 5a, 5b, and 5c almost certainly involve ionic species as well.

Acknowledgment

We thank Daniel Billen for use of the Maxitron x-ray unit. This work was supported by Atomic Energy Commission Contract No. AT-(40-1)-3106 and by the University of Florida Nuclear Science Program. This is Document Number ORO-3106-23.

Literature Cited

(1) Askew, W. C., Reed, III, T. M., Mailen, J. C., *Radiation Res.* **33,** 282 (1968).
(2) Butler, J. N., *J. Am. Chem. Soc.* **84,** 1393 (1962).
(3) Doepker, R. D., Ausloos, P., *J. Chem. Phys.* **44,** 1641 (1966).
(4) Fajer, J., MacKenzie, D. R., Bloch, F. W., *J. Phys. Chem.* **70,** 935 (1966).
(5) Fallgatter, M. B., Hanrahan, R. J., *J. Phys. Chem.* **69,** 2059 (1965).
(6) Fallgatter, M. B., Hanrahan, R. J., "Abstracts of Papers," 154th Meeting, ACS, Sept. 1967, V-75.
(7) Feigl, F., "Spot Tests in Inorganic Analysis," 5th English Ed., pp. 269-271, Elsevier, New York, 1958.
(8) Heckel, E., Hanrahan, R. J., in preparation.
(9) Hine, G. J., Brownell, G. L., "Radiation Dosimetry," pp. 625, 627, Academic Press, New York, 1956.
(10) Kevan, L., Hamlet, P., *J. Chem. Phys.* **42,** 2255 (1965).
(11) Kevan, L., *J. Chem. Phys.* **44,** 683 (1966).
(12) Lifshitz, A., Carroll, H., Bauer, S., *J. Chem. Phys.* **39,** 1661 (1963).
(13) MacKenzie, D. R., Block, F. W., Wiswall, Jr., R. H., *J. Phys. Chem.* **69,** 2526 (1965).
(14) Majer, J. R., *Advan. Fluorine Chem.* **2,** 55 (1961).
(15) Miller, C. D., Winefordner, J. D., *Microchemical J.* **8,** 334 (1964).
(16) Miller, G. H., Dacey, J. R., *J. Phys. Chem.* **69,** 1434 (1965).
(17) Patrick, C. R., *Advan. Fluorine Chem.* **2,** 23 (1961).
(18) Pritchard, G. O., Miller, G. H., Dacey, J. R., *Can. J. Chem.* **39,** 1968 (1961).
(19) Rajbenbach, L. A., *J. Am. Chem. Soc.* **88,** 4275 (1966).
(20) Rajbenbach, L. A., Kaldor, U., *J. Chem. Phys.* **47,** 242 (1967).
(21) Sagert, N. H., *Can. J. Chem.* **46,** 95 (1968).
(22) Sokolowska, A., Kevan, L., *J. Phys. Chem.* **71,** 2220 (1967).
(23) Spinks, J. W. T., Woods, R. J., "An Introduction to Radiation Chemistry," pp. 215-218, 319-322, Wiley, New York, 1964.

RECEIVED January 8, 1968.

7

Vapor-Phase γ-Radiolysis of Benzene, Toluene, Ethylbenzene, and the Xylenes

K. E. WILZBACH and LOUIS KAPLAN

Argonne National Laboratory, Argonne, Ill. 60439

Publication Date: January 1, 1968 | doi: 10.1021/ba-1968-0082.ch007

Benzene, toluene, ethylbenzene, and the three xylenes have been irradiated in the vapor phase with gamma rays. Products and yields have been compared with those in liquid-phase radiolysis. G values for disappearance in the vapor phase range from 6 to 10, more than five times greater than in the liquid phase. The principal product in each case is "polymer." All of the identified products are also found in the liquid phase, but relative yields are markedly different. The high yields of acetylene and some other products in the vapor phase suggest that ionic processes are more important here than in the liquid phase.

The stability of aromatic hydrocarbons to radiation has been cited so frequently in the literature that it has come to be accepted (*5, 6*) as a characteristic of aromaticity, a consequence of electron delocalization. These conclusions are based on the results of irradiations in the liquid phase. That they may not apply to the isolated aromatic molecule, however, is suggested by the few reported studies of the radiolysis of aromatic hydrocarbons in the vapor phase. Such studies have thus far been limited to two compounds—benzene (*8, 10, 11*) and isopropylbenzene (cumene) (*9*), and differences in the character of the radiation or the conditions of irradiation preclude a simple assessment of the effect of phase on these systems.

To provide further information on this point, we have investigated the γ-radiolysis of benzene, toluene, ethylbenzene, and the xylenes in the vapor phase and have determined yields of the gaseous products, "polymer," and some products of intermediate volatility. These results are compared with those of parallel irradiations of liquid toluene and *o*-xylene and with published (*2, 12*) data for the other hydrocarbons in the liquid phase.

In Radiation Chemistry; Hart, E.;
Advances in Chemistry; American Chemical Society: Washington, DC, 1968.

Experimental

Chemicals. The *o*-xylene was an American Petroleum Institute standard sample, with stated impurities of 0.005 ± 0.004 mole %. Other hydrocarbons were purified by gas chromatography. Purity was checked by gas chromatography on three columns of different selectivity: except for 0.02% *p*-xylene in the *m*-xylene, no more than 0.002% of any impurity was detected. Samples were stored *in vacuo*.

Irradiation. Samples were irradiated in the Argonne high level gamma irradiation facility. γ-Rays, from spent reactor fuel elements, ranged in energy from 0.22 to 2.5 Mev., with an average of about 0.75 Mev. The dose rates for various samples varied from 1×10^4 to 4×10^4 rads per minute. The temperature of the samples was about 30°C.

Dosimetry. The intensity of the flux at the sample site was measured periodically with a ferrous sulfate dosimeter, using $G_{Fe(III)} = 15.5$. Energy absorbed in liquid samples was based on this dosimetry and was corrected for the electron density of the samples. To determine energy absorbed in the vapor samples, nitrous oxide was irradiated, at comparable electron densities, in the vessel used for the hydrocarbons; the *G* value for nitrogen production was taken to be 11.0 (7).

Procedure. For liquid-phase studies, weighed samples (*ca.* 0.5 ml.) were irradiated in sealed, evacuated glass tubes (*ca.* 0.7 ml.). Vapor samples were irradiated in a 700-ml. glass cylinder. Small weighed samples (12–77 mg.) of hydrocarbon were introduced into the vessel in sealed thin-walled capillary tubes prior to evacuation and sealing-off. Irradiated samples were processed on the vacuum line to yield a noncondensable gas fraction ($H_2 + CH_4$), a fraction containing the C_2 to C_4 hydrocarbons, and a liquid fraction containing the C_6 to C_{10} components. The weight of "polymer" was taken to be the difference between the initial weight of hydrocarbon and the sum of the measured weight of the liquid fraction and the calculated weights of the gaseous fractions. The residual polymeric material was not investigated further.

Analysis of Products. The three fractions collected from each sample were analyzed by gas chromatography. The noncondensable fraction, containing hydrogen and methane, was analyzed on silica gel at room temperature. The fraction containing C_2–C_4 hydrocarbons was analyzed at 75°C. on silica gel treated with didecyl phthalate. Aliquots of the liquid fraction were analyzed on three columns of different selectivity: Bentone-34–didecyl phthalate; silicone SE-30; and *m*-polyphenyl ether (five-ring). Products were identified, and their yields were determined by comparison of retention volumes and peak areas with values for known amounts of authentic samples.

The analytical procedure did not permit reliable analyses for C_3 to C_5 hydrocarbons. C_3 and C_4 products are formed from all of the alkylbenzenes, especially from ethylbenzene. A few unidentified peaks were observed in the analyses of the liquid fractions but generally in low yield.

Results

Our results on the γ-radiolysis of benzene, toluene, ethylbenzene, and the xylenes in the vapor phase, and of toluene and *o*-xylene in the

liquid phase, are shown in Tables I and II. The results listed are those of specific experiments; duplicate runs gave product yields which agreed within 5–10% with those tabulated. The yields of products were closely proportional to dose over the limited range investigated, 20–100 Mrads. No systematic study of effects of dose rate and of pressure on yields was carried out; increasing the pressure of toluene from 7 to 22 torr produced no significant change. Included in the tables are the results of Burns and Jones (*2*) on the ^{60}Co radiolysis of liquid benzene and of Verdin (*12*) on the ^{60}Co radiolysis of ethylbenzene and *m*- and *p*-xylene in the liquid phase. To the extent that they overlap, our results on liquid *o*-xylene agree reasonably well with those of Verdin (*12*) as do our results on liquid toluene with those of Weiss and Collins (*14*).

Comparison of the results of vapor- and liquid-phase radiolysis shows that the yields of all products from each hydrocarbon are markedly greater in the vapor phase. As in the liquid phase, "polymer" is the predominant product, accounting for 83–96% of the hydrocarbon consumed. The 100-e.v. yields (*G* values) of "polymer" increase with alkyl substitution from 6 for benzene to 8.7 for ethylbenzene; the yield in each case is about five to six times that observed in the liquid phase.

The gaseous products (hydrogen, methane, and the C_2 hydrocarbons) are formed also with high *G* values in the vapor-phase radiolyses. Yields of H_2 increase markedly with alkyl substitution, from 0.15 for benzene to about 0.8 for ethylbenzene and *p*-xylene, paralleling the trend in the liquid phase but about four times greater in each case. Methane and ethane yields also increase with alkyl substitution; from the alkylbenzenes the yields of methane are 10–20 times greater and those of ethane are more than 100 times greater in the vapor than in the liquid phase. Yields of ethylene and acetylene are also much higher in the vapor phase. Acetylene yields are decreased slightly by alkyl substitution; ethylene yields are increased markedly by ethyl substitution but only moderately by methyl substitution.

The liquid products include compounds in which alkyl groups have been replaced by hydrogen and vice versa. In vapor-phase radiolysis, *G* values for replacement of a single alkyl group (*e.g.*, benzene from toluene and ethylbenzene; toluene from xylenes and ethylbenzene) are *ca.* 0.3, about 10 to 20 times those in the liquid phase. Replacement of two alkyl groups is still an important process in the radiolysis of the xylene vapors although almost negligible in liquid *o*-xylene. Replacement of hydrogen by methyl occurs both in the ring and in side chains. In the vapor phase, the replacement of an aromatic hydrogen is affected by its position; *G* values range from 0.007 to 0.06, with the order of preference being meta > ortho > para. In the liquid phase, the corresponding process is essentially statistical, with a *G* value of 0.001 per

Publication Date: January 1, 1968 | doi: 10.1021/ba-1968-0082.ch007

hydrogen. In the vapor, side-chain hydrogens are substituted about as readily as ring hydrogens, with the alpha position favored over the beta (as judged from ethylbenzene).

Table I. γ–Radiolysis of Benzene, Toluene, and Ethylbenzene in Vapor and Liquid Phase

	Vapor Phase			*Liquid Phase*		
Conditions	*Benzene*	*Toluene*	*Ethylbenzene*[a]	*Benzene*[b]	*Toluene*	*Ethylbenzene*[c]
Pressure, torr	26.4	7.5	7.6	liq.	liq.	liq.
Dose, e.v. gram^{-1} × 10^{-21}	8.8	9.1	1.7		8.7	
Rate, e.v. gram^{-1} sec.$^{-1}$ × 10^{-16}	6.1	2.3	2.8		2.2	
Products	$G_{product}$			$G_{product}$		
Hydrogen	0.15	0.47	0.76	0.039	0.11	0.158
Methane	0.018	0.15	0.51		0.017	0.0259
Ethane	0.004	0.06	0.92		0.0001	0.0057
Ethylene	0.08	0.10	0.40		0.0004	0.0071
Acetylene	0.73	0.64	0.56	0.019	0.007	0.0021
Benzene		0.20	0.38		0.018	0.016
Toluene	0.02		0.34			0.018
Ethylbenzene	0.007	0.07			0.001	
o-Xylene		0.02	0.02		0.002	< 0.002
m-Xylene		0.06	0.01		0.002	
p-Xylene		0.007			0.001	
Propylbenzene		0.003	0.034			
i-Propylbenzene			0.11			
o-Ethyltoluene		0.002	0.035			
m-Ethyltoluene		0.003	0.10			
p-Ethyltoluene		0.002	0.012			
"Polymer"	6.0	6.3	8.7	0.94	1.16	

[a] Products found also include propane, butanes, butylbenzenes, and diethylbenzenes.
[b] Data of Burns and Jones (*2*).
[c] Data of Verdin (*10*).

In radiolysis of xylenes, the products include benzocyclobutene and the isomeric xylenes. The former is formed from *o*-xylene in the vapor phase with a *G*-value of 0.08, 40 times that in the liquid phase. Its yield from the other xylenes is much smaller. The *G* values for isomerization of the xylenes in the vapor phase are about 0.3. In each case both possible isomers are formed with significant yields. In the liquid phase, the isomerization of *o*-xylene is much more selective; *m*-xylene is produced with a *G* of 0.01; the para isomer could not be detected.

Publication Date: January 1, 1968 | doi: 10.1021/ba-1968-0082.ch007

Table II. γ–Radiolysis of *o*-, *m*-, and *p*-Xylene in Vapor and Liquid Phase

	Xylene Vapor			*Xylene Liquid*		
Conditions	o-	m-	p-	o-	m-[a]	p-[a]
Pressure, torr	4.7	3.0	2.9	—	—	—
Dose, e.v. gram^{-1} × 10^{-21}	8.2	8.4	8.0	8.2		
Rate, e.v. gram^{-1} sec.$^{-1}$ × 10^{-16}	1.9	1.8	1.7	5.7		
Products	$G_{product}$			$G_{product}$		
Hydrogen	0.65	0.65	0.84	0.18	0.184	0.209
Methane	0.26	0.32	0.33	0.025	0.0142	0.0144
Ethane	0.39	0.41	0.41	0.0002		0.0001
Ethylene	0.16	0.14	0.15	0.0004		0.0002
Acetylene	0.53	0.56	0.59	0.0028		0.0033
Benzene	0.13	0.10	0.15	0.001	<0.05	<0.002
Toluene	0.36	0.21	0.38	0.031	<0.05	0.014
Ethylbenzene	0.028	0.012	0.011	<0.0003		
o-Xylene		0.10	0.08		<0.05	<0.002
m-Xylene	0.18		0.26	0.012		
p-Xylene	0.07	0.11		<0.0003		
Benzocyclobutene	0.08	0.01	0.004	0.002		
o-Ethyltoluene	0.13	0.002	0.001	0.0028		
m-Ethyltoluene	0.004	0.10	0.004			
p-Ethyltoluene	0.001	0.002	0.11			
1,2,3-Trimethylbenzene	0.065	0.010	0.001	0.0021		
1,2,4-Trimethylbenzene	0.027	0.018	0.12	0.0028		
1,3,5-Trimethylbenzene		0.062				
"Polymer"	7.2	6.4	6.6	1.44	0.99	1.10

[a] Verdin (*10*).

Discussion

The results clearly demonstrate that aromatic hydrocarbons are markedly less resistant to radiation in the vapor phase than in the liquid; *G* values for their disappearance in the vapor phase (6.3 to 10) are, in fact, not much smaller than those of comparable saturated hydrocarbons. In aromatic liquids neutralization of the ions produced by radiolysis is rapid; the excited states, produced either directly or by ion recombination, degrade mostly to the parent hydrocarbon (*6*). Those chemical reactions which excited species, or radicals derived from them, undergo in the liquid phase should also occur in the vapor and might be enhanced by

longer lifetimes of excited states and lower probabilities for radical recombination. In addition, the longer lifetimes of the ions might result in ionic decompositions and rearrangements and ion-molecule reactions not observed in the liquid phase. Elucidation of the pathways by which the various products of vapor phase radiolysis are actually formed is beyond the scope of this study. It would require, *inter alia,* information concerning the composition of the "polymer" and the effects of dose rate, pressure, and added scavengers on the yields of each product. It may, however, be worthwhile to consider briefly some features of the vapor-phase radiolyses.

For toluene and *o*-xylene, where analyses are directly comparable, there are no significant products found in the vapor- which are not also produced in liquid-phase irradiation. Further, all of these products except ethylene, acetylene, and benzocyclobutene are also formed in vapor-phase photolyses (*17*) at 2537 A.; even these exceptions have been detected in photolyses of *o*-xylene at shorter wavelengths. Benzocyclobutene was found (*13*) among the products of photolysis at 1600–2100 A.; this product, as well as acetylene and ethylene, was observed (*18*) on irradiation with an unfiltered mercury resonance lamp.

It would appear, therefore, that all of the products identified in the vapor-phase radiolyses could be formed from excited molecules. Some products, however, are so much more abundant in vapor-phase radiolysis than in photolysis or liquid-phase radiolysis as to suggest the likelihood of additional precursors. In particular, the formation of acetylene, the isomerization of the xylenes, and the replacement of aromatic hydrogen by methyl groups are difficult to explain solely in terms of reactions of excited molecules.

As indicated, acetylene is formed by photolysis of *o*-xylene at 1849 A. In contrast to the situation in vapor-phase radiolysis, however, its yield is small compared with that of other products. The quantum yield for its formation is not known, but it is probably close to 0.01, reported (*3*) for benzene vapor photolyzed at the same wavelength. So small a quantum yield could not account for the observed *G* value of 0.5 of acetylene from *o*-xylene vapor (or of 0.7 from benzene vapor). A plausible source of the excess acetylene is the direct decomposition of ions formed in the radiolysis. [The possibility that more highly excited states than those investigated thus far might give higher yields of acetylene (and other products) cannot be excluded.] Decomposition of ions from aromatic hydrocarbons to acetylene is known to occur in the mass spectrometer: A metastable peak at mass 34.7 in the spectrum of benzene (*1*) corresponds to the reaction $C_6H_6^+ \rightarrow C_4H_4^+ + C_2H_2$; processes yielding acetylene from abundant ions in the spectra of toluene and the C_8 aromatic hydrocarbons are also known (*4*). Assuming that the pattern of

Publication Date: January 1, 1968 | doi: 10.1021/ba-1968-0082.ch007

ions formed in radiolysis is similar to that in the mass spectrometer (*1*), and using a *W* value of 30 e.v. per ion pair, one can calculate *G* values of 1 to 1.5 for production of acetylene from the various aromatic hydrocarbons—more than enough to account for the observed yields.

The isomerization of *o*-xylene in liquid-phase radiolysis, as well as in vapor-phase photolysis either at 2537 A. (*17*) or in the vacuum ultraviolet (*13*), gives a very high ratio of meta to para isomer. The more nearly statistical distribution of isomers observed in the vapor-phase radiolysis may again be rationalized in terms of an ionic process. Mass spectral studies (*4*) of isotopically labeled *p*-xylene indicate extensive randomization of carbon atoms in the abundant $C_8H_9^+$ ion. It is not known whether such randomization ocurs in the parent ion or whether randomized ions could revert to xylenes, but the rearomatization of a randomized species has been demonstrated (*19*) in the radiolysis of toluene-7-^{14}C vapor.

The products resulting from replacement of aromatic H by CH_3, in the vapor-phase radiolyses of the alkylbenzenes, show a strong preference for meta orientation. That these products are derived from radicals is suggested by our observation that no xylenes are formed when toluene vapor is radiolyzed in the presence of iodine. The distribution of isomers does not, however, correspond to the preferential ortho substitution found (*16*) in the homolytic methylation of toluene, nor does it resemble the nearly statistical distribution observed in liquid phase radiolysis or in vapor-phase photolysis at 2537 A. (*17*). The process is obviously complex, and there is little direct evidence on which to base a mechanism. It may, nevertheless, be of interest that the $C_8H_9^+$ ion is observed (*15*) in the mass spectrum of toluene at moderate pressures. Neutralization of such an ion could lead to radicals and ultimately to aromatic products. It is also of interest that the "high pressure" mass spectrum shows (*15*) abundant formation of dimeric ions, which may well be involved in the enhanced production of dimer and higher polymeric products in the vapor phase radiolysis.

Publication Date: January 1, 1968 | doi: 10.1021/ba-1968-0082.ch007

Acknowledgment

We are indebted to M. P. Cava for supplying us with a sample of benzocyclobutene.

Literature Cited

(1) API Project 44, "Catalog of Mass Spectral Data," Chemical Thermodynamics Properties Center, Texas A & M University, College Station, Tex., 1947 *et seq.*
(2) Burns, W. G., Jones, J. D., *Trans. Faraday Soc.* **60**, 2022 (1964).

(3) Foote, J. K., Mallon, M. H., Pitts, J. N., Jr., *J. Am. Chem. Soc.* **88,** 3698 (1966).
(4) Grubb, H. M., Meyerson, S., "Mass Spectrometry of Organic Ions," F. W. McLafferty, Ed., Chap. 10, Academic Press, New York, 1963.
(5) Haissinsky, M., "Nuclear Chemistry and its Applications," p. 407, Addison-Wesley, Reading, Mass., 1964.
(6) Hardwick, T. J., "Actions Chimiques et Biologiques des Radiations," Dixième Série, M. Haissinsky, Ed., p. 180, Masson, Paris, 1966.
(7) Hearne, J. A., Hummel, R. W., *Radiation Res.* **15,** 254 (1961).
(8) Henri, V. P., Maxwell, C. R., White, W. C., Peterson, D. C., *J. Phys. Chem.* **56,** 153 (1952).
(9) Hentz, R. R., *J. Phys. Chem.* **66,** 1622 (1962).
(10) Huyskens, P., *Bull. Soc. Chim. Belg.* **68,** 89 (1959).
(11) Manion, J. P., Burton, M., *J. Phys. Chem.* **56,** 560 (1952).
(12) Verdin, D., *J. Phys. Chem.* **67,** 1263 (1963).
(13) Ward, H. R., *J. Am. Chem. Soc.* **89,** 2367 (1967).
(14) Weiss, J., Collins, C. H., *Radiation Res.* **28,** 1 (1966).
(15) Wexler, S., Clow, R. P., *J. Am. Chem. Soc.*, in press.
(16) Williams, G. H., "Homolytic Aromatic Substitution," p. 106, Pergamon Press, New York, 1960.
(17) Wilzbach, K. E., Kaplan, L., *J. Am. Chem. Soc.* **86,** 2307 (1964).
(18) Wilzbach, K. E., Kaplan, L., unpublished data.
(19) Wilzbach, K. E., "Mass Spectrometry of Organic Ions," F. W. McLafferty, Ed., p. 522, Academic Press, New York, 1963.

RECEIVED January 15, 1968. Work performed under the auspices of the U. S. Atomic Energy Commission.

8

A Pulsed-Radiolysis Study of the Gas-Phase Reaction of Oxygen Atoms with Benzene and Related Compounds: Rate Constants and Transient Spectra

INDER MANI and MYRAN C. SAUER, JR.

Chemistry Division, Argonne National Laboratory, Argonne, Ill.

Publication Date: January 1, 1968 | doi: 10.1021/ba-1968-0082.ch008

Pulsed-radiolysis of gas-phase systems containing CO_2 or N_2O results in the production of oxygen atoms, which are in the triplet ground state. In the presence of small amounts of benzene, for example, an optical absorption is found to be formed after the pulse, with a maximum at 275 mμ and a shoulder in the region of 300 mμ. Similar absorption spectra are found for other compounds. Rate constants for the process $O(^3P) + X \rightarrow$ products are, where the compound X is given in parentheses and the rate constant is in units of 10^8 liter mole^{-1} sec.$^{-1}$, 0.36 (benzene), 1.4 (toluene), 3.2 (ethylbenzene), 6.7 (o-xylene), 7.7 (m-xylene), 4.5 (p-xylene), 3.1 (chlorobenzene), 0.27 (fluorobenzene), and 1.0 (pyridine). The estimated limits of error are about ±25%.

The production of oxygen atoms by the pulsed-radiolysis of gas-phase systems containing CO_2 or N_2O has been described (*6*) and the reaction with molecular oxygen has been studied. The conclusion was reached that the oxygen atoms are most likely in the ground state (^3P) when they undergo reaction with the oxygen. In the present work, we have studied the reactions of oxygen atoms produced in such systems with various aromatic molecules and have obtained information on the absolute rate constants of these reactions and on the optical absorption spectra of the resulting transients.

In Radiation Chemistry; Hart, E.;
Advances in Chemistry; American Chemical Society: Washington, DC, 1968.

Experimental

The experimental details of the preparation of samples, the pulse-irradiation procedure, and the recording and analysis of data have all been described (*6*, *7*, *9*). Product analysis was done as previously described (*9*), using temperature programmed gas chromatography (25°C. to 230°C.) and a 2% Versamid-900 on silanized Chromosorb (white, acid washed, 60–80 mesh) column.

Results and Discussion

Transient Spectra. The spectra are shown in Figures 1, 2, and 3 and were obtained point by point, as has been previously described (*1*, *8*),

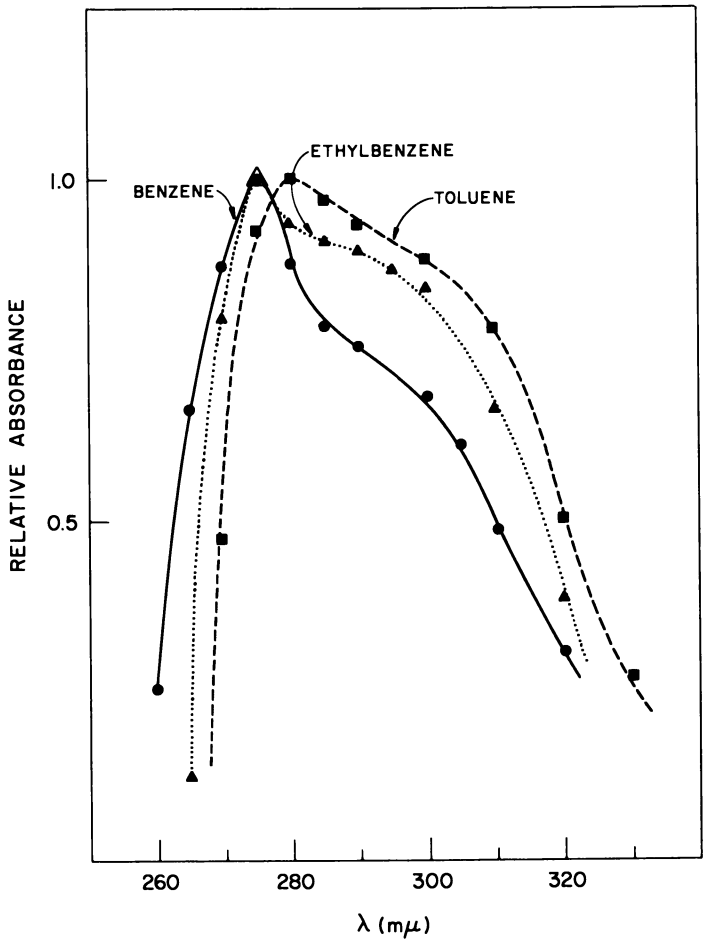

Figure 1. Transient absorption spectra resulting from reaction of oxygen atoms with benzene, toluene, and ethylbenzene

taking readings every 5 mμ. The absorption spectra shown correspond to a time approximately 20 μsec. after the electron pulse. As will be discussed in the section on transient decay, the absorption decayed little over a time of a few milliseconds at wavelengths around the maximum, but the shoulder at longer wavelengths decayed to a plateau (about 50% of the maximum O.D.) in a time of less than a millisecond.

Although absorption coefficients could not be determined accurately, they are estimated to be in the range of 10^3–$10^4 M^{-1}$ cm.$^{-1}$ based on what is known about the concentration of oxygen atoms produced per pulse. The spectrum for each compound shown in Figures 1–3 is normalized to 1.0 at the maximum.

In the case of benzene, one possible species absorbing in the region of 275 mμ is phenol. By measuring the absorption of phenol vapor in one atm. of air at 24°C. in a Cary spectrophotometer, we found the absorption coefficient to be 4–5 × $10^3 M^{-1}$ cm.$^{-1}$ at 275.7 mμ; however, the absorption peak at 275.7 was very sharp, the absorption reaching zero by about 280 mμ. We do not know how much the 50 fold increase in pressure used in the pulsed-radiolysis experiment would affect the width of the absorption, but it is very unlikely that phenol is the only absorbing species. In a recent study (*10*) on the synthesis of benzene oxide (*A*) in isooctane solution, this compound was found to have a maximum absorption at 271 mμ, and to be in equilibrium with oxepin (*B*), with a maximum at 305 mμ.

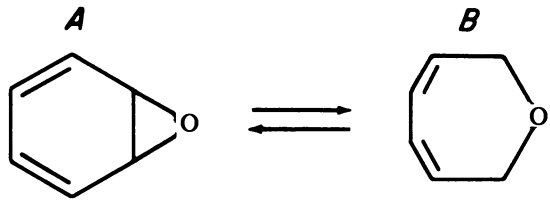

The equilibrium is about 2:1 in favor of *B* at room temp. in isooctane solution. As will be discussed in the section on transient decay, these species are possible products of the reaction of oxygen atoms with benzene. In addition, the biradical (*C*) produced

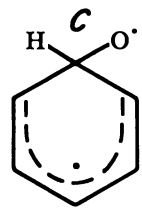

Publication Date: January 1, 1968 | doi: 10.1021/ba-1968-0082.ch008

when triplet ground state oxygen atoms react with benzene may have a long enough lifetime with respect to conversion to *A*, *B*, or phenol to be responsible for part of the absorption. (It should be noted, however, that work on the gas-phase reaction of triplet oxygen atoms to olefins (3) indicates that the lifetime of the biradical must be much shorter than the approximately 100 μsec. lifetime which would be required here.)

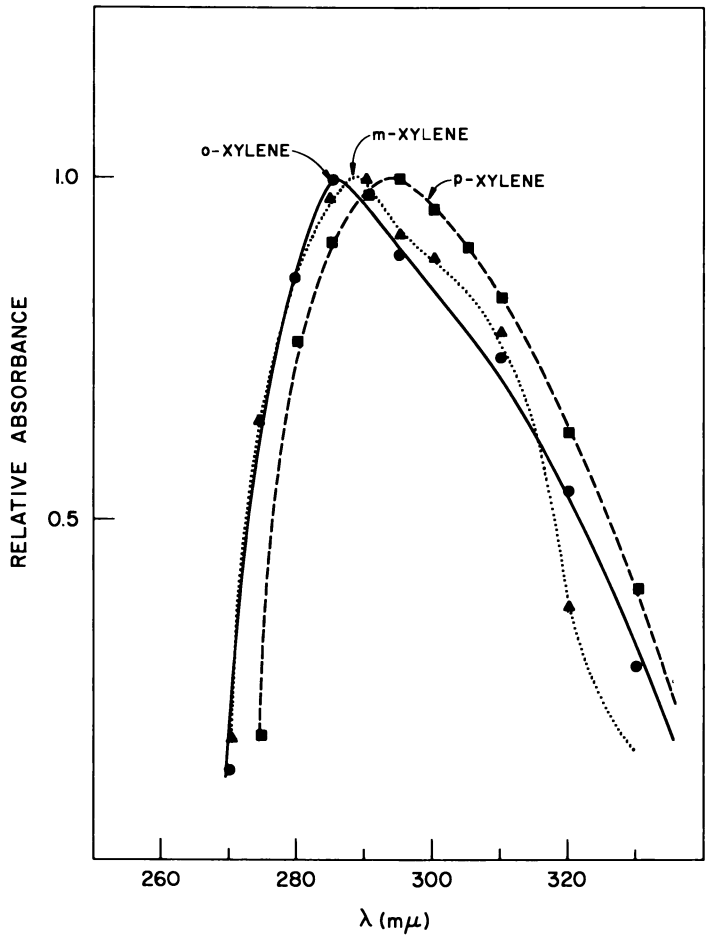

Figure 2. Transient absorption spectra resulting from reaction of oxygen atoms with o-, m-, and p-xylene

In the case of the other compounds studied, the spectra are similar, as are the decays of the longer wavelength parts of the spectra. However, we can only surmise that analogous transient species are involved.

Publication Date: January 1, 1968 | doi: 10.1021/ba-1968-0082.ch008

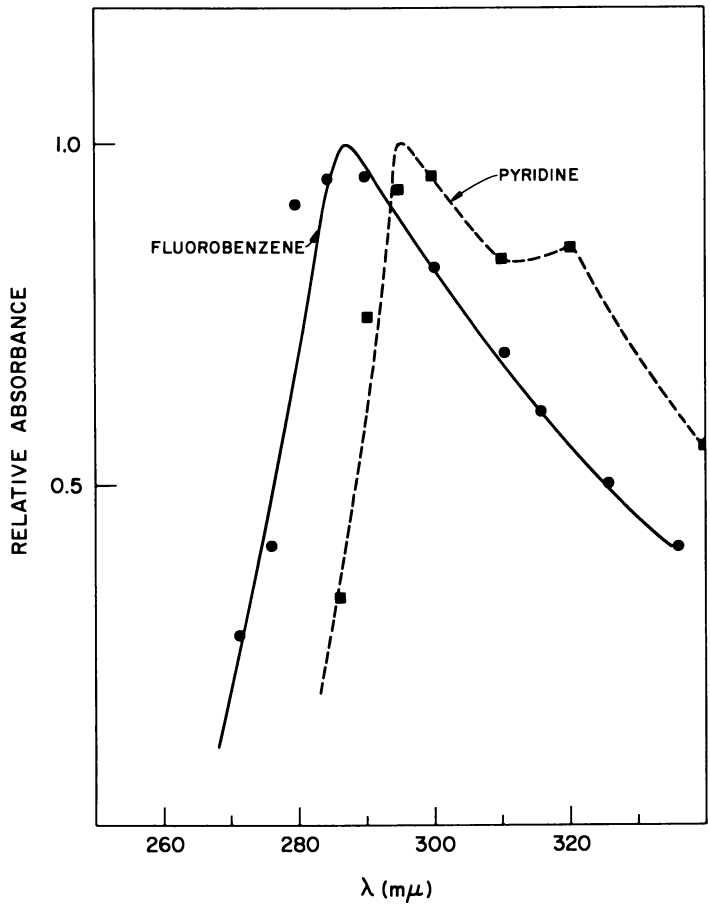

Figure 3. Transient absorption spectra resulting from reaction of oxygen atoms with fluorobenzene and pyridine

Transient Formation. That oxygen atoms in the ^3P ground state are produced when a system of argon and CO_2 is pulse irradiated has been previously demonstrated (*6*). Furthermore, the oxygen atoms were shown to be formed nearly simultaneously with the microsecond pulse. When a small amount of benzene (1 to 8 cm.) is added to the system, optical absorption is found in the region of 275 mμ, the spectrum being shown in Figure 1. This absorption was observed to form with a half time of about 4 μsec. or greater, depending on the benzene pressure. A typical formation curve is shown in Figure 4. It was found that the first order rate constant derived from such transient curves was independent of benzene concentration, as expected, with the following qualifications. As the benzene concentration was lowered, it was found that high values

Publication Date: January 1, 1968 | doi: 10.1021/ba-1968-0082.ch008

were obtained for the rate constant unless progressively lower intensity pulses were used. (Of course, the optical density was thereby lowered, and more amplification had to be used, resulting in greater noise levels. However, analysis of the curves was possible, several curves being analyzed at each intensity and the results averaged.) This behavior can be explained if the formation of the transient by Reaction 1

$$O + C_6H_6 \rightarrow C_6H_6O \quad (1)$$

is interfered with by any reaction involving two transient species such as

$$O + C_6H_6O \rightarrow \text{products} \quad (2)$$

$$O + O \rightarrow O_2 \quad (3)$$

$$C_6H_6O + C_6H_6O \rightarrow \text{products} \quad (4)$$

Lower pulse intensity makes smaller the probability of Reactions 2, 3, and 4 occurring during the formation of C_6H_6O by Reaction 1.

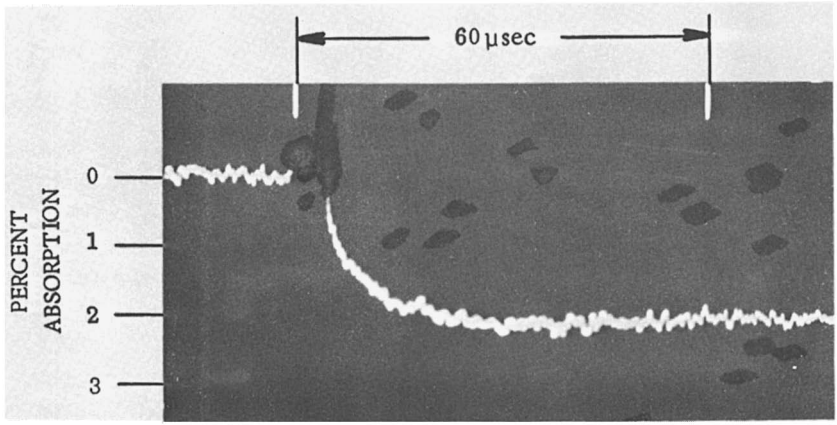

Figure 4. Transient formation at 285 $m\mu$ in system containing 56 atm. Ar, 2 atm. CO_2, and 0.09 atm. benzene. The pulse was 80 ma. and 0.4 μsec.; the optical pathlength was 26 cm.

The rate constant obtained for Reaction 1 was $3.6 \pm 0.7 \times 10^7 M^{-1}$ sec.$^{-1}$ independent of benzene pressure from 2 to 8 cm. (However, at 1 cm. benzene, low enough pulse intensity could not be used to overcome the importance of Reactions 2, 3, and 4 relative to 1, and the apparent rate constant obtained was higher.) Within 20%, the same rate constant for Reaction 1 was obtained in systems containing 30 to 90 atm. Ar plus about 2 atm. CO_2, 50 atm. Ar plus about 2 atm. N_2O, and 15 atm. CO_2

(no Ar). Also, the use of C_6D_6 had no effect on k_1. (It should be emphasized that the rate constants reported here are actually a sum of the rate constants for all reaction paths by which the oxygen atom reacts with a given compound. The intermediate C_6H_6O formed in Reaction 1, for example, may represent more than one species.)

As has been discussed previously (*6*, *7*), the oxygen atom which reacts with benzene is likely to be ^3P, and therefore the C_6H_6O species produced in Reaction 1 must be initially the biradical species *C*. Although we do not know the lifetime of this species, it may be rapidly converted to species *A* and/or *B*, and thereby not contribute directly to the observed absorption. These species will be further considered in the section on transient decay.

Similar transient formation curves were obtained when other organic molecules, listed in Table I, were used instead of benzene. The rate constants obtained are given in Table I along with that obtained for benzene. The values for benzene and toluene are in good agreement with the relative rate constants given by Cvetanovic (*3*).

Although the estimated error limits are rather large (approximately 25%), the general trends in reactivity are clear. In the series benzene, toluene, xylenes, the rate constant for the reaction of oxygen atoms with the molecule increases by a factor of approximately 20. It is clear that increasing the number of methyl groups has the effect of increasing the rate constant, although the differences between the three xylenes may not be meaningful since the rate constants are the same within the estimated error. The same order of reactivity (and approximately the same absolute rate constants) have been observed for the reaction of hydrogen atoms with these substances (*4*, *9*). The values obtained (*9*) for the reaction of hydrogen atoms with benzene and toluene are 0.37 and $1.0 \times 10^8 M^{-1}$ sec.$^{-1}$, both of which are within the experimental error of the corresponding oxygen atom results in Table I. In the case of xylenes, preliminary results (*4*) on the reactions of hydrogen atoms indicate that the rate constants are about half as great as the corresponding values of Table I. The rate constant for the reaction of H· with ethylbenzene is likewise about half that of oxygen atoms with ethylbenzene. Chlorobenzene shows about the same rate constant for both hydrogen and oxygen atoms, as does pyridine. Fluorobenzene shows the greatest difference, the hydrogen atom reaction being about 2.5 times faster than the oxygen atom reaction.

Cvetanovic (*3*) has concluded that the reaction of triplet oxygen with olefins is electrophilic, and that the reaction of hydrogen atoms is free radical in nature, the oxygen atom reaction rate constants showing larger variations with structural changes in the olefins. In view of the

Publication Date: January 1, 1968 | doi: 10.1021/ba-1968-0082.ch008

similarity of the rate constants for hydrogen atom and oxygen atom reactions with the compounds in Table I, the question arises as to whether the same classifications are reasonable for the reactions with aromatic compounds.

Table I. Gas Phase Rate Constants for Reactions of Oxygen Atoms with Organic Compounds

	Pressures (atm.) of Sample Constituents			$10^{-8} \times$ *Rate Constant*
	Ar	CO_2	*Organic*	*liter mole^{-1} sec.$^{-1}$*
Toluene	97	2.5	0.032	1.4 ± 0.3
Ethylbenzene	51	2	0.011	3.2 ± 0.8
o-Xylene	54	2	0.007	6.7 ± 1.6
m-Xylene	54	2	0.009	7.7 ± 2.0
p-Xylene	58	2	0.011	4.5 ± 1.4
Chlorobenzene	58	2	0.012	3.1 ± 0.8
Fluorobenzene	55	2	0.09	0.27 ± 0.06
Pyridine	28, 54	2	0.024	1.0 ± 0.3
Benzene	[a]			0.36 ± 0.07

[a] Various conditions, *see* text.

The classification of the hydrogen atom reactions as "free radical" seems reasonable, as the presence of any of the substituents tested on the benzene ring has an activating effect, as would seem to be expected (*11*); furthermore, the rather small changes in rate constants caused by the different constituents supports the "free radical," *i.e.*, homolytic classification (*11*). However, several puzzling aspects of the oxygen atom rate constants in Table I should be pointed out with respect to the question of the electrophilic nature of the oxygen atom reactions. The increase in reactivity in the series benzene, toluene, xylenes is expected in view of the expected hyperconjugative effect of the added methyl groups which would make more electrons "available" to the ring, but on this basis, ethylbenzene should react more slowly than toluene because of the smaller hyperconjugative effect of ethyl compared with methyl. Thus, the data require an additional electron donating effect, which is stronger for ethyl than methyl. This is in agreement with work on the formation of π-complexes in solutions of HCl in these aromatic compounds (*2*), where the conclusion was reached that the alkyl groups promote the formation of the π-complex with HCl primarily through their inductive effect, which is expected to be stronger for ethyl than for methyl. Therefore, in the oxygen atom reactions, the alkyl groups must contribute to the electron density of the aromatic nucleus primarily through the inductive effect. The rate constant for chlorobenzene is also higher than one would expect in view of the ex-

Publication Date: January 1, 1968 | doi: 10.1021/ba-1968-0082.ch008

pected inductive effect of the chlorine atom, which would be expected to decrease the electron density in the ring. However, recent work (5) which considers the effect of substituents on the optical absorption spectrum of benzene leads to the conclusion that a chlorine atom substituent contributes electrons to the ring by the mesomeric effect, which qualitatively supports our data on chlorobenzene. At the same time, the latter work finds a very small mesomeric effect for the fluorine atom, which correlates with the low value for $O\cdot$ + fluorobenzene in Table I.

Therefore, we conclude that the attack of oxygen atoms on the compounds in Table I may be of an electrophilic nature, but that the rather small differences in comparison with the analogous hydrogen atom reactions leaves some doubt as to the meaning and correctness of this conclusion.

Decay of Transient Absorption. The optical absorption decayed significantly over a few milliseconds only at the longer wavelength side of the maximum absorption—*i.e.*, in the region of 300 mμ. (The behavior of the absorption on appreciably longer time scales was obscured by the combination of low optical density and fluctuations in lamp intensity.)

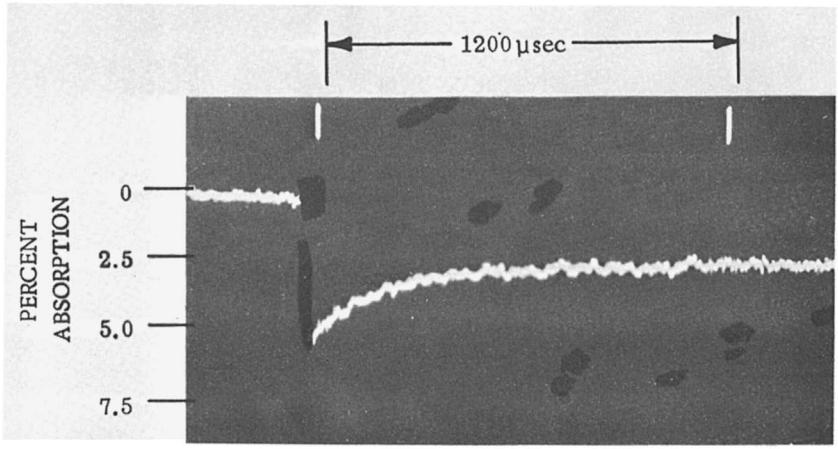

Figure 5. Transient decay at 305 mμ in system containing 56 atm. Ar, 2 atm. CO_2, and 0.09 atm. benzene. The pulse was 80 ma. and 0.4 μsec.; the optical pathlength was 26 cm.

A typical oscilloscope trace is shown in Figure 5. (The decay rate did not change when the argon pressure was varied from 58 to 95 atm., or when the benzene pressure was changed from 2 to 8 cm.). The absorption did not decay to zero, but seemed to reach a plateau of about half of the maximum optical density. Because of "noise" and the difficulty of establishing the plateau, first and second order tests on such decay

Publication Date: January 1, 1968 | doi: 10.1021/ba-1968-0082.ch008

curves were ambiguous. However, by varying the intensity, and thereby the concentration of transient, it was found that the decay became faster with increasing intensity in a manner which indicates that the main path of decay is by bimolecular interaction between transient species except at the lowest intensities where a first order decay of the transient perhaps begins to contribute to the decay. (The first order rate constant is $\gtrsim 2 \times 10^3$ sec.$^{-1}$). The fact that use of deuterated benzene had no appreciable effect on the decay substantiates the argument that the decay is mainly bimolecular, since a first order process such as

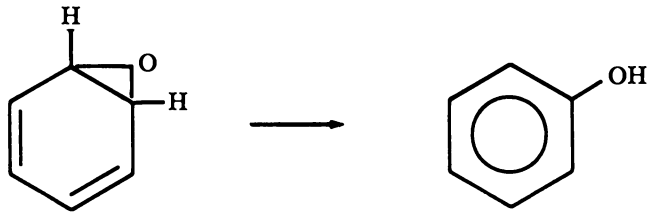

would be expected to be slower with deuterated benzene.

The bimolecular decay of the transient which absorbs at 300 mμ is probably not caused by the interaction of two bi-radical species—*e.g.*,

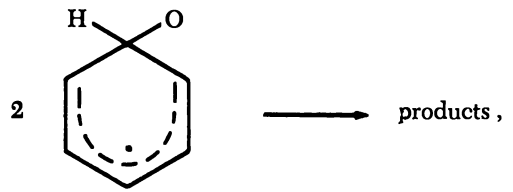

because this would leave unexplained the adsorption at lower wavelengths which does not decay. However, fortuitous combinations of absorption spectra can be imagined which would allow the decay to be ascribed to the bi-radical species (*C*) being converted to *A*, *B*, or phenol. (This phenomenon of partial decay of the longer wavelength portion of the spectrum was also observed for the transients formed from the other organic compounds studied, and the intensity behavior was in general similar.) It is possible that the decay may be related in some way to a conversion involving one or more of the isomeric species benzene oxide (*A*), oxepin (*B*), and phenol. The species *A* and *B* were found (*10*) to be stable in isooctane solution, and to exist in equilibrium with each other and to have optical absorptions at 271 and 305 mμ respectively. Phenol absorbs in the vapor phase at 275.5 mμ, as has been mentioned. Hence, it is tempting to ascribe the decay observed at 305 mμ to a

Publication Date: January 1, 1968 | doi: 10.1021/ba-1968-0082.ch008

disappearance of oxepin. However, it is not clear why this would be a second order decay, and if the oxepin converted to benzene oxide or phenol, the absorption in the 275 region should increase, which was not observed. It appears that there is not enough information to permit a conclusive statement as to which species are responsible for absorptions in the wavelength regions mentioned.

It should be mentioned that an end-product analysis was carried out by gas chromatography. The only product detected corresponded to the retention time of phenol. However, if benzene oxide and oxepin were present, they may have isomerized to phenol during the process of collection and passage through the chromatographic column, or the retention times may have been indistinguishable from that of phenol. (Authentic samples of oxepin and benzene oxide were not available to test these points).

Publication Date: January 1, 1968 | doi: 10.1021/ba-1968-0082.ch008

Acknowledgment

The authors wish to thank B. E. Cliftt, B. J. Naderer, and D. Donkersloot for operating the Linac.

Literature Cited

(1) Arai, S., Sauer, M. C., Jr., *J. Chem. Phys.* **44**, 2297 (1966).
(2) Brown, H. C., Brady, J. D., *J. Am. Chem. Soc.* **74**, 3570 (1952).
(3) Cvetanovic, R. J., "Advances in Photochemistry," Vol. 1, p. 142, W. A. Noyes, Jr., *et al.*, eds., Interscience Publishers, New York and London, 1963.
(4) Mani, I., Sauer, M. C., Jr. (unpublished work).
(5) Murrell, J. N., *Lecture Series 1963*, **No. 2**, The Royal Institute of Chemistry, London, p. 6.
(6) Sauer, M. C., Jr., *J. Phys. Chem.* **71**, 3311 (1967).
(7) Sauer, M. C., Jr., Dorfman, L. M., *J. Am. Chem. Soc.* **87**, 3801 (1965).
(8) Sauer, M. C., Jr., Arai, S., Dorfman, L. M., *J. Chem. Phys.* **42**, 708 (1965).
(9) Sauer, M. C., Jr., Ward, B., *J. Phys. Chem.* **71**, 3971 (1967).
(10) Vogel, E., Günther, H., *Angew. Chem. Intern. Ed.* **6**, 385 (1967).
(11) Williams, G. H., "Homolytic Aromatic Substitution," p. 19, 25, Pergamon Press, New York, 1960.

RECEIVED January 8, 1968. Based on work performed under the auspices of the U. S. Atomic Energy Commission.

Dipole Effects on Hydrogen Atom Transfer in Ion-Molecule Reactions

G. G. MEISELS and L. J. LEGER[1]

University of Houston, Houston, Tex. 77004

Publication Date: January 1, 1968 | doi: 10.1021/ba-1968-0082.ch009

Proton and hydrogen atom transfer has been investigated in the methanol-acetaldehyde system. Combinations of CH_3OH, CD_3OH, CH_3CHO, CD_3CDO, CD_3CHO, and CH_3CDO were employed to allow evaluation of the position from which the transfer occurs, and the ratio plot method (variation of ionizing voltage near the onset of methanol-ion formation) was used to distinguish between proton and hydrogen atom transfer. Proton transfer appears to be determined chiefly by the energetics of the competitive processes, while hydrogen atom transfer is favored from the acetyl and hydroxyl groups by a factor of 3.

In spite of the extensive investigations of ion-molecule reactions by mass spectrometry (*1*), relatively little attention has been paid to the participation of permanent dipoles in the reaction mechanism. Early work noted that the cross section for reactions involving methanol and other species having permanent dipoles appeared to be larger (*25*) than one would expect on the basis of simple ion-induced dipole interaction (*8*). This observation was confirmed by Moran and Hamill (*23*) who proposed a qualitative explanation based on the participation of the permanent dipole and "lock-in" of the dipole on the ion to account for the larger cross section. Walton (*29*) has estimated rate constants but used averaged quantities throughout, an approach already demonstrated to be inadequate even for non-polar systems (*8*). Dugan and Magee subsequently showed that lock-in was an oversimplification, and these authors calculated complete sets of classical trajectories for the collisions in such a system. This resulted in complex relationships which were evaluated by numerical techniques (*7*). In all cases, the main concern was with the effect of the permanent dipole on overall cross section for reaction.

[1] Present address: Manned Spacecraft Center, Houston, Tex.

In Radiation Chemistry; Hart, E.;
Advances in Chemistry; American Chemical Society: Washington, DC, 1968.

The possibility that atom transfer may occur preferentially from the electronegative group has been recognized for some time (*5*). Preliminary work on methylamine suggested that transfer was favored from the NH_2 group (*13*), but this was withdrawn later (*17*).

Harrison has investigated the ion-molecule reactions in a series of specifically labeled polar molecules, but no preference for transfer from the electronegative group was evident, except in such cases where a transfer from the electropositive end of the molecule was endothermic (*11*). Sieck *et al.* (*28*) have also investigated the ion-molecule reactions of specifically labeled methanol and found that transfer from the hydroxyl and the methyl group was equally probable, whether the transferred species was a hydrogen atom or a hydrogen ion. However, with the exception of the methanol system, there is no other experimental support for such a supposition. Lack of specificity might be considered to suggest that the transfer mechanism does not involve a long-lived complex in which the reacting entities can assume a minimum energy configuration before species transfer occurs. Such a mechanism may be indicated in the work of Henglein (*14*), Herman and Wolfgang (*15*), and others.

In attempts to assess the probability of transfer from a particular group, it is necessary to distinguish between the proton and the hydrogen atom transfer since the secondary ion formation by transfer of the charged entity would not necessarily be expected to depend on dipole moment. Separation of these two types of reactions in a homomolecular system is experimentally possible only by the use of tandem mass spectrometers (*28*) or by double resonance ion cyclotron measurements (*2*). However, when mixtures are employed, variations in the ionizing voltage can be used to change the relative abundance of the reacting ions, making possible the quantitative determination of the relative probability of the concurrent ion-molecule reactions leading to the same product (*10, 12, 16, 26, 27*). We have employed this method to assess the extent to which the transfer reactions occur in the methanol-acetaldehyde system.

Experimental

The experiments were performed on a C.E.C. Model 21-103C mass spectrometer modified by including a mercury battery-powered repeller circuit and provisions for low ionizing voltage. All experiments were carried out at a nominal repeller voltage of 2.27 volts as measured on a J. A. Fluke Model 883 differential voltmeter using electron beam currents of 30 and 6 μamp., without affecting results. The linearity of the ion source pressure with the inlet pressure as read on a C.E.C. micromanometer was checked by measuring total ionization (obtained by summing all peaks at 10 e.v. ionizing voltage) and was within experimental error over the pressure range used for the ion-molecule reaction studies.

Publication Date: January 1, 1968 | doi: 10.1021/ba-1968-0082.ch009

The method of evaluating the relative contributions of hydrogen atom and proton transfer depends on measurements at several ionizing voltages. Therefore, experiments were performed as follows. Mixtures of the two compounds under investigation were prepared and admitted into the inlet system at the maximum pressure to be investigated. The mass spectra were taken at ionizing voltages which had previously been shown to lead to a variation of a factor of *ca.* 5 in the relative abundance of the parent ions of the mixture. Five or six determinations were made in this manner; thereafter the pressure was reduced, and the mass spectrum taken once more at the same nominal ionizing voltages. This procedure was repeated three or four times, and the pressure in the inlet system was measured after each expansion using a Trans-sonics, Inc. Equibar micromanometer. Ionizing voltages could be reproduced within about ± 0.01 e.v.

Ordinary acetaldehyde and methanol were obtained in the purest commercially available grade (Matheson, Coleman, and Bell). CD_3OH, CD_3CH_2OH and CD_3CDO were obtained from Merck, Sharp, and Dohme of Canada and had an isotopic purity of approximately 99%. This was verified by low voltage mass spectrometry. CH_3CDO was prepared as described by Leitch (*21*). The desired product was obtained with a yield of only a few percent but of an isotopic purity of better than 90%, as again checked by low voltage mass spectrometry. Moreover, microwave spectrometry was used to assess isotopic purity of these compounds.

Publication Date: January 1, 1968 | doi: 10.1021/ba-1968-0082.ch009

Results

It is qualitatively apparent that reactions of methanol ion will be enhanced at higher ionizing voltages since the ionization potential of methanol exceeds that of acetaldehyde by approximately 0.64 e.v. (*30*). Unfortunately, quantitative measurements in the range where only acetaldehyde ions should be observed is not practical with our equipment because of lack of sensitivity and the energy spread of the electron beam. However, earlier investigations by Hutchison and Pobo (*16*) and Harrison *et al.* (*10, 12, 26, 27*) have shown that relative cross sections can be obtained quantitatively on the following basis.

Consider the reactions

$$CH_3CDO^+ + CH_3OH \rightarrow CH_3OHD^+ + CH_3CO \quad (1)$$

$$CH_3CDO + CH_3OH^+ \rightarrow CH_3OHD^+ + CH_3CO \quad (2)$$

where the product CH_3OHD^+ can result by either of two mechanisms but only if the intermediate complex is heteromolecular. If we designate the phenomenological cross sections as Q_1 and Q_2 and the distance between the electron beam and the exit slit in the ion source as Z the following relationships hold for the secondary ion current.

$$i(CH_3OHD)^+ = ZQ_1 i(CH_3CDO^+) \cdot [CH_3OH] + ZQ_2 i(CH_3OH^+) \cdot [CH_3CDO] \quad (I)$$

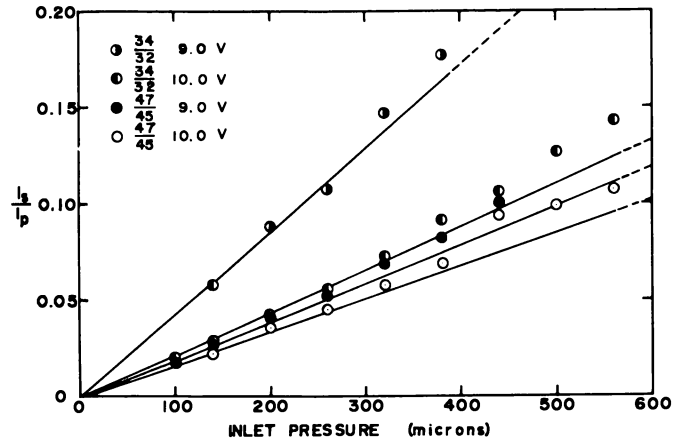

Figure 1. Variation of ion current ratios in mixtures of CH_3CDO and CH_3OH with reservoir pressure. Voltages are nominal

Reaction 1 clearly represents deuteron transfer and Reaction 2 deuterium atom transfer.

The ratio of the secondary ion current to the adjacent methanol primary ion current is given by

$$i(CH_3OHD^+)/i(CH_3OH^+) = ZQ_2[CH_3CDO] + ZQ_1[CH_3OH]\frac{i(CH_3CDO^+)}{i(CH_3OH^+)} \quad \text{(II)}$$

Now the ratio of the primary ion currents on the right side is independent of pressure. The secondary ion current should be directly proportional to pressure provided that a constant mixture composition is maintained. Figure 1 demonstrates that the data are consistent with Equation II. An upward deviation from linearity at higher pressures is expected because of attenuation of the primary ion beam. Since total pressure corresponds to the sum of the concentrations of the reactants, the initial slopes of the plots in Figure 1 are

$$SP = i_s/(i_p \cdot P_{total}) = ZQ_2x(CH_3CDO) + ZQ_1x(CH_3OH)\frac{i(CH_3CDO^+)}{i(CH_3OH^+)} \quad \text{(III)}$$

where x represents the mole fraction of the component. Maintaining constant composition but varying the relative amounts of the parent primary ions by changing ionizing voltage allows one to assess the cross section for the hydrogen atom transfer from the intercept and that of the proton transfer from the slope of the appropriate plot of SP against

Publication Date: January 1, 1968 | doi: 10.1021/ba-1968-0082.ch009

the ratio of the primary ion currents. A mole fraction near 0.5 was used for experimental evaluations to maximize the rate of secondary ion formation from the heteromolecular complex. Typical results are shown in Figures 2 and 3 and are summarized for the four mixtures in Table I, indicated errors representing the average deviation from the mean of three replicate evaluations. While these results are corrected for ^{13}C and ^{18}O isotope contributions, no allowance is made for incomplete deuteration since the experimental error far exceeds any error that could be introduced by the 2 or 3% isotopic impurity.

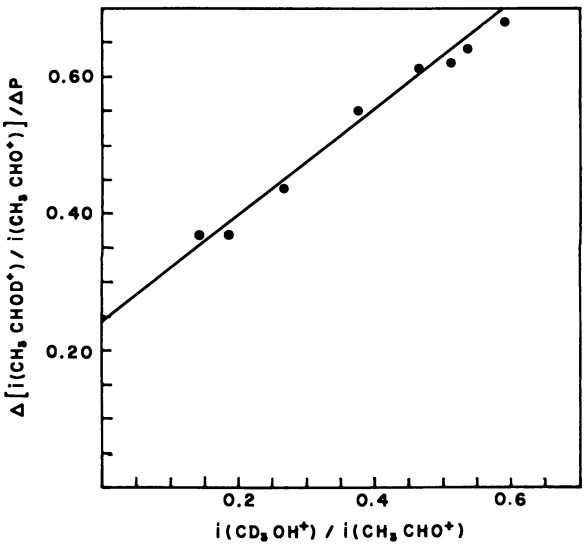

Figure 2. Variation of slopes of plots such as in Figure 1 with primary ion current ratio. Relative cross sections for D and D^+ transfer to acetaldehyde are evaluated from intercept and slope of this plot

The approach was checked for self-consistency by obtaining relative cross sections for the reactions of the undeuterated pure components and their mixtures. Results are summarized in Table II. The slope given in Table II for mixture *G* and designated $Q_{sG} = 8.3$ should be the sum of the cross sections of the reactions which contribute to it: $Q_{pA} + Q_{pB} = 6.0$. The discrepancy is within experimental error. Similarly, $Q_{pC} + Q_{pD} = 7.6$ is within experimental error of $Q_H = 9.0$, while $Q_{iG} = 12.4$ may be compared with $Q_E + Q_{aA} + Q_{aB} = 14.7$ and $Q_{iH} = 14.6$ with $Q_F + Q_{aC} + Q_{aD} = 14.9$.

Although this method appears to give reasonably satisfactory and self-consistent results, there are many complications. The variation of

Publication Date: January 1, 1968 | doi: 10.1021/ba-1968-0082.ch009

ionizing voltage and the change of pressure and hence ion current may affect space charge, contact potentials, collection efficiencies and other parameters with a consequent effect on reaction probability and ion energy. As noted previously, the success of this method and its reproducibility are its best justification (*12, 26*).

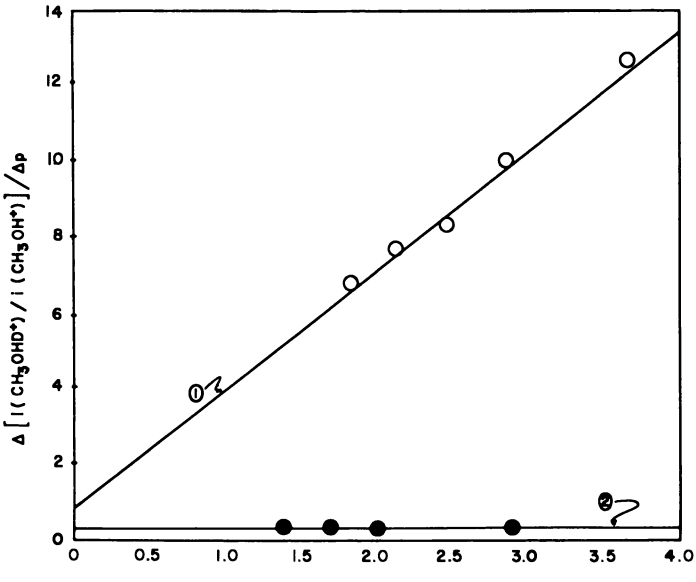

Figure 3. Evaluation of probabilities of hydrogen atom and hydrogen ion transfer from methyl and acyl groups of acetaldehyde to methanol

Curve 1: $i_p(CH_3CDO^+)/i_p(CH_3OH^+)$.
Curve 2: $i_p(CD_3CHO^+)/i_p(CH_3OH^+)$.

Other and probably more severe problems are the formation of fragment ions of low appearance potential and that of long-lived excited ions. Clearly such fragments as CHO^+ which undergo proton transfer reactions with the reactant molecules could seriously alter the results. We have evaluated appearance potentials with reference to Ar and find $AP(CH_3CHO^+) = 10.25 \pm 0.1$ e.v. in good agreement with the literature (10.21 e.v.) (*31*), and $AP(CHO^+) = 13.0 \pm 0.2$ e.v., which may be compared with 12.5 e.v. obtained by the RPD technique (*18*) and *ca.* 13.0 by the second differential method (*6*). The participation of CH_3CO^+, whose appearance potential is approximately 10.5 e.v. (*6*) to 10.9 e.v. (*19*), in ion-molecule reactions is not likely to lead to protium or proton transfer but probably leads to hydride transfer. To minimize the contribution from such reactions the increase in ionizing voltage was terminated

Publication Date: January 1, 1968 | doi: 10.1021/ba-1968-0082.ch009

when fragment ion currents exceeded 10% of the parent ion current. The experimental points at the lowest CH_3OH^+/CH_3CHO^+ ion current ratios must therefore be regarded as more reliable. Unfortunately, it is also in this range that ion currents are reduced significantly so that the signal-to-noise ratio becomes poorer. We have not found any evidence for the charge transfer reaction

$$CH_3OH^+ + CH_3CHO \rightarrow CH_3OH + CH_3CHO^+ \quad (3)$$

which is energetically allowed. This reaction would have been observed under our conditions if it occurred with a cross section of the order of that for proton transfer reactions.

Discussion

If one assumes that every collision leads to a long-lived intermediate complex, one might regard the summary in Table II as a comparison of the fate of intermediates differing only in energy content. Since the ionization potential of methanol is higher, there is 0.64 e.v. additional energy available when the reactant ion is CH_3OH^+. However, the colliding partners will initiate their encounter on different potential energy surfaces.

Table I. Relative Cross Sections of Specific Hydrogen Atom and Hydrogen Transfer Reactions Estimated

		Mixture	
Cross Section	*Ion Current Ratio*	*Proton Transfer* Q_p	*Hydrogen Atom Transfer* Q_a
(A) $CH_3CDO + CH_3OH$	CH_3OHD^+/CH_3OH^+	0. ± 0.2	0.5 ± 0.2
(B) $CD_3CHO + CH_3OH$	CH_3OHD^+/CH_3OH^+	6. ± 1.	1.8 ± 1.
(C) $CD_3CDO + CD_3OH$	CD_3CDOH^+/CD_3CDO^+	4.1 ± 0.6	3.0 ± 0.1
(D) $CH_3CHO + CD_3OH$	CH_3CHOD^+/CH_3CHO^+	3.5 ± 1.	0.8 ± 0.3

Table II. Cross Sections of Ion-Molecule Reactions in Undeuterated Components and Mixtures

		Cross Section	
Mixture	*Ion Current Ratio*	*Intercept* Q_i	*Slope* Q_s
(E) CH_3OH	$CH_3OH_2^+/CH_3OH^+$	12.4	
(F) CH_3CHO	CH_3CHOH^+/CH_3CHO^+	11.1	
(G) $CH_3OH + CH_3CHO$	$CH_3OH_2^+/CH_3OH^+$	12.4	8.3
(H) $CH_3OH + CH_3CHO$	CH_3CHOH^+/CH_3CHO^+	14.6	9.0

Table III. Reactions of CH_3CHO^+ and Reactions of CH_3OH^+

	Relative Cross Section	ΔH(*kcal. mole*$^{-1}$)
(4) $CH_3CHO^+ + CH_3OH \rightarrow CH_3OH_2^+ + CH_3CO$	6. ± 1.	−17.0
(5) $CH_3CHO^+ + CH_3OH \rightarrow CH_3OH_2^+ + CH_2CHO$	0.	−4.0
(6) $CH_3CHO^+ + CH_3OH \rightarrow CH_3CHOH^+ + CH_3O$	3.0 ± .1	−4.0 (+13.0)
(7) $CH_3CHO^+ + CH_3OH \rightarrow CH_3CHOH^+ + CH_2OH$	0.8 ± .3	−5.0 (+12.0)
	$\Sigma Q_M = 9.8 \pm 1.5$	
(8) $CH_3OH^+ + CH_3CHO \rightarrow CH_3CHOH^+ + CH_3O$	4.1 ± .6	−18.0 (−1.0)
(9) $CH_3OH^+ + CH_3CHO \rightarrow CH_3CHOH^+ + CH_2OH$	3.5 ± 1.	−19.0 (−2.0)
(10) $CH_3OH^+ + CH_3CHO \rightarrow CH_3OH_2^+ + CH_3CO$	1.8	−32.0
(11) $CH_3OH^+ + CH_3CHO \rightarrow CH_3OH_2^+ + CH_2CHO$	0.5	−19.0
	$\Sigma Q_A = 9.9 \pm 2$	

There exists more serious objection to any comparison based merely on the energetics: the impossibility of assigning a critical collision radius within which orbiting or capture occurs, and thus the probable absence of any long lived intermediate complex. Therefore, it is preferable to compare the fates of encounters when reaction is initiated only by acetaldehyde ions or solely by methanol ions. Such a regrouping of reactions is shown in Table III, and the energetics of each process (*4*, *19*) are included for comparison. The ion $C_2H_5O^+$ can exist in two configurations (*24*), CH_3CHOH^+ having the lower energy content. The thermodynamic values in parentheses are those calculated for $CH_3CH_2O^+$. It is apparent that the formation of this ion can be excluded from several reactions on energetic grounds.

If product formation proceeded *via* an intermediate long-lived ion whose dissociation were governed by competitive channeling of energy into the possible dissociation coordinates, one would expect the complex to fragment at the weakest bond—*i.e.*, in the most thermodynamically favorable direction. This is clearly not the case. The most exothermic reaction (*17*) does not dominate the fate of the complex formed by collision of methanol ion with acetaldehyde. Similarly, one would expect Reaction 4 to be favored and Reactions 5, 6, and 7 to occur with about equal probability.

An alternate approach to analysis of these results may be based on the separation of hydrogen atom and proton transfer reactions. This

Publication Date: January 1, 1968 | doi: 10.1021/ba-1968-0082.ch009

would indicate that the position from which proton transfer occurs is determined by the energetics of the dissociation since the more exothermic Reaction 4 proceeds at the exclusion of 5, and the thermodynamically nearly equal Reactions 8 and 9 are equally probable. On the other hand, the hydrogen atom transfer, where one might expect participation of the permanent dipole in selecting the group from which transfer occurs, shows a clear preference by a factor of over 3:1 for transfer from the electronegative end of the neutral species.

Such a separation of hydrogen atom and proton transfer reactions implies that the two reaction paths are predestined before the collisions. Although it would be tempting to associate one of these with ion-induced dipole and the other with ion-permanent dipole long-range forces in the manner in which maximum cross sections (*9, 23*) and averaged cross sections (*29*) are calculated, this does not represent the physical reality of the collision process (*7*) which clearly demonstrates the inseparability of these contributions. This is further supported by simple considerations of maximum cross sections based on known polarizabilities and dipole moments (*20, 22*). The ion-induced dipole interaction (*23*) is independent of the nature of the reactant ion in this instance since the disparity of the polarizabilities is exactly balanced by the difference in masses. The ion-dipole interaction should be 16% larger for reactions initiated by methanol ions assuming dipole "lock-in." Our relative cross section measurements are too uncertain to assess the veracity of a slightly higher cross section for CH_3OH^+ but suggest (Table III) that the specificity of the atom transfer from the negative group is independent of dipole moment and that over-all contribution of the neutral transfer is actually smaller when the dipole interaction cross section should be larger. The simple theory of maximum cross sections based on lock-in of the dipole (*9, 23*) cannot readily account for these observations.

Another way in which the reaction rates could be determined *a priori* would be association of one of the two processes with an intimate collision (complex formation) and the other with a transfer at longer ranges, perhaps by a stripping mechanism (*14, 15*). This differs only slightly from the assignment of critical reaction separations completely devoid of the assumption of any contribution of long-lived complexes. In view of the inability to assign a critical capturing radius on theoretical grounds (*7*) the last alternate appears to be the most attractive one.

Acknowledgments

We are indebted to the U.S. Atomic Energy Commission for their support of this research, and to the Manned Spacecraft Center of the National Aeronautics and Space Administration for permission to use

their facilities. We thank James Kluetz for providing the analyses by microwave spectrometry.

Literature Cited

(1) ADVAN. CHEM. SER. **58** (1966).
(2) Baldeschwieler, J. M., *J. Am. Chem. Soc.* **89**, 4569 (1967).
(3) Blatt, A. H., ed., "Organic Synthesis," p. 541, Vol. II, Wiley, New York, 1943.
(4) Calvert, J. G., Pitts, J. N., "Photochemistry," p. 817, Wiley, New York, 1966.
(5) Derwish, G. A. W., Galli, A., Giardini-Guidoni, A., Volpi, G. G., *J. Chem. Phys.* **39**, 1599 (1963).
(6) Dorman, F. H., *J. Chem. Phys.* **42**, 65 (1965).
(7) Dugan, J. V., Magee, J. L., *J. Chem. Phys.* **47**, 3103 (1967).
(8) Gioumousis, G., Stevenson, D. P., *J. Chem. Phys.* **29**, 294 (1958).
(9) Gupta, S. K., Jones, E. G., Harrison, A. G., Myher, J. J., *Can. J. Chem.* **45**, 3107 (1967).
(10) Harrison, A. G., *Can. J. Chem.* **41**, 236 (1963).
(11) Harrison, A. G., Myer, J. J., Thynne, J. C. J. ADVAN. CHEM. SER. **58**, 150 (1963).
(12) Harrison, A. G., Tait, J. M. S., *Can. J. Chem.* **40**, 1986 (1962).
(13) Henchman, M., Ogle, C. H., *Discussions Faraday Soc.* **39**, 63 (1965).
(14) Henglein, A., ADVAN. CHEM. SER. **58**, 63 (1966).
(15) Herman, Z., Kerstetter, J. D., Rose, T. L., Wolfgang, R., *Discussions Faraday Soc.*, in press; *J. Chem. Phys.* **46**, 2844 (1967).
(16) Hutchison, D., Pobo, L., *Proc. Meeting Mass. Spectrometry, 9th*, Chicago, June 1961.
(17) Hyatt, D. J., Dodman, E. A., Henchman, M. J., ADVAN. CHEM. SER. **58**, 131 (1966).
(18) Konomata, I., *Bull. Chem. Soc. Japan* **34**, 1864 (1961).
(19) Lampe, F. W., Franklin, J. L., Field, F. H., *Prog. Reaction Kinetics* **1**, 69 (1961).
(20) Landolt, H. H., Bornstein, R., "Zahlenwerte und Funktionen," p. 515, 6th ed., **Vol. I**, Part III, Springer Verlag Berlin, 1950.
(21) Leitch, L. C., *Can. J. Chem.* **33**, 400 (1965).
(22) Maryott, A. M., Buckley, F., *Natl. Bur. Std. (U.S.) Circ.* **537** (1953).
(23) Moran, R. F., Hamill, W. H., *J. Chem. Phys.* **39**, 1413 (1963).
(24) Munson, M. S. B., Franklin, J. L., *J. Chem. Phys.* **68**, 3191 (1964)
(25) Schissler, D. O., Stevenson, D. J., *J. Chem. Phys.* **24**, 926 (1956).
(26) Shannon, T. W., Harrison, A. G., *J. Chem. Phys.* **43**, 4201 (1965).
(27) *Ibid.*, p. 4206.
(28) Sieck, L. W., Abramson, F. P., Futrell, J. H., *J. Chem. Phys.* **45**, 2859 (1966).
(29) Walton, J. C., *J. Phys. Chem.* **71**, 2763 (1967).
(30) Watanabe, Nakayama, Mottl, *J. Quant. Spectry. Radiative Transfer* **2**, 369 (1962).

RECEIVED January 25, 1968.

ESR Studies of Free Radicals Condensed from Vapors of Acetone, Ethylene, Methyl Alcohol, Ethyl Alcohol, and *tert*-Butyl Alcohol after Irradiation by 1 Mev. He^+ Ions

Publication Date: January 1, 1968 | doi: 10.1021/ba-1968-0082.ch010

W. A. SEDDON and D. R. SMITH

Research Chemistry Branch, Atomic Energy of Canada, Ltd., Chalk River Nuclear Laboratories, Chalk River, Ontario, Canada

Paramagnetic species, generated in the vapor phase in a "crossed-beam" experiment by irradiation with 1 Mev. He^+ ions, have been trapped at 77°K. and detected by electron spin resonance (ESR). This paper describes the results obtained from irradiated methyl-, ethyl-, and tert*-butyl alcohol, acetone, and ethylene. Trapped electrons together with the radicals $\cdot CH_2OH$, $CH_3\dot{C}HOH$, and $(CH_3)_2C(OH)CH_2\cdot$ and $(CH_3)_3C\cdot$ are formed in methyl-, ethyl-, and* tert*-butyl alcohol respectively. Ethyl radicals are formed from ethylene. Acetone gives rise to $CH_3COCH_2\cdot$ and CH_3 radicals and appears to form trapped electrons in the deposit. The results are compared with the radiation chemistry of these systems in the solid and vapor phase.*

Recent studies using a "cross-beam" technique have shown that free radicals produced in the vapor phase by irradiation with 100 e.v. electrons (*18, 22, 23*), 40 Kev. Ar^+ ions (*39*), or 1 Mev. He^+ ions (*34*), can be trapped at 77°K. and studied by ESR. Experiments on water vapor irradiated by 100 e.v. electrons (*22*), or by 1 Mev. He^+ ions (*34*), showed the formation of trapped electrons, e^-_t—a species thought to be the HO_2 radical—and provided indirect evidence for hydrogen atoms (*34*). Cyclohexane, cyclopentane, and benzene gave the same results from 1 Mev. He^+ irradiation (*40*) as from 40 Kev. Ar^+ irradiation (*39*)

In Radiation Chemistry; Hart, E.;
Advances in Chemistry; American Chemical Society: Washington, DC, 1968.

producing cyclohexyl, cyclopentyl, and cyclohexadienyl (C_6H_7) and phenyl (C_6H_5) radicals, respectively. Neither water nor ethyl alcohol formed trapped electrons from Ar^+ irradiation, although earlier results on the He^+ irradiation of water (*34*), and the work on ethyl alcohol reported below, indicate the formation of trapped electrons with the familiar sample coloration and ESR signal. However, the possible introduction of electron scavenging impurities from the Ar^+ apparatus cannot be excluded and may explain the difference between the two methods.

In the belief that the above results have shown the usefulness of the technique for physically demonstrating the identity of paramagnetic species formed in vapor-phase radiolysis, we decided to study some additional compounds, from which it seemed probable that evidence for electrons, hydrogen atoms, or molecular radicals might be obtained. Since the vapor is condensed about 10^{-5} sec. after irradiation, an effort is made to correlate the observed species with the results of conventional radiolysis studies.

This paper reports the results from the 1-Mev. He^+ irradiation of CH_3OH, C_2H_5OH, $(CH_3)_3COH$, CH_3COCH_3, CD_3COCD_3, and C_2H_4. Results of the photolysis of the trapped species are also described. Although these are of separate interest, they often facilitate identifying the initially trapped species since the products are structurally related.

Publication Date: January 1, 1968 | doi: 10.1021/ba-1968-0082.ch010

Experimental

The experimental technique and associated physical parameters have been described in detail (*34, 39*), and only a brief description is included here. A cut-away illustration of the experimental configuration is shown in Figure 1. A stream of deaerated vapor admitted through a nozzle at room temperature is intersected by a well-focused 100-μamp beam of 1 Mev. helium ions in the evacuated (10^{-5} torr) chamber of a Van de Graaff accelerator. The irradiated vapor flows across a 0.8 cm. gap and is then condensed at 77°K. on the quartz cold finger of the Dewar assembly depicted in Figure 1. The resulting deposit is isolated under vacuum by mating the outer quartz finger with the Dewar by a double O-ring seal, and the assembly is then transferred to the sample cavity of a Varian V-4502-04 ESR spectrometer for subsequent analysis. Microwave power measurements were made with a Hewlett Packard 431C power meter and a 3 dB directional coupler. Unless stated otherwise all ESR measurements were made at a cavity input power of 8×10^{-5} watt. Samples can be kept for 8 hours or more allowing subsequent photolysis experiments to be conducted on the deposit. These have been done outside the ESR cavity. Post-irradiation photolysis (photobleaching) of the deposit was accomplished by illuminating with white light or light of wavelength $>$ 5600 A. (filtered through a Corning glass filter No. 3480) from a 500-watt tungsten filament lamp. Ultraviolet light of wavelength 2537 A. was produced with a Mineralight UVS-11 (Ultra-Violet Products, Inc.) and light of wavelength 2500–4000 A. from a PEK

109 high pressure mercury arc lamp filtered through a Corning glass filter No. 9863.

Acetone and methanol (A.R. grade) were used without further purification. *tert*-Butyl alcohol (BDH) was dried over CaO, distilled under vacuum into an ice bath, and recrystallized before use. Absolute ethyl alcohol was dried over CaO and redistilled. Methyl iodide (Baker and Adamson) was singly distilled. Research grade ethylene (Matheson, Ltd.) and acetone-D_6 (99.5% D, Stohler Isotope Chemicals) were used as received. Deaerated samples were prepared either in the vapor phase in a 5-liter flask or distilled directly into the irradiation chamber from the pure liquid stored in a tube.

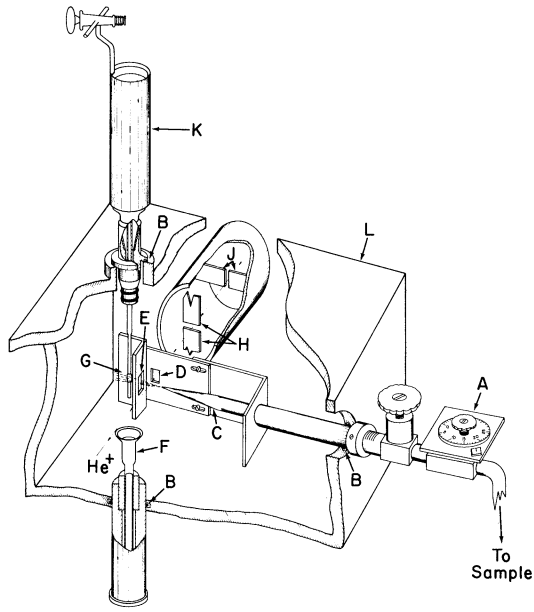

Figure 1. Cut-away view of irradiation chamber

A: Needle valve
B: O ring seals
C: Nozzle
D: He^+ beam aperture
E: Vapor aperture
F: Outer quartz finger
G: Deposit
H and J: Collimating and energy stabilization slits
K: Dewar
L: Target chamber

Results

Methyl-, Ethyl-, and *tert*-Butyl Alcohol. In each case the deposits were noticeably colored, those from methyl- and ethyl alcohol being red-

dish and that from *tert*-butyl alcohol being blue. For methyl- and ethyl alcohol the color and spectra are very similar to the results of previously published work on γ-irradiated methyl- and ethyl alcohol glasses at 77°K. (*1, 8*). As such the spectra are readily assigned to the presence of e^-_t, in addition to the radicals $\cdot CH_2OH$ and $CH_3\dot{C}HOH$, respectively. The $\cdot CH_2OH$ triplet gave an average peak-to-peak hyperfine splitting $A_{H_1} = 19.0 \pm 0.5$ *G*, and the $CH_3\dot{C}HOH$ quintet $A_{H_2} = 22.2 \pm 0.8$ *G*. Photobleaching with visible light removed the red color and associated central ESR singlet and at the same time increased the intensity of the underlying triplet or quintet absorption. However, in both cases even after prolonged photobleaching (30 minutes) a small spike remained superimposed on the central absorption. Within experimental error (± 10–20%) the integrated intensities of the spectra remained the same both before and after photobleaching. In ethyl alcohol the relative concentrations of e^-_t to $CH_3\dot{C}HOH$ were estimated from the integrated areas and the low field line of the radical spectrum giving the ratio 0.2:1.0. The ratio appears similar in methyl alcohol but is more difficult to estimate since the e^-_t signal overlaps the low and high field lines of the radical spectrum. Irradiating the photobleached methyl alcohol spectrum with ultraviolet light (2537 A.) transforms a fraction of the $\cdot CH_2OH$ radicals into formyl radicals, $\cdot CHO$ (*1, 8, 29*), giving the well-recognized doublet, $A_{H_3} = 130$ *G*.

Figure 2A shows the ESR spectrum obtained from *tert*-butyl alcohol. This spectrum is composed of at least three distinct species. A central sin-

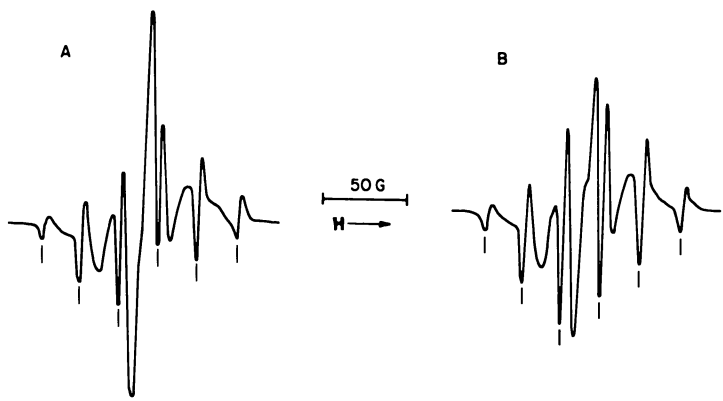

Figure 2. First derivative ESR spectra observed at 77°K. from irradiated $(CH_3)_3COH$ vapor

A: $(CH_3)_3COH$
B: After photobleaching sample in A (equivalent spectrometer gain)
The lines indicate the position of the $(CH_3)_2\dot{C}$· radical

Publication Date: January 1, 1968 | doi: 10.1021/ba-1968-0082.ch010

glet with a peak-to-peak line width $\Delta H_{ms} = 10.4 \pm 0.1$ *G*, is superimposed on an underlying triplet $A_{H_4} \sim 22$ *G*. Six narrow lines, $A_{H_5} = 22.9 \pm 0.2$ *G* are also clearly defined and superimposed on the triplet and singlet spectra. The latter lines are the six most intense of a symmetrical 10-line spectrum, the outer 4 of which can be resolved only at a higher cavity input power (3.5 mwatt) and higher gain. Photobleaching with visible light rapidly removed the blue color and at the same time diminished the intensity of the central singlet absorption (Figure 2B). In addition, the intensity of the 10-line spectrum increased by about 20%. Within experimental error the integrated intensities of the spectra before and after photobleaching were identical.

Acetone. Figure 3A shows the ESR spectrum obtained from CH_3COCH_3. The deposit was pale grey-yellow. This spectrum consists predominantly of a triplet, $A_{H_6} = 21.2 \pm 0.2$ *G*, with a sharp singlet, ΔH_{ms} 7–8 *G*, superimposed on the central line. Photobleaching with visible light or light of wavelength > 5600 A. removes the color of the deposit, decreases the intensity of the singlet, and increases the intensity of the underlying triplet (Figure 3B. The integrated areas of the spectra remained the same before and after photobleaching. At the same time the additional quartet structure (assigned to CH_3 radicals $A_{H_7} = 23.1 \pm 0.2$ *G*) poorly resolved in the unbleached sample becomes more evident. Ultraviolet photolysis of the photobleached sample in Figure 3B with light of wavelength 2537 A. did not affect the spectrum. However, photolysis with ultraviolet light of wavelength 2500–4000 A. for about 20 minutes produced the spectrum shown in Figure 3C. This spectrum is recognized as the original triplet with diminished intensity on which are superimposed CH_3 lines of increased intensity. Photolysis of an acetone blank for a similar period did not produce any ESR signal.

Figure 3D shows the ESR spectrum obtained from irradiated CH_3COCH_3 vapor in the presence of 10 mole % CH_3I. In this case the deposit was rusty brown. The central singlet peak was reduced relative to that in the absence of CH_3I by about 40%, and the relative intensity of the triplet spectrum increased by 100%. In addition the relative intensity of the CH_3 radical spectrum was significantly greater than that in the absence of CH_3I (*cf.* Figures 3A or B).

Deuterated Acetone (CD_3COCD_3). Figure 4A shows the ESR spectrum obtained from CD_3COCD_3. The deposit was pale yellow. Photobleaching with visible light removed the color and an associated ESR absorption giving the seven-line spectrum (Figure 4B), with a hyperfine splitting $A_{D_1} = 3.6$ *G*, superimposed on a broad line. Irradiation with ultraviolet light (2500–4000 A.) gave the spectrum shown in Figure 4C. In addition to a slight improvement in resolution the spectrum differs from that in Figure 4B in that the septet has become more intense, and

Publication Date: January 1, 1968 | doi: 10.1021/ba-1968-0082.ch010

the broad underlying line has been eliminated. Again within experimental error the integrated intensities of the spectra remained the same before and after photobleaching.

Ethylene. In this case a 12-line spectrum was observed arising from the $CH_3CH_2\cdot$ radical (*2*, *12*), giving $A_{H\alpha} = 27.0 \pm 0.8$ *G*, and $A_{H\beta} = 21.1 \pm 1.0$ *G*.

Discussion

Identifying the Radicals. METHYL- AND ETHYL ALCOHOL. The identities of the principal species formed from methyl- and ethyl alcohol are e^-_t, and the radicals $\cdot CH_2OH$ and CH_3CHOH respectively.

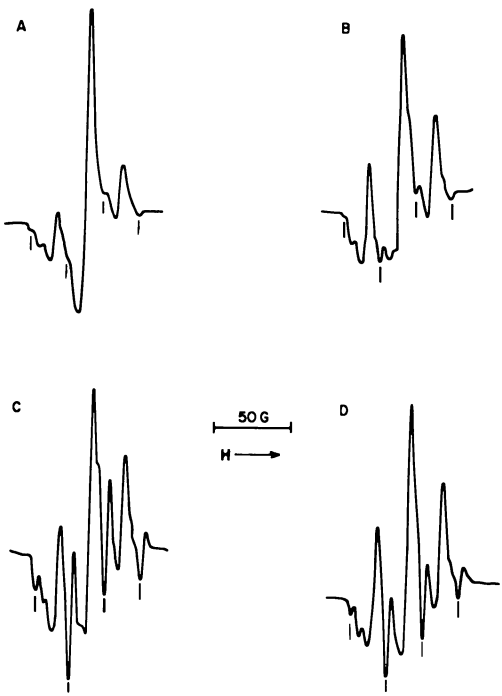

Figure 3. First derivative ESR spectra observed at 77°K. from irradiated CH_3COCH_3 vapor

A: CH_3COCH_3
B: After photobleaching sample in A; relative spectrometer gain, 1.46 × A
C: After ultraviolet (2500–4000 A.) photolysis of sample in B; relative spectrometer gain 1.96 × A
D: CH_3COCH_3 containing 10 mole % CH_3I
The lines indicate the position of the $CH_3\cdot$ radical

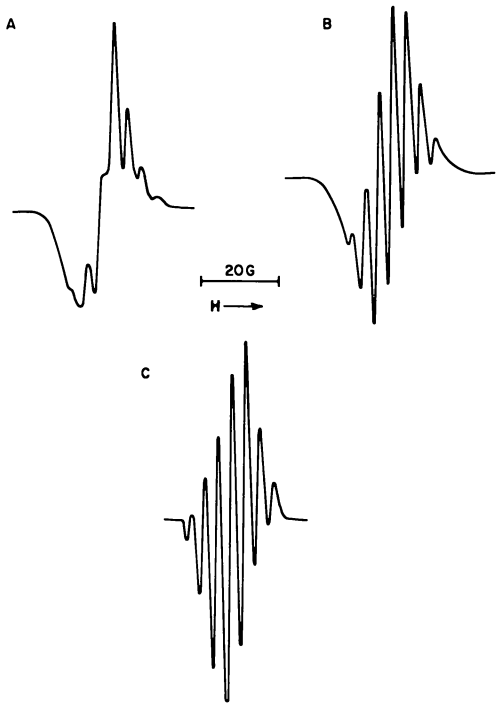

Figure 4. First derivative ESR spectra observed at 77°K. from irradiated CD_3COCD_3 vapor

A: CD_3COCD_3
B: After photobleaching of the sample in A; relative spectrometer gain 1.07 × A
C: After ultraviolet (2500–4000 A.) photolysis of sample in B; relative spectrometer gain 0.95 × A

Publication Date: January 1, 1968 | doi: 10.1021/ba-1968-0082.ch010

The behavior on photobleaching is similar to that of electrons trapped in normal alcohols after γ-irradiation at 77°K. (*1*, *8*, *38*). Likewise, the formation of $\cdot CHO$ radicals from $\cdot CH_2OH$ on irradiation with ultraviolet light leaves no doubt as to the identity of the primary radical (*1*, *8*, *29*). The presence of a small spike on the central peak of both radical spectra after prolonged photobleaching suggests that a small fraction of alkoxy or peroxy radicals may be present.

tert-Butyl Alcohol. The blue color and associated ESR singlet arise from e^-_t. Trapped electrons in *tert*-butyl alcohol have an optical absorption spectrum with a maximum around > 7000 A. (*5*) and appear blue, whereas in methyl- and ethyl alcohol this is shifted toward 5000 A. (*1*). The triplet would be expected from the radical $(CH_3)_2C(OH)CH_2\cdot$. The

value A_{H_4} compares well with that of 21.3 *G* obtained for this radical in aqueous solutions of *tert*-butyl alcohol by Dixon and Norman (*10*), and 21 ± 1 *G* in γ-irradiated *tert*-butyl alcohol at 77°K. (*9*). The 10-line spectrum is assigned to the *tert*-butyl radical $(CH_3)C\cdot$, and the value of A_{H_5} agrees with previous values for this radical of 22.5 ± 0.8 *G* (*2*), and 22.7 *G* (*12*).

Trapped electrons are not produced in *tert*-butyl alcohol by γ-irradiation in the solid phase (*7*, *9*). They are produced and trapped in this matrix by a special technique of depositing alkali-metal atoms on *tert*-butyl alcohol at 77°K. as demonstrated by Bennett *et al.* (*5*). The ultimate fate of these trapped electrons was not established since no additional radical species were observed on photo- or thermal bleaching (*6*). In our case *tert*-butyl radicals are produced on photobleaching the trapped electrons. Possible reasons for this difference are discussed later.

ACETONE. The spectra obtained in this study are similar to those previously reported by Pukhal'skaya *et al.* (*32*), in γ-irradiated acetone at 77°K. Again the central superimposed singlet absorption is thought to be caused by e^-_t. This singlet disappears on photobleaching to produce a corresponding amount of the underlying triplet absorption. Pukhal'skaya *et al.* (*32*) also observed such a singlet but did not discuss its identity or fate on photobleaching. The triplet splitting is attributed to the acetonyl radical $CH_3COCH_2\cdot$, the value of A_{H_6} agreeing well with the corresponding constants for this radical of 20 *G* in a similar matrix (*32*) and 19.75 and 20.3 *G* in acetone solutions (*11*, *44*). This assignment is confirmed by the results of ultraviolet photolysis on the deposit. The acetonyl radical photolyzes with light of wavelength ~ 3000 A. as in Reaction 1, to give ketene and CH_3 radicals (*32*, *44*).

$$CH_3COCH_2\cdot \xrightarrow{h\nu} CH_2{=}C{=}O + CH_3\cdot \qquad (1)$$

The growth of CH_3 radicals is apparent in Figure 3C.

DEUTERATED ACETONE. In this case the initial spectra, Figure 4A, can be attributed to the presence of a singlet caused by e^-_t and a septet caused by CD_3 superimposed on a wide line arising from $CD_3COCD_2\cdot$ (the quintet is unresolved). Photobleaching with visible light removes the e^-_t singlet and enhances the resolution of the CD_3 septet (Figure 4B), but the underlying $CD_3COCD_2\cdot$ spectrum remains unresolved. Subsequent irradiation with 2500–4000-A. light removes the $CD_3COCD_2\cdot$ radical and its underlying spectrum *via* Reaction 1, leaving only the CD_3 radical (Figure 4C). Taking the known ratio of H:D hyperfine splitting constants as 6.5 (*12*), and the proton hyperfine splitting $A_{H_7} = 23.1$ *G* for CH_3 radicals, then the calculated value for $A_{D_1} = 3.55$ *G*, in excellent agreement with the experimental value of 3.6 *G* for $CD_3\cdot$ radicals.

Publication Date: January 1, 1968 | doi: 10.1021/ba-1968-0082.ch010

ETHYLENE. The radical obtained here is the ethyl radical. The values for A_{H_α} and A_{H_β} compare well with values in the literature (*2, 12*).

Radiolysis Mechanisms. In the earlier work (*34*) with water vapor a number of parameters relevant to understanding the experimental system were discussed in detail. These are summarized in Table I for H_2O and D_2O. Briefly, it can be calculated that given a pressure in the irradiated vapor stream of $\sim$ 0.05 torr, second- or third-order processes of radical decay cannot occur in the vapor phase on a time scale $< 10^{-5}$ sec. On the other hand, ion-molecule reactions with a rate constant $k \sim 5 \times 10^{-10}$ cc./molecule-sec. (*16*), could have reaction half-lives of this order and may go to completion before condensation at 77°K. However, it is possible for radical-scavenger reactions to occur in this system. For example, it was shown that 0.14 mole % CH_3I reacts readily with electrons produced from irradiated water vapor to give CH_3 radicals (*34*). We suggested that this reaction may occur in the transient liquid phase immediately before solidification at 77°K. Irrespective of the phase where such a reaction occurs, it can be used for detecting the presence of electrons.

Table I. Parameters Used

Deposition rate	$\sim$	0.1 gm./15 minutes
Pressure	=	0.05 torr
Velocity of molecules in vapor stream	=	5.5×10^4 cm./sec.
Transit time between irradiation and deposition	=	1.4×10^{-5} sec.
Ion beam	=	100 μamp, 1 Mev. He^+
$-dE/dX$	=	1.6 Kev./μgram/sq. cm.
Dose		3.5×10^{19} e.v./gram
Vapor collection efficiency	$\sim$	40%

METHYL-, ETHYL-, AND *tert*-BUTYL ALCOHOL. Reactions 2 and 3a may be written for methyl alcohol and are well established in the solid and vapor phase (*8, 19, 33*).

$$CH_3OH \rightarrow CH_3OH^+ + e^- \quad (2)$$

$$CH_3OH^+ + CH_3OH \rightarrow \cdot CH_2OH + CH_3OH_2^+ \quad (3a)$$

The alternative reaction (3b), is expected to produce $CH_3O\cdot$ radicals in approximately equal quantities (*19*), but we cannot be certain of their presence in our experiment.

$$CH_3OH^+ + CH_3OH \rightarrow CH_3O^\cdot + CH_3OH_2^+ \quad (3b)$$

Further, conversion of alkoxy to hydroxy alkyl radicals is exothermic (*15*).

The results of recent mass spectrometric studies by Sieck *et al.* (*37*) support the occurrence of a reaction analogous to Reaction 3a in ethyl alcohol. This work corrects the earlier suggestion by Ryan *et al.* (*33*) that only the ion CH_3CHOH^+ contributes significantly to the formation of $CH_3CH_2OH_2^+$ in ethyl alcohol at elevated pressures. Myron and Freeman (*30*) indicate that Reaction 4 occurs only in the liquid phase radiolysis of ethyl alcohol.

$$CH_3CH_2OH^+ + CH_3CH_2OH \rightarrow CH_3CH_2OH_2^+ + CH_3CH_2O\cdot \qquad (4)$$

This may be possible in our system during the condensation process.

In *tert*-butyl alcohol a reaction analogous to Reaction 2 followed by Reaction 5 is consistent with the formation of $(CH_3)_2C(OH)CH_2\cdot$ radicals and trapped electrons.

$$(CH_3)_3COH^+ + (CH_3)_3COH \rightarrow (CH_3)_2C(OH)CH_2\cdot + (CH_3)_3COH_2^+ \qquad (5)$$

An alternative process involving fragmentation of the parent positive ion cannot be excluded. *tert*-Butyl radicals may be formed by the charge neutralization process.

$$(CH_3)_3COH_2^+ + e^- \rightarrow (CH_3)_3C\cdot + H_2O \qquad (6)$$

This reaction could also be responsible for the formation of *tert*-butyl radicals on photobleaching the trapped electrons. No such effect was observed by Bennett *et al.* (*6*) because Na^+ is the parent ion in their experiment. In their system protonated alcohol ions are not formed, and Reaction 6 is not possible. Apparently in *tert*-butyl alcohol the electrons on photobleaching do not react with the parent alcohol contrary to the behavior observed with alcohols containing an α-hydrogen atom (*6, 36*). In γ-irradiated *tert*-butyl alcohol both $(CH_3)_2C(OH)CH_2\cdot$ and $(CH_3)_3C\cdot$ are observed (*9*), and the electrons presumably disappear by Reaction 6 rather than becoming trapped.

ACETONE. In acetone the predominant species is the acetonyl radical, $CH_3COCH_2\cdot$. Acetone is well known as an electron scavenger in the radiation chemistry of aqueous solutions (*17*), and it was thought that the acetone negative ion, $CH_3COCH_3^-$, might have been detected. Instead a species thought to be trapped electrons was observed, which on photobleaching gave rise to additional $CH_3COCH_2\cdot$ radicals. In support of this we find that adding 10 mole % CH_3I decreases the intensity of the singlet superimposed on the acetonyl triplet and at the same time produces additional CH_3 radicals. This is consistent with Reaction 7, followed by Reaction 8 in competition with the trapping process

$$CH_3COCH_3 \rightarrow CH_3COCH_3^+ + e^- \ (\rightarrow e^-_t) \qquad (7)$$

Publication Date: January 1, 1968 | doi: 10.1021/ba-1968-0082.ch010

$$CH_3I + e^- \rightarrow CH_3\cdot + I^- \quad (8)$$

In the vapor phase the formation of acetonyl radicals *via* neutral dissociation and free radical processes (Reactions 9 and 10), is well established in both photochemistry (*21*) and radiation chemistry (*3, 41, 42*).

$$CH_3COCH_3^* \rightarrow CH_3COCH_2\cdot + H\cdot \quad (9)$$

$$CH_3COCH_3 + H\cdot \rightarrow CH_3COCH_2\cdot + H_2 \quad (10)$$

In the photolysis of liquid acetone, Reaction 11, also involving an excited state of acetone, is an important source of acetonyl radicals (*44*).

$$CH_3COCH_3^* + CH_3COCH_3 \rightarrow (CH_3)_2\dot{C}OH + CH_3COCH_2\cdot \quad (11)$$

We have no definite evidence for the presence of $(CH_3)_2\dot{C}OH$ radicals although a weak unidentified absorption, detected at high gain, is present in the "wings" of the spectrum shown in Figure 3A. Acetonyl radicals could also be produced by an ion-molecule reaction such as Reaction 12.

$$CH_3COCH_3^+ + CH_3COCH_3 \rightarrow CH_3COCH_2\cdot + (CH_3COCH_3)H^+ \quad (12)$$

Shida and Hamill (*35*) indicate that Reaction 12 does occur in the mass spectrometer.

Positive ions must be associated with trapped electrons in the deposit since the negative potential otherwise generated at the cold finger would give a field strength of about 10^7 volts/cm. (*34*). This situation is most unlikely. Since on photobleaching the total number of paramagnetic species remains constant, the fate of the electron can be ascribed to either Reaction 13 or 14.

$$CH_3COCH_3^+ + e^- \rightarrow CH_3\dot{C}OCH_2 + H\cdot \ (\rightarrow H_2) \quad (13)$$

$$(CH_3COCH_3)H^+ + e^- \rightarrow CH_3\dot{C}OCH_2 + H_2 \quad (14)$$

The vapor-phase radiolysis of acetone is known to yield mainly CO, CH_4, C_2H_6, C_2H_4, and H_2 (*3, 41*). Methane together with acetonyl radicals results from the reaction of CH_3 radicals with acetone *via* Reaction 15.

$$CH_3\cdot + CH_3COCH_3 \rightarrow CH_4 + CH_3\dot{C}OCH_2 \quad (15)$$

Some evidence that this can also occur in our system is seen from the increased yield of acetonyl radicals in the presence of CH_3I. This is consistent with the occurrence of Reaction 8 followed by Reaction 15. A similar sequence of reactions can be written for deuterated acetone.

In γ-irradiated acetone at 77°K. Shida and Hamill (*35*) observed a broad optical absorption band assigned to the presence of $CH_3COCH_3^+$ and $CH_3COCH_3^-$ molecular ions. No ESR signal of the anion was detected in their work, and its absence was attributed to extreme dipolar broadening. The ESR spectrum of the anion is known to be a septet, $\Delta H = 16.1$ *G* (*4*), whereas the ESR spectrum of γ-irradiated acetone at

Publication Date: January 1, 1968 | doi: 10.1021/ba-1968-0082.ch010

77°K. consists of a singlet superimposed on a triplet (*1, 32*), the triplet spectrum being assigned to the acetonyl radical. Blandamer *et al.* (*7*) and Nitta *et al.* (*31*) also observed a singlet assigned to trapped electrons in γ-irradiated acetone at 77°K.

ETHYLENE. The radiolysis and photolysis of ethylene have been studied extensively, and again both dissociation and free radical processes are well established. A review by Meisels (*28*) and the references therein discuss the mechanisms in detail. In our experiment the detection of ethyl radicals clearly indicates the prior formation of H atoms, a major primary radical in ethylene radiolysis (*27*).

$$C_2H_4 + H\cdot \rightarrow C_2H_5\cdot \qquad (16)$$

The importance of ion-molecule reactions in ethylene involving the primary ions $C_2H_4^+$, $C_2H_3^+$, and $C_2H_2^+$ is now well documented in mass spectrometry (*13, 20, 43*), photolysis (*14*), and radiation chemistry (*24, 25, 26, 28*). However, electrons were not detected in this work, and hence their fate was not established.

Publication Date: January 1, 1968 | doi: 10.1021/ba-1968-0082.ch010

Conclusions

Our results are consistent with the radiation chemistry data for most of these systems in the solid phase and with the occurrence of reactions well established in vapor phase radiolysis. In the alcohols (and to some extent in acetone) the formation of the principal radical species seems best explained on the basis of ionization, followed by an ion-molecule reaction and subsequent trapping of the appropriate radicals in the frozen matrix at 77°K. As in the case of water (*34*), electrons can be stabilized in a non-glassy matrix.

The main value of this method lies in identification of the paramagnetic species produced in the vapor phase. Less significance should be attached to the relative yields of e^-_t and/or radicals because of the large uncertainty in the ratio of the number formed to these actually trapped in the deposit.

Acknowledgment

We are grateful to P. E. Bindner for technical assistance and to G. A. Sims for his operation of the accelerator and preparation of some of the diagrams.

Literature Cited

(1) Alger, R. S., Anderson, T. H., Webb, L. A., *J. Chem. Phys.* **30,** 695 (1959).
(2) Ayscough, P. B., Thomson, C., *Trans. Faraday Soc.* **58,** 1477 (1962).

(3) Ausloos, P., Paulson, J. F., *J. Am. Chem. Soc.* **80,** 5117 (1958).
(4) Bennett, J. E., *Nature* **203,** 514 (1964).
(5) Bennett, J. E., Mile, B., Thomas, A., *J. Chem. Soc.* **A,** 1393 (1967).
(6) Bennett, J. E., Mile, B., Thomas, A., *J. Chem. Soc.* **A,** 1399 (1967).
(7) Blandamer, M. J., Shields, L., Symons, M. C. R., *J. Chem. Soc.* **1965,** 1127.
(8) Chachaty, C., Hayon, E., *J. Chim. Phys.* **61,** 1115 (1964).
(9) Chachaty, C., Perrin, F., *Compt. rend., Sér. C.* **259,** 2219 (1964).
(10) Dixon, W. T., Norman, R. O. C., *J. Chem. Soc.* **1963,** 3119.
(11) Dixon, W. T., Norman, R. O. C., Buley, A. L., *J. Chem. Soc.* **1964,** 3625.
(12) Fessenden, R. W., Schuler, R. H., *J. Chem. Phys.* **39,** 2147 (1963).
(13) Field, F. H., *J. Am. Chem. Soc.* **83,** 1523 (1961).
(14) Gorden, R., Jr., Ausloos, P., *J. Chem. Phys.* **47,** 1799 (1967).
(15) Gray, P., Shaw, R., Thynne, J. C. J., *Progr. Reaction Kinetics* **4,** 63 (1967).
(16) Harrison, A. G., Myher, J. J., Thynne, J. C. J., ADVAN. CHEM. SER. **58,** 150 (1966).
(17) Hart, E. J., Gordon, S., Thomas, J. K., *J. Phys. Chem* **68,** 1271 (1964).
(18) Horani, M., Leach, S., *J. Chim. Phys.* **58,** 825 (1961).
(19) Hyatt, D. J., Dodman, E. A., Henchman, M. J., ADVAN. CHEM. SER. **58,** 131 (1966).
(20) Kebarle, P., Hogg, A. M., *J. Chem. Phys.* **42,** 668 (1965).
(21) Leiga, A. G., Taylor, H. A., *J. Chem. Phys.* **41,** 1247 (1964).
(22) Marx, R., Leach, S., Horani, M., *J. Chim. Phys.* **60,** 726 (1963).
(23) Marx, R., Maruani, J., *J. Chim. Phys.* **61,** 1604 (1964).
(24) Meisels, G. G., *J. Chem. Phys.* **42,** 2328 (1965).
(25) *Ibid.*, p. 3237.
(26) Meisels, G. G., Sworski, T. J., *J. Phys. Chem.* **69,** 2867 (1965).
(27) Meisels, G. G., *J. Am. Chem. Soc.* **87,** 950 (1965).
(28) Meisels, G. G., ADVAN. CHEM. SER. **58,** 243 (1966).
(29) Milliken, S. B., Johnsen, R. H., *J. Phys. Chem.* **71,** 2116 (1967).
(30) Myron, J. J. J., Freeman, G. R., *Can. J. Chem.* **43,** 1484 (1965).
(31) Nitta, I., Ohnishi, S., Sugimoto, S., Kuwata, K., *Ann. Rept. Japanese Assoc. Radiation Res. Polymers* **6,** 283 (1964-1965).
(32) Pukhal'skaya, G. V., Kotov, A. G., Pshezhetskii, S. Ya., *Russ. J. Phys. Chem.* **40,** 382 (1966).
(33) Ryan, K. R., Sieck, L. W., Futrell, J. H., *J. Chem. Phys.* **41,** 111 (1964).
(34) Seddon, W. A., Smith, D. R., Bindner, P. E., *Can. J. Chem.* **46,** 1747 (1968).
(35) Shida, T., Hamill, W. H., *J. Am. Chem. Soc.* **88,** 3683 (1966).
(36) *Ibid.*, p. 3689.
(37) Sieck, L. W., Abramson, F. P., Futrell, J. H., *J. Chem. Phys.* **45,** 2859 (1966).
(38) Smaller, B., Matheson, M. S., *J. Chem. Phys.* **28,** 1169 (1958).
(39) Smith, D. R., Tole, J. C., *Can. J. Chem.* **45,** 779 (1967).
(40) Smith, D. R., Seddon, W. A., unpublished results.
(41) Stief, L. J., Ausloos, P., *J. Phys. Chem.* **65,** 1560 (1961).
(42) Strong, J. D., Burr, J. G., *J. Am. Chem. Soc.* **81,** 775 (1959).
(43) Wexler, S., Marshall, R., *J. Am. Chem. Soc.* **86,** 781 (1964).
(44) Zeldes, H., Livingston, R., *J. Chem. Phys.* **45,** 1946 (1966).

RECEIVED December 26, 1968. Issued as AECL No. 3105.

11

Collisional Excitation Transfer in the Gas Phase

TSUTOMU WATANABE[1]

Radiation Laboratory, University of Notre Dame, Notre Dame, Ind.

Publication Date: January 1, 1968 | doi: 10.1021/ba-1968-0082.ch011

The cross sections of processes $A^* + A \rightarrow A + A^*$, $A^* + B \rightarrow A + B^*$, *and* $A^* + B \rightarrow A + B^+ + e$ *have been studied theoretically. The cross sections are sometimes large (of the order of* $10^2 \sim 10^3$ *sq. A. at thermal energies) compared with those of other processes. Some typical examples of the calculated cross sections are listed, mainly for "optically allowed" excitations. Calculations for other cases are mentioned briefly. Relations with gas-phase experiments (*e.g., *the pressure effect of excitation transfer, the temperature effect of spectral line width, etc.) are also discussed.*

The importance of electronic excitation transfer processes is sometimes emphasized in radiation chemistry. In both the condensed and gas phase this process should be taken into account. The cross sections of such transfer processes are sometimes extremely large (of the order of $10^2 \sim 10^3$ sq. A. at thermal energies) compared with gas kinetic cross sections. The excitation transfer processes can be represented by:

(Case 1: discrete-discrete exact resonant process)

$$A^* + A \rightarrow A + A^* \quad (1)$$

(Case 2: discrete-discrete near-resonant process) and

$$A^* + B \rightarrow A + B^* \quad (2)$$

(Case 3: discrete-continuum process)

$$A^* + B \rightarrow A + B^+ + e \quad (3)$$

A and B denote atoms, and A* and B* denote their electronically excited states. The discrete-discrete nonresonant process is excluded from this

[1] Permanent address: Department of Applied Physics, University of Tokyo, Bunkyo-ku, Tokyo, Japan.

In Radiation Chemistry; Hart, E.;
Advances in Chemistry; American Chemical Society: Washington, DC, 1968.

discussion because the cross section will be of the same order as gas-kinetic cross sections or less. The discrete-continuum process is always possible if the excitation energy of A exceeds the ionization potential of B.

There are many theoretical and experimental investigations concerning a charge transfer process like $A^+ + B \rightarrow A + B^+$ (*27, 28, 49*). On the other hand, a theoretical investigation of the electronic excitation transfer problem had already been undertaken by Kallmann, London, and Rice (*24, 32, 57*) in the early stages of the development of quantum mechanics. Nevertheless, the excitation transfer problem has not yet been actively studied because it is difficult to measure the cross section directly. For the last few years, theoretical calculations for these processes have been attempted by several authors. This paper describes recent studies on the excitation transfer between atoms in gas phase. Most excitations treated here are optically allowed. The transfer processes of metastable excitation are briefly mentioned. Relations with some experiments are also discussed.

Publication Date: January 1, 1968 | doi: 10.1021/ba-1968-0082.ch011

Impact Parameter Method

When colliding particles are heavy and their interactions are long range, the impact parameter method conveniently describes the problem (*9, 10, 32, 57*). This method is based on the concept that the motion of nucleus is described classically and that of electrons is described quantum mechanically. If the angular momentum of colliding system is larger than $\hbar$, the trajectory of an incident or a scattered particle can be defined. The impact parameter method will be useful where the total scattering is determined mainly by these processes.

Like a charge transfer process ($A^+ + B \rightarrow A + B^+$), this method is available for an excitation transfer process. Figure 1 is a schematic of the trajectory of the nucleus with impact parameter R_o. Here, we take a straight-line trajectory approximation for nuclear motion as in the charge transfer process (*26*). The equivalence of the Born approximation in the quantum mechanical treatment to the straight line trajectory in the impact parameter treatment has been discussed and verified (*3*). The straight-line approximation here is more easily applied than that for charge transfer process. The trajectory will hardly be affected by the interaction between neutral particles. The straight-line approximation is valid if incident kinetic energy is much larger than the potential energy of an incident particle in interacting region (*69*). Let us suppose Ψ the total electronic wavefunction of the system (A +A or A + B), and H a total Hamiltonian. H consists of a time-independent unperturbed Hamiltonian H_o and a time-dependent perturbing one $H'(t)$. Ψ is

assumed to be expressed in terms of linear combinations of eigenfunctions of H_o, *i.e.*, ψ_i, as

$$\Psi = \sum_i C_i(t)\psi_i e^{-iE_i t/\hbar}. \tag{4}$$

Here the coefficient C_i is a function of time. The function ψ_i satisfies the equation:

$$H_o\psi_i = E_i\psi_i \tag{5}$$

which is independent of time, and ψ_i can be expressed by a simple (or an antisymmetrized, if necessary) product of each atomic orbital as

$$\psi_1 = \phi_{A*}\phi_B \text{ or } \phi_A\phi_{B*}. \tag{6}$$

Here we denote A and B as the incident and target atom, respectively (even for Case 1). By substituting Equation 6 into the Schrödinger equation of the system $[i\hbar(\partial/\partial t)\Psi = H\Psi]$, and with aid of Equation 5 we obtain simultaneous equations for $C_i(t)$:

$$i\hbar \frac{dC_i(t)}{dt} = \sum_j H_{ij}'(t)C_j(t). \tag{7}$$

Here $H_{ij}'(t)$ is the i-j component of the interaction representation matrix, *i.e.*, $< \psi_i|H'(t)|\psi_j >$ exp $(-i(E_i - E_j)t/\hbar$. If we set an initial condition $C_i(-\infty) = 1$ and $C_j(-\infty) = 0$ for $i \neq j$ (time goes from $-\infty$ to ∞), a transition probability for $i \to j$ of a given trajectory (or a given impact parameter) is written by

$$P_{i\to j} = |C_j(\infty)|^2. \tag{8}$$

A cross section for $i \to j$ is given by the integration of $P_{i\to j}$ over impact parameter R_o as

$$\sigma(i \to j) = 2\pi \int P_{i\to j} R_o dR_o. \tag{9}$$

We introduce a vector **C** which consists of $Ci(t)$ $(i = 1, 2 \ldots)$. *i.e.*,

$$\mathbf{C} = \begin{bmatrix} C_1(t) \\ C_2(t) \\ \cdot \\ \cdot \\ C_i(t) \\ \cdot \\ \cdot \\ \cdot \end{bmatrix}, \tag{10}$$

and an interaction matrix **A** whose $i - j$ component is $H_{ij}'(t)/i\hbar$. Equation 7 can be rewritten by a single operator-differential equation:

$$\frac{d}{dt}\mathbf{C}(t) = \mathbf{A}\mathbf{C}(t) \tag{11}$$

Publication Date: January 1, 1968 | doi: 10.1021/ba-1968-0082.ch011

This time-evolution equation can be solved by iteration. A solution at $t = t$ is given by

$$\mathbf{C}(t) = \left(\sum_{n=0}^{\infty} \mathbf{B}_n \right) \mathbf{C}(-\infty) \tag{12}$$

where

$$\mathbf{B}_n = \int_{-\infty}^{t} \mathbf{A}(t_1)dt_1 \int_{-\infty}^{t_1} \mathbf{A}(t_2)dt_2 \cdots \int_{-\infty}^{t_{(n-1)}} \mathbf{A}(t_n)dt_n$$

and $\mathbf{B}_0 = \mathbf{1}$ (unit matrix). We denote $\mathbf{u}_j$ unit vector whose components are $u_i = 1$ for $i = j$ and $u_i = 0$ for $i \neq j$. The projection of the vector $\mathbf{C}(t)$ to jth component $C_j(t)$ can be obtained by the inner product of $[\mathbf{u}_j \cdot \mathbf{C}(t)]$. If $\mathbf{C}(-\infty) = \mathbf{u}_i$, $P_{i \to j}$ is written by

$$P_{i \to j} = |(\mathbf{u}_j \cdot \mathbf{C}(\infty))|^2. \tag{13}$$

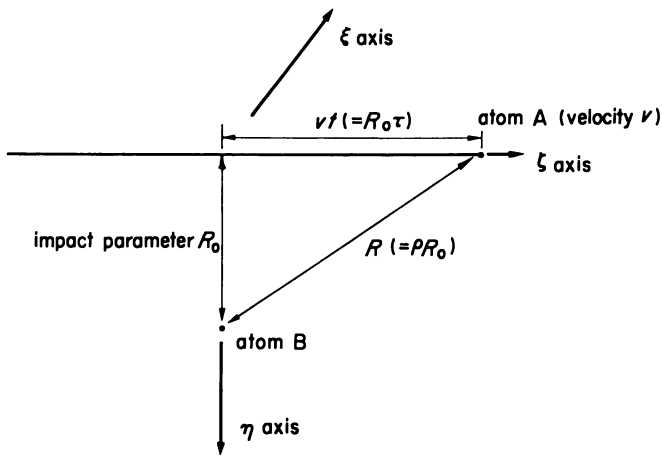

Figure 1. Schematic of the colliding system and direction of the coordinates used. Atom B is located at rest at a distance R_0 *from the incident path, and atom A moves along the straight line with constant velocity* v

S-P Type Interaction

Discrete-Discrete Resonant Process. We consider a case where A, A*, B, and B* are in *S,P,S,* and *P* states or *P,S,P,* and *S* states (with respect to total angular momenta), respectively (*47, 67, 68*). In this case the transfer of the excitation occurs by the so-called induced dipole-dipole interaction. In like-atom case (Case 1), calculations for the probability and the cross section can be obtained.

Publication Date: January 1, 1968 | doi: 10.1021/ba-1968-0082.ch011

The interaction Hamiltonian $H'(t)$ is a usual interatomic type, and is written

$$H'(t) = \frac{Z_A Z_B e^2}{R} - \sum_{\mu} \frac{Z_B e^2}{r_{b\mu}} - \sum \frac{Z_A e^2}{r_{a\nu}} + \sum_{\mu > \nu} \frac{e^2}{r_{\mu\nu}}, \tag{14}$$

where e is electronic charge, Z_A, Z_B are the nuclear charge of A and B, in e unit and R, $r_{b\mu}$, $r_{a\nu}$, and $r_{\mu\nu}$ are distances between A-B, B-μ, A-ν and μ-ν. Here μ and ν are labeled on electrons, and μ and ν belong to A and B, respectively. If $R >$ atomic dimensions, the interaction $H'(t)$ can be expanded in terms of Legendre polynomials (multipole expansion). In the case of S-P type interactions $H'(t)$ can be reduced to a dipole-dipole type interaction:

$$H'(t) = \frac{e^2}{R^3} \{ \sum_{\mu\nu} (\mathbf{r}_{a\mu} \cdot \mathbf{r}_{b\nu}) - 3 \sum_{\mu,\nu} r_{a\mu} \cos \theta_{a\mu} r_{b\nu} \cos \theta_{b\nu} \} \tag{15}$$

where $\mathbf{r}_{a\mu}$, r_{au} are a position vector of μ from nucleus A and its magnitude, and $\theta_{a\mu}$ is an angle between $\mathbf{r}_{a\mu}$ and coaxis AB, and so on. Other terms except Equation 15 in the Legendre expansion disappear by integrating these terms over angular parts of electron coordinates. Since Equation 15 depends on time only through R, $\theta_{a\mu}$, $\theta_{b\nu}$, and the mutual angle between $\mathbf{r}_{a\mu}$ and $\mathbf{r}_{b\nu}$, the time dependence of each matrix element of $\mathbf{A}$ in Equation 11 becomes a simple form. Every matrix element in Equation 12 can be obtained by numerical multifold integration and by making matrix products. The probability of Equation 13 can be given by the solution $\mathbf{C}(\infty)$ of the iteration formula (Equation 12). If we note $< \phi_{A^*} | \sum_{\mu} \mathbf{r}_{a\mu} | \phi_A > = \boldsymbol{\mu}_A$, $< \phi_{B^*} | \sum_{\nu} \mathbf{r}_{b\nu} | \phi_B > = \boldsymbol{\mu}_B$, $|\boldsymbol{\mu}_A| = \mu_A$, $|\boldsymbol{\mu}_B| = \mu_B$ ($\mu_A = \mu_B = \mu$ for Case 1) and $\mathbf{R} = \mathbf{v}t$, $|\mathbf{v}| = v$, the transfer probability and the cross section for $i \rightarrow j$ is written in terms of v (relative incident velocity) and of μ (the optical transition dipole moment).

The probability of excitation transfer depends on the direction of initial p-state (from a particular i to all transferred states $\sum_j$). Figure 2 illustrates the probability of transfer $P_{i \rightarrow f}$ *vs.* impact parameter R_o in the term $e\mu(\hbar v)^{-1/2}$ (*67*). In Figure 2, P_ξ, P_η, and P_ζ are the probabilities for cases where the initial direction of P is along ξ, η, and ζ axes respectively (Figure 1). The mean cross section over the initial P-direction can be obtained by

$$\sigma = \tfrac{1}{3}(\sigma_\xi + \sigma_\eta + \sigma_\zeta) \tag{16}$$

where $\sigma_s = 2\pi \int P_s R_o dR_o$, $s = \xi$, η, or ζ. The mean cross sections are universally calculated as

$$\sigma = 2.26\pi\mu^2 e^2/\hbar v. \tag{17}$$

Publication Date: January 1, 1968 | doi: 10.1021/ba-1968-0082.ch011

Omont (*53*, *54*) has made a similar calculation for this process. He has given a result of $\sigma = 2.28\pi\mu^2e^2/\hbar v$ which is in good agreement with our results. At thermal velocity the cross section is

$$\sigma = 160\mu^2\sqrt{M}$$

where M is the mass number of the atom. Some typical cross sections at room temperature for the like-atom S-P case are given in Table I.

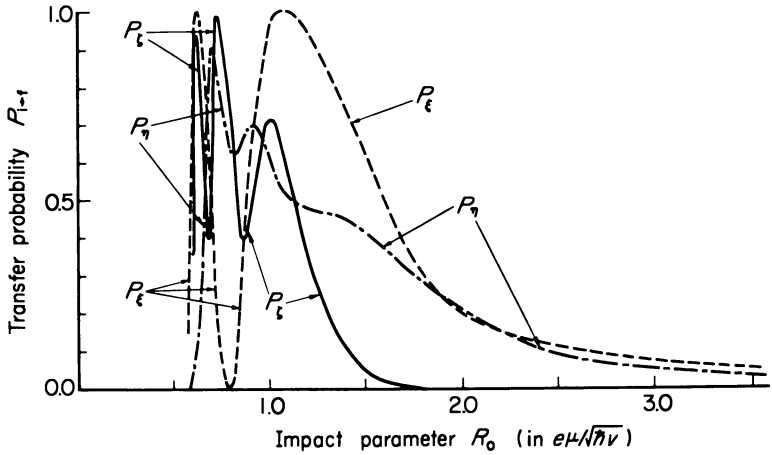

Figure 2. Relations between transition probabilities and impact parameter R_0 *for* $A^* + A \rightarrow A + A^*$ *(S-P type interaction).* P_ξ, P_η, *and* P_ζ *are the transfer probabilities where the initial P-state angular momenta have the direction* ξ, η, *and* ζ

One difficulty in performing the calculations comes from the fact that Equations 7 and 11 with degenerate angular momentum states have two sets of three P states. Furssow and Wlassow (*24*) assumed that the initial state is always in a definite component state of P, whereas the final states are in three P states. The assumption will be valid when $P_{i\to f}(R_0) \leqslant 1/2$ in Equation 8. Further, these authors considered that inside the critical impact parameter R_{oc} defined by $R_{i\to f}(R_{oc}) = 1/2$, $P_{i\to f}$ is always 1/2 because of the oscillation between zero and unity. They obtained the shift in the line shape of the spectrum. According to their scheme, Halstein *et al.* (*27*) estimated the excitation transfer cross section as $(4/\sqrt{3})\pi e^2\mu^2/\hbar v$. We can simplify the problem by making some assumptions with respect to the direction of P-state during collision (fixed and rotating P-state approximation). With these approximation, the cross sections are $(2/3)\pi^2\mu^2e^2/\hbar v$ and $2\pi^2\mu^2e^2/\hbar v$, respectively (*47*).

Publication Date: January 1, 1968 | doi: 10.1021/ba-1968-0082.ch011

Table I. Cross Sections of Excitation Transfer between Identical Atoms in Thermal Energy

Atom[a]	*Ground and Excited States (transition)*	*Cross Section of Excitation Transfer (sq. A.)*	*Lower Critical Pressure* P_l *at 0°C. (mm. Hg)*	*Higher Critical Pressure* P_h *at 0°C. (mm. Hg)*
H (1)	$1S–2P$	7.80×10^2	2.2	1.3×10^3
	$–3P$	1.26×10^2	3.8	2.0×10^4
He (4)	$1^1S–2^1P$	4.98×10^2	2.7	2.5×10^3
	$–3^1P$	1.54×10^2	2.7×10	1.5×10^4
Li (7)	$2^2S–2^2P$	1.9×10^4	1.4×10^{-1}	1.0×10
	$–3^2P$	1.1×10^2	1.4×10^{-1}	2.2×10^4
Be (9)	$2^1S–2^1P$	1.98×10^4	3.1×10^{-1}	1.0×10
Ne (20)	$2p^6\ {}^1S_o$ $–2p^5(^2P_{1/2})3s^1P_1$	1.1×10^4	1.6×10^{-1}	2.7×10
Na (23)	$3^2S_{1/2}–3^2P_{1/2}$	1.4×10^4	5.9×10^{-2}	1.6×10
	$–3^2P_{3/2}$	2.9×10^4	2.1×10^{-2}	5.6
Mg (24)	$3^1S–3^1P$	3.766×10^4	1.8×10^{-1}	3.8
Al (27)	$3^2P_{1/2}–4^2S_{1/2}$ $3^2P_{3/2}–4^2S_{3/2}$	4.0×10^3	6.7×10^{-2}	1.1×10
Ar (40)	$3p^6\ {}^1S_o$ $–3p^5(^2P_{1/2})4s^1P_1$	2.6×10^2	3.6	6.9×10^3
K (39)	$4^2S_{1/2}–4^2S_{1/2}$	2.6×10^3	2.7×10^{-1}	2.2×10^2
	$–4^2P_{3/2}$	5.2×10^3	1.3×10^{-1}	7.6×10
Cs (133)	$6^2S_{1/2}–6^2P_{1/2}$	5.2×10^4	1.6×10^{-2}	2.3×10
Ba (137; 11%)	$6^1S_o–6^1P_1$	2.10×10^5	1.3×10^{-2}	2.9×10^{-1}
(138; 72%)		2.10×10^5		
Hg (200; 23.13%)	$6^1S_o–6^1P_1$	4.785×10^4	6.5×10^{-1}	2.7×10
(202; 29.80%)		4.809×10^4		

[a] Mass number (M) in parentheses.

Discrete-Discrete Near-Resonant Process. We assume the commutative relation between the matrices $\mathbf{A}(t)$ and $\mathbf{B}(t)$, as $[\mathbf{A}(t), \mathbf{B}(t)] = 0$ where [ ] means the commutator bracket and $\mathrm{B}(t) = \int_{-\infty}^{t} A(t')dt'$. This assumption is acceptable for the near-resonant case (*18, 19, 46, 47*). Together with this assumption we assume that the direction of P-state points to the other atom throughout collision (the rotating atom approximation). The rotating atom approximation has been employed and discussed by Bates *et al.* (*6, 7, 8*) in some collision problems. In our excitation transfer problem this approximation would also be available.

In Radiation Chemistry; Hart, E.;
Advances in Chemistry; American Chemical Society: Washington, DC, 1968.

Judging from the calculation of the coupled equation (without the rotating atom approximation) in the resonant case and the discrete-continuum case, the error from the rotating atom approximation would not change the order of the magnitude (*67, 68, 70*). With these approximations, the process can be described in terms of the resonance defect $[\omega = (E_i - E_f)/\hbar]$ and the transition matrix dipole moments of A and B μ_A and μ_B. By Nakamura's calculation (*50*), the transfer probability is written as

$$P_{i\to f}(R_0, v) = \sin^2\{4\alpha^2\beta K_1(\alpha R_0)/\alpha R_0\} \tag{19}$$

where $\alpha = \omega/v$, $\beta = \mu_A\mu_B e^2/v$ and $K_1(x)$ is the first-order modified Bessel function. The cross section for the excitation transfer is given by

$$\sigma_{i\to f}(v) = \frac{2\pi}{\alpha^2}\int_0^\infty x \sin(4\alpha^2\beta)\frac{K_1(x)}{x}\,dx \tag{20}$$

If we consider the case $H(1s) + D^*(2p) \rightarrow H^*(2p) + D(1s)$ the resonance defect (ω) is 22.4 cm.$^{-1}$. The results are illustrated in Figure 3 as a function of the incident velocity v. This kind of theoretical work together with the exact resonant case had already appeared by 1930 (*24, 32, 57*). Bates (*11*) and Rosen and Zener (*59*) also investigated the near-resonant type problem. The work by Vainshtein *et al.* (*65*) can be applicable to the process.

Generally, one of the characteristic features of Case 1 is a monotonic dependence on the incident velocity (v) as mentioned later. For instance,

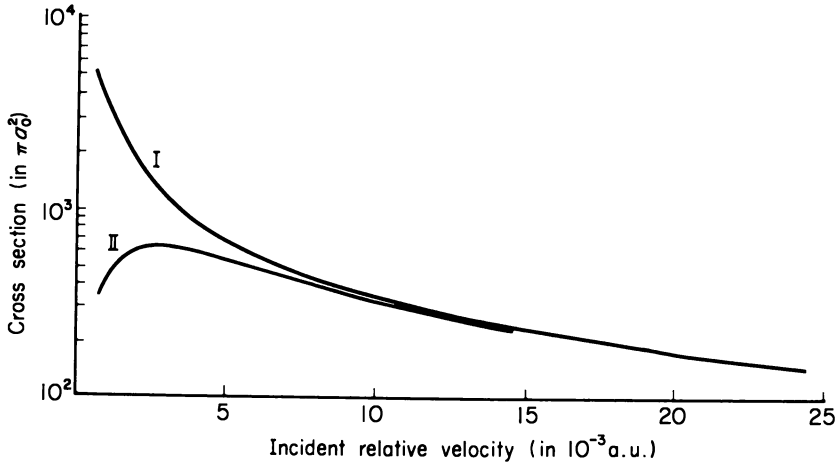

Figure 3. Relation between cross section and incident relation velocity
(I): $H^*(2p) + H(1s) \rightarrow H(1s) + H^*(2p)$
(II): $D^*(2p) + H(1s) \rightarrow D(1s) + H^*(2p)$

Publication Date: January 1, 1968 | doi: 10.1021/ba-1968-0082.ch011

the cross section of S-P case is proportional to v^{-1}. However, in the near-resonant case the dependence of the transfer cross section is not a monotonic function of v and should have a maximum. The maximum of the cross section occurs at about $v = \omega/2\pi\bar{a}$ where $\bar{a}$ has a dimension of length and is of the order of interaction range. In the incident velocity energy range higher than $\omega/2\pi\bar{a}$, the property of near-resonant process disappears and approaches that of a resonant process. If the resonant defect ω is larger than 200 cm.$^{-1}$ (1.02×10^{-3} a.u.), the transfer cross section will be fairly small compared with that of the S-P resonant case.

Discrete-Continuum Process. For Case 3, the basic operator-differential equation (Equation 11) involves continuum states. $\mathbf{A}(t)$ will be a continuously infinite row-column matrix. If excitation of A is optically allowed, the matrix components corresponding to discrete-continuum components of $\mathbf{A}(t)$ are predominant—*i.e.*, $\mathbf{A}(t)$ can be regarded as

$$\mathbf{A}(t) = \left[\begin{array}{c|c} 0 & \mathbf{A}_{jk} \\ \hline \mathbf{A}_{ki} & 0 \end{array}\right] \tag{21}$$

where upper and left halves correspond to discrete states, opposite halves to continuum states, and k is a wave vector of an ejected electron. Using Equation 21 and with some approximation, Equation 11 can be simplified.

Equation 11:

$$\frac{d}{dt}\mathbf{C} = \mathbf{A}(t)\mathbf{C} \tag{11}$$

with the initial condition $\mathbf{C}(-\infty) = \mathbf{C}_0$ is equivalent to a integral equation:

$$\mathbf{C} = \mathbf{C}_0 + \int_{-\infty}^{t} \mathbf{A}(t)\mathbf{C}dt. \tag{22}$$

If we substitute Equation 22 into Equation 11, we obtain

$$\frac{d}{dt}\mathbf{C} = \mathbf{A}\mathbf{C}_0 + \mathbf{A}\int_{-\infty}^{t} \mathbf{A}\mathbf{C}dt. \tag{23}$$

We divide C into two sub-vectors which represent continuum and discrete components, respectively:

$$\mathbf{C} = \left[\begin{array}{c} \mathbf{C}_c \\ \hline \mathbf{C}_d \end{array}\right] = \left[\begin{array}{c} \mathbf{C}_c \\ \hline 0 \end{array}\right] + \left[\begin{array}{c} 0 \\ \hline \mathbf{C}_d \end{array}\right]. \tag{24}$$

Our initial state of the system is discrete. The continuum component $\mathbf{C}_c$ is zero, *i.e.*,

$$\mathbf{C}_0 = \left[\begin{array}{c} 0 \\ \hline \mathbf{C}_d \end{array}\right]. \tag{25}$$

Publication Date: January 1, 1968 | doi: 10.1021/ba-1968-0082.ch011

Then, using Equation 25 the discrete component of $\mathbf{AC}_o = 0$. Equation 23 has a form of

$$\frac{d}{dt}\begin{bmatrix}\mathbf{C}_c(t)\\ \mathbf{C}_d(t)\end{bmatrix} = \begin{bmatrix}\sum_i \mathbf{A}_{ki}\mathbf{C}_i\\ 0\end{bmatrix} \tag{26}$$

$$+\int_{-\infty}^{t}\begin{bmatrix}\sum_i \mathbf{A}_{ki}(t)\mathbf{A}_{ik'}(t) & 0\\ 0 & \int \mathbf{A}_{jk}(t)\mathbf{A}_{ki}(t')d\mathbf{k}\end{bmatrix}\cdot\begin{bmatrix}\mathbf{C}_c(t')\\ \mathbf{C}_d(t')\end{bmatrix}dt'$$

which can be separated into two parts. For $\mathbf{C}_d$:

$$\frac{d}{dt}\mathbf{C}_d(t) = \int_{-\infty}^{t}\mathbf{K}(t,t')\mathbf{C}_d(t')dt'. \tag{27}$$

Here, $\mathbf{K}(t,t')$ is a matrix whose i-j component is expressed by

$$\mathrm{K}_{ij}(t,t') = \int \mathrm{A}_{ik}(t)\mathrm{A}_{kj}(t')d\mathbf{k}. \tag{28}$$

The transfer probability $P_{i\to f}$ can be obtained by

$$P_{i\to f} = 1 - |\mathbf{C}_d(\infty)|^2.$$

If the matrix $\mathbf{K}(t,t')$ in Equation 28 can be reduced to a simple form as $\int_{-\infty}^{t'}\mathbf{K}(t,t')\ \mathbf{C}(t') = \mathbf{J}(t)\ \mathbf{C}(t)$, Equation 27 can be solved easily by iteration (Equation 12).

Two approximations can be used to simplify the matrix $\mathbf{K}(t,t')$. Mori and Fujita (*44*, *45*, *46*) assumed the commutative relationship between $\mathbf{A}(t)$ and $\mathbf{B}(t)$ as for the near-resonant process, and gave a formula for the error which would arise from the commutative assumption. Katsuura and Watanabe (*33*, *70*) did not make such assumption but assumed that the transition dipole moment of $\mathrm{B} \to \mathrm{B}^+ + e$ depends little on the energies of an ejected electron. In both approximations, the dependence of $\mathbf{J}(t)$ on interatomic distance becomes $\propto R^{-2n}$ if the interatomic Hamiltonian $H' \propto R^{-n}$. This property predicts the velocity dependence of the cross section (discussed later). In Mori-Fujita calculation, the rotating atom approximation was used. In Watanabe-Katsuura's (W-K) paper (*70*) the solution without rotating atom approximation was obtained. Figure 4 shows the relation between the transfer probability $P_{i\to f}$ for $\mathrm{A}^* + \mathrm{B} \to \mathrm{A} + \mathrm{B}^+ + e$ and impact parameter R_o, by W-K calculation. Taking the integration over R_o, the transfer cross sections for Case 3 can be obtained. For the direction of angular momentum P, an approximation method can be used. This method gives upper and lower bounds of the cross section, obtainable from Equation 11 (*70*). Smirnov and Firsov also calculated for the same process using a similar but slightly different method (*60*, *61*), taking the P-direction

Publication Date: January 1, 1968 | doi: 10.1021/ba-1968-0082.ch011

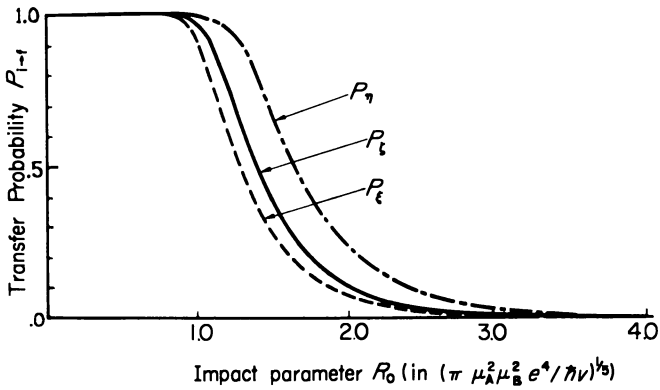

Figure 4. Relation between transition probabilities and impact parameter R_0 *for* $A^* + B \rightarrow A + B^+ + e$ *(S-P type interaction).* P_ξ, P_η, *and* P_ζ *are the same as in Figure 2*

Table II. Various Formulas of Cross Sections for Ionization by Excited Atoms

Investigator	*Cross Section* × $(\mu_A^2\mu_B^2e^4/\hbar v)^{2/5}$	*Reference*
Katsuura	18.14	*33*
Smirnov-Firsov	13.29	*61*
Smirnov-Firsov	13.8	*60*
Mori-Fujita	15.04	*44, 45*
Watanabe-Katsuura	13.88	*70*

Table III. Rate Constants and Cross Sections for Ionization by Collision with Excited Atoms

$(A^* + B \rightarrow A + B^+ + e)$

Excited Atom and Transition $(A^* \rightarrow A)$	*Atom and Molecule to Be Ionized (B)*	*Ionization Rate Constant* $k(10^{-9}$ *cc./sec., 300°K.)*	*Ionization Cross Section* σ_{th}*(sq. A., 300°K.)*
$He(2^1P \rightarrow 1^1S)$ (584 A.)	Ar	0.91–0.98	78–84
$He(2^1P \rightarrow 1^1S)$ (584 A.)	Kr	0.96–0.99	84–86
$He(2^1P \rightarrow 1^1S)$ (584 A.)	Xe	0.86–0.90	75–80
$He(2^1P \rightarrow 1^1S)$ (584 A.)	CH_4	0.95–0.96	76–77
$Ne[2p^5(^2P_{1/2})3s^1P_1 \rightarrow 2p^6\ ^1S_o]$ (736 A.)	Ar	0.52–0.58	85–95
$Ne[2p^5(^2P_{1/2})3s^1P_1 \rightarrow 2p^6\ ^1S_o]$ (736 A.)	Kr	0.59–0.63	106–113
$Ne[2p^5(^2P_{1/2})3s^1P_1 \rightarrow 2p^6\ ^1S_o]$ (736 A.)	Xe	0.58–0.65	109–121
$Ne[2p^5(^2P_{1/2})3s^1P_1 \rightarrow 2p^6\ ^1S_o]$ (736 A.)	CH_4	0.70	94
$Hg(6^1P_1 \rightarrow 6^1S_o)$ (1849 A.)	Li	1.07	124
$Hg(6^1P_1 \rightarrow 6^1S_o)$ (1849 A.)	Na	0.14	28

Publication Date: January 1, 1968 | doi: 10.1021/ba-1968-0082.ch011

effect into consideration. The results by several authors are tabulated in Table II. At present, the W-K calculation seems most rigorous. Table II shows that the cross section can be written by a factor $(\mu_A^2\mu_B^2e^4/\hbar v)^{2/5}$ regardless of the method used. Further, the error from simplifications on the P-direction is about 25% at most for Case 3, with S-P type interaction. Some typical cross sections calculated from the coupled equation are tabulated in Table III. The cross sections of Case 3 are sometimes large compared with gas kinetic dimensions.

Cases Other than S-P Type Interaction

Velocity Dependence of the Cross Section. For S-P type interaction, the excitation transfer cross section was proportional to v^{-1} for Case 1, and to $v^{-2/5}$ for Case 3. For Case 2 the velocity dependence was not as simple. Here the ratio of the angular frequency of the resonant defect [$\omega = (E_i - E_f/\hbar)$] to the relative incident velocity (v)—*i.e.*, $\alpha = \omega/v$ is the most important parameter. If the ratio is small compared with the reciprocal of the interaction range $\bar{a}^{-1}$, the transfer will approach that of Case 1 (exact resonance). The cross section will decrease monotonically with v at higher velocities. If $\alpha \geqslant \bar{a}^{-1}$, the cross section will be fairly small compared with that of exact resonance. Further, in the limit of $v \to 0$, the cross section would be zero, and would increase with v at low velocity region. Then, it will reach a maximum in between these regions for Case 2. This feature will hold for all inter-multipole types of interaction including the S-P type. However, the detailed and quantitative discussion on the velocity dependence for Case 2 is not this simple. On the other hand, the velocity dependence of the cross section for the resonance type excitation transfer (Cases 1 and 3) can be discussed more straightforwardly, not only for the S-P interaction case but also for other interaction cases (*48*, *69*).

If we can confine the problem to a two-level case—*i.e.*, one initial and one final state—the velocity dependence of the excitation transfer cross section can easily be obtained. If the interaction has the form $C \cdot R^{-n}$, $\sigma(i \to f)$ can be expressed as

$$\sigma(i \to f) = \tfrac{1}{2}\pi\left(1 + \frac{2}{n-2}\right) \cdot \left[\frac{C}{\hbar}\frac{f(n)}{v}\right]^{2/(n-1)}, \tag{29}$$

where $f(n)$ is a numerical constant. This was obtained by Massey and Mohr (*39*) using semiclassical (with respect to nuclear motion, WKBJ) method. For Case 3, an extension of above result is possible. Equation 28 after integrating over k shows that $\mathbf{K}(t,t')$ is proportional to R^{-2n} $\mathbf{K}(t,t')$ and is most significant when $t = t'$. When $\mathbf{C}_d$ has one component, the problem is identical to one with a R^{-2n} potential in Equation 29. If there is more than one channel of excitation transfer (not a two-level problem),

Publication Date: January 1, 1968 | doi: 10.1021/ba-1968-0082.ch011

the velocity dependence can be obtained by the dimension analysis technique (69). If **A** in Equation 11 or **K** in Equation 27 can be factored out by $(e^2M_A^2 \cdot R_0^{-n})$ or $[e^2M_A^2(dM_B^2/dE)_{k0} \times R_0^{-2n}]$, we can derive the same velocity dependence of the cross section. Here M_A^2 and $(dM_B^2/dE)_{k_0}$ are the square of multipole moment of $A \rightarrow A^*$ and that of $B \rightarrow B^+ + e$ with energy interval dE at wave number k_o, respectively. The cross sections are expressed as

$$\sigma(i \rightarrow f) = K_A \left(\frac{e^2M_A^2}{v}\right)^{2/(n-1)} \qquad \text{for Case 1} \qquad (30)$$

where

$$K_A = \frac{4\pi}{n-1}\int_0^\infty |<\mathbf{C}(\infty)|\mathbf{F}(a,\infty)|\,\mathbf{C}(-\infty)>|^2 a^{-(n+1)/(n-1)}da,$$

and

$$\sigma(i \rightarrow f) = K_B \left\{\frac{\pi e^4}{\hbar v} M_A^2 \cdot \left(\frac{dM_B^2}{dE}\right)k_0\right\}^{2/(2n-1)} \qquad \text{for Case 3} \qquad (31)$$

where

$$K_B = \frac{4\pi}{2n-1}\int_0^\infty [1 - |<\mathbf{C}_d(\infty)|\mathbf{G}(b,\infty)|\,\mathbf{C}_d(-\infty)>|^2] b^{-(2n+1)/(2n-1)}\mathrm{db} \qquad (32)$$

Here $\mathbf{F}(a, \infty)$ and $\mathbf{G}(b, \infty)$ are matrices which give the solution vector $\mathbf{C}(\infty)$ and $\mathbf{C}_d(\infty)$ as $\mathbf{C}(\infty) = \mathbf{F}(a, \infty) \cdot \mathbf{C}(-\infty)$ and $\mathbf{C}d(\infty) = \mathbf{G}(a, \infty)\mathbf{C}_d(-\infty)$. The parameters a and b are dimensionless and given by $a = (R_0e^2/\hbar v) \times (M_A^2/R_0^n)$ and $b = (\pi R_0/\hbar v)(e^2/R_0^{2n}) \times M_A^2(dM_B^2/dE)_{k0}$. It is interesting to see the difference of the velocity dependences for these processes. When the final state is discrete, the velocity dependence is $v^{-2/(n-1)}$, and when the final state is continuous, the dependence is $v^{-2/(2n-1)}$. If the final state has finite line width, the exponent of the dependence will be between $-2/(n-1)$ and $-2/(2n-1)$. The change from n to $2n$ in the exponent depends on the line width of the final state.

The temperature dependencies of the thermal cross sections (σ_{th}) and the reaction constants (k) can be obtained by taking the Boltzmann average of these over velocities. These are

$$\sigma_{th} = 2\pi^{-1/2}\Gamma\left[\frac{3}{2} - (n-1)^{-1}\right] K_A(e^2M_S^2/\hbar)^{2/(n-1)} \times (M^*/2k_\beta T)^{1/(n-1)} \qquad (33)$$

$$k = 2\pi^{-1/2}\Gamma\,[2 - (n-1)^{-1}] \cdot K_A(e^2M_A^2/\hbar)^{2/(n-1)} \times (M^*/2k_\beta T)^{-1/2+[1/(n-1)]} \qquad (34)$$

Publication Date: January 1, 1968 | doi: 10.1021/ba-1968-0082.ch011

for Case 1, and

$$\sigma_{th} = 2\pi^{-1/2}\Gamma\left[\frac{3}{2} - (2n-1)^{-1}\right] K_B[(e^4\pi/\hbar) \cdot M_A^2 \cdot (dM_B^2/dE)_{k_0}]^{2/(2n-1)} \times (M^*/2k_\beta T)^{-1/(2n-1)} \quad (35)$$

$$k = 2\pi^{-1/2}\Gamma[2 - (2n-1)^{-1}] K_B[(e^4\pi/\hbar) M_A^2 (dM_B^2/dE)_{k_0}]^{2/(2n-1)} \times (M^*/2k_\beta T)^{-1/2+[1/(2n-1)]} \quad (36)$$

for Case 3. Here k_β is Boltzmann constant, and M^* is the reduced mass of the incident partners.

Bates *et al.* (*12*) obtained the velocity dependence of $\sigma(i \rightarrow f)$ for Case 3 from the viewpoint of a simple classical collision theory as:

$$\sigma(i \rightarrow f) = \pi\left(\frac{C(n-2)}{M^* v^2}\right)^{\frac{2}{n}}\left(\frac{n}{(n-2)}\right) \cdot P_i f_W, \quad (37)$$

where M^* is the reduced mass and where $P_i \cdot f_W$ is the probability of ionization when the colliding particles are in interaction region. The factor $P_i f_W$ is considered independent of velocity. The velocity dependence in Equation 37 is different from that predicted from Equation 29, equating $n \rightarrow 2n$. This discrepancy comes from the difference in the physical picture. Equation 37 is valid for a case where the ionization cross section is small, whereas Equation 31 is for a case where the cross section is comparatively large. The processes of Equation 37 will occur within a narrow region. Nevertheless, there remain some points of controversy on this discrepancy of the velocity dependence.

Collisions with Metastable Excited Atoms and PSS Method. When an excitation in Case 1 is metastable or optically forbidden, the interaction between A and B is not long range. A question of the validity of the impact parameter method arises. The interaction can not be expanded by Legendre polynomials. Buckingham and Dargarno (*4*) and Matsuzawa and Nakamura (*40*) calculated the transfer cross section for metastable excitation transfer processes. The perturbed stationary state method (PSS method) can be used for this problem rather than the impact parameter method (IP method). The PSS method is based on the concept that the motion of nucleus is treated in quantum mechanical way, the wavefunction of the total system can be divided into one of nuclear motion and one of electronic motion, and the electronic wavefunction is determined by the electronic Hamiltonian for a "fixed" nuclear configuration at every moment of nuclear motion during collision. The PSS method has been used for $He^* + He \rightarrow He + He^*$ by Buckingham and Dalgarno (*4*). In Matsuzawa-Nakamura's paper (*40*), the two (IP and PSS) methods were compared for the process $H^*(2s) + H(1s) \rightarrow H(1s) + H^*(2s)$. The results for hydrogen are illustrated in Figure 5.

Publication Date: January 1, 1968 | doi: 10.1021/ba-1968-0082.ch011

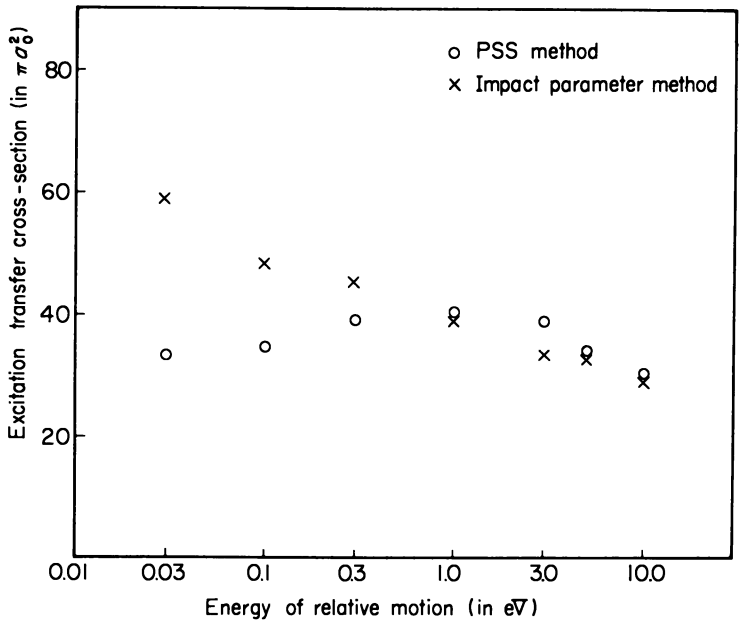

Figure 5. Cross sections for metastable excitation transfer process $H^*(2s) + H(1s) \rightarrow H(1s) + H^*(2s)$ *vs. incident energy*

○: Calculated by PSS method
×: Calculated by IP method

The data show that the impact parameter calculation agrees with that of PSS above the energy region of 1.0 e.v. Inaccuracy in IP calculation arises mainly from the straight-line trajectory approximation (*see* Figure 1). The cross section from PSS calculation is greatly influenced by the small hill of the adiabatic potential of AB at about 5-a.u. internuclear separation. The IP calculation would be markedly improved if we take a distorted trajectory affected by interatomic interaction. The calculation with the PSS method shows that the transfer cross section for an optically forbidden excitation can become large (of the order of 10 sq. A.) compared with geometrical cross section. The PSS method was applied also to $H^*(2p) + H(1s) \rightarrow H(1s) + H^*(2p)$ by Nakamura and Matsuzawa (*51*). In this process the interaction is long range. The results are in excellent agreement with that of IP method (with straight-line trajectory). Thus, the IP method with straight-line trajectory was proved to be useful for long-range interactions, as expected.

Processes like $A^* + B \rightarrow A^{*\prime} + B$ have also been investigated (*18, 19, 23, 37, 38, 62, 63*). Although they may be important in some gas-phase experiments, we would like to exclude them from this discussion because they are not the excitation transfer type. If the potential crossing occurs

Publication Date: January 1, 1968 | doi: 10.1021/ba-1968-0082.ch011

in the case of nonresonant process, the problem will be different. The cross section for the transfer will be significant at the crossing point (*13*). Besides the famous Landau-Zener formula (*36, 71*), Stuckelberg (*64*) extended the theory for the potential crossing problem. This can be used for Case 2.

The PSS method was also used for $He^*(1s2s, {}^3S) + He^*(1s2s, {}^3S) \rightarrow He(1s^2, {}^1S) + He^+(1s) + e$ by von Roos (*58*). The cross section was estimated to be 10^{-2} sq. A. at 293°K. and is much smaller compared with experimental data (*56*). Besides the above, Ferguson (*22*) and Bates *et al.* (*12*) investigated similar process by simple collision theory. The processes include metastable excitation as well as the *S-P* case. Their procedures are similar. According to Bates *et al.*, the rate coefficient for the ionization is expressed as

$$k_p = f_w P_i k_c \tag{38}$$

where f_w is the fraction of the close collision from which any state of the continuum can be reached without Wigner's spin conservation rule being violated, where P_i is the probability of ionization occurring in one of these close collisions, and where k_c is the rate coefficient for close collisions. The rate coefficient k_c is obtained from the classical orbital theory (*25*). The probability P_i is obtained from the ionization rate which is determined by the initial-final matrix element of interelectronic Coulomb interaction. They estimated k_p's for the processes: $H^*(2s - p) + H^*(2s - p) \rightarrow H(1s) + H^+ + e$ and $He^*(1s2s, {}^3S) + He^*(1s2s, {}^3S) \rightarrow He(1s^2, {}^1S) + He^+(1s) + e$. The cross section can be obtained by dividing k_p by the mean velocity. The estimated values for the cross section are 1.8×10^2 sq. A. for the H case and 1.1×10^2 sq. A. for the He case. The interatomic potential in calculating k_c was considered to be the dipole-dipole type ($\propto R^{-3}$) for the H case and the van der Waals type ($\propto R^{-6}$) for He case. This is in agreement with the experimental value of $0.9 \sim 1.2 \times 10^2$ sq. A. at $300 \sim 520$°K. They also discussed P_i for the process of Penning ionization like $He^*(1s2s, {}^3S) + Ar({}^1S) \rightarrow He(1s^2, {}^1S) + Ar^+ + e$ and compared their results with Ferguson's (*22*). The order of cross section for these processes is considered about 10 sq. A. at 300°K. experimentally (*14, 16, 30, 34, 63*). The theoretical cross section ($k_p/<\text{velocity}>$) is about $100 \sim 200$ sq. A. by Bates *et al.* and 40 sq. A. by Ferguson. The P_i's for these processes are about $0.05 \sim 0.3$.

Relation with Experiments. The resonant type excitation transfer has been investigated since about 1930 (*24, 57*). Attempts were made mainly to interpret the line profile of the spectrum. Now the theory of the resonant optical-allowed type transfers are well established and have been tested experimentally in several cases. On the contrary, near resonant and discrete-continuum theory have not been as well established.

Publication Date: January 1, 1968 | doi: 10.1021/ba-1968-0082.ch011

They still include some controversy. Direct measurement is difficult except for metastable excitation. We can find many experimental works on the metastable excitation transfer processes (*15, 28, 55, 56*). There are, however, only a few theoretical attempts done on these processes because of the difficulty of the problem. In lighter-atom case, the discrimination of an optically allowed state from a forbidden state is strict but, in heavier-atom cases, such as Hg, this becomes obscure because of *l-s* coupling. Thus, the S-*P* type transfer theory will be available for a metastable excitation transfer of heavier atom.

In gas-phase experiments which contain excited atoms, the pressure range of the gas can be classified into three regions from the viewpoint of excitation transfer. At low pressure, each atom behaves as if it were isolated. Atom excitation can not be transferred to other atoms within the lifetime of the excitation. At the intermediate pressure region, atom excitation can transfer to another atom within its lifetime. In this region, the pressure is, however, considered to be low enough so that the mean interatomic distance is not smaller than the mean radius of excitation transfer $(\sigma_{th})^{1/2}$. The highest pressure region is defined as that where the mean interatomic distance is smaller than $(\sigma_{th})^{1/2}$. We shall call these pressure regions independent excitation region, excitation transfer region, and collective excitation region. In the collective excitation region, the excitation of an isolated atom is not a good eigenstate. Here, we note P_h and P_l the higher and lower critical pressures of the excitation transfer region. P_h and P_l can be expressed in terms of the excitation transfer cross section σ_{th}. That is,

$$P_h = k_\beta T(\sigma_{th})^{-3/2} \tag{39}$$

$$P_l = k_\beta T(k\tau_o)^{-1} \tag{40}$$

where τ_0 is the lifetime of the excitation. For Case 1 with S-*P* type interaction, the relationships between P_h and P_l and the transition dipole moment (μ) of $A \rightarrow A^*$ are shown in Figure 6. Some typical P_l and P_h at room temperature are shown in Table I. The excitation transfer will play a role even in a comparatively low pressure region.

The excitation transfer of an atom with like atoms (Case 1) can affect the spectrum. If either an upper or a lower state is connected to the ground state by optically allowed transitions and these excited atoms are surrounded by ground state like-atoms, the Lorentzian spectrum half-line width (w) of the transition is expressed in terms of k (*1, 5*) as

$$w = \frac{2\pi N}{(n-1)} \frac{k}{K_A} \int [<\mathbf{C}(\infty)|1 - \mathbf{F}(a, \infty)|\mathbf{C}(-\infty)>]_{av} a^{-(n+1)/(n-1)} da \tag{41}$$

where N is the density of perturbes, and av means that over all the initial states. Experiments on $He^{**} \rightarrow He^* + h\nu$ and on $Ne^{**} \rightarrow Ne^* + h\nu$

Publication Date: January 1, 1968 | doi: 10.1021/ba-1968-0082.ch011

(*35, 66*) shows that the observed data are in excellent agreement with calculations by Omont and Watanabe (*53, 54, 68, 69*) for Case 1. Equation 41 shows that w is proportional to k, and its temperature effect will be the same as k of Equation 34.

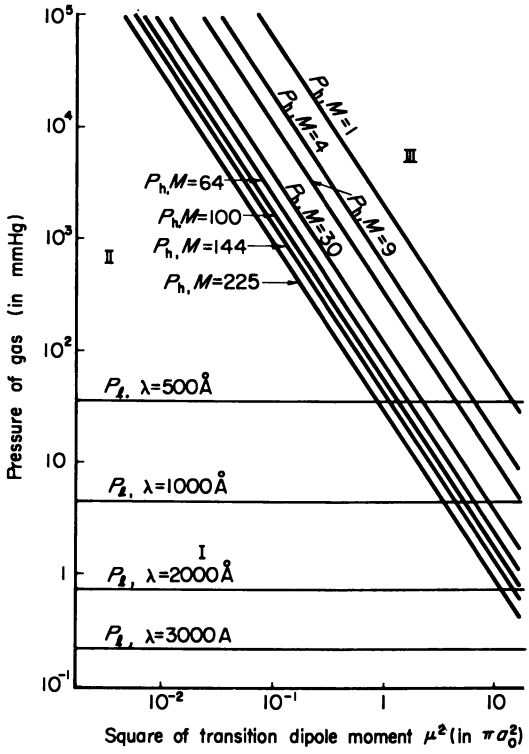

Figure 6. Higher (P_h) and lower (P_l) critical pressures of excitation transfer process $A^* + A \rightarrow A + A^*$. M = mass number of atom A; λ = wavelength of transition $A \rightarrow A^*$

The line width w is proportional to $\langle \mathbf{C}(\infty)|1 - \mathbf{F}(a, \infty)|\mathbf{C}(-\infty)\rangle$ and $\sigma(i \rightarrow f)$ is proportional to $|\langle \mathbf{C}(\infty)|\mathbf{F}(a, \infty)|\mathbf{C}(-\infty)\rangle|^2$. Generally speaking, w cannot be obtained from $\sigma(i \rightarrow f)$ or vice-versa in the strict sense. If the matrix **A** in Equation 11 has only off-diagonal components, $\langle \mathbf{C}(\infty)|1 - \mathbf{F}(a, \infty)|\mathbf{C}(-\infty)\rangle$ becomes real. The integrations in Equations 30 and 41 are mainly determined by a small value of a because of the weighting factor $a^{-(n+1)/(n-1)}$. In other words, the transfer probabilities $P_{i \rightarrow f}$ and $\langle \mathbf{C}(\infty)|1 - \mathbf{F}(a, \infty)|\mathbf{C}(-\infty)\rangle$ are determined by larger R_0 because of weighting factor R_0. In this sense a kind of "mean"

Publication Date: January 1, 1968 | doi: 10.1021/ba-1968-0082.ch011

cross section $\bar{\sigma}$ can be connected to w as $w = 2N\overline{\sigma v}$ as a crude approximation. Equation 41 rewritten as

$$w = K\frac{e^2 f}{8mc^2\nu} \qquad (\text{in cm.}^{-1}) \qquad (42)$$

where f is the oscillator strength and ν is the wavenumber of the resonance transition. K is a universal constant and can be calculated from collision theory. Several authors have estimated K with impact theory, with the following results: Byron and Foley (*17*), 1.33; Watanabe (*69, 70*), 1.44; Ali and Griem (*1, 2*), 1.41, Omont (*53, 54*), 1.45. Omont (*54*) has recently discussed the various forms of theory. Omont and Watanabe's calculations are essentially the same and seem the most rigorous. The latter performed the calculation over a wider range of impact parameters.

With magnetic resonance of excited gas-phase atoms one can also measure the cross section of excitation transfer (*20, 21, 41, 42, 52, 53*). Using a gas-laser technique, particular direction of [a particular m(azimuthal) state of] the angular momentum of atoms can be pumped under a static magnetic field with a polarized resonance radiation. If the excitation transfers to other atoms, this pumping efficiency will decrease. From this decrease one can measure the excitation transfer cross section. The Zeeman splitting of the levels is proportional to the strength of the magnetic field. If one observes the excitation transfer cross section as a function of magnetic field strength, these data will give information on the resonance defect (ω) dependence of the excitation transfer for the near-resonant case (Case 2).

Of course, Case 3 together with Cases 1 and 2, is an important process in W-value measurements of gaseous materials (*16, 31*). However, these measurements are indirect, and the data do not correspond directly to each primary process. At present the experimental data are too scant to explain in detail each process which results in electron and ion production. Case 3 may also be important in magneto-hydrodynamic power generation experiments (*61*).

Acknowledgments

The radiation laboratory is operated by the University of Notre Dame under contract with the U. S. Atomic Energy Commission. This is AEC document number COO-38-602.

Literature Cited

(1) Ali., A. W., Griem, H. R., *Phys. Rev.* **140,** A1044 (1965).
(2) Ali, A. W., Griem, H. R., *Phys. Rev.* **144,** A366 (1968).
(3) Arthurs, A. M., *Proc. Cambridge Phil. Soc.* **57,** 904 (1962).

(4) Backingham, R. A., Dalgarno, A., *Proc. Roy. Soc.* **A213,** 206 (1952).
(5) Baranger, M., "Atomic and Molecular Processes," D. R. Bates, ed., Chap. 13, Academic Press, New York, 1962.
(6) Bates, D. R., *Proc. Roy. Soc.* **A243,** 15 (1957).
(7) *Ibid.*, **A240,** 437 (1957).
(8) *Ibid.*, **A245,** 299 (1958).
(9) Bates, D. R., "Quantum Theory I. Elements," p. 254-259, Academic Press, New York, 1961.
(10) Bates, D. R., "Atomic and Molecular Process," p. 578-587, Academic Press, New York, 1962.
(11) Bates, D. R., *Discussions Faraday Soc.* **33,** 7(1962).
(12) Bates, D. R., Bell, K. L., Kingston, A. E., *Proc. Phys. Soc.* **91,** 288 (1967).
(13) Bates, D. R., Massey, H. S. W., *Phil. Mag.* **45,** 111 (1954).
(14) Benton, E. E., Ferguson, E. E., Matsen, F. A., Robertson, W. W., *Phys. Rev.* **128,** 206 (1962).
(15) Biondi, M. A., *Phys. Rev.* **82,** 543 (1951).
(16) *Ibid.*, **88,** 660 (1952).
(17) Byron, F. W., Foley, H. M., *Phys. Rev.* **134,** A625 (1964).
(18) Callaway, J., Bauer, E., *Phys. Rev.* **140,** A1072 (1965).
(19) Callaway, J., Bartling, J. Q., *Phys. Rev.* **150,** 69 (1966).
(20) Colegrove, F. D., Schearer, L. D., Walters, G. K., *Phys. Rev.* **135,** A353 (1964).
(21) Faroux, J. P., Baossel, J., *Compt. Rend.* **262,** 41 (1966).
(22) Ferguson, E. E., *Phys. Rev.* **128,** 210 (1962).
(23) Field, G. B., "The Distribution and Motion of Interstellar Matter in Galaxies," L. Woltjer, ed., Benjamin, New York, 1962.
(24) Furssov, W., Wlassow, A., *Physik Z. Sowjetunion* **10,** 378 (1936).
(25) Gioumousis, G., Stevenson, D. P., *J. Chem. Phys.* **29,** 294 (1958).
(26) Gurnee, H. F., Magee, J. L., *J. Chem. Phys.* **26,** 1237 (1957).
(27) Hasted, J. B., "Atomic and Molecular Processes," D. R. Bates, ed., Chap. 18, Academic Press, New York, 1962.
(28) Hasted, J. B., "Physics of Atomic Collisions," Chaps. 12 and 13, Butterworth and Co., London, 1964.
(29) Holstein, T., Alpert, D., McCoubrey, A. O., *Phys. Rev.* **85,** 985 (1952).
(30) Hury, W. B., *J. Chem. Phys.* **45,** 2713 (1966).
(31) Jesse, W. P., Sadauskis, J., *Phys. Rev.* **100,** 1755 (1955).
(32) Kallmann, H., London, F., *Z. Physik. Chem.* **2,** 207 (1929).
(33) Katsuura, K., *J. Chem. Phys.* **42,** 3771 (1965).
(34) Kruithof, A. A., Druyvestyn, M. J., *Physica* **4,** 456 (1937).
(35) Kuhn, H. G., Lewis, E. L., *Proc. Roy. Soc.* **A299,** 423 (1967).
(36) Landau, L. D., *Z. Phys. Soviet Union* **2,** 46 (1932).
(37) Lees, J. H., Skinner, H. W. B., *Proc. Roy. Soc.* **A137,** 186 (1932).
(38) Lin, C. C., Fowler, R. G., *Ann. Phys. (N. Y.)* **15,** 461 (1961).
(39) Massey, H. S. W., Mohr, C. B. O., *Proc. Roy. Soc.* **A144,** 188 (1934).
(40) Matsuzawa, M., Nakamura, H., *J. Phys. Soc. Japan* **22,** 392 (1967).
(41) Meunier, J., Omont, A., Brossel, J., *Compt. Rend.* **261,** 5033 (1965).
(42) Meunier, J., Omont, A., *Compt. Rend.* **262,** 260 (1966).
(43) Mitchell, A., Zemansky, M. W., "Resonance Radiation and Excited Atoms," Cambridge University Press, London, 1934.
(44) Mori, M., *J. Phys. Soc. Japan* **21,** 979 (1966).
(45) *Ibid.*, **23,** 1086 (1967).
(46) Mori, M., Fujita, H., *J. Phys. Soc. Japan* **20,** 432 (1965).
(47) Mori, M., Watanabe, T., Katsuura, K., *J. Phys. Soc. Japan* **19,** 380, 1504 (1964).
(48) Mott, N. F., Massey, H. S. W., "The Theory of Atomic Collisions," 3rd edition, p. 630-p. 654, Oxford Press, 1965.

(49) Mott, N. F., Massey, H. S. W., "Theory of Atomic Collisions," 3rd edition, p. 654-p. 670, Oxford Press, 1965.
(50) Nakamura, H., *J. Phys. Soc. Japan* **20,** 2272 (1965).
(51) Nakamura, H., Matsuzawa, M., *J. Phys. Soc. Japan* **22,** 248 (1967).
(52) Omont, A., *Compt. Rend.* **260,** 3331 (1965).
(53) Omont, A., *J. Phys. Radium (Paris)* **26,** 26(1965).
(54) Omont, A., *Compt. Rend.* **262,** 190 (1966).
(55) Phelps, A. V., *Phys. Rev.* **99,** 1307 (1955).
(56) Phelps, A. V., Molnar, J. P., *Phys. Rev.* **89,** 1202 (1953).
(57) Rice, O. K., *Phys. Rev.* **38,** 1943 (1931).
(58) von Roos, O., *J. Chem. Phys.* **30,** 729 (1959).
(59) Rosen, N., Zener, C., *Phys. Rev.* **40,** 502 (1932).
(60) Smirnov, B. M., private communication (1966).
(61) Smirnov, B. M., Firsov, O. B., *Zh. Exper. Theor. Fis. Pis'ma* **2,** 478 (1965); English transl.: *Soviet Physics-JETP Letters* **2,** 297 (1965).
(62) Smith, F. J., *Planet. Space Sci.* **14,** 937 (1966).
(63) St. John, R. M., Fowler, R. G., *Phys. Rev.* **122,** 1813 (1961).
(64) Stuckelberg, E. C. G., *Helv. Phys. Acta* **5,** 365 (1932).
(65) Vainshtein, L., Presnyakov, L., Sobel'man, I., *Zh. Eksperim. i Teor. Fiz.* **43,** 518 (1962); English transl.: *Soviet Phys.-JETP* **16,** 370 (1963).
(66) Vaugham, J. M., *Proc. Roy. Soc.* **A295,** 164 (1966).
(67) Watanabe, T., *Phys. Rev.* **138,** A1573 (1965), **140,** AB5, (1965).
(68) Watanabe, T., *J. Fac. Eng. Univ. Tokyo* **28,** 81 (1965).
(69) Watanabe, T., *J. Chem. Phys.* **46,** 3741 (1967).
(70) Watanabe, T., Katsuura, K., *J. Chem. Phys.* **47,** 800 (1967).
(71) Zener, C., *Proc. Roy. Soc.* **A137,** 969 (1932).

RECEIVED December 26, 1967.

Primary Processes in the Radiolysis of Gaseous Ammonia

G. R. A. JOHNSON and M. SIMIC

Laboratory of Radiation Chemistry, School of Chemistry, The University, Newcastle upon Tyne, 1, England

Publication Date: January 1, 1968 | doi: 10.1021/ba-1968-0082.ch012

The H atom and molecular H_2 yields from irradiated NH_3 gas, measured by organic scavengers are $G_H = 7.2 \pm 0.5$ and $G_{H_2} = 0.8 \pm 0.2$. The depression of the H_2 yield from the system $NH_3 + C_3H_8$ (1.5 mole%) by the electron scavenger SF_6, $\Delta G(H_2) = 3.9 \pm 0.6$, corresponds closely to $G_{NH_4^+} = 3.8$, calculated from $W(NH_3)$. The total $G(H_2)$ and $\Delta G(H_2)$ in this system are temperature independent (20° to 200°C.). The N_2 yield from $NH_3 + C_3H_8$ (> 3%) + N_2O (1.5%), $G(N_2) = 3.8 \pm 0.2$, is equal to G_{e^-}, suggesting that in this system N_2 is formed only as a result of electron capture by N_2O. The formation of HD from $NH_3 + D_2$ occurs by a chain reaction both at 20° and 120°C. $G(HD)$ depends on temperature and on D_2 concentration.

Several previous studies of the radiolysis of gaseous ammonia have shown that nitrogen and hydrogen are the only products formed in significant amounts under static conditions (*1, 3, 14, 28*), and certain evidence suggests that these products are formed by the reactions of the free radicals NH_2 and H, whose production is the main consequence of the primary ionization and excitation processes (*21, 22*). Until recently, however, no attempt has been made to determine the total yields of the free radicals, the separate contributions of the various primary processes to these yields, and the mechanism by which the free radicals react to give the products.

The initial aim of this work was to determine the total primary yield of H atoms and the extent to which ion neutralization processes contribute to the formation of this species. The mechanism of the radiation-induced decomposition of NH_3 is discussed in the light of the results obtained. A preliminary account of part of this work has been published (*10*).

In Radiation Chemistry; Hart, E.;
Advances in Chemistry; American Chemical Society: Washington, DC, 1968.

Experimental

The gases used (NH_3, Matheson, pure grade; C_3H_8 and C_3H_6, Phillips, research grade; SF_6, I.C.I., 99.95%; N_2O, British Oxygen Gases, medical grade) were condensed at 77°K. and distilled. Irradiations were carried out in borosilicate glass vessels ($\sim$ 400 ml.) fitted with breakseals. Before filling, the vessels were baked in air at 500°C. for at least 6 hours and pumped to $< 10^{-5}$ torr. Gases were introduced by condensing the required quantity into the vessel at 77°K. The technique used for the water vapor experiments has been described (*11*). During irradiation (^{60}Co γ-rays) the vessels were maintained at the required temperature ($\pm$ 2°C.) either by heating in an oven or cooling in a deep-freeze cabinet.

The dose rate was measured by the N_2O dosimeter assuming $G(N_2) = 10.0$ (*13*). The energy absorbed in each component of the gas mixtures was calculated from the energy absorbed in N_2O using the ratio of stopping powers per molecule given by Meisels (*20*). The dose rate was approximately 10^{13} e.v./ml. sec. in NH_3 at 760 torr, 20°C.

Gases present after irradiation, which were noncondensable at 77°K., were transferred to a gas buret by a one-stage diffusion pump and a Toepler pump. After PVT measurement, the gas composition was determined mass spectrometrically.

Results

Pure Ammonia. The yields of hydrogen and nitrogen from pure ammonia over the temperature range −20° to 200°C. are given in Figure 1. At all temperatures, the ratio $G(H_2)/G(N_2) = 3$ is that expected if these are the sole products. The maximum yield of hydrazine, therefore, corresponds to the experimental uncertainty in determining $G(H_2)$ and $G(N_2)$ and is estimated to be $G(N_2H_4) \leqslant 0.4$. The product yields at 41°C., measured at different NH_3 pressures, were unchanged over the NH_3 density range 3.5×10^{-4} to 2.1×10^{-3} gm./cc.

Effects of Scavengers. Except as otherwise stated, the G values quoted refer to the events in the NH_3 fraction of the mixtures. Appropriate corrections are made to allow for the dose absorbed by the scavenger fraction assuming the measured yield of a product, X, to be given by $G(X) = f_a\, G(X)_a^\circ + f_b\, G(X)_b^\circ$, where f_a and f_b are the fractions of energy absorbed by the ammonia and the scavenger, and $G(X)_a^\circ$ and $G(X)_b^\circ$ are the yields at $f_b = 0$ and $f_a = 0$, respectively.

PROPANE. In the presence of C_3H_8, $G(H_2) = 8.0 \pm 0.3$ and is independent of the C_3H_8 concentration between 1.5 and 6.0 mole % and of temperature between −20° and 200°C. (Figure 2). Over most of the temperature range, $G(N_2)$ is significantly smaller than the yield from pure NH_3, but the actual value is uncertain. We have frequently found small quantities of N_2, comparable with the amounts obtained in these experiments, to be apparently produced by radiolysis of gaseous systems

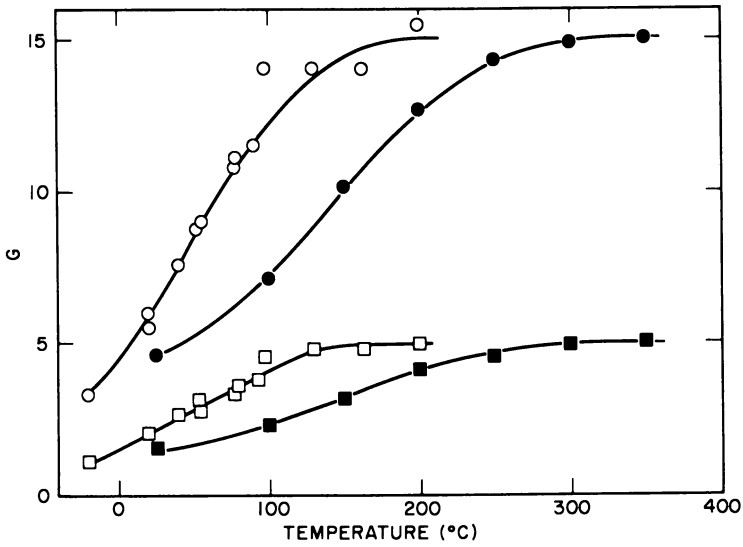

Figure 1. Hydrogen and nitrogen yields from the radiolysis of ammonia. Dependence on temperature. ○, hydrogen. □, nitrogen. Filled points are data of Jones and Sworski (14)

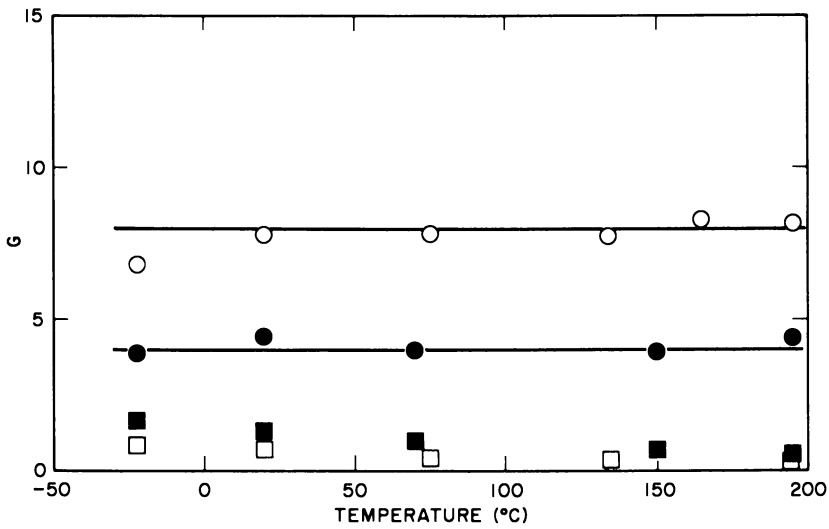

Figure 2. Hydrogen and nitrogen yields from the radiolysis of $NH_3 + C_3H_8$ (1.5 mole %). Dependence on temperature. ○, hydrogen. □, nitrogen. Filled points are with SF_6 (0.2 mole %) present

under conditions where the formation of N_2 as a product can be excluded. The origin of the N_2 is uncertain, but possibly it is desorbed from the vessel walls during irradiation. Hence, the values given for $G(N_2)$ from NH_3 irradiated in the presence of organic scavengers should be regarded as upper limits. At −22°C., $G(H_2)$ and $G(N_2)$ depend on the C_3H_8 concentration (Figure 3).

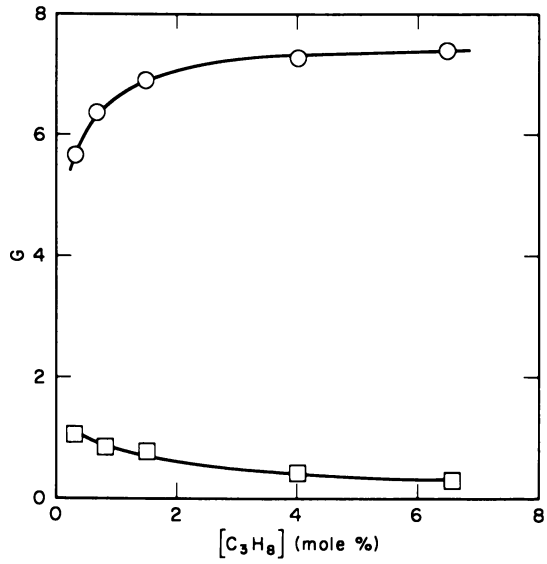

Figure 3. Dependence of $G(N_2)$ and $G(H_2)$ on C_3H_8 concentration at −22°C. ○, hydrogen. □, nitrogen

PROPANE + SULFUR HEXAFLUORIDE. The H_2 yield from $NH_3 + C_3H_8$ is decreased to $G(H_2) = 4.1 \pm 0.3$ by SF_6 (0.1 mole %), and this value is independent of temperature (−22° to 200°C.) (Figure 2). $G(N_2)$ is approximately the same as in the absence of SF_6, except at −22°C. where a slightly higher value, $G(N_2) = 1.6$, is observed.

PROPENE, BENZENE. Experiments with C_3H_6 (1.5 mole %) or C_6H_6 (3 mole %) gave $G(H_2) = 0.8 \pm 0.2$ and $G(N_2) \leqslant 0.3$ (20°C.).

DEUTERIUM. The yields of H_2, HD, and N_2 from $NH_3 + D_2$ mixtures at 20° and 120°C. are given in Table I. $G(N_2)$ is independent of D_2 concentration within experimental uncertainty. $G(HD)$ increases markedly with increasing D_2 concentration, the effect being more pronounced at the higher temperature.

Table I. Yields from the Radiolysis[a] of $NH_3 + D_2$

Temperature, °C.	*D_2 Concentration, mole %*	*G(HD)*	*$G(H_2)$*	*$G(N_2)$*
20	0	—	5.7	1.9
	0.38	3.4	8.3	2.1
	0.70	4.5	5.7	1.6
	1.43	7.8	5.1	1.4
	2.65	12.7	4.7	1.9
	4.70	17.2	3.4	1.5
120	0.33	6.6	13.6	2.8
	0.65	11.8	11.8	3.6
	4.00	41.3	8.9	3.9

[a] Conditions: $P_{NH_3} = 760$ torr. Dose rate $= 10^{13}$ e.v./ml. sec.

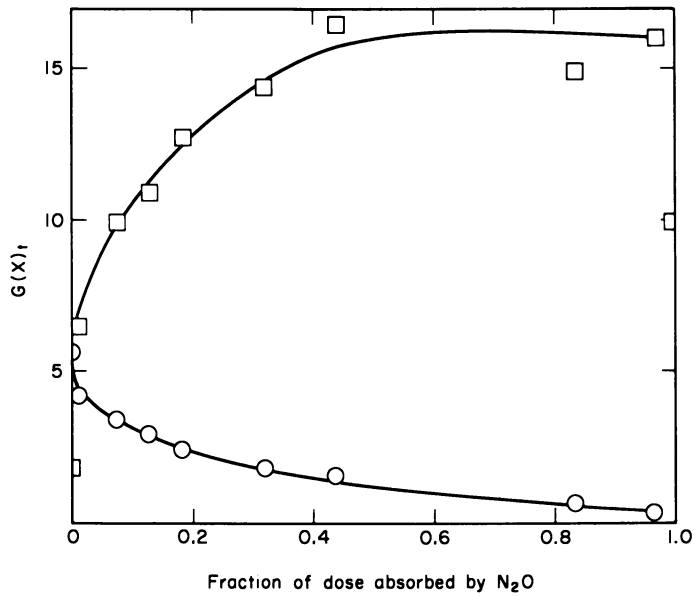

Figure 4. Hydrogen and nitrogen yields from the radiolysis of $NH_3 + N_2O$ mixtures. ○, hydrogen. □, nitrogen

NITROUS OXIDE. The yields of N_2 and H_2 from $NH_3 + N_2O$ mixtures, given as a function of the energy fraction absorbed in the NH_3 in Figure 4, show a marked dependence on the composition of the mixture, and the simple mixture law is not obeyed. The dependence of $G(H_2)$ and $G(N_2)$ from $NH_3 + N_2O$ (1.5 and 3.8 mole %) on C_3H_8 concentration is shown in Figure 5.

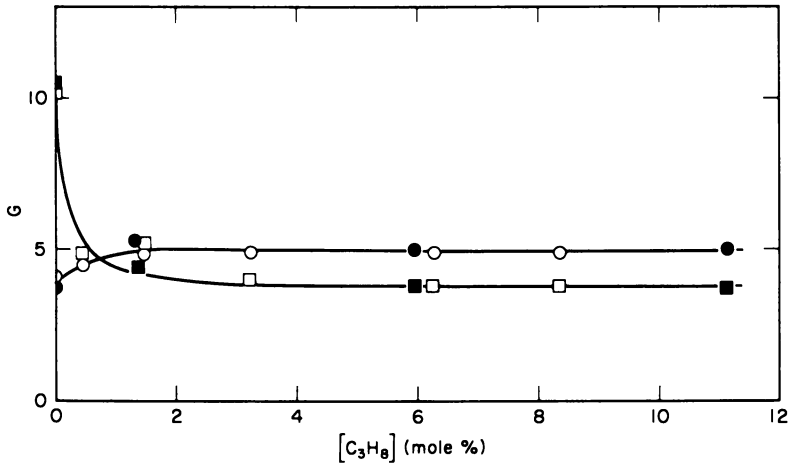

Figure 5. Hydrogen and nitrogen yields from $NH_3 + N_2O$. Dependence on C_3H_8 concentration. ○, hydrogen. □, nitrogen. Open points, N_2O = 1.5 mole %. Closed points, N_2O = 3.0 mole %

WATER VAPOR + AMMONIA. Yields of H_2 and N_2 from H_2O and NH_3 mixtures were measured as a function of NH_3 concentration and temperature. Figure 6 shows the dependence of $G(H_2)$ and $G(N_2)$ on temperature for NH_3 = 3 mole %. The yields at 150°C. were independent of NH_3 concentration between 0.5 and 3.0 mole %.

Discussion

Primary Processes. Detailed discussions of the primary events in irradiated NH_3 have been given recently (*14, 19*), and it is necessary here only to summarize the relevant information. Mass spectrometric data suggest that the main ionization processes will be Reactions 1 and 2.

$$NH_3 \longrightarrow NH_3^+ + e^- \quad (1)$$

$$NH_3 \longrightarrow NH_2^+ + H + e^- \quad (2)$$

The ion abundance ratio determined by mass spectrometry $NH_2^+/NH_3^+ \sim 0.4$ (*21, 22*), but the relative importance of Reactions 1 and 2 under radiolytic conditions is not known. The ion-molecule Reactions 3, 4, and 5

$$NH_3^+ + NH_3 \rightarrow NH_4^+ + NH_2 \quad (3)$$

$$NH_2^+ + NH_3 \rightarrow NH_3^+ + NH_2 \quad (4)$$

$$NH_2^+ + NH_3 \rightarrow NH_4^+ + NH \quad (5)$$

Publication Date: January 1, 1968 | doi: 10.1021/ba-1968-0082.ch012

occur with rate constants greater than $10^{11}M^{-1}$ sec.$^{-1}$ (*7*, *8*) and, at the NH_3 pressures and the dose rates considered here, are rapid compared with ion neutralization. When neutralization occurs, therefore, only the ammonium ion is present, and there is evidence that this will be in a clustered form, $NH_4^+ \, nNH_3$ (where $n \geq 4$) (*9*). The extent of negative ion formation in pure NH_3 is negligible (*21*, *22*), so that ion neutralization involves only recombination of ammonium ions and electrons.

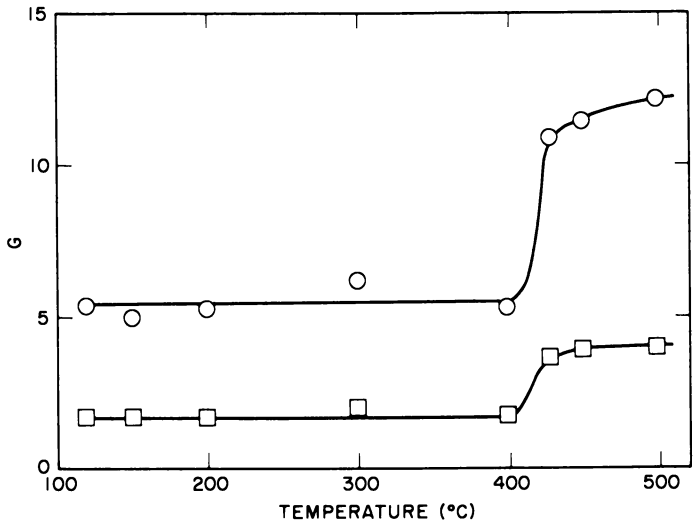

Figure 6. Hydrogen and nitrogen yields from the radiolysis of $H_2O + NH_3$ (3 mole %). Dependence on temperature. ○, hydrogen. □, nitrogen

Photochemical studies indicate that the Reaction 6, 7, and 8 can result from electronic excitation.

$$NH_3 \xrightarrow{h\nu} NH_2 + H \quad (6)$$

$$NH_3 \xrightarrow{h\nu} NH + H_2 \quad (7)$$

$$NH_3 \xrightarrow{h\nu} NH + 2H \quad (8)$$

Reaction 7 contributes less than 4% to the photolytic decomposition at 1849 A. and about 14% at 1236 A. (*18*). The formation of NH at $\lambda <$ 1600 A. has been demonstrated by flash photolysis (*2*). There is no direct evidence for the postulated intermediates in the radiolysis except for the NH radical, which has been detected by pulsed radiolysis experiments (*19*).

Publication Date: January 1, 1968 | doi: 10.1021/ba-1968-0082.ch012

NH_3 + C_3H_8. In pure NH_3 the free radicals, H and NH_2, can participate in a variety of reactions (discussed below). C_3H_8 scavenges H atoms by Reaction 9,

$$H + C_3H_8 \rightarrow H_2 + C_3H_7 \quad (9)$$

and also may be expected to react with NH_2 according to Reaction 10,

$$NH_2 + C_3H_8 \rightarrow NH_3 + C_3H_7 \quad (10)$$

these reactions competing with the alternative reactions of H and NH_2. Since $G(H_2)$ is independent of C_3H_8 concentration between 1.5 and 6.0 mole %, it is concluded that a C_3H_8 concentration of 1.5 mole % is sufficient to scavenge all of the H atoms at 20°C. and above. At −20°C., a concentration above 6.6 mole % appears necessary to scavenge all the H atoms.

The possibility that C_3H_8 can interfere with ionic reactions can be excluded since the reactions of the NH_4^+ ion with C_3H_8, either by charge transfer (Reaction 11) or proton transfer (Reaction 12) are energetically unfavorable

$$NH_4^+ + C_3H_8 \rightarrow NH_3 + H + C_3H_8^+ \qquad \Delta H = 6.9 \text{ e.v.} \quad (11)$$

$$NH_4^+ + C_3H_8 \rightarrow NH_3 + C_3H_9^+ \qquad \Delta H = 5.0 \text{ e.v.} \quad (12)$$

(ΔH is calculated from proton affinities of NH_3 (9.3 e.v.) and C_3H_8 (4.3 e.v.) and ionization potentials of H (13.6 e.v.) and C_3H_8 (11.2 e.v.)).

When all H atoms are scavenged by C_3H_8, $G(H_2) = 8.0 \pm 0.3 = G_H + G_{H_2}$—*i.e.*, the sum of the H atom yield (G_H) and the molecular yield (G_{H_2}) in this system.

$G(N_2)$ is markedly lowered by C_3H_8, suggesting that NH_2 radicals, which react to give N_2 as one of the products in pure NH_3, are removed, presumably by Reaction 10. The results indicate that, at 20°C. and above, NH_2 reacts exclusively by Reaction 10 when the C_3H_8 concentration exceeds 1.5 mole %, whereas at −22°C. concentrations of C_3H_8 higher than this are required to remove the NH_2 radicals (Figure 5). NH radicals, which are formed in minor amounts, may not react readily with C_3H_8 although they apparently do react rapidly with C_3H_6 (*19*), and the small yield of N_2 found with C_3H_8 present could possibly include some contribution from NH radicals.

NH_3 + C_3H_6. C_3H_6 is an efficient scavenger for H atoms and the H_2 yield in this system can be equated with the molecular yield $G_{H_2} = 0.8 \pm 0.2$. This value is close to that recently reported in two independent studies using C_2H_4 and C_3H_6 as scavengers (*14*, *23*).

NH_3 + C_3H_8 + SF_6. The reaction of thermal electrons with SF_6 is extremely rapid, with a rate constant of $1.8 \times 10^{14} M^{-1}$ sec.$^{-1}$ reported (*17*) for Reaction 13.

Publication Date: January 1, 1968 | doi: 10.1021/ba-1968-0082.ch012

$$e^- + SF_6 \xrightarrow{(M)} SF_6^- \quad (13)$$

The value of SF_6 as an efficient electron scavenger, which reacts only slowly if at all with free radicals, has been demonstrated (*6, 11, 12*). In the radiolysis of water vapor (*11*) neutralization of the hydronium ion (H_3O^+) by electrons gives one H atom per ion, whereas neutralization by SF_6^- ions does not give any H atoms. The effect of SF_6 in NH_3 can be interpreted in a similar fashion Thus, the depression of $G(H_2)$ by SF_6, $\Delta G(H_2) = 3.9 \pm 0.6$, corresponds closely to the yield of NH_4^+ ions $G_{NH_4^+} = 3.8$, calculated from $W(NH_3) = 26.5$ e.v. per ion pair (*20*). $\Delta G(H_2)$ is independent of temperature (Figure 2), which suggests that the yield of H_2 from NH_4^+ + electron recombination is independent of temperature, and there seems to be no evidence to support the hypothesis (*1*) that the extent of clustering of the NH_4^+ ion, varying with temperature, influences the hydrogen yield.

$NH_3 + C_3H_8 + N_2O$. The effect of N_2O (1.5 mole %) on the yield of H_2 in this system is similar to that of SF_6 and again can be interpreted in terms of a change in the ion neutralization process from reaction of the NH_4^+ ion with electrons to its reaction with negative ions. The residual yield $G(H_2) = 5.0 \pm 0.5$ is, however, somewhat greater than that observed with SF_6.

For water vapor, the formation of N_2 when C_3H_8 and N_2O are present as scavengers has been attributed (*11*) to Reaction 14,

$$e^- + N_2O \rightarrow N_2 + O^- \quad (14)$$

and since $G(N_2)$ from this system is approximately equal to the electron yield, it was concluded that the O^- ion reacts with water (Reaction 15).

$$O^- + H_2O \rightarrow OH^- + OH \quad (15)$$

This reaction was assumed to compete favorably with Reaction 16,

$$O^- + N_2O \rightarrow N_2 + O_2^- \quad (16)$$

which has been postulated to account for the N_2 yields from hydrocarbon + N_2O mixtures (*12, 31*).

The N_2 yield from $NH_3 + N_2O$ (1.5 mole %) decreases with increasing C_3H_8 concentration from $G(N_2) = 10$, in the absence of C_3H_8, to $G(N_2) = 3.8 \pm 0.2$ at a C_3H_8 concentration greater than 3 mole % (Figure 5). It is possible that the high N_2 yields in the absence of C_3H_8 are caused by the reaction of NH_2 radicals with N_2O according to Reaction 17 (*cf.*, Ref. 5):

$$NH_2 + N_2O \rightarrow NH_2O + N_2 \quad (17)$$

The results with $NH_3 + N_2O$ (Figure 4) indicate that a chain reaction

Publication Date: January 1, 1968 | doi: 10.1021/ba-1968-0082.ch012

leading to N_2 can occur; however, a more detailed study is required before a detailed mechanism can be given for this process. The effect of C_3H_8 can be attributed to competition between Reactions 10 and 17, and at sufficiently high concentrations of C_3H_8, the constant $G(N_2) = 3.8 \pm 0.2$ suggests that under these conditions N_2 is formed only by the reaction of electrons with N_2O and that Reaction 16 does not occur in this system. The proton transfer Reaction 18:

$$O^- + NH_3 \rightarrow NH_2^- + OH \qquad (18)$$

which is analogous to Reaction 15 is improbable on energetic grounds, and it is suggested (*27*) that Reaction 18 may be unfavorable in this system because of clustering of the O^- ion by NH_3 molecules.

Decomposition of Pure NH_3. In the presence of C_3H_8 the total yield of H_2, and the contribution of NH_4^+ ion neutralization, are independent of temperature; it seems reasonable to suppose that, in the unscavenged system also, the primary decomposition yield is independent of temperature. However, this system is complicated since the free radicals can react to give the products or combine to give NH_3, a variety of interradical reactions being possible. It is difficult, therefore, to deduce the primary yields from the measured product yields. In the photolysis of NH_3 ($\lambda = 1849$ A.), primary decomposition gives H and NH_2, and it might be expected that the reactions which occur will be similar to those in the radiolysis. In static photolysis (*16*) there is only a low stationary concentration of N_2H_4, but in a flow system much higher yields of this intermediate are observed since rapid removal from the reaction zone prevents decomposition by secondary reactions. Recent flow studies (*15*) have similarly shown that N_2H_4 is an important intermediate in the radiolysis.

The photolysis results have been interpreted (*16*) in terms of Reactions 19 to 24:

$$H + NH_2 + M \rightarrow NH_3 + M \qquad (19)$$

$$H + H + M \rightarrow H_2 + M \qquad (20)$$

$$NH_2 + NH_2 \rightarrow N_2H_4 \qquad (21)$$

$$N_2H_4 + H \rightarrow N_2H_3 + H_2 \qquad (22)$$

$$N_2H_3 + H \rightarrow N_2 + 2H_2 \qquad (23)$$

$$2N_2H_3 \rightarrow 2NH_3 + N_2 \qquad (24)$$

It is of interest to compare the dependence of NH_3 decomposition we found with that reported by Jones and Sworski (*14*), who used 1.0-Mev. electron irradiation with dose rates greater by a factor of about 10^3 than those we used. The results are given in Figure 1. In both cases the

Publication Date: January 1, 1968 | doi: 10.1021/ba-1968-0082.ch012

yield increases with temperature, ultimately reaching a plateau corresponding to $G(H_2) = 15$. There is, however, a significant difference between the two sets of results, both in the temperature range over which the increase is observed and the temperature at which the plateau is reached. Jones and Sworski attribute the temperature effect to a competition between Reaction 25

$$H + NH_3 \rightarrow H_2 + NH_2 \qquad (25)$$

and Reactions 19 and 20, the former reaction predominating as the temperature is increased because of its higher activation energy. However, the activation energy of Reaction 25 is in the region 10–15 kcal./mole (*24, 25*), and since the activation energies of the radical combination Reactions 19 and 20 are negligible compared with this, the observed temperature effect is not consistent with this mechanism.

It is possible, on the other hand, to interpret the temperature effect in terms of a mechanism similar to that suggested (*16*) for the photolytic decomposition of NH_3. Thus, the dependence of the yield on temperature may be attributed to the competition between Reactions 19 and 22. In this case, if the direct molecular formation of H_2 is neglected, the H_2 yield is given by Equation I.

$$G(H_2)^{max}/G(H_2)^T = 1 + k_{19}[NH_2]/k_{22}[N_2H_4] \qquad (I)$$

$G(H_2)^T$ is the yield at temperature T, $G(H_2)^{max}$ is the yield at the plateau of the yield-temperature curve, and $[NH_2]$ and $[N_2H_4]$ are the stationary state concentrations during radiolysis. Assuming that the temperature effect arises from the difference between the activation energies of Reactions 19 and 22, $\Delta E = E_{22} - E_{19}$, the Arrhenius equation gives Equation II:

$$\log(G(H_2)^{max}/G(H_2)^T) = \Delta E/2.303\,RT + A[NH_2]/[N_2H_4] \qquad (II)$$

where A is the ratio of the pre-exponential factors of Reactions 19 and 22. The concentration ratio $[NH_2]/[N_2H_4]$ might be expected to depend on temperature; however, the plot of log $(G(H_2)^{max}/G(H_2)^T)$ against $1/T$ (Figure 7), which includes our data and these of Sworski and Jones, is linear, suggesting that $[NH_2]/[N_2H_4]$ does in fact remain approximately constant over the temperature range used, for a given NH_3 pressure and dose rate. There is reasonable agreement between the values of $\Delta E = 2100 \pm 200$ and 1700 ± 100 cal./mole obtained from the two sets of data. Furthermore, these values are consistent with the suggested competition between radical combination reactions, with activation energies close to zero, and Reaction 22, whose activation energy of 2000 cal./mole has been measured (*24*). The difference between the intercepts at $1/T = 0$ in Figure 7 is understandable since the dose rates in the two investigations were different, and different pressures were employed. These

Publication Date: January 1, 1968 | doi: 10.1021/ba-1968-0082.ch012

parameters would be expected to affect the stationary state ratio $[NH_2]/[N_2H_4]$.

The mechanism proposed here to explain the temperature effect implies that Reaction 25 does not play a part in the radiolysis over the temperature range studied.

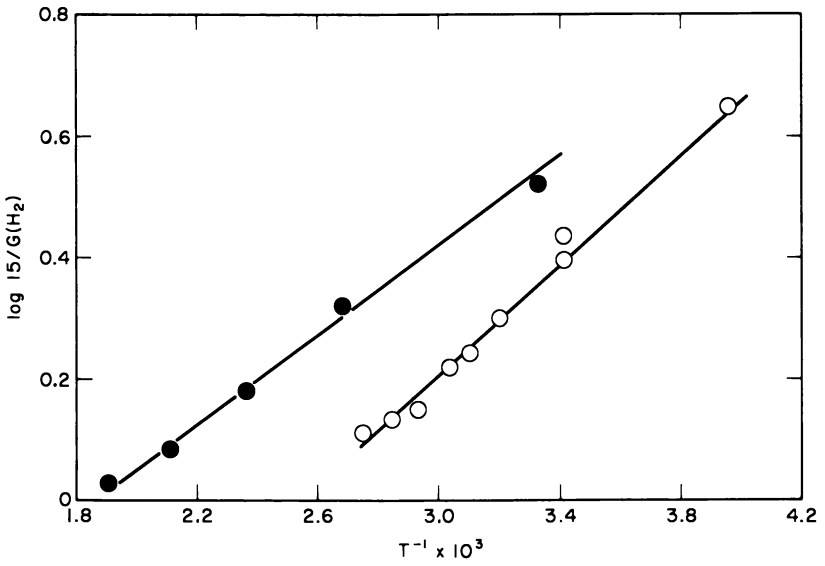

Figure 7. Arrhenius plot for hydrogen formation from the radiolysis of NH_3. Open points from present work, filled points from Jones and Sworski (14)

$NH_3 + D_2$. Experiments with D_2 as scavenger were carried out in the hope of using the exchange Reaction 26

$$H + D_2 \rightarrow HD + D \qquad (26)$$

to determine G_H. However, the yield of HD depends on the D_2 concentration up to the highest concentrations used, and the values attained (Table I) indicate that HD is formed by a chain reaction. Possible propagation steps are Reactions 26 and 27,

$$D + NH_3 \rightarrow NH_2D + H \qquad (27)$$

where the dependence of $G(HD)$ on D_2 concentration is caused by competition between Reaction 26 and other reactions of H atoms, including Reactions 19, 20, 22, and 23. Increased temperatures should favor Reaction 26 (E_{26} = 7300 cal./mole (25)). Increased dose rates favor the combination reactions compared with Reaction 26 at a given D_2

Publication Date: January 1, 1968 | doi: 10.1021/ba-1968-0082.ch012

concentration. This could account for the different yields of HD obtained by Jones and Sworski (*14*). Using a dose rate approximately 10^3 times ours, they observed only a small increase in $G(HD)$ with D_2 concentration at 23°C. (from 0.67 at 1.6 mole % to 5.6 at 14.3 mole % D_2) and concluded that a chain reaction did not occur under these conditions, although a chain reaction was observed at 200°C.

In view of our results, we are doubtful whether any meaningful conclusions about the primary yields can be drawn from the measurements of the exchange yield in this system.

Primary Yields in NH_3 and in $NH_3 + C_3H_8$. The yields from pure NH_3 show that the decomposition yield at the high temperature plateau of the yield-temperature plot (Figure 1) is at least $G(-NH_3) = 2G(N_2)^{max} = 10$. On the other hand, the experiments with C_3H_8 as scavenger indicate $G(-NH_3) = G_H + G_{H_2} = G(H_2) = 8.0 \pm 0.4$. This discrepancy suggests that C_3H_8 reacts with or prevents the formation of an intermediate, which in pure NH_3 contributes to the decomposition. The possibility that an excited state of NH_3 is formed, which dissociates in pure NH_3 but is deactivated by C_3H_8, cannot be excluded. However, this seems improbable since it implies that the postulated excited state is quenched by $4 \times 10^{-4}M$ C_3H_8 but not by $4 \times 10^{-2}M$ NH_3.

It is possible that neutralization of NH_4^+ ions by electrons may not lead directly to H atoms according to Reaction 28,

$$NH_4^+ + e^- \rightarrow NH_3 + H \qquad (28)$$

but that NH_4 radicals may be formed (Reaction 29).

$$NH_4^+ + e^- \rightarrow NH_4 \qquad (29)$$

The existence of NH_4 has been suggested previously on the basis of mass spectrometric evidence and theoretical considerations (*21, 22*). The two neutralization Reactions 28 and 29 may not be distinguishable with C_3H_8 as scavenger since both Reaction 9 and Reaction 30

$$NH_4 + C_3H_8 \rightarrow H_2 + C_3H_7 + NH_3 \qquad (30)$$

would result in the formation of one molecule of H_2 per ion. However, in pure NH_3 it is possible that interaction of NH_4 with other free radicals in the system might result in an extra decomposition of NH_3, over that observed in the presence of C_3H_8, up to a maximum corresponding to $G_{NH_4^+} = 3.8$.

Some evidence for a decomposition of NH_3 resulting from NH_4^+ neutralization has been obtained from experiments with water vapor + NH_3 mixtures (Figure 6). Radiolysis of water vapor results in the formation of H atoms by Reactions 31 to 34 (*cf.* Ref. *11*)

$$H_2O \rightsquigarrow H_2O^* \rightarrow H + OH \qquad (31)$$

$$H_2O \longrightarrow H_2O^+ + e^- \quad (32)$$

$$H_2O^+ + H_2O \rightarrow H_3O^+ + OH \quad (33)$$

$$H_3O^+ + e^- \rightarrow H + H_2O \quad (34)$$

In the presence of NH_3, the proton-transfer Reaction 35

$$H_3O^+ + NH_3 \rightarrow H_2O + NH_4^+ \quad (35)$$

can occur so that, as in the case of pure NH_3, it is the NH_4^+ ion which undergoes neutralization. In this system, decomposition of NH_3 can conceivably result from attack by H atoms (Reaction 25), by OH radicals (Reaction 36)

$$OH + NH_3 \rightarrow H_2O + NH_2 \quad (36)$$

or from the neutralization of NH_4^+. The results with pure NH_3 discussed above show that Reaction 25 does not occur, at least at temperatures up to 200°C., and it can therefore be excluded, at these temperatures, in the $H_2O + NH_3$ system. The decomposition yield in H_2O at 120°C., $G(-NH_3) = 2\,G(N_2) = 3.4 \pm 0.4$ is independent of the concentration of NH_3 between 0.5 and 3.0 mole %. This appears to exclude Reaction 36 as being responsible since for 0.5 mole % of NH_3 to scavenge all the OH radicals, the specific rate of Reaction 36 would have to be greater than that of Reaction 9, which is highly improbable. It is possible, however, that decomposition is initiated by neutralization (Reaction 28) followed by reactions of NH_4 to give N_2. The value of $G(N_2)$ agrees with this interpretation since it is equal to $\frac{1}{2}\,G\,(NH_4^+) = \frac{1}{2}\,G\,(e^-) \sim 1.5$. The higher yields from $H_2O + NH_3$ at temperatures above 400°C. are possibly caused by Reaction 36, and the results indicate the activation energy of this reaction to be *ca.* 15 kcal./mole.

Publication Date: January 1, 1968 | doi: 10.1021/ba-1968-0082.ch012

Literature Cited

(1) Anderson, A. R., Winter, J. A., "The Chemistry of Ionization and Excitation," p. 197, Taylor & Francis, London, 1967.
(2) Becker, K. H., Welge, K. H., *Z. Naturforsch.* **19A,** 1006 (1964).
(3) Burtt, B. P., Baurer, T., *J. Chem. Phys.* **23,** 466 (1955).
(4) *Ibid.*, **26,** 846 (1957).
(5) Dainton, F. S., Skwarski, T., Smithies, D., Wezranowski, E., *Trans. Faraday Soc.* **60,** 1068 (1964).
(6) Davidow, R. S., Lee, R. A., Armstrong, D. A., *J. Chem. Phys.* **45,** 3364 (1966).
(7) Dorfman, L. M., Noble, P. C., *J. Phys. Chem.* **63,** 980 (1959).
(8) Harrison, A. G., Thynne, J. C. J., *Trans. Faraday Soc.* **62,** 2804 (1966).
(9) Hogg, A. M., Haynes, R. M., Kebarle, P., *J. Am. Chem. Soc.* **88,** 28 (1966).
(10) Johnson, G. R. A., Simic, M., *Nature* **216,** 479 (1967).
(11) Johnson, G. R. A., Simic, M., *J. Phys. Chem.* **71,** 1118 (1967).
(12) Johnson, G. R. A., Warman, J. M., *Trans. Faraday Soc.* **61,** 1709 (1965).
(13) Jones, F. T., Sworski, T. J., *J. Phys. Chem.* **70,** 1546 (1966).
(14) Jones, F. T., Sworski, T. J., *Trans. Faraday Soc.* **63,** 2411 (1967).

(15) *Ibid.*, p. 2426.
(16) MacDonald, C. C., Kahn, A., Gunning, H. E., *J. Chem. Phys.* **22,** 908 (1954).
(17) Mahan, B. H., Young, C. E., *J. Phys. Chem.* **44,** 2192 (1966).
(18) McNesby, J. R., Tanaka, T., Okaba, H., *J. Chem. Phys.* **36,** 605 (1962).
(19) Meaburn, G. M., Gordon, S., *J. Phys. Chem.* **72,** 1592 (1968).
(20) Meisels, G. G., *J. Chem. Phys.* **41,** 51 (1964).
(21) Melton, C. E., *J. Chem. Phys.* **45,** 4414 (1966).
(22) *Ibid.*, **46,** 4275 (1967).
(23) Nishikawa, M., Shinohara, N., Matsuura, N., *Bull. Chem. Soc. Japan* **40,** 1993 (1967).
(24) Oganasyan, K. T., Nalbandyan, A. B., *Dokl. Akad. Nauk SSSR* **160,** 162 (1965).
(25) Schiavello, M., Volpi, G. G., *J. Chem. Phys.* **37,** 1510 (1962).
(26) Schultz, W. R., LeRoy, D. J., *Can. J. Chem.* **42,** 2480 (1964).
(27) Simic, M., Redpath, J. L., in press.
(28) Sorokin, Y. A., Pshezhetskii, S. Y., *Russ. J. Phys. Chem.* **38,** 434 (1964).
(29) *Ibid.*, **39,** 1037 (1965).
(30) Toi, Y., Petterson, D. B., Burton, M., *Radiation Res.* **17,** 399 (1962).
(31) Warman, J. M., *J. Phys. Chem.* **71,** 4066 (1967).
(32) Wourtzel, E., *Radium* **11,** 319 (1919).

RECEIVED January 17, 1968.

13

ESR Study of Free Radicals Produced in the Gas Phase by Low Energy Electrons

Energy Effect on the Production of NH_2 in NH_3

R. MARX and G. MAUCLAIRE

Laboratoire de Physico-Chimie des Rayonnements, Faculté des Sciences, 91 Orsay, France

Publication Date: January 1, 1968 | doi: 10.1021/ba-1968-0082.ch013

An apparatus allowing the ESR study of free radicals produced by electron bombardment of gases is described. The energy of the electrons can be varied from 5 to a few hundred e.v. The free radicals are trapped on a cold finger. For ammonia, between 8 and 30 e.v., there are at least three different processes responsible for producing $\cdot NH_2$ radicals. Two of them, which have nearly the same threshold energies as NH_3^+ and NH_2^+ ions (10.4 and 15.7 e.v.) are ion-molecule reactions. The third, appearing near 18 e.v. is thought to be caused by the decomposition of a highly excited state of NH_3 molecules. The production of $\cdot NH_2$ below the first ionization potential of NH_3 cannot be excluded.

Primary processes in radiation chemistry are largely caused by secondary electrons whose energies are less than 100 e.v. This is why direct study of the transient species produced by low energy electrons is so important for understanding the results of radiation chemistry. Most investigations have been carried out by mass spectrometry techniques (*e.g.*, by Derwish *et al.* (*3*) and Melton (*9*) for NH_3) and a few by optical spectroscopy (*6*). Mass spectrometry gives much information about ions and some of their reactions and neutral species (radicals) but in an indirect way.

Since ESR spectrometry provides a direct method to study free radicals, it may also give some interesting information (*7*, *10*). We report here some results concerning radicals formed when gaseous ammonia is bombarded with electrons of energy ranging from 5 to 100 e.v. Ammonia

In Radiation Chemistry; Hart, E.;
Advances in Chemistry; American Chemical Society: Washington, DC, 1968.

was chosen for the first investigation of this kind because there are many results available on ionization, photoionization, and radiation chemistry of this compound. Moreover, it is a simple compound from an experimental point of view—*i.e.*, it produces only a small amount of insulating deposit on the electrodes, it is easy to condense at liquid nitrogen temperature, and it can give only a small number of free radical types.

Experimental

Apparatus. The experimental apparatus, an ion source coupled to an ESR spectrometer, has been described (7). However, with our first ion source we could not obtain enough electrons of energy lower than 15 e.v., and we could not operate at high pressure because pyrolysis of products on the hot filament gave spurious spectra and corroded the filament.

The apparatus used in this work is shown in Figure 1. The stainless steel ion source is divided in two parts, each of which is pumped by separate diffusion pumps (limiting vacuum 10^{-6} mm. Hg). The electron gun contains the filament, 4 (tungsten ribbon 0.4 mm. wide 0.05 mm. thick), and two stainless steel electrodes, 5 and 6. The interaction chamber contains usually only the collector, 8, but some other electrodes may be added—a retarding grid to measure the energy spread of the electron beam and two parallel plates to extract the positive ions. The two compartments are separated by Electrode 7 with a 10-mm. long rectangular channel to give a pressure drop between the two parts of the source. The same voltage, V, which determines the energy of the electrons is applied to Electrodes 7 and 8 and to the walls of the reaction chamber. Electrode 8 is isolated from the end plate of the ion source and connected to the power supply through a microammeter to measure the intensity of the electron beam after its passage through the reaction chamber.

One end of the filament is connected to Electrode 5. The accelerating voltage on Electrode 6 is maintained lower than V. Under these conditions, the energy spread of the electron beam is large with a half-width of about 2 e.v.

Since the axis of the ion source is parallel to the axis of the electromagnet of the ESR spectrometer, 12, the electrons are collimated in such a way that, after passing through the channel, the intensity of the electron beam is still high even at low energies. For example, for a 5-e.v. electron beam, with very clean electrodes, we obtain currents as high as 50 μamp. If there is an insulating deposit on Electrode 7, the intensity is considerably decreased.

Owing to the pressure drop between the two compartments the intensity remains almost constant when the pressure in the reaction chamber is raised to 10^{-3} or 10^{-2} mm. Hg.

The gaseous samples are introduced through a pin hole, 9, (ϕ = 0.4 mm.). The flow rate is regulated by a valve between the exit hole and a reservoir containing the compound. The reservoir must be kept at

Publication Date: January 1, 1968 | doi: 10.1021/ba-1968-0082.ch013

Publication Date: January 1, 1968 | doi: 10.1021/ba-1968-0082.ch013

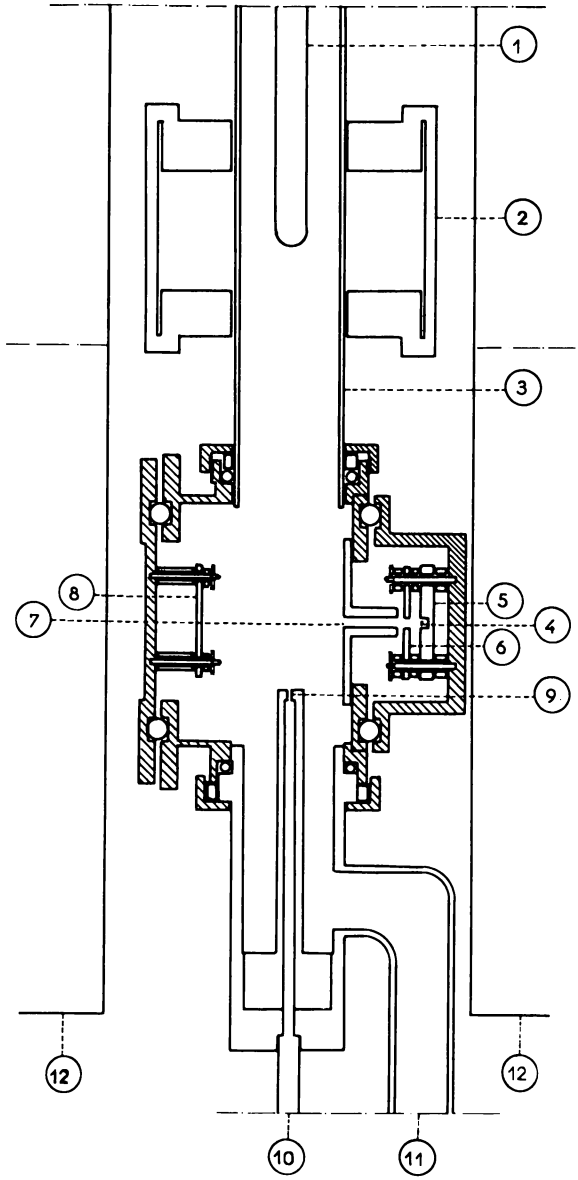

Figure 1. The ion source

(1) Cold finger to trap free radicals
(2) ESR cavity (cylindrical H_{011})
(3) Quartz tube
(4) Filament of electron gun
(5, 6, 7, 8) Stainless steel electrodes
(9) Exit hole for gas sample
(10) To valve and gas reservoir
(11) To pressure gage
(12) Pole pieces of electromagnet

a suitable temperature to keep the pressure on the valve below 1 atm. Under these conditions we do not have a molecular beam, and the pressure measured in 11 may be considered uniform throughout the whole reaction chamber.

After crossing the electron beam, the gas flow, which contains both the reaction products and the unreacted molecules, is condensed on a cold finger, 1, located in the cavity of the ESR spectrometer, 2. The temperature of the cold finger may be varied to 77°K. The ratio of the pressures in the two compartments of the ion source is approximately 30, so that the amount of pyrolysis products trapped on the cold finger is very low.

Conditions. NH_3 gas is introduced into the source from a reservoir kept at −40°C. In most of these experiments the pressure in the ion source was 3×10^{-3} torr (10^{14} molecules/cc.). The pumping rate is 5 liters/sec. when the cold finger is filled with liquid nitrogen, the flowing rate being 6×10^{17} molecules/sec., and the transit time of molecules between the interaction zone and the cold finger $\simeq 2 \times 10^{-3}$ sec.

During the electron bombardment the strength of the magnetic field was only 300 oe., sufficient to obtain a well-focused electron beam. The very slow secondary electrons produced in the reaction chamber may diffuse across the magnetic field, but they are in low concentration ($\simeq$ 1/1000 of the electron current), and their effects can be neglected.

Since the reaction chamber is surrounded by an equipotential surface, we may assume that there is no electric field acting on the ions produced by electron impact. Therefore, those ions have only the kinetic energy of the molecules, and they may diffuse across the magnetic field at much higher rates than the electrons. However, the component of their velocity perpendicular to the magnetic field is less than the velocity parallel to the field by a factor $\frac{1}{1 + (\omega\tau)^2}$, where ω is the cyclotron frequency of the ions in the magnetic field, and τ is the time between collisions.

Consequently, the relative efficiency of ion reactions in the volume of the chamber and of neutralization on the walls depends not only on pressure and reaction cross sections but also on magnetic field strength.

Electron bombardment was carried out for 30 min. at energies below 14 e.v. and for 15 min. at higher energies. When the pressure is less than $\simeq 10^{-2}$ mm. Hg, the amount of trapped radicals is proportional to the duration of the experiment as long as it is shorter than 60 min.

The intensity of the electron beam, measured on Electrode 8 in the absence of gas ($P \simeq 10^{-6}$ mm. Hg) was fixed at 50 μamp. for all energies used. Below the threshold energy for radical production, this intensity remains practically constant when ammonia is admitted in the ion source. At higher energies its value depends, of course, on the reactions involving ions and electrons which occur in the source.

Publication Date: January 1, 1968 | doi: 10.1021/ba-1968-0082.ch013

Results

ESR Spectrum. At all energies between 5 and 100 e.v. we observe only the spectrum of $\cdot NH_2$ radical (Figure 2A). The shape of this spectrum corresponds to the calculated shape for $\cdot NH_2$ radicals rigidly held in a polycrystalline matrix of parent molecules (8) ("quenched $\cdot NH_2$"). Some experiments at lower pressure (10^{-4} mm. Hg) gave a slightly different spectrum (Figure 2B); besides the lines owing to quenched $\cdot NH_2$ there are some additional lines which may arise from rapidly reorientating $\cdot NH_2$. The difference between the two kinds of $\cdot NH_2$ radicals was attributed to differences in the crystalline structure of the matrix around the trapping sites (8).

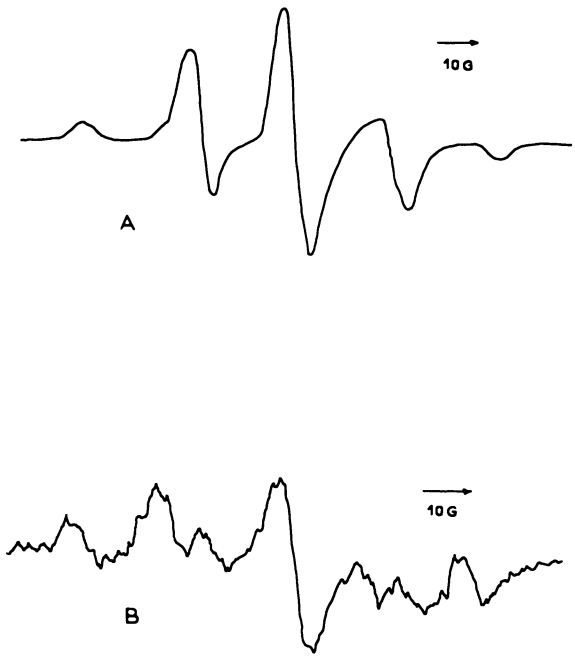

Figure 2. ESR spectra of $\cdot NH_2$ radicals trapped on the cold finger

(A) Quenched $\cdot NH_2$ obtained at 3×10^{-3} mm. Hg
(B) Rotating + quenched $\cdot NH_2$ obtained at 3×10^{-4} mm. Hg

In our case the difference may arise between trapping sites inside the solid deposit (quenched $\cdot NH_2$) and trapping sites near the surface (rotating $\cdot NH_2$). For the same deposit time, the ratio of rotating over quenched $\cdot NH_2$ increases when pressure decreases since the volume of

deposit decreases with pressure while its surface remains approximately constant. H atoms which may be produced in our experiments cannot be trapped at 77°K. in an ammonia matrix.

Radical Production as a Function of Electron Energy. Figure 3 shows the number of trapped $\cdot NH_2$ radicals as a function of the energy of the incident electrons up to 50 e.v. The intensity of the beam, ammonia pressure, and the deposit time were the same in all the experiments. Only a small fraction of electrons collides, so that the chance that an electron makes two collisions is negligible even for electrons of 50 e.v.

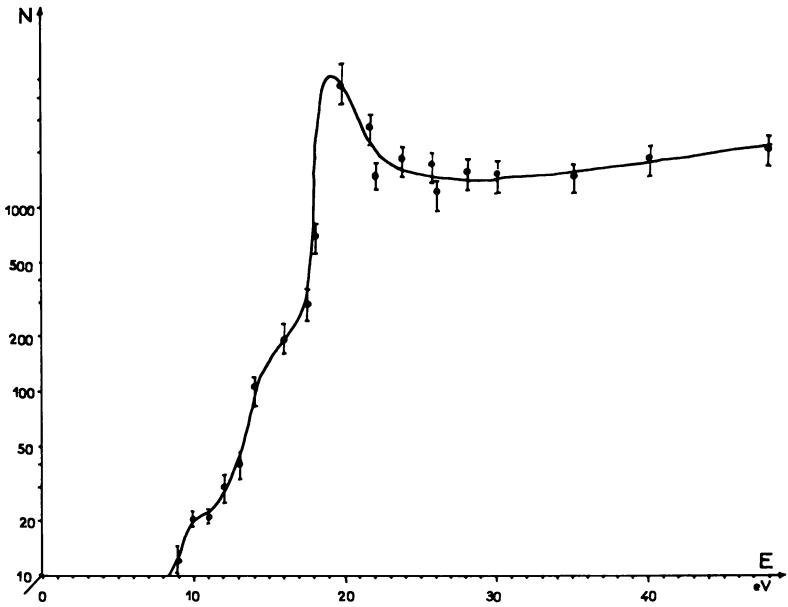

Figure 3. Number of radicals (logarithmic scale, arbitrary unit) vs. *mean energy of the electron beam*

The step-like shape of this curve indicates that different processes for $\cdot NH_2$ production occur at definite electron energies. The first step appears between 8 and 11 e.v., the second between 13 and 15 e.v., and a third sharp step near 18 e.v. There is a maximum near 20 e.v., and between 23 and 50 e.v. we have practically no change in $\cdot NH_2$ concentration.

The energy distribution of the electron beam is too high to give a good determination of the threshold energy for the different steps. Further, V is the voltage measured between the cathode (filament) and the two end plates. The true energy of the electrons may be slightly different and depends on the interelectrodes contact potentials.

Publication Date: January 1, 1968 | doi: 10.1021/ba-1968-0082.ch013

Nevertheless, the three steps in Figure 3 are fairly well reproducible even for different values of the magnetic field strength, but the amount of trapped radicals for a given energy of the electron-beam varies in large proportions with the magnetic field. Hence, the radical concentrations are given in arbitrary units. For example, with a magnetic field of 300 oe, the amount of radicals trapped in 30 min. is about 5×10^{15} for 25 e.v. electrons and 2×10^{13} (corresponding to a signal-to-noise ratio of ~ 3) for 8 e.v. electrons. Hence, for the moment we must consider these results only as qualitative.

Discussion

Processes Occurring at Energies Lower than 18 e.v. Much work has been done on the ionization potential of ammonia (*see* Table I, Ref. *4*). The first ionization potential as determined by electron impact experiments (*5*) is 10.4 e.v.

$$NH_3 + e \rightarrow NH_3^+ + 2e \quad (1)$$

The second ionization process appearing at about 15 e.v. is thought to be caused by the ionization of a strongly bonding orbital of NH_3 (*4*). Therefore, NH_3^+ produced by electrons of energy higher than 15 e.v. must produce fragment ions easily. The mechanism of fragmentation occurring near 15 e.v. has been established recently by Brehm and Puttkamer (*2*) who investigated simultaneously the NH_3^+ and NH_2^+ ions formed and the photoelectrons ejected by 21.2 e.v. photons acting on NH_3.

Between 15.02 and 15.73 e.v. they observed NH_3^+ ions only, while above 15.73 e.v., NH_3^+ and NH_2^+ ions are produced

$$NH_3 + h\nu \rightarrow NH_3^+ + e \quad (2)$$

$$NH_3 + h\nu \rightarrow NH_2^+ + H + e \quad (3)$$

Taking account the fact that the energy of our electron beam is not as well defined as theirs was, there is good correlation between the appearance potential of NH_3^+ and NH_2^+ and the two first steps of our curve (Figure 3). The production of $^{\cdot}NH_2$ by electrons of energy up to $\simeq$17 e.v. may therefore be interpreted as being caused by the two ion-molecule reactions (*3, 9*) below

$$NH_3^+ + NH_3 \rightarrow {}^{\cdot}NH_2 + NH_4^+ \quad (4)$$

$$NH_2^+ + NH_3 \rightarrow {}^{\cdot}NH_2 + NH_3^+ \quad (5)$$

Neutralization of NH_4^+ on the wall of the reaction chamber may also give NH_2 (*9*) by:

$$NH_4^+ + e \rightarrow {}^{\cdot}NH_2 + H_2 \quad (6)$$

Publication Date: January 1, 1968 | doi: 10.1021/ba-1968-0082.ch013

If we take:

$$\sigma_4 = 55.10^{-16} \text{ sq. cm.}$$

$$\sigma_5 = 70.10^{-16} \text{ sq. cm.}$$

for the cross sections of Reactions 4 and 5 (*3, 9*), and if we evaluate the diffusion rate of the ions under our experimental conditions of pressure and magnetic field strength, it is easy to show that more than 90% of the ions collide effectively, giving $^{\cdot}NH_2$ before they are neutralized on the electrodes or walls of the reaction chamber.

On the contrary, it is difficult to compare the efficiency of $^{\cdot}NH_2$ production at different energies with the ionization cross sections for the primary ions NH_3^+ and NH_2^+. In the literature one finds ionization cross sections for 21.2 e.v. photons (*2, 4*) and for 100 e.v. electrons (*9*), but none of these data are directly applicable to our experimental procedure.

However, at least for two values of the magnetic field, the ratio $[^{\cdot}NH_2]_{16\,e.v.}/[^{\cdot}NH_2]_{12\,e.v.}$ (about 6 for 700 oe. and 9 for 300 oe.) is close to the ratio of ejected photoelectrons and ions produced by 21.2 e.v. photons (*2, 4*).

Below the first ionization potential, $^{\cdot}NH_2$ radical production has been proposed and attributed to a dissociative electron attachment occurring near 3.9 e.v. (*9*).

$$NH_3 + e \rightarrow {}^{\cdot}NH_2 + H^- \qquad (7)$$

Moreover, Lassettre (*11*) shows a sharp excitation peak at 6.38 e.v. for 300 e.v. electrons. In our experiments we have been unable to observe any radical produced below 8 e.v., but this may be caused by the low cross section of the processes occurring in this region and by the limiting sensitivity of our spectrometer.

The long tail of our curve below the first ionization potential (between 8 and 10.4 e.v.) may be caused by different processes: (a) the energy spread of the electron beam, allowing Reactions 1 and 4, or (b) decomposition processes like Reaction 7 or more probably:

$$NH_3 + e \rightarrow (NH_3)^* + e \rightarrow {}^{\cdot}NH_2 + H + e \qquad (8)$$

Processes Occurring at Energies Higher than 18 e.v. Besides the processes just described, others must occur near 18 e.v. The increase in radical production is important indeed and is accompanied by an emission of blue light.

With our experimental device it has not been possible yet to analyze the light emitted; this could be done in the apparatus used by Horani for H_2O (*6*). However, we think that at these energies the decomposition

Publication Date: January 1, 1968 | doi: 10.1021/ba-1968-0082.ch013

of a highly excited state of NH_3 becomes important. We tentatively propose

$$NH_3 + e \rightarrow (NH_3)^{**} + e \rightarrow {}^{\cdot}NH_2 + H^* + e \qquad (9)$$

The blue light emission could be caused then by excited hydrogen atoms.

A process of the same kind has been observed by Beyer and Welge (*1*) who studied the photodecomposition of NH_3 in the region 843–743 A. (15–18 e.v.).

Moreover, in the excitation spectrum of NH_3 by 300 e.v. electrons (*11*) there is a peak at 17.36 e.v. The energetics of Reaction 9 show that it may occur above 17.6 e.v.:

$$D_{N\text{-}H} + IP(H) = 4.1 + 13.5 = 17.6 \text{ e.v.}$$

This corresponds fairly well to the 18-e.v. threshold energy of our experiments. Furthermore a mechanism like Reaction 9 would have a first-order dependence on pressure and be independent of the magnetic field strength.

We made some preliminary experiments on the pressure dependence of ${}^{\cdot}NH_2$ production. At 25 e.v. it was nearly first order while at 16 e.v. it was closer to second order. We cannot say anything about magnetic field dependence. To explain the increase in radical yield observed at higher magnetic field (700 oe.), it is necessary to perform more elaborate calculations on the magnetic field dependence of the ion-molecule reactions (4 and 5).

Conclusion

Between 8 and 30 e.v. there are at least three different processes responsible for producing ${}^{\cdot}NH_2$ radicals by electron impact on NH_3 molecules. Two of them are ion-molecule reactions, the primary ions being NH_3^+ and NH_2^+. Another process occurring near 18 e.v. is probably the decomposition of a highly excited neutral state of NH_3.

Further experiments to determine more precisely the threshold energy for the different processes, the origin of the light emission observed above 18 e.v., and the influence of magnetic field strength are planned for the near future. We intend also to study the ions in the reaction chamber by a cyclotron resonance mass spectrometry technique.

Literature Cited

(1) Beyer, K. D., Welge, K. H., *Z. Naturforsch.* **22a**, 1161 (1967).
(2) Brehm, B., Von Puttkamer, E., *Intern. Conf. Mass Spectrometry, Berlin, 1967.*
(3) Derwish, G. A. W., Galli, A., Giardini-Guidoni, A., Volpi, G. G., *J. Chem. Phys.* **39**, 1599 (1963).

Publication Date: January 1, 1968 | doi: 10.1021/ba-1968-0082.ch013

(4) Frost, D. C., McDowell, C. A., Vroom, D. A., *Can. J. Chem.* **45,** 1343 (1967).
(5) Frost, D. C., McDowell, C. A., *Can. J. Chem.* **36,** 39 (1958).
(6) Horani, M., Leach, S., *J. Chim. Phys.* **58,** 825 (1961).
(7) Mauclaire, G., Marx, R., *J. Chim. Phys.* **65,** 213 (1968).
(8) Marx, R., Maruani, J., *J. Chim. Phys.* **61,** 1604 (1964).
(9) Melton, C. E., *J. Chem. Phys.* **45,** 4414 (1966).
(10) Smith, D. R., Tole, J. C., *Can. J. Chem.* **45,** 779 (1967).
(11) Skerbele, A., Lassettre, E. N., *J. Chem. Phys.* **42,** 395 (1965).

RECEIVED February 19, 1968.

14

The Study of Electron Decay in Pulse-Irradiated Gases by a Microwave Technique

RICHARD W. FESSENDEN and JOHN M. WARMAN

Radiation Research Laboratories, Mellon Institute, Carnegie-Mellon University, Pittsburgh, Pa. 15213

Publication Date: January 1, 1968 | doi: 10.1021/ba-1968-0082.ch014

A microwave technique for measuring the decay of electrons in pulse irradiated gases is described. The technique involves the measurement of the change in resonant frequency of a microwave cavity caused by a change in the complex conductivity within the cavity when electrons are present. Single pulses of 3 Mev. electrons from a Van de Graaff accelerator are used to ionize the gas. Electron densities as low as 10^7 cm.$^{-3}$ (total dose $\sim$ 0.3 rad at 10 torr) can be measured accurately. In the absence of diffusion the method can be used to study electron loss by electron capture or electron-ion recombination for pressures as low as 1 torr and as high as at least 200 torr. The potential of the technique is illustrated by results obtained with pulse-irradiated air.

The presence in the gas phase of electrons within a microwave cavity is indicated by a shift of the cavity resonance frequency from that in the absence of electrons. This shift, Δf, is related to the concentration of electrons according to Equation A (*2, 3*):

$$\frac{\Delta f}{f} = \frac{A}{2\pi} \cdot \frac{e^2}{mf^2} \cdot \frac{N_e}{1 + \left(\frac{\nu_c}{2\pi f}\right)^2} \qquad \text{(A)}$$

where f is the resonant frequency, in the absence of electrons, in cycles/sec. (Hz), N_e is the mean number density of electrons in cm.$^{-3}$, e is the charge of the electron in e.s.u., m is the mass of the electron in gram, ν_c is the collision frequency of electrons with neutral gas molecules and A is a constant determined by the geometry of the cavity and the spatial distribution of the electrons within it ($A = 1$ for a uniform distribution

In Radiation Chemistry; Hart, E.;
Advances in Chemistry; American Chemical Society: Washington, DC, 1968.

within the cavity). For the relationship between electron concentration and complex conductivity *see* Ref. 6; for the relationship between the complex conductivity in a microwave cavity and the resonant frequency *see* Ref. 9.

The first use of this technique, to observe the decay of electrons in an ionized gas, was made by Biondi and Brown in 1949 (*1*). Since that time the technique has been used by several workers to determine electron attachment and electron-ion recombination rate constants, diffusion coefficients and electron collision frequencies. Sources of plasmas have included microwave discharges (*2*), photoionization (*7*), and particle accelerators (*11*). The first of these sources has two main disadvantages: (1) interference in the detecting circuitry is caused by the high power microwave pulse required to produce the discharge, and (2) the high ratio of excited to ionic species initially formed can result in considerable ionization after the pulse. Photoionization requires the presence in the system of a substance having a suitably low ionization potential and high photoionization cross section, and ideally a low electron capture cross section. The formation of ions in a gas by a high energy ($>$ 1 Mev.) electron beam has none of the above disadvantages and has several important advantages. Among these are the possibility of producing a uniform concentration of electrons throughout the cavity, continuous variation of pulse width and beam current over several orders of magnitude and the possibility of absolute calibration of the technique *via* chemical dosimetry.

The availability of pulsed particle accelerators in radiation laboratories and the interest of radiation chemists in the chemistry of the electron would indicate this technique to be of considerable use in this field. The purpose of the present paper is therefore to detail the experimental procedure involved and to illustrate the potential of the technique.

Publication Date: January 1, 1968 | doi: 10.1021/ba-1968-0082.ch014

Experimental

As shown by Equation A measurement of electron concentration reduces to measurement of changes in the resonant frequency of a microwave cavity. The early approaches involved a point-by-point method (*2*) of following the decay of concentration and hence were slow and subject to error. In more recent work (*7*) the detection cavity formed part of a frequency discriminator thereby providing an output proportional to cavity frequency. The technique used in the work reported here is an obvious extension of this approach.

The frequency used is in the X-band region (3 cm., 9500 MHz) because of the convenient size of the components and their ready availability. A block diagram of the apparatus is shown in Figure 1 (its similarity to an ESR spectrometer will be noted). The klystron signal after passing through an isolator is sampled to provide a reference bias signal of

adjustable phase for the balanced mixer. The microwave power travels to the sample cavity through an attenuator and magic tee; the arm of the "tee" opposed to the cavity is terminated. The signal from the fourth arm of the "tee" goes to the balanced mixer. In operation the phase shifter is adjusted so that the reference signal and power reflected by the cavity at its resonant frequency are in quadrature. The difference between the two crystal detector outputs is of the same form as that of a frequency discriminator. This output after amplification is applied to the klystron reflector supply (which can be viewed as just an amplifier) to electronically tune the klystron and to hold its frequency at the center of the cavity resonance. For very high gain of the feedback loop, the output voltage to the oscilloscope per MHz of frequency deviation depends only upon the gain of the klystron power supply and the MHz/volt factor of the klystron. In our arrangement the klystron reflector supply can be viewed as a flat amplifier from d.c. to several MHz. The loop gain of the feedback circuit was around 20 under the usual conditions (microwave power in the cavity of ~ 50 μwatts). The response time was found to be less than 0.5 μsec. as measured by injecting a chopped microwave signal into the normally terminated arm of the magic tee. The width of the cavity response curve (loaded Q = 5000) probably is the limiting factor in this response time. No special efforts have been made to reduce the noise level since sufficient signal is usually available at small radiation doses. The detectors used are standard 1N23E diodes and give a noise level corresponding to ~ 5 kHz change in the cavity frequency.

Publication Date: January 1, 1968 | doi: 10.1021/ba-1968-0082.ch014

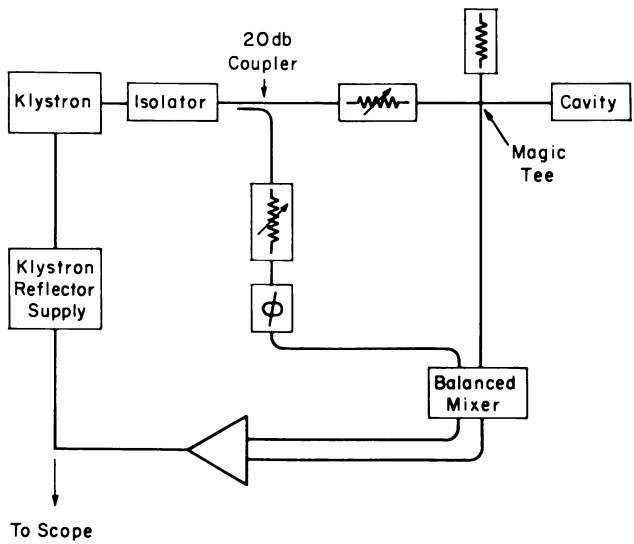

Figure 1. Block diagram of apparatus used to detect electrons in the gas phase. Symbols for fixed and variable resistance indicate respectively a termination and variable attenuator and the letter ϕ indicates an adjustable phase shifter

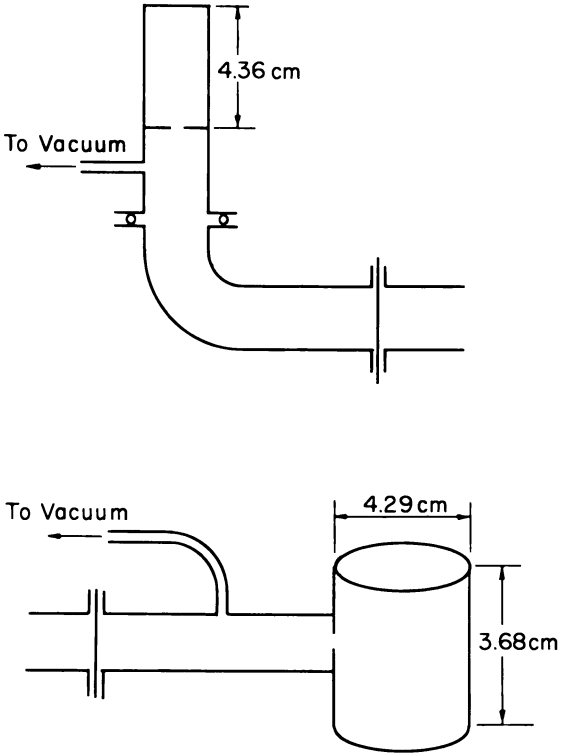

Figure 2. Two microwave cavity configurations which have been used in these experiments. Upper: rectangular $TE_{1,0,2}$ mode in standard X-band waveguide; lower: cylindrical, radially symmetric $TE_{0,1,1}$ mode. Both use a Mylar film and stopcock grease for a vacuum seal and the upper has an additional "O"-ring seal. Irradiation is from above in both cases

The use of feedback to provide frequency control of the klystron has the obvious advantage that the usable range of frequency deviation is much larger. Also the real component of electron conductivity encountered at high pressures (and which changes the cavity Q) can have an effect only on the error signal ($\sim$ 5%) in the feedback loop rather than upon the whole signal as in the case of no feedback.

Two cavity arrangements which have been used are shown in Figure 2. The rectangular $TE_{1,0,2}$ mode has given results indicating that diffusion to the walls is important below 10 torr pressure for electron lifetimes of 100 μsec. The radially symmetric mode $TE_{0,1,1}$ is used in the second configuration to provide the longest possible distances for diffusion. This also has the advantage that there is no microwave electric field at the walls thereby reducing the effect of those electrons close to the walls (which would have the shortest diffusion lifetime).

The gas is ionized by a single pulse of 2.8 Mev. electrons from a Van de Graaff accelerator. The cavity is sufficiently far removed from the beam exit port to ensure uniform irradiation within the cavity (tested for using blue cellophane). The beam enters the cavity through an 0.018 inch (0.46 mm.) stainless steel window, maximum attenuation 0.8 Mev. Gas pressures were measured with a mercury manometer (20–760 torr) or a Dubrovin gauge (1–20 torr) on a vacuum line connected to the waveguide by a metal to glass seal, Figure 2. The air used was analyzed mass spectrometrically and contained 21.2% O_2. Drying, by passing the gas through an elongated semi-immersed spiral trap at −72°C., did not change the results.

Since the decay process in the present experiments is pseudo-first order, absolute calibration of the electron concentration was not necessary. However, an indication of the sensitivity of the technique is of interest and can be obtained using Equation A. Thus, the noise level of 5 kHz mentioned above corresponds to an electron concentration of $\sim 10^6$ cm.$^{-3}$. The electron concentration immediately after the pulse (2 μsec., $\sim$ 10 μA) in Figure 3 (upper) is $\sim 5 \times 10^7$ cm.$^{-3}$.

Results and Discussion

The decrease of electron concentration, N_e, in air following a 2 μsec. pulse of irradiation was studied as a function of pressure, from 4.0 to 80 torr. The results obtained at 6.0 and 36 torr, using the rectangular cavity, are shown in Figure 3. Using the rectangular cavity deviation from a purely exponential decay was found below 10 torr indicating a contribution to the decay from diffusion to the cavity walls. Single points, taken from the continuous decay curves, when plotted as log N_e *vs.* time after pulse were linear, for at least four half-lives, at all pressures using the cylindrical cavity. The pseudo-first order process involved is presumably electron attachment to oxygen, Reaction 1a

$$e + O_2 \xrightarrow{k_{eff}} O_2^- \qquad (1a)$$

as suggested previously in other studies of electron loss mechanisms in oxygen and oxygen-nitrogen mixtures (*4, 5, 12*). The half-life of electrons, $\tau_{1/2}$, determined from plots of log N_e *vs.* time is related to the rate constant for Reaction 1a,

$$\tau_{1/2} = \frac{0.693}{k_{eff} N_{O_2}}$$

where N_{O_2} is the concentration of oxygen in molecules cm.$^{-3}$. The initial step in the electron capture process must be the formation of the O_2^- ion with excess vibrational energy equal to the sum of the electron affinity of O_2 and the kinetic energy of the incident electron,

$$e + O_2 \xrightarrow{k_1} O_2^{*-} \qquad (1b)$$

The reverse reaction, (2), can then occur and permanent electron attachment is not attained unless part, at least, of the excess energy of the ion is removed.

$$O_2^{*-} \xrightarrow{k_2} O_2 + e \qquad (2)$$

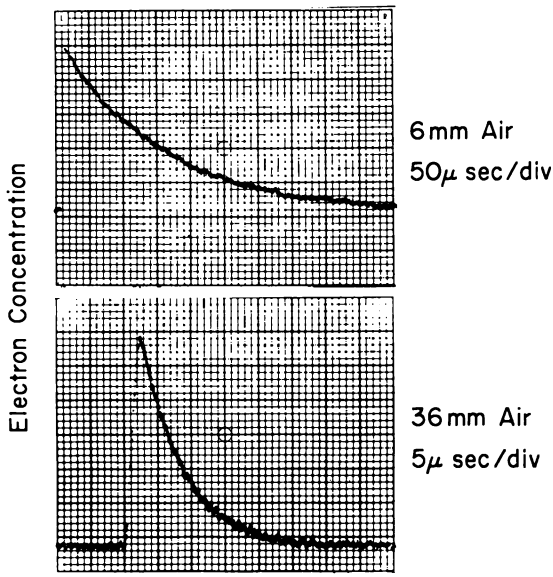

Figure 3. Oscilloscope traces of the electron decay in pulse-irradiated air at pressures of 6.0 and 36 torr. Electron concentration in arbitrary units. Time scale refers to heavy vertical divisions

It was first suggested by Bloch and Bradbury (3) that stabilization could be accomplished by collisional deactivation,

$$O_2^{*-} + M \xrightarrow{k_3} O_2^- + M^* \qquad (3)$$

If the concentration of O_2^{*-} is small compared with the electron concentration then, from the above reactions, the electron decay is described by the expression.

$$-\frac{dN_e}{dt} = \frac{k_1}{1 + \frac{k_2}{k_3 N_M}} N_e \cdot N_{O_2} \qquad (B)$$

where N_M, N_e and N_{O_2} are the concentrations of neutral molecules, elec-

trons and oxygen respectively. The effective two body rate constant is then

$$k_{eff} = \frac{k_1}{1 + \frac{k_2}{k_3 N_M}} \quad (C)$$

At low pressures (C) approximates to

$$k_{eff} = \frac{k_1 k_3}{k_2} N_M \quad (D)$$

and electron capture is effectively a three body reaction

$$e + O_2 + M \rightarrow O_2^- \quad (4)$$

of rate constant k_1k_3/k_2 cm.^{6} sec.$^{-1}$. A plot of $\tau_{1/2}P_{O_2}$ ($\sim 1/k_{eff}$) *vs.* $1/P_{air}$ is shown in Figure 4 for air pressures from 14 to 80 torr. The linearity of this plot is in accord with the expected pseudo-three body nature of electron capture by oxygen as has been found by other workers (*4, 5, 8, 10, 12*). The three body rate constant derived from the slope of the line in Figure 4 is 0.65×10^{-30} cm.^{6}/sec. The relative efficiencies of O_2 and N_2 as third bodies in Reaction 4 have been determined to be $O_2/N_2 \simeq 20$ (*8, 12*). Using this value and the known composition of the air sample (21.2% O_2) the three body rate constant for electron capture in oxygen alone is calculated to be 2.6×10^{-30} cm.^{6}/sec. This value is in good agreement with previous values of 2.1×10^{-30} (*12*) and 2.0×10^{-30} (*8*) obtained by microwave and drift tube methods respectively.

In terms of the above discussion the intercept in Figure 4 corresponds to a limiting (infinite pressure) two body rate constant, k_1, of 4×10^{-12} cm.^{3} sec.$^{-1}$. This value is considerably lower than the minimum values for k_1 which can be estimated from several other studies [2.5×10^{-11} (*13*), 4×10^{-11} (*5*), 7×10^{-11} (*8, 10*)]. Because of this inconsistency the value of k_1 determined from the present results should be considered to be in doubt. Experiments are presently being carried out to clarify this point.

Conclusion

The advantages of the use of an electron accelerator for production of ionization in studies of electron reactions is evident from the preceding example. Preliminary experiments with N_2O and with N_2O in propane show that electron capture by N_2O occurs in a way which also depends on the total pressure and so is apparently also a three-body process. The success of these experiments at pressures as high as 200 torr illustrates the relevance to radiation chemistry as compared with other methods such as mass spectrometry which only operate at much lower pressures.

Publication Date: January 1, 1968 | doi: 10.1021/ba-1968-0082.ch014

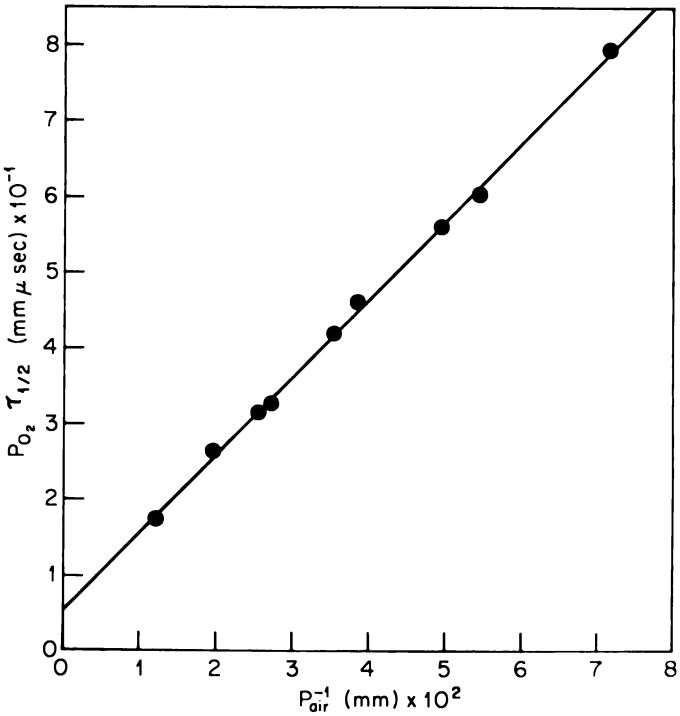

Figure 4. Dependence of the product of the electron half-life and the oxygen pressure (proportional to the reciprocal of the effective two body rate constant, see text) on the reciprocal air pressure

The sensitivity of the method is extremely high so that no problems with build-up of products of the radiolysis are likely. Conversely, however, problems with impurities will be serious. The radiolytic method allows the possibility of pre-irradiation as a partial cure.

This method is being extended to detailed studies of electron capture by N_2O and other compounds. Several other applications of importance to radiation chemistry are immediately apparent such as studies of ion recombination and the dependence of its rate on the nature of the positive ion.

Literature Cited

(1) Biondi, M. A., Brown, S. C., *Phys. Rev.* **75,** 1700 (1949).
(2) Biondi, M. A., *Rev. Sci. Instr.* **22,** 500 (1951).
(3) Bloch, F., Bradbury, N. E., *Phys. Rev.* **38,** 689 (1935).
(4) Chanin, L. M., Phelps, A. V., Biondi, M. A., *Phys. Rev.* **128,** 219 (1962).

(5) Hurst, G. S., Bortner, T. E., *Phys. Rev.* **114,** 116 (1959).
(6) McDaniel, E. W., "Collision Phenomena in Ionized Gases," p. 121, Wiley, New York, 1964.
(7) Mahan, B. H., Young, C. E., *J. Chem. Phys.* **44,** 2192 (1966).
(8) Pack, J. L., Phelps, A. V., *J. Chem. Phys.* **44,** 1879; **45,** 4316 (1966).
(9) Slater, J. C., *Rev. Mod. Phys.* **18,** 659 (1946).
(10) Stockdale, J. A., Christophorou, L. G., Hurst, G. S., *J. Chem. Phys.* **47,** 3267 (1967).
(11) Van Lint, V. A. J., Parez, J., Trueblood, D. L., Wyatt, M. E., *Rev. Sci. Instr.* **36,** 521 (1965).
(12) Van Lint, V. A. J., Wikner, E. G., Trueblood, D. L., *Bull. Am. Phys. Soc.* **5,** 122 (1960).
(13) Young, B. G., Johnsen, A. W., Carruthers, J. A., *Can. J. Phys.* **41,** 625 (1963).

RECEIVED January 12, 1968. This work was supported in part by the U. S. Atomic Energy Commission.

Effect of Oxygen on the Radiolysis of Gaseous Carbon Dioxide

A. R. ANDERSON and J. V. F. BEST

Chemistry Division, Atomic Energy Research Establishment, Harwell, Berkshire, England

Publication Date: January 1, 1968 | doi: 10.1021/ba-1968-0082.ch015

Measurements are described of the effects of added O_2, CO, and SF_6 on the proton irradiation of gaseous CO_2 and on the radiation-induced exchange of ^{14}C between ^{14}CO and CO_2. The oxidation of CO is enhanced by adding small concentrations of O_2 but is inhibited at higher concentrations of O_2 by increased dose rate and on adding SF_6. The data are interpreted on the basis of two principal oxidizing species —the CO_3 radical and the negative ion O_2^-, which is in equilibrium with ions of higher molecular weight such as CO_4^-. Both the species, CO_3 and O_2^-, participate in the radiolysis of pure CO_2, but its apparent radiation stability is attributed primarily to oxidation of CO by the O_2^- ion.

The apparent stability of gaseous carbon dioxide under ionizing radiation, in contrast to its photolytic decomposition, has been ascribed to the efficient reoxidation of the product carbon monoxide. Although the exact nature of the oxidation process has not been elucidated, various mechanisms have been postulated involving the species ozone (*16*), carbon suboxides (*14*), the CO_3 radical (*1*), and the ions O_2^- and O_2^+ (*8, 9*). The work of Dominey *et al.* (*9, 10*) on the radiation-induced isotope exchange reaction between ^{14}CO and CO_2 showed the importance of a species (probably ionic) derived from molecular oxygen, and that added oxygen enhanced the yield of $^{14}CO_2$ from the oxidation of ^{14}CO. These observations and general conclusions were confirmed in later work on the γ-radiolysis of liquid CO_2 (*6*) and on the proton radiolysis of gaseous CO_2 at high dose rates (*2*). However, Anbar and Perlstein (*1*) also studied the effect of added oxygen on the yields of various radiation-induced isotopic exchange reactions in mixtures of CO_2 and CO, and they have queried the importance of molecular oxygen in controlling the

In Radiation Chemistry; Hart, E.;
Advances in Chemistry; American Chemical Society: Washington, DC, 1968.

radiation-induced oxidation of CO in gaseous CO_2. A careful examination (*4*) of their data has shown that their conclusions are equivocal, and in the present work, which extends our previous studies on the proton radiolysis of CO_2 (*2*), we have attempted *inter alia* to reconcile the apparently conflicting data on the effect of O_2 on the radiation-induced isotopic exchange reactions. We have also studied the effects of an electron scavenger, SF_6, and of changes in the ratio of CO and O_2 concentrations on both the $^{14}CO/CO_2$ exchange reaction and on the radiolysis of CO_2.

To understand fully the inferences drawn from the data, it is perhaps necessary to point out the general significance of the yields obtained with gas mixtures involving ^{14}CO. The philosophy underlying studies of the radiation-induced exchange reaction is that measurements of the oxidation of ^{14}CO can be related to the primary decomposition processes in irradiated CO_2. Even though the concentrations of added CO are generally low, they are often in excess of the steady-state concentrations for the radiolysis of pure CO_2, and hence experimental data must be used carefully in making deductions about the radiolysis of CO_2. However, by varying the concentrations of additives—*viz.* ^{14}CO, O_2, SF_6—it is possible to draw conclusions about the nature of the species which can oxidize CO and which may be relevant to understanding the details of the processes which account for the radiation stability of gaseous CO_2.

Publication Date: January 1, 1968 | doi: 10.1021/ba-1968-0082.ch015

Experimental

The irradiation techniques, gas purification methods, and analytical procedures have been described (*2, 3*). Borosilicate glass cells with mica windows and all-silica cells were used at a gas pressure of about 300 mm. at ambient temperatures. The energy of the incident protons was about 1.5 Mev. which was reduced to about 1.2 Mev. on passage through the cell window (3–4 mg./sq. cm.). Dose rates were varied from 2×10^{16} to 2×10^{18} e.v. $cc.^{-1}$ $sec.^{-1}$ at STP.

A mercury-free system was used for filling the irradiation cells. Carbon dioxide from cylinders (Distillers Company Ltd.) was purified by passage over copper oxide at 800°C. to oxidize hydrogen and hydrocarbons, followed by passage over activated copper at 170°C. to remove oxygen, and finally over silica gel previously dried at 200°C. *in vacuo*. The purified gas, which contained 1-2 p.p.m. oxygen and $<$ 0.5 p.p.m. water vapor, was used directly in the once-through gas flow experiments or stored in 8-liter vessels for use in the static gas runs. ^{14}C-labeled carbon monoxide (Radiochemical Centre, Amersham) was mixed with carbon dioxide in a 1-liter bulb to achieve the desired concentration. Oxygen was dried over molecular sieve (Linde 5A) before use.

In the gas-flow experiments, carbon dioxide from the purification line was allowed to flow through the irradiation cell and condensed in a large cold trap cooled in liquid nitrogen; the noncondensible gases (oxygen and carbon monoxide) were removed continuously by a Toepler pump and transferred to the sample loop of a gas chromatograph, where

carbon monoxide and oxygen were determined. For the static gas experiments the irradiated carbon dioxide was condensed, and the noncondensible gases were removed as above. To determine the extent of ^{14}C exchange, the effluent gas from the gas chromatograph was passed through a low volume gas scintillation counter which measured the activity in each peak as it was eluted from the chromatograph.

For ozone determinations, the irradiated gas was pumped through a trap containing 10 ml. of KI reagent; the absorption of the I_3^- peak was subsequently measured on a Hilger Uvispek at 3500A., using a value of 2.5×10^4 for the extinction coefficient of I_3^-. In the flowing gas experiments the efficiency of this bubble trap was improved by filling with small glass balls which prevented splashing over of the reagent. Tests with a second trap showed that $> 95\%$ of the ozone was collected in one trap even at gas flow rates of 500 cc. per min.

SF_6 [Kingsley and Keep (London)] was purified by three distillations at liquid nitrogen temperature and could be analyzed quantitatively as a peak on the gas chromatogram with a retention time slightly greater than that for CO_2 on a SiO_2–gel column.

Results

Steady-State Values in the Presence of Added O_2 and CO. It has been shown previously (*2*) that the steady-state values of O_2 and CO obtained on irradiating pure CO_2 at high dose rates (3×10^{16}–1.3×10^{18} e.v. cc.$^{-1}$ sec.$^{-1}$) are approximately proportional to (dose rate)$^{1/2}$. When either CO or O_2 was added initially to the CO_2, the steady-state levels were changed, and for small additions of CO the steady-state values of oxygen $[O_2]_{ss}$ were approximately proportional to $[CO]_{ss}^{-1}$. However, where increasing amounts of O_2 were added to pure CO_2, the resulting $[CO]_{ss}$ level increased, and ozone was detected. Figure 1 shows the steady-state levels (expressed as percentage or parts per million by volume) at 20°C. for two dose rates, with $[CO]_{ss}$ passing through a minimum corresponding to the values obtained in pure CO_2 (*2*). At oxygen concentrations > 2000 p.p.m. (0.2%) significant amounts of ozone were detected, and the steady-state concentrations of both CO and ozone became independent of dose rate at slightly higher oxygen concentrations. In this region of oxygen concentration the steady-state concentration of ozone was approximately equal to $[O_2]/50$ at either dose rate, but the ratio $[O_2]/[CO]_{ss}$ increased progressively with increasing O_2 concentration.

Radiolysis of CO_2 in the Presence of SF_6. On adding SF_6 to CO_2, the production of CO and O_2 was linear with dose up to concentrations at least four times greater than the steady-state values obtained on irradiating initially pure CO_2. In the presence of SF_6 there was no indication of any deviation from linearity of CO and O_2 production at doses three times higher than those required to attain steady-state conditions in pure

CO_2. Over the range of dose rate from 2×10^{16} to 2×10^{18} e.v. cc.$^{-1}$ sec.$^{-1}$ constant yields of CO and O_2 were obtained in the presence of 1% SF_6, but with 0.05% SF_6 there was a slight effect of dose rate on yields (Table I).

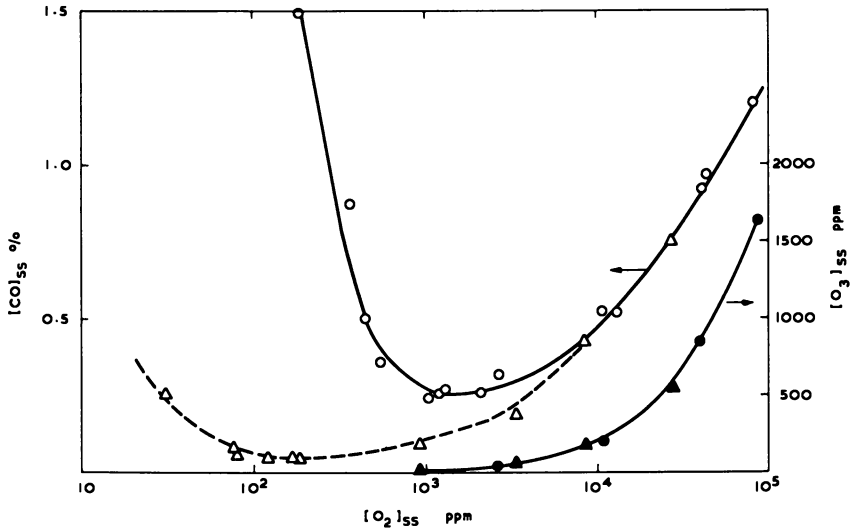

Figure 1. Steady-state concentrations of CO, O_2, and O_3 in irradiated CO_2

△ CO, ▲ O_3 } *Dose rate* $= 7 \times 10^{16}$ *e.v. cc.*$^{-1}$ *sec.*$^{-1}$

○ CO, ● O_3 } *Dose rate* $= 7 \times 10^{17}$ *e.v. cc.*$^{-1}$ *sec.*$^{-1}$

Table I. Yields of CO and O_2 from Mixtures of CO_2 and SF_6

Dose Rate, e.v. cc.$^{-1}$ sec.$^{-1}$	$[SF_6]$, %	G(CO)	$G(O_2)$
2×10^{16}	0.05	0.94	0.42
	1.0	0.94	0.42
7×10^{17}	0.05	1.24	0.56
	1.0	0.93	0.42
2×10^{18}	0.05	1.38	0.61
	1.0	0.94	0.41

Radiation-Induced $^{14}CO/CO_2$ Exchange Reaction. Yields of the exchange reaction, which are a measure of the radiolytic oxidation of the added ^{14}CO, are expressed as $G(^{14}CO_2)$ and calculated as described elsewhere (2). Where concentrations of CO and/or O_2 are changing significantly during the measurements of ^{14}C exchange, the quoted values for $G(^{14}CO_2)$ are calculated from the tangent to the plot of log $(1\text{-}F)$ using the measured CO concentration at the relevant dose. This method

Publication Date: January 1, 1968 | doi: 10.1021/ba-1968-0082.ch015

gives "instantaneous" values of $G(^{14}CO_2)$ and fulfills the requirement that the expression used to calculate exchange values (*2*) is only applicable where there is no over-all change in the gas composition.

Measurements in the Absence of Added O_2. We have reported (*2*) a value of $G(^{14}CO_2) = 4.6$ for the exchange reaction which is increased by adding O_2, in agreement with data for ^{60}Co γ-irradiations (*9, 10*). To establish firmly the limiting value in the absence of added O_2, we have carried out further measurements with different concentrations of ^{14}CO and have investigated the effect of adding SF_6. The results obtained at a dose rate of $\sim 2 \times 10^{16}$ e.v. cc.$^{-1}$ sec.$^{-1}$ are shown in Table II. No O_2 accumulates during any of these irradiations, and there is no change in the concentrations of CO.

Table II. Yields of $^{14}CO_2$ at Various Concentrations of CO

Dose Rate $= 2 \times 10^{16}$ e.v. cc.$^{-1}$ sec.$^{-1}$

$[CO]$, %	$G(^{14}CO_2)(\pm 0.3)$
0.27	4.61
1.2	4.62
2.8	4.72
3.85	4.2
5	4.8
5 (+ 1% SF_6)	5.0
	Mean 4.66

The values of $G(^{14}CO_2)$ are calculated from the energy absorbed in the CO_2 alone and are corrected for the contribution arising from the radiolysis of CO on the basis of $G(-CO) = 8$ (*3*).

Measurements in the Presence of Added O_2. In a series of measurements with 1% CO at a dose rate of $\sim 2 \times 10^{16}$ e.v. cc.$^{-1}$ sec.$^{-1}$ the addition of O_2 at first enhanced the yield of $^{14}CO_2$, but at higher concentrations (> 3 $[O_2]_{ss}$ in pure CO_2) the yield decreased to reach values lower than those in the absence of added O_2 (Figure 2). The significance of the measured yield at the highest concentration of O_2 used (20%) is uncertain since a significant fraction of the energy is absorbed directly by O_2. The corresponding yields for CO disappearance showed a complementary trend to the values of $G(^{14}CO_2)$—*e.g.*, at the minimum of the curve the net yield of CO (Figure 2) is $G(CO) = -4.4$, which together with the initial yield of 4.7 leads to a gross yield $G(CO) = -9.1$, in close agreement with the oxidation yield, $G(^{14}CO_2) = 9.4$. At low concentrations of O_2 the values of $2G(O_2)$ are probably more reliable

than the measurements of $G(CO)$ and should equal the latter if the simple stoichiometry represented by Reaction 1 is obeyed.

$$2CO_2 \rightarrow 2CO + O_2 \qquad (1)$$

At high concentrations of O_2 (2–3%) the yield of $^{14}CO_2$ increases with increasing concentration of CO (Table III).

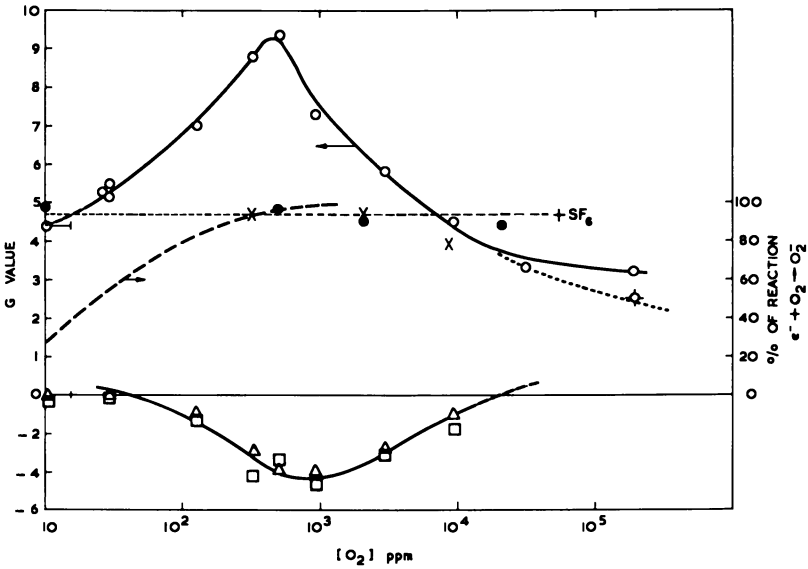

Figure 2. Yields of $^{14}CO_2$ and CO from irradiation of $^{14}CO/CO_2$ mixtures in the presence of O_2. Dose rate = 2×10^{16} e.v. cc.$^{-1}$ sec.$^{-1}$; [CO] = 1%

○ $G(^{14}CO_2)$
◇ *Based on total energy absorption*
△ $G(CO)$
□ $2G(O_2)$
Minimum yields in the presence of SF_6 { ● *0.5–3% CO* × *1% CO (at dose rate = 7×10^{17} e.v. cc.$^{-1}$ sec.$^{-1}$)*
---- *Calculated curve (see text).*

Table III. Yields of $^{14}CO_2$ at High Concentrations of O_2

[CO], %	[O_2], %	[SF_6], %	$G(^{14}CO_2)$[a]
1.0	2.0	—	3.8
3.0	2.2	—	5.7
6.3	2.7	—	6.9
1.25	2.0	4.5	4.9
1.35	2.6	0.6	4.4

[a] Based on total energy absorption.

Publication Date: January 1, 1968 | doi: 10.1021/ba-1968-0082.ch015

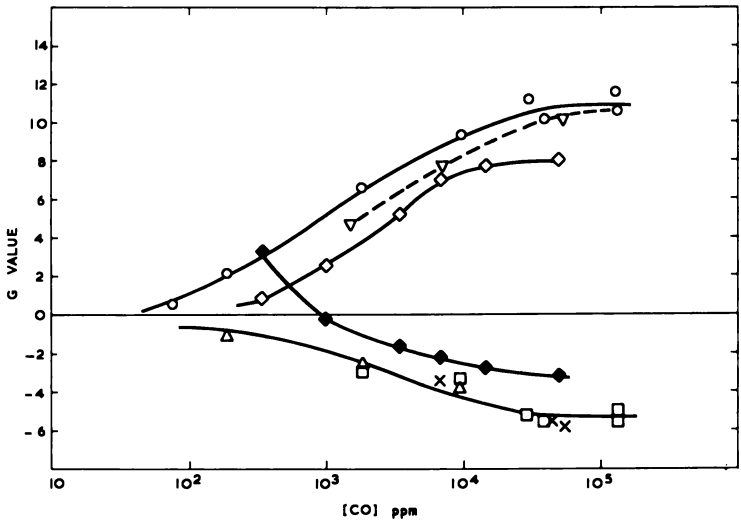

Figure 3. Yields of $^{14}CO_2$ and CO from irradiation of $CO_2/O_2/^{14}CO$ mixtures as a function of CO concentration

Dose rate = 2×10^{16} e.v. cc.$^{-1}$ sec.$^{-1}$, 500 p.p.m. O_2
○ $G(^{14}CO_2)$
△ $G(CO)$
□ $2G(O_2)$
Dose rate = 2×10^{16} e.v. cc.$^{-1}$ sec.$^{-1}$, 2000 p.p.m. O_2
▽ $G(^{14}CO_2)$
× $2G(O_2)$
Dose rate = 6×10^{17} e.v. cc.$^{-1}$ sec.$^{-1}$, 1000 p.p.m. O_2
◇ $G(^{14}CO_2)$
◆ $G(CO)$

To investigate further the competition between CO and O_2 for some oxidizing species, we have irradiated mixtures in which the O_2 concentration was constant and that of CO was varied. The most complete set of data was obtained at an O_2 concentration of $\sim$ 500 p.p.m., corresponding to the maximum value for $G(^{14}CO_2)$ in Figure 2. Under these conditions little reaction was observed at concentrations of CO $<$ 80 p.p.m., but at the higher concentrations the yield of $^{14}CO_2$ rose to a maximum, $G(^{14}CO_2) \sim 11$ at CO concentrations $\geq$ 3% (Figure 3). The corresponding values of $G(CO)$ or $2G(O_2)$ decreased with increasing CO concentration to a limiting value of approximately -5.5 to -6, which, together with the initial yield of $G(CO) = 4.7$, corresponds closely to the oxidation yield. With a higher concentration of O_2 ($\sim$ 2000 p.p.m.) a similar trend in yields was observed.

Similar measurements in the presence of 1000 p.p.m. O_2 at a dose rate about 30 times greater ($\sim 6 \times 10^{17}$ e.v. cc.$^{-1}$ sec.$^{-1}$) also gave an increase in the yield of $^{14}CO_2$ with increasing concentration of CO, but

in this case the yield approached an upper limit of $G(^{14}CO_2) \sim 8$ (Figure 3).

Measurements of $^{14}CO/CO_2$ Exchange in the Presence of O_2 and SF_6. Adding SF_6 at the lower dose rate ($\sim 2 \times 10^{16}$ e.v. cc.$^{-1}$ sec.$^{-1}$) led to a maximum decrease in $G(^{14}CO_2)$ of ~ 6 at $\sim 0.1\%$ SF_6, as shown in Table IV. The data at high SF_6 concentration (ionization potential = 19.3 e.v. (*28*)) are somewhat uncertain owing to the significant amount of energy absorbed directly by the high molecular weight molecule, SF_6, and the possibility of energy transfer to CO_2 or O_2.

Table IV. Effect of SF_6 on Yields of $^{14}CO_2$

Dose Rate 2×10^{16} e.v. cc.$^{-1}$ sec.$^{-1}$

$[CO]$, %	$[O_2]$, %	$[SF_6]$, %	$G(^{14}CO_2)$[a]	$-\Delta G(^{14}CO_2)$
3	0.05	—	11	—
3	0.05	0.02	6.0	5.0
3	0.05	0.04	5.6	5.4
3	0.05	0.10	4.8	6.2
3	0.05	2	(5.8)	(5.2)
3	0.05	6.5	(5.3)	(5.7)
0.1	0.05	—	5.2	—
0.1	0.05	0.7	3.0	2.2
0.5	0.2	—	7.2	—
0.5	0.2	0.05	4.4	2.8

[a] Based on total energy absorption.

At relatively low O_2 concentrations (Table IV, Lines 3 and 4) the maximum decrease in $G(^{14}CO_2)$ is obtained when the ratio $[SF_6]/[O_2] \leqslant 2$, but at the high O_2 concentration of $\sim 2\%$ (Table III) the same ratio of SF_6 to O_2 concentrations does not decrease the yield of $^{14}CO_2$.

The marked effect of SF_6 on the $^{14}CO/CO_2$ exchange reaction is clearly shown in Figure 2, where data at two different dose rates show that the minimum yield of $^{14}CO_2$ in the presence of SF_6 is independent of O_2 concentration over a wide range and is equal to the value in the absence of added O_2.

Yields of Ozone from Mixtures of CO_2 and O_2. Steady-state concentrations of ozone obtained in the presence of added O_2 are given in Figure 1, and we have also measured the initial yield of ozone in CO_2/O_2 mixtures in a gas flow system. At a dose rate of $\sim 7 \times 10^{16}$ e.v. cc.$^{-1}$ sec.$^{-1}$ and a high gas flow rate (0.6–0.9 volume changes per sec.) yields calculated from the energy absorbed in the CO_2 fraction were $G(O_3) = 4.48$ and 4.92 for 5 and 10% concentrations of O_2 in CO_2. Some ozone will arise from the energy absorbed by the O_2 fraction of the gas, and published values (*18*, *22*) for $G(O_3)$ in pure O_2 range from 1–12. If a value

Publication Date: January 1, 1968 | doi: 10.1021/ba-1968-0082.ch015

$G(O_3) = 6$ is assumed for pure O_2, the above yields can be corrected for the different O_2 concentrations and become 4.30 and 4.43 at 5 and 10% O_2 respectively; there is probably no significant difference between these two values.

Discussion

General Conclusions. The main conclusion we draw from these data is that there are two principal species which participate in the radiolytic oxidation of CO in irradiated CO_2. They are an electrically neutral species (probably CO_3), derived from electronically excited states of CO_2, and a negatively charged ion (probably O_2^-). We also infer that the charge neutralization reactions in irradiated CO_2 are nondissociative at gas pressures $\geq$ 300 mm. Hg. The oxidation of CO by the negative ion is inhibited by increasing dose rate and at high concentrations of O_2. Oxidation of CO by the electrically neutral species, however, is not significantly affected by changes in dose rate or by the presence of O_2 when the ratio of concentrations $[O_2]/[CO] < 1$. Our observations on the effect of O_2 on the $^{14}CO/CO_2$ exchange reaction also largely explains the apparent anomaly between the data of Dominey *et al.* (*9*, *10*), and of Anbar and Perstein (*1*) since the latter workers always used gas mixtures containing about 1% of O_2 where the oxidation yields are similar to or lower than those in the absence of added O_2. We shall now justify these conclusions by a detailed discussion of the significant experimental data, summarized below.

Important Results. The significant experimental data which must be incorporated into an over-all reaction mechanism are as follows:

(a) Adding 1% SF_6 to CO_2 leads to the production of CO and O_2 with initial yields $G(CO) \sim 0.9$ and $G(O_2) \sim 0.4$, in contrast to the situation with pure CO_2 where steady-state concentrations of CO and O_2 are established at lower doses.

(b) In the presence of SF_6, the yield of $^{14}CO_2$ from the oxidation of ^{14}CO is not affected markedly by the presence of O_2 (Tables II, III, IV, Figure 2).

(c) With mixtures of CO_2 and O_2 in the absence of CO the initial yield of ozone is $G(O_3) \approx 4.4$.

(d) On adding O_2 to mixtures of ^{14}CO and CO_2 the yield of $^{14}CO_2$ first increases with increasing O_2 concentration, then decreases (Figure 2).

(e) Adding SF_6 has no effect on the yield of $^{14}CO_2$ from $^{14}CO/CO_2$ mixtures in the absence of O_2 (Table II), decreases $G(^{14}CO_2)$ to a minimum of $\sim$ 4.8 at the concentration of O_2 (0.05%) which gives the peak value in Figure 2, but has little effect at a concentration of $O_2 \sim 2\%$ (Table III).

(f) The maximum yield of $^{14}CO_2$ from irradiation of $CO_2/^{14}CO/O_2$ mixtures decreases with increasing dose rate (Figure 3).

Publication Date: January 1, 1968 | doi: 10.1021/ba-1968-0082.ch015

Steady-State Data. The steady-state data in Figure 1 show that the species which oxidizes CO, thus leading initially to a decrease in $[CO]_{ss}$ with increasing concentration of O_2, can also react with O_2 to give a product which cannot oxidize CO rapidly. If this were not true, the steady-state concentration of CO would simply decrease to zero with increasing concentration of O_2. The competitive reaction between CO and O_2 for the oxidizing species at high O_2 concentrations seems to depend only on the relative concentrations of CO and O_2 since their measured steady-state concentrations and that of O_3 are independent of dose rate at O_2 concentrations $\gtrsim 0.5\%$.

Effect of SF_6 on the Radiolysis of CO_2. The above steady-state data give no indication of the number of oxidizing species involved, and the first evidence for the participation of more than one species is provided by the results obtained on adding SF_6 to pure CO_2. As an electron scavenger, SF_6 could affect the steady-state concentrations in one of two ways. If the charge neutralization reaction involving CO_2^+ is dissociative (Reaction 2), participation of SF_6^- ions could lead to a nondissociative reaction (Reaction 3) since the energy released on charge neutralization will be reduced owing to the electron affinity of SF_6.

$$CO_2^+ + e^- \rightarrow CO_2^* \rightarrow CO + O \quad (2)$$

$$CO_2^+ + SF_6^- \rightarrow CO_2 + SF_6 \quad (3)$$

The result of this process, however, would be simply a reduction in the rate of production of CO and O from the primary ions (without affecting the species produced directly from electronically excited molecules) and a consequent reduction in the measured steady-state concentrations of CO and O_2. Since the experimental data show exactly the opposite behavior, we conclude tentatively that SF_6 must be interfering with the production of a negative ion which can oxidize CO efficiently. Moreover, since the measured values $[G(CO) \sim 0.9$ and $G(O_2) \sim 0.4]$ in the presence of SF_6 are significantly lower than the initial values $[G(CO) = 4.5 \pm 0.5$ and $G(O_2) = 2.2 \pm 0.2]$ measured in other ways (*4*), some species other than the negative ion must be capable of oxidizing CO under these conditions with a yield, $G(\text{-CO}) \sim 3.5$.

Ozone Yields in Mixtures of CO_2 and O_2. It can be inferred from the above discussion on the effect of SF_6 that the charge neutralization of CO_2^+ in pure CO_2 is nondissociative, possibly caused by the participation of other negative ions and/or the formation of ion clusters, *e.g.*, $CO_2^+(CO_2)_n$. The data on ozone yields from the gas flow experiments support this inference of nondissociative charge neutralization. We argue that the limiting yield of ozone at high gas flow rates, $G(O_3) \sim 4.4$ is equal to the yield of an electrically neutral oxidizing species formed solely from the dissociation of electronically excited CO_2 molecules.

Publication Date: January 1, 1968 | doi: 10.1021/ba-1968-0082.ch015

The yield of ozone agrees with the yield of $^{14}CO_2$ from $^{14}CO/CO_2$ mixtures in the absence of O_2, $G(^{14}CO_2) = 4.7$ (Table II), and if this latter yield is caused solely by the reaction of an electrically neutral oxidizing species, as we argue more fully later, then the species could arise from two sources—*viz.*, dissociation of excited CO_2 molecules (Reaction 4) and dissociative charge neutralization of CO_2^+ ions (Reaction 2). Thus, the over-all yield [$G(^{14}CO_2) = 4.7$] would be derived from the sum of the following processes (Reactions 2 and 4), since $W(CO_2) = 32.7 - 34.2$ e.v. (*17, 21, 30*).

$$CO_2^+ + e^- \rightarrow CO_2^* \rightarrow CO + O \quad G = 3 \tag{2}$$

$$CO_2 \xrightarrow{\wedge\wedge\wedge} CO_2^* \rightarrow CO + O \quad G = 1.7 \tag{4}$$

In mixtures of CO_2 and O_2, however, the principal positive ion participating in the charge neutralization reaction is O_2^+ owing to the rapid ion-molecule Reaction 5 for which $k_5 = 10^{-10}$ cc. molecule^{-1} sec.$^{-1}$ (*25*).

$$CO_2^+ + O_2 \rightarrow CO_2 + O_2^+ \tag{5}$$

The major negative ion will be of the form CO_4^- as shown by Phelps *et al.* (*24, 27*); if we postulate that the charge neutralization reaction in the presence of O_2 is nondissociative—*e.g.*, Reaction 6—then $G(O_3)$ would be 1.7 since only the contribution arising from Reaction 4 remains.

$$O_2^+ + CO_4^- \rightarrow 2O_2 + CO_2 \tag{6}$$

On the other hand, if we postulate that the charge neutralization reaction is dissociative (Reaction 7), although this seems highly improbable, then the yield of O_3 will be $G(O_3) = 1.7 + 2 \times 3 = 7.7$. Neither of these postulates fit the observed yield.

$$O_2^+ + CO_4^- \rightarrow 2O + O_2 + CO_2 \tag{7}$$

Examination of the possible reactions of the ions with O_2 also suggests that in mixtures of CO_2 and O_2 no O_3 will be formed by these processes. It is known that excited O_2^+ ions can react with O_2 to form O_3, but the reaction is significant only when the O_2^+ ions are ~ 5 e.v. above the ground state (*13*). Since charge transfer Reaction 5 will produce O_2^+ ions only 1.7 e.v. above the ground state (owing to the difference in ionization potentials, $CO_2 = 13.79$ e.v., $O_2 = 12.08$ e.v.), it is a reasonable conclusion that O_3 will not be produced by reaction of these ions. There is no evidence for the formation of O_3 from reactions of CO_4^- ions (*24*), and we return to this point in discussing the effect of high concentrations of O_2 on the yield of $^{14}CO_2$.

Fehsenfeld *et al.* (*11*) observed a series of negative ion reactions (Reactions 8–10) which could lead to a reduction in the yield of O_3, but these processes are unlikely to be important here since at very low

Publication Date: January 1, 1968 | doi: 10.1021/ba-1968-0082.ch015

concentration of O_3 the most likely reaction of O_2^- is with CO_2 (*24, 27*), and the O atoms will act preferentially with the high concentrations of O_2 or CO_2.

$$O_2^- + O_3 \rightarrow O_3^- + O_2 \quad (8)$$

$$O_3^- + CO_2 \rightarrow CO_3^- + O_2 \quad (9)$$

$$CO_3^- + O \rightarrow O_2^- + CO_2 \quad (10)$$

Thus, we conclude that in mixtures of CO_2 and O_2 neither negative nor positive ions participate in the formation of O_3 and that the maximum observed yield, $G(O_3) \sim 4.4$, is caused solely by the reaction of electrically neutral species, derived principally from electronically excited states of CO_2.

Yields and Reactions of the Electrically Neutral Oxidizing Species. The interpretation of the above data suggests that an electrically neutral oxidizing species, with a yield of $G = 4.5 \pm 0.2$, is formed from electronically excited CO_2 molecules produced directly from the absorption of radiation. This view is further confirmed by the effect of SF_6 on the exchange reaction between ^{14}CO and CO_2. In the presence of SF_6 and 1–3% CO we obtain a yield $G(^{14}CO_2) \sim 4.7$ which is largely independent of the concentration of O_2 from zero to 2% (Figure 2). Measurements of the reactions of O atoms and O_2 (*19*) show that SF_6 simply acts as an efficient third body and does not react with O atoms. Also we have not observed any experimentally significant changes in SF_6 concentrations before and after irradiation showing that it is acting catalytically. Thus, it seems clear that in irradiated CO_2, SF_6 is acting simply as an electron scavenger, and the minimum yields of $^{14}CO_2$ which we obtain in its presence are caused by the reaction of an electrically neutral species. Since this species can still oxidize CO when the ratio of concentrations $[O_2]/[CO] \sim 2$ (Table III), it cannot be identified as the $O(^3P)$ atom for previous estimates (*4, 9*) based on rate constants for reaction of $O(^3P)$ have shown that Reaction 11 will eliminate Reaction 12 at low $[O_2]/[CO]$.

$$O(^3P) + O_2 + M \rightarrow O_3 + M \quad (11)$$

$$O(^3P) + CO \rightarrow CO_2 \quad (12)$$

These estimates are based on rate constants for Reaction 12 measured at low pressures, but it has been pointed out (*4*) that they must be viewed cautiously since the order of Reaction 12 (and its rate constant) may increase at the higher gas pressures used in radiolysis studies.

The possible nature of this electrically neutral species has been considered exhaustively by Anbar and Perlstein (*1*), who identify it as the CO_3 radical. We support this view but recognize that in the absence of measurements over a range of pressures, our kinetic data could also be explained by reactions of long-lived excited CO_2 molecules.

Publication Date: January 1, 1968 | doi: 10.1021/ba-1968-0082.ch015

We suggest that the observations on irradiated CO_2 with only SF_6 added are entirely consistent with the postulate that the sole chemical reactions occurring are similar to those in the ultraviolet photolysis of CO_2, leading to a buildup of CO and O_2 (and O_3?) which is linear with dose.

Reactions and Nature of the Negative Ion Oxidizing Species. Evidence for the participation of a negative ion oxidizing species is shown clearly by the effect of SF_6 on the steady-state concentrations of CO and O_2 from pure CO_2, and by its effect in reducing the enhanced yields of $^{14}CO_2$ from mixtures of ^{14}CO and CO_2 in the presence of O_2 (Table IV). This effect suggests that the increase in yields of $^{14}CO_2$ on adding O_2 arises from electron capture by O_2 (Reaction 13) followed by oxidation reactions such as 14 and 15.

$$e^- + O_2 + M \rightarrow O_2^- + M \quad (13)$$

$$O_2^- + CO \rightarrow CO_2 + O^- \quad (14)$$

$$O^- + CO \rightarrow CO_2 + e^- \quad (15)$$

These reactions are plausible since Reaction 14 is exothermic by 23 kcal./mole and $k_{15} = 8 \times 10^{-10}$ cc. molecule^{-1} sec.$^{-1}$ (*24*). However, Ferguson and Fehsenfeld (*12*) have recently found that Reaction 14 is unlikely since $k_{14} < 10^{-12}$ cc. molecule^{-1} sec.$^{-1}$, so that arguments based on the exothermicity of the reaction are inadequate. A more plausible sequence may involve the ion CO_3^-—*e.g.*, Reactions 16 and 17.

$$CO + O_2^- \rightarrow CO_3^- \quad (16)$$

$$CO + CO_3^- \rightarrow 2CO_2 + e^- \quad (17)$$

Reactions 15 and 17 could also occur in the absence of O_2 owing to the occurrence of the dissociative attachment process, Reaction 18, but since this reaction is at least 3.8 e.v. endothermic, it is unlikely to make a significant contribution to the radiation chemistry of CO_2.

$$CO_2 + e^- \rightarrow CO + O^- \quad (18)$$

Explanations based on participation of the ion O_2^- are complicated further by the data of Phelps *et al.* (*24, 27*), which show that in mixtures of CO_2 and O_2 the stable negative ion is CO_4^- which has an energy of dissociation into O_2^- and CO_2 of 0.8 e.v. (*27*). It is difficult to decide (*24*) whether CO_4^- is formed from O_2^- (Reaction 19) or in a three-body collision (Reaction 20), but values for the effective rate constants are $k_{19}(CO_2) = 9 \times 10^{-30}$ cm.^{6} molecule^{-2} sec.$^{-1}$ and $k_{19}(O_2) = 2 \times 10^{-29}$ cm.^{6} molecule^{-2} sec.$^{-1}$ (*24*)

$$O_2^- + CO_2 + M \rightarrow CO_4^- + M \quad (19)$$

$$e^- + O_2 + CO_2 \rightarrow CO_4^- \quad (20)$$

Publication Date: January 1, 1968 | doi: 10.1021/ba-1968-0082.ch015

Moruzzi and Phelps (*24*) also observed that at source pressures above 3 mm. the CO_4^- current decreased, so unfortunately it is not possible to use their data to decide unequivocally which negative ion species will predominate at the pressure of our measurements ($\sim$ 300 mm.). It seems clear, however, that there will be an equilibrium between O_2^-, CO_4^-, and possibly higher molecular weight ions which may depend *inter alia* on the concentration of O_2 since $k_{19}(O_2) > k_{19}(CO_2)$.

Since k_{13} is in the range 10^{-30}–10^{-29} cm.^{6} molecule^{-2} sec.$^{-1}$ (*26*) and $k_2 = 4 \times 10^{-7}$ cc. molecule^{-1} sec.$^{-1}$ (*29*), it can be shown that at a dose rate of 2×10^{16} e.v. cc.$^{-1}$ sec.$^{-1}$ and gas pressure of 300 mm., electron capture by O_2 will predominate over charge recombination of CO_2^+ and electrons when the concentration of $O_2 \geq 500$ p.p.m. The line in Figure 2 is calculated for $k_{13} = 3 \times 10^{-30}$ cm.^{6} molecule^{-1} sec.$^{-1}$. Thus, electron capture by O_2 followed by oxidation of CO by either O_2^- or CO_4^- could account for the increased yields of $^{14}CO_2$ observed in the presence of O_2 (Figure 2).

The subsequent decrease in $G(^{14}CO_2)$ at higher concentrations of O_2 cannot be accounted for by charge exchange Reaction 21 since this will not affect the concentration of O_2^-, but it could possibly be explained by competition between reactions such as 22 and 23.

$$O_2^- + O_2 \rightarrow O_2 + O_2^- \quad (21)$$

$$CO_4^- + CO \rightarrow CO_2 + CO_3^- \quad (22)$$

$$CO_4^- + O_2 \rightarrow CO_3^- + O_3 \quad (23)$$

However, there is no indication of a reaction such as 23 from the work of Moruzzi and Phelps (*24*), and we have not found any high yields of ozone in the relevant mixtures of CO_2, CO, and O_2. With 5% O_2 and 1% CO where $G(^{14}CO_2)$ is reduced by about 6 below the maximum value at 0.05% O_2 (Figure 2), the maximum yield of ozone was $1.1 \geqslant G(O_3) \leqslant 2$; this yield can be accounted for by competition between O_2 and CO for the CO_3 radical. These observations lead us to suggest that the subsequent reduction in yields of $^{14}CO_2$ with increasing concentration of O_2 may result from a change in the complex equilibria involving electrons, O_2, CO_2, and the negative ions. At relatively low concentrations of O_2 (*see* Figure 2) the principal negative ion (say O_2^-) can oxidize CO to CO_2, but as the concentration of O_2 is increased, the oxidizing ion is converted to another ion or ions—*e.g.*, through Reaction 20 which is a three-body process involving electrons which cannot oxidize CO or react with O_2 to form O_3. The ultimate fate of the nonoxidizing ion will be charge neutralization without the formation of O atoms or CO_3 radicals.

The decrease in the maximum yield of $^{14}CO_2$ with increasing dose rate (Figure 3) is attributed to competition between charge neutralization reactions (*e.g.*, Reaction 6) and oxidation of CO by the negative ion

Publication Date: January 1, 1968 | doi: 10.1021/ba-1968-0082.ch015

species, or to competition between formation of O_2^- and charge neutralization of CO_2^+ or O_2^+.

SF_6 can interfere with all these processes involving negative ions of O_2 and CO_2–O_2 by capturing electrons. The electron affinity of SF_6, 34 ± 5 kcal. (*20*) is higher than that for O_2, 0.4 e.v., *i.e.*, 9.2 kcal. (*26*), or than the effective electron affinity of CO_4, 1.2 e.v., *i.e.*, 27.6 kcal. (*27*). It is difficult to compare the rate constants for reactions such as 13–17 with the appropriate value for electron attachment to SF_6 since a number of measurements (*5, 7, 15, 23*) have given values for $k(SF_6 + e^- \rightarrow SF_6^-)$ which vary from 2.9×10^{-13} cc. molecule^{-1} sec.$^{-1}$ (*15*) to 3.1×10^{-7} cc. molecule^{-1} sec.$^{-1}$ (*23*). Thus, it is possible only to conclude that independent evidence does not invalidate the above mechanism, but it cannot be justified further at present than on the basis that it provides the most plausible way to explain our extensive data obtained over a wide range of conditions.

Relevance to the Radiation Stability of Gaseous CO_2. Two oxidizing species are necessary to explain the apparent radiation stability of gaseous CO_2 owing to rapid oxidation of the product CO. One of these is probably the CO_3 radical, as suggested by Anbar and Perlstein (*1*), and the other is a negative ion which we tentatively identify as O_2^-, as suggested by Dainton (*8*). When the effect of this negative oxidizing ion is removed, as shown by adding SF_6 to CO_2, no approach to steady-state gas concentrations is observed, but a continuous production of CO and O_2 is obtained, as in ultraviolet photolysis. This situation probably represents reactions of the CO_3 radical alone, which reactions appear to be inadequate to explain the radiation stability of CO_2, even though the ratio of the rates of reaction of CO_3 with CO and O_2 is apparently much higher than the corresponding ratio for reactions of $O(^3P)$. Moreover, if CO_3 is the exclusive oxidizing species, it is extremely difficult to reconcile the marked experimental differences between the photolysis and radiolysis of gaseous CO_2 (*4*).

The important additional reaction in determining the apparent radiation stability of CO_2 is rapid oxidation of CO by a negative ion species (say O_2^-). This reaction becomes important once a small concentration of molecular O_2 has accumulated in irradiated CO_2, and it is the addition of this process to reactions involving the CO_3 radical which accounts for the difference between the radiolysis and ultraviolet photolysis of gaseous CO_2.

Acknowledgment

We are grateful to C. B. Amphlett for helpful discussions during this work and to E. E. Ferguson for permission to quote his data for k_{14} before publication.

Literature Cited

(1) Anbar, M., Perlstein, P., *Trans. Faraday Soc.* **62,** 1803 (1966).
(2) Anderson, A. R., Best, J. V. F., *Trans. Faraday Soc.* **62,** 610 (1966).
(3) Anderson, A. R., Best, J. V. F., Willett, M. J., *Trans. Faraday Soc.* **62,** 595 (1966).
(4) Anderson, A. R., Dominey, D. A., *Radiation Rev.*, to be published.
(5) Asundi, R. K., Craggs, J. D., *Proc. Phys. Soc. (London)* **83,** 611 (1964).
(6) Baulch, D. L., Dainton, F. S., Willix, R. L. S., *Trans. Faraday Soc.* **61,** 1146 (1965).
(7) Buchel'nikova, I. S., *Soviet Phys. JEPT* **8,** 783 (1959).
(8) Dainton, F. S., *Discussions Faraday Soc.* **36,** 237 (1963).
(9) Dominey, D. A., Palmer, T. F., *Discussions Faraday Soc.* **36,** 35 (1963).
(10) Dominey, D. A., Palmer, T. F., Robertson, J. C., *U.K.A.E.A. Rept.* AERE-R 481 (1965).
(11) Fehsenfeld, F. C., Schmeltekopf, A. L., Schiff, H. I., Ferguson, E. E., *Planet. Space Sci.* **15,** 373 (1967).
(12) Ferguson, E. E., Fehsenfeld, F. C., unpublished data.
(13) Dong, P., Cottin, M., *J. Chim. Phys.* **57,** 557 (1960).
(14) Harteck, P., Dondes, S., *J. Chem. Phys.* **23,** 902 (1955); **26,** 1727 (1957).
(15) Hasted, J. B., Beg, S., *Brit. J. Appl. Phys.* **16,** 1779 (1965).
(16) Hirschfelder, J. O., Taylor, H. S., *J. Chem. Phys.* **6,** 783 (1938).
(17) Jesse, W. P., Sadauskis, J., *Phys. Rev.* **97,** 1668 (1955).
(18) Johnson, G. R. A., Warman, J. M., *Discussions Faraday Soc.* **37,** 87 (1964).
(19) Kaufman, F., Kelso, J. R., *J. Chem. Phys.* **46,** 4541 (1967).
(20) Kay, J., Page, F. M., *Trans. Faraday Soc.* **60,** 1042 (1964).
(21) Klots, C. E., *J. Chem. Phys.* **44,** 2715 (1966).
(22) Lind, S. C., "Radiation Chemistry of Gases," Reinhold, New York, 1961.
(23) Mahan, B. H., Young, C. L., *J. Chem. Phys.* **44,** 2192 (1966).
(24) Moruzzi, J. L., Phelps, A. V., *J. Chem. Phys.* **45,** 4617 (1966).
(25) Norton, R. B., Ferguson, E. E., Fehsenfeld, F. C., Schmeltekopf, A. L., *Planet. Space Sci.* **14,** 969 (1966).
(26) Pack, J. L., Phelps, A. V., *J. Chem. Phys.* **44,** 1870 (1966).
(27) Pack, J. L., Phelps, A. V., *J. Chem. Phys.* **45,** 4316 (1966).
(28) Reed, T. M., *J. Phys. Chem.* **59,** 428 (1955).
(29) Weller, C. S., Biondi, M. A., *Phys. Rev. Letters* **19,** 59 (1967).
(30) Whyte, G. N., *Radiation Res.* **18,** 265 (1963).

RECEIVED January 25, 1968.

Yields of the Reducing Species in the Vapor-Phase Radiolysis of Isopropyl Alcohol and Water-Isopropyl Alcohol Mixtures

R. S. DIXON and M. G. BAILEY

Atomic Energy of Canada Limited, Whiteshell Nuclear Research Establishment, Pinawa, Manitoba

Publication Date: January 1, 1968 | doi: 10.1021/ba-1968-0082.ch016

In the γ-radiolysis of water-isopropyl alcohol mixtures in the vapor phase, the total yields of hydrogen, methane, and carbon monoxide are linear over the whole concentration range, in the presence and absence of electron scavengers. The majority of the hydrogen produced from energy absorption by both water and isopropyl alcohol is formed by H-atom abstraction from isopropyl alcohol. Part of the H-atom yield is formed by electron-positive ion neutralization and part by processes not involving electrons. As far as the formation of H atoms is concerned, both electron-positive ion and ion-ion neutralizations appear to be independent of the composition of the positive ion cluster. A yield of molecular hydrogen is also present in both water and isopropyl alcohol.

There is now substantial agreement that at atmospheric pressure and at temperatures within the range 110° to 140°C., the hydrogen yield from H_2O or D_2O irradiated in the presence of an organic additive has a value $G \sim 8$ (*5, 6, 12, 18*). The use of specific scavengers has shown the major precursors of the hydrogen yield to be the electron and the hydrogen atom (*7, 11, 12, 18*). A value $G(N_2) = g(e) = 3.0 \pm 0.3$ was found in water vapor containing nitrous oxide (*7, 11*) which is in reasonable agreement with the value expected from the *W*-value of 30 e.v. in water vapor (*8, 30*). (Experimental yields are written as $G(X)$ and "primary" yields as $g(X)$ molecules per 100 e.v. energy absorbed.) The value for $g(e)$ may be compared with the reduction in hydrogen yield when electron scavengers are added to water vapor containing an organic

In Radiation Chemistry; Hart, E.;
Advances in Chemistry; American Chemical Society: Washington, DC, 1968.

additive (*7, 12, 18*). This reduction represents the number of H atoms arising from electron-positive ion neutralization and the possibility that the number of H atoms could differ with different additives, or that products other than H atoms may be formed during neutralization, is apparent in previous studies (*3, 12*).

Recent mass spectrometric studies have shown that clustered ions may play an important role in the radiation chemistry of water vapor and other gases (*19, 20*). In pure water vapor, the neutralization reaction which produces H atoms is probably of the form

$$e^- + H_3O^+(H_2O)_n \rightarrow H + (n + 1)H_2O$$

where $H_3O^+(H_2O)_n$ represents the clustered or hydrated hydronium ion. However, in water vapor containing a polar additive such as methanol, the ion cluster will contain both water and methanol molecules, and the numbers of each in the cluster will depend on the concentrations of water and methanol in the mixture (*20*). The effects which the composition of the clustered ion will have on the neutralization reaction are not known and we have, therefore, chosen to study the water-isopropyl alcohol system over the whole concentration range, in the presence and absence of electron scavengers. We have also studied the effects of some hydrogen atom scavengers by competitive methods, to obtain information about the total and individual yields of the various hydrogen precursors in pure water and pure isopropyl alcohol vapors. The formation of other gaseous products has been discussed briefly in terms of ionic and non-ionic reactions.

Publication Date: January 1, 1968 | doi: 10.1021/ba-1968-0082.ch016

Experimental

Materials. Water: ordinary distilled water was redistilled in an all-quartz bidistillation apparatus, first from alkaline permanganate and then alone. Nitrous oxide and sulfur hexafluoride (Matheson research grade), carbon tetrachloride (Fisher certified), ethylene and propylene (Phillips research grade) and perfluoromethylcyclohexane (Aldrich Chemical Co.) were used as supplied. Isopropyl alcohol (Baker Instra-Analysed) was quoted as 99.9+% pure and contained 0.02% water. In most of the experiments it was used as supplied. The gas chromatogram showed a small impurity peak with the same retention time as ethyl alcohol, but a positive identification was not made. Several experiments with pure isopropyl alcohol were made, after it had been refluxed over dinitrophenylhydrazine and barium oxide for 24 hours each and then distilled, retaining the middle fraction. These gave the same yields of the gaseous products measured as did the unpurified isopropyl alcohol.

Technique. The irradiation vessels were ~ 250 cc. cylindrical borosilicate glass cells equipped with a thermocouple well and break-seal. Before filling, the vessels were heated in air at 500°C. for 16 hours, cooled,

and evacuated to 10^{-6} torr at room temperature. The weighed water-isopropyl alcohol sample was deaerated by several freeze-pump-thaw cycles and distilled into the irradiation vessel immersed in liquid nitrogen. Additives were introduced by condensing a gas sample of known PVT into the vessel. The vessel and contents were finally evacuated to 10^{-6} torr at 77°K. before sealing off.

The vessel was mounted in a furnace kept at 125 ± 2°C. during irradiation, the temperature being constant to ±1°C. over the whole vessel. The total pressure during irradiation was generally ~ 700 torr. Irradiations were carried out in triplicate using ^{60}Co γ-rays from a Gammacell 220 (Atomic Energy of Canada Limited). After irradiation, the gases not condensible at 77°K. were measured volumetrically and the composition determined by gas chromatography.

Dosimetry. The dose rate of 2.0×10^{18} e.v. grams^{-1} min.$^{-1}$ in water vapor was based on the yield of hydrogen from ethylene, using $G(H_2) = 1.31$ (*23*). Using this dosimetry, the yield of nitrogen from 700 torr N_2O irradiated in the same experimental set-up at room temperature was $G(N_2) = 10.0 \pm 0.3$. The relative dose rate was checked periodically with the Fricke dosimeter. The energy absorbed by each component in a mixture was calculated, assuming it to be directly proportional to the electron density of that component.

Publication Date: January 1, 1968 | doi: 10.1021/ba-1968-0082.ch016

Results

The number of molecules of product X formed per 100 e.v. energy absorbed by water, isopropyl alcohol, and the total mixture are designated $G(X)_w$, $G(X)_p$ and $G(X)_t$, respectively. The respective fractions of the energy absorbed are represented by $f_w = E_w/E_t$ and $f_p = E_p/E_t$, where E_w, E_p, and E_t are the energies absorbed by water, isopropyl alcohol and the total mixture. The yields obtained by extrapolating to $f_p = 0$ and $f_w = 0$ are designated $G(X)_w°$ and $G(X)_p°$, respectively.

Water-Isopropyl Alcohol Mixtures. The plots of $G(H_2)_t$, $G(CH_4)_t$, and $G(CO)_t$ against f_w and f_p for water-isopropyl alcohol mixtures are shown in Figures 1 and 2. The plots are all linear with composition, though $G(CH_4)_t$ has possibly a small positive deviation at higher values of f_p. Extrapolation to $f_p = 0$ gives $G(H_2)_w° = 8.1 \pm 0.2$, $G(CH_4)_w° = 0$ and $G(CO)_w° = 0$. Extrapolation to $f_w = 0$ gives $G(H_2)_p° = 8.9 \pm 0.2$, $G(CH_4)_p° = 5.4 \pm 0.3$ and $G(CO)_p° = 0.5 \pm 0.1$. Experiments using total pressures between 300–700 torr showed an increase of about 0.5 G units in $G(H_2)$ with decreasing pressure. In pure isopropyl alcohol, the yields showed no dose effect within the range 2.0×10^{19} to 1.2×10^{20} e.v.g.$^{-1}$.

Water-Isopropyl Alcohol + Additives. SULFUR HEXAFLUORIDE. The effect of SF_6 on the hydrogen, methane, and carbon monoxide yields from water-isopropyl alcohol mixtures is shown in Figures 1 and 2. Extrapolation to $f_p = 0$ gives $G(H_2)_w° = 5.5 \pm 0.3$, $G(CH_4)_w° = 0$

and $G(CO)_w^\circ = 0$. Extrapolation to $f_w = 0$ gives $G(H_2)_p^\circ = 5.4 \pm 0.3$, $G(CH_4)_p^\circ = 6.5 \pm 0.5$ and $G(CO)_p^\circ = 0.5 \pm 0.1$. Runs at $f_w = 0$ and $f_w = 0.42$ showed that SF_6 concentration within the range of 0.1 to 5 mole % had no effect on $G(H_2)_t$. Figure 2 shows possibly a slight increase in $G(CH_4)_t$ with increasing SF_6 concentration.

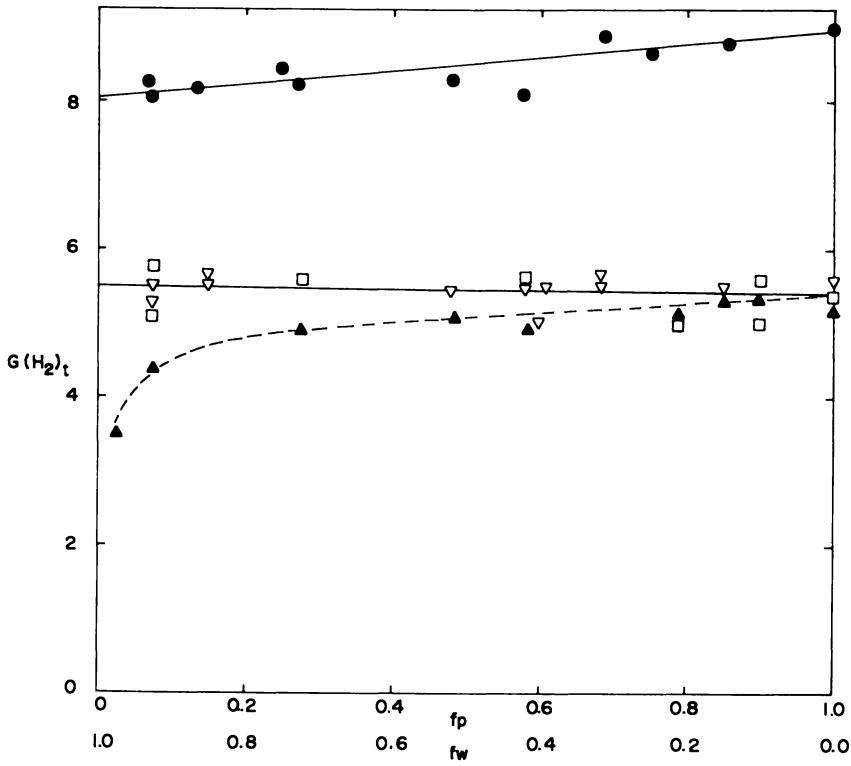

Figure 1. Radiolysis of water-isopropyl alcohol vapor mixtures at 125°C. in the presence and absence of electron scavengers. Dependence of $G(H_2)_t$ on the fraction of dose absorbed by water (f_w) and isopropyl alcohol (f_p)

● *No additive*
▽ *With 1% SF_6*
□ *With 1% C_7F_{14}*
▲ *With 1% CCl_4*

PERFLUOROMETHYLCYCLOHEXANE. The effect of C_7F_{14} is similar to that of SF_6 with $G(H_2)_w^\circ = 5.5 \pm 0.3$, $G(CH_4)_w^\circ = 0$, $G(H_2)_p^\circ = 5.4 \pm 0.3$ and $G(CH_4)_p^\circ = 6.0 \pm 0.5$ (Figures 1 and 2). Carbon monoxide was not measured.

CARBON TETRACHLORIDE. The effect of 1 mole % CCl_4 is similar to that of SF_6 and C_7F_{14} except for $G(H_2)_t$ at lower values of f_p (Figures

1 and 2). Values of $G(CH_4)_w^\circ = 0$, $G(H_2)_p^\circ = 5.4 \pm 0.3$ and $G(CH_4)_p^\circ = 5.8 \pm 0.3$ are estimated. $G(H_2)_t$ begins to fall off rapidly below $f_p = 0.5$, making the estimation of $G(H_2)_w^\circ$ difficult. Carbon monoxide was not measured.

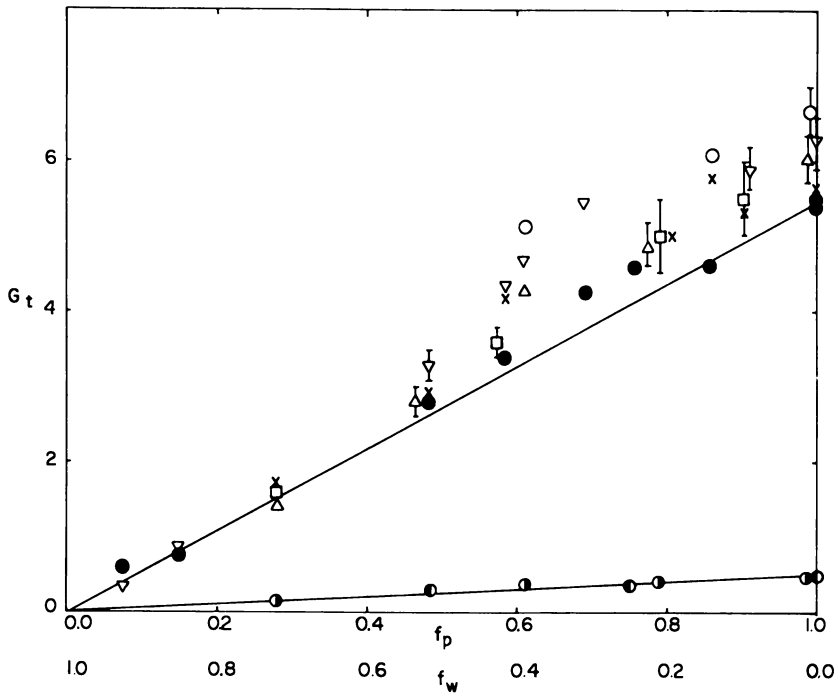

Figure 2. Radiolysis of water-isopropyl alcohol vapor mixtures at 125°C. in the presence and absence of electron scavengers. Dependence of $G(CH_4)_t$ and $G(CO)_t$ on the fraction of dose absorbed by water (f_w) and isopropyl alcohol (f_p)

CH_4 yields ● *No additive*
□ *With 1% C_7F_{14}*
× *With 1% CCl_4*
△ *With 0.1% SF_6*
▽ *With 1% SF_6*
○ *With 5% SF_6*
CO yields ◐ *No additive*
◑ *With 1% SF_6*

The effect of CCl_4 concentration on $G(H_2)_w$ from water vapor containing 1 mole % isopropyl alcohol is shown in Figure 3, $G(H_2)_w$ falls rapidly from 8.1 at zero CCl_4 concentration to 4.75 at 0.13 mole % CCl_4, then more slowly to 1.5 at 7.7 mole % CCl_4. A few runs with H_2O—C_3H_7OH—CCl_4 containing 1 mole % SF_6 gave values of $G(H_2)_w$ which fall on the same curve as those in the absence of SF_6.

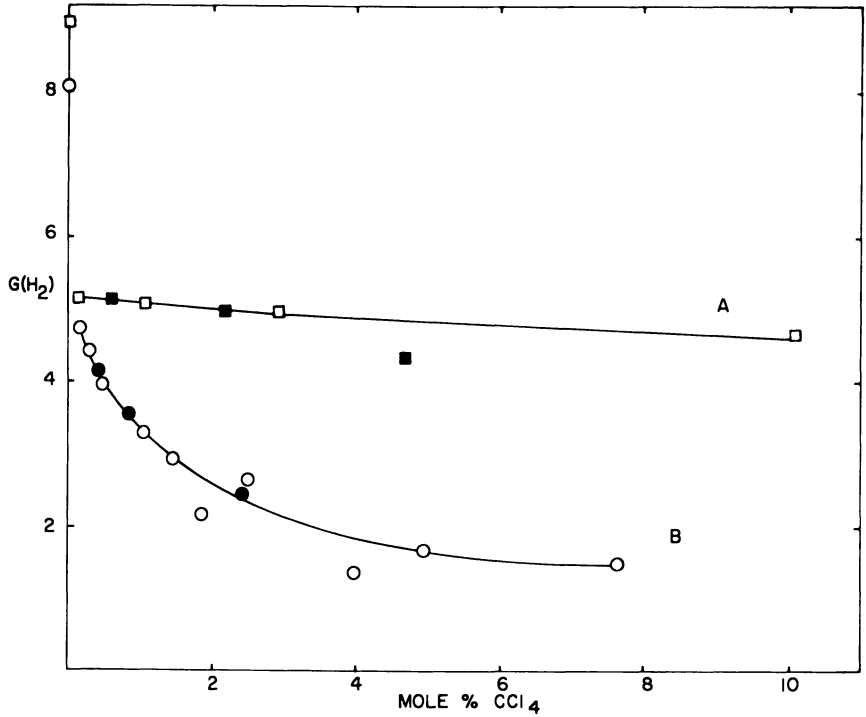

Figure 3. Effect of carbon tetrachloride concentration on the hydrogen yields from pure isopropyl alcohol (Curve A) and from water containing 1 mole % isopropyl alcohol (Curve B)

Curve A—$G(H_2)_p$ □ *No SF_6*
■ *With 1% SF_6*
Curve B—$G(H_2)_w$ ○ *No SF_6*
● *With 1% SF_6*

PROPYLENE. Values of $G(H_2)_w$ from water vapor containing various concentrations of isopropyl alcohol and propylene are shown in Table I.

Isopropyl Alcohol + Additives. CARBON TETRACHLORIDE. The effect of CCl_4 in pure isopropyl alcohol is shown in Figure 3. $G(H_2)_p$ falls steeply from 8.9 at zero CCl_4 to 5.2 at 0.11 mole % CCl_4, then slowly to 4.7 at 10 mole % CCl_4. Again the presence of 1 mole % SF_6 gave values of $G(H_2)$ which fall on the same line as those in the absence of SF_6.

PROPYLENE. The effect of propylene concentration on $G(H_2)_p$ from isopropyl alcohol, both in the presence and absence of 1 mole % SF_6, is shown in Figure 4. In the absence of SF_6, $G(H_2)_p$ falls smoothly from 8.9 at zero propylene to 3.5 at 9.4 mole % propylene. In the presence of 1% SF_6, $G(H_2)_p$ falls from 5.4 at zero propylene to 2.9 at 4.8 mole % propylene. $G(CH_4)_p$ was unaffected by propylene concentration up to

1 mole % but decreased by about 20% between 1–10 mole % propylene, both in the presence and absence of SF_6.

In all samples containing propylene, corrections for H_2 production from the propylene were made using $G(H_2)_{propylene} = 1.2$ (*4*).

Table I. Hydrogen Yields from Water Vapor Containing Isopropyl Alcohol and Propylene[a]

C_3H_7OH (Mole %)	C_3H_6 (Mole %)	$G(H_2)_w$
0.90	3.41	0.44
0.93	1.05	0.55
8.83	0.67	1.70
4.02	0.14	2.19
8.87	0.17	3.02

[a] Pressure ~ 700 torr and temperature 125°C.

Publication Date: January 1, 1968 | doi: 10.1021/ba-1968-0082.ch016

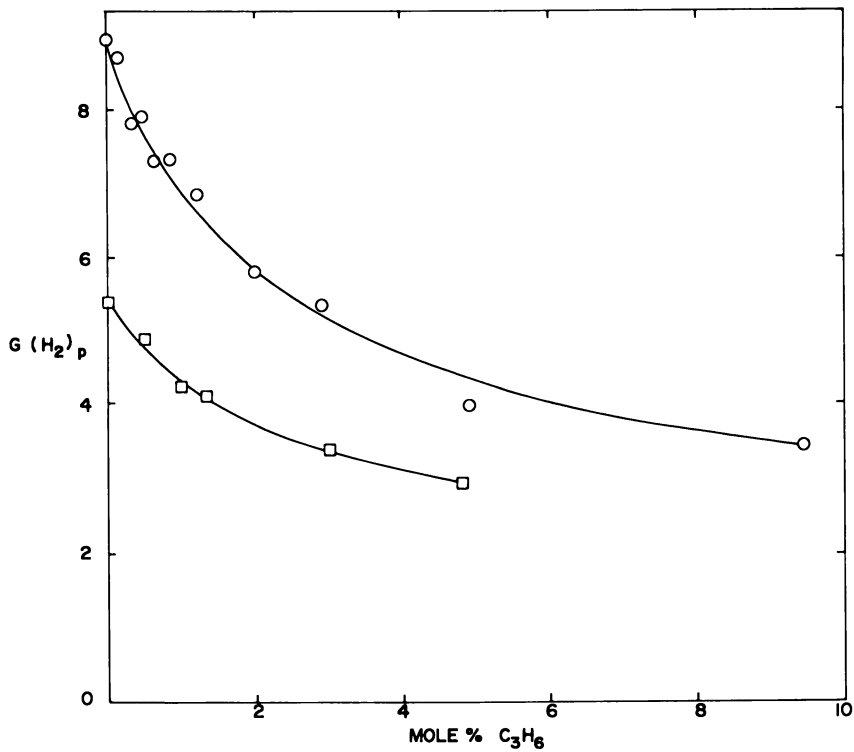

Figure 4. Effect of propylene concentration on the hydrogen yield from isopropyl alcohol vapor in the presence and absence of SF_6 at 125°C.

○ *No SF_6*
□ *With 1% SF_6*

Discussion

Hydrogen Yields from Water-Isopropyl Alcohol Mixtures. Figure 1 shows that both water and isopropyl alcohol contribute to the total hydrogen yield, and the linear dependence of $G(H_2)_t$ on the fraction of energy absorbed by each component may be expressed by the relationship

$$G(H_2)_t = f_w G(H_2)_w{}^\circ + f_p G(H_2)_p{}^\circ$$

where $G(H_2)_w{}^\circ = 8.1 \pm 0.2$ and $G(H_2)_p{}^\circ = 8.9 \pm 0.2$ are the values at $f_p = 0$ and $f_w = 0$, respectively. We will now consider the formation of hydrogen in water, isopropyl alcohol, and mixtures of the two, in terms of the probable ionic and non-ionic reactions occurring.

Pure water vapor is decomposed little by ionizing radiation (*2, 15*). On addition of an alcohol, however, $G(H_2)_w$ increases rapidly and reaches a limiting value of $\sim$ 8 at less than 1 mole % alcohol (*5, 12*). In water vapor, H atoms are generally considered to be formed *via* Reactions 1 to 5.

$$H_2O \rightsquigarrow H_2O^+, e^-, H_2O^* \quad (1)$$

$$H_2O^+ + H_2O \rightarrow H_3O^+ + OH \quad (2)$$

$$H_3O^+ + xH_2O \rightarrow H_3O^+(H_2O)_x \quad (3)$$

$$e^- + H_3O^+(H_2O)_x \rightarrow H + (x+1)H_2O \quad (4)$$

$$H_2O^* \rightarrow H + OH \quad (5)$$

where Reaction 3 represents the clustering or solvation of the hydronium ion by water molecules. At the limiting value of $G(H_2)_w$, all H atoms formed *via* Reactions 1, 2, 3, 4, and 5 abstract from the alcohol giving hydrogen. In the present system the minimum isopropyl alcohol concentration was 2 mole %, and since isopropyl alcohol has a weak α carbon-hydrogen bond, this will be sufficient to capture all available H atoms. In the present work, therefore, $G(H_2)_w{}^\circ$ represents the number of H atoms arising from all precursors plus the molecular hydrogen yield in water vapor.

In pure isopropyl alcohol, the major neutralization reaction producing H atoms will probably be

$$e^- + C_3H_7OH_2^+(C_3H_7OH)_y \rightarrow H + (y+1)C_3H_7OH \quad (6)$$

which is analogous to Reaction 4 in water vapor. (For convenience the isopropyl alcohol molecule will be written simply as C_3H_7OH and similarly for radicals and ions formed from isopropyl alcohol.) Although we have not made a detailed product analysis in pure isopropyl alcohol, it may be useful to speculate on the possible ion-molecule reactions occurring.

In pure isopropyl alcohol vapor, the mass spectrum using 50 e.v. electrons (*16*) shows a number of positive ions, the most abundant of which are: CH_3CHOH^+ (55.4%), $C_2H_3^+$ (6.3%), CH_3CO^+ (5.9%), COH^+ (4.5%), $C_3H_5^+$ (4.2%), $C_3H_7^+$ (3.6%), CH_3^+ (3.6%), $C_3H_3^+$ (3.3%), CH_2OH^+ (2.9%), $(CH_3)_2COH^+$ (2.1%), and $C_3H_6^+$ (1.4%). These ions, therefore, are likely to be produced in gamma-radiolysis, though not necessarily in the same proportions as in the mass spectrometer. Many of these ions are protonated forms of stable molecules or radicals and may be expected to transfer a proton under favorable conditions. The proton affinity of isopropyl alcohol is not known, but in view of the relative inductive effects in methanol, ethyl alcohol, and isopropyl alcohol, it is probably greater than that of ethyl alcohol *viz.* 193 ± 9 kcals./mole (*28*). From the heats of formation of the appropriate ions (*14*), with the above assumption regarding the proton affinity of isopropyl alcohol, it can be shown that proton transfer from CH_3CHOH^+, $C_2H_3^+$, COH^+, $C_3H_5^+$, $C_3H_7^+$, CH_2OH^+, and $(CH_3)_2COH^+$ to isopropyl alcohol is exothermic.

From an energetic point of view, therefore, and considering the large excess of isopropyl alcohol, proton transfer to isopropyl alcohol is not unreasonable. This would leave $C_3H_7OH_2^+$ as the major positive ion. However, Wilmenius and Lindholm (*29*) have pointed out that proton transfer in ethyl alcohol may be followed by the further dissociation of $C_2H_5OH_2^+$, and this is supported by the results of Sieck and Johnsen in the radiolysis of ethyl alcohol vapor (*25*). They find that in some cases, proton transfer to ethyl alcohol leads to dissociation and formation of H_3O^+ but since this can react further with ethyl alcohol by proton transfer, the major ion present is still $C_2H_5OH_2^+$. In view of this we cannot discount the further dissociation of $C_3H_7OH_2^+$ following proton transfer, but if reactions similar to those in ethyl alcohol vapor occur, this will not necessarily affect the overall formation of $C_3H_7OH_2^+$. Hydride ion transfer may also occur—*e.g.*, with CH_3^+

$$CH_3^+ + C_3H_7OH \rightarrow CH_4 + C_3H_6OH^+ \qquad (7)$$

and this would probably be followed by proton transfer from $C_3H_6OH^+$ to isopropyl alcohol.

It therefore seems likely that $C_3H_7OH_2^+$ will be the major positive ion remaining in pure isopropyl alcohol after ion-molecule reactions, though it will be of the clustered form $C_3H_7OH_2^+(C_3H_7OH)_y$, and that neutralization will proceed *via* Reaction 6. The mercury photosensitized decomposition of isopropyl alcohol shows a high quantum yield of H atoms (*21*) and a yield of H atoms from dissociation of excited isopropyl alcohol molecules might also be expected in the radiolysis. Hence, as for water vapor, the yield of H atoms from pure isopropyl alcohol will have

Publication Date: January 1, 1968 | doi: 10.1021/ba-1968-0082.ch016

both ions and excited molecules as precursors, and the total hydrogen yield will be the sum of the total H atom yield from all precursors plus the molecular hydrogen yield.

In water-isopropyl alcohol mixtures, the ion-molecule reactions occurring will be even more complicated. The reaction

$$H_3O^+ + C_3H_7OH \rightarrow H_2O + C_3H_7OH_2^+ \qquad (8)$$

is probably exothermic by at least 10 kcals./mole, and this would indicate $C_3H_7OH_2^+$ to be the major positive ion undergoing neutralization in water-isopropyl alcohol mixtures. However, Kebarle (*20*) found that α-particle irradiation of water-methanol vapor mixtures under conditions where ion-molecule reactions occurred gave predominantly ion clusters of the type $H^+(H_2O)_x(CH_3OH)_y$. Here x and y vary according to the concentrations of water and methanol in the mixture and the size of the cluster, methanol being taken up preferentially in clusters with $x + y < 9$. These findings imply that the proton is not bound more strongly to one molecule or the other, and since the same situation probably applies in water-isopropyl alcohol mixtures, the dominant positive ion which undergoes neutralization will be $H^+(H_2O)_x(C_3H_7OH)_y$.

$$e^- + H^+(H_2O)_x(C_3H_7OH)_y \rightarrow H + xH_2O + yC_3H_7OH \qquad (9)$$

Here x and y will depend on the concentrations of H_2O and C_3H_7OH in the mixture, with $x = 0$ at $f_w = 0$ and $y = 0$ at $f_p = 0$.

Despite the changing composition of this positive ion cluster with changes in f_w and f_p, $G(H_2)_t$ is linear with isopropyl alcohol concentration both in the presence and absence of electron scavengers (Figure 1). Thus, there is no evidence that the composition of the positive ion affects either the conversion of electrons to H atoms *via* Reaction 9, or ion-ion neutralization in the presence of electron scavengers. This, however, is not completely unambiguous, particularly in view of the numerical similarities between $G(H_2)_w°$ and $G(H_2)_p°$ in the presence and absence of electron scavengers.

Hydrogen Yields in the Presence of Electron Scavengers. The total hydrogen yield also behaves linearly in the presence of certain additives (Figure 1). Both sulfur hexafluoride and carbon tetrachloride have been found to capture electrons in water vapor containing methanol (*12*). Perfluorocyclocarbons have also been used as electron scavengers and are known to reduce hydrogen yields from liquid hydrocarbons (*24*). In the presence of these additives, therefore, electron-positive ion neutralization will be replaced completely by ion-ion neutralization, assuming that sufficient additive is present to capture all electrons. Most of the results in Figure 1 were carried out at 1 mole % additive, but experiments with SF_6 in the concentration range 0.1 to 5.0 mole % showed

Publication Date: January 1, 1968 | doi: 10.1021/ba-1968-0082.ch016

no effect of concentration on $G(H_2)_t$. Since essentially the same effect was found with all three additives, it may be concluded that complete electron capture takes place. Hence, the reduction in hydrogen yields $\Delta G(H_2)_w°$ and $\Delta G(H_2)_p°$ will represent the yields of H atoms caused by electron-positive ion neutralization in water and isopropyl alcohol vapors, respectively, unless ion-ion neutralization results in the formation of H atoms.

In alkane gases, neither ion-ion neutralization in the gas phase (*17*) nor at the walls of the vessel on application of an electric field (*31*) produce H atoms. Similarly in D_2O-propane mixtures (*18*), Johnson and Simic have shown that neutralization of D_3O^+ by negative ions formed from N_2O and SF_6 does not result in D atom formation. In our system SF_6, C_7F_{14} and CCl_4 have essentially the same effect on $G(H_2)$ over the whole H_2O–C_3H_7OH concentration range. If ion-ion recombination resulted in H atom production, then the negative ions from all these additives would have to produce H atoms to the same extent, which is unlikely. It, therefore, seems likely that ion-ion neutralization does not lead to H atoms in our system, irrespective of the composition of the positive ion cluster. Thus, $\Delta G(H_2)_w°$ and $\Delta G(H_2)_p°$, the reductions in hydrogen yield in water and isopropyl alcohol, respectively, on addition of electron scavengers, represent the number of H atoms arising from electron-positive ion neutralization in water and isopropyl alcohol vapors.

The reductions in hydrogen yield for all three electron scavengers are in close agreement and lead to values of $g(H)_w{}^e = 2.6 \pm 0.5$ and $g(H)_p{}^e = 3.5 \pm 0.5$, where these represent the number of H atoms which have the electron as a precursor in water and isopropyl alcohol vapors, respectively. The value 2.6 ± 0.5 in water vapor is essentially the same as that found in D_2O (*18*) and may be compared with the expected value of 3.3 from the *W*-value of 30 e.v. (*8*, *30*). The value 3.5 ± 0.5 in isopropyl alcohol suggests that the energy required to produce an ion-pair in isopropyl alcohol is about 28 e.v., assuming that all electrons are converted to H atoms in pure isopropyl alcohol vapor.

In the presence of carbon tetrachloride, $G(H_2)_t$ begins to fall rapidly at values of f_p lower than 0.5. This is caused by reaction with H atoms in competition with their abstraction reaction from isopropyl alcohol. However, the values of $G(H_2)_t$ at high values of f_p indicate that the reduction in hydrogen yield owing to electron capture by CCl_4 is similar to those in the presence of SF_6 and C_7F_{14}. Any possibility that the effect of these additives is owing to reaction with H atoms may be excluded. SF_6 reacts much too slowly with H atoms (*13*) to compete with isopropyl alcohol at the concentrations used, and since C_7F_{14} has the same effect as SF_6, it too must react too slowly with H atoms to compete with their abstraction reaction from isopropyl alcohol.

Publication Date: January 1, 1968 | doi: 10.1021/ba-1968-0082.ch016

The hydrogen which remains in the presence of electron scavengers represents the sum of the "residual" H atoms plus the molecular hydrogen yield, designated $g(H)$ and $g(H_2)$, respectively. The results show $g(H)_w + g(H_2)_w = 5.5 \pm 0.3$ and $g(H)_p + g(H_2)_p = 5.4 \pm 0.3$.

Competition Kinetic Analysis. PROPYLENE. Propylene is known to add H atoms rapidly giving the isopropyl radical

$$H + C_3H_6 \rightarrow C_3H_7 \qquad (10)$$

The simple alkenes have negative electron affinities and therefore will not capture electrons. At the pressure of water vapor used, Reaction 2 is fast enough to preclude other reactions of H_2O^+ (*22*). Charge or proton transfer to propylene may also be excluded on energetic grounds. The effect of propylene on $G(H_2)_w$ from water vapor containing small amounts of isopropyl alcohol will therefore be owing to the capture of H atoms in competition with their abstraction reaction from isopropyl alcohol

$$H + C_3H_7OH \rightarrow H_2 + C_3H_6OH \qquad (11)$$

This simple competition for H atoms leads to the following relationship for the measured hydrogen yield $G(H_2)_w$:

$$G(H_2)_w = g(H_2)_w + \frac{g(H)_w^e + g(H)_w}{1 + \dfrac{k_{10}[C_3H_6]}{k_{11}[C_3H_7OH]}}$$

Hence, the reduction in hydrogen yield, ΔG, on addition of propylene may be expressed by the equation

$$\frac{1}{\Delta G} = \frac{1}{g(H)_w^e + g(H)_w}\left(1 + \frac{k_{11}[C_3H_7OH]}{k_{10}[C_3H_6]}\right) \qquad (12)$$

where $\Delta G = g(H_2)_w + g(H)_w^e + g(H)_w - G(H_2)_w = 8.1 - G(H_2)_w$. The plot of $1/\Delta G$ *vs.* $[C_3H_7OH]/[C_3H_6]$ from the results in Table I is shown in Figure 5. The plot is a good straight line in agreement with the above scheme, and from it the values $g(H)_w^e + g(H)_w = 7.6$ and $k_{10}/k_{11} = 90$ are obtained. The value $g(H)_w^e + g(H)_w = 7.6$ is lower than $G(H_2)_w$ in the absence of propylene. This shows that a small yield of hydrogen is present in water vapor, $g(H_2)_w = 0.5 \pm 0.2$ which does not arise from H atom precursors. This is in good agreement with the molecular yield found by non-competitive methods (*1*, *32*). Hence, the number of H atoms arising from processes not involving the electron, $g(H)_w = 5.0 \pm 0.5$.

The effect of propylene concentration on $G(H_2)_p$ from pure isopropyl alcohol (Figure 4) will also be owing to capture of H atoms. The

Publication Date: January 1, 1968 | doi: 10.1021/ba-1968-0082.ch016

kinetic relationship will be analogous to that in water containing isopropyl alcohol *viz.*

$$\frac{1}{\Delta G} = \frac{1}{g(H)_p{}^e + g(H)_p}\left(1 + \frac{k_{11}[C_3H_7OH]}{k_{10}[C_3H_6]}\right) \qquad (13)$$

where $\Delta G = 8.9 - G(H_2)_p$.

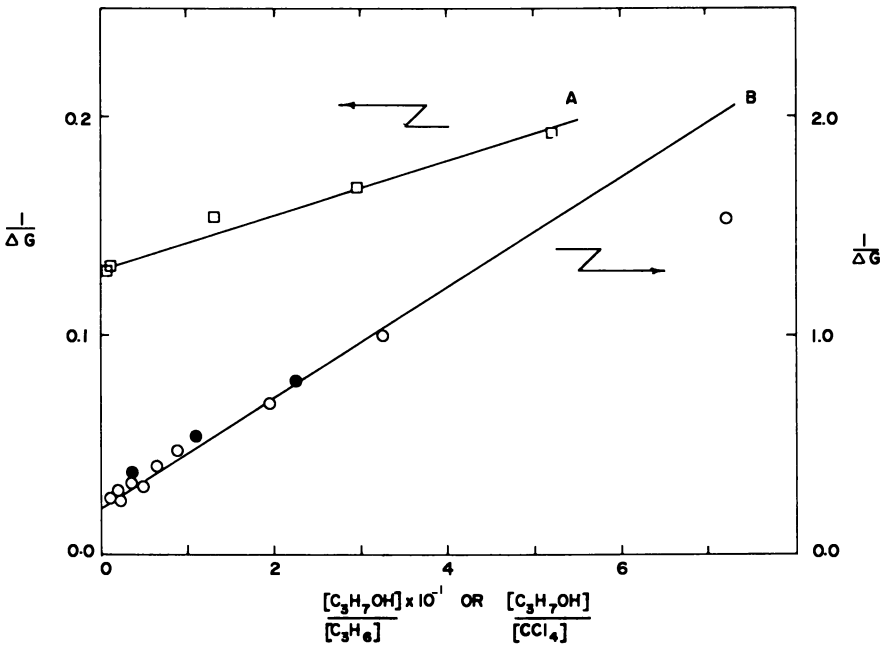

Figure 5. H atom competition plots in water vapor containing isopropyl alcohol + propylene (Curve A) or isopropyl alcohol + carbon tetrachloride (Curve B)

□ *$H_2O + C_3H_7OH + C_3H_6$ plotted according to Equation 12*
○ *$H_2O + C_3H_7OH + CCl_4$ plotted according to Equation 17 (no SF_6)*
● *With 1% SF_6*

The plot of $1/\Delta G$ *vs.* $[C_3H_7OH]/[C_3H_6]$ is shown in Figure 6. From the slope and intercept, values of $g(H)_p{}^e + g(H)_p = 7.2$ and $k_{10}/k_{11} = 40$ are deduced. Since $G(H_2)_p = 8.9$ in pure isopropyl alcohol in the absence of propylene, these results show the presence of a substantial molecular hydrogen yield, $g(H_2)_p = 1.7 \pm 0.2$ which does not arise from H atom precursors. Hence, the number of H atoms arising from processes not involving electrons, $g(H)_p = 3.7 \pm 0.5$ in pure isopropyl alcohol.

Publication Date: January 1, 1968 | doi: 10.1021/ba-1968-0082.ch016

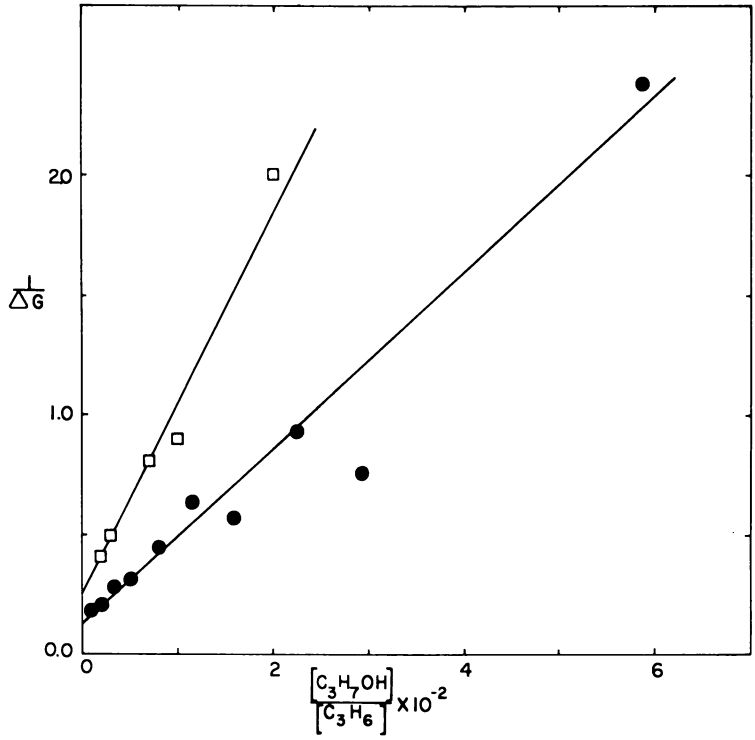

Figure 6. H atom competition plots for isopropyl alcohol-propylene system with and without SF_6

● *According to Equation 13 (no SF_6)*
□ *According to Equation 14 (with 1% SF_6)*

In isopropyl alcohol containing 1 mole % SF_6, the H atoms arising from electron-positive ion combination will be completely suppressed. Propylene will therefore suppress the hydrogen yield by capturing the residual H atoms in competition with isopropyl alcohol. Since $G(H_2)_p = 5.4$ in the presence of SF_6 at zero propylene, the competition will be governed by the relationship

$$\frac{1}{\Delta G} = \frac{1}{g(H)_p}\left(1 + \frac{k_{11}[C_3H_7OH]}{k_{10}[C_3H_6]}\right) \qquad (14)$$

where $\Delta G = g(H_2)_p + g(H)_p - G(H_2)_p = 5.4 - G(H_2)_p$. The plot of $1/\Delta G$ *vs.* $[C_3H_7OH]/[C_3H_6]$ is also shown in Figure 6 and gives values of $g(H)_p = 3.7$ and $k_{10}/k_{11} = 35$. By subtraction, the molecular hydrogen yield $g(H_2)_p = 1.7$. These results are in excellent agreement with those in the absence of SF_6 and show that SF_6 does not interfere with H atom reactions or with molecular hydrogen production.

Publication Date: January 1, 1968 | doi: 10.1021/ba-1968-0082.ch016

The three values of the rate constant ratio found above in water and isopropyl alcohol vapor give an average value $k_{10}/k_{11} = 60 \pm 30$.

CARBON TETRACHLORIDE. The rapid decrease in $G(H_2)_w$ upon adding 0.13 mole % CCl_4 to water vapor containing 1 mole % isopropyl alcohol, followed by a slower fall-off as the CCl_4 concentration increases, is indicative of more than one precursor of hydrogen reacting with CCl_4. These may be identified as the electron and H atom, in view of their known reaction with CCl_4 in the vapor phase (*11*, *26*)

$$e^- + CCl_4 \rightarrow CCl_3 + Cl^- \quad (15)$$

$$H + CCl_4 \rightarrow HCl + CCl_3 \quad (16)$$

and the analogous effect in water vapor containing methanol (*12*). Our experiments also show that, in the presence of sufficient SF_6 to capture all electrons, values of $G(H_2)_w$ fall on the same curve as those in the absence of SF_6. This shows that, in the absence of SF_6, carbon tetrachloride captures all available electrons at all concentrations studied. Since the consumption of CCl_4 owing to electron capture is small at the CCl_4 concentrations used, the reduction in hydrogen yield may be expressed in a form similar to those with added propylene *viz.*

$$\frac{1}{\Delta G} = \frac{1}{g(H)_w}\left(1 + \frac{k_{11}[C_3H_7OH]}{k_{16}[CCl_4]}\right) \quad (17)$$

where $\Delta G = g(H_2)_w + g(H)_w - G(H_2)_w = 5.5 - G(H_2)_w$. The plot of $1/\Delta G$ *vs.* $[C_3H_7OH]/[CCl_4]$ is shown in Figure 5 and gives $g(H)_w = 4.9$ and $k_{11}/k_{16} = 1.2$. By subtraction the molecular yield in water vapor $g(H_2)_w = 0.6$. Since the molecular yield persists at high CCl_4 concentrations, this is further evidence that it does not have either thermal electrons or H atoms as precursors.

The effect of CCl_4 on $G(H_2)_p$ from pure isopropyl alcohol (Figure 3) is as predicted from these results. The rapid decrease in $G(H_2)_p$ on addition of only 0.11 mole % CCl_4 is because of efficient electron capture and the slower fall-off at higher CCl_4 concentrations is the result of H atom scavenging. Again the addition of 1 mole % SF_6 has no effect on $G(H_2)_p$ at any particular CCl_4 concentration, showing that, in the absence of SF_6, all available electrons are captured by CCl_4 at all concentrations studied.

Thus, the use of appropriate additives which react with specific intermediates allows us to estimate the yields of the various hydrogen precursors in water and isopropyl alcohol vapors. These yields are summarized in Table II.

Formation of Methane and Carbon Monoxide. Ionization of isopropyl alcohol using 50 e.v. electrons leads to the formation of CH_3 (55.4%), CH_3^+ (3.6%), and CH_4 (6.3%) in the mass spectrometer (*16*).

Publication Date: January 1, 1968 | doi: 10.1021/ba-1968-0082.ch016

Table II. Yields of the Hydrogen Precursors in Water and Isopropyl Alcohol Vapors

	H_2O	C_3H_7OH
g(H)[a]	2.6 ± 0.5	3.5 ± 0.5
g(H)	5.0 ± 0.5	3.7 ± 0.5
$g(H_2)$	0.5 ± 0.2	1.7 ± 0.2

[a] Pressure ~ 700 torr and temperature 125°C.

Assuming that a similar effect occurs in γ-radiolysis, that all methyl radicals abstract from isopropyl alcohol

$$CH_3 + C_3H_7OH \rightarrow CH_4 + C_3H_6OH \quad (18)$$

and that CH_3^+ undergoes the hydride transfer reaction

$$CH_3^+ + C_3H_7OH \rightarrow CH_4 + C_3H_6OH^+ \quad (7)$$

then the primary ionization and secondary decomposition of primary fragments could result in methane formation with $G \sim 2.3$. Calculations of G values by quantitative correlations of this type are not strictly justified but, qualitatively, they indicate that a major fraction of the methane yield is probably produced by the above reactions. The lack of a dose effect indicates that methane formation is not affected by secondary reactions of the radiolysis products at the doses used. Since little CH_4 is likely to be produced *via* ion-molecule reactions of the remaining primary and secondary ions, part of the methane yield probably arises *via* decomposition of excited isopropyl alcohol molecules.

Since much of the methane yield appears to be produced *via* methyl radicals, the yield should be affected by propylene concentration. We found little effect below 1 mole % propylene but the yield fell by ~ 20% as the propylene concentration increased to 10 mole %, both in the presence and absence of SF_6. These results, however, do not indicate how much methane is formed from CH_3 precursors and how much by "molecular" processes. The effect of propylene is being studied further in an attempt to obtain this information. The electron scavengers appear to increase the methane yield slightly. Since they do not decrease the yield, this probably means that electron-positive ion neutralization does not produce methane. The reason for the increase in $G(CH_4)$ is not clear but it could occur if ion-ion neutralization produced methane, or if some physical interaction caused a transfer of energy from the additives to isopropyl alcohol. The slight increase in CH_4 yield with SF_6 concentration tends to favor the latter assumption.

In the mass spectrum, about 4.5% of the ions produced are COH^+ (*16*). As discussed earlier, proton transfer from COH^+ to isopropyl alcohol is likely and if the same situation applies to γ-radiolysis, this could

Publication Date: January 1, 1968 | doi: 10.1021/ba-1968-0082.ch016

lead to a small yield of carbon monoxide. Up to 5 mole % SF_6 had no noticeable effect on $G(CO)$ showing that little or none is produced by electron-positive ion or ion-ion neutralization. Up to 60 mole % propylene had no effect on the CO yield. As with methane, part of the yield of carbon monoxide is probably produced from decomposition of excited isopropyl alcohol molecules.

Molecular Hydrogen Formation. In the mass spectrum of isopropyl alcohol vapor with 50 e.v. electrons, about 18% of the total ionization leads to molecular hydrogen as a product (*16*). Assuming a similar cracking pattern in γ-radiolysis, this would account for $G \sim 0.7$ in pure isopropyl alcohol. Again, this figure may not strictly apply to the radiolysis, but it appears that about half the molecular yield probably arises from decomposition of excited isopropyl alcohol molecules. Production of molecular hydrogen *via*

$$C_3H_7OH \xrightarrow{\wedge\wedge\wedge} H_2 + H_2C\underset{H}{\overset{O}{\diagup\diagdown}}C{-}CH_3 \qquad (19)$$

has been postulated in the radiolysis of the liquid (*27*). If this proceeds *via* decomposition of excited isopropyl alcohol molecules, it might be expected to occur more favorably in the vapor phase.

Our results give no positive evidence for either of the two possible modes of formation of molecular hydrogen in water vapor *viz.* decomposition of an excited molecule

$$H_2O^* \rightarrow H_2 + O \qquad (20)$$

or *via* the hydride ion

$$e^- + H_2O \rightarrow H^- + OH \qquad (21)$$

$$H^- + H_2O \rightarrow H_2 + OH^- \qquad (22)$$

However, our value for $g(H)_w{}^e$ is somewhat lower than that predicted from the *W*-value of 30 e.v. in water vapor (*8, 30*) and is in good agreement with $G(N_2)$ from water vapor containing N_2O, after correcting to the same dosimetry (*7, 11*). This may be indicative of some electrons reacting *via* other processes such as Reaction 21. Since the appearance potential of H^- from H_2O is $\sim$ 5 e.v. (*9*), the electron scavengers would not be expected to compete with Reaction 21 in view of their known cross-sections for electron capture in this energy range and the high concentration of water (*see* Ref. 11).

Conclusions

Hydrogen, methane, and carbon monoxide yields in the vapor phase radiolysis of water-isopropyl alcohol mixtures at 125°C. are linear over

Publication Date: January 1, 1968 | doi: 10.1021/ba-1968-0082.ch016

the whole concentration range. From the effects of electron scavengers on the hydrogen yields, we estimate the number of H atoms resulting from electron-positive ion neutralization, $g(H)^e$, to be 2.6 ± 0.5 and 3.5 ± 0.5 in water and isopropyl alcohol, respectively. Both electron-positive ion and ion-ion neutralizations appear to be independent of the composition of the positive ion cluster. The effects of carbon tetrachloride and propylene give values for the number of H atoms which do not have the electron as a precursor, $g(H) = 5.0 \pm 0.5$ and 3.7 ± 0.5 in water and isopropyl alcohol, respectively. Molecular hydrogen yields are also formed with $g(H_2) = 0.5 \pm 0.2$ in water and 1.7 ± 0.2 in isopropyl alcohol. The rates of reaction of H atoms with carbon tetrachloride, isopropyl alcohol, and propylene were found to be in the approximate ratio 1:1:60.

Publication Date: January 1, 1968 | doi: 10.1021/ba-1968-0082.ch016

Acknowledgment

The authors would like to thank P. J. Dyne for his helpful comments on the manuscript.

Literature Cited

(1) Anderson, A. R., Knight, B., Winter, J. A., *Nature* **201,** 1026 (1964).
(2) Anderson, A. R., Knight, B., Winter, J. A., *Trans. Faraday Soc.* **62,** 359 (1966).
(3) Anderson, A. R., Winter, J. A., "Chemistry of Ionization and Excitation," p. 197, G. R. A. Johnson, G. Scholes, eds., Taylor and Francis Ltd., London, 1967.
(4) Back, R. A., Woodward, T. W., McLauchlan, K. A., *Can. J. Chem.* **40,** 1380 (1962).
(5) Baxendale, J. H., Gilbert, G. P., *Discussions Faraday Soc.* **36,** 186 (1963).
(6) Baxendale, J. H., Gilbert, G. P., *J. Am. Chem. Soc.* **86,** 516 (1964).
(7) Baxendale, J. H., Gilbert, G. P., *Science* **147,** 1571 (1965).
(8) Booz, J., Ebert, H. G., *Z. Angew. Phys.* **13,** 376 (1961).
(9) Buchel'nikova, I. S., *Zh. Eksperim. i Teor. Fiz.* **35,** 1119 (1958).
(10) Cvetanovic, R. J., "Advances in Photochemistry," Vol. 1, p. 115, W. A. Noyes, G. S. Hammond, J. N. Pitts, eds., Interscience, New York, N. Y., 1963.
(11) Dixon, R. S., Bailey, M. G., *Can. J. Chem.* **46,** 1181 (1968).
(12) Dixon, R. S., Bailey, M. G., *Can. J. Chem.* (in press).
(13) Fenimore, C. P., Jones, G. W., *Combust. Flame* **8,** 231 (1964).
(14) Field, F. H., Franklin, J. H., "Electron Impact Phenomena," Academic Press, New York, N. Y., 1957.
(15) Firestone, R. F., *J. Am. Chem. Soc.* **79,** 5593 (1957).
(16) Friedman, L., Long, F. A., Wolfsberg, M., *J. Chem. Phys.* **27,** 613 (1957).
(17) Johnson, G. R. A., Warman, J. M., *Trans. Faraday Soc.* **61,** 1709 (1965).
(18) Johnson, G. R. A., Simic, M., *J. Phys. Chem.* **71,** 1118 (1967).
(19) Kebarle, P., Searles, S. K., Zolla, A., Scarborough, J., Arshadi, M., *J. Am. Chem. Soc.* **89,** 6393 (1967).
(20) Kebarle, P., Haynes, R. N., Collins, J. G., *J. Am. Chem. Soc.* **89,** 5753 (1967).

(21) Knight, A. R., Gunning, H. E., *Can. J. Chem.* **40,** 1134 (1962).
(22) Lampe, F. W., Field, F. H., Franklin, J. L., *J. Am. Chem. Soc.* **79,** 6132 (1957).
(23) Meisels, G. G., *J. Chem. Phys.* **41,** 51 (1964).
(24) Rajbenbach, L. A., *J. Am. Chem. Soc.* **88,** 4275 (1966).
(25) Sieck, L. W., Johnsen, R. H., *J. Phys. Chem.* **69,** 1699 (1965).
(26) Steacie, E. W. R., "Atomic and Free Radical Reactions," Vol. 2, p. 657, Reinhold, New York, N. Y., 1954.
(27) Sweeney, M. A., Ph.D. Thesis, p. 78, Lawrence Radiation Laboratory, University of California, 1962.
(28) Tal'roze, V. K., Frankevich, E. L., *J. Am. Chem. Soc.* **80,** 2344 (1958).
(29) Wilmenius, P., Lindholm, E., *Arkiv Fyzik* **21,** 97 (1961).
(30) Wingate, G., Gross, W., Failla, G., *Radiation Res.* **8,** 411 (1958).
(31) Woodward, T. W., Back, R. A., *Can. J. Chem.* **41,** 1463 (1963).
(32) Yang, J. Y., Marcus, I., *J. Am. Chem. Soc.* **88,** 1625 (1966).

RECEIVED January 29, 1968.

Properties and Reactions of Electrons in γ-Irradiated and Photoionized Organic Glasses

MICHAEL A. BONIN, JACOB LIN, KOZO TSUJI, and FFRANCON WILLIAMS

University of Tennessee, Knoxville, Tenn. 37916

Publication Date: January 1, 1968 | doi: 10.1021/ba-1968-0082.ch017

The ways in which the radiation-induced generation and stability of trapped electrons in hydrocarbon glasses are affected by the presence of polar additives have been studied by ESR and optical techniques. Adding 5 mole % triethylamine (TEA) enhances the radiation chemical yields; $G(e^-)$ *is increased from 0.30 to 0.98 for methylcyclohexane, from 0.69 to 1.08 for 3-methylpentane, but only from 0.89 to 0.96 for 3-methylhexane. At higher TEA concentrations, the yield is reduced by incipient crystallinity effects. The presence of a polar substance retards thermal decay of the trapped electron after irradiation. Acetonitrile in methyltetrahydrofuran glass undergoes efficient dissociative electron capture to give methyl radicals on photobleaching after γ-irradiation. This reaction may involve resonance capture of the optically excited electron.*

There is now a considerable literature on the subject of localized electrons in liquids and rigid glasses. It is natural that polar solvents have claimed the most attention, partly because both chemical and radiation techniques can be used to generate the solvent-trapped electron in many of these systems and also because of the appreciable stability of the solvated electron in several polar media. Only recently has the trapped electron (e^-) been positively identified in nonpolar materials such as the saturated hydrocarbons, and here the observations have been confined to matrix-isolation studies with γ-irradiated and photoionized glasses (*8, 9, 13, 14, 19, 22, 23, 24*). Several fundamental questions are posed by these newer findings, and in view of the present theoretical

In Radiation Chemistry; Hart, E.;
Advances in Chemistry; American Chemical Society: Washington, DC, 1968.

state of the subject (*11, 17*), it is necessary to seek clarification by further experiments.

First, we describe studies on the generation and thermal stability of trapped electrons in hydrocarbon glasses, and show how the results are modified by the presence of polar molecules in the matrix. It will be useful to analyze these findings to obtain evidence for or against the specific role of polar molecules in the process of electron trapping because there is much theoretical interest focused on this question. Another problem on which this research should throw some light concerns the mechanism of thermal decay for the trapped electron. A process of positive charge transfer has been suggested by some authors (*7, 9*), so it is necessary to distinguish between the contributions caused by hole and electron mobility in the dark. In considering this subject, we expand upon the results presented previously (*12*).

Secondly, we discuss the chemical reactivity of the excited state of the electron e^{-*} produced by optical excitation of (e^-). To avoid confusion, we shall describe this species as the excited electron in contrast to the mobile electron, and this latter term will be used to describe (e^-) when it undergoes what is essentially translational motion through the matrix. It is also necessary to introduce the concept of a delocalized electron, which may be defined as belonging to the ionized state of a molecule before the electron either becomes trapped as (e^-) or is captured by an electron scavenger. The system which has been studied, and which will be discussed in connection with these ideas, consists of acetonitrile in a 2-methyltetrahydrofuran glass. Its behavior does not fit the conventional description of an electron scavenger in a rigid matrix, and this provides the opportunity to learn something new about electronic processes in radiation and photochemistry.

Publication Date: January 1, 1968 | doi: 10.1021/ba-1968-0082.ch017

Experimental

Materials. Tetrahydro-2-methylfuran (MTHF), 2-methylbutane (isopentane), triethylamine (TEA), and *N,N,N′,N′*-tetramethyl-*p*-phenylenediamine dihydrochloride (TMPD) were obtained from Eastman Organic Chemicals. Trimethylamine (99.0%) was obtained from Matheson, and 3-methylpentane (3-MP, chromatoquality) from Matheson, Coleman, and Bell. Acetonitrile (Baker Analyzed Reagent) was supplied by the J. T. Baker Co. Samples of acetonitrile-d_3 were obtained from E. Merck, AG (Darmstadt) and from Stohler Isotope Chemicals.

Preparation of Samples. All materials available in the form of bulk liquids were pretreated according to accepted purification techniques and then distilled before use. These methods and the sample preparation techniques have been described (*14*). Acetonitrile was dried *in vacuo* over magnesium sulfate. Optical cells were made from extruded quartz

tubing of square or rectangular cross section. The samples for the ESR work were prepared in Spectrosil or Suprasil tubes about 4 mm., o. d.

Radiation Sources. Cobalt-60 γ-ray sources provided dose rates of 1.4×10^{18} and 2.9×10^{17} e.v. gram^{-1} min.$^{-1}$ as determined by Fricke dosimetry. The source of ultraviolet radiation was a high pressure mercury arc lamp (General Electric Co. A-H6 or B-H6), and the output was passed through a Corning 9863 filter and a quartz optical cell (1 cm.) filled with a saturated aqueous solution of nickel sulfate. This filtration system gives a suitable passband in the 320-n.m. region corresponding to the absorption maximum for TMPD. The samples were generally irradiated at 77°K., but in some experiments it was desirable to obtain lower irradiation temperatures (*ca.* 71°K.) by using the cryogenic cooling technique (*16*), which involves bubbling helium gas through the liquid nitrogen. The γ-irradiations were carried out in the dark, and care was taken to prevent sample exposure to stray (unfiltered) light during ultraviolet irradiation.

Optical Measurements. The methods of Hamill *et al.* (*8, 9, 18*) were employed without any significant modification. Spectra were recorded against air as a reference. The near infrared spectrum of the trapped electron was then plotted as the difference between the two spectra obtained before and after bleaching the sample with an intense source of infrared light ($\lambda > 1000$ n.m.). Other details will be given with the results.

ESR Measurements. Our equipment and the experimental arrangements have been described (*14*). Photoionization studies were carried out by irradiating the sample with ultraviolet light in the cavity. The spectra were usually obtained at low microwave power (0.01 mwatts) such that the trapped electron signal was not saturated. For 3-MP and mixtures containing low concentrations of TEA in 3-MP, the γ-irradiated samples had to be maintained below 77°K. as described before to prevent thermal decay of the ESR signal (*14*). Also, the decay of photoionized samples after irradiation could be completely arrested at 71°K. At the higher amine concentrations, the ESR signal was much more stable at 77°K., and the measurements were made routinely at this temperature. Almost all the kinetic measurements of thermal decay were made at 77°K. All manipulations involving transfer, etc., of samples were carried out in the dark. The arrangements for subsequent optical bleaching of the γ- and ultraviolet-irradiated samples are described below.

Results

Hydrocarbon-Amine Glasses. Optical studies on irradiated glasses consisting of binary mixtures of 3-MP and TEA were first made by Gallivan and Hamill (*8, 9*). This system is suitable for studying the effect of polarity on the trapped electron because the optical and bleaching characteristics of (e^-) are remarkably similar over the entire composition range. Thus, λ_{max} is located at 1600 n.m., and (e^-) is readily bleached by infrared light ($\lambda > 1000$ n.m.) in these mixtures. This

Publication Date: January 1, 1968 | doi: 10.1021/ba-1968-0082.ch017

constancy in the properties and behavior of (e^-) does not apply to some other nonpolar-polar mixtures, such as 3-MP and MTHF (9).

The results of our optical measurements on γ-irradiated samples are illustrated in Figure 1, where two effects are immediately apparent. First,

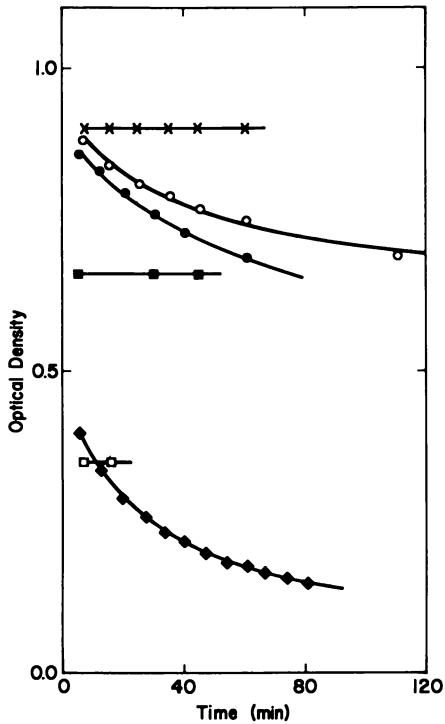

Figure 1. Optical densities at 1600 n.m. of 3-methylpentane–triethylamine glasses after γ irradiation at 77°K. All values normalized to 1-cm. path length and dose of 1.4 × 10^{18} e.v. gram^{-1} for each mixture. For pure 3-MP, the dose was 2.8 × 10^{18} e.v. gram^{-1} and the path length 1 cm.; for pure TEA, the dose was 7.0 × 10^{18} e.v. gram^{-1} and the path length 0.23 cm.
Symbols: ◆, pure 3-MP; ●, 2 mole % TEA; ○, 5 mole % TEA; ×, 25 mole % TEA; ■, 50 mole % TEA; □, pure TEA. Dose rate, 1.4 × 10^{18} e.v. gram^{-1} min.$^{-1}$

the postirradiation thermal decay of (e^-) at 77°K. becomes progressively slower as the concentration of TEA in the mixture is increased; secondly, the optical density of (e^-) extrapolated to zero time after irradiation in-

Publication Date: January 1, 1968 | doi: 10.1021/ba-1968-0082.ch017

creases remarkably with TEA concentration for dilute solutions of TEA in 3-MP; however, at higher TEA concentration the optical density of (e^-) declines, and the value obtained for pure TEA is actually somewhat lower than for 3-MP alone. The second effect was described by Gallivan and Hamill (*9*).

Much the same behavioral pattern emerges from the ESR results shown in Figure 2, except for the notable difference that the signal decay rates at 77°K. are faster than those observed in the corresponding optical experiments. The reason for this apparent difference in the absolute decay rates as measured by optical and ESR methods for samples of the same composition is not completely understood at this time, and the problem has been discussed elsewhere (*14*) in connection with 3-MP. It is unlikely that the effect is caused simply by temperature differences between the optical and ESR Dewars. It should be added that results such as those shown in Figure 2 do not permit accurate extrapolations to be made for the initial yield when the decay is rapid, as is the case for the dilute range of TEA concentrations. Obviously, plots of signal intensity, measured at some arbitrary time after the irradiation, *vs.* composition, give a false indication of the true yields under these conditions of fast decay, and this comment applies particularly to some data we obtained earlier for the 3-MP-trimethylamine system (*24*) under similar circumstances. To counter the effect of fast decay in the dilute TEA systems at 77°K., γ-irradiation and the subsequent ESR measurements were made at 71°K., where there was almost no thermal decay of the signal.

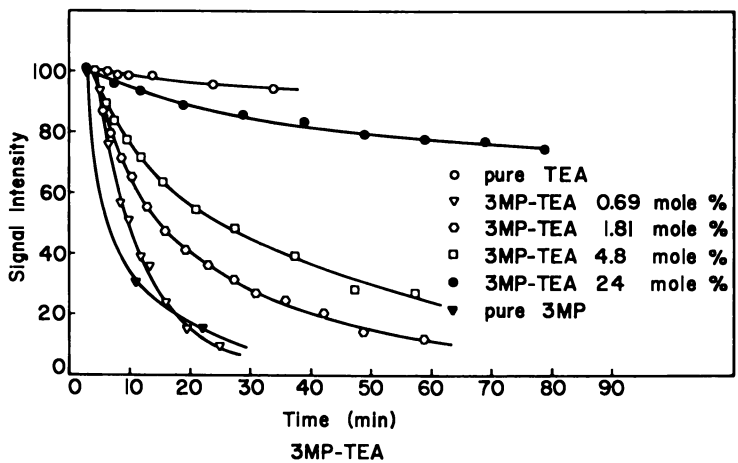

Figure 2. ESR signal intensity of (e^-) vs. *time after irradiation at 77°K. for 3-methylpentane–triethylamine mixtures γ-irradiated for 10 minutes at a dose rate of* 2.9×10^{17} *e.v. gram*$^{-1}$ *min.*$^{-1}$. *Intensity scale normalized to an initial value of 100 for pure TEA*

Publication Date: January 1, 1968 | doi: 10.1021/ba-1968-0082.ch017

In Figure 3, the ESR determinations of $G(e^-)$ are plotted against composition. The numerical values are based on a comparison with $G(e^-) = 2.6$ for MTHF as the standard (*4, 18, 21*). These results obtained under conditions where there was no thermal decay clearly show that the yield is definitely enhanced at low amine concentrations. For comparison, the optical densities are also given; these data are corrected for the relatively small amount of postirradiation decay (Figure 1) which occurred under the experimental conditions, and the numerical values have been normalized so that the optical density for pure 3-MP actually corresponds to the $G(e^-)$ value based on the molar extinction coefficient $\epsilon(e^-) = 3 \times 10^4\ M^{-1}\ \text{cm.}^{-1}$ (*8*). Therefore, if this value of $\epsilon(e^-)$ were also to apply for the binary mixtures, the normalized optical densities would in fact represent the optical $G(e^-)$ values. As it is, we see that there is a good qualitative correlation between the ESR and optical results. As mentioned before, similar plots of optical data were obtained by Gallivan and Hamill (*8, 9*), and the only slight disagreement between this work and their results concerns the value obtained for TEA. This discrepancy may be the result of crystallinity effects which will be mentioned later.

An enhancement in the yield of (e^-) by adding a polar substance (TEA or MTHF) was a general effect for several hydrocarbon glasses

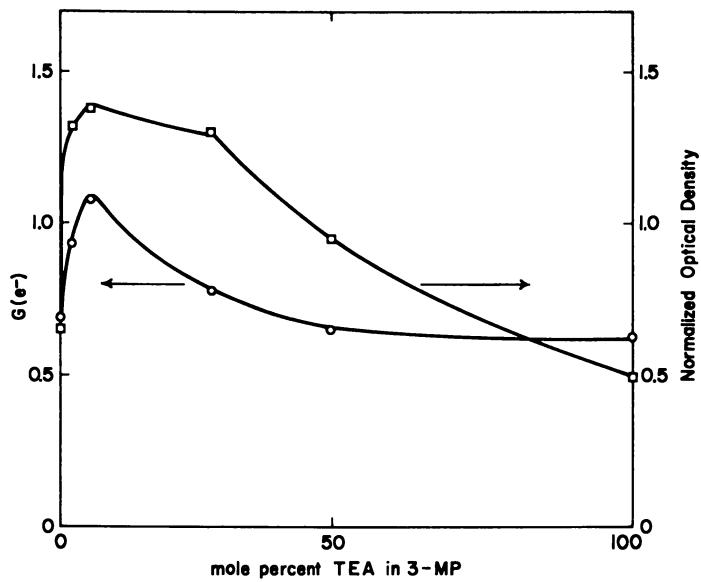

Figure 3. $G(e^-)$ vs. *mole % triethylamine in 3-methylpentane Symbols:* ○, *by ESR spectroscopy;* □, *optical densities normalized to the* G *value for 3-MP* (see *text*)

Publication Date: January 1, 1968 | doi: 10.1021/ba-1968-0082.ch017

even where there was no significant thermal decay of (e^-) at 77°K. A summary of the pertinent yields is given in Table I. Hence, these results provide further evidence that this "polarity effect" is not simply a consequence of arresting a thermal decay of some electron population which disappears too rapidly to be measurable in the hydrocarbon alone. An interesting fact is that the magnitude of this polarity effect varies from one hydrocarbon to another; the largest increase is observed for methylcyclohexane where the yield for the pure hydrocarbon is low, whereas the effect is much smaller for 3-methylhexane, which has the highest value of $G(e^-)$ for any pure hydrocarbon glass examined in our studies (*14*).

Publication Date: January 1, 1968 | doi: 10.1021/ba-1968-0082.ch017

Table I. G Values (100 e.v. yields) of Trapped Electrons in γ-Irradiated Organic Glasses at 77°K.

Glass	*ESR*[a] G(e^-)	*Optical*[b] G(e^-)
3-MP (3-methylpentane)	0.69[c]	0.65[d]
5% TEA (triethylamine) in 3-MP	1.08[c]	1.38
3-MP[k]	0.59[c]	
TEA	0.63	0.58[c]
TEA[k]	0.54	
MTHF (methyltetrahydrofuran)	2.6[f]	2.6
MCH (methylcyclohexane)	0.38	0.30[c]
5% TMA (trimethylamine) in MCH	0.88	
5% TEA in MCH		0.98
7% MTHF in MCH	1.33	
3-MHX (3-methylhexane)	0.87	0.89
3-MHX[g]	0.54	
5% TEA in 3-MHX	0.95	0.96
3-MHP (3-methylheptane)	0.68	0.58[c]
5% TEA in 3-MHP	0.81	0.62

[a] Reproducibility of ESR data is ± 10%.
[b] Optical determinations are all based on $\epsilon(e^-) = 3 \times 10^4 M^{-1}$ cm.$^{-1}$ at λ_{max} (*8*), except for MTHF (*4*, *18*).
[c] At 71°K. by helium bubbling (*see* text).
[d] Extrapolated for decay at 77°K.
[e] In cells of ≃ 2 mm. path length.
[f] Value taken as a standard for the ESR determinations (*21*).
[g] Sample (1 ml.) from Chemical Samples Co., Columbus, Ohio.
[k] Polycrystalline in part (opaque).

Among the factors which influence the yield of trapped electrons, any partial crystallinity in the glassy sample appears to exert a significant effect. Some compounds such as methylcyclohexane and TEA crystallize readily, and in these cases, clear glasses for optical work could be obtained only by shock cooling in thin cells (path length ≃ 2 mm.). In

larger cells, a clear glass would often be formed initially only to "crack" on further standing, rendering the sample unsuitable for optical work. On occasion, a 3-MP glass cooled in an ESR tube from 77° to 71°K. underwent partial crystallization and became opaque, and the yield on subsequent γ-irradiation was invariably smaller, although the decay rate was actually less than that for a glassy sample where measured at the same temperature. A lower $G(e^-)$ yield was also observed for semi-crystalline TEA compared with that obtained for a glassy sample (Table I), according to the ESR method. A similar result was obtained by Tsujikawa *et al.* (*25*). One related observation on TEA was made fortuitously during optical studies. A clear glass was formed in a 3.1-mm. cell and γ-irradiated to a total dose of 7×10^{18} e.v. gram^{-1}; after an optical density of 0.40 had been measured at 1600 n.m., the sample crystallized spontaneously on standing in the optical Dewar, and the corresponding optical density was then reduced to 0.32. This final value was obtained by difference after bleaching, whereas the initial value before crystallization was obtained by subtraction of the spectrum of the blank unirradiated sample. Since the optical density of the crystallized material would presumably have been considerably less than 0.32 in the absence of scattering by the crystals, it appears as if the process of crystallization causes some of the trapped electrons to disappear.

At least some of the above effects observed in the γ-irradiation studies have their counterparts in the photoionization work. A particularly striking demonstration is provided by the effect of added amine on the photolysis of TMPD in isopentane. No trapped electron can be observed in this hydrocarbon matrix alone either after γ-irradiation or even during the steady state of TMPD photoionization at 77°K. On the other hand, when 7% TEA was present in the matrix, the ESR signal of (e^-) could be detected during photoionization (Figure 4), although the decay of the signal after ultraviolet irradiation was extremely rapid ($t_{1/2} \simeq 5$ sec.). Isopentane is a very soft glass with a viscosity at 77°K. close to 10^6 poise (*15*), and it is remarkable that the presence of the amine stabilizes (e^-) sufficiently to permit direct observation. In the more rigid 3-MP glass which has a viscosity approaching 10^{12} poise (*15*), the effect of added amine was not so marked on the strong steady-state ESR signal of (e^-) set up during photoionization. This photodynamic equilibrium (*10, 13*) is not affected by thermal decay under these conditions. However, the rate of thermal decay after photoionization was profoundly affected by the composition of the matrix as shown in Figure 5, and obviously the effect of amine is quite similar to that observed after γ-irradiation, as revealed in Figures 1 and 2.

Effects resulting from partial crystallinity in the specimen were again comparable with the findings in the γ-ray work. Thus, the signal intensity

Publication Date: January 1, 1968 | doi: 10.1021/ba-1968-0082.ch017

in the steady state was reduced, and the subsequent thermal decay rate was slower for semicrystalline TEA than for a glassy sample examined under the same photoionization conditions.

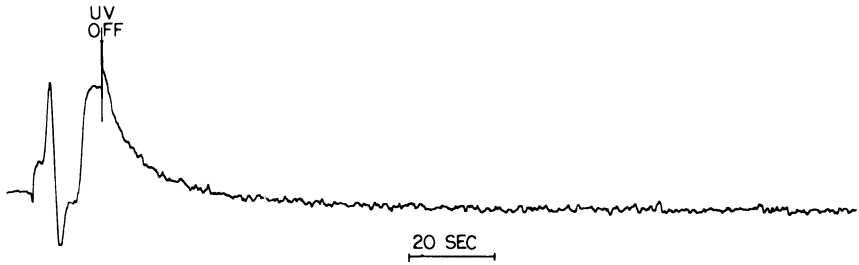

Figure 4. Photograph of recorder trace showing decay of ESR signal after ultraviolet irradiation at 77°K. of isopentane glass containing 7 mole % TEA and 0.02 mole % TMPD. The experimental technique used to obtain the trace has been described in Ref. 14

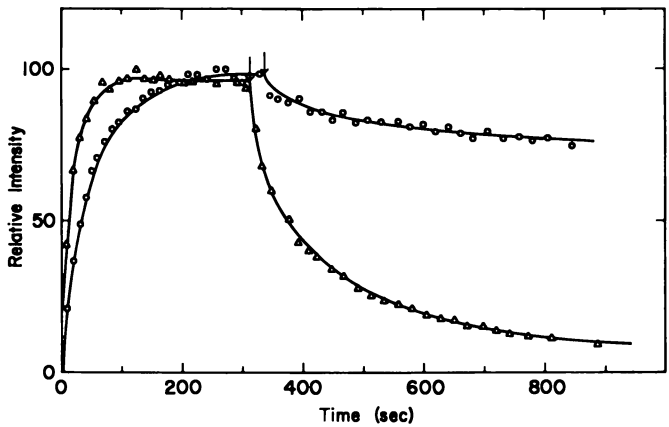

Figure 5. Growth and decay of ESR signal at 77°K. caused by (e^-) *induced by ultraviolet irradiation of 3-MP* (△) *and 3-MP-5 mole % trimethylamine* (○), *each containing 0.02 mole % TMPD. Arrows represent the time when the ultraviolet light was turned off*

Methyltetrahydrofuran–Acetonitrile (MTHF–CH_3CN) Glasses. The effects of γ-radiation and the subsequent photochemical changes have been investigated primarily by ESR spectroscopy. Most of the results relate to the γ-irradiation of clear glasses containing up to 25 mole % CH_3CN in MTHF. The samples were irradiated in the dark at 77°K. and then optically bleached inside the ESR cavity. The light from a

Publication Date: January 1, 1968 | doi: 10.1021/ba-1968-0082.ch017

1-kwatt tungsten lamp was focused by a lens arrangement and passed through filters. In the majority of studies, either Corning filter No. 4305 (passband 340-600 n.m.) or No. 2030 ($\lambda > 600$ n.m.) was used. In addition to the γ-irradiation studies, some complementary photoionization experiments are reported.

A typical experiment is illustrated by the ESR spectra in Figure 6. Spectrum A, taken immediately after γ-irradiation, shows a prominent singlet caused by the trapped electron and an underlying seven-line spectrum which has been attributed to the paramagnetic species formed

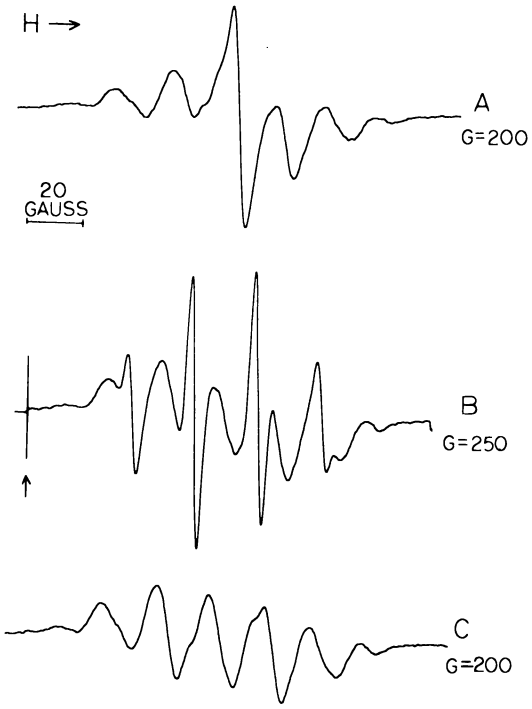

Figure 6. ESR spectra for sample containing 20 mole % acetonitrile in methyltetrahydrofuran after γ-irradiation for 28 minutes at a dose rate of 2.9×10^{17} e.v. gram^{-1} min.$^{-1}$. Sample at 77°K. during and after irradiation. A: After gamma irradiation. B: Immediately after bleaching with 1 kwatt W lamp using Corning filter No. 2030. Arrow represents time when lamp was turned on. Scan rate was 100 gauss per minute, response time 0.3 sec. C: Spectrum 27 minutes after start of photobleaching. Microwave power is 0.01 mwatt in each case

Publication Date: January 1, 1968 | doi: 10.1021/ba-1968-0082.ch017

from MTHF (*21*). The relative intensity of the singlet was reduced compared with the spectrum obtained from the irradiation of pure MTHF, but otherwise there was no recognizable difference between the two spectra. However, when the sample was bleached with visible or red light, the quartet spectrum of the methyl radical appeared very clearly, as shown in Spectrum B. After the methyl radicals had been allowed to decay out thermally at 77°K., only the underlying spectrum of the MTHF radical remained (Spectrum C). These experiments were repeated for a range of samples containing up to 40 mole % acetonitrile. Above 25 mole % CH_3CN, the shock-cooled samples were occasionally polycrystalline, but only glassy samples were used for irradiation studies.

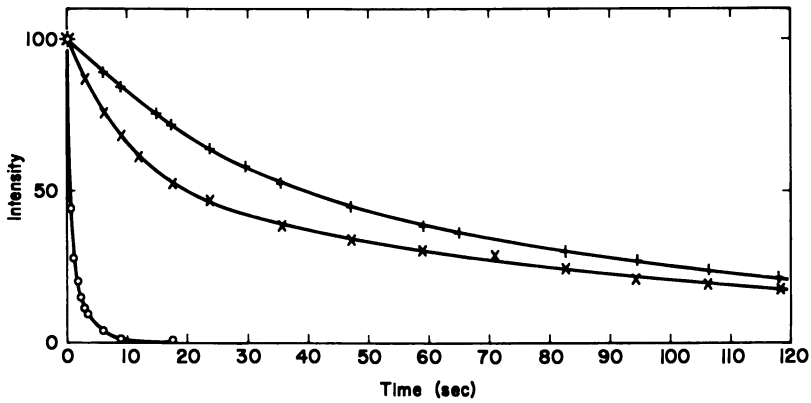

Figure 7. Decay of ESR signal of (e^-) *at 77°K. during photobleaching with 1-kwatt W lamp using Corning filter No. 2030* (λ *>640 n.m.). Symbols: +, Photoionized methyltetrahydrofuran containing 0.02 mole % TMPD. ×, γ-Irradiated methyltetrahydrofuran, dose 8.9 × 10¹⁸ e.v. gram⁻¹. ○, γ-Irradiated methyltetrahydrofuran containing 10 mole % acetonitrile, dose 8.9 × 10¹⁸ e.v. gram⁻¹. Intensity scale represents the percentage of the original signal in each case. Magnitudes of original signal were in the ratio +, 1.0; ×, 2.4; and ○, 1.0. Individual curves obtained in a manner* [cf. (14)] *similar to Figure 4; points used to normalize the curves*

Kinetic studies were carried out to obtain further information about the nature of the bleaching reaction. The decay of the trapped electron singlet under standard bleaching conditions became more rapid as the concentration of CH_3CN was increased in the γ-irradiated sample until at 10 mole % CH_3CN, $t_{1/2}$ was reduced to 0.03 of the value obtained for pure MTHF. Two of the decay curves given in Figure 7 further illustrate this point. At CH_3CN concentrations greater than 5 mole %, both the decrease in the electron singlet and the appearance of the methyl radical

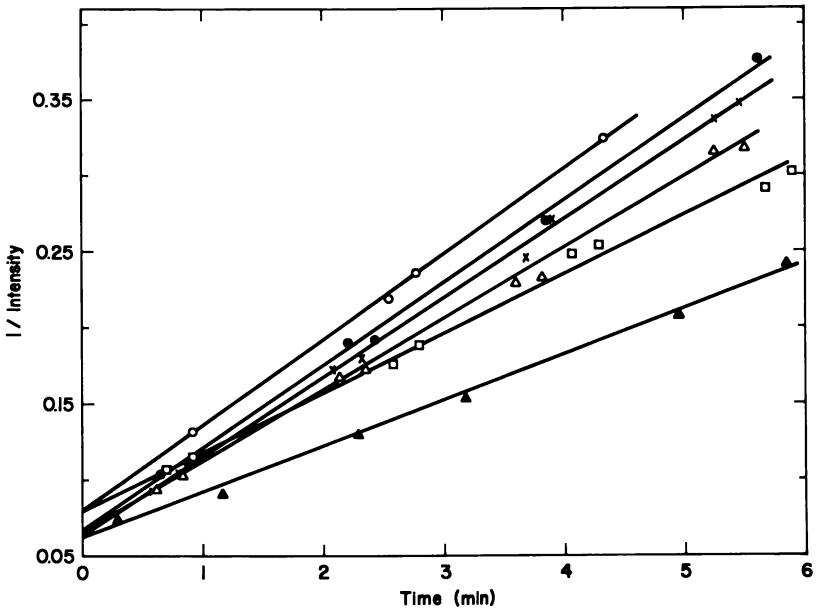

Figure 8. Second-order plots showing reciprocal of signal intensity caused by methyl radicals vs. *time after start of photobleaching following γ-irradiation at 77°K. to a dose of 8.9 × 10¹⁸ e.v. gram⁻¹. Composition in mole % CH_3CN in MTHF:* ○, *6;* ●, *10;* ×, *15.1;* △, *19.9;* ▲, *35.7;* □, *40.1. Intensity scale (in arbitrary units) refers to ESR measurements uncorrected for variation in spectrometer sensitivity in order of increasing CH_3CN concentration: 1, 0.91, 0.91, 0.91, 1.11, 1.67*

spectrum occurred rapidly and simultaneously under our experimental conditions. The subsequent thermal decay of the methyl radicals fitted second-order kinetics (Figure 8), and this decay was unaffected by continued irradiation with the light used for photobleaching. This result was demonstrated in cases where the methyl radicals were formed almost instantaneously in the photobleaching reaction. For a glass containing 2 mole % CH_3CN in MTHF, the bleaching of the ESR signal caused by the trapped electron was only slightly faster than in pure MTHF, and there was enough time in this case to follow the decay of (e^-) as well as the growth of the $CH_3\cdot$ signal through a maximum. The results are presented in Figure 9, and the time dependence of the $CH_3\cdot$ intensity is characteristic of an intermediate in consecutive reactions.

At 10 mole % CH_3CN in MTHF, the γ-irradiated samples showed virtually no difference either in the rate of production or in the total "initial" intensity of the $CH_3\cdot$ radicals generated as a result of changing the wavelength of the bleaching light from the visible (340–600 n.m.) to the red ($\lambda > 600$ n.m.) end of the spectrum. A 1-kwatt tungsten lamp

Publication Date: January 1, 1968 | doi: 10.1021/ba-1968-0082.ch017

served as the source in each case. In a blank experiment, there was no $CH_3\cdot$ radical production on illuminating a typical sample (15 mole % CH_3CN) which had not been preirradiated in the γ-ray source.

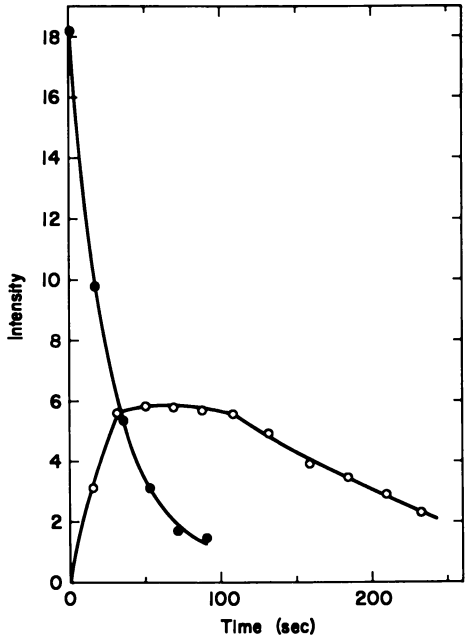

Figure 9. ESR signal intensities of methyl radicals, ○, and (e^-), ●, vs. time during photobleaching of glass at 77°K. containing 2.1 mole % CH_3CN in MTHF previously γ-irradiated to a dose of 8.9×10^{18} e.v. gram^{-1}. Intensity scale proportional to the concentration for each species

The concentration dependence of the results is shown in Figure 10. The intensity of the electron singlet measured before bleaching declines with increasing CH_3CN concentration in the glass until a shallow minimum is reached at about 25 mole %. Actually, it is questionable whether the singlet spectrum at high CH_3CN concentration is in fact the same species as (e^-) in the dilute solutions because the microwave saturation behavior was not completely identical in the two cases. Therefore, some reservation must be used in considering these results at high ($>$ 25 mole %) CH_3CN concentration. The "initial" methyl radical intensities produced on bleaching were computed from the extrapolated values of the second-order kinetic plots (Figure 8). Signal intensities have been

Publication Date: January 1, 1968 | doi: 10.1021/ba-1968-0082.ch017

plotted on the same scale in Figure 10 by assuming that the proportionality constant K in the intensity expression KW^2H is the same for the (e^-) singlet as for each of the lines in the methyl quartet. In the above expression, W is the line-width and H is the height or peak-to-peak amplitude of the signal. The total $CH_3\cdot$ intensity was obtained by adding the contributions from the four lines.

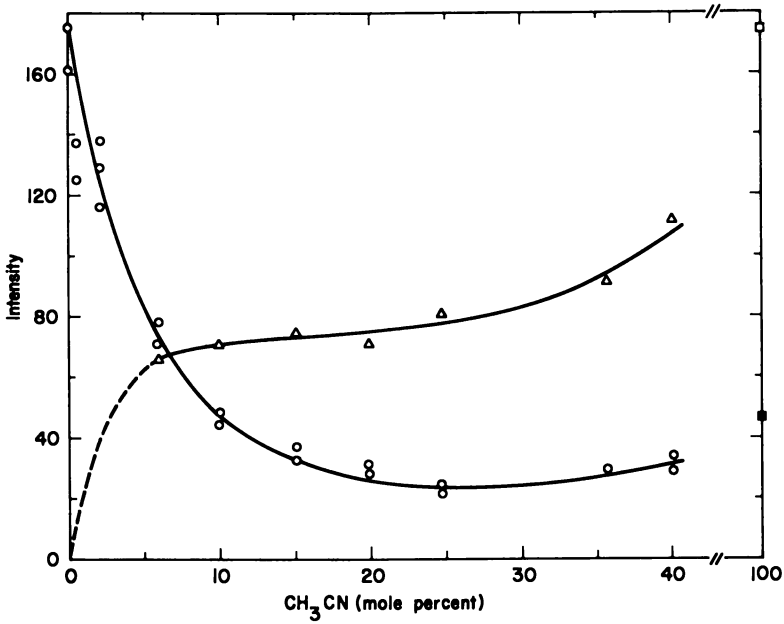

Figure 10. ESR signal intensities of initial (e^-), ○, *and photoinduced methyl radicals,* △, *produced in* γ*-irradiated* CH_3CN*–MTHF mixtures (dose* 8.9×10^{18} *e.v. gram*$^{-1}$*) at 77°K. Intensity scale proportional to concentration for each species. Intensity of methyl radicals produced from* γ*-irradiation at 77°K. of pure (polycrystalline)* CH_3CN *(dose* 8.9×10^{18} *e.v. gram*$^{-1}$*) before* ■, *and after* □, *photobleaching under the same conditions*

Also included in Figure 10 are the results for $CH_3\cdot$ production from a γ-irradiated sample of pure (polycrystalline) CH_3CN before and after bleaching. The plateau value of the $CH_3\cdot$ intensity reached in Figure 9 falls reasonably close to the broken line used in Figure 10 to represent the $CH_3\cdot$ radical intensity attained in dilute CH_3CN solutions.

Independent evidence for the decrease in (e^-) yield with added CH_3CN was obtained by a parallel optical experiment. For 6 mole % CH_3CN in MTHF, the optical density at λ_{max} for (e^-) was reduced to 26% of the value obtained for pure MTHF. This should be compared with a reduction to 42% in the ESR singlet intensity at this concentration

Publication Date: January 1, 1968 | doi: 10.1021/ba-1968-0082.ch017

(Figure 10). If the minimum value reached in the ESR intensity curve of (e^-) at high CH_3CN concentration can be regarded as a measure of some other paramagnetic species, this would help to explain the quantitative difference between these ESR and optical results.

In contrast to the results obtained by the optical bleaching of γ-irradiated samples, thermal bleaching of two samples containing 2.1 and 6 mole % did not produce any $CH_3\cdot$ radicals during the warmup. In each case the electron singlet decayed out completely at about 95°K., and the radical spectrum disappeared at 97°K.

Competitive experiments were carried out with *tert*-butyl bromide, a known electron scavenger (*3, 20*). The presence of 1.4 mole % $(CH_3)_3CBr$ in a mixture of 15 mole % CH_3CN in MTHF prevented the production of the singlet by γ-irradiation, and the 10-line spectrum of the $(CH_3)_3C\cdot$ radical was clearly visible at medium power (0.4 mwatt). Spectrum A, at low power (0.01 mwatt) immediately after irradiation, is shown in Figure 11, and while only eight of the 10 lines caused by $(CH_3)_3C\cdot$ can be seen in this case, this spectrum shows clearly that there is no evidence for a strong center line corresponding to (e^-). However, when this sample was bleached with visible light (340–600 n.m.), there was a small but significant increase in the intensity of the four center lines (Spectrum B) indicating the formation of some $CH_3\cdot$

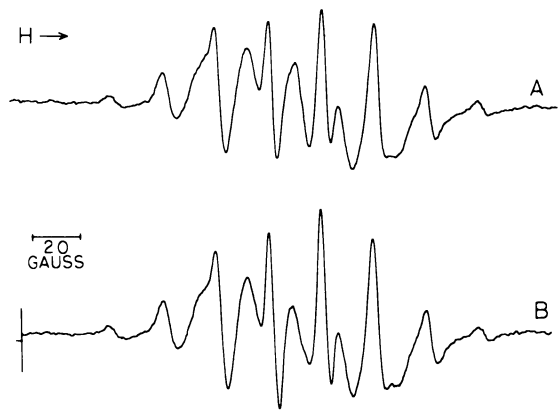

Figure 11. ESR spectra of γ-irradiated sample containing 1.4 mole % $(CH_3)_3$ CBr and 15 mole % CH_3CN in MTHF (dose 8.9 × 10^{18} e.v. $gram^{-1}$). A: after γ-irradiation. B: after photobleaching with 1-kwatt W lamp using Corning Filter No. 2030 (λ >640 n.m.). Vertical line (left) represents point at which the lamp was turned on. Scan rate 100 gauss per minute. γ-Irradiation and subsequent ESR measurements at 77°K. Microwave power 0.01 mwatt

radicals under these conditions. This contribution decayed out on standing in the dark at 77°K., and the spectrum reverted to the one obtained before illumination (A). It was estimated that the $CH_3\cdot$ radical production in this experiment was only 10% of the yield obtained in a corresponding experiment without *tert*-butyl bromide.

When we used glasses containing 6 and 20 mole % CD_3CN in MTHF, there was no $CD_3\cdot$ production on bleaching a γ-irradiated sample under any of the conditions which applied successfully for CH_3CN. Despite this nonappearance of $CD_3\cdot$, the γ-induced singlet disappeared readily on bleaching in a manner similar to that already described for the CH_3CN mixtures. We have also observed considerable differences in the postirradiation behavior of γ-irradiated CH_3CN (*1*) and CD_3CN in the crystalline state; this will be taken up in a separate report.

A number of photoionization experiments were also performed. As shown by the ESR spectrum in Figure 12, methyl radicals were produced during the photoionization of TMPD in a CH_3CN–MTHF glass, and no trapped electron was observed, in contrast to the result obtained with pure MTHF (*12*). Therefore, the presence of the CH_3CN in the matrix causes the electron to react and form $CH_3\cdot$ radicals in the steady-state photoionization. This conclusion was confirmed by another experiment in which 1.6 mole % *tert*-butyl bromide was added to 15 mole % CH_3CN in MTHF containing TMPD. Photoionization of this glass produced only the recognizable 10-line spectrum of $(CH_3)_3C\cdot$ radicals, as expected for electron capture by the halide. It appears, therefore, as though the *tert*-butyl bromide competes efficiently with the acetonitrile for the electrons under these conditions.

Again the behavior of a 15-mole % CD_3CN glass did not follow that of CH_3CN. A weak signal which might be caused by a trapped electron was observed in the CD_3CN–MTHF matrix during photoionization, and $CD_3\cdot$ radicals were not identified in this case, although a

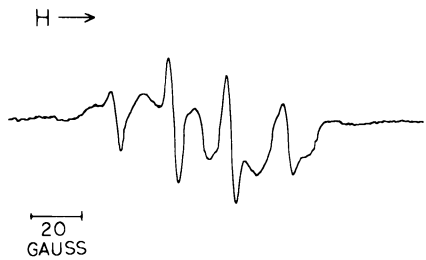

Figure 12. ESR spectrum during photoionization of sample containing 15 mole % CH_3CN and 0.02 mole % TMPD in MTHF at 77°K.

Publication Date: January 1, 1968 | doi: 10.1021/ba-1968-0082.ch017

more complex ESR spectrum was produced. Blank experiments without TMPD were always carried out to verify that the observed effects in the various systems were genuinely associated with photoionization.

Finally, we wish to draw attention to the comparison in Figure 7 between the optical bleaching rates of (e^-) in γ-irradiated MTHF and in the photoionized MTHF–TMPD system under the same conditions, using red light ($\lambda > 600$ n.m.). The decay rate is slightly greater for the γ-irradiated MTHF, but this difference is minor compared with the much faster decay which is observed when more than 5 mole % CH_3CN is present in the matrix of the γ-irradiated sample.

Discussion

Polarity and Crystallinity Effects. Our work shows that the presence of polar molecules (amines) in a nonpolar hydrocarbon matrix can cause two distinct effects concerning trapped electrons. First, thermal decay in a soft matrix is retarded by polar additives. This was observed repeatedly for both γ-irradiated and photoionized systems and therefore does not seem to be related to the nature of the cation in the system. The argument for this point of view has been presented previously (*12*), and the more detailed results of this paper are in full agreement with that interpretation. Thus, the effect is logically interpreted as being caused by a decrease in (thermal) electron mobility when polar molecules are embedded in the matrix. In naive terms, one might say that once the electron diffuses (after it has become trapped) to the site of the polar molecule, it is less constrained to move under thermal motion because of the strong charge-dipole interaction. The effect could also be compared in some ways with the familiar asymmetric drag of an ion atmosphere on the motion of ions in solution, except that the "ion atmosphere" in the present case consists of dipolar species which may not be able to move as freely as the electron in diffusive motion. Our concept of the "mobile" electron under thermal activation is essentially that of an electron moving between adjacent traps or cavities (*6*) so that its mean free path is extremely short, and it spends virtually all its time in the solvated or trapped condition. This idea is fundamentally different from the notion (*5*) that the electron can be thermally excited into a conduction band and "hops" relatively large distances between traps. If this were the mechanism, it would require that the amines furnish deeper traps. Yet it is clear that in the TEA–3–MP system, both the optical absorption (λ_{max} constant at 1600 n.m.) and the bleaching behavior (with infrared light) of the solvated electron are unaffected by adding amine.

The second effect is the enhancement of $G(e^-)$ by adding amine to a hydrocarbon matrix. This was first observed by Gallivan and Hamill

Publication Date: January 1, 1968 | doi: 10.1021/ba-1968-0082.ch017

(*9*), and the effect has been confirmed in similar systems by the present study. The former authors attributed this increase in yield to the stabilizing effect of positive charge transfer, and in another communication (*24*), two of us speculated that proton transfer might also be an important factor in permitting the electron to be detected more easily by ESR in γ-irradiated 3-MP when amine is present. In the light of subsequent experiments (*12, 13*) by the TMPD photoionization technique, the suggestion must be withdrawn. This has forced us to re-examine the entire problem. The enhancement effect could well be caused by positive charge (or proton) transfer as Gallivan and Hamill (*8, 9*) suggest if the positive charge transfer is visualized as taking place very rapidly ($< 10^{-13}$ sec.) from the ionized state of the original molecule before the electron-hole pair recombines. For reasons already given, we do not feel that a mechanism of positive charge transfer is generally applicable to explain slow thermal decay in the amine systems once the electron is already trapped; hence, we restrict the meaning of positive charge transfer to the possibility of a very fast process occurring "instantaneously" during ionization.

Another possibility which could explain the enhancement effect is that the electron is trapped preferentially at the site of a polar molecule. Since the electron in a delocalized Rydberg state of the preionized molecule is presumably best represented by a wavefunction, a probability distribution will determine its effective range of interaction with the environment, and in turn this will dictate its eventual fate. Among the general possibilities are capture by an electron scavenger, solvation, or recombination with the positive hole. According to this idea, competition between the two latter events could be determined by the presence of suitably oriented polar molecules (*2*) as well as by the number of pre-existing cavities in the glass. Returning to the experimental facts, it is difficult to understand why small amounts of added amine should increase the number density of pre-existing physical traps. If this were the responsible factor, it would be hard to explain why mixtures of hydrocarbons behave differently, and give yield-composition plots which are concave (negative deviations) rather than convex (positive deviations) to the composition axis (*14*).

It is also necessary to explain the decrease in the yield of (e^-) at the high amine concentrations in the glass. We believe that this effect occurs because of increasing order in the glass. For example, it is much easier to make a crystalline sample of pure TEA than 3-MP at 77°K. Therefore, according to this view, the "crystallinity effect" outweighs the "polarity effect" at high TEA concentrations, and the yield of (e^-) is thereby reduced. Whatever the complete explanation, it is difficult to escape the conclusion that the degree of structural organization in the

Publication Date: January 1, 1968 | doi: 10.1021/ba-1968-0082.ch017

glassy state (*6, 14, 25*) is of particular importance, and that this consideration can modify other effects of a more specific molecular nature.

Reactivity of Electrons. Electron capture by additives during γ-irradiation is well established (*18, 20*). This process occurs efficiently even in rigid glasses such as MTHF, where the trapped electron formed in the absence of additive is thermally stable. Therefore, the electron-capture process cannot occur through the intermediacy of trapped electrons. Rather, the electrons must be captured directly from the delocalized state of the preionized molecule, and the process is electronic and comparatively unaffected by thermal motions. Therefore, the physical mechanism is entirely different from the diffusive reactions of hydrated and solvated electrons in liquids, although the chemical products may sometimes be similar.

In this study we have observed a different type of electron-capture process. Here, the electron does not react chemically with acetonitrile in an MTHF glass during γ-irradiation, although we do not rule out the possibility that some kind of weak physical association takes place. However, when the trapped electron is optically excited after gamma irradiation, a reaction does take place efficiently with the formation of methyl radicals. This can be represented as follows:

$$(e^-) + h\nu \rightarrow e^{-*}$$

$$e^{-*} + CH_3CN \rightarrow CH_3\cdot + CN^-$$

The experimental evidence in support of this interpretation is overwhelming. First, the optical excitation causes the trapped electron to disappear more rapidly when CH_3CN is present in the matrix, and methyl radicals are produced simultaneously. Secondly, the removal of the trapped electron by using a conventional electron scavenger (*tert*-butyl bromide), acting through dissociative capture during γ-irradiation, greatly reduces the subsequent effect of the optical bleaching. Third, methyl radicals are produced during the photoionization of TMPD in an MTHF-CH_3CN matrix, and the stationary-state concentration of trapped electrons is negligible compared with that obtained in the control experiment without CH_3CN. In the case of photoionization, the electrons are being continuously excited out of their traps during irradiation, and the rapid reaction with acetonitrile prevents the accumulation of the (e^-) concentration corresponding to that obtained in the simple photodynamic equilibrium (*13*) indicated below.

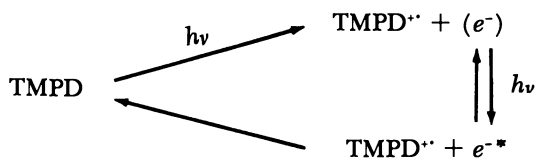

Publication Date: January 1, 1968 | doi: 10.1021/ba-1968-0082.ch017

Finally, the presence of a competitive electron scavenger during photoionization prevents the appearance of methyl radicals.

The distinction we have drawn between the delocalized state of the electron in the preionized molecule and in the excited state produced by optical excitation of (e^-) may be considered a matter of taste although the behavioral difference is real enough. One could argue, for instance, that the reason the electron does not react with CH_3CN during γ-irradiation is because the latter is a poor electron scavenger with a small thermal capture cross section, but that under optical excitation the electron is excited and re-trapped many times so that the cumulative probability for reaction is increased. It must be admitted that the experimental results do not distinguish adequately between these suggestions, although there is one piece of evidence which supports our first proposition. In the experiment with *tert*-butyl bromide and acetonitrile in the MTHF matrix (Figure 11), methyl radicals are formed in preference to *tert*-butyl radicals on bleaching, although the effect of γ-radiation alone clearly favored electron capture by the *tert*-butyl bromide. This observation is difficult to reconcile with any theory which does not distinguish between the state (energy) of the electron in the two cases. It may well be that we are in fact observing a resonance capture process with CH_3CN on optical bleaching since it appears that the reaction does not proceed during γ-irradiation when only thermal electron capture is generally considered to occur.

The failure to observe methyl radicals during the warmup of CH_3CN–MTHF glasses after gamma irradiation is a further indication that "mobile" electrons released by thermal activation may behave differently from "excited" electrons produced by photobleaching. It is imperative that such differences in the chemical reactivity of electrons should be recognized and further explored.

At the higher concentrations of CH_3CN in MTHF, the results are less easy to interpret. There is a seeming lack of parity between the initial concentration of "trapped electrons" and the methyl radicals produced on subsequent bleaching (Figure 10). In the polycrystalline CH_3CN, recent work has shown that an ESR signal attributable to the trapped electron can be observed after γ-irradiation, and methyl radicals are produced both during γ-irradiation and on subsequent optical bleaching. Ayscough *et al.* (*1*) studied this system, and we have confirmed some of their general findings. We have also extended the investigation to cover polycrystalline CD_3CN. In this case the behavior is substantially different from CH_3CN and will be described elsewhere.

A puzzling feature of the present work is the failure of CD_3CN to produce $CD_3\cdot$ radicals on optical bleaching of γ-irradiated glassy systems

Publication Date: January 1, 1968 | doi: 10.1021/ba-1968-0082.ch017

under conditions similar to those which apply for CH_3CN. It is difficult to see why small differences in zero-point energies should affect the course of these bleaching reactions. Further work is needed on various cyanides to determine the generality of dissociative electron capture in these compounds.

Acknowledgment

Part of this work was carried out (by J. L. and F. W.) at the Radiation Laboratory of The University of Notre Dame during the summer of 1967. We thank Milton Burton and many staff members at the Radiation Laboratory for their help, advice, and encouragement. The generous assistance of Robert B. Taylor in some phases of this work, including dosimetry, is much appreciated.

Literature Cited

(1) Ayscough, P. B., Collins, R. G., Kemp, T. J., *J. Phys. Chem.* **70,** 2220 (1966).
(2) Blandamer, M. J., Shields, L., Symons, M. C. R., *J. Chem. Soc.* **1965,** 1127.
(3) Claridge, R. F. C., Willard, J. E., *J. Am. Chem. Soc.* **87,** 4992 (1965).
(4) Dyne, P. J., Miller, O. A., *Can. J. Chem.* **43,** 2696 (1965).
(5) Fowler, J. F., *Proc. Roy. Soc. (London)* **A 236,** 464 (1956).
(6) Funabashi, K., Herley, P. J., Burton, M., *J. Chem. Phys.* **43,** 3939 (1965).
(7) Funabashi, K., Magee, J. L., *J. Chem. Phys.* **45,** 1851 (1966).
(8) Gallivan, J. B., Hamill, W. H., *J. Chem. Phys.* **44,** 1279 (1966).
(9) *Ibid.*, p. 2378.
(10) Johnson, G. E., Albrecht, A. C., *J. Chem. Phys.* **44,** 3162 (1966).
(11) Jortner, J., Rice, S. A., Kestner, N. R., "Modern Quantum Chemistry," Part II, p. 133, Academic Press, New York, 1965.
(12) Lin, J., Tsuji, K., Williams, F., *Chem. Phys. Letters* **1,** 66 (1967).
(13) Lin, J., Tsuji, K., Williams, F., *J. Chem. Phys.* **46,** 4982 (1967).
(14) Lin, J., Tsuji, K., Williams, F., *J. Am. Chem. Soc.* **90,** 2766 (1968).
(15) Lombardi, J. R., Raymonda, J. W., Albrecht, A. C., *J. Chem. Phys.* **40,** 1148 (1964).
(16) Lytle, F. W., Stoner, J. T., *Science* **148,** 1721 (1965).
(17) Onsager, L., "Modern Quantum Chemistry," Part II, p. 123, Academic Press, New York, 1965.
(18) Ronayne, M. R., Guarino, J. P., Hamill, W. H., *J. Am. Chem. Soc.* **84,** 4230 (1962).
(19) Shirom, M., Claridge, R. F. C., Willard, J. E., *J. Chem. Phys.* **47,** 286 (1967).
(20) Skelly, D. W., Hayes, R. G., Hamill, W. H., *J. Chem. Phys.* **43,** 2795 (1965).
(21) Smith, D. R., Pieroni, J. J., *Can. J. Chem.* **43,** 876, 2141 (1965).
(22) *Ibid.*, **45,** 2723 (1967).
(23) Tsuji, K., Yoshida, H., Hayashi, K., *J. Chem. Phys.* **46,** 810 (1967).

(24) Tsuji, K., Williams, F., *J. Am. Chem. Soc.* **89**, 1526 (1967).
(25) Tsujikawa, H., Fueki, K., Kuri, Z., *J. Chem. Phys.* **47**, 256 (1967).

RECEIVED December 26, 1967. Research performed under the auspices of the U. S. Atomic Energy Commission at the Radiation Laboratory of the University of Notre Dame, and under Contract No. AT-(40-1)-2968 at The University of Tennessee. This is AEC Document No. ORO-2968-31.

Publication Date: January 1, 1968 | doi: 10.1021/ba-1968-0082.ch017

Ionic Processes in γ-Irradiated 3-MP Glass

I. KOSA SOMOGYI and J. BALOG

Central Research Institute for Physics, P.O.B. 49, Budapest 114, Hungary

Studies of the electrical conductivity as a function of temperature on gamma-irradiated 3-methylpentane glass are reported. During irradiation steady-state currents of 1.7 $\times$ 10^{-8} and 5.7 $\times$ 10^{-10} amp. have been measured at 290° and 77°K., respectively. The temperature dependence of the conductivity curves during warming reveals three populations of charge carriers which can be freed from traps to the conduction band at 77°, 85°–185° and 200°K. The two thermoluminescence intensity peaks observed at 100° and 163°K. confirm charge migration in these temperature ranges, but no intensity peak appears at 77°K.

Publication Date: January 1, 1968 | doi: 10.1021/ba-1968-0082.ch018

In recent years the investigation of ionic processes has become one of the main efforts in radiation chemistry. The existence of the "blue electrons" predicted by Platzman's theory (*17*) has been confirmed in different irradiated materials, and their properties and reactions have been extensively studied. This progress in our knowledge about the radiation-induced ionic processes arises mainly from the use of pulse radiolysis, flash photolysis, and matrix isolation techniques.

Despite the fact that one of the most characteristic properties of hydrated and solvated electrons is their electric charge, surprisingly few investigations have covered the conductivity of the current induced by the migration of these charges. This applies particularly to simple organic solids, including organic glasses, though the latter are extensively used for the optical identification of ions formed by irradiation.

This is probably caused partly by the fact that no satisfactory theory is available for interpreting the data obtainable from current measurements during and after irradiation, partly by the experimental difficulties involved in using sensitive electrometers and high resistance measuring cells required for the measurements.

The electric current induced in organic liquids by irradiation was studied by Freeman (*7, 8, 9*), Hummel and Allen (*12, 13*), and Gibaud

In Radiation Chemistry; Hart, E.;
Advances in Chemistry; American Chemical Society: Washington, DC, 1968.

(*11*), who measured steady-state current at low applied field. Under these conditions most of the charge carriers recombine before reaching the electrodes, and the measured "free electron" yields are much lower than those obtained by other methods.

Conductivity measurements on irradiated solids (*2, 4, 5*) revealed the similarity of the mechanisms of photo- and radiation-induced conductivity and indicated the importance of the role of traps and recombination centers which may exist at positions of disorder in the liquid or solid structure. Radiation-produced impurities can also act as traps.

Only a few conductivity measurements on organic glasses have been reported. Albrecht *et al.* (*14, 15*) studied the photoconductance of 3-methylpentane (3-MP) while Viseall and Willard (*18*) determined the conductivity of the same compound after γ-irradiation. In an earlier paper (*16*) we reported the observations on the conductivity of irradiated 2-methyltetrahydrofuran. The presence of trapped electrons and ions that can be freed by illumination or thermally can be inferred from the current increase caused by their movements. The temperature dependence of the conductivity in these glasses suggested the occurrence of structural changes and indicated the existence of traps with different depths.

This paper reports measurements of the electrical conductivity and the thermoluminescence of γ-irradiated 3-MP.

Publication Date: January 1, 1968 | doi: 10.1021/ba-1968-0082.ch018

Experimental

3-MP was purified by stirring with concentrated H_2SO_4, followed by several passages through 1.50 meters of freshly activated silica gel, then fractional distillation from P_2O_5. The end product was stored in evacuated ampoules provided with breakseals.

Diphenyl was distilled at 10^{-2} torr, repeatedly recrystallized from high purity ethyl alcohol, and sublimated in high vacuum.

A lead borosilicate cell of about 5 cc. capacity was used. The leads from the two plane-parallel 1-sq. cm. Pt electrodes were coated with glass. The electrode spacing was 1 mm. The dimensions of the cell are shown in Figure 1. Long leadouts were used to reduce as much as possible the conductivity caused by vapor condensation on the wires since the protective effect of the hydrophobic silicone coating proved insufficient at the temperatures used. The background current of the evacuated empty cell was measured as less than 10^{-12} to 10^{-13} amp. and that of the unirradiated sample as less than 10^{-12} amp. at 5×10^3 volts/cm. From about 200°K. up the blank current through the empty cell gradually increased, in some cases up to 10^{-10} amp. at 500 volts. The measured values were corrected for the blank currents. To eliminate the probable changes in resistivity owing to irradiation, the cell was heated to 300°C. in an oven after each measuring cycle (blank with empty cell, unirradiated sample; irradiated sample, blank with irradiated empty cell).

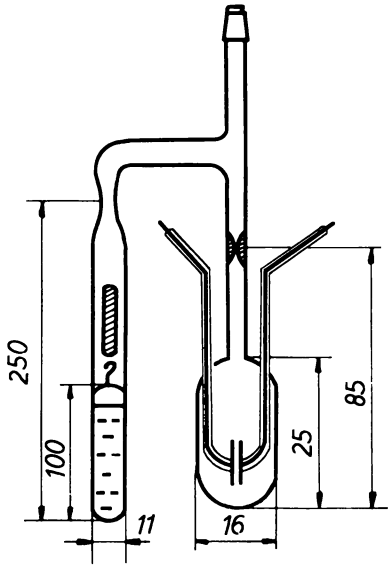

Figure 1. Conductivity cell with sidearm for 3-MP. Dimensions in mm.

The purified 3-MP was distilled into the cell from the sidearm (Figure 1) which was subsequently sealed off, and the system was evacuated by the usual pumping-thawing-freezing technique to a pressure of 10^{-6} torr.

The samples were irradiated in a ^{60}Co gamma source at a dose rate of 0.9×10^{17} e.v./ml. min. The electrical conductivity of the samples was measured either during or after irradiation. In the latter case the conductivity (or the optical) measurements were begun about 1 minute after termination of the irradiation. The samples were protected from the incidence of light when transported from irradiation to measurement.

The circuit consisted of a stabilized voltage supply, KFKI type P-13-1RK, and the conductivity cell that was connected with the electrometer in series. The lower limit of the SEA type 6-ATCC-5 electrometer sensitivity was 10^{-13} amp. The variations in the output current were displayed on a Graphispot, type GR4VAD recorder. The sample was warmed by two different methods, both essentially spontaneous. The sample was either exposed to the surrounding air or left to warm slowly inside of the metal block that was cooled to liquid nitrogen temperature before the measurement. The sample temperature was measured by recording the thermo e.m.f. *vs.* time of an iron constantan thermocouple put in the middle of the opened sample. The temperature was measured to a $\pm 5°$ accuracy.

During the connection of the samples to the electrometer charge loss to grounding was unavoidable. Thus, the current peaks appearing at 77°K. had to be ignored in interpreting the measured data.

Publication Date: January 1, 1968 | doi: 10.1021/ba-1968-0082.ch018

For optical measurements, either a Unicam Sp-700 recording spectrophotometer with low temperature cell holder, or spectrofluorimeter displaying the whole emission spectrum with 1-second repetition frequency was used.

Results

The temperature dependence of the current in a nonirradiated 3-MP sample measured at an applied field of 3×10^4 volts/cm. is shown in Figure 2. Before the increase in slope at about 200°K. in some cases a "negative" (opposite to the direction of the field) current peak is observable. A definite, broad peak that, however, does not exceed 5×10^{-12} amp. also appears in the temperature range 90°–140°K.

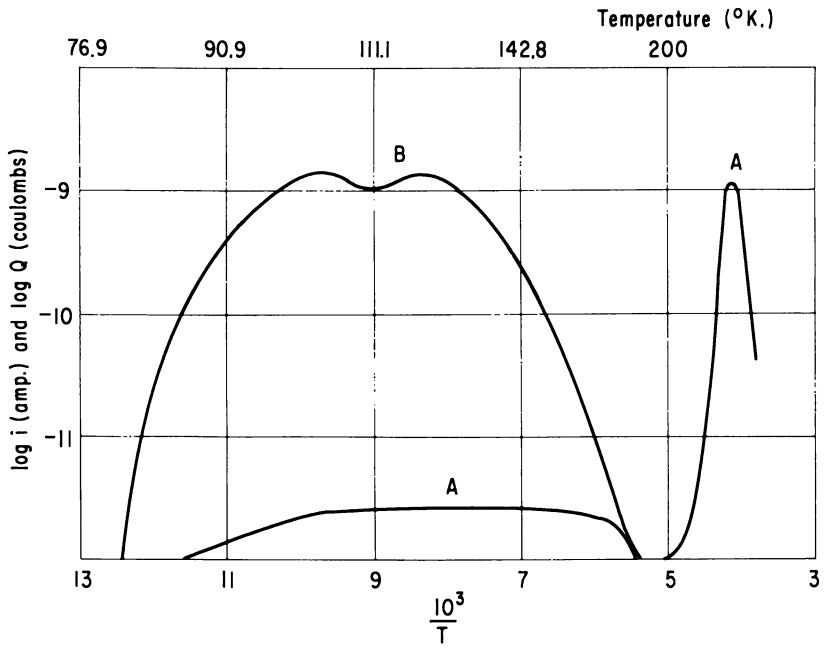

Figure 2. Current vs. sample temperature before irradiation (A) and after irradiation (B) with a dose of 1.6×10^{18} e.v./gram

After irradiation, the current *vs.* temperature curve changes considerably (Figure 2). The current surges accompanying the connection of the cell to the measuring circuit indicate the availability of free charges at 77°K. The decay of currents at 77°K. was studied and described by Viseall *et al.* (*18*).

The main difference in the temperature dependence after irradiation from that before irradiation is the current peak in the range from 85° to 185°K. with a maximum at 110°K. After this peak the current decreases to its blank value and rises again at about 200°K. as for the nonirradiated sample. At higher doses the position of this peak shifts to somewhat higher temperatures and is preceded by a "negative" peak of increasing magnitude as the dose increases.

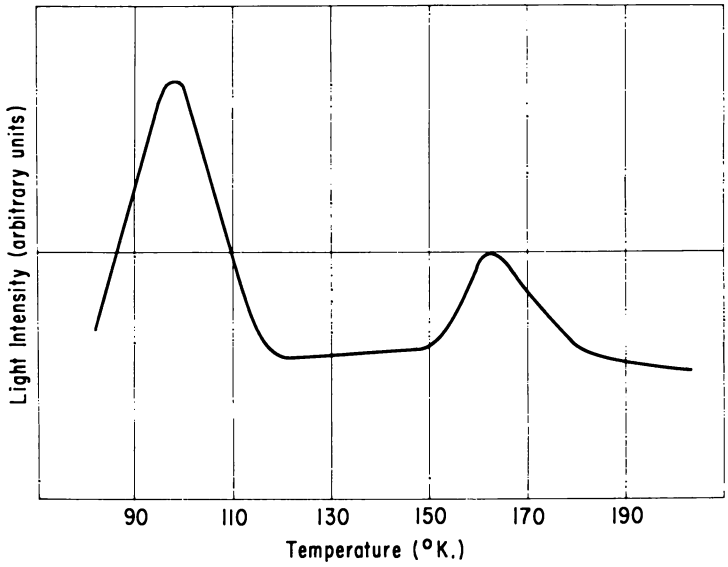

Figure 3. Radiothermoluminescence curves as a function of temperature

To observe the possible effects of molecular movements and structural changes on the resistivity of the sample, thermoluminescence measurements were performed which are known to be very sensitive to these changes (*1, 3*). Figure 3 shows the thermoluminescence curve for 3-MP containing $10^{-4}M$ diphenyl. Two peaks appear—one at about 100°K., the other at 163°K. The spectral distribution of the emitted light (Figure 4) that remains unchanged during the heating period and the decay of the emission show that diphenyl phosphorescence takes place.

On bleaching the irradiated sample with the light from a tungsten lamp, the second current peak between 85° and 180°K. becomes appreciably lower (Figure 5) but does not disappear completely.

Steady-state current values obtained during irradiation in the source are summarized in Table I. Separate measurements show that these values

Publication Date: January 1, 1968 | doi: 10.1021/ba-1968-0082.ch018

contain a contribution from the ionization of the surrounding air which, however, does not induce any appreciable error. The steady-state current was recorded during the spontaneous warming of the sample while in the gamma source. The value of the current changes smoothly from that measured at 77°K. to that obtained at room temperature; thus it does not follow the behavior pattern of the conductivity after irradiation.

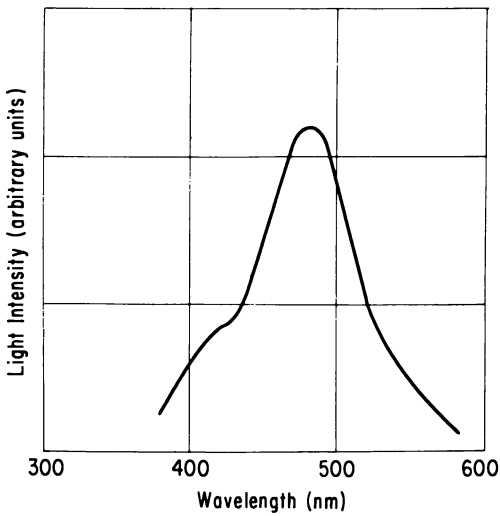

Figure 4. Luminescence spectrum of gamma-irradiated 3-MP glass containing 10^{-4}M diphenyl

There were no detectable changes in the absorption spectra of 3-MP after an absorbed dose of 3×10^{18} e.v./gram. A sample with a dose of 4×10^{20} e.v./gram showed two small peaks, at 322 and 555 mμ, but the peak in the near infrared (*10*) was not detected in our samples even at this high dose.

Discussion

The thermoluminescence curve suggests that two different kinds of charges are migrating while the sample is left to warm, provided the light emission is caused mainly by the recombination of charged particles. Earlier conductivity data (*6*) obtained on irradiated frozen hydrocarbons as well as the results of ESR and optical measurements indicate that the first entities freed from traps in the temperature range 77°–115°K. with small volume expansion are electrons, while the second peak above 200°K. is caused by ions needing more space for their migration.

Publication Date: January 1, 1968 | doi: 10.1021/ba-1968-0082.ch018

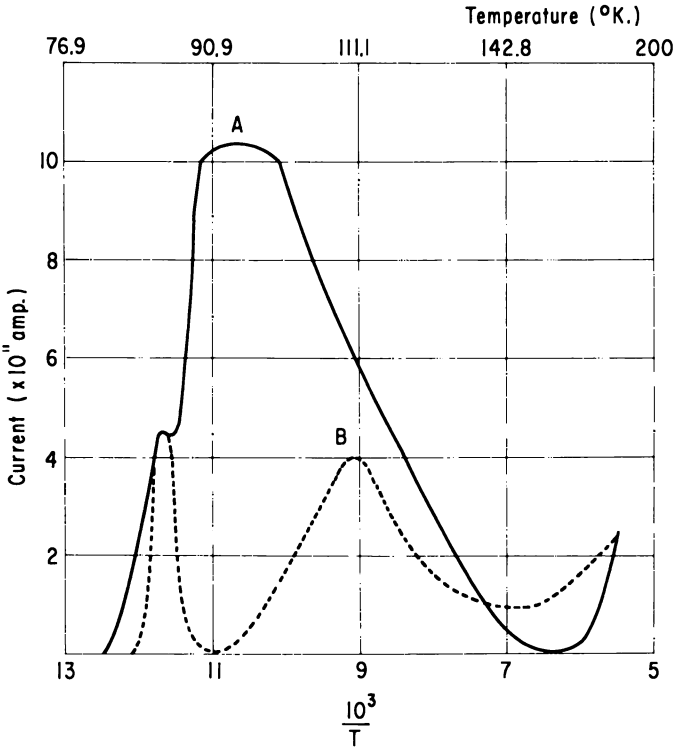

Figure 5. Current vs. *temperature curves for gamma-irradiated sample; dose = 10^{18} e.v./ml. (Curve A). Curve B, taken under the same conditions plus 10 minutes bleaching at 77°K. with the unfiltered light of a 100 watt tungsten lamp*

Table I. Steady-State Currents in Irradiated 3-MP at Different Temperatures[a]

Temperature, °K.	*Current, amp.*
290	1.74×10^{-8}
	1.68×10^{-8}
320	2.00×10^{-8}
77	5.72×10^{-10}
	5.72×10^{-10}
	5.95×10^{-10}

[a] Dose rate = 0.9×10^{17} e.v./ml. min. Voltage = 300 volts. The values of the current at the same temperature were measured on the same sample that was cooled down several times to 77°K. after warming to room temperature.

Publication Date: January 1, 1968 | doi: 10.1021/ba-1968-0082.ch018

There seems to be good agreement between the above picture and the temperature profile of the current. Accordingly, the first row of trapped electrons seems to be liberated at 85°K., ignoring, of course the electrons causing current surges at 77°K. The current caused by the movements of the released electrons has a maximum at about 115°K., then decreases to the value of the dark current to which it becomes equal at 185°K. This means that the freed electrons can be raised to the conduction band by rearranging the glass structure needing only a very small activation energy.

The summing of the charges under the electron peak permits one to evaluate the "virtual" electron yield $G(e)$ if the absorbed dose is known. The "virtual" value may be substantially different from the true radiation-chemical yield since a major fraction of the free electrons is lost by recombination during their migration and thus does not contribute to the current. The electron peak of a sample irradiated at 77°K. by a dose of 1.6 to 10^8 e.v./gram was caused by the passage of 6.5×10^{-9} coulomb charges—*i.e.*, the virtual $G(e) = 2.5 \times 10^{-5}$ electrons/100 e.v. Thus, the number of charges so small that 1 in 10^4 of the molecules in the monolayer adjacent to the electrodes would be able to produce them if they had any charge.

Conductivity measurements on solids after irradiation do not seem to yield sufficient information for evaluating the radiation chemical electron yield since the number of the radiation-produced charge carriers cannot be determined by this method alone. The conductivity data are, however, useful for identifying these charge carriers, and they permit determination of the temperature range at which the charge carriers react and the rate constants of their reactions. The temperature behavior of the conductivity can be related to the structural changes expected to occur.

Investigation must be continued for a better understanding of the mechanism of the radiation-induced electronic movements.

Literature Cited

(1) Bagdassarian, Kh. S., Milutinskaya, R. I., Kovalev, Yu. V., *High Energy Chemistry* (in Russian) **1**, 127 (1967).
(2) Bube, R. H., "Photoconductivity of Solids," p. 120, Wiley, New York, 1960.
(3) Buben, N. Ya., Goldanskii, V. I., *Dokl. Akad. Nauk. USSR* **162**, 370 (1965).
(4) Frankevich, E. L., Tal'roze, V. L., *Proc. Symp. Radiation Chem. 2nd, AN USSR Moscow, 1962*, p. 651.
(5) Frankevich, E. L., Tal'roze, V. L., *Solid State Phys.* **3**, 180 (1961).
(6) Frankevich, E. L., *Uspehi Chim.* **35**, 1161 (1966).
(7) Freeman, G. R., *J. Chem. Phys.* **39**, 988 (1963).
(8) *Ibid.*, p. 1580.

(9) Freeman, G. R., Fayadh, J. M., *J. Chem. Phys.* **43,** 86 (1965).
(10) Gallivan, J. B., Hamill, W. H., *J. Chem. Phys.* **44,** 2378 (1966).
(11) Gibaud, R., *J. Chim. Phys.* **64,** 521 (1967).
(12) Hummel, A., Allen, A. O., *J. Chem. Phys.* **44,** 3426 (1966).
(13) Hummel, A., Allen, A. O., Watson, F. H., *J. Chem. Phys.* **44,** 3431 (1966).
(14) Johnson, G. E., Albrecht, A. C., *J. Chem. Phys.* **44,** 3162 (1966).
(15) *Ibid.*, p. 3179.
(16) Kosa Somogyi, I., "The Chemistry of Ionization and Excitation," p. 116, Taylor & Francis, London, 1967.
(17) Platzman, R. L., *U. S. Natl. Res. Council Publ.* **305,** 34 (1953).
(18) Wiseall, B., Willard, J. E., *J. Chem. Phys.* **46,** 4387 (1967).

RECEIVED January 16, 1968.

19

Radiation Chemistry of *n*-Pentane in the Solid Phase

C. BIENFAIT, J. CEULEMANS, and P. CLAES

Department of Physical Chemistry III, University of Louvain, Schapenstraat, 39, Louvain, Belgium

Publication Date: January 1, 1968 | doi: 10.1021/ba-1968-0082.ch019

n-Pentane was irradiated in the solid phase at 77°K. by ^{60}Co γ-rays to doses ranging from 1 to 12 Mrads. The concentration of dimers was measured by gas-liquid partition chromatography after melting the irradiated sample; the amount of unsaturated hydrocarbons was determined by bromine titration. The yields of these various products are independent of the absorbed dose. The following yield values were measured: G(dimer) = 0.56 molecules/100 e.v., G(trimer) = 0.03 molecules/100 e.v., and G(C=C) = 3.31 double bonds/100 e.v. Dimer production arises from radical and ionic processes. Occurrence of ion-molecule reactions is proposed to explain the formation of trimers. Unsaturated compounds are formed by radical disproportionation or by molecular fragmentation.

The aggregation state is known to exert a great influence on radiation chemistry processes. In the gas phase, active species formed by decomposition of a parent molecule can easily escape recombination. In the liquid phase, diffusion competes with recombination in the cage formed by the surrounding molecules. In the solid phase, diffusion is very limited, and the most probable fate of fragments issued from a parent molecule is recombination.

Smaller and Matheson (*14*) have shown that radicals are trapped in hydrocarbons irradiated at liquid nitrogen temperature. ESR studies point out that these radicals are nearly always formed by C-H bond rupture (*6, 14, 16*), owing to a cage effect—*i.e.*, only hydrogen atoms can diffuse out of the cage in which they are formed. In a few cases only, C-C bond cleavage is observed; for example, *tert*-butyl radicals are

In Radiation Chemistry; Hart, E.;
Advances in Chemistry; American Chemical Society: Washington, DC, 1968.

formed in neopentane irradiated at 77°K. (*6, 16*). Then, radicals are generated by detachment of a methyl radical. However, diffusion of heavier hydrocarbon radicals seems not to occur in solid hydrocarbons at 77°K.

Moreover, ESR studies show that when the temperature of the sample is raised, trapped radicals recombine just below a transition point or below the melting point (*2, 13, 15, 16*). When the melting point of the irradiated hydrocarbon is low, the only fate for a trapped radical is recombination with another radical. Indeed, at low temperature, the rate constants of the other reactions are very small. After melting, trapped radicals will be found as dimers, olefins, or parent molecules. This work completes the ESR study of the radiolysis of solid hydrocarbons at low temperature and reports the first results on the radiolysis of *n*-pentane. We studied only heavy and unsaturated products.

Publication Date: January 1, 1968 | doi: 10.1021/ba-1968-0082.ch019

Experimental

Materials. *n*-Pentane was Fluka product, purest grade, 99.98 mole % minimum purity.

Irradiations. The hydrocarbon was degassed by a repeated freeze-pump-thaw cycle, then distilled into borosilicate glass tubes, sealed under vacuum. Each cell contains about 1 gram of *n*-pentane.

Samples were irradiated at the Nuclear Center of Mol with ^{60}Co γ-rays. The dose rate was about 0.5×10^6 rads per hour, and the absorbed doses ranged from 10^6 to 12×10^6 rads. During irradiation, the samples were maintained in a Dewar flask containing liquid nitrogen. After irradiation, the temperature of the samples was raised to ambient temperature.

Fricke dosimeter was used. The energy absorption by liquid nitrogen and the difference between the absorption coefficients of the dosimeter and of the hydrocarbon were taken into account.

Analysis. HEAVY PRODUCTS. High molecular weight hydrocarbons were analyzed by gas-liquid chromatography. A known volume of undecane was added to the irradiated sample as internal standard. The stationary phase was silicone oil on Chromosorb W. The column was 1.50 meters long; its diameter was 3 mm. A flame ionization detector was used.

UNSATURATED PRODUCTS. The irradiated sample was condensed at 77°K. An excess of a standard acid solution of bromate and bromide was added, and the temperature was raised. When the reaction was complete, the mixture was treated with excess iodide. Free iodine was titrated with thiosulfate. A blank analysis was substracted from the measured volume.

Results

Heavy Products. Figure 1a is a chromatogram of the heavy products of the radiolysis of *n*-pentane in the solid phase. Column temperature was 50°C. Small amounts of linear paraffins from C_6 to C_{10} were

added to the same sample. This mixture yielded the chromatogram in Figure 1b. Peaks located between those of the normal hydrocarbons are caused by branched chain products. Identification is performed using a plot of the retention time of various hydrocarbons *vs.* their vapor pressure at the column temperature. This graph allows the calculation of the boiling points of the radiolysis products. These temperatures are then compared with those calculated by the Kenney's formula for various decane structures.

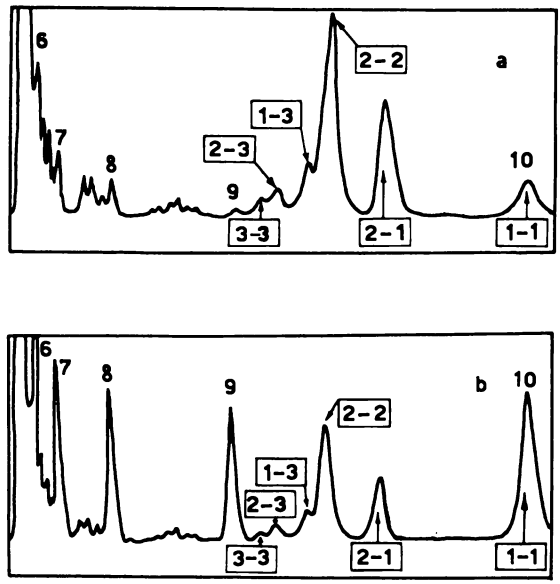

Figure 1. Chromatograms of dimers produced by radiolysis of solid n-*pentane before (a) and after (b) adding small amounts of* n-*hexane(6),* n-*heptane(7),* n-*octane(8),* n-*nonane(9), and* n-*decane(10) to sample. Column temperature, 50°C.; carrier gas flow, 30 cc./min.*

The following dimers could be formed by condensation of two molecules of *n*-pentane:

Dimer 3-3: 3,4-diethylhexane
Dimer 2-3: 3-ethyl-4-methylpentane
Dimer 1-3: 3-ethyloctane
Dimer 2-2: 4,5-dimethyloctane
Dimer 1-2: 4-methylnonane
Dimer 1-1: *n*-decane

Publication Date: January 1, 1968 | doi: 10.1021/ba-1968-0082.ch019

In this sequence, the boiling points and thus the retention times increase from the first compounds to the last. Table I gives the yields of dimers at various doses. These yields are given in dimer molecules/100 e.v. Yields are independent of the absorbed dose. The last line of Table I gives the mean value of the yields measured at the various absorbed doses.

Table I. Dimer Yields

Dose, Mrads	G(3-3)	G(2-3)	G(1-3)	G(2-2)	G(2-1)	G(1-1)
4.2	0.008	0.016	0.012	0.23	0.17	0.11
6.3	0.009	0.020	0.012	0.23	0.17	0.08
8.4	0.010	0.023	0.015	0.28	0.17	0.07
10.5	0.009	0.023	0.018	0.33	0.20	0.08
12.6	0.008	0.016	0.013	0.28	0.17	0.06
Mean value	0.009	0.020	0.014	0.27	0.17	0.08

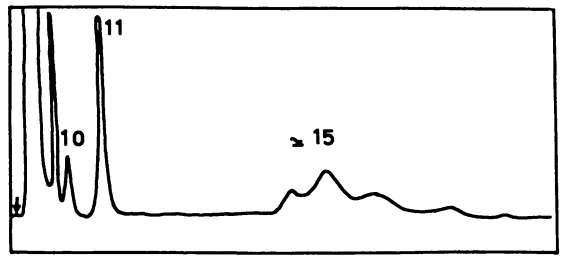

Figure 2. Chromatogram of the high molecular weight products. Column temperature, 140°C.; carrier gas flow, 30 cc./min.

(1) n-*Decane*
(11) n-*Undecane (internal standard)*
(15) Trimers

Figure 1 shows that linear and branched chain products in C_6, C_7, C_8, and C_9 are also formed by the radiolysis. Figure 2 is a chromatogram obtained with the same column at 140°C. It shows a series of peaks with retention times higher than those of dimers. The same identification method was used as for the dimers. Figure 3 is a logarithmic plot giving the retention times of various hydrocarbons *vs.* their vapor pressure at the column temperature. Using this plot, the boiling points of these high molecular weight products can be determined. Those of the most abundant compounds lie between 234 and 240°C. The boiling points of some heavy hydrocarbons are given in Table II. They are calculated using the Kenney's formula. When retention times were available, the corresponding boiling points were determined by using the graph of Figure 3. These

Publication Date: January 1, 1968 | doi: 10.1021/ba-1968-0082.ch019

temperatures are also quoted in Table II (experimental b.p.). When comparison is possible, rather good agreement is observed. In view of these values, it seems reasonable to identify these heavy products as

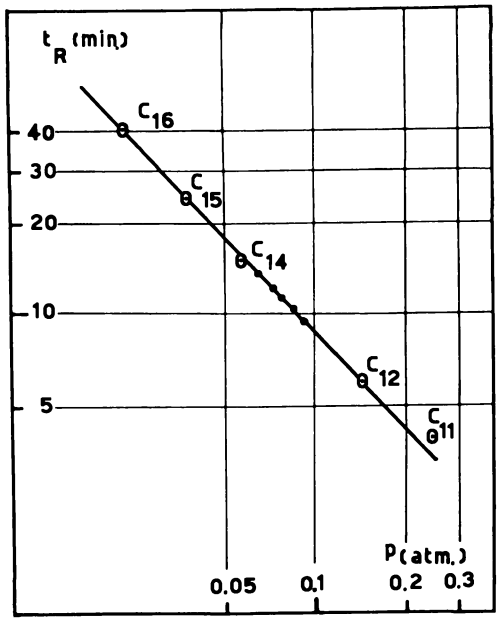

Figure 3. Identification of the high molecular weight fraction. Experimental line obtained by plotting retention times of linear hydrocarbons vs. *their vapor pressure at column temperature (140°C.)*

○ *Calibration products*
● *Retention times of radiolysis products*

Table II. Boiling Points of Some High Molecular Weight Hydrocarbons

Hydrocarbon	*Boiling Point, °C.*	
	Calculated	*Experimental*
6,7-Dimethyldodecane (C_{14})	242	240
n-Tetradecane (C_{14})	252	251
3-Ethyl-4-propyl-4,5-dimethyloctane (C_{15})	234	
4,5,6-Trimethyl-5-propylnonane (C_{15})	239	
4,6-Dimethyl-5,5-diethylnonane (C_{15})	240	
6-Methyl-7-ethyldodecane (C_{15})	255	252
4,5-Dimethyl-5-propyldecane (C_{15})	262	
n-Pentadecane (C_{15})	270	271
6,7-Diethyldodecane (C_{16})	267	264
n-Hexadecane (C_{16})	286	283

Publication Date: January 1, 1968 | doi: 10.1021/ba-1968-0082.ch019

branched chain pentadecanes—*i.e.*, trimers of the irradiated hydrocarbon. The amount of trimer products was determined by planimetry, and a total G(trimer) value of about 0.03 molecules/100 e.v. was found.

Olefins. Figure 4 shows the dependence of the amount of double bonds formed in 1 gram of hydrocarbon upon the absorbed dose. The slope of the line yields a $G(C{=}C)$ value of 3.31 double bonds/100 e.v.

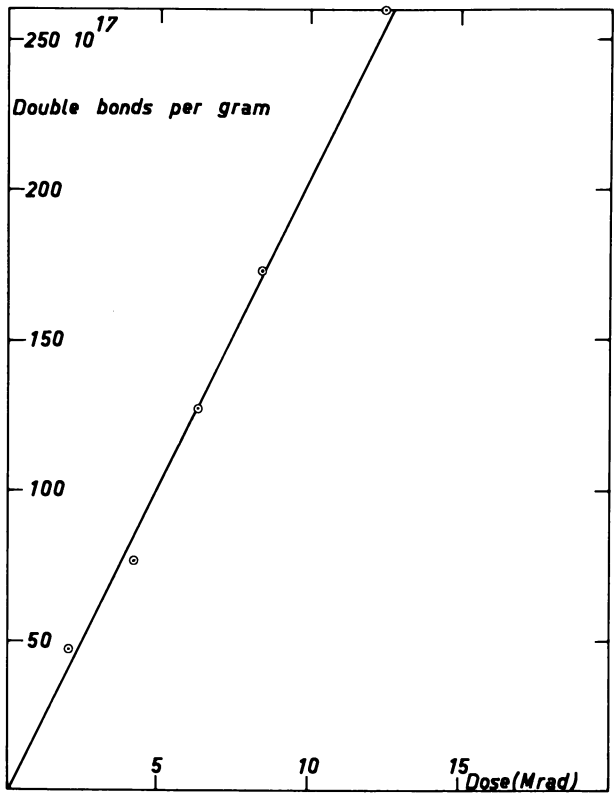

Figure 4. Number of double bonds formed per gram of irradiated sample vs. *absorbed dose*

Discussion

The following sequence of events is generally postulated to occur during the radiolysis of saturated hydrocarbons (7). Radiation first produces ions (Reaction 1) or excited molecules (Reaction 2).

$$C_5H_{12} \xrightarrow{\text{MM}} C_5H_{12}^{+} + e^{-} \quad (1)$$

$$C_5H_{12} \xrightarrow{\text{MM}} C_5H_{12}^{*} \quad (2)$$

Publication Date: January 1, 1968 | doi: 10.1021/ba-1968-0082.ch019

Recombination of the positive ion with the electron leaves a highly activated molecule (Reaction 3).

$$C_5H_{12}^+ + e^- \rightarrow C_5H_{12}^* \quad (3)$$

Excited molecules can revert to their ground state without chemical change (Reaction 4) or by energy transfer to other molecules. This latter process is ineffective for pure hydrocarbons.

$$C_5H_{12}^* \rightarrow C_5H_{12} \quad (4)$$

These excited molecules may decompose directly and form stable molecular fragments (Reaction 5).

$$C_5H_{12}^* \rightarrow C_5H_{10} + H_2 \quad (5)$$

Radicals may also be formed either by C—C (Reaction 6) or by C—H (Reaction 7) bond scission.

$$C_5H_{12}^* \rightarrow C_2H_5^{\cdot} + C_3H_7^{\cdot} \quad (6)$$

$$C_5H_{12}^* \rightarrow C_5H_{11}^{\cdot} + H^{\cdot} \quad (7)$$

ESR results show that in most cases only Reaction 7 occurs in the solid phase; a C—C bond rupture yields fragments that recombine immediately in the cage.

ESR work (*16*) shows that 2-pentyl radicals (CH_3—CH_2—CH_2—$\dot{C}H$—CH_3) are trapped in solid *n*-pentane irradiated at 77°K. Careful examination of the ESR signal indicates that other radicals are produced with much lower yields than 2-pentyl radicals. The measurements do not allow the identification of these minor products. When the temperature of the sample is raised, the ESR signal disappears just below the melting point of the *n*-pentane matrix.

Weiss (*18*), Kevan, Davis, and Libby (*3, 9*) proposed ion-molecule reactions to explain dimer formation. Radical scavenging studies have lead Falconer and Salovey (*4, 5, 12*) to the conclusion that radical reactions produce at least 40% of the dimer. Other authors (*17, 19*) give much more importance to radical processes.

Recombination of the trapped radicals at the melting point necessarily produces dimer molecules by addition (Reaction 8) or pentene molecules by disproportionation (Reaction 9).

$$2\,C_5H_{11}^{\cdot} \rightarrow C_{10}H_{22} \quad (8)$$

$$2\,C_5H_{11}^{\cdot} \rightarrow C_5H_{10} + C_5H_{12} \quad (9)$$

The disproportionation-combination ratio is temperature dependent. For *sec*-butyl radicals, this ratio is 2.3 at 375°K. (*11*) and 11 at 90°K. (*10*). Adopting the same values for pentyl radicals we calculate a ratio of 7.5 at 143°K. (melting point of *n*-pentane) at which recombination occurs.

Publication Date: January 1, 1968 | doi: 10.1021/ba-1968-0082.ch019

If dimers are formed only by combination of pentyl radicals after melting of the sample, then 4,5-dimethyloctane must be characterized by a much higher yield than all other dimers. Indeed, this dimer is formed by combination of 2-pentyl radicals that are found to be the most abundant species in the irradiated solid (*16*). Table I shows effectively that the highest yield is measured for dimer 2-2. High values are also obtained for 1-1 and 1-2 isomers. Table I allows calculation of the individual yields of pentyl radicals if it is assumed that the disproportionation-combination ratio is the same for all pentyl radicals formed in the solid during radiolysis. If k is a constant and if $[R_1^{\cdot}]$, $[R_2^{\cdot}]$, and $[R_3^{\cdot}]$ are the concentrations of 1-, 2-, and 3-pentyl radicals respectively, then:

$$[R_2^{\cdot}] = k\,(G_{12} + 2\,G_{22} + G_{23}) = 0.73\,k$$
$$[R_1^{\cdot}] = k\,(2\,G_{11} + G_{12} + G_{13}) = 0.34\,k$$
$$[R_3^{\cdot}] = k\,(G_{13} + G_{23} + 2\,G_{33}) = 0.052\,k$$

Although 2-pentyl radicals are found to be the major product of the radiolysis, it is surprising to find such a high yield for 1-pentyl radicals. This contrasts with ESR results indicating only traces of paramagnetic species other than 2-pentyl radicals. Production of the corresponding dimers by ways other than combination of trapped radicals would explain this discrepancy. On the other hand, combination prevails over disproportionation for primary radicals (*7*). This would explain that larger amounts of dimers containing radical 1-pentyl would be formed. Our results do not allow selection of one of these explanations; they possibly intervene together.

However, although radical reactions can explain dimerization, they cannot account for the production of trimers. It is possible to explain the formation of polymers in liquid-phase radiolysis by the following sequence. Reaction of a pentyl radical with a pentene molecule would yield a decyl radical (*10*).

$$C_5H_{11}^{\cdot} + C_5H_{10} \rightarrow C_{10}H_{21}^{\cdot} \qquad (10)$$

Combination of a pentyl radical with this dimer radical leaves a trimer molecule (*11*).

$$C_5H_{11}^{\cdot} + C_{10}H_{21}^{\cdot} \rightarrow C_{15}H_{32} \qquad (11)$$

Such mechanisms were proposed to account for radiopolymerization of liquid cyclohexane (*1, 7*). In our case, however, Reaction 10 cannot occur. ESR results show that radical recombination is complete at the melting point of the matrix (143°K.). At such a low temperature Reaction 10 must be negligible, owing to its relatively high activation energy. Indeed, this reaction is characterized by an activation energy of about

Publication Date: January 1, 1968 | doi: 10.1021/ba-1968-0082.ch019

6 kcal./mole (7). On the other hand, radical combination requires negligible activation energy. Kerr and Trotman-Dickenson (8) have measured the rate constant of the addition reaction of *sec*-propyl radials on ethylene; they report a value

$$\log k \text{ (cc./mole-sec.)} = 11.4 - \frac{6.900}{2.303\,RT}$$

With $T = 143°K.$, this equation yields $k_{10} = 8.52$ cc./mole-sec. A value $k_{11} = 10^{13}$ cc./mole-sec. (7) is adopted for the rate constant of the recombination reaction of alkyl radicals.

Let us calculate the rate of both reactions when a sample of solid pentane irradiated at a dose of 10 Mrads is allowed to melt. Assuming the yield of pentyl radicals is twice that of the dimers and using the experimental G values, concentrations of 3.5×10^{-5} mole/gram and of 1.2×10^{-5} mole/gram are found respectively for the olefins and the pentyl radicals. The ratio of the rates of the two reactions is then:

$$\frac{k_{11}[R^{\cdot}]^2}{k_{10}[R^{\cdot}][C{=}]} = \frac{10^{13}\,(1.2 \times 10^{-5})^2}{8.52\,(1.2 \times 10^{-5})(3.5 \times 10^{-5})} = 3.5 \times 10^{11}$$

Reaction of pentyl radicals with olefins may thus be neglected at 143°K.

Furthermore, relatively high yields of light olefins are formed during the radiolysis—*e.g.*, ethylene yield is found to be about 0.60 molecules/100 e.v. If addition of pentyl radicals on olefins was possible, one would find at least traces of dodecane among the radiolysis products. The absence of products with molecular weights intermediate between those of dimers and pentadecanes excludes occurrence of this reaction.

On the other hand, trimer production can be easily explained by the occurrence of the Weiss ion-molecule reaction (*18*). Reaction of a parent ion with a hydrocarbon molecule yields a dimer ion (*12*) which after neutralization leaves an excited decane molecule (Reaction 13). The latter can decompose leaving a decyl radical (Reaction 14) trapped in the matrix.

$$C_5H_{12}^{+} + C_5H_{12} \rightarrow C_{10}H_{22}^{+} + H_2 \quad (12)$$

$$C_{10}H_{22}^{+} + e^{-} \rightarrow C_{10}H_{22}^{*} \quad (13)$$

$$C_{10}H_{22}^{*} \rightarrow C_{10}H_{21}^{\cdot} + H^{\cdot} \quad (14)$$

When the temperature is raised, the decyl radicals react with pentyl radicals yielding pentadecane by combination (Reaction 11), decanes, decenes, pentenes, and pentane by disproportionation (*15, 16*).

$$C_{10}H_{21}^{\cdot} + C_5H_{11}^{\cdot} \rightarrow C_{10}H_{20} + C_5H_{12} \quad (15)$$

$$C_{10}H_{21}^{\cdot} + C_5H_{11}^{\cdot} \rightarrow C_{10}H_{22} + C_5H_{10} \quad (16)$$

These ion-molecule reactions would thus also occur in the formation of

Publication Date: January 1, 1968 | doi: 10.1021/ba-1968-0082.ch019

dimers. The measured yield G(trimer) is small (0.025 molecules/100 e.v.). However, if the disproportionation-combination ratio is sufficient at 143°K., the Weiss ion-molecule reaction could yield a relatively high total $G(C_{10})$ value.

Figure 4 indicates that the yields of olefins produced by radiolysis are independent of the absorbed dose. These unsaturated products are pentene, light hydrocarbons, and eventually decenes produced by Reaction 15. Cage disproportionation of alkyl radicals produced by C—C bond scission and molecular fragmentation account for the formation of light olefins. Pentene would be formed either by elimination of molecular hydrogen (Reaction 5) or by disproportionation of radicals when the temperature of the sample is raised (Reactions 9 and 16). The latter process is thus a postirradiation production of pentene.

The straight line of Figure 4 implies that reactions of unsaturated radiolysis products with active species diffusing in the solid (hydrogen atoms for instance) are not important. This is in agreement with the conclusions of Falconer and Salovey (*4*).

Publication Date: January 1, 1968 | doi: 10.1021/ba-1968-0082.ch019

Conclusion

Dimers and trimers are produced by radiolysis of *n*-pentane in the solid phase. The yields of the various dimers have been measured. These yields suggest a much higher production of 1-pentyl radicals than does the ESR study of these transformations. Occurrence of non-radical processes in dimer production would account for this discrepancy. Trimer production strongly suggests the occurrence of ion-molecule reactions. These reactions would also yield dimers. Dimers would thus be formed by ionic and by radical processes.

Acknowledgments

The authors are indebted to P. Huyskens, Director of the Department. This work received financial assistance from the F.N.R.S. (Fonds National de la Recherche Scientifique de Belgique) and from the F.R.S.F.C. (Fonds de la Recherche Scientifique Fondamentale et Collective).

Literature Cited

(1) Barker, R., Hill, M. J. R., *Nature* **194,** 277 (1962).
(2) Bensasson, R., Durup, M., Dworkin, A., Magat, M., Marx, R., Szwarc, H., *Discussions Faraday Soc.* **36,** 177 (1963).
(3) Davis, D. R., Libby, W. F., *Science* **144,** 991 (1964).
(4) Falconer, W. E., Salovey, R., *J. Chem. Phys.* **44,** 3151 (1966).
(5) Falconer, W. E., Salovey, R., *J. Chem. Phys.* **46,** 387 (1967).

(6) Fessenden, R. W., Schuler, R. H., *J. Chem. Phys.* **33,** 935 (1960).
(7) Hardwick, T. J., *Actions Chim. Biol. Radiations* **10,** 125 (1966).
(8) Kerr, J. A., Trotman-Dickenson, A. F., *Trans. Faraday Soc.* **55,** 921 (1959).
(9) Kevan, L., Libby, W. F., *J. Chem. Phys.* **39,** 1288 (1963).
(10) Klein, R., Scheer, M. D., Kelley, B., *J. Phys. Chem.* **68,** 598 (1964).
(11) Kraus, J. W., Calvert, J. G., *J. Am. Chem. Soc.* **79,** 5921 (1957).
(12) Salovey, R., Falconer, W. E., *J. Phys. Chem.* **70,** 3203 (1966).
(13) Semenov, N. N., *Pure Appl. Chem.* **4,** 353 (1962).
(14) Smaller, B., Matheson, M. S., *J. Chem. Phys.* **23,** 1169 (1958).
(15) Szwarc, H., *J. Chim. Phys.* **39,** 1067 (1962).
(16) Thyrion, F., Dodelet, J. P., Fauquenoit, C., Claes, P., *J. Chim. Phys.* **65,** 227 (1968).
(17) Wagner, C. D., Geymer, D. O., *J. Phys. Chem.* **71,** 1551 (1967).
(18) Weiss, J., *J. Polymer Sci.* **29,** 425 (1958).
(19) Widmer, H., Gaumann, T., *Helv. Chim. Acta* **46,** 944 (1963).

RECEIVED January 2, 1968.

An Electron Spin Resonance Study of Energy Transfer in the γ-Irradiated System Benzene/Silica Gel

OVE EDLUND, PER-OLOF KINELL, ANDERS LUND, and AKIRA SHIMIZU[1]

The Swedish Research Council's Laboratory, Studsvik, Nyköping, Sweden

Publication Date: January 1, 1968 | doi: 10.1021/ba-1968-0082.ch020

Benzene/silica gel has been irradiated at 77°K. with ^{60}Co γ-rays at a dose rate of 300–350 krads/hour. At a low benzene content the monomeric benzene cation is observed, while at higher concentrations the singly charged dimer is predominant. Cyclohexadienyl is formed from hydrogen atoms, radiolytically liberated from surface hydroxyl groups. The ions are created at other sites. At higher temperatures radical reactions occur between benzene and cyclohexadienyl or the positive ion. The dependency of the yields on the dose shows that only a limited number of sites, 7×10^{14} per sq. meter. Brunauer-Emmett-Teller (BET) surface, is available for the oxidation of benzene. Cyclohexadienyl yields do not saturate to the same extent. The magnitude of energy transfer is estimated.

In a previous paper (*14*) a study of the yields of free radicals formed by γ-irradiating *n*-hexane adsorbed on silica gel at 77°K. showed that a transfer of energy occurred from the silica gel to the adsorbed hydrocarbon phase. This transfer was particularly pronounced at very low coverages. A saturation effect was observed; the yields of radicals increased rapidly with the amount of hydrocarbon up to the electron fraction of 0.02, then a leveling off occurred. A decrease in the $g = 2.0080$ signal from the silica gel was observed at the same time, and at the electron fraction of 0.02 this signal had completely disappeared. From the saturation data the number of active sites on the silica gel surface

[1] Present address: Mizonokuchi Research Laboratory, Mitsubishi Petrochemical Co. Ltd., Kawasaki-shi, Japan.

In Radiation Chemistry; Hart, E.;
Advances in Chemistry; American Chemical Society: Washington, DC, 1968.

was estimated to 10^{17} per sq. meter BET surface. These observations indicate an interaction between molecules in the adsorbed hydrocarbon layer and radiation induced centers in the silica gel. No complete assignment of the radicals formed could be made, mainly because of the limited resolution of the electron spin resonance spectra obtained.

The occurrence of energy transfer has been confirmed by preliminary determinations of the yield of hydrocarbon products formed (*15*). The dependence of the yields of various products on the amount of *n*-hexane shows a rapid increase at low hydrocarbon electron fractions. The curves then flatten out demonstrating that the active sites on the silica gel surface have been used up. There is a difference in saturation behavior for various hydrocarbon products; the combination of two *n*-hexyl radicals to form *n*-dodecane indicates a saturation at an electron fraction of 0.05, whereas the formation of 5-methylundecane from *n*-hexyl and 2-hexyl radicals reaches saturation first at the electron fraction of 0.2. The same general behavior is observed also for C_{10}, C_9, and C_8 products.

In the continuation of our work a study has also been made of the system benzene/silica gel. When irradiating this system at 77°K. it was found that the silica gel could stabilize both monomeric and dimeric cation radicals of benzene (*6*). Furthermore, the high resolution of the electron spin resonance lines indicated a high degree of mobility for the benzene molecules in the adsorbed layer. No spectrum from trapped electrons could be observed although this could very well be hidden behind the strong cation absorption. However, ethylene, and isobutylene in the adsorbed state at low temperature gave spectra from shortlived species identified as trapped electrons (*7*).

The present investigation is concerned with the type of radical formed in the benzene/silica gel systems and with the yields of these radicals at different benzene contents. An explanation of the yields is given on the basis of an energy transfer mechanism.

Publication Date: January 1, 1968 | doi: 10.1021/ba-1968-0082.ch020

Experimental

Materials. Silica gel (AB Kebo, Stockholm) for chromatographic purpose, 100–200 mesh, was used. The specific surface area (BET) was 667 sq. meters/gram. The main impurities of silica gel as determined by spectral analysis were Al(350 p.p.m.), Fe(136 p.p.m.), Cu(10 p.p.m.) and Mn(< 4 p.p.m.).

The benzene (Fluka AG., Buchs SG) used was 99.93 mole % pure with toluene as the most probable impurity (6 p.p.m.). Benzene-d_6 (Merck's Reagenzien) with a minimum degree of deuteration of 99% was used.

Sample Preparation. Varying amounts of carefully degassed benzene were vacuum distilled onto silica gel which had first been dried at 500°C. at 10^{-4}–10^{-5} torr for 17 hours. The amount of benzene was

determined by measuring the pressure of the hydrocarbon vapor in a known volume at room temperature. The composition of the system expressed as electron fraction of benzene, x_1, was determined from the weight of the sample after completing the ESR experiment. Samples with $x_1 = 0.0005$–0.40 benzene were prepared. Benzene contents higher than $x_1 = 0.40$ gave samples with a moist appearance. Before irradiation the samples were stored at room temperature for some days to obtain a homogeneously adsorbed hydrocarbon layer.

Irradiation. The samples were irradiated with ^{60}Co γ-rays at 77°K. in ampoules sealed at 10^{-4}–10^{-5} torr. The ampoules were made from Suprasil quartz which on irradiation gave an ESR signal which was very small compared with the intensity of the sample absorption. The dose rate of the radiation source varied within 300–350 krads/hour. The dose was 3.4 Mrads for most of the experiments. The dose dependence of the radical formation was investigated in the dose range 0.02–10 Mrads.

ESR-spectrometer. The electron spin resonance spectra were recorded with a Varian V-4502-11 spectrometer operating at a wavelength of 3 cm. The magnetic field sweep of the Varian Fieldial unit was calibrated by means of the splitting in the $ON(SO_3)_2^{2-}$ radical prepared from Fremy's salt (*28*). *g*-Factors were measured by comparison with a solid diluted sample of DPPH (α,α'-diphenyl-2-picrylhydrazyl), $g = 2.0037$, kept in the Varian V-4532 dual cavity together with the sample under investigation.

Radical Concentration. The absorption intensities were obtained from the spectra by calculating the first moment of the derivative curves. To obtain the correct intensity of a central component (*cf.* Figure 1) the contribution from the broader parts of the spectrum was subtracted. The sensitivity of the spectrometer was gauged by the DPPH sample retained throughout in the dual cavity. Absolute concentrations were measured by comparing the absorption intensity with the signal strength from a sample of Cu(II)dithiocarbamate in benzene solution recorded at room temperature (*22*). A correction for the difference in temperature was applied. Determination of radical concentration is reproducible to about 25% as judged from earlier measurements of a similar type (*13*). The microwave power was for these determinations kept below 2 mw.

Variable Temperature. The changes in the radical spectra with temperature were studied by slowly heating the samples in a stream of cold nitrogen gas passing through a double walled quartz tube placed in the microwave cavity.

Results

Spectra. The gross feature of the spectrum from the composite benzene/silica-gel system obtained at 77°K. is a strong narrow component overlapping the central part of a weak broad component. The strong component is shown in Figure 1 at different benzene concentrations. For a benzene content of $x_1 = 0.001$ (Figure 1a) the spectrum consists of seven asymmetric main lines, separated by about 4.4 G. The septet is

Publication Date: January 1, 1968 | doi: 10.1021/ba-1968-0082.ch020

caused by the benzene monomeric cation as has been reported previously (*6*). Other lines are just recognized between those of the main components; with increasing hydrocarbon concentration ($x_1 = 0.02$)

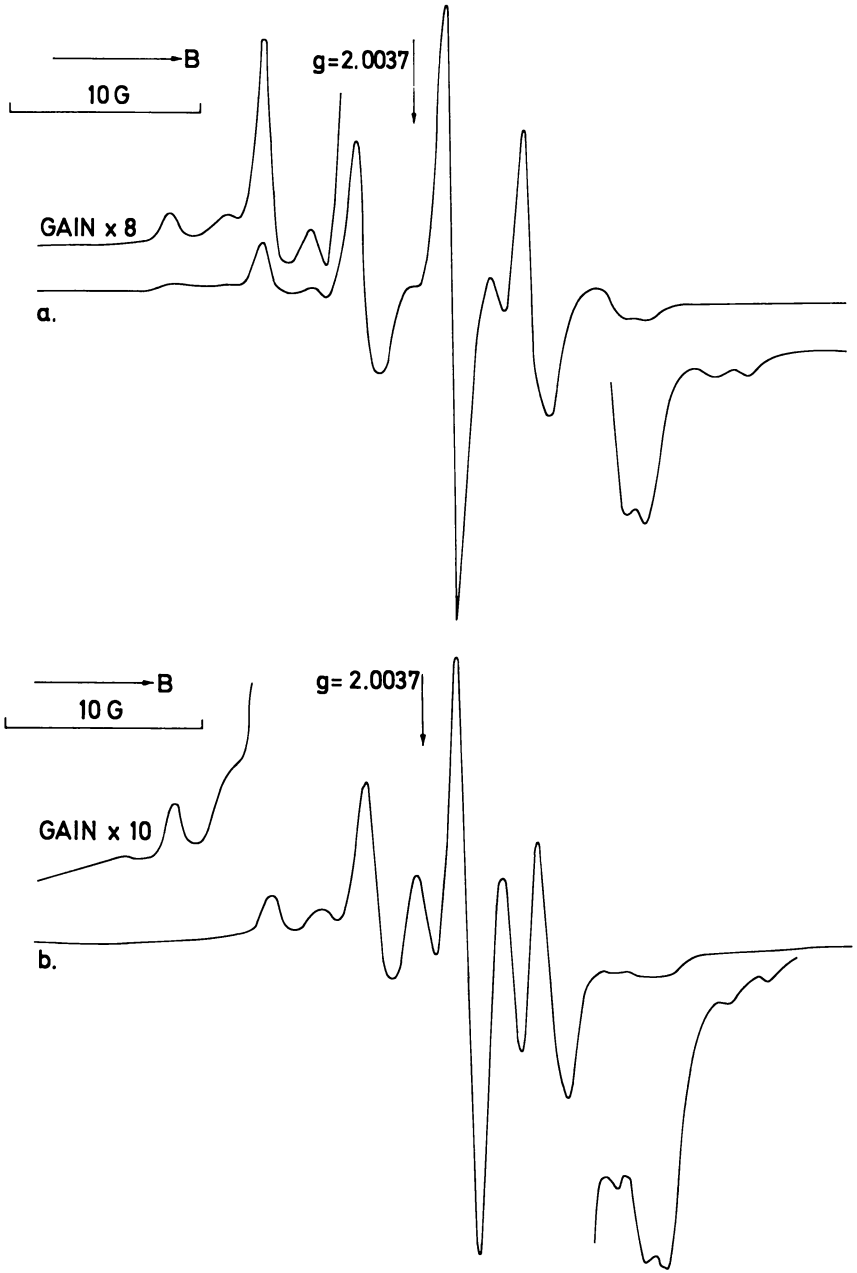

Publication Date: January 1, 1968 | doi: 10.1021/ba-1968-0082.ch020

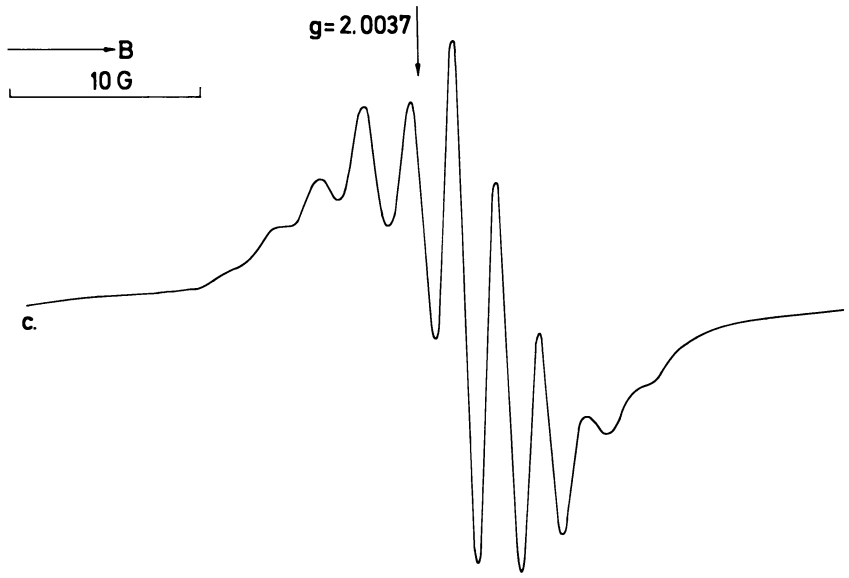

Figure 1. The strong narrow component of benzene/silica gel first derivative ESR spectrum at 77°K. at the following electron fractions of benzene; (a) $x_1 = 0.001$, *(b)* $x_1 = 0.02$, *and (c)* $x_1 = 0.06$

these lines grow in intensity (Figure 1b). At a benzene content of $x_1 = 0.06$ it is possible to resolve 9 lines with an average separation of 2.2 G (Figure 1c). This spectrum mainly originates from the singly charged dimeric cation of benzene (*6*).

As in the previous work on *n*-hexane (*14*) only traces of atomic hydrogen could be found. The wings of the weak component in the spectrum at 77°K. (Figure 2a) can be resolved into two quartets which are identified as belonging to the spectrum from cyclohexadienyl, C_6H_7 (*8, 9, 21*). The intensity ratio between the strong and the weak components decreases with increasing benzene concentration. The third quartet of the cyclohexadienyl spectrum hidden behind the central absorption is indicated in the stickplot diagram. The outer lines of this quartet can be observed at the benzene content $x_1 = 0.40$. The triplet separation is measured to 48.5 ± 1 G. The separation of the lines in the quartets is 10.2 ± 0.5 G. The integrated intensity ratio of the peaks in the quartets is about 1:2:2:1; these intensities deviate from the theoretical values partly because of a possible non-equivalency of the *o*- and *p*-protons (*8*). The line width is 6.5 ± 0.5 G. At a higher resolution an additional splitting of 2.5 G is obtained. If every line in the quartets

Publication Date: January 1, 1968 | doi: 10.1021/ba-1968-0082.ch020

constitutes an unresolved triplet the individual triplet line width is estimated to be about 3 G.

Influence of Temperature. The intensity of the monomeric cation spectrum decreases relative to that of the dimeric cation when the temperature of the sample in the cavity is raised above 77°K. Above 185°K. no signal could be detected. The change in the complete spectrum of a sample with a benzene content $x_1 = 0.02$ with increasing temperature is shown in Figure 2. The relative intensities of the lines in the quartets change (Figure 2b), and when the sample is kept at about 140°K. for a few minutes the outermost lines are transformed into a shoulder. Additional peaks become apparent near the central absorption. The positions of these lines do not coincide with those expected for the outer peaks of the central quartet of the cyclohexadienyl radical. When the temperature is further increased to 219°K., the spectrum in Figure 2c is obtained. In this spectrum all ionic species are supposed to have decayed. The most prominent feature of the spectrum can be accounted for by a pair of quartets as shown in the stickplot in Figure 2c. The spectrum has a doublet coupling constant of 35 ± 1 G and a quartet line separation of 11.5 ± 0.5 G. The line width is 5.5 ± 0.5 G. The remaining lines on the wings could be annealed only by keeping the sample at 255°K. or higher for at least 10 minutes. Additional hyperfine structure of about 2.5 G can partly be resolved at a low modulation amplitude. When the central line is recorded in an expanded magnetic field sweep it is resolved into two lines. The *g*-factors of these lines are 2.0031 and 2.0008. The latter of these values coincides with that of the narrow peak from irradiated silica gel.

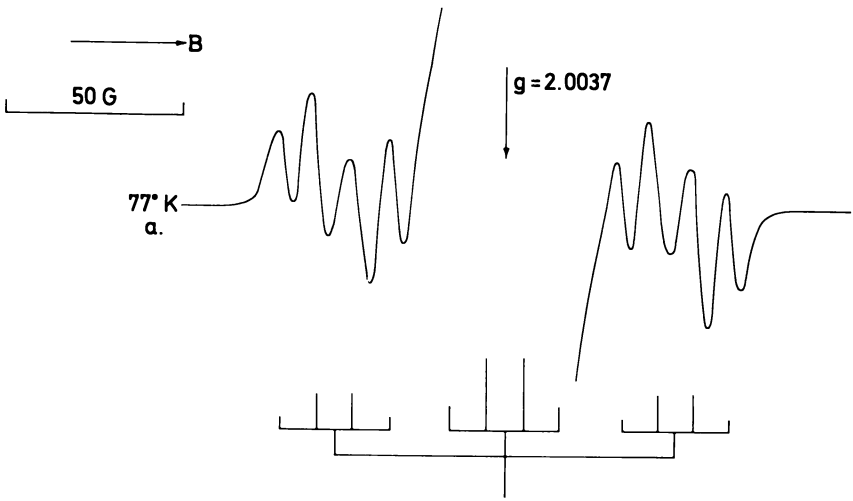

Publication Date: January 1, 1968 | doi: 10.1021/ba-1968-0082.ch020

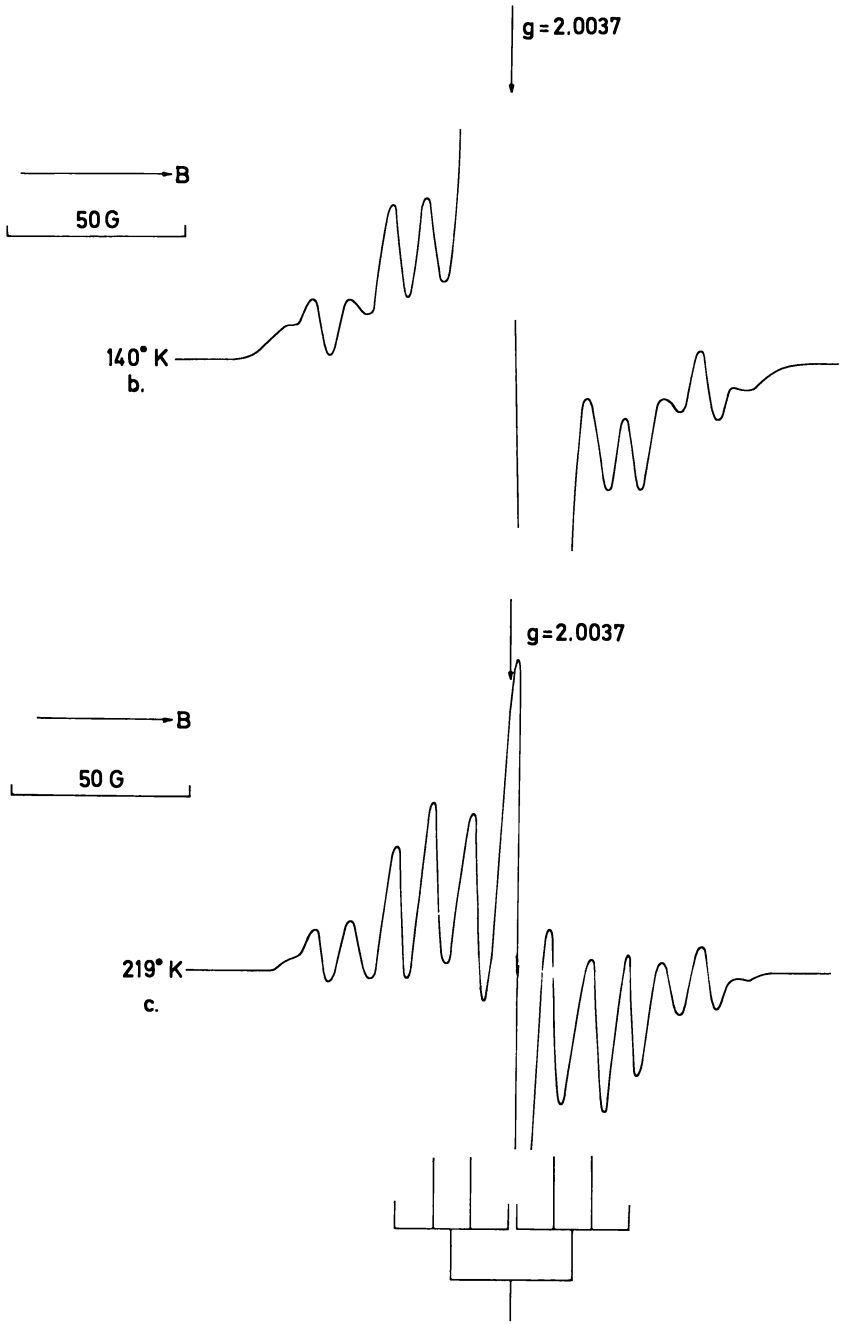

Figure 2. The complete first derivative ESR spectrum of benzene/silica gel at $x_1 = 0.02$ *recorded at different temperatures. (a) 77°K., (b) 140°K., and (c) 219°K.*

Benzene-d_6/Silica Gel System. A sample containing $x_1 = 0.02$ benzene-d_6 adsorbed on silica gel dried at 500°C. was irradiated to a dose of 3.4 Mrads at 77°K. In this case the ESR spectrum (Figure 3) agrees in its outer parts with that obtained from the radical $C_6D_6H^\cdot$ in an alcoholic glass (*21*). When the silica gel sample was dried at 700°C. for 17 hours, only a single line with $g = 2.0022$ and the line width 3.5 G was observed. This over-all width approximately equals the $C_6H_6^+$ value divided by 6.514 (the ratio of the nuclear g-factor for H and D). These data corroborate the existence of the $C_6D_6^+$ cation radical.

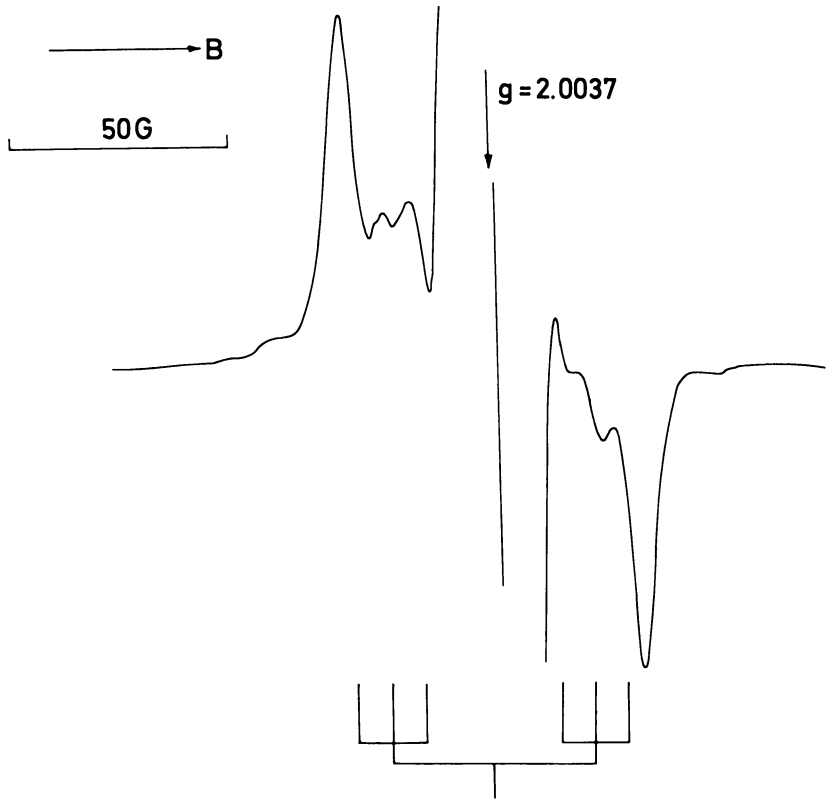

Figure 3. ESR first derivative spectrum of benzene-d_6/silica gel at 77°K. $x_1 = 0.02$. Silica gel dried at 500°C.

Yields. The number of spins per meter BET surface area as a function of the dose are given in Figure 4. The yield, G_{app}—*i.e.*, the number of paramagnetic species per 100 e.v. of energy released in the benzene/silica gel system, at a dose of 3.4 Mrads is plotted against the benzene content

Publication Date: January 1, 1968 | doi: 10.1021/ba-1968-0082.ch020

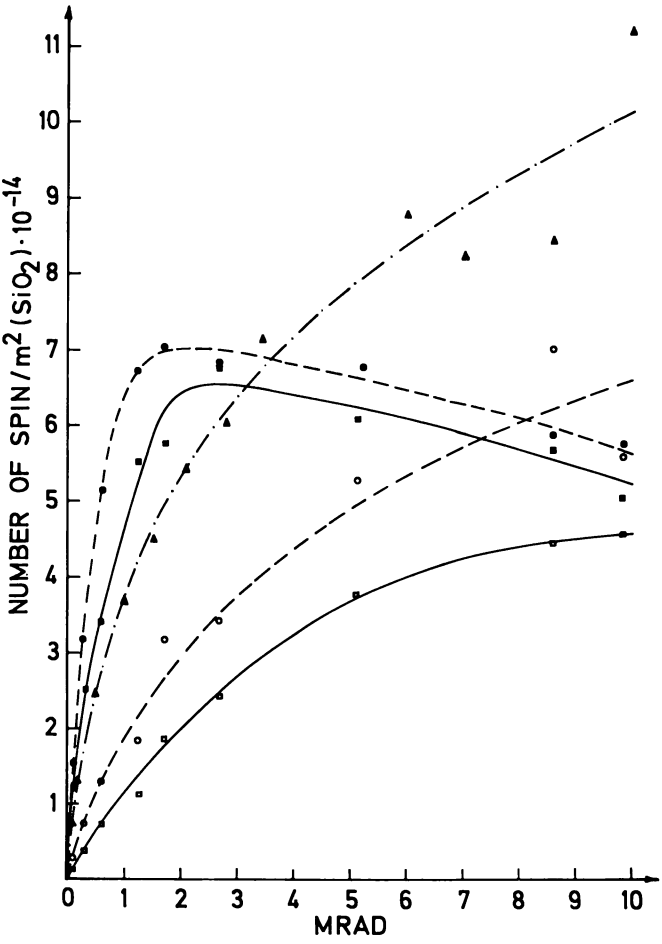

Figure 4. The dose dependence of the number of spins per unit surface area. Cation radicals, $x_1 = 0.01$ (■), $x_1 = 0.05$ (●). *Neutral radicals* $x_1 = 0.01$ (□), $x_1 = 0.05$ (○). *Silica gel defects* (▲)

in Figure 5 for both the ionic and the neutral radicals. The *G* values are mean values over the dose range. The initial values are 4–5 times greater than the mean values.

Discussion

Benzene Ions. In a previous paper (*6*) evidence was presented that the strong central absorption in the γ-irradiated benzene/silica gel system is caused by singly charged positive ions. The data obtained are in

complete agreement with those later found by Carter and Vincow (3) for benzene cations formed by photooxidation in a rigid sulfuric acid matrix. At low benzene concentrations the ions are present as monomers (Figure 1a) but at higher contents the dimeric cation is also observed (Figure 1b and 1c). The separation between the lines, 2.2 G, is half as large as the value, 4.4 G, observed for the monomeric ion. The same ratio of line separations is found for corresponding complexes formed on oxidation of condensed aromatic compounds by $SbCl_5$ (*11, 18*).

The narrow, although somewhat asymmetric lines observed at 77°K. for the ions are typical for a complex with a restricted ability to tumble.

Publication Date: January 1, 1968 | doi: 10.1021/ba-1968-0082.ch020

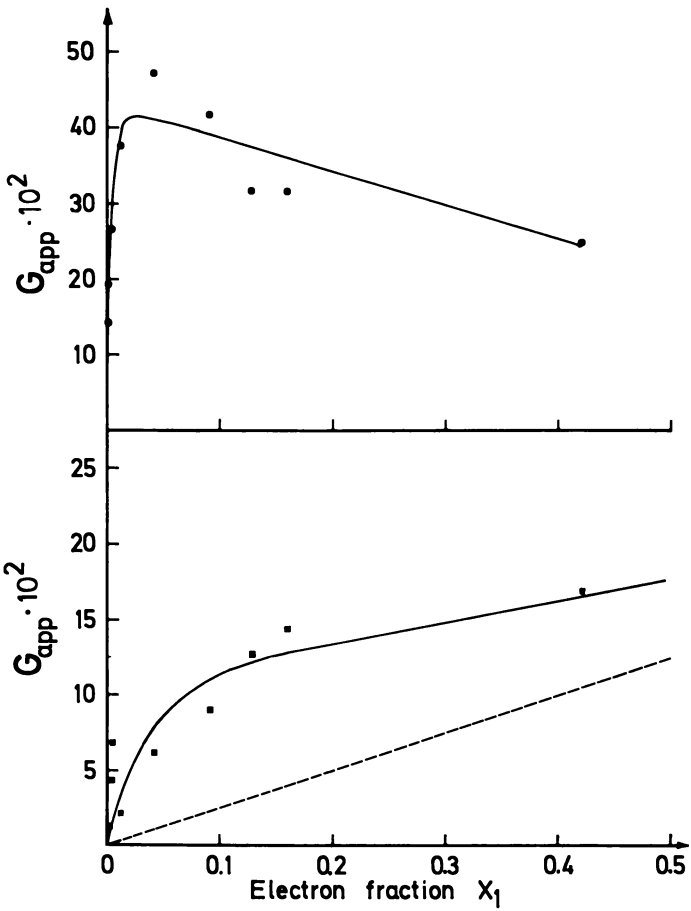

Figure 5. Apparent yields of cation (above) and neutral radicals (below) as function of the benzene electron fraction x_1. The dashed line represents no interaction. The solid lines are obtained from the equations given in the text

It seems reasonable that rapid rotation around the sixfold axis could occur more easily than any other reorientation (*30*). If the anisotropic hyperfine coupling for the protons is of the same form as that observed for other π-electron hydrocarbon radicals (*20*), then the anisotropy would be averaged out by a rapid rotation around this axis. However, the small asymmetry observed indicates an incomplete averaging. The additional structure of the two outermost lines on the high field side may be an anisotropy effect. Alternatively, an underlying spectrum—*e.g.*, from cyclohexadienyl—may also distort the line shape.

A Jahn-Teller distortion should occur for radicals, like the positive benzene ion, possessing an orbitally degenerate ground state. However, this static splitting is probably small (*4*), and the ion is continually passing between the two configurations of lowest energy as it vibrates in its ground vibronic state. McConnell and McLachlan (*19*) considered the dynamical effect on the benzene negative ion in the fluctuating field from a dipolar solvent. In this case the spin density distribution fluctuates with time. When the correlation time for the interaction $\tau << (2\pi\Delta\nu)^{-1}$, where $\Delta\nu$ is the hyperfine splitting, seven equidistant lines with binomial intensities are obtained. A line broadening occurs when $\tau \approx (2\pi\Delta\nu)^{-1}$. A similar mechanism may apply to the positive benzene ion reorienting in the perturbing field of the silica gel matrix. It may also happen that the ion vibrates so as to simulate reorientation. Different hyperfine lines will broaden to various extents (*10*). This is also observed (Figure 1a). Unfortunately this mechanism of line broadening cannot easily be isolated from other contributions—*e.g.*, the incomplete averaging of dipolar hyperfine interactions discussed previously. Indications that interactions with polar solvents may lift the degeneracy have been reported (*16*), although the evidence is far from conclusive. One possibility to study this effect would be to lower the temperature to a point where reorientation becomes slow and/or vibrational states become unpopulated. At present we have no direct evidence for a Jahn-Teller distortion in the benzene ion adsorbed on silica gel.

It seems reasonable to assume that the dimeric benzene ion has a sandwich conformation. A similar structure has been invoked to explain excimer spectra from neutral benzene molecules in solution where stable dimers are observed (*27*). Also Howarth and Fraenkel (*11*) have suggested that the two hydrocarbon moieties of the dimeric ion of naphthalene lie in parallel planes. Ishitani and Nagakura (*12*) have suggested a sandwich structure for paracyclophane anions but they also consider the possibility of a diphenyl type of structure.

Dimers should preferably be formed at high benzene contents where adsorption in double and multiple layers can be expected. From the BET area of 667 sq. meters/grams and an assumed area of 33 sq. A. (*29*) occu-

Publication Date: January 1, 1968 | doi: 10.1021/ba-1968-0082.ch020

pied by an adsorbed benzene molecule one finds that complete coverage corresponds to $x_1 = 0.25$. However, even at $x_1 = 0.001$ lines caused by the dimeric ions are observed. The reasons for the formation of dimers at this low concentration may be several. The maximum heat of adsorption of benzene on a silica gel surface has been found to be 0.45–0.50 e.v. (*29*). The exchange interaction energy between the benzene rings in the paracyclophane anions has been estimated to be 0.83 e.v. It can be assumed that the energy is about the same for cations and thus dimerization is energetically favored. This is also evidenced by the increase in the number of dimeric ions in comparison with that of monomers when the samples are warmed above 77°K. The possibility of a diffusion at 77°K. of neutral benzene molecules to sites with monomeric ions and the subsequent formation of dimers seems unlikely in view of the stability of the monomeric species.

Cyclohexadienyl Radicals. The lines on the wings of the spectra from irradiated benzene/silica gel mixtures owing to the cyclohexadienyl radical are better resolved than in the spectrum obtained from pure benzene at the same temperature, 77°K. The main cause for line broadening in radical spectra of polycrystalline samples is the anisotropy of the hyperfine coupling. To average out this anisotropy, rapid tumbling is required, the rate of reorientation has to be at least the same magnitude as the anisotropic part of the hyperfine coupling tensor. The measured splittings of the α-protons in the ortho and para positions are about 10 G, while the anisotropic contribution is about 50% of the isotropic coupling (*20*). This indicates that the tumbling frequency is at least 15 Mc/sec.

The cyclohexadienyl is formed in a secondary reaction between benzene and atomic hydrogen. Hydrogen atoms may be created by the homolytic scission of a C–H–bond in the benzene molecule. Alternatively they may be formed by rupture of the hydrogen-oxygen bonds of surface hydroxyl groups. In the former case phenyl radicals will also appear. From phenyl radicals produced in the adsorbed state by photolyzing iodobenzene, a spectrum suggested to be a triplet of triplets, $a_{ortho} = 18$ G, $a_{meta} = 7$ G (*26*) has been observed. The same interpretation was reached for spectra obtained in solid matrices at 77°K. using sodium and iodobenzene (*1*). Ultraviolet induced phenyl radicals from pure benzene at 77°K. give a six line spectrum interpreted as a doublet of triplets, $a_{ortho} = 12$ G, $a_{para} = 6$ G (*25*). In the present system the central part of a phenyl signal would be obscured at 77°K. by the strong absorption owing to the ionic species. In spectra obtained from samples warmed to temperatures above 77°K. neither the total width nor the line separation conform with the reported data of phenyl spectra. The abstraction of hydrogen atoms from the benzene molecules seems unlikely in the present

Publication Date: January 1, 1968 | doi: 10.1021/ba-1968-0082.ch020

system. Further the neutral radical observed in the irradiated benzene-d_6/silica gel system is mainly $C_6D_6H^{\cdot}$, which clearly shows that the cyclohexadienyl radical is formed by a reaction with atomic hydrogen released from the silica gel. This is also confirmed by using deuterated silica gel (*23*).

Free Radical Reactions. As is shown in Figure 2 the spectra obtained from samples irradiated at 77°K. gradually change their shape when the temperature is raised. The strong central line (Figure 2c) is mainly caused by one of the paramagnetic centers in the silica gel. The three lines on each side and the two outer lines on each wing apparently belong to different radicals. The change in the appearance of the spectra may be attributed to a radical reaction according to the scheme

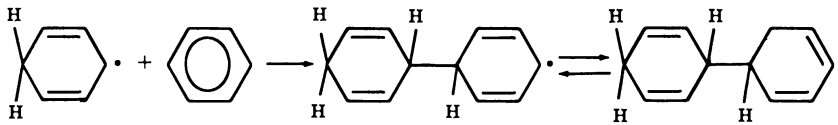

In this reaction cyclohexadienyl behaves as if it initiates a radical polymerization process.

The spectrum of the radical should contain a quartet splitting from the ortho and para protons and an additional doublet splitting owing to the β-proton. The outermost lines are probably caused by cyclohexadienyl radicals which are firmly bound to the gel surface. Such radicals may be more stabilized and thus less reactive. The spectrum may be modified owing to a distorted conformation.

Energy Transfer Mechanism. In the earlier work on *n*-hexane (*14*) it was found that the broad line in the spectrum of the paramagnetic species in the silica gel decreased in intensity as the amount of hydrocarbon increased. For ethylene and isobutylene (*7*) only the narrow line at $g = 2.0008$ from the silica gel has been observed. Because of the strong absorption from the cation radicals no direct observation could be made of the change in intensity of the silica gel peaks in the present system. After thermal annealing, however, the only line remaining from the silica gel is the narrow one. This accordingly indicates that in the case of benzene the radical species forms by the action of excitations arising from irradiation of the gel. The cation radicals are most certainly formed at sites different from those responsible for the cyclohexadienyl radicals. The results from the benzene-d_6 system show that the OH groups on the silica gel surface are necessary for cyclohexadienyl formation. Furthermore, cation radicals were the only species formed after drying the gel at 700°C., at which temperature most of the OH groups had disappeared (*5*). It seems likely that the sites for cation formation are localized at surface Si–O–Si bridges.

Publication Date: January 1, 1968 | doi: 10.1021/ba-1968-0082.ch020

The dose variation of the number of radical cations per unit surface area does not appear to be very dependent upon the content of benzene (Figure 4). This indicates that only a limited number of active sites are available for cation formation. The simplest model for this process follows from Equations 1 and 2.

$$S \xrightarrow{M} S^* \quad (1)$$

$$S^* + B \rightarrow B^+ + e \quad (2)$$

S* denotes an active site that has been formed at the surface by an excitation originally created in the solid S and then transferred to the surface (*2, 24*). B is a benzene molecule adsorbed on a site, which can be transformed to S*. This assumption is in accordance with the previously used model (*1*). If $B > S_{max}$, the limiting number of B^+ will be equal to S_{max} independently of the number of B. This case applies to the cation formation and the data in Figure 4 give $S_{max} = (6\text{–}7) \times 10^{14}$ sites/sq. meter. When $B < S_{max}$, the limiting number of B^+ will of course be equal to B.

In forming cyclohexadienyl the number of hydroxyl groups (about 10^{18} OH/sq. meter) is large enough compared with the number of benzene molecules (about 10^{16} C_6H_6/sq. meter) to prevent saturation within the dose range used, as is evident from Figure 4.

The concentration of paramagnetic species in the pure silica gel is apparently slightly lower than the content of ionic species. This does not contradict the proposed mechanism since all the species can not be detected owing to the width of the line. The detectable microwave absorption in silica gel increases when—*e.g.*, hydrogen gas is added to the sample (unpublished results).

In a previous paper (*14*) two simple models were proposed to explain the change in yield with composition. It was assumed that the silica gel surface could adsorb molecules on active sites, where radicals are formed with a yield G_{ads}. Molecules not situated on active sites gave free radicals with the same yield as in the homogeneous phase G_{hom}. Applying this model to the case of cation formation we have $G_{hom} = 0$. Thus

$$G_{app} = G_{ads} \frac{x_1^s}{1 - x_1^s}(1 - x_1)\left[1 - \exp\left(-\frac{1 - x_1^s}{x_1^s}\,\frac{x_1}{1 - x_1}\right)\right]$$

where x_1^s is the hydrocarbon content when all active sites are saturated. The experimental data give $G_{ads} = 95 \pm 25$ and $x_1^s = 0.0045 \pm 0.0010$ (*see* Figure 5). From the latter value and the area occupied by each benzene molecule, 33 sq. A. (*29*), we find that about 2% of the BET area is active. This corresponds to 5×10^{16} sites/sq. meter. The number

Publication Date: January 1, 1968 | doi: 10.1021/ba-1968-0082.ch020

of the sites is of the same magnitude as that found in the hexane/silica gel system, 10^{17} sites/sq. meter.

There is a considerable difference between the number of active sites as determined from the limiting number of spins 7×10^{14}/sq. meter, and from the saturation composition. This can be partly explained by the magnitude of the experimental errors involved. Some prohibiting mechanism may exist which has not been taken into account in the model. Thus, use of a site for cation formation may render inactive a certain number of neighboring sites.

From the data for the cyclohexadienyl yields (Figure 5) one obtains using $G_{hom} = 0.25$ the values $G_{ads} = 3.0 \pm 1.0$ and $x_1^s = 0.035 \pm 0.008$. The number of active sites will be 5×10^{17}/sq. meter. This is of the same order of magnitude as the number of hydroxyl groups.

The ionization energy of gaseous benzene, 9.6 e.v., gives an upper limit of $G = 10$ for cation formation in pure benzene vapor. In order to explain the value for G_{ads} of 95 transfer to the hydrocarbon of about 5% of the energy released in the silica gel must occur. In the adsorbed state the ionization energy is probably lower than in the gaseous state. Still the amount of energy needed for creating one ionization is likely to exceed the ionization potential and the fraction of transferred energy will thus be of at least the estimated magnitude. For cyclohexadienyl radicals the values $G_{hom} = 0.25$ and $G_{ads} = 3.0$ give an energy transfer of 25%. However, in this case the mechanism proposed does not necessarily require energy transfer.

Literature Cited

(1) Bennet, J. E., Mile, B., Thomas, A., *Proc. Roy. Soc.* **A293,** 246 (1966).
(2) Caffrey, Jr., M. M., Allen, A. O., *J. Phys. Chem.* **62,** 33 (1958).
(3) Carter, M. K., Vincow, G., *J. Chem. Phys.* **47,** 292 (1967).
(4) Coulson, C. A., Golebiewski, A., *Mol. Phys.* **5,** 71 (1961).
(5) Davydov, V. Ya., Kiselev, A. V., Zhuralev, L. T., *Trans. Faraday Soc.* **60,** 2254 (1964).
(6) Edlund, O., Kinell, P.-O., Lund, A., Shimizu, A., *J. Chem. Phys.* **46,** 3679 (1967).
(7) Edlund, O., Kinell, P.-O., Lund, A., Shimizu, A., *Polymer Letters* (in the press).
(8) Fessenden, R. W., Schuler, R. H., *J. Chem. Phys.* **39,** 2147 (1963).
(9) Fischer, H., Kolloid-Z. Z. *Polym.* **180,** 64 (1962).
(10) Freed, J. H., *J. Chem. Phys.* **43,** 1427 (1965).
(11) Howarth, O. W., Fraenkel, G. K., *J. Am. Chem. Soc.* **88,** 4514 (1966).
(12) Ishitani, A., Nagakura, S., *Mol. Phys.* **12,** 1 (1967).
(13) Kinell, P.-O., Lund, A., Vänngård, T. *Arkiv Kemi* **23,** 193 (1964).
(14) Kinell, P.-O., Lund, A., Vänngård, T., *Acta Chem. Scand.* **19,** 2113 (1965).
(15) Kinell, P.-O., "Progress Report Nuclear Chemistry," **AE-232,** AB Atomenergi, Stockholm, 1966.

(16) Köhnlein, W., Böddeker, K. W., Schindewolf, U., *Angew. Chem.* **79,** 318 (1967).
(17) Leone, I. A., Koski, W. S., *J. Am. Chem. Soc.* **88,** 224 (1966).
(18) Lewis, I. C., Singer, L. S., *J. Chem. Phys.* **43,** 2712 (1965).
(19) McConell, H. H., McLachlan, A. D., *J. Chem. Phys.* **34,** 1 (1961).
(20) Morton, J. R., *Chem. Rev.* **64,** 453 (1964).
(21) Ohnishi, S., Tanei, T., Nitta, I., *J. Chem. Phys.* **37,** 2402 (1962).
(22) Pettersson, R., Vänngård, T., *Arkiv Kemi* **17,** 249 (1961).
(23) Strelko, V. V., Suprunenko, K. A., *Teor. Eksp. Khim.* **2,** 694 (1966).
(24) Sutherland, J. W., Allen, A. O., *J. Am. Chem. Soc.* **83,** 1040 (1961).
(25) Tanei, T., *Bull. Chem. Soc. Japan* **40,** 2456 (1967).
(26) Tolkachev, V. A., Chkheidze, I. I., Buben, N. Ya., *Zh. Strukt. Khim.* **3,** 709 (1962).
(27) Vala, M. T. Jr., Hilber, I. H., Rice, S. A., Jortner, J., *J. Chem. Phys.* **44,** 23 (1966).
(28) Valenzula, J. A., Bard, A. J., *J. Phys. Chem.* **72,** 286 (1968).
(29) Whalen, J. W., *J. Phys. Chem.* **71,** 1557 (1967).
(30) Woesner, D. E., *J. Phys. Chem.* **70,** 1217 (1966).

RECEIVED January 4, 1968.

Some Effects of Crystal Structure on Production of Radicals in Irradiated Organic Crystals

MAX T. ROGERS and L. D. KISPERT

Michigan State University, East Lansing, Mich. 48823

Publication Date: January 1, 1968 | doi: 10.1021/ba-1968-0082.ch021

A series of anhydrous and hydrated polycrystalline metal acetates has been irradiated at 77°K. with 1-Mev. electrons and the ESR spectra observed. The principal stable free radical found in the hydrated materials is methyl whereas other species predominate in the anhydrous acetates and methyl radical is not observed or is only a minor product. The absolute yield of methyl radicals, as well as the ratio of methyl to other species, appears to increase with the number of molecules of water of crystallization. The radicals obtained by breaking C–C bonds are also found in irradiated sodium perfluorosuccinate hexahydrate and acetamide and it appears that such species may be favored in crystals whose structures are largely determined by hydrogen bonding.

Radicals produced in irradiated crystals usually may be identified by their ESR spectra, and detailed studies of single crystals lead to a rather complete picture of their structures (*1, 21*). There is now enough information concerning the nature of the radicals produced under given conditions so that one can hope to predict the products of radiation damage of organic crystals in favorable cases. In order to be able eventually to select conditions to observe a given radical of interest, however, it will first be necessary to study in detail the factors which influence the nature of the radicals produced. These include the structure of the species irradiated, the crystal structure, the nature of the radiation used and the thermal history of the crystal.

Where a large enough series of chemically related species has been irradiated it is often possible to formulate some rules governing the radical species likely to be found. Studies of aliphatic amides (*27*) show that

In Radiation Chemistry; Hart, E.;
Advances in Chemistry; American Chemical Society: Washington, DC, 1968.

C–H bonds on carbon adjacent to nitrogen are likely to be broken preferentially, and where these are absent (in the unsubstituted amides) C–H bonds on carbon adjacent to the carbonyl group tend to be broken. Some general rules can also be formulated for simple carboxylic acids, dicarboxylic acids (*35, 36*) and amino acids (*6, 7, 8, 33*) since these have been extensively studied. Aliphatic fluorine compounds appear to behave similarly to the corresponding hydrogen compounds. Thus, the C–F bond of the group adjacent to –COOH or $-CONH_2$ is preferentially broken in $CF_3CF_2CONH_2$ (*17*) and in $HOOC-CF_2-CF_2-COOH$ (*28*). However, as mentioned below, C–C bonds are also broken in some cases, and the present work is part of a general study to determine the conditions under which C–C bond breakage is favored over other processes.

The temperature at which crystals are irradiated and observed and the thermal history of the crystals after irradiation prove to be of major importance in determining the nature of the radicals, their orientation in the crystal lattice, and their thermal motions. Recent studies (*6, 7, 8, 33, 34 35*) have shown that for many molecules irradiated at low temperature (often 77°K.) the first paramagnetic species is produced by adding an electron (or hole). This species is usually not stable at higher temperatures and decays to give a "primary neutral radical" (*6, 7, 8*). In some cases this radical may change its orientation in the lattice as the temperature is raised or may rearrange or react to give the final species seen at high temperature. Thus, irradiation of alanine (*33*) leads first to the ion-radical $CH_3CH(NH_3^+)COOH^-$, stable at 77°K., followed by loss of NH_3 to give $CH_3\dot{C}HCOOH$ at 140°–150°K. and eventually to reorientation of this radical by room temperature to give the arrangement responsible for the room temperature spectrum. In the interesting case of irradiated α-aminoisobutyric acid (*9*) the radical $(CH_3)_2\dot{C}COO^-$ stable at intermediate temperatures gives three different sets of ESR spectra corresponding to three distinct environments for the radical at different temperatures.

It is often the case that the electron (or hole) attachment product is not seen at 77°K. but that a different radical is stable at 77°K. from that seen at 25°C. Irradiation of sodium acetate trihydrate at 77°K. gives methyl radical (*29*) but at 25°C. the principal product (*31*) is $\cdot CH_2COO^-$; also, irradiation of CF_3CONH_2 leads to $\cdot CF_3$ at 77°K. but to $\cdot CF_2CONH_2$ at room temperature (*18, 30*).

Reactions of radicals first formed with other species in the crystal may also occur on warming or on standing. Intermolecular transfer of spins has been demonstrated in deuterium substituted alanine where

Publication Date: January 1, 1968 | doi: 10.1021/ba-1968-0082.ch021

$CH_3\dot{C}HCOO^-$ comes to equilibrium with $CD_3\dot{C}DCOO^-$ and partly deuterated species on standing at room temperature for a year or on heating at 150°C. for an hour (*19*). The radical $\cdot CF_2COO^-$ produced in irradiated sodium chlorodifluoroacetate reacts with ions of the lattice, on standing for a year, to give $\cdot CFClCOO^-$ (*31*) and also reacts readily with oxygen gas to give a peroxide radical (*32*).

The effect of radiation on the nature of the stable radicals produced has not been systematically studied to any extent. Rather random observations available at present indicate that x-rays, γ-rays, and high-energy electrons give about the same radicals. Photolysis often leads to similar radicals, but by varying the wavelength of irradiation, the products may be varied (*5*). It has also been found that where irradiation by γ-rays or by electrons produces two or more different species a single one may often be obtained by bombardment with hydrogen atoms (*11*, *12*). Saturated organic compounds suffer hydrogen abstraction whereas unsaturated molecules add a hydrogen atom in the examples studied (*11*, *12*). Some control over the nature of the products is thus possible by the proper choice of radiation.

One factor about which little is as yet known is the effect on the nature of the radicals produced of changes in the structure of the host crystal. It has been reported that the CO_2^- radical, which is obtained on irradiating sodium formate (*24*), is also present in the irradiated potassium salt and in several other irradiated metal formates (*4*). Similarly, irradiation of the potassium, calcium, and lithium salts of glycollic acid (*2*, *3*, *14*), as well as the acid itself (*2*), leads to the radical $H\dot{C}(OH)CO_2^-$. It is interesting that some of the hyperfine splittings differ substantially for irradiated anhydrous lithium glycollate (*25*), and it has been proposed that the geometry of the radical is slightly different in this lattice. Cases are also known where essentially the same radical is produced on irradiating chemically different materials. The radical $\cdot CH_2COO^-$ (or its protonated form) is observed (*31*) in sodium acetate trihydrate irradiated at 25°C. but is also a product of the irradiation of glycine (*6*, *7*, *8*, *22*, *23*). The radical $HOOCCH_2\dot{C}HCOOH$ is obtained from room temperature irradiation of succinic acid (*26*), maleic acid (*13*) and *dl*-aspartic acid (*15*).

We report here some observations on irradiated metal salts of acetic acid which suggest that changing the crystal structure by changing the number of molecules of water of crystallization may lead to quite different stable radicals at 77°K. It is hoped that further studies of the effects of crystal structure on the nature of the free radicals obtained on irradiation may aid in choosing conditions under which a given desired radical might be stable.

Publication Date: January 1, 1968 | doi: 10.1021/ba-1968-0082.ch021

Table I. Production of $\cdot CH_3$ and $\cdot CH_2COO^-$ Radicals in Irradiated

Substance	*A(·CH₃)*	*g(·CH₃)*	*·CH COO⁻ Observed*
CH_3COONa	None	—	Yes
CH_3COOK	None	—	Yes
$(CH_3COO)_2Hg$	None	—	?
$(CH_3COO)_2Ag$	None	—	?
CH_3CONH_2	23.1		$\cdot CH_2CONH_2$
CH_3COONH_4	23.0	2.0028	No
$(CH_3COO)_2Ca \cdot H_2O$	23.0	2.0027	No
$(CH_3COO)_2Zn \cdot 2H_2O$	22.8	2.0027	No
$(CH_3COO)_2Pb \cdot 3H_2O$	22.5	2.0029	No
$CH_3COONa \cdot 3H_2O$	22.5	2.0028	No
$(CH_3COO)_2Mg \cdot 4H_2O$	22.5	2.0026	No

[a] All irradiations and ESR observations were at 77°K. with about the same radiation hyperfine splittings is estimated to be ±0.5 G.

Publication Date: January 1, 1968 | doi: 10.1021/ba-1968-0082.ch021

Experimental

The metal acetates were commercial reagent grade materials. Single crystals, where used, were grown from saturated aqueous solutions of the salts. Trapped radicals were produced by irradiation with the 1-Mev. beam of a General Electric resonant transformer, and crystals could be irradiated at 77°K. and observed at that temperature.

ESR spectra were taken with a Varian V-4200-10A spectrometer equipped with 100 KHz modulation. Hyperfine splittings were obtained by placing proton markers on the spectra, and *g*-values were obtained from a measurement of the klystron frequency.

Results

The ESR spectra of polycrystalline acetates irradiated and observed at 77°K. lead to the *g*-values and hyperfine splitting constants shown in Table I. Details of the analysis of the spectra, where available, are given under the heading *Comments*. The spectra for three representative crystals are shown in Figure 1.

Discussion

It may be seen (Table I and Figure 1) that the methyl radical becomes relatively more stable, and more are produced for a given dosage of radiation, as the number of molecules of water of crystallization increases. The spectra of the anhydrous acetates are too complex to interpret in detail, but both the absolute concentration and the relative amount of the methyl radical compared with other radical species must be small.

Polycrystalline Acetates and Other Crystals at 77°K.

	Comments[a]
	Principal A values are 28.5, 20, 9 *G*
	Principal A values 32, 23.6, 14.5 *G*, pattern asymmetric
	Radicals not identified, very asymmetric pattern
	Triplet observed at low microwave power
	Both radicals present
	Very asymmetric pattern, other radicals present
$\cdot CH_3$	predominates, lines saturate easily
	Also a center line at $g = 2.0024$
	Lines are 100× intensity of those for CH_3COONa

dosage and the same microwave power attenuation (15 db). The error in the proton

A detailed analysis of the single-crystal ESR spectra of sodium acetate trihydrate at 77°K. has been given (*29*); in that crystal the hyperfine interaction is nearly isotropic, with $A \cong 23$ G, presumably as a result of rapid reorientation of the methyl group about its threefold axis combined with accidental near equality of $(A_{xx} + A_{yy})$ and A_{zz} for the anisotropic C–H interactions. The radical was identified as $\cdot CH_3$ (rather than $CH_3\dot{C}OO^{2-}$) by the ^{13}C hyperfine interactions which are observed for $^{13}CH_3COONa \cdot 3H_2O$ but not for $CH_3{}^{13}COONa \cdot 3H_2O$. On this basis we assign the quartets with $A_H \cong 23$ G to $\cdot CH_3$ in all the irradiated acetates although ^{13}C substituted materials have not been examined. The methyl radical is also apparently present in irradiated acetamide and ammonium acetate although, in the absence of ^{13}C hyperfine interaction data, there is also the possibility that these quartets with $A \cong 23$ G are from radicals formed by electron attachment to a molecule of the lattice (or electron loss).

The precursor radical-ion $CH_3\dot{C}OO^{2-}$ with $A_H = 21.0$ G and $g = 2.0030$ has been reported (*10*) in irradiated sodium acetate (presumably the trihydrate, but this is not stated) at 77°K. We have thus far failed to observe a radical characterized by these parameters in either the irradiated anhydrous salt or in the trihydrate. In the latter we observed only the quartet ($A_H = 22.5$ G, $g = 2.0028$) even with γ-irradiation under conditions chosen to prevent the sample temperature from rising above 77°K. at any time. These lines almost certainly arise from the methyl radical itself since irradiation of $^{13}CH_3COONa \cdot 3H_2O$ produces a spectrum characteristic of the $^{13}CH_3$ radical (*29*).

Irradiated anhydrous sodium or potassium acetate shows a complex ESR pattern (Figure 1) with no lines owing to $\cdot CH_3$ apparent. The radicals giving the dominant lines have anisotropic hyperfine interactions,

Publication Date: January 1, 1968 | doi: 10.1021/ba-1968-0082.ch021

and the estimated principal values of the hyperfine splitting tensors, ($\pm$28.5, $\pm$20, $\pm$9 G) and ($\pm$32, $\pm$23.6, $\pm$14.5 G), are not greatly different from values typical of the proton interactions in $\cdot CH_2COO^-$. In irradiated malonic acid at 25°C. (*21*) the principal tensor components for $\cdot CH_2COO^-$ are (−32.8, −21, −13.2) and (−32.5, −19.7, −10.7), while in $CH_3COONa \cdot 3H_2O$ at room temperature the values (*31*) are ($\pm$31.3, $\pm$19.0, $\pm$8.0). On the basis of these observations the major radical present in irradiated CH_3COONa and CH_3COOK is believed to be $\cdot CH_2COO^-$.

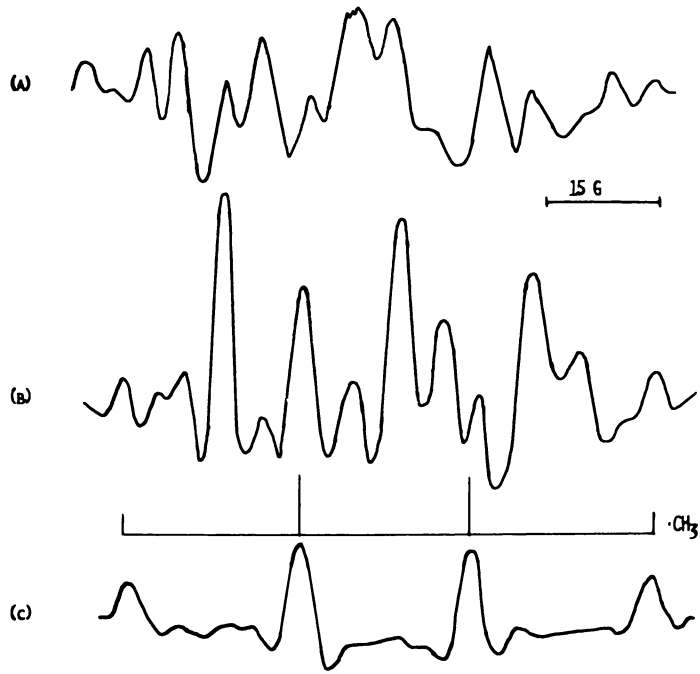

Figure 1. Second-derivative ESR spectra of polycrystalline (A) potassium acetate, (B) calcium acetate monohydrate, and (C) magnesium acetate tetrahydrate irradiated and observed at 77°K. with 15db attenuation

It appears that the methyl radical is more stable in crystals with the more open structure characteristic of two- or three-dimensional hydrogen-bonded networks. The structure of zinc acetate dihydrate, for example, is known (*37*), and the acetate ions are tied together by hydrogen bonds in two-dimensional sheets with only weak Van der Waals forces between layers. Since the formation of $\cdot CH_3$ in hydrated acetates presumably is the result of dissociation of a precursor of the type $CH_3\dot{C}OO^{2-}$, which

Publication Date: January 1, 1968 | doi: 10.1021/ba-1968-0082.ch021

would be formed from the ion by gain (or possibly loss) of an electron, the CO_2 might be more readily lost in the more open crystal structure. In the anhydrous salt abstraction of a hydrogen atom from an ion of the lattice by the precursor radical to give $\cdot CH_2COO^-$ can be postulated. Spin-flip satellites, which are displaced from the main lines by ±5.6 G, are observed for $\cdot CH_3$ in the hydrated salts; they show that the radicals interact weakly with neighboring protons. The $\cdot CH_3$ lines disappear on warming for all the crystals in which they appear and are replaced at higher temperatures by the lines of $\cdot CH_2COO^-$. We believe this change is the result of hydrogen abstraction by methyl (*31*). Strangely enough methyl radicals do not appear to be an important product of the irradiation of acetic acid itself at 77°K. (*20*).

There is also some evidence that C–C bonds may be broken in amides. The methyl radical appears to be a product of the irradiation of acetamide (Table I), and the trifluoromethyl radical has been conclusively shown to be the principal product of the irradiation of CF_3CONH_2, at 77°K. (*30*). Evidence that $\cdot CCl_3$ is the principal product of the irradiation of CCl_3CONH_2 (*31*) has also been found. Until complete single-crystal data are available for acetamide there remains a possibility that the quartet could arise from a species such as $(CH_3CONH_2)^{+ \text{ or } -}$ rather than $\cdot CH_3$; however, the molecule-ion, if present, should show extra hyperfine interactions which we do not see.

Another example of a hydrated salt which gives the stable radicals obtained from C–C bond breakage is sodium perfluorosuccinate hexahydrate. When irradiated at room temperature the principal product is $^-OOC–CF_2–\dot{C}F–COO^-$ (*28*) but at 77°K. the ESR spectrum of $\dot{C}F_2COO^-$ is also seen (*31*). In this case the magnitude of the fluorine hyperfine splitting rules out the electron attachment products such as $^-OOC–CF_2–CF_2–\dot{C}OO^{2-}$ since β-fluorine splittings are much smaller. In a detailed study of the 77°K. irradiation products of succinic acid (*8*) only the radical-ion $HOOC–CH_2–CH_2–\dot{C}OOH^-$ was mentioned. More recently it is claimed (*16*) that some of the weak lines are from $HOOC–CH_2–CH_2\cdot$, but $HOOC–CH_2\cdot$ has not been reported.

It has been shown that the nature of the stable radicals produced on irradiation of a given species, in this case acetate ion, can be influenced in an important way by the crystal structure of the host. At 77°K. the anhydrous alkali metal acetates give $\cdot CH_2COO^-$ as a principal product, but the hydrated metal acetates give $\cdot CH_3$. We conclude that the products of breaking C–C bonds are more stable in crystals with water of hydration than in anhydrous crystals and tentatively suggest that one should expect such species to be favored in crystals where hydrogen bonding is important in determining the structure. The products of the

Publication Date: January 1, 1968 | doi: 10.1021/ba-1968-0082.ch021

irradiation of acetamide, trifluoroacetamide, and sodium perfluorosuccinate hexahydrate are in agreement with this hypothesis, but much more extensive data will be needed to develop a full understanding of this subject.

Acknowledgment

This work was supported through a contract with the Atomic Energy Commission and this is AEC Document No. COO-1385-20. We are indebted to the Department of Agricultural Engineering, Michigan State University, for the irradiations.

Literature Cited

(1) Atherton, N. M., Parker, A. J., Steiner, H., *Ann. Rept. Progr. Chem. (Chem. Soc. London)* **58,** 62 (1966).
(2) Atherton, N. M., Whiffen, D. H., *Mol. Phys.* **3,** 1 (1960).
(3) *Ibid.*, **3,** 103 (1960).
(4) Atkins, P. W., Keen, N., Symons, M. C. R., *J. Chem. Soc.* **1962,** 2873.
(5) Ayscough, P. B., Collins, R. B., Dainton, F. S., *Nature* **205,** 965 (1965).
(6) Box, H. C., Freund, H. G., Budzinski, E. E., *J. Chem. Phys.* **46,** 4470 (1967).
(7) Box, H. C., Freund, H. G., Budzinski, E. E., *J. Am. Chem. Soc.* **88,** 658 (1966).
(8) Box, H. C., Freund, H. G., Lilga, K., *J. Chem. Phys.* **42,** 1471 (1965).
(9) Box, H. C., Freund, H. G., *J. Chem. Phys.* **44,** 2345 (1966).
(10) Cadena, D. G., Mendez, V., Rowlands, J. R., *Mol. Phys.* **13,** 157 (1967).
(11) Cole, T., Heller, H. C., *J. Chem. Phys.* **42,** 1668 (1965).
(12) Heller, H. C., Schlick, S., Cole, T, *J. Phys. Chem.* **71,** 97 (1967).
(13) Cook, J. B., Elliott, J. P., Wyard, S. J., *Mol. Phys.* **12,** 185 (1967).
(14) Grant, P. M., Ward, R. B., Whiffen, D. H., *J Chem. Soc.* **1958,** 4635.
(15) Jaseja, T. S., Anderson, R. S., *J. Chem. Phys.* **36,** 3727 (1962).
(16) Klinck, R. E., *Bull. Am. Phys. Soc.* **11,** 314 (1966).
(17) Lontz, R. J., *J. Chem. Phys.* **45,** 1339 (1966).
(18) Lontz, R. J., Gordy, W., *J. Chem. Phys.* **37,** 1357 (1962).
(19) Miyagawa, I., Itoh, K., *Proc. Symp. Mol. Struct. Spectr.*, Tokyo, Sept. 1962, **D-202.**
(20) Miyagawa, I., Gordy, W., *J. Am. Chem. Soc.* **83,** 1036 (1961).
(21) Morton, J. R., *Chem. Rev.* **64,** 453 (1964).
(22) Morton, J. R., *J. Am. Chem. Soc.* **86,** 2235 (1964).
(23) Collins, M. A., Whiffen, D. H., *Mol. Phys.* **10,** 317 (1966).
(24) Ovenall, D. W., Whiffen, D. H., *Mol. Phys.* **4,** 135 (1961).
(25) Pooley, D., Whiffen, D. H., *Trans. Faraday Soc.* **57,** 1445 (1961).
(26) Pooley, D., Whiffen, D. H., *Mol. Phys.* **4,** 81 (1961).
(27) Rogers, M. T., Bolte, S. J., Rao, P. S., *J. Am. Chem. Soc.* **87,** 1875 (1965).
(28) Rogers, M. T., Whiffen, D. H., *J. Chem. Phys.* **40,** 2662 (1964).
(29) Rogers, M. T., Kispert, L. D., *J. Chem. Phys.* **46,** 221 (1967).
(30) *Ibid.*, **46,** 3193 (1967).
(31) Rogers, M. T., Kispert, L. D. (unpublished results).
(32) Rogers, M. T., Kispert, L. D., *U. S. At. Energy Comm.*, AEC Document **No. COO-1385-18.**
(33) Sinclair, J. W., Hanna, M. A., *J. Phys. Chem.* **71,** 84 (1967).

(34) Srygley, F., Gordy, W., *J. Chem. Phys.* **46,** 2245 (1967).
(35) Tamura, M., Collins, M. A., Whiffen, D. H., *Trans. Faraday Soc.* **62,** 2534 (1966).
(36) Tsvetkov, Y. D., Rowlands, J. R., Whiffen, D. H., *J. Chem. Soc.* **1963,** 810.
(37) van Niekirk, J. N., Schoening, F. R. L., Talbot, J. H., *Acta Cryst.* **6,** 720 (1953).

RECEIVED January 11, 1968.

Ion Neutralization Times in the Gamma or Electron Radiolysis of Several Dielectric Liquids with Different Dielectric Constants

GORDON R. FREEMAN

University of Alberta, Edmonton, Alberta, Canada

Publication Date: January 1, 1968 | doi: 10.1021/ba-1968-0082.ch022

The recently developed nonhomogeneous kinetics model for the reaction of ions produced during radiolysis of dielectric liquids is applied to the estimation of the lifetimes of these ions in water, ethyl alcohol, acetone, and cyclohexane. Calculated lifetime spectra are given. The use of the complex dielectric constant in the calculations is discussed and found to be necessary for alcohols, but not for water, acetone, or hydrocarbons. The model predicts that the yield of ions observed at time t *after an instantaneous pulse of radiation would be about 10% greater than* G_{fi} *at 0.3 nsec. in water, 2 nsec. in ethyl alcohol, 3 nsec. in acetone, and 400 nsec. in cyclohexane. The calculated results are consistent with the limited measurements that have been published.*

A recently proposed nonhomogeneous kinetics model (*5*) has been moderately successful in the interpretation of the rates of reactions of ions produced during the γ-radiolysis of dielectric liquids. A wide range of dielectric liquids has been tested, from hydrocarbons (*5, 14, 20*) to alcohols (*16, 17*) and water (*18*). The same model explains the variation in the yield of free ions—*i.e.*, ions that have escaped geminate neutralization—from one liquid to another (*6*). The model is still in a rather crude form and has many shortcomings. Its only strength is the degree to which it provides a quantitative interpretation of experimental results.

The crudest part of the model is the discontinuous (step) function $N(y)$ used to describe the initial distribution of separation distances between the positive ions and thermalized electrons (*5, 6*). When enough

In Radiation Chemistry; Hart, E.;
Advances in Chemistry; American Chemical Society: Washington, DC, 1968.

experience has been gained with the model in its present form and with the types of experiment required to test it, a suitable continuous function will be sought to replace the function now in use. In fact, a start has already been made in that direction (*23*).

With the continuing improvement in the time resolution of pulsed radiation equipment, it should soon be possible to measure the lifetimes of a significant portion of the ions that undergo geminate neutralization. This information will be valuable in determining the distribution of ion separation distances.

In view of the moderate success of the kinetics model in its present form, it might be useful to present the radiolytic ion lifetime spectra that are predicted by the model for several different dielectric liquids. In anticipation of what follows, the very limited results of the few experiments that have attempted to measure these lifetimes [in cyclohexane (*11*) and in water (*9*)] are consistent with the present calculations. More extensive experiments are needed.

Publication Date: January 1, 1968 | doi: 10.1021/ba-1968-0082.ch022

Theory

The System. Consider the ions produced in a dielectric liquid by an instantaneous pulse of radiation:

$$A \longrightarrow [B^+ + C^-] \qquad (1)$$

(square brackets around reactants or products indicate that the species are inside a spur). The majority of ionizations in an irradiated system occur by the ejection of relatively low energy ($<10^3$ e.v.) electrons from molecules (*12*). These electrons lose their excess energy by exciting and ionizing the medium through which they pass. In a molecular dielectric liquid, when the electrons have been sufficiently de-energized they apparently become localized either by attachment to a single molecule, as probably occurs in acetone, or by interacting more or less equally with several molecules, as apparently occurs in water, ethyl alcohol, and cyclohexane, among others. This article is concerned only with the physical process of ion neutralization, so the possible occurrence of ion-molecule reactions and the precise nature of the ions B^+ and C^- are only of secondary importance (they are unimportant except insofar as they affect the charge mobilities).

The ions formed in Reaction 1 can follow two quite different paths to neutralization. The electron initially becomes localized—*i.e.*, the species C^- is formed—at a distance y from the ion B^+. The coulombic attraction between the pair of charges tends to draw them back together:

$$[B^+ + C^-] \rightarrow [\text{geminate neutralization}] \qquad (2)$$

On the other hand, random diffusive forces tend to drive them apart:

$$[B^+ + C^-] \rightarrow B^+ + C^- \text{ (free ions)} \quad (3)$$

Thus, some pairs of ions undergo geminate neutralization and others become free ions. The free ions diffuse at random in the liquid and ultimately meet other free ions from other spurs and undergo neutralization:

$$B^+ + C^- \rightarrow \text{random neutralization} \quad (4)$$

In the calculation of the ion lifetime spectrum, Reactions 2 and 4 are considered separately. Reaction 4 is assumed to obey simple second order kinetics, so it presents no problem if the fraction of the total ions that becomes free ions can be determined. The nonhomogeneous kinetics model allows one to estimate this fraction (*6*) as well as the lifetimes of the ions that undergo Reaction 2 (*5*).

The model contains many approximations which can be criticized and discussed at length. In this article, however, the approximations are simply stated and briefly commented upon.

The Approximations. First, there is only one ion pair per spur. This assumption is probably wrong for about half of the spurs. However, the error introduced by this approximation may be partly cancelled by that introduced by the next one.

Second, the $N(y)$ *vs.* y distribution—*i.e.*, the initial distribution of B^+–C^- separation distances—can be estimated by the simple method previously described (*5*). The method is very rough. However, no refined method yet exists to determine this distribution, because too little is known about such things as electron energy degradation spectra and the ranges of low energy electrons in liquids. The experimental measurement of radiolytic ion lifetimes in liquids may help to determine more accurate $N(y)$ *vs.* y distributions.

Third, the static dielectric constant of the liquid can be used. This assumption will be discussed later in this paper.

Fourth, the mobilities of the ions depend on their identities, but it is assumed that in a pure solvent the mobilities do not change after the first 10^{-12} sec. of the charge lifetimes. This assumption becomes progressively less important with increasing ion lifetime.

Ion Lifetime Calculations. The yield G_{fi} of the radiolytic ions that become free ions is given by

$$G_{fi} = \frac{\Sigma N(y) e^{-r/y}}{\Sigma N(y)} \times G_o \quad (I)$$

where G_o is the total initial ionization yield and

$$r = \xi^2/\epsilon kT \quad (II)$$

Publication Date: January 1, 1968 | doi: 10.1021/ba-1968-0082.ch022

where ξ is the charge on the electron, ϵ is the dielectric constant of the liquid, k is Boltzmann's constant and T is the absolute temperature. Equation I is solved numerically, using the appropriate $N(y)$ *vs.* y distribution (*6*).

The yield G_{gn} of the ions that undergo geminate neutralization is given by

$$G_{gn} = G_o - G_{ft} \qquad \text{(III)}$$

Consider the decrease of the number of ions in a liquid as a function of time after an instantaneous pulse of radiation. The ions that undergo geminate neutralization move together under the influence of their mutual electric field. The relative velocity v of a pair of ions with respect to each other is negative and is given by the negative product of the electric field strength between them and the sum of their mobilities:

$$v = -1.44 \times 10^{-7} (u_+ + u_-)/\epsilon r^2, \text{ cm./sec.} \qquad \text{(IV)}$$

where u_+ and u_- are the mobilities (sq. cm./volt sec.) of the positive and negative ions, respectively, and r is the distance (cm.) between the ions of a pair. The time t_{gn} required for a pair of ions to move together from their initial separation distance y is

$$t_{gn} = \int_y^{r_o} \frac{dr}{v} = \epsilon(y^3 - r_o^3)/4.32 \times 10^{-7} (u_+ + u_-), \text{ sec.} \qquad \text{(V)}$$

where the value of r_o depends on the nature of the final charge transfer step that results in neutralization. The value of r_o can be appreciably greater than zero if the final charge transfer step occurs by electron tunnelling, but in the present work it will be assumed that $r_o^3 << y^3$.

Equation V is used to convert values of y to corresponding values of t_{gn}. Thus, an $N(y)$ *vs.* y spectrum is transformed into an $N(t_{gn})$ *vs.* t_{gn} spectrum. Since a step function was used for $N(y)$ in the present work, $N(t_{gn})$ is also a step function and it is too coarse for present purposes. It is transformed into a continuous function as follows. The total number $N(t)$ of ions that survive at time t after an instantaneous pulse of radiation is given by

$$N(t) = \sum_{t_{gn}=t}^{\infty} N(t_{gn})(1 - e^{-r/\nu}) + \sum N(y) e^{-r/\nu} \qquad \text{(VI)}$$

Equation VI takes into account the formation of free ions, which have relatively long lifetimes. However, it neglects the neutralization of the free ions, which will be considered separately.

By drawing a smooth curve through a plot of $N(t)$ *vs.* t, a continuous function $n(t)$ is obtained.

Publication Date: January 1, 1968 | doi: 10.1021/ba-1968-0082.ch022

The yield of C^- ions, $G'(C^-)_t$, that would be observed spectroscopically at time t can be approximately calculated from $n(t)$ according to Equation VII.

$$G'(C^-)_t = \frac{n(t)}{n(0)} \times G(C^-)_o \qquad \text{(VII)}$$

where $n(0)$ is the number of C^- ions at $t = 0$ and $G(C^-)_o$ is the corresponding 100 e.v. yield.

The effect of neutralization of the free ions must be superimposed on Equation VII. Since the lifetimes of the free ions are greater than those of the ions that undergo geminate neutralization, this can be done as follows. Reaction 4 obeys simple second order kinetics, so the fraction $F_{fi}(t)$ of the free ions that survive at time t is given by

$$F_{fi}(t) = \frac{1}{1 + [fi]_o k_4 t} \qquad \text{(VIII)}$$

where $[fi]_o$ = initial concentration of each type of free ion B^+ and C^-

$$= \frac{G_{fi} \times \text{pulse dose (e.v./ml.)}}{6.02 \times 10^{22}}, \text{ molar} \qquad \text{(IX)}$$

If the value of k_4 has not been measured directly, it can be estimated to within a factor of about two from Equation X:

$$k_4 = 2 \times 10^{10}/\epsilon\eta, \text{ liter/mole sec.} \qquad \text{(X)}$$

where η is the viscosity, in poise, of the liquid. Equation X was deduced from data in Ref. 2, and from theoretical considerations of diffusion controlled reactions between oppositely charged ions (*3*, *4*, *5*).

The over-all lifetime spectrum of the C^- ions, based upon Reactions 1, 2, 3, and 4, is calculated from the product of Equations VII and VIII:

$$G(C^-)_t = G'(C^-)_t \cdot F_{fi}(t) \qquad \text{(XI)}$$

The value of $F_{fi}(t)$ depends upon the initial free ion concentration (*see* Equation VIII), which in turn depends on the irradiation dose delivered in the instantaneous pulse (*see* Equation IX). If such a large dose were used that $F_{fi}(t)$ became appreciably less than unity before geminate neutralization had been completed, this would indicate the occurrence of spur overlap and would alter the calculation somewhat.

It can be shown that in the liquids of interest the factor $F_{fi}(t)$ is within one percent of unity under the following conditions: for times up to 1×10^{-6} sec., doses up to 200 rad; for times only up to 1×10^{-7} sec., doses up to 2000 rad; for times up to 1×10^{-8} sec., doses up to 2×10^4 rad; and so on. The curves in Figure 1 extend from 10^{-12} to 3×10^{-6} sec.

Publication Date: January 1, 1968 | doi: 10.1021/ba-1968-0082.ch022

and it has been assumed that $F_{fi}(t)$ is unity throughout, so for a precision of one percent, the right ends of the curves apply to pulse doses less than about 100 rads.

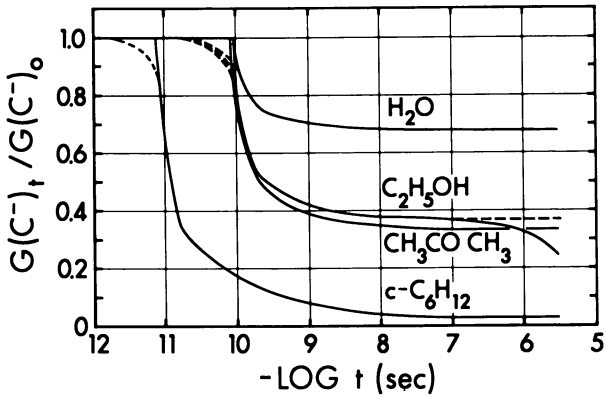

Figure 1. Calculated spectra of lifetimes of solvated electrons after an instantaneous pulse of high energy electrons or x-rays in pure water, ethyl alcohol and cyclohexane. The calculated spectrum of lifetimes of ions in acetone is also included. Liquid temperature, 20°C.; pulse dose < 100 rads. The dashed curves on the left side of the figure were drawn arbitrarily. The dashed line on the right end of the ethyl alcohol spectrum indicates the sum of (e^-_{solv} + $C_2H_5O^-$)

Figure 1 shows calculated plots of $G(C^-)_t/G(C^-)_o$ against t for the pure liquids water, ethyl alcohol, acetone, and cyclohexane. Other relevant information is listed in Table I. In pure water and pure cyclohexane the C^- ions are probably solvated electrons throughout the times shown in Figure 1. In acetone, C^- is assumed to be a negative molecular ion. In ethyl alcohol, the decomposition reaction

$$e^-_{solv} \rightarrow H + C_2H_5O^-_{solv} \qquad (5)$$

has a half-life of 5 ± 2 μsec. at room temperature (*15*), so $k_5 \approx 1.4 \times 10^5$ sec.$^{-1}$. The pure ethyl alcohol curve in Figure 1 has been drawn to account for this decay of the free ion solvated electrons; free ions continue to exist for a longer period, but their identities change from solvated electrons to ethoxide ions. To obtain the solvated electron curve, the factor $F_{fi}(t)$ in Equation XI was replaced by $F_e\text{-}(t)$, which is given by

$$F_e\text{-}(t) = e^{-k_5 t} \qquad (XII)$$

The upper end of each calculated curve contains a sharp angle because the $N(y)$ *vs.* y spectra are very crude in this region. The real life-

Publication Date: January 1, 1968 | doi: 10.1021/ba-1968-0082.ch022

Table I. Data Relevant to the Ion Lifetime Spectra

Liquid	ϵ	ρ[a]	$(u_+ + u_-)$ *(sq. cm./volt sec.)*	G_{fi}/G_o[b]
water	80	1.00	5.4×10^{-3}[d]	0.68
ethyl alcohol	25	1.19	3×10^{-3}[c]	0.37
acetone	21	1.22	3×10^{-3}[c]	0.33
cyclohexane	2.0	1.22	3×10^{-3}[c, e]	0.027

[a] Multiplication factor used to adjust the y values from those in water; *see* Ref. 6.
[b] Calculated from the model.
[c] Assumed.
[d] *See* Ref. 19.
[e] *See* Ref. 5.

time curves would probably be rounded, as indicated qualitatively by the dashed lines.

Lifetime spectra of specific types of ions in irradiated solutions could readily be calculated by the method used in the present work. Reactions that occur at times greater than about 10^{-8} sec. after the instantaneous pulse occur mainly by homogeneous kinetics. At times shorter than 10^{-8} or 10^{-9} sec., the nonhomogeneous kinetics become progressively more important (*see* Figure 1).

If the radiolytic ion is neutralized by an ionic scavenger, *e.g.*,

$$e^-_{solv} + H_3O^+ \rightarrow H_3O \rightarrow H + H_2O \qquad (6)$$

this reaction can readily be included in the kinetic treatment.

The Value of the Dielectric Constant Used in Equations II, IV, and V. The curves in Figure 1 were calculated by using the static value of the dielectric constant for each liquid. However, the dielectric constant of a medium is time dependent, because it requires a certain amount of time for the medium to attain its new polarization equilibrium after the sudden application of an electric field. In a polar liquid the permanent molecular dipoles require a certain time to rotate to line up with the electric field. When the value of t_{gn} is in the vicinity of or smaller than that of the dielectric relaxation time τ of the liquid—*i.e.*, when $t_{gn} \lesssim 10\tau$,—then a time-averaged complex dielectric constant should be used in Equations II, IV, and V. At a time t after the instantaneous application of a d.c. electric field, the dielectric constant of the medium in the field is given approximately by

$$\epsilon(t) = \epsilon_0 + \frac{\epsilon_\infty - \epsilon_0}{1 + (\tau/t)^2} \qquad (XIII)$$

where ϵ_0 is the $t = 0$ value and ϵ_∞ is the $t = \infty$ value of the dielectric constant. The equation for the real part of the complex dielectric constant in an oscillating electric field of frequency ν is

$$\epsilon'(\nu) = \epsilon_0 + \frac{\epsilon_\infty - \epsilon_0}{1 + (2\pi\nu)^2\tau^2} \qquad (XIV)$$

Publication Date: January 1, 1968 | doi: 10.1021/ba-1968-0082.ch022

To convert this equation for use at time t after the instantaneous application of a constant electric surface charge, the angular velocity $2\pi\nu$ of the oscillating field has been equated to $1/t$; hence, Equation XIII. (For discussions of complex dielectric constants *see* Refs. 1, 7, and 22).

The time averaged value of the dielectric constant, ϵ_{ave}, during the period from $t = 0$ to $t = t_{gn}$, is

$$\begin{aligned}\epsilon_{ave} &= \int_0^{t_{gn}} \epsilon(t)dt \Big/ \int_0^{t_{gn}} dt \\ &= \epsilon_\infty - (\epsilon_\infty - \epsilon_0)\left(\frac{\tau}{t_{gn}}\right)\tan^{-1}\left(\frac{t_{gn}}{\tau}\right)\end{aligned} \tag{XV}$$

It is difficult to know what value of τ to use in Equation XV. The dielectric relaxation time of a liquid is commonly determined from its microwave absorption spectrum. The energy of a microwave photon in the region of the absorption maximum, which is usually at greater than 1 cm. wavelength, is less than 1×10^{-4} e.v. This is much smaller than kT, which is 2.6×10^{-2} e.v. at 25°C. The microwaves therefore do not appreciably perturb the normal thermal agitation of the system during the measurement. However, the sudden creation of a charged species in a liquid would significantly alter the normal thermal motion of the neighboring molecules. The ion-dipole interactions would increase the speed with which the nearest-neighbor dipoles would line up with the field of the ion. This means that the ion-dipole interactions would decrease the dielectric relaxation time in the immediate vicinity of the ion.

Ethyl alcohol will be used as an example. The present discussion is especially pertinent to the radiolysis of alcohols because they have relatively long relaxation times (*8, 10, 21*).

From a plot of dielectric relaxation data in Ref. *21* it was determined that molecular rotation in liquid ethyl alcohol has an activation energy of 4.6 kcal./mole. In ethyl alcohol at 20°C., $\tau = 1.4 \times 10^{-10}$ sec. (*21*), so one can write for the unperturbed relaxation time

$$\tau_{C_2H_5OH} \approx 5.4 \times 10^{-14}\, e^{4600/RT} \tag{XVI}$$

The ion-dipole interaction exerts a torque on the dipole, which reduces the activation energy of the rotation. For randomly oriented molecules, the average torque U exerted on a molecule with dipole moment μ by a singly charged ion at a distance r through a medium of dielectric constant ϵ is roughly

$$\begin{aligned}U &= \int_0^{\pi/2} \frac{\xi\mu}{\epsilon r^2} \sin\theta\, d\theta \Big/ \int_0^{\pi/2} d\theta \\ &= 0.64\, \xi\mu/\epsilon r^2\end{aligned} \tag{XVII}$$

Publication Date: January 1, 1968 | doi: 10.1021/ba-1968-0082.ch022

where $\xi = 4.80 \times 10^{-10}$ e.s.u. It is difficult to make meaningful calculations concerning dielectrics on a molecular level, but by treating each layer of molecules around the ion separately, it appears that the rotational relaxation time of the ethyl alcohol molecules between an ion and a localized electron that are separated by 20 A. would be reduced by about an order of magnitude. In addition to the perturbation caused by U, for the molecular layers outside the first the enhanced rate of reorientation of an inner layer would collisionally increase the "effective temperature" of the adjacent outer layer. Furthermore, the effect of the field of the positive ion would enhance that of the localized electron on dipoles situated between them.

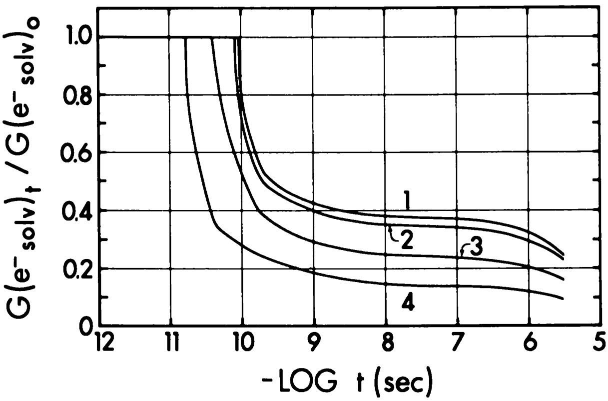

Figure 2. Effect of the assumed value of the dielectric relaxation time on the calculated spectrum of lifetimes of solvated electrons in ethyl alcohol. For Curve 1, as in Figure 1, $\epsilon = \epsilon_\infty$ was used for all values of y; *time-averaged complex dielectric constants were used for Curves 2, 3, and 4. For Curve 2, $\tau_p = 1 \times 10^{-11}$ sec.; Curve 3, $\tau_p = 3 \times 10^{-11}$ sec.; Curve 4, $\tau_{up} = 1.4 \times 10^{-10}$ sec. was used at all* y

The value of U, and hence the perturbation of the relaxation time, rapidly becomes negligible with increasing r. To simplify the calculations involving Equation XV, the unperturbed value of τ, designated τ_{up}, was used for all values of $y > 31$ A. For $y \leqslant 31$ A., a value for the perturbed τ, designated τ_p, was used. Although the appropriate value of τ_p may be an order of magnitude smaller than that of τ_{up}, the former is uncertain. Therefore, three sets of calculations were done, using different values of τ_p. Values of ϵ_{ave} were thereby calculated from Equation XV, and electron lifetime curves were calculated from Equations VI, XI, and XII. In Figure 2, Curves 2, 3, and 4 correspond to the use of $\tau_p/\tau_{up} = 0.07$, 0.2, and 1.0, respectively. Curve 1 in Figure 2 is the ethyl alcohol curve

taken from Figure 1, for which the static dielectric constant was used at all values of y.

Curves 1 and 4 in Figure 2 correspond to the upper and lower limits, respectively, of the electron lifetime spectrum in γ-irradiated ethyl alcohol, according to the present model. The true spectrum probably lies between Curves 2 and 3.

A test of the relative appropriateness of the curves in Figure 2 is the value of G_{fi} that each predicts. It appears that $G(e^-_{solv})_0 \approx 4.0$ in ethyl alcohol (*16*), so the predicted values of G_{fi} are 1.5 for Curve 1, 1.4 for Curve 2, 0.9 for 3 and 0.5 for 4. Many workers have experimentally estimated $G_{fi} = 1.0$ in ethyl alcohol, and the results of a recent, more complete, scavenger study are consistent with a value of $G_{fi} = 1.5$ (*16*). It may therefore be concluded that the lifetime spectrum lies above Curve 3, and may be in the vicinity of Curve 2.

The behavior of radiolytic ions in other liquids such as water, acetone, and cyclohexane, can be similarly treated. Equation XVI can be generalized to

$$\tau_{up} = A_\tau e^{E_\tau/RT} \qquad \text{(XVIII)}$$

Values of the constants in Equations XIII, XVII, and XVIII for water, acetone and cyclohexane at 20°C., are listed with those for ethyl alcohol in Table II.

Table II. Dielectric Data for Liquids at 20°C.

	H_2O	C_2H_5OH	CH_3COCH_3	$c\text{-}C_6H_{12}$
ϵ_0 [c]	5.2	4.3	1.90	2.02
ϵ_∞ [c]	80.4	25.1	21.2	2.02
$A_\tau(10^{-14}$ sec.) [a]	0.26	5.4	22.	—
E_τ(kcal./mole) [a]	4.8	4.6	1.9	—
μ(debye) [d]	1.84	1.69	2.75	0
$\tau_{up}(10^{-11}$ sec.) [b]	0.95	14.	0.33	—

[a] $\tau_{up} = A_\tau e^{E_\tau/RT}$. The listed values refer to temperatures between 0° and 40°C. and were derived from data in Ref. *21*.
[b] $\tau_{up} = \lambda_c/2\pi c$, where λ_c is the critical wavelength and c is the velocity of light; values of λ_c taken from Ref. *21*.
[c] *See* Ref. *21*.
[d] *See* Ref. *13*.

For cyclohexane, $\epsilon_0 = \epsilon_\infty$, so the dielectric constant is independent of time. The cyclohexane curve in Figure 1 is therefore not altered by using the complex dielectric constant.

It turns out that the water and acetone curves in Figure 1 are also not appreciably altered by the use of their respective complex dielectric constants, even if one uses τ_{up} for all ion separation distances. This is because the dielectric relaxation times of these liquids are so short that a negligible amount of ion neutralization occurs during an interval equal to τ_{up}.

Publication Date: January 1, 1968 | doi: 10.1021/ba-1968-0082.ch022

Since t_{gn} varies as $(u_+ + u_-)^{-1}$, the upper limit of the dielectric relaxation time, τ_{lim}, for which it is permissible to use ϵ_∞ at all values of y is proportional to $(u_+ + u_-)^{-1}$. To sum up, when $(u_+ + u_-) = 5 \times 10^{-3}$ sq. cm./volt sec., one may use ϵ_∞ at all values of y in liquids that have dielectric relaxation times $\leqslant 1 \times 10^{-11}$ sec., and $\tau_{lim} \alpha (u_+ + u_-)^{-1}$. When $t_{gn} < 10\tau$, the time-averaged complex dielectric constant is required; the perturbed relaxation time τ_p should be used for τ in Equation XV. The estimation of ion lifetimes in the radiolysis of ethyl alcohol, and of all alcohols, appears to require the use of the complex dielectric constant, but ϵ_∞ may be used in the calculations for water, acetone, and hydrocarbons.

Comparison of Measured and Calculated Ion Lifetimes. The yield of biphenyl or anthracene ions in cyclohexane, observed by pulse-radiolysis-absorption-spectroscopy, was 10%–20% greater at a few tenths of a microsecond than it was at 2–3 microseconds (*11*). Each of these solutes captures both positive and negative charges, so in each case the observed neutralization reaction was

$$S^+ + S^- \rightarrow \text{product} \qquad (7)$$

where S represents the solute. Thus, $(u_+ + u_-) \approx 7 \times 10^{-4}$ cm.^{2}/volt sec. (*5*). Using the present model, the calculated value of $G(S^+ + S^-)$ at 2×10^{-7} sec. is 20% higher than that at 2×10^{-6} sec., in agreement with experiment.

More recently it was observed that there was no significant decay in the yield of solvated electrons in water between 5×10^{-9} and 5×10^{-8} sec. (*9*). Time was measured from the beginning of the 3×10^{-9} sec. pulse of 3 m.e.v. electrons (pulse dose $\approx 1 \times 10^3$ rad). Within experimental error, there was no decay at times greater than 5×10^{-10} sec. (*9*). The present model predicts that there would be only one percent decay of solvated electrons in water between 5×10^{-9} and 5×10^{-8} sec., and six percent decay between 5×10^{-10} and 5×10^{-8} sec. These values are consistent with the observations.

Literature Cited

(1) Brown, W. F., "Handbuch der Physik," Vol. 17, pp. 119-121, Springer-Verlag, Berlin, 1956.
(2) Dorfman, L. M., Matheson, M. S., *Progr. Reaction Kinetics* **3**, 237 (1965).
(3) Freeman, G. R., *J. Chem. Phys.* **39**, 988 (1963).
(4) *Ibid.*, **41**, 901 (1964).
(5) Freeman, G. R., *J. Chem. Phys.* **46**, 2822 (1967).
(6) Freeman, G. R., Fayadh, J. M., *J. Chem. Phys.* **43**, 86 (1965).
(7) Fröhlich, H., "Theory of Dielectrics," p. 73, Clarendon Press, Oxford, 1949.
(8) Garg, S. K., Smyth, C. P., *J. Phys. Chem.* **69**, 1294 (1965).
(9) Hunt, J. W., Thomas, J. K., *Radiation Res.* **32**, 149 (1967).

Publication Date: January 1, 1968 | doi: 10.1021/ba-1968-0082.ch022

(10) Imanov, L. M., Mirzoev, F. G., Zul'fugarzade, K. E., *Russ. J. Phys. Chem.* **39,** 1518 (1965).
(11) Keene, J. P., Land, E. J., Swallow, A. J., *J. Am. Chem. Soc.* **87,** 5284 (1965).
(12) Lea, D. E., "Actions of Radiations on Living Cells," 2nd ed., Chap. 1, Cambridge University Press, 1955.
(13) Partington, J. R., "An Advanced Treatise on Physical Chemistry," Vol. 5, pp. 507, 522, Longmans, Green & Co., London, 1962.
(14) Robinson, M. G., Freeman, G. R., *J. Chem. Phys.* **48,** 983 (1968).
(15) Russell, J. C., Freeman, G. R., *J. Phys. Chem.* **71,** 755 (1967).
(16) *Ibid.*, **72,** 808 (1968).
(17) *Ibid.*, **72,** 816 (1968).
(18) Russell, J. C., Freeman, G. R., *J. Chem. Phys.* **48,** 90 (1968).
(19) Schmidt, K., Buck, W., *Science* **151,** 70 (1966).
(20) Stover, E. D., Freeman, G. R., *J. Chem. Phys.* (in press).
(21) "Tables of Dielectric Dispersion Data," *Nat. Bur. Std. Circ.* **589** (1958).
(22) von Hipple, A. R., "Dielectric Materials and Applications," Chap. 1, John Wiley & Sons, New York, 1954.
(23) Walker, L. G., Ph.D. Thesis, University of Alberta, 1967.

RECEIVED December 5, 1967.

Nanosecond Pulse Radiolysis of Carbon Tetrachloride

R. COOPER[1] and J. K. THOMAS

Chemistry Division, Argonne National Laboratory, Argonne, Ill. 60439

Publication Date: January 1, 1968 | doi: 10.1021/ba-1968-0082.ch023

A positive ion of CCl_4 is observed in the nanosecond pulse radiolysis of pure CCl_4. The ion which has an absorption maximum at 4750 A. where ϵ is 2.34×10^4, shows an initial rapid first order decay, $t_{1/2} = 15 \pm 2$ nsec. followed by a much slower decay over several μsec. The slow decay is 4% of the fast decay. Many solutes remove the positive ion forming solute positive ions with spectra in the visible which also exhibit a rapid and slow decay. At the same time, long-lived species are observed with absorptions towards the ultraviolet and these may be caused by Cl atom/solute complexes or free radicals.

In the γ radiolysis of glasses of carbon tetrachloride containing various solutes, the positive ions of these solutes are formed by electron transfer to the positive ion of the host, (CCl_4) (*10*). Recent experiments in the γ irradiation at 20°K. of 3-methylpentane glasses with 1 mole % of CCl_4 show that the species Cl_2^- is formed (*5*). No evidence of the positive ion of carbon tetrachloride with an absorption maximum at 4800 A. was obtained at 20°K., although this species is observed at higher temperatures (*5, 12*).

The pulse radiolysis of carbon tetrachloride and solutions of carbon tetrachloride shows that transient species are produced with absorption spectra from 3000 to 7000 A. (*3*). These species have been assigned to chlorine atom-solute charge transfer complexes (*4*). No assignment was made to positive ions as in the glassy state.

It is possible that the lifetimes of the ions are too short to be observed by conventional μsec. pulse radiolysis (*14*), but may be observed by nanosecond pulse radiolysis techniques.

[1] Present address: Chemistry Department, University of Melbourne, Australia.

In Radiation Chemistry; Hart, E.;
Advances in Chemistry; American Chemical Society: Washington, DC, 1968.

Experimental

The nanosecond pulse radiolysis technique has been described (*8*, *14*). Carbon tetrachloride was purified as follows: Matheson Research grade CCl_4 was dried over anhydrous potassium carbonate for several days, and subsequently distilled, discarding initial and final fractions. However, untreated research grade CCl_4 gave identical results to that treated as above. Zone refined naphthalene, anthracene, biphenyl, and *N,N,N′,N′*-tetramethyl-paraphenylenediamine (TMPD) were used; pyrene, 1:2 benzanthracene were recrystallized from absolute alcohol, and aniline was purified as described in an earlier paper (*6*). Normal hexane, cyclohexane, 3-methylpentane, benzene, and toluene were Matheson research grade; methanol and ethyl alcohol were analytical grade.

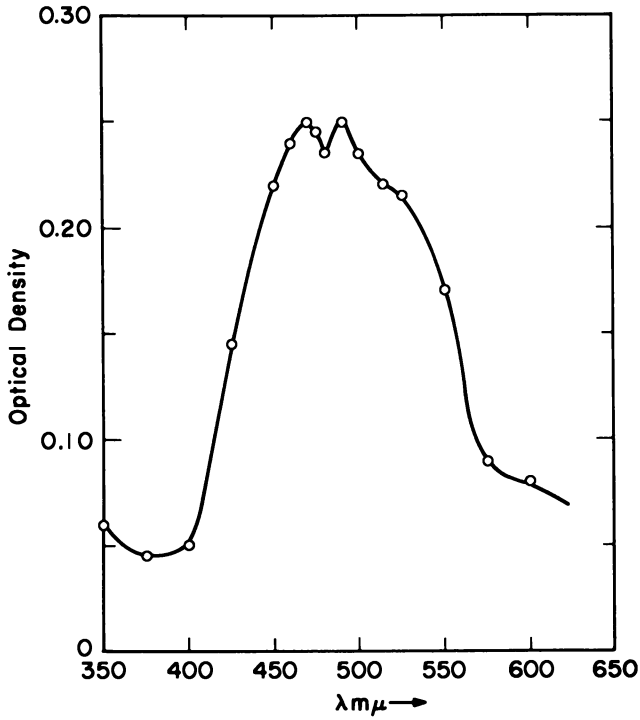

Figure 1. Spectrum in pure CCl_4

Results

Pure CCl_4. Figure 1 shows the spectrum of the species observed directly after a 12 nsec. pulse in degassed CCl_4; at 4750 A. $G\epsilon$ is measured as 1.88×10^4. The decay of the species is shown in Figure 2 and may be divided into two time periods: (a) the decay immediately following

the pulse which is first order over three half-lives with $t_{1/2} = 15 \pm 2$ nsec. and (b) a much slower decay over μsecs. The long-lived absorption has an identical spectrum to that observed directly after the pulse, showing that only one species is observed, and that it decays with two different time dependent decay modes; the amount decaying over a short period being twenty-five times greater than that decaying over the longer period.

Oxygen or nitrous oxide have no effect on this species.

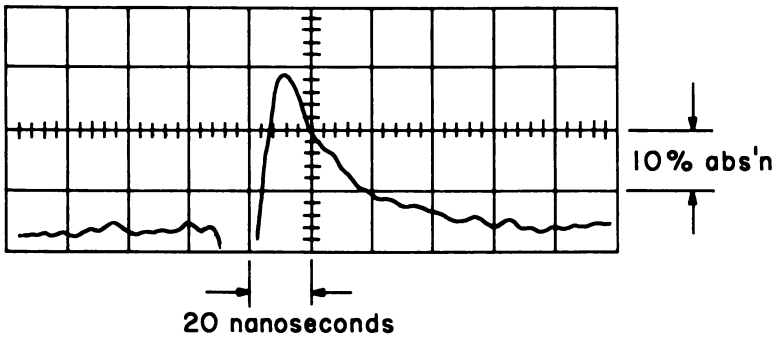

Figure 2. Decay of species at 4750 A. in pure CCl_4

Solutions of Aniline or TMPD. Adding TMPD removes the species with a spectrum shown in Figure 1, while the spectrum characteristic of $(TMPD)^+$ is produced. Similarly, aniline also removes the spectrum in Figure 1 while the $(aniline)^+$ ion is produced. This spectrum has a peak at 4100 A. and agrees well with that found for $(aniline)^+$ in water (*9*), CCl_4 glass (*11*), and pure aniline (*6*). Figure 3 shows that the decrease in the species in Figure 1 is matched by the appearance of the positive ion of aniline. This indicates that the species in Figure 1 is a positive ion: the limiting plateau yield of aniline positive ion is 0.8 at and above $10^{-2}M$ (calculated from $\epsilon = 12{,}050$ cm.^{2}/mole), and if this is equivalent to the yield of the CCl_4 positive ion then the extinction coefficient of this ion at 475 mμ is 2.34×10^4. The yield of 0.8 for CCl_4^+ is lower than that found in solid CCl_4 (*11*).

Solutes that Produce no New Intermediates. Methanol, ethyl alcohol, cyclohexene, cyclohexane, *n*-hexane, 3-methylpentane, and biacetyl also remove the absorption spectrum attributed to (CCl_4^+), but no additional new spectra are observed from 3500 to 6000 A. Millimolar concentrations of these solutes remove the long-lived portion of (CCl_4^+) while 0.1*M* of all solutes apart from cyclohexane completely removes the short and long-lived (CCl_4^+); cyclohexane 0.1*M* increases the decay rate of the positive ion. Adding 10 m*M* methanol and 20 m*M* *n*-hexane decreases the $t_{1/2}$

Publication Date: January 1, 1968 | doi: 10.1021/ba-1968-0082.ch023

of the decay of (CCl_4^+) from 15 nsec. to 12 nsec. and 11 nsec., respectively, the kinetics remaining first order. This shows that these solutes are reacting with the positive ion with rate constants of about $10^{10}M^{-1}$ sec.$^{-1}$—*i.e.*, at every collision.

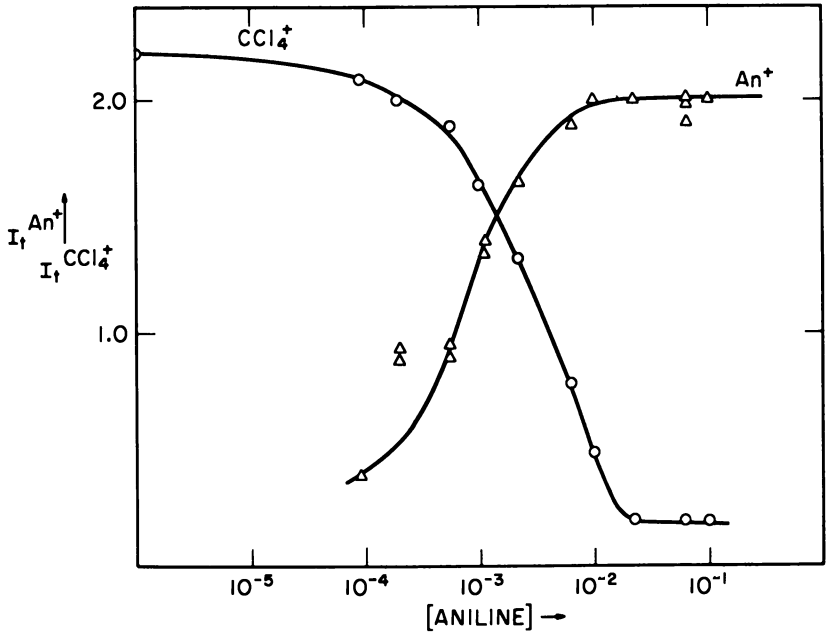

Figure 3. Yield of CCl_4^+ and (aniline)$^+$

Solutes that Produce New Intermediates. BIPHENYL. Biphenyl removes the spectrum of the positive ion of CCl_4 and produces new transitory spectra, some of which have long lifetimes (μsec.) while others are short-lived—*i.e.*, 10's of nanoseconds. Figure 4 shows the spectra of the transients produced immediately after the pulse, at 40 nsec. after the pulse, and at 500 nsec. after the pulse. The spectra at the end of the pulse and at 40 nsec. after the end of the pulse are calculated as the difference between the total absorption observed and the long-lived absorption (500 nsec.). A typical oscilloscope trace illustrates the decay of the spectrum at 5000 A.

TOLUENE AND BENZENE. Figure 5 shows the spectra produced in 0.1*M* toluene in CCl_4, the positive ion being removed by the toluene. The spectra are calculated as in Figure 4 and are shown at the end of the pulse, 40 nsec. after the end of the pulse, and at 500 nsec. after the pulse.

Publication Date: January 1, 1968 | doi: 10.1021/ba-1968-0082.ch023

Similar data is shown in Figure 6 for 0.1*M* benzene in CCl_4, the spectra are shown at the end of the pulse, and at 500 nsec. after the pulse.

ANTHRACENE AND PYRENE. Both anthracene and pyrene remove the (CCl_4^+) ion and give new transitory species shown in Figures 7 and 8. In Figure 7 the spectra are shown at the end of the pulse and at 500 nsec. after the pulse, while in Figure 8 the spectra are shown at the end of the pulse minus the long-lived absorption measured at 500 nsec., and as the long-lived absorption.

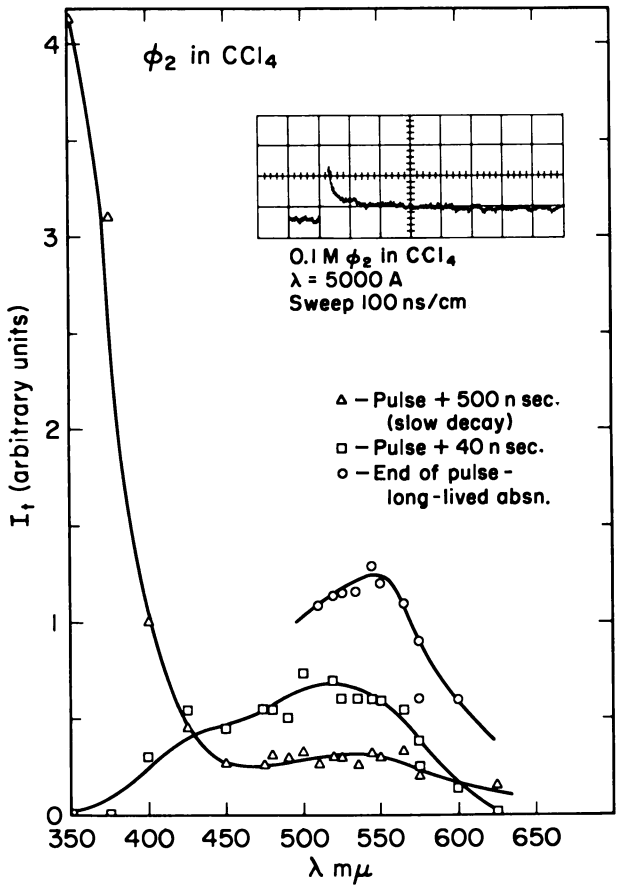

Figure 4. Spectra produced in 0.1M biphenyl, and decay of spectrum at 5000 A.

NAPHTHALENE AND 1:2 BENZANTHRACENE. Solutions of naphthalene and 1:2 benzanthracene, both of which removed the CCl_4^+ ion, showed only a long-lived transient with an absorption maximum below 4000 A.

Publication Date: January 1, 1968 | doi: 10.1021/ba-1968-0082.ch023

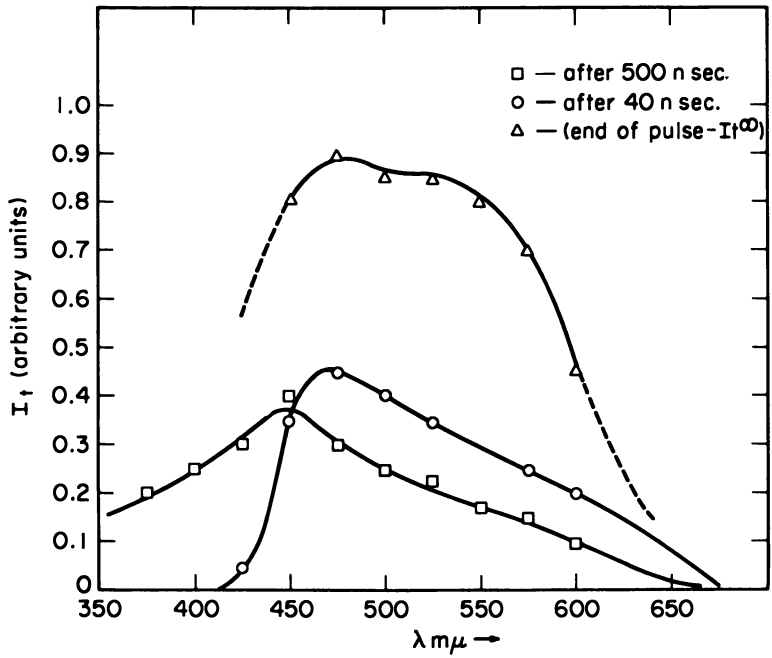

Figure 5. Spectra produced in 0.1M toluene

Discussion

The rapid and long-lived decay of the species with spectrum in Figure 1 is similar to that observed for the decay of negative and positive ions in water, alcohols, aniline, and cyclohexane (*6, 13, 14*). The removal of this species by aniline and TMPD to produce the positive ions of these solutes, confirms that this species is a positive ion. The position of the absorption maximum is similar to that observed in glasses containing CCl_4 (*7, 12*). The removal of this positive ion by all solutes of lower ionization potential than CCl_4 indicates that the positive ions of these solutes may be formed by electron transfer. It is commonly assumed that the negative ion, namely, the electron, is rapidly captured by CCl_4 giving CCl_4^-, which may decay rapidly giving Cl^- and CCl_3. The attractive force between the positive ion (CCl_4^+) and the negative ion (Cl^- or CCl_4^-) causes a rapid neutralization of the ions. The time of recombination depends on the separation of the ions, which in turn depends on the energy of the ejected electron and the rate of thermalization of the electron before capture by the CCl_4. A whole span of separations will be produced leading to a whole span of recombination times from nanoseconds to μseconds, as is observed experimentally. The resulting kinetics are

heterogeneous and it is to be expected that solute positive ions might also show a rapid decay followed by a much slower decay, as exhibited by the parent (CCl_4^+) ion. Other factors as yet unknown also influence the recombination time, for example, the recombination of the positive ions of aniline and TMPD with negative ions in C_6H_{12} is much slower than the corresponding reactions of hydrocarbon positive ions such as (biphenyl)$^+$, etc. (*6*).

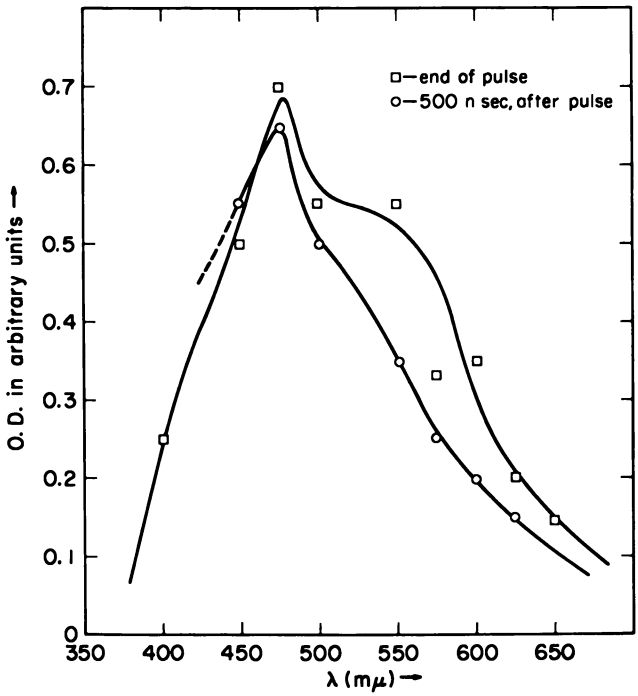

Figure 6. Spectra produced in 0.1M benzene

For biphenyl, benzene, toluene, anthracene, and pyrene, the above heterogeneous kinetic behavior was observed at 5500 A., approximately 5500 A., approximately 5500 A., 5750 A., and 6000 A., respectively. In the case of benzene this agrees quite well with the absorption maximum of 5600 A. quoted in the literature for the benzene cation (*2*). Anthracene and pyrene spectra attributed to positive ions have been observed in concentrated sulfuric at about 450 mμ for pyrene, and in the 300 mμ and 700 mμ regions for anthracene (*1*). In the irradiation of CCl_4 glasses, spectra attributed to positive ions are observed in the 500–600 mμ region for benzene and toluene and in the 600–700 mμ region for anthracene (*10*). The agreement between the sulfuric acid and CCl_4

Publication Date: January 1, 1968 | doi: 10.1021/ba-1968-0082.ch023

glass data, and the present data are satisfactory. However, in the case of biphenyl, an absorption attributed to O_2^+ is observed at 550 mμ in the present work, while the CCl_4 glass data show peaks at 350 mμ and 700 mμ (*10*).

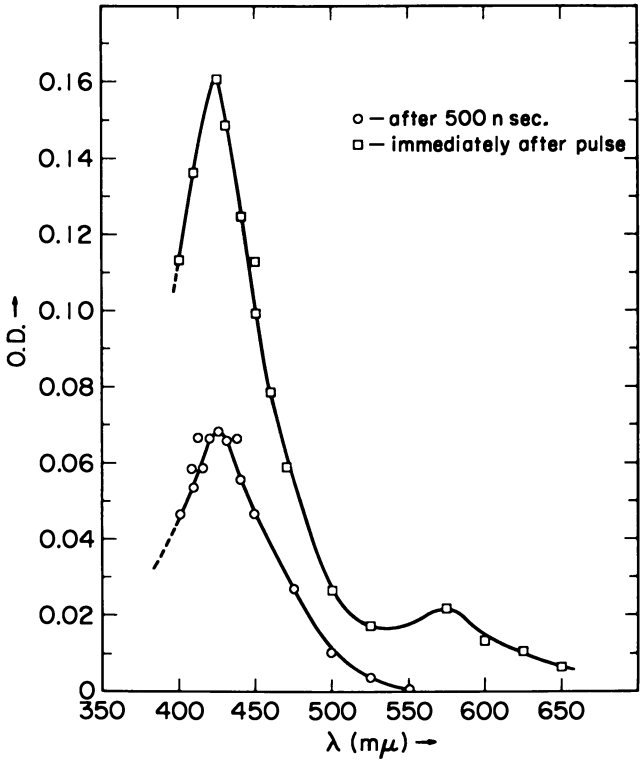

Figure 7. Spectra produced in 10mM anthracene

In all cases, a larger and much longer-lived asborption is also observed in the ultraviolet. Oxygen has no effect on these absorptions and these may be correlated in the benzene and toluene cases with the Cl-atom-solute complexes proposed by Bühler. However, with the other solutes the maxima are removed much further into the ultraviolet. For anthracene the long-lived absorption corresponds to the position of the triplet excited state, but saturating the solution with oxygen only produces a slight enhancement of the natural decay to a $t_{1/2}$ of 1.0 μsec. At this concentration of oxygen, approximately $10^{-2}M$, the quenching of anthracene triplet by the oxygen would have a $t_{1/2}$ of about 7 nsec. Hence, the longer $t_{1/2}$ that is observed indicates that the species is not a triplet state of anthracene. At lower anthracene concentrations this transient actually shows a growth after the pulse which is

Publication Date: January 1, 1968 | doi: 10.1021/ba-1968-0082.ch023

dependent on the anthracene concentration. This species may be a radical of anthracene produced by the addition of a Cl atom.

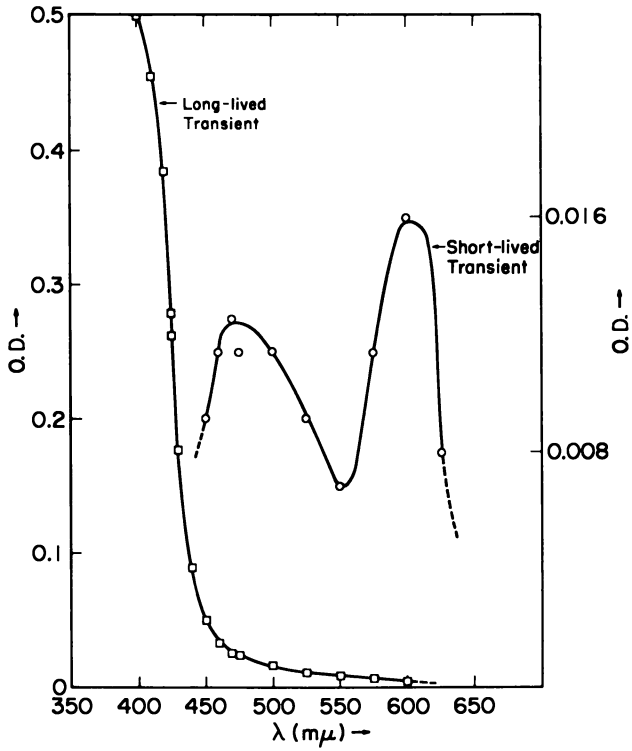

Figure 8. Spectra produced in CCl_4 saturated with pyrene

If the longer-lived species are indeed Cl atom-solute complexes, they may be formed at diffusion controlled rates with $k \sim 10^{10} M^{-1}$ sec.$^{-1}$. In the presence of 0.1*M* solute these species are observed directly after the pulse, so the Cl atoms must be formed in less than 1 nsec. The decay of the positive ion is much longer than this, and it seems that the Cl atoms are not formed by the ion-neutralization reaction.

Literature Cited

(1) Aalbersberg, W. Ij., Hoijtink, G. J., Mackor, E. L., Weijland, W. P., *J. Chem. Soc.* **3049**, 3055 (1959).
(2) Barachevskii, V. A., Terenin, A. N., *Opt. Spectr. (USSR) (English Transl.)* 17, 161 (1964).
(3) Bühler, R. E., Gäumann, T., Ebert, M., "Pulse Radiolysis," p. 279, Ebert, M., *et al.* eds., Academic Press, 1966.

(4) Bühler, R. E., Ebert, M., *Nature* **214,** 1220 (1967).
(5) Claridge, R. F. C., Iyer, R. M., Willard, J. E., *J. Phys. Chem.* **71,** 3527 (1967).
(6) Cooper, R., Thomas, J. K., in press.
(7) Guarino, J. P., Hamill, W. H., *J. Am. Chem. Soc.* **86,** 777 (1964).
(8) Hunt, J. W., Thomas, J. K., *Radiation Res.* **32,** 149 (1967).
(9) Land, E. J., Porter, G., *Trans. Faraday Soc.* **59,** 2027 (1963).
(10) Shida, T., Hamill, W. H., *J. Chem. Phys.* **44,** 2375 (1966).
(11) Shida, T., Hamill, W. H., *J. Chem. Phys.* **44,** 2369 (1966).
(12) Skelly, D. W., Hamill, W. H., *J. Phys. Chem.* **70,** 1630 (1966).
(13) Thomas, J. K., Bensasson, R. V., *J. Chem. Phys.* **46,** 4147 (1967).
(14) Thomas, J. K., Johnson, K., Klippert, T., Lowers, R., *J. Chem. Phys.*, in press.

RECEIVED January 22, 1968. This work was performed under the auspices of the U. S. Atomic Energy Commission.

Liquid-Phase Ion-Molecule Reactions: The Ion Injection Method Applied to Isobutylene

N. S. VISWANATHAN and L. KEVAN

University of Kansas, Lawrence, Kan. 66044

Publication Date: January 1, 1968 | doi: 10.1021/ba-1968-0082.ch024

tert-Butyl carbonium ion is produced by vapor phase photolysis of isobutylene with a krypton resonance lamp. The tert-$C_4H_9^+$ is separated from its concomitant electron and injected into liquid isobutylene by an electric field. Only C_8 and C_{12} products are observed; the relative C_8 and C_{12} yields are dose dependent. The C_8 products are 2,2,4-trimethylpentane (4%); 2,4,4-trimethylpentene-2 (49%); 2,2,3-trimethylpentane (19%) and 3,4,4-trimethylpentene-2 (28%). Proton transfer is the most important neutralization step but hydride transfer also occurs. The tert-$C_4H_9^+$ is vibrationally excited and reacts equally at both double-bond carbons in isobutylene. Added argon deexcites tert-$C_4H_9^+$ which then primarily reacts at the terminal double-bond carbon in isobutylene.

Reactions of specific hydrocarbon ions in the liquid phase are difficult to study directly. Ions may be produced in the liquid by direct liquid radiolysis, but the situation is complicated because many other reactive species such as electrons, radicals, and excited states are produced simultaneously. This complex situation may be simplified by producing specific ions in the vapor phase and injecting them by means of an electric field into a liquid or solid matrix. Under such conditions the positive ion is separated from its concomitant electron and is accelerated into the liquid or solid alone. We call this the ion injection method. It shows considerable promise for studying specific ion-molecule reactions in the liquid phase and should allow new types of studies on positive ion trapping in inert matrices to be made.

Here we describe a successful ion injection method for one component systems which is based on previous experiments by Schlag and Sparapany (*7*, *8*). By this method *tert*-butyl carbonium ion is formed in

In Radiation Chemistry; Hart, E.;
Advances in Chemistry; American Chemical Society: Washington, DC, 1968.

the vapor from photoionization of isobutylene. After injection into liquid isobutylene the reactions of *tert*-butyl carbonium ion with isobutylene to form C_8 and C_{12} carbonium ions have been ascertained. It has also been possible to study the effect of vibrational excitation on the reaction selectivity of *tert*-butyl carbonium ions.

Experimental Techniques

Resonance Lamps. Krypton resonance lamps were constructed of borosilicate glass as shown in Figure 1. An O-ring joint is provided to attach to the sample cell. A 2 mm. thick by 20 mm. diameter LiF window (Optovac, Inc.) was attached to each lamp with Torr-Seal (Varian Vacuum Products Division). Torr-Seal was applied so as to not be exposed to the inside of the lamp. Lamps were attached to a greaseless vacuum line used only for lamp filling and were evacuated to about 10^{-5} torr for 24 hours while being heated with heating tape to about 300°C. The lamps were then cooled and filled with about 1.0 torr of research grade krypton to provide maximum photon output (*6*) and sealed off. The lamp discharge is maintained by a 125 watt Raytheon 2450 Mc./sec. microwave generator; it is initiated with a Tesla coil. The lamp was operated with one end in a liquid nitrogen trap to remove condensable impurities.

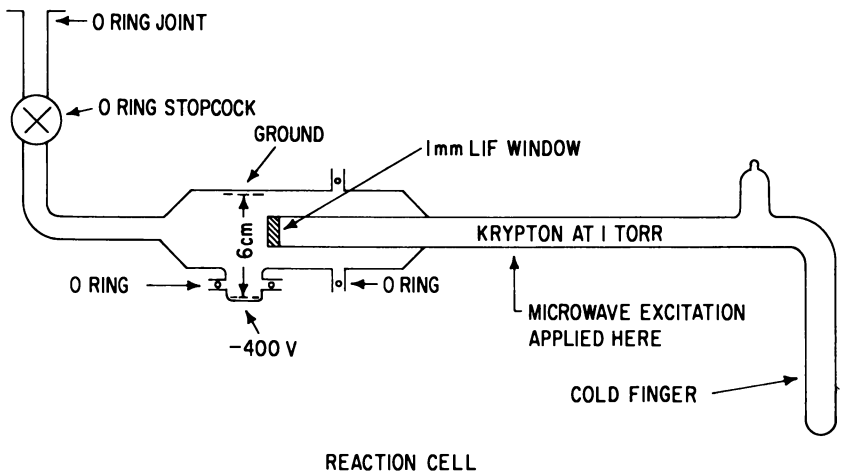

Figure 1. Right angle reaction cell and vacuum ultraviolet photolysis lamp

Under normal operating conditions about 40% of full power from the microwave generator was used. The discharge had to be in contact with the LiF window for maximum intensity (9); if not the intensity dropped by about tenfold. Good lamps lasted for 60–90 hours of operation before the impurity level increased so that the lamp would not operate.

Publication Date: January 1, 1968 | doi: 10.1021/ba-1968-0082.ch024

Current-voltage saturation curves for krypton resonance lamps were determined in a special cell with two internal rectangular (1.1 × 1.7 cm.) nickel electrodes 1.6 cm. apart. The LiF window extended between the electrodes. For 1.3 torr NO the saturation current was typically about 2.5 μamp. The lamp intensities were usually about 10^{15} quanta/sec. Lamp intensities were monitored at about 10 hour intervals of operation.

The spectral output from several used lamps was examined on a McPherson vacuum ultraviolet monochromator. Strong krypton resonance lines were observed at 1236 A. and 1165 A. with relative intensities of about 4 to 1 respectively. A number of much weaker lines at longer wavelengths were observed which were mostly attributable to H_2O. Some H_2O was apparently released from the borosilicate glass walls during the operation of the lamp. As will be seen later a weak lamp intensity at wavelengths longer than 1236 A. does not affect the ion chemistry of the isobutylene system.

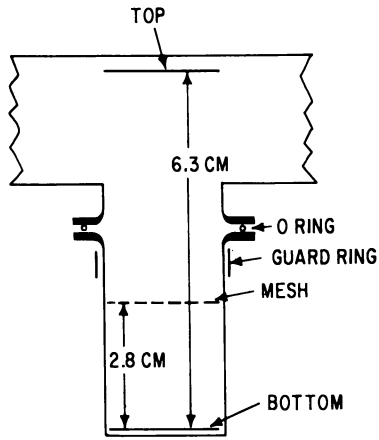

Figure 2. Electrode configuration in right angle reaction cell

Cell Designs. Several different reaction cell designs were tested. Two basic designs (right angle and direct) with various electrode configurations in each were finally used. Most of the experiments were performed in the right angle cell shown in Figure 1. O-ring joints and greaseless stopcocks were used to minimize contamination. The electrodes (1-2 sq. cm.) were made of nickel and in early experiments were attached external to the cell with Silastic RTV 731 (Dow Corning Corp.). It is interesting to note that the ion injection method will work with both electrodes external. However, to measure reaction cell characteristics the top electrode was normally internal as shown in Figure 2. The bottom electrode was also normally internal. In some experiments a mesh electrode made of electroformed nickel mesh with 85% optical transmittance

was used between the top and bottom solid nickel electrodes. The positioning of the electrodes for the right angle reaction cell is illustrated in Figure 2. A copper foil guard ring was attached externally and grounded to minimize surface leakage currents.

Sample Treatment. Research grade isobutylene (99.5 mole % purity) was used after degassing by the freeze-pump-thaw method for most experiments. The only impurity detected by gas chromatographic analysis was 0.02% isobutane. C_8 and C_{12} compounds which were used as gas chromatographic standards were obtained from the Chemical Samples Co. (Cleveland). Research grade rare gases were used.

A block diagram of the experimental set-up is shown in Figure 3. The lower part of the reaction cell which held the liquid matrix extended into a Dewar. The temperature was controlled to ±2°C. by a cooled air stream which was regulated by a differential flow controller and flowmeter. The temperature could be decreased by increasing the flow rate. The temperature was monitored by a platinum resistance probe attached to a digital readout unit (Digitec Model 531).

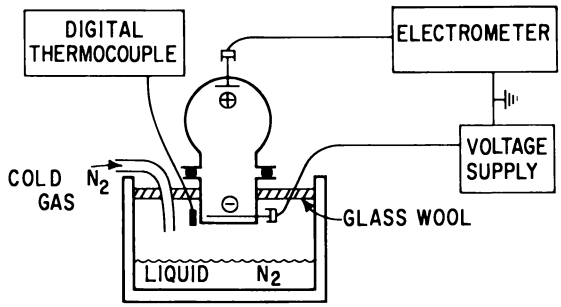

Figure 3. Experimental set-up for the ion injection method

Voltage from a Keithley 240A power supply was applied to the electrodes during photolysis and the current was monitored by a Keithley 610B electrometer. Normal experiments were carried out with a temperature of −128°C., −400 volts applied to the bottom electrode and 10^{-7} to 10^{-8} amp of current.

The experimental procedure was as follows. Isobutylene was expanded into a glass vacuum system and condensed into the reaction cell with liquid N_2. *PV* relations were used to calculate the amounts taken. Photolysis was usually carried out for 120 minutes although times as short as 30 minutes were also used. After photolysis the cell was warmed to 0°C. and the isobutylene was expanded back into a vacuum system of known volume. The remaining high molecular weight products in the reaction cell were dissolved in 1 ml. of hexane and subjected to gas chromatography.

In the experiments involving added rare gases a measured amount of isobutylene was condensed into the cell first. Then the rare gas was added (Ar at −150°C. and Ne at −196°C.) to the desired pressure.

In those experiments which incorporated a mesh electrode the mesh blocked access to the sample for gas chromatographic sampling. Therefore, the entire reaction mixture was distilled out of the reaction cell into a detachable cold finger on the vacuum line at −196°C. The isobutylene was then evacuated at 0°C., and 1 ml. hexane was added to dissolve the C_8 and C_{12} products. This procedure discriminated against complete C_{12} product recovery and invalidated C_8/C_{12} ratios. However, the relative amounts of C_8 products were still accurate.

Gas chromatography was carried out on an Aerograph Model 202 with thermal conductivity detection and helium carrier gas at 45 ml./min., and on an Aerograph Model 600D with flame ionization detection and nitrogen carrier gas at 24 ml./min. C_8 and C_{12} groups were separated at 90°C. on a 6 feet 6 inches long by 1/4 inch o.d. SE30 (25% w/w on Chromosorb W) column. C_8 products were resolved at 50°C. on a 14 feet 9 inches long by 3/16 inch o.d. SE30 (30% w/w on Chromosorb W) column and at 20°C. on a 14 feet 2 inches long by 1/4 inch o.d. $AgNO_3$/benzyl cyanide column. C_{12} products were analyzed on the same columns at 150°C. (SE30 column) and at 20°C. ($AgNO_3$ column).

For mass spectral measurements products were trapped from the gas chromatographic stream on silica sand at −196°C. The trapped samples were degassed and injected into a Nuclide 12-90G mass spectrometer for analysis.

Results

Reaction Cell Characteristics—Gas Phase. The right angle reaction cell with an applied electric field is effectively an ionization chamber. Current-voltage curves for different electrode configurations are shown in Figure 4 for 2 torr isobutylene at room temperature. Good saturation currents are achieved with internal electrodes. When the bottom electrode was external to the reaction cell, no saturation current plateau was found.

The different electrode connections are top to bottom (T-B), top to mesh (T-M) and top to mesh + bottom (T-MB). The average ion current values at −400 volts and 2 torr are 2.8, 5.8 and 7.5 μamp respectively for the different electrode connections. The mesh electrode collects a large fraction of the total current. Ideally the T-B current plus the T-M current should equal the T-MB current. The results show that the T-MB current is a little lower than expected. This is probably because of an artificially high T-M current caused by some transmitted ions being attracted back to the mesh electrode. Thus, in the T-B or T-MB connections $2.8/7.5 = 38\%$ of the ions are transmitted through the mesh electrode.

Figure 5 shows the dependence of saturation current in isobutylene *vs.* pressure in the reaction cell. The saturation current increases to a plateau at 4 torr. Above 4 torr all of the incident photons are absorbed

Publication Date: January 1, 1968 | doi: 10.1021/ba-1968-0082.ch024

by isobutylene. At pressures above 8 torr the saturation current decreases because of incomplete ion collection by the electrodes.

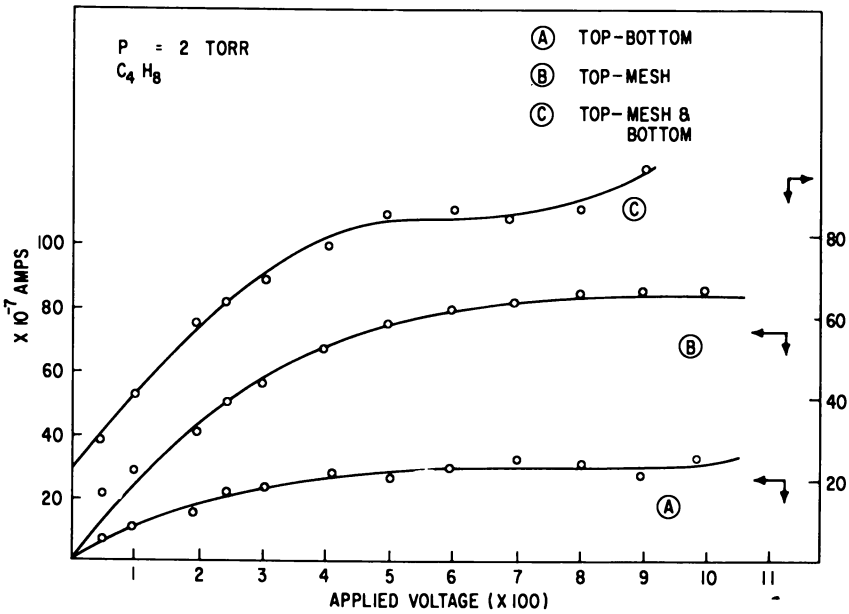

Figure 4. Current-voltage saturation curves for different electrode configurations in 2 torr isobutylene

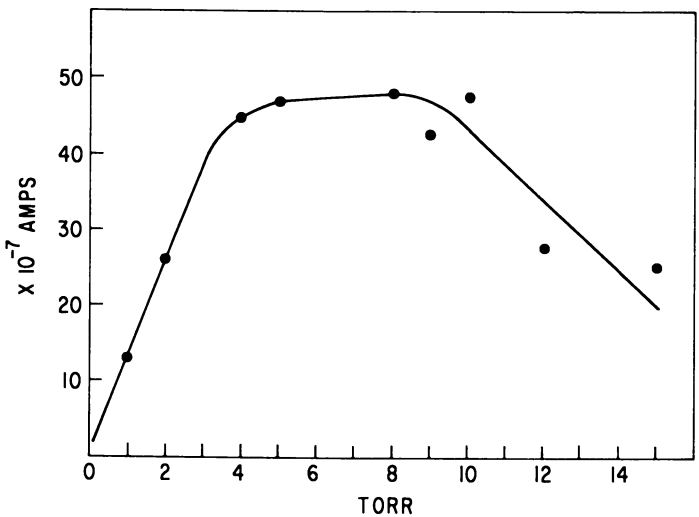

Figure 5. Saturation current vs. isobutylene pressure

Reaction Cell Characteristics—Liquid Phase. In order to determine the reaction cell characteristics under actual experimental conditions, saturation current measurements were made at −128°C. with about 1 mm. of liquid isobutylene covering the bottom electrode. The results for different electrode configurations are shown in Figure 6. Saturation current curves analogous to those for the gas phase are observed. The magnitudes of the saturation currents are 15-fold smaller in the liquid case because the vapor pressure of isobutylene at −128°C. is only 40 microns. The current magnitudes are quite similar to those observed for gaseous isobutylene at 40 microns at room temperature. Thus, the presence of an isobutylene layer over the bottom electrode has little effect on the magnitude or shape of the current-voltage curves obtained in the reaction cell. The saturation current plateau begins at about 400 volts so this voltage was chosen for most experiments.

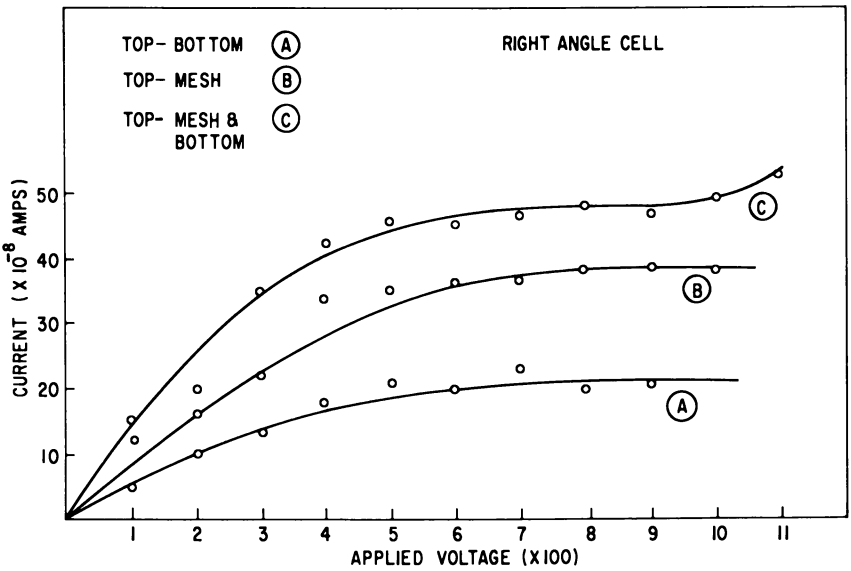

Figure 6. Current-voltage saturation curves for different electrode configurations at −128°C. with liquid isobutylene present

The sum of the saturation currents for the T-M and T-B electrode connections is about 10% greater than the saturation current for the T-MB connection. The T-B over T-MB current ratio is 41% and is taken as the percent of ions that are transmitted through the mesh electrode into the liquid. This percentage is the same as found for the all gas system and indicates that essentially all ions injected into the liquid are collected at the bottom electrode. Therefore, the bottom electrode can be used

just as reliably as the mesh electrode to monitor the number of ions injected into the liquid. The remaining purpose of the mesh electrode is to provide a field-free region between the mesh and bottom electrodes for the T-MB connection. It was found that the presence of a field-free region did not affect the product distribution and that it lowered the total product yield by the fraction of ions collected on the mesh electrode. Thus, a mesh electrode was only in place for part of the experiments.

Product Identification. Gas chromatography showed that C_8 and C_{12} compounds comprised all detectable products. No products between C_8 and C_{12} were observed. A careful search was made for C_{16} compounds but none could definitely be detected. Material balance calculations showed indeed that the C_8 and C_{12} compounds detected constituted over 95% of the reacted isobutylene. It seems that all important products were detected and that C_{16} products, if present, are minor.

The C_8 products were analyzed on a $AgNO_3$/benzyl cyanide column which discriminates between alkenes and alkanes, and on a SE-30 column which discriminates according to boiling point. These two columns clearly distinguish the alkenes from the alkanes. The products were identified by retention time comparison on both columns with C_8 standards (Table I). Identification of the more abundant olefins was confirmed by mass spectrometry.

Table I. Gas Chromatographic Retention Times of C_8 Products from *tert*-$C_4H_9^+$ Reaction with Liquid Isobutylene

	Retention Time[a]	
Product	*SE-30 Column 50°C.*	*$AgNO_3$ Column 20°C.*
2,2,4-Trimethylpentane	19.7 min.	7.8 min.
2,4,4-Trimethylpentene-1	23.7 min.	12.0 min.
2,4,4-Trimethylpentene-2	27.8 min.	11.8 min.
2,2,3-Trimethylpentane	30.3 min.	10.0 min.
3,4,4-Trimethylpentene-2	35.8 min.	15.0 min.

[a] ±0.3 min.

Since the amount of 2,4,4-trimethylpentene-1 was only 5% of the amount of 2,4,4-trimethylpentene-2, resolution was not normally achieved. The relative C_8 yields at 120 minutes of photolysis at −128°C. are given in Table III. It will be seen that the individual C_8 isomers reveal the probable structure of the C_8 carbonium ions and how they are neutralized. The relative C_8 yields are only slightly dependent on dose (*see* the section on dose effects).

The C_{12} products were not resolved into separate isomers or clearly identified. The gas chromatographic retention times for the C_{12} peak

Publication Date: January 1, 1968 | doi: 10.1021/ba-1968-0082.ch024

and several known standards are shown in Table II. On a $AgNO_3$ column *n*-alkanes have longer retention times than isomeric branched alkanes. Furthermore, highly branched alkenes have shorter retention times than linear alkenes. Therefore, the C_{12} product seems to consist of one or more highly branched alkenes.

Table II. Gas Chromatographic Retention Times of Standards and C_{12} Products from *tert*-$C_4H_9^+$ Reaction with Liquid Isobutylene

	Retention Time	
Compound	*$AgNO_3$ Column 20°C.*	*SE-30 Column 150°C.*
2-Dodecene	126 min.	49 min.
Methylundecene-2	118 min.	—
Dodecane	94 min.	—
C_{12} product	104 min.	37 min.

Table III. Phase and Temperature (Vapor Pressure) Effects on C_8 Products from *tert*-$C_4H_9^+$ Reaction with Isobutylene

Vapor Pressure (Microns)	*Temp. (°C.)*	*Percent C_8 in Products*[a]	*224-TMP*[b] *(% of C_8)*	*244-TMP-2*[c] *(% of C_8)*	*223-TMP*[d] *(% of C_8)*	*344-TMP-2*[e] *(% of C_8)*
540	−110	75	4	49	20	27
280	−115	70	4	52	16	28
140	−120	74	5	49	17	29
80	−124	73	5	50	18	27
40	−128	76	4	49	19	28
6	−138	76	5	60	14	21
4	−140[f]	80	6	84	4	6
1	−145[g]	91	7	84	3	6

[a] 120 min. photolysis time.
[b] 2,2,4-trimethylpentane, ± 1%.
[c] 2,4,4-trimethylpentene-2, ± 4% (includes 2,4,4-trimethylpentene-1 to about 5%).
[d] 2,2,3-trimethylpentane, ± 2%.
[e] 3,4,4-trimethylpentene-2, ± 3%.
[f] Freezing point.
[g] Solid.

Dose Effects. The percent conversion of isobutylene is linear to at least 120 minutes of photolysis time (Figure 7). The conversion rate is typically 0.01%/min. The relative amounts of C_8 and C_{12} products change with photolysis time (Figure 8). Thus, the C_{12} products seem to be secondary in nature. This observation is consistent with the absence of observable amounts of C_{16} products. The relative yields of C_8 products change only slightly with dose. At longer doses the total percentage of C_8 alkenes drops by a few percent.

Publication Date: January 1, 1968 | doi: 10.1021/ba-1968-0082.ch024

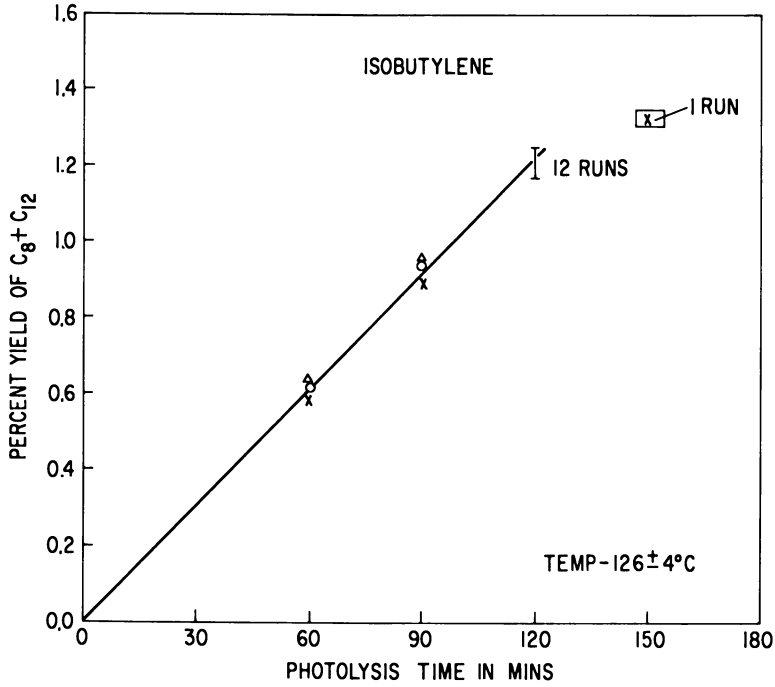

Figure 7. Isobutylene conversion vs. *krypton resonance photolysis time*

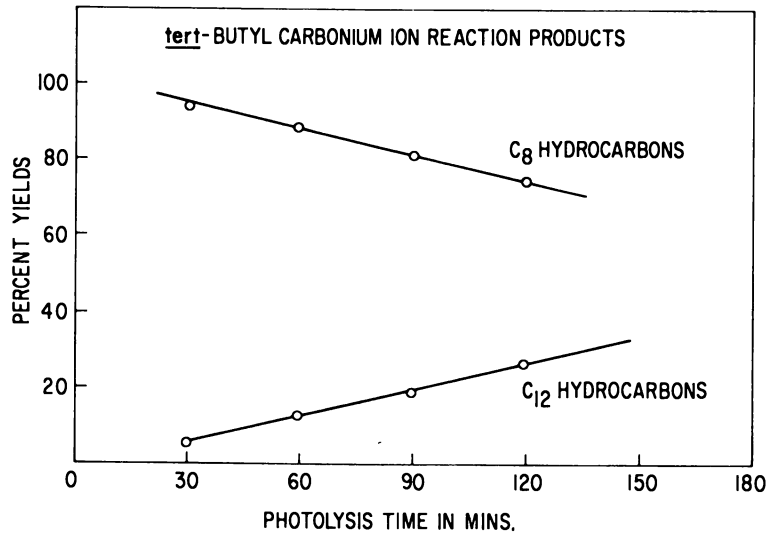

Figure 8. Relative C_8 and C_{12} product yields from isobutylene vs. *krypton resonance photolysis time*

Reversed Field Experiments. The experiments are normally performed with a negative voltage applied to the bottom electrode to inject positive ions into the liquid. When the field is reversed and +400 volts are applied to the top electrode so that positive ions are not injected into the liquid, no C_8 or C_{12} products were found. Very low yields of isobutylene fragmentation products were observed but were not measured quantitatively. The C_8 yields, observed in normal field experiments, were 20–100 times greater than these yields. PV measurements showed that the total isobutylene decomposition for the reversed field (+400 volts at top electrode) was only about 5% of the decomposition for the normal field (−400 volts at bottom electrode). These reversed field experiments support the contention that the C_8 and C_{12} products are formed from positive ions in the liquid phase.

Table IV. Effect of Added Argon and Neon on C_8 Products from *tert*-$C_4H_9^+$ Reaction with Liquid Isobutylene[a]

Added Gas		*C_8 Product Distribution (%)*[b]			
Type	*Pressure (torr)*	*224-TMP*[c]	*244-TMP-2*[d]	*223-TMP*[e]	*344-TMP-2*[f]
None		4	49	19	28
Ar	0.05	4	55	16	25
Ar	0.10	4	59	14	23
Ar	0.20	3	62	13	22
Ar	0.50	3	67	12	18
Ar	1.0	4	65	11	18
Ar	2.0	4	71	10	15
Ar	3.0	4	76	7	13
Ar	5.0	5	76	8	11
Ar	10.0	4	78	8	10
Ar	12.0	4	77	7	12
Ar	15.0	5	76	8	11
Ne	1.0	5	52	17	26
Ne	2.0	5	55	15	25
Ne	5.0	4	51	17	28
Ne	10.0	4	49	18	29

[a] Conditions: −400 volts, 120 minutes photolysis, −128°C. (0.04 torr isobutylene).
[b] Relative C_8 yield and C_8/C_{12} ratio is constant for all experiments.
[c] 2,2,4-trimethylpentane, ± 1%.
[d] 2,4,4-trimethylpentene-2, ± 4% (includes 2,4,4-trimethylpentene-1 to about 5%).
[e] 2,2,3-trimethylpentane, ± 2%.
[f] 3,4,4-trimethylpentene-2, ± 2%.

Applied Field Dependence. The magnitude of the applied voltage is expected to change the energy of the positive ions striking the liquid. The applied voltage was varied from −100 to −1200 volts at the bottom electrode. No change was seen in the relative yields of C_8 to C_{12} products or in the distribution among the C_8 products. Above −400 volts the total

yield of products was also constant. So in the voltage range investigated no applied field effects are observable.

Gas Phase Photolysis. Two experiments were performed in the gas phase at 23°C. at a pressure of 5 torr isobutylene, 120 minute photolysis time and −400 volts applied field. No C_8 or C_{12} products were observed.

Temperature and Phase Effects. As the liquid temperature of isobutylene is lowered, the vapor pressure is decreased. The freezing point of isobutylene is −140°C. Table III shows the effects of temperature and phase on the percentage of C_8 products and on the C_8 product distribution. The apparent decrease in the percentage of C_8 products is artificial; the decrease simply corresponds to a lower conversion of isobutylene and does not reflect a phase effect. The C_8 product distribution remains about constant from −110° to −128°C. At lower liquid temperatures and in the solid phase the percentage of C_8 products with a 2,2,4-structure increases with respect to the C_8 products with a 2,2,3-structure.

Added Rare Gases. Added rare gases can collide with the gas phase ions and de-excite any excited ions. The effect of added argon and neon on the C_8 product distribution is shown as a function of rare gas pressure in Table IV. Krypton was not used because it would absorb the photons from the krypton resonance lamp. Neon has little effect on the C_8 product distribution, but argon causes the C_8 products with a 2,2,4-structure to increase relative to the C_8 products with a 2,2,3-structure.

Publication Date: January 1, 1968 | doi: 10.1021/ba-1968-0082.ch024

Discussion

Nature of Ion Injected into Liquid Isobutylene. The krypton resonance lamp emits photons at 1236 A. (10.0 e.v.) and 1165 A. (10.6 e.v.) with relative intensities of 1.00 and 0.28 respectively (*5*). The ionization potential of isobutylene is 9.4 e.v., and the lowest appearance potential for a fragment ion from isobutylene is 11.3 e.v. ($C_4H_7^+$) (*1*). Therefore, the only ion produced is the parent $C_4H_8^+$.

Several mass spectrometric examinations of ion-molecule reactions in isobutylene have been carried out (*2, 4, 10*). Reaction 1 constitutes 76% of the total cross section; the secondary ions $C_4H_7^+$ and $C_5H_9^+$ each

$$C_4H_8^+ + C_4H_8 = C_4H_9^+ + C_4H_7 \qquad (1)$$

constitute about 12% of the total cross section (*4*). The $C_4H_9^+$ ion is considered to have the tertiary butyl cation structure because of its great stability.

The $C_4H_8^+$ will be formed about 5 cm. above the liquid isobutylene in an electric field of 60 volts/cm. at 400 volts applied so on the average it will take 2×10^{-6} sec. to reach the liquid. The vapor pressure of isobutylene at −128°C. is 0.04 torr; at this pressure collisions occur about

every 2×10^{-6} sec. Hence, the $C_4H_8^+$ ion will make about one collision before reaching the liquid which will allow Reaction 1 to occur.

The cross section for Reaction 1 is undoubtedly dependent on the kinetic energy of $C_4H_8^+$. However, the liquid phase products show no applied field effect between 100–1200 volts and are characteristic of $C_4H_9^+$ reactions. We conclude that most of the ions striking the liquid are *tert*-$C_4H_9^+$. There may also be small amounts of $C_4H_8^+$, $C_4H_7^+$, and $C_5H_9^+$.

Reactions of *tert*-$C_4H_9^+$. The major product of *tert*-$C_4H_9^+$ in liquid isobutylene is 2,4,4-trimethylpentene-2. *tert*-$C_4H_9^+$ can react with the two double-bonded carbons in iso-C_4H_8. The reaction with the terminal carbon in isobutylene is shown in Reaction 2. This reaction is estimated to be

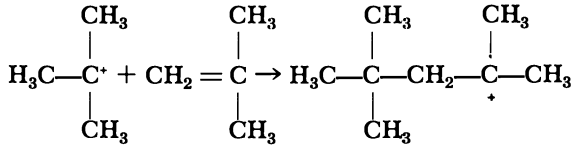

(2)

about 15 kcal./mole exothermic from extrapolated heats of formation, and it gives the correct carbon skeleton for the major product. There are two basic neutralization reactions for C_8 carbonium ions: one is hydride transfer to the carbonium ion to yield an alkane plus $C_4H_7^+$ and the other is proton transfer from the carbonium ion to give an alkene plus $C_4H_9^+$. It is also possible that proton transfer occurs to trace amounts of water. Both the 2,2,4-alkene and alkane are observed; their relative abundances show that proton transfer predominates by 10:1.

An alternative possibility for alkane formation is neutralization of the C_8 ion on the internal electrode, followed by H abstraction to produce an alkane. However, the alkane/alkene ratio is the same for internal or external bottom electrodes.

The other two C_8 products indicate somewhat surprisingly that *tert*-$C_4H_9^+$ also reacts at the tertiary carbon is isobutylene. This yields the 2,2,3,3-tetramethylbutyl primary carbonium ion shown in Reaction 3.

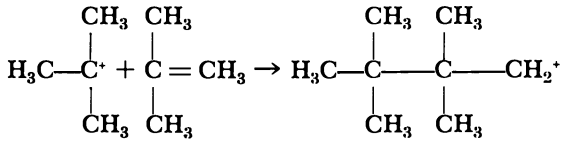

(3)

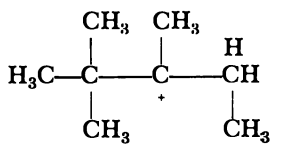

(4)

Publication Date: January 1, 1968 | doi: 10.1021/ba-1968-0082.ch024

Primary carbonium ions as in Reaction 3 are expected to rearrange rapidly as in Reaction 4 to give the tertiary 2,2,3-trimethylpentyl structure because the tertiary carbonium ion is so much more stable. Proton transfer from and hydride transfer to this carbonium ion lead to the observed 3,4,4-alkene and 2,2,3-alkane respectively. For this carbonium ion the results show that proton transfer again predominates, but only by 2:1.

The principal neutralization reaction to form C_8 products from both carbonium ions is proton transfer. The proton transfer Reaction 5 is

$$tert\text{-}C_8H_{17}^+ + i\text{-}C_4H_8 \rightarrow tert\text{-}C_4H_9^+ + tert\text{-}C_8H_{16} \quad (5)$$

estimated to be exothermic by a few kcal./mole. This exothermicity arises from the conversion of an iso-C_4 olefin to a *tert*-C_8 olefin; the greater branching in the tertiary structure lowers its heat of formation compared with a secondary structure. Reaction 5 produces a chain reaction. Non-chain propagating neutralization can take place by reaction at the walls, at the electrode, to form alkane, or with trace water impurities.

It is striking that the total reactivity of *tert*-$C_4H_9^+$ at both the primary and tertiary carbons in isobutylene is about 50%. Since *tert*-$C_4H_9^+$ shows so little selectivity in this situation it was suggested that it was vibrationally excited (*11*). Evidence supporting this supposition is discussed later.

The C_{12} products have not been characterized as completely as the C_8 products. Reactions 6 and 7 are both possible pathways to C_{12} formation.

$$tert\text{-}C_8H_{17}^+ + i\text{-}C_4H_8 \rightarrow tert\text{-}C_{12}H_{25}^+ \quad (6)$$

$$tert\text{-}C_4H_9^+ + tert\text{-}C_8H_{16} \rightarrow tert\text{-}C_{12}H_{25}^+ \quad (7)$$

The retention time data on a $AgNO_3$/benzyl cyanide gas chromatographic column suggests that only C_{12} olefins are formed. Thus, proton transfer seems to predominate as the neutralization reaction. Since no resolution of the C_{12} gas chromatographic peak has been obtained, it is possible that the C_{12} product is largely one compound. In Reaction 6 it is expected that the *tert*-$C_8H_{17}^+$ ion will be a thermal ion since it is formed in the liquid, and that it will react preferentially at the terminal carbon of isobutylene to give one olefinic product. However, in Reaction 7 *tert*-$C_4H_9^+$ is vibrationally excited (*see* last section of Discussion) and should react at both double-bond carbons in C_8H_{16} to give two olefinic products. The dose effects discussed in the next section do not clearly distinguish between Reactions 6 and 7 since *tert*-$C_8H_{17}^+$ can be formed from *tert*-C_8H_{16} by proton transfer. Both Reactions 6 and 7 are estimated to be exothermic reactions by about 15 and 7 kcal./mole respectively. On the basis of existing evidence either or both Reactions 6 and 7 contribute to C_{12} formation.

Publication Date: January 1, 1968 | doi: 10.1021/ba-1968-0082.ch024

Dose Effects on Molecular Weight. A dose effect is clearly exhibited in Figure 8. As the photolysis time increases the percent of C_8 products decreases linearly while the percent of C_{12} products increases linearly. The C_8's extrapolate to 100%, and the C_{12}'s extrapolate to 0% at 10 minutes of photolysis time. The data do not guarantee that 10 minutes of photolysis time is significantly different from 0 minutes, but they do indicate that an induction period is present before the dose dependence of the product yields begins. The relative rise of C_{12} products together with the decrease in C_8 products can be explained by Reaction 7 or by Reaction 8. The relationship shown in Figure 8

$$tert\text{-}C_{12}H_{25}^{+} + tert\text{-}C_8H_{16} \rightarrow tert\text{-}C_8H_{17}^{+} + tert\text{-}C_{12}H_{24} \qquad (8)$$

indicates that low concentrations of *tert*-C_8H_{16} can compete with *i*-C_4H_8 for carbonium ions. Similar dose effects are noted in the ionic polymerization of irradiated ethylene in the solid phase (*12*).

Evidence for Excited *tert*-$C_4H_9^+$. Vibrationally excited ions exhibit less selectivity in their reactions than thermal ions. Ions produced in the liquid phase are expected to be thermalized rapidly at the time of formation. However, vibrationally excited ions are commonly produced in the gas phase both by electron or photon impact and by ion-molecule reactions. In the ion injection method ions are produced in the gas phase and injected into the liquid. Thus, the possibility arises for injecting excited ions into the liquid and for examining whether excited ions will show reactive selectivity in the liquid phase. The formation and reaction of *tert*-$C_4H_9^+$ in isobutylene by the ion injection method illustrate these possibilities.

The C_8 reaction products in Table III illustrate that *tert*-$C_4H_9^+$ reacts nonselectivity at both the primary and tertiary carbons in isobutylene. *tert*-$C_4H_9^+$ is formed by Reaction 1 which is estimated to be 10–20 kcal./mole exothermic in the gas phase. It is postulated that vibrationally excited *tert*-$C_4H_9^+$ is formed in the gas phase and exhibits this by nonselective reactivity in the liquid phase. Two independent sets of experiments support this. When *tert*-$C_4H_9^+$ is de-excited in the gas phase by collisions with added argon, its reaction selectivity towards liquid isobutylene increases. When Reaction 1 takes place in the liquid phase, nonexcited *tert*-$C_4H_9^+$ is formed which exhibits considerable reaction selectivity towards 2-butene.

The reaction selectivity of *tert*-$C_4H_9^+$ can be measured quantitatively from the C_8 products. The percent of 2,2,4-trimethylpentane plus 2,4,4-trimethylpentene-2 represents the percentage of attack of *tert*-$C_4H_9^+$ at the primary double-bond carbon in isobutylene. And the percent of 2,3,3-trimethylpentane plus 3,4,4-trimethylpentene-2 represents the percentage of attack of tert-$C_4H_9^+$ at the tertiary double-bond carbon in

Publication Date: January 1, 1968 | doi: 10.1021/ba-1968-0082.ch024

isobutylene. Thermal ions preferentially attack at the primary double-bond carbon.

Argon and neon were tested as de-exciters for *tert*-$C_4H_9^+$. Both can de-excite vibrational levels of molecules as well as act as moderators for translational energy (3). Table IV shows that reaction selectivity for the primary carbon increases from 53% with no added argon to 76% with 3 torr and above added argon. However, from 1 to 10 torr of neon shows no effect on the C_8 distribution. If neon and argon were acting entirely as translational energy moderators 3 torr Ar would be equivalent to 4.5 torr neon.

The absence of ion translational energy effects on the C_8 distribution is also indicated by the lack of an applied field effect. We conclude that vibrational de-excitation is occurring and that argon is much more effective for vibrational de-excitaton than is neon. Such a large difference in vibrational deactivation efficiency between neon and argon is somewhat surprising. However, deactivation of ions may be more sensitive to polarizability effects than is deactivation of neutral molecules.

The de-excitation experiments were done at a liquid isobutylene temperature of −128°C. where the vapor pressure is 0.04 torr. $C_4H_9^+$ makes 1–2 collisions before reaching the liquid at this pressure. Maximum effective de-excitation by argon occurs at 3–4 torr which means that about 100 collisions of $C_4H_9^+$ with argon are necessary for maximum reaction selectivity. The selectivity of de-excited $C_4H_9^+$ never rises above 78% whereas percentages approaching 90–100% are expected. The limiting observed value of 78% may be caused by those $C_4H_9^+$ ions that are formed in a narrow layer above the liquid and are not de-excited before being injected.

Table III shows that the reaction selectivity of *tert*-$C_4H_9^+$ can also be increased by lowering the liquid temperature. Lowering the temperature lowers the isobutylene vapor pressure. At 0.04 torr and above $C_4H_8^+$ makes one or more gas-phase collisions with isobutylene to form vibrationally excited *tert*-$C_4H_9^+$. However, below 0.04 torr more and more of the $C_4H_8^+$ ions are directly injected into the liquid. Reaction 1 then occurs in the liquid phase and the product *tert*-$C_4H_9^+$ ion is vibrationally de-excited. At vapor pressures of only 0.004 torr the reaction selectivity reaches 90%. This suggests that thermal energy *tert*-$C_4H_9^+$ ions are indeed quite selective in their reaction with isobutylene. In fact, 2,4,4-trimethylpentene-2 accounts for 84% of all the C_8 products.

Acknowledgment

This research was supported by the Air Force Rocket Propulsion Laboratory. We thank R. Koob for help with lamp evaluation, J. Futrell

for the mesh electrode suggestion, and S. Lipsky for use of a vacuum ultraviolet monochromator.

Literature Cited

(1) Field, F. H., Franklin, J. L., "Electron Impact Phenomena," Table 45, Academic Press, New York, 1957.
(2) Fuchs, R., Z. *Naturforsch* **16a,** 1026 (1961).
(3) Kondrat'ev, V. N., "Chemical Kinetics of Gas Reactions," Chap. 6, Addison-Wesley Inc., Reading, Mass., 1964.
(4) Koyano, I., *J. Chem..Phys.* **45,** 706 (1966).
(5) McNesby, J. R., Okabe, H., "Advances in Photochemistry," p. 157, Vol. 3, W. A. Noyes, G. S. Hammond, J. N. Pitts, eds., Wiley Interscience, New York, 1964.
(6) Okabe, H., *J. Opt. Soc. Am.* **54,** 478 (1965).
(7) Schlag, E. W., Sparapany, J. J., *J. Am. Chem. Soc.* **86,** 1875 (1964).
(8) Sparapany, J. J., *J. Am. Chem. Soc.* **88,** 1357 (1966).
(9) Stief, L. J., Mataloni, R. J., *Appl. Opt.* **4,** 1674 (1965).
(10) Talroze, V. L., Lyubimova, A. K., *Dokl. Acad. Nauk. SSSR* **86,** 909 (1952).
(11) Viswanathan, N. S., Kevan, L., *J. Am. Chem. Soc.* **89,** 2482 (1967).
(12) Wagner, C. D., *J. Phys. Chem.* **66,** 1158 (1962).

RECEIVED January 8, 1968.

25

Rate Constants and Equilibrium Constants for Electron Transfer Reactions of Aromatic Molecules in Solution

SHIGEYOSHI ARAI and LEON M. DORFMAN

The Ohio State University, Columbus, Ohio 43210

Publication Date: January 1, 1968 | doi: 10.1021/ba-1968-0082.ch025

Absolute rate constants for electron transfer reactions of aromatic molecules in solution have been determined by the pulse radiolysis method for three additional pairs of aromatic compounds. In two of these cases in which an electron transfer equilibrium is established, the rate constant for the back reaction has also been determined. The equilibrium constant has been estimated from the kinetic data. A correlation of the experimental rate constants with the theory for homogeneous electron transfer rates is considered.

Absolute rate constants for electron transfer reactions of some aromatic molecules in solution have been reported in our earlier work (*2*) using the pulse radiolysis method. The transfer of an electron from various radical anions to a second aromatic compound in solution was observed directly. Of the rate constants for nine donor-acceptor pairs investigated, two were found to be lower than the diffusion controlled values, and a correlation with such parameters as the reduction potential difference of the pair was considered. These measurements have been extended to additional transfer pairs for which the reduction potential difference is small. The objective of this work, in addition to furnishing new data for electron transfer rates, is to provide an adequate test of theories of the rate of homogeneous electron transfer in polar liquids (*10, 11, 12, 13, 14, 15, 16, 17*).

Experimental

The details of our experimental method, using a Varian V-7715A linear accelerator as the pulsed electron source, have been adequately

In Radiation Chemistry; Hart, E.;
Advances in Chemistry; American Chemical Society: Washington, DC, 1968.

described (*2, 7*). The electron pulse used ranged from 100 nsec. to 1 μsec. The fast optical detection method and the reaction cell arrangement were the same as before (*2*).

The reactions were carried out in isopropyl alcohol. This compound was selected as solvent because the natural lifetime of the aromatic radical anion with respect to protonation (*1, 3*) is longer than in methyl alcohol or ethyl alcohol. The isopropyl alcohol was obtained from Matheson, Coleman, and Bell and was freshly distilled over sodium metal through a glass-packed column for each set of runs. Anthracene from Matheson, Coleman and Bell, pyrene from Aldrich Chemical Co., *m*-terphenyl and *p*-terphenyl from City Chemical Corp. were purified as described (*2*). 9,10-Dimethylanthracene obtained from K and K Laboratories, Plainview, N. Y., was recrystallized from isopropyl alcohol solution.

Publication Date: January 1, 1968 | doi: 10.1021/ba-1968-0082.ch025

Results and Discussion

The donor-acceptor pairs investigated were pyrene-anthrace, pyrene-9,10-dimethylanthracene and *m*-terphenyl-*p*-terphenyl. The radical anions of these compounds may be observed at the appropriate optical absorption bands, the maxima of which are as follows: *m*-terphenyl, 7400 A., a broad weak band; *p*-terphenyl, 8770 A.; pyrene, 4900 A.; anthracene, 7200 A.; and 9,10-dimethylanthracene, 7300 A. For most of the systems we have studied in this and earlier work (*1, 2, 3*) these absorption bands have been known (*4, 6, 8*) from work on solutions in which the radical anions are stable. In the systems involving pyrenide anion as donor the decay of the donor anion and the formation of the acceptor could be observed simultaneously since their absorption bands do not overlap extensively.

Rate Constants. The sequence of reactions taking place in a two-component solute system, as discussed previously (*2*), are the formation by attachment of the solvated electron, the decay by proton transfer and by counter-ion combination, and the electron transfer.

$$e_{sol}^- + \text{arene} = \text{arene}^- \quad (1)$$

$$\text{arene}^- + i\text{-PrOH} = \text{arene H}\cdot + i\text{-PrO}^- \quad (2)$$

$$\text{arene}^- + i\text{-PrOH}_2^+ = \text{arene H}\cdot + i\text{-PrOH} \quad (3)$$

$$\text{arene}_a^- + \text{arene}_b = \text{arene}_a + \text{arene}_b^- \quad (4)$$

At sufficiently high concentrations of arene so that Reaction 1 is complete at the end of the pulse, and at sufficiently low pulse intensity so that the rate of Reaction 3 is negligible, the differential rate expression for the decay of the radical anion is adequately represented (*2*) by:

$$\frac{-d[A_a^-]}{dt} = k_{4a}[A_a^-][A_b] + k_{2a}[A_a^-][i\text{-PrOH}] \quad (5)$$

If the composition of the system is such that $k_{1a}[A_a] >> k_{1b}[A_b]$, the radical anion A_a^- will have been formed preferentially at the end of the pulse. This condition obtained for most of the runs. These are, of course, equilibrium systems with respect to the electron transfer, and in those cases in which the equilibrium is not overwhelmingly on the side of the acceptor anion the back reaction may occur. If there is a significant rate of the back reaction, 4b, Equation 5 becomes:

$$\frac{-d[A_a^-]}{dt} = k_{4a}[A_a^-][A_b] - k_{4b}[A_b^-][A_a] + k_{2a}[A_a^-][i\text{-PrOH}] \quad (6)$$

If the formation curve for A_b^- is observed, the analysis may be carried out by considering the analogous equation for $d[A_b^-]/dt$. This was done for only the *m*-terphenyl–*p*-terphenyl system, in which case the *m*-terphenylide band is obscured by a strong absorption of the *p*-terphenylide.

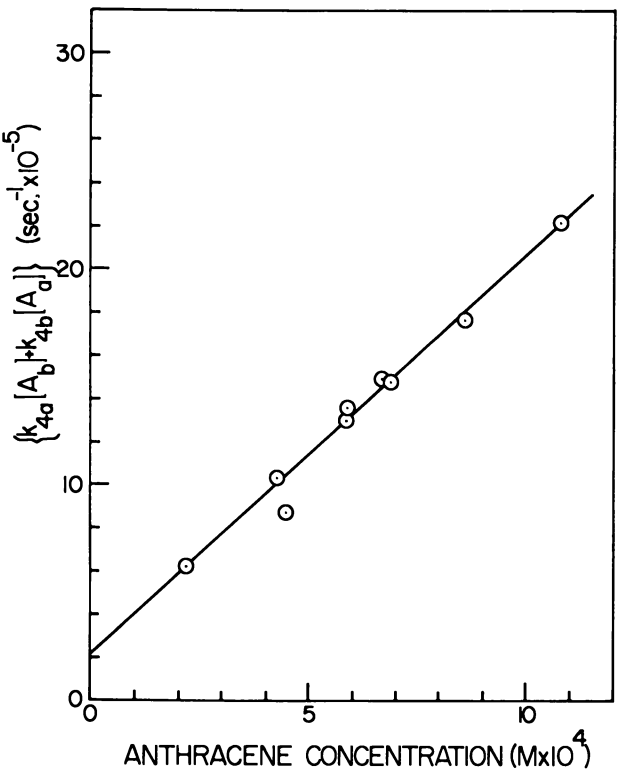

Figure 1. Plot of $\{k_{4a}[A_b] + k_{4b}[A_a]\}$, *from decay curves of pyrenide anion, against concentration of anthracene. The concentration of pyrene is constant and is equal to* 1.0×10^{-2}M. *The slope gives* $k_{4a} = 1.8 \times 10^9 M^{-1}$ *sec.*$^{-1}$ *at 25°C.*

Publication Date: January 1, 1968 | doi: 10.1021/ba-1968-0082.ch025

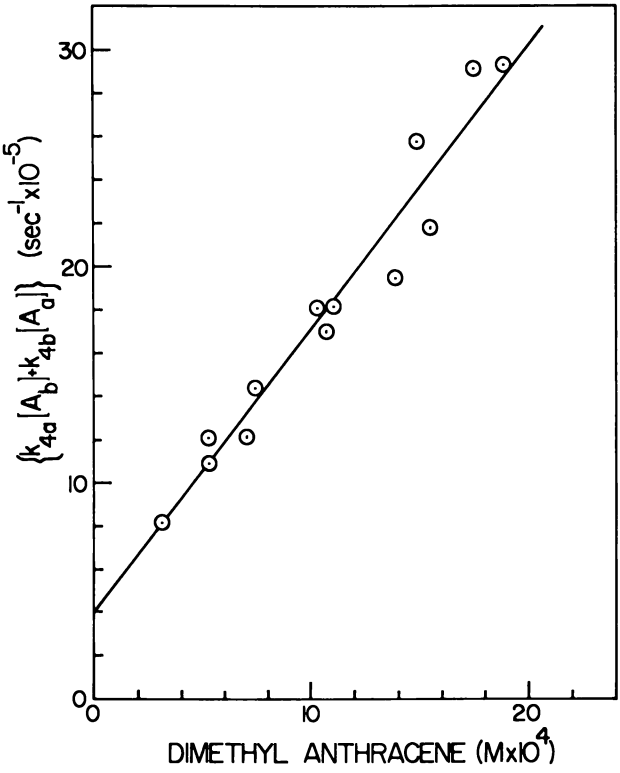

Figure 2. Plot of $\{k_{4a}[A_b] + k_{4b}[A_a]\}$, *from decay curves of pyrenide anion, against concentration of 9,10-dimethylanthracene. The concentration of pyrene is constant and is equal to 1.1* $\times$ 10^{-2}M. *The slope gives* $k_{4a} = 1.3 \times 10^{9}$M^{-1} *sec.*$^{-1}$ *at 25°C.*

If the concentration of the acceptor, A_b, is sufficiently high, the rate of Reaction 2a is negligible compared with the electron transfer rate and the integrated form of Equation 6 is:

$$[A_a^-]_t - [A_a^-]_e = C_1 \exp - (k_{4a}[A_b] + k_{4b}[A_a])t \qquad (7)$$

where $[A_a^-]_e$ is the concentration of A_a^- at equilibrium and C_1 is a constant. In terms of the optical density, D, this becomes:

$$2.303 \log_{10} (D_t - D_e) = -(k_{4a}[A_b] + k_{4b}[A_a])t + C_2 \qquad (8)$$

A plot of the left-hand side as a function of time gives a straight line with slope $-(k_{4a}[A_b] + k_{4b}[A_a])$. In this way, values of $(k_{4a}[A_b] + k_{4b}[A_a])$ are obtained for different $[A_b]$ holding $[A_a]$ constant. A plot of this term against $[A_b]$ gives a straight line from the slope of which k_{4a} may be determined. The rate constant for the back reaction, k_{4b}, may be

determined from the intercept. The uncertainty in k_{4b} is considerably larger than in k_{4a}. Such a plot is shown in Figure 1 for pyrene-anthracene, and in Figure 2 for pyrene-9,10-dimethylanthracene, both of which are pairs for which the back reaction rate is not negligible, and in which equilibrium is attained. The values for k_{4a} and k_{4b} are shown in Table I.

Table I. Electron Transfer Rate Constants for Aromatic Radical Anions in Isopropyl Alcohol at 25°C.

Donor-Acceptor Pair	*Forward Rate Constant,* k_{4a} (M^{-1} *sec.*$^{-1}$)	*Back Rate Constant,* k_{4b} (M^{-1} *sec.*$^{-1}$)
Pyrene–anthracene	$(1.8 \pm 0.3) \times 10^9$	$(2.1 \pm 0.9) \times 10^7$
Pyrene–9,10-dimethyl anthracene	$(1.3 \pm 0.3) \times 10^9$	$(3.7 \pm 1.7) \times 10^7$
m-Terphenyl–*p*-terphenyl	$(2.3 \pm 0.4) \times 10^9$	—

The value of D_e, in Equation 8, is taken from the almost horizontal portion of the rate curve, which represents the attainment of equilibrium between the two radical anions, at the region in which the fast portion of the decay curve becomes asymptotic to this horizontal. Such a rate curve, taken at two different sweep times, is shown in Figure 3. The uncertainty in the value of D_e is very small since the linear portion of the curve is nearly horizontal. This linear portion is not perfectly horizontal when examined on a long time-scale simply because the rates of Reactions 2 and 3 are not completely negligible. Another observation which is indicative of the establishment of equilibrium with respect to Reaction 4 may be made in the following way. If one observes the slow decay of the two radical anions at their respective wavelengths, which in the system pyrene-anthracene would be 490 mμ for the former and 720 mμ for the latter, both anion spectra are found to be present for many tens of microseconds. Moreover, the ratio of the optical densities at these two wavelengths remains constant over this extended period. The same is found for pyrene-dimethylanthracene.

In the case of *m*-terphenyl–*p*-terphenyl, the kinetics were observed for the formation of *p*-terphenylide anion. The rate of the back reaction is negligible at the *m*-terphenyl concentration used, $6 \times 10^{-4}M$. This may be seen from the fact that the decay of *p*-terphenylide anion with this concentration of *m*-terphenyl present, does not differ appreciably from its decay rate when only *p*-terphenyl is present. The decay rate of *m*-terphenylide anion in Reaction 2, is however, much higher than that of *p*-terphenylide anion. A plot of $\log_{10} (D_\infty - D_t)/D_\infty$ against time, from the formation curves of this pair, gives a straight line from the slope of which we determine $(k_{4a}[A_b] + k_{2a}[i\text{-PrOH}])$, since the decay rate

Publication Date: January 1, 1968 | doi: 10.1021/ba-1968-0082.ch025

of *p*-terphenylide anion by Reaction 2 is negligible. A subsequent plot of this term against $[A_b]$ gives k_{4a} from the slope. The value is shown in Table I.

Equilibrium Constant. For those cases in which the electron transfer equilibrium is overwhelmingly on the side of the acceptor anion, the rate of the back reaction, as has been pointed out (*2*), is negligible. In some cases where this is not true, as for diphenyl-naphthalene, the equilibrium with respect to Reaction 4 may be "quenched" by the protonation of the acceptor anion in Reaction 2. In the case of pyrene-anthracene and pyrene-9,10-dimethylanthracene, where equilibration occurs, the back reaction has a measurable effect upon the electron transfer kinetics, and k_{4b} has been determined. From these data, the equilibrium constant may also be reliably estimated since it is given by the ratio: $K_e = k_{4a}/k_{4b}$. The values obtained at 25°C. are: (1) pyrene-anthracene ~86 and (2) pyrene-9,10-dimethylanthracene ~35. These values for K_e may also be determined from the difference in the reduction potentials of the pair as measured potentiometrically (*5, 8, 9, 18*). The equilibrium constant is related to the reduction potential difference, ΔF, by:

$$\Delta F = RT \ln K_e \qquad (9)$$

Equilibrium constants of 81 and 30 for the two foregoing pairs in tetrahydrofuran are calculated from such data, in excellent agreement with the values from our kinetic method.

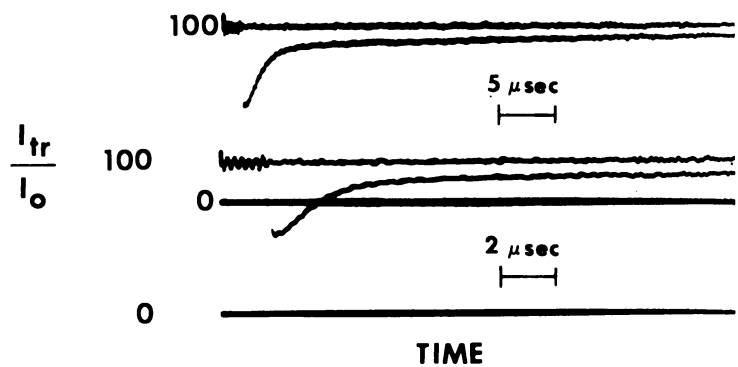

Figure 3. Decay curves of pyrenide anion in isopropyl alcohol solution containing 4.9 × 10⁻⁴M anthracene. The concentration of pyrene is 8.5 × 10⁻⁵M. The sweep time for the upper curve is 5 μsec./div., and for the lower 2 μsec./div.

Correlation with Theory. A general theory for homogeneous electron transfer reactions has been developed and discussed by Marcus (*10, 11, 12, 13, 14 15, 16, 17*). The rate constant in this model, as applied to

Table II. Correlation with Theory of Experimental Rate Constants

Donor, Acceptor Pair	$\Delta F^{\circ\prime}$ *(kcal./mole)*	ΔF^{*} *(kcal./mole)*
Diphenyl$^-$, naphthalene	−0.99	3.4
Anthracene$^-$, pyrene	+2.61	5.34
9,10-dimethylanthracene$^-$, pyrene	+2.01	4.99
Diphenyl$^-$, phenanthrene	−3.28	2.46
Pyrene$^-$, 9,10-dimethylanthracene	−2.01	2.99
Pyrene$^-$, anthracene	−2.61	2.73
Diphenyl$^-$, pyrene	−12.2	0.20
Diphenyl$^-$, anthracene	−14.8	0.012

[a] The calculated values are based on a reorganization parameter, $\lambda = 16$ kcal./mole and upon $Z = 10^{11}M^{-1}$ sec.$^{-1}$.

our systems, depends upon the dielectric behavior of the solvent and upon the difference in reduction potentials of the donor-acceptor pair as well as upon such collision parameters as the encounter radii. The dependence upon the dielectric properties of the liquid reflects the energy of reorientation of the solvent dipoles in the formation of the activated complex. The difference in reduction potentials is a major contribution to the value of the exponential term in the rate constant expression, and is therefore an important parameter.

The bimolecular rate constant for electron transfer, k_{bi}, in the notation of Marcus (*10, 11, 13*), is given by:

$$k_{bi} = Ze^{-\Delta F^*/RT} \tag{10}$$

where ΔF^* is the free energy of activation. Z is the collision number, which has been taken by Marcus to be about $10^{11}M^{-1}$ sec.$^{-1}$, equivalent to the collision number in the gas phase, and thus not dependent upon solvent properties. It is defined (*13*) as equivalent to $(8\pi kT/m^*)^{1/2}r^2$ where m^* is the reduced mass of the reactants and r is the distance between the centers in the collision complex. The free energy of activation is given (*13*) by:

$$\Delta F^* = w + \frac{\lambda}{4} + \frac{\Delta F^{\circ\prime}}{2} + \frac{(\Delta F^{\circ\prime})^2}{4\lambda} \tag{11}$$

w is the difference in the work of bringing together the reactants and separating the products. With one reactant uncharged, as in our systems, this does not involve a coulombic interaction, and w should therefore be small. $\Delta F^{\circ\prime}$ is the standard free energy of reaction, which is taken as the difference in reduction potentials of the donor-acceptor pair. The reorganization parameter, λ, is given by:

$$\lambda = \left(\frac{1}{2a_1} + \frac{1}{2a_2} - \frac{1}{r}\right)\left(\frac{1}{D_{op}} - \frac{1}{D_s}\right)(\Delta e)^2 \tag{12}$$

for Electron Transfer of Aromatic Molecules in Solution[a,b]

Experimental k_{bi} (M^{-1} *sec.*$^{-1}$)	*Calculated* k_{bi} (M^{-1} *sec.*$^{-1}$)	*Experimental* $(k_{bi})_n/(k_{bi})_1$	*Calculated* $(k_{bi})_n/(k_{bi})_1$
2.6×10^8	3.0×10^8	1.0[c]	1.0[c]
2.1×10^7	1.2×10^7	0.081	0.041
3.7×10^7	2.2×10^7	0.14	0.074
6×10^8	1.6×10^9	2.3	5.3
1.3×10^9	6.5×10^8	5.0	2.2
1.8×10^9	1.0×10^9	6.9	3.4
5.0×10^9	7.2×10^{10}	19	240
6.4×10^9	9.8×10^{10}	25	330

[b] Those donor-acceptor pairs not from the present work are from Reference 2.
[c] k_{bi} for the diphenyl$^-$-naphthalene pair is taken as the reference constant.

Publication Date: January 1, 1968 | doi: 10.1021/ba-1968-0082.ch025

The contribution from intramolecular vibrational reorganization, which is small for strong internal bonding, has been neglected. The effective radii for the encounter, a_1 and a_2, include in addition to the molecular radii of the reactants, a saturated monolayer of solvent around the molecular anion. r is taken as $a_1 + a_2$. D_{op}, the optical dielectric constant, is equal to the square of the refractive index, and D_s is the static dielectric constant, Δe is the change in charge of the donor, which for our case is $+1$.

If we take $a_1 = a_2 \cong 5$A. for all of our molecules, and hence $r =$ 10A., we obtain $\lambda = 16$ kcal./mole from Equation 12. If $w << \{\lambda/4 + \Delta F^{\circ\prime}/2 + (\Delta F^{\circ\prime})^2/4\lambda\}$, we may obtain ΔF^* directly from Equation 11. We may then obtain an absolute value of k_{bi} from Equation 10 if a value is assumed for the collision number, Z. Or alternatively the theory may be tested by examining the internal consistency of the calculated values, compared with our data, of the ratio $(k_{bi})_n/(k_{bi})_1$ for a series of rate constants relative to one reference constant, assuming, as a first approximation, that the collision number Z is the same for all our pairs, and therefore cancels out.

Table II shows experimental values for the rate constant from this and earlier work (2), and calculated values for $\lambda = 16$ kcal./mole for both k_{bi} (taking $Z = 10^{11}$) and $(k_{bi})_n/(k_{bi})_1$ referred to diphenyl-naphthalene. Reasonable agreement is obtained for k_{bi} for those cases tested for which the rate constant is significantly lower than the diffusion-controlled value. The ratio $(k_{bi})_n/(k_{bi})_1$ also shows good agreement for these cases.

For those cases for which the experimental rate constant corresponds to the diffusion-controlled value (diphenyl-pyrene or diphenyl-anthracene) a direct comparison of the calculated value with experiment is not

meaningful, but must be understood on the basis of the relation (*17*):

$$1/k_{obs} = 1/k_{act} + 1/k_{diff} \quad (13)$$

where k_{act} is the value calculated from Equation 10, and k_{diff} is the diffusion-controlled value. Thus, for diphenyl-pyrene and diphenyl-anthracene, where $k_{diff} << k_{act}$, the observed value is, $k_{obs} = k_{diff}$ or approximately (2) $4 \times 10^9 M^{-1}$ sec.$^{-1}$. The direct correlation is, of course, most meaningful for the lowest values (10^7 to $10^8 M^{-1}$ sec.$^{-1}$) where $k_{act} << k_{diff}$.

If, in the correlation, a_1 and a_2 are both taken as 4A., we obtain $\lambda =$ 20 kcal./mole; a_1 and a_2 taken as 6A. gives $\lambda = 13$ kcal./mole. The values of $(k_{bi})_n/(k_{bi})_1$ calculated with either of these values for λ are not very different from the values in Table II for those cases with $k_{obs} < k_{diff}$, the important parameter being the difference in reduction potentials.

Acknowledgment

This work was supported by the U.S. Atomic Energy Commission. We are grateful to R. A. Marcus with whom we have discussed the theory. We are indebted to E. G. Wendell for operating the linear accelerator and maintaining the detection equipment.

Literature Cited

(1) Arai, S., Dorfman, L. M., *J. Chem. Phys.* **41,** 2190 (1964).
(2) Arai, S., Grev, D. A., Dorfman, L. M., *J. Chem. Phys.* **46,** 2572 (1967).
(3) Arai, S., Tremba, E. L., Brandon, J. R., Dorfman, L. M., *Can. J. Chem.* **45,** 1119 (1967).
(4) Balk, P., Hoijtink, G. J., Schreurs, J. W. H., *Rec. Trav. Chim.* **76,** 813 (1957).
(5) Chaudhuri, J., Jagur-Grodzinski, J., Szwarc, M., *J. Phys. Chem.* **76,** 3063 (1967).
(6) De Boer, E., Weissman, S. I., *Rec. Trav. Chim.* **76,** 825 (1957).
(7) Felix, W. D., Gall, B. H., Dorfman, L. M., *J. Phys. Chem.* **71,** 384 (1967).
(8) Gill, D., Jagur-Grodzinski, J., Szwarc, M., *Trans. Faraday Soc.* **60,** 1424 (1964).
(9) Jagur-Grodzinski, J., Feld, M., Yang, S. L., Szwarc, M., *J. Phys. Chem.* **69,** 628 (1965).
(10) Marcus, R. A., *J. Chem. Phys.* **24,** 966 (1956).
(11) *Ibid.*, **26,** 867 (1957).
(12) *Ibid.*, **26,** 872 (1957).
(13) *Ibid.*, **43,** 679 (1965).
(14) *Ibid.*, **43,** 2654 (1965).
(15) Marcus, R. A., *Discussions Faraday Soc.* **29,** 21 (1960).
(16) Marcus, R. A., *J. Phys. Chem.* **67,** 853 (1963).
(17) Marcus, R. A., *J. Chem. Phys.* **43,** 3477 (1965).
(18) Slates, R. V., Szwarc, M., *J. Phys. Chem.* **69,** 4124 (1965).

RECEIVED January 4, 1968.

Excited States in Irradiated Aromatic Solvents

R. B. CUNDALL and W. TIPPETT

University of Nottingham, University Park, Nottingham, NG7 2RD, England

Publication Date: January 1, 1968 | doi: 10.1021/ba-1968-0082.ch026

The radiation induced cis-trans isomerization of 2-butene in benzene, benzene-d_6, toluene, and pyridine has been studied. The triplet yield in benzene is 4.7 molecules per 100 e.v.; benzene-d_6 is similar. The yield in toluene is ~ 6 molecules per 100 e.v. Nitrous oxide reduces the isomerization yield by about 40%. This indicates a G value of about 2 for excited states produced by the recombination of benzene ions with electrons. Xenon and krypton (up to 1M) increase the isomerization yield from 2.4 to 3.1 and 2.9 respectively, whereas argon has no effect. From the effect of xenon, which is attributed in part to enhanced intersystem crossing, it is estimated that the yield of singlet states which do not cross to the triplet in unperturbed benzene solutions is 1.3 molecules per 100 e.v.

Ionizing radiations may produce electronically excited states of the components of organic solutions as a result of charge recombination and direct excitation by impact with fast and slow electrons. The initially formed excited states can undergo intersystem crossing, internal conversion, or mutual interactions such as triplet-triplet annihilation which can give rise to excited singlet or quintet states (*2*). The relative importance of these different processes is uncertain, and experimental data are rarely capable of being uniquely interpreted. The nature of the excited state involved—singlet, triplet or higher multiplet—is usually unknown, and identification techniques need to be developed further. Scintillation methods can be used for fluorescent molecules (*30*), and more recently pulse radiolysis has been used to study triplet states in irradiated systems (*31*). These techniques are restricted by their nature to systems with

In Radiation Chemistry; Hart, E.;
Advances in Chemistry; American Chemical Society: Washington, DC, 1968.

suitable photochemical characteristics. Energy transfer between molecules can be used to detect and measure the yields of electronically excited states if excitation produces an observable chemical change, as in the cis-trans isomerization of olefins. Golub indicated the possibility of a triplet-triplet transfer process to explain the cis-trans isomerization of polybutadiene in benzene (*23*). The radiation induced isomerization of 2-butene in hydrocarbon solutions has been studied in some detail (*14*), and for benzene it was used to study the behavior of the $^3B_{iu}$ state (*15*). Subsequently, other workers have carried out similar studies with 2-pentene (*24*), 2-hexene (*24*), 2-octene (*24, 25*), stilbene (*7, 22, 27, 36*), 1,2-diphenylpropene (*7*), piperylene (*7*), *p*-nitro-*p*-methoxystilbene (*45*), and dimethyl maleate (*40*). The 2-butene system has some advantages over stilbene; it is not as susceptible to ionic catalysis, and singlet-singlet transfer is not of prime importance. Isomerization techniques are reliable only if accompanied by careful examination of the mechanism in each case.

Publication Date: January 1, 1968 | doi: 10.1021/ba-1968-0082.ch026

Experimental

Phillips Research Grade benzene was used without further purification. Toluene (BDH) was shaken with concentrated sulfuric acid, washed with aqueous sodium carbonate and water, dried over silica gel, and distilled. In later experiments, the distillate was further purified by preparative gas chromatography using a Carbowax-20M column. *Cis*- and *trans*-2-butene (Phillips Research Grade) were used without further purification other than degassing and vacuum distillation. Other materials were purified by distillation.

Solutions were made up under vacuum in borosilicate glass breakseal tubes, usually 10-ml. volume, cleaned by baking at 540°C. and flaming at 10^{-6} torr. Where gases of limited solubility were involved tubes of 2-ml. capacity were used to reduce dead space. Inert gas concentrations were calculated using the data of Clever *et al.* (*8*). Solvent (usually 1 ml.) was put into the breakseal tube, and measured amounts of 2-butene or other additive were introduced before sealing. Irradiations were carried out using a ^{60}Co γ-ray source (300 c). The sample tubes were mounted in a holder which rotated the samples around the cylindrical source. Dosimetry was performed by the Fricke method ($G_{Fe^{3+}} = 15.6$, $E_{Fe^{3+}} = 2209$ at 304 nm. and 25°C.). The differing electron densities of the dosimeter and other solutions were corrected for. After irradiation the gaseous materials were removed by low temperature distillation. Gases volatile at −196°C. were collected, measured in a gas buret, and analyzed by gas chromatography on a Linde 5A molecular sieve column. Gases collected at −78°C. were analyzed on a silver nitrate–ethylene glycol column. All irradiations were carried out at 1.46×10^{15} e.v. gram^{-1} sec.$^{-1}$ for 24 hours. Conversions were typically 2%. All irradiations were carried out at room temperature, 24 ∓ 1°C.

Results

2-Butene–Benzene Solutions. The earlier results for the cis-trans conversion were confirmed (*14, 15*). Apparently the original studies of the trans-cis conversion were insufficient for accurate assignment of the yield of benzene triplet, and more experiments have been done. The measurement is not as precise as the cis-trans conversion at low percentage conversions since cis follows trans in the chromatogram and the cis impurity in the trans isomer is higher than the trans in cis. Some experiments were done using benzene-d_6 as solvent (Figure 1). Examination of the benzene solvent after extraction showed the presence of a small amount of benzene–2-butene adduct (*50*) (*ca.* 1% of the extent of isomerization).

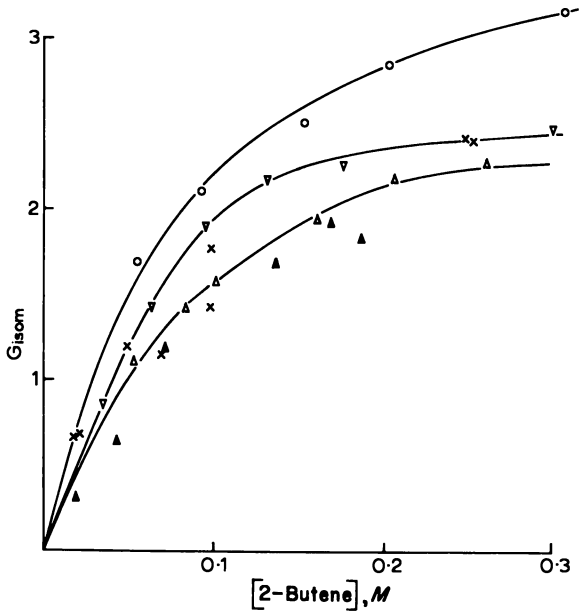

Figure 1. G_{isom} vs. *2-butene concentration in benzene*

▽, *cis* → *trans*; △, *trans* → *cis*; ▲, *trans* → *cis* (14); ×, *cis* → *trans in* C_6D_6; ○, *cis* → *trans in the presence of 0.25M xenon*

***cis*-2-Butene–Toluene Solutions.** The effect of varying *cis*-2-butene concentration on the isomerization yield in toluene at room temperature (24°C.) is shown in Figure 2. The hydrogen yield was 0.14 molecules per 100 e.v. at all 2-butene concentrations.

Publication Date: January 1, 1968 | doi: 10.1021/ba-1968-0082.ch026

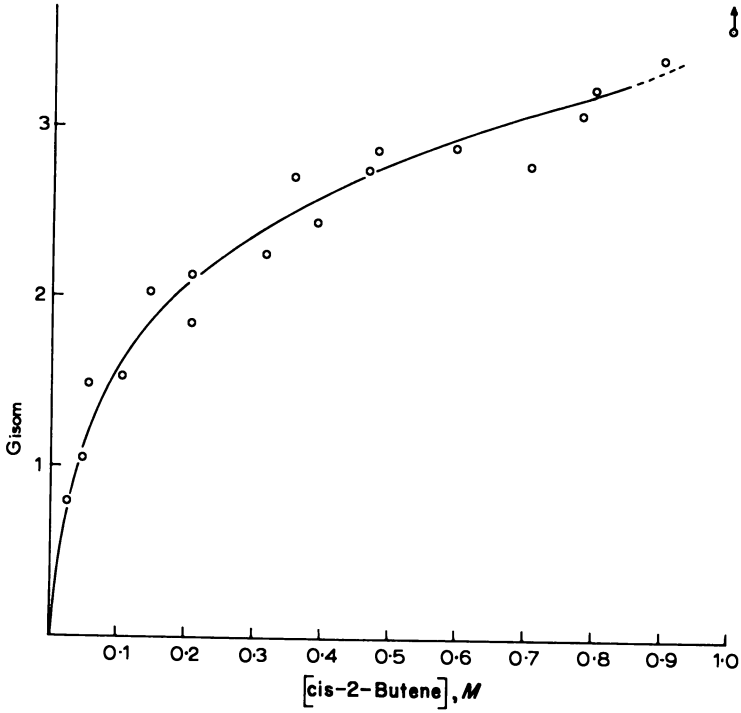

Figure 2. G_{isom} vs. cis-2-*butene concentration in toluene*

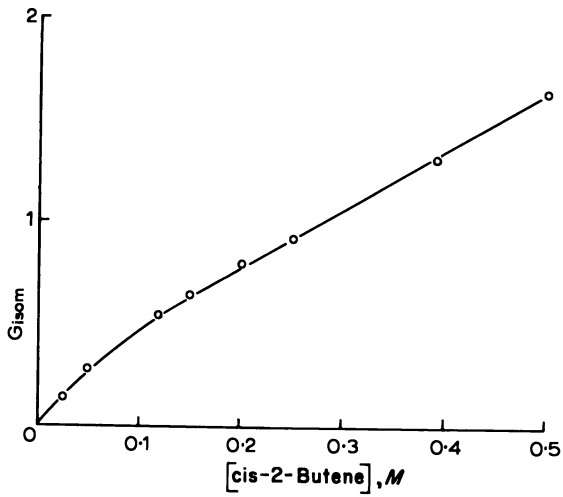

Figure 3. G_{isom} vs. cis-2-*butene concentration in pyridine*

***cis*-2-Butene–Pyridine Solutions.** Isomerization in pyridine solutions is presented in Figure 3. Irradiated solutions turned yellow, and the hydrogen yield was constant at all 2-butene concentrations ($G_{H_2} = 0.03$).

Effect of Nitrous Oxide on Benzene–2-Butene Solutions. The yield of nitrogen increased with increasing concentration of nitrous oxide, in agreement with the work of Sato and co-workers (*43*). The isomerization showed a marked decrease at low nitrous oxide concentrations. Figure 4 summarizes the results.

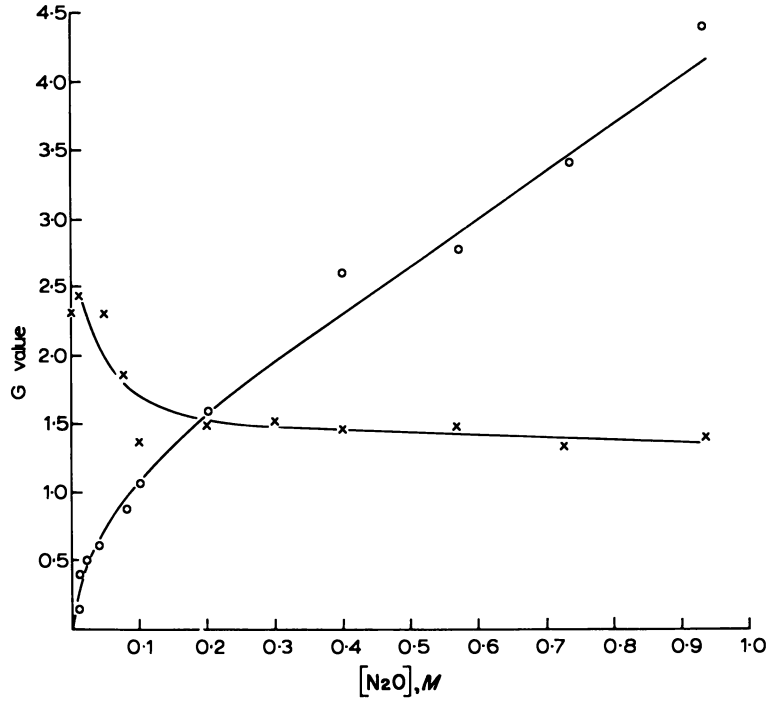

Figure 4. G_{N_2} *and* G_{isom} vs. *nitrous oxide concentration for* cis-2-*butene (0.25*M*) in benzene.* ×, G_{isom}; ○, G_{N_2}

Effect of Argon, Krypton, and Xenon on Benzene–2-Butene Solutions. Both krypton and xenon affected the isomerization yield as shown in Figure 5. Argon had no effect. The effect of 0.25*M* xenon on the cis-trans isomerization at different olefin concentrations is shown in Figure 1. *G* values are for the total energy deposited in the solutions.

Effect of Additives on Benzene–2-Butene Solutions. In a previous report (*14*) the effect of additives was studied. The results of further similar studies are summarized in Table 1.

Publication Date: January 1, 1968 | doi: 10.1021/ba-1968-0082.ch026

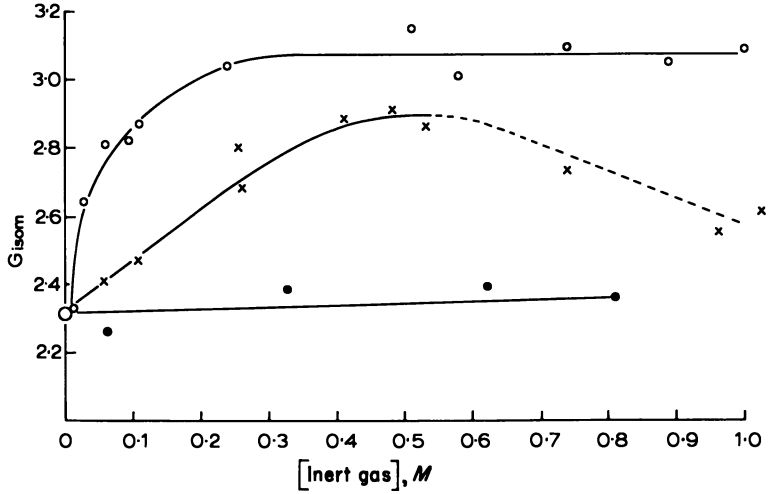

Figure 5. Effect of inert gases on G_{isom} for cis-2-butene (0.25M) in benzene. ○, Xenon; ×, krypton; ●, argon

Table I. The Effect of Various Additives on the cis-trans Isomerization of 0.25M *cis*-2-Butene in Benzene[a]

Additive	*Conc.*, M	G_{isom}	$G_{perm.\ gas}$
CO_2	0.90	very high	
	1.10	very high	
	0.039	20	
SF_6	0.89	very high	
	0.04	very high	
H_2O	0.024	2.34	
	0.024	2.23	
CCl_4	0.20	6	
CCl_4/C_2H_5OH	0.20 (both)	6	
C_2H_5OH	0.20	2.21	
N_2O/C_2H_5OH	0.20 (both)	2.30	
Piperidine	0.20	1.79	0.07 (H_2)
	0.20	1.89	0.07 (H_2)
Piperidine/N_2O	0.20 (both)	1.71	(0.07) (H_2) 1.80 (N_2)
	0.20 (both)	1.94	(0.07) (H_2) 1.80 (N_2)
Pyridine	0.20	2.03	0.04 (H_2)
	0.20	2.06	0.04 (H_2)
CH_3NO_2	0.20	0.70	
	0.10	0.91	

[a] Dose rate, 1.46×10^{15} e.v. gram^{-1} sec.$^{-1}$. Temperature, 24°C. Irradiation time, 24 hours.

Publication Date: January 1, 1968 | doi: 10.1021/ba-1968-0082.ch026

Discussion

The following mechanism has been used to explain the earlier work with benzene–2-butene solutions (*14*, *15*):

$$C_6H_6 \xrightarrow{\wwvy} C_6H_6^* \quad (1)$$

$$C_6H_6^* + 2\text{-}C_4H_8 \rightarrow 2\text{-}C_4H_8^* + C_6H_6 \quad (2)$$

$$2\text{-}C_4H_8^* \rightarrow \textit{cis}\text{- or }\textit{trans}\text{-}2\text{-}C_4H_8 \quad (3)$$

$$C_6H_6^* \rightarrow C_6H_6 \quad (4)$$

$C_6H_6^*$ is the triplet state of benzene formed directly or indirectly from ground state benzene molecules. Complexities which arise from the effects of radical quenching and triplet-triplet annihilation have been discussed by Burns *et al.* (*6*). These effects are significant only at higher dose rates and LET than used in this work. An examination of homogeneous and nonhomogeneous kinetic models shows that simple kinetics can be applied to the results. The usual steady-state assumption gives

$$1/G_{\text{isom}} = 1/k' + k_4/k'k_2(2\text{-}C_4H_8)$$

where k' is a constant. Experiments with a range of different additives show that k_2 must be approximately diffusion controlled (*15*), and estimates of the lifetimes of the triplet states of benzene or other solvents can be made.

The earlier papers showed that the fluorescence of the $^1B_{2u}$ state and the lowest excimer singlet state ($^1B_{1g}$) of benzene are not quenched by 2-butene. 2-Butene, by reason of its lower lying triplet excited state, is able to quench the benzene $^3B_{1u}$ state. It is remarkable that the lifetime of the benzene triplet is so short compared with the value (of the order of several seconds) in the solid state. It has been suggested (*46*) that this could be caused by triplet dimer production. An alternative possibility is that the triplet is not the $^3B_{1u}$ state but perhaps some other state such as the $^3E_{1u}$ which does not internally convert $^3E_{1u} \rightarrow {}^3B_{1u}$. This type of behavior is consistent with that found by Lipsky (*4*) which shows that intersystem crossing and/or internal conversion from higher excited to lower excited states is not facile.

Isomerization in Different Solvents. It has been confirmed that the value of k_2/k_4 is 21.2 in benzene. Figure 6 is a plot of $1/G_{\text{isom}}$ *vs.* $1/(\textit{cis}\text{-}2\text{-}C_4H_8)$ for toluene, from which it can be deduced that k_2/k_4 is 12.1. From the data for pyridine similar analysis gives 0.2 for k_2/k_4. The result for toluene is similar to that of Dubois (*46*) obtained for biacetyl–toluene solutions, and the triplet lifetime may be about half that for benzene, *ca.* 10^{-8} sec. The slow increase in G_{isom} even at the higher olefin concentrations suggests that an ionic contribution to the isomerization cannot be disregarded. The k_2/k_4 ratio is deduced from the results at

Publication Date: January 1, 1968 | doi: 10.1021/ba-1968-0082.ch026

lower olefin concentrations when such effects are small. Dubois and van L. Sels (*20*) have found evidence for singlet-singlet energy transfer by solvent-solvent resonance transfer (octopole-octopole). Such an effect could make k_2 greater in toluene than in benzene. This would make the lifetime of the toluene triplet less than that for benzene (possibly by a factor of 4). Our attempts to detect the pyridine triplet by energy transfer from photoactivated (2537 A.) pyridine to biacetyl and 2-butene have been negative. It must be concluded that the photoexcited pyridine singlet rapidly undergoes internal conversion (or valence isomerization) or forms a very short-lived triplet state (*i.e.*, $k_4 \approx 10^{10}$ sec.$^{-1}$). If Reactions 1–4 are applicable to irradiated pyridine solutions, the triplet state must be very short lived. The validity of these reactions depends on the energy states of the pyridine molecule. If there are low energy ($n-\pi^*$) excited states (below 3 e.v.) of pyridine excitation transfer and subexcitation electron activation of the 2-butene would be unimportant. Positive ion mechanisms are improbable in pyridine.

The new data on the trans → cis isomerization require a revised estimate of the benzene triplet yield (G_T) from the sum of $G_{c \to t} + G_{t \to c}$ (2.44 + 2.25) at high (0.3*M*) olefin concentrations—*i.e.*, 4.7 within the limits of error. This is in closer agreement with other published values—5.0 (*24, 25*), 5.0 (*22*), and 5.4 (*27*). If $G_{t \to c} = G_{c \to t}$, agreement is excellent. An accurate value of G_T cannot be assessed for toluene owing to the failure to achieve a limiting value. A yield in excess of 7 may be deduced from Figure 2, but in view of the high solute concentrations this must be an upper limit. Extrapolating the low solute concentration data in Figure 6 allows an approximate yield of 6 to be deduced; this is probably more reliable. Deuteration does not seem to affect the triplet yield for benzene, but the lifetime is reduced slightly.

Charge transfer processes which may be involved are

$$S^+ + 2\text{-}C_4H_8 \rightarrow S + 2\text{-}C_4H_8^+ \quad (5)$$

$$S^- + 2\text{-}C_4H_8 \rightarrow S + 2\text{-}C_4H_8^- \quad (6)$$

where S is benzene, toluene, or pyridine. Gas-phase ionization potentials for benzene, toluene, pyridine, and 2-butene (cis and trans) are 9.2, 8.8, 9.8, and 9.24 e.v., respectively (*21*). Reaction 5 would not appear probable for toluene since *IP* ($C_6H_5CH_3$) < *IP* (2-C_4H_8). Olefins have negative electron affinities, and Reaction 6 is improbable (*10, 11, 47, 48*). Ion yields observed in pulse radiolysis are much less than the isomerization observed in benzene (*35*). The absence of side products indicates that ion-molecule reactions do not occur. Direct production of excited states of the solute by subexcitation electrons (*41*) is a possibility for which there is no firm evidence.

Publication Date: January 1, 1968 | doi: 10.1021/ba-1968-0082.ch026

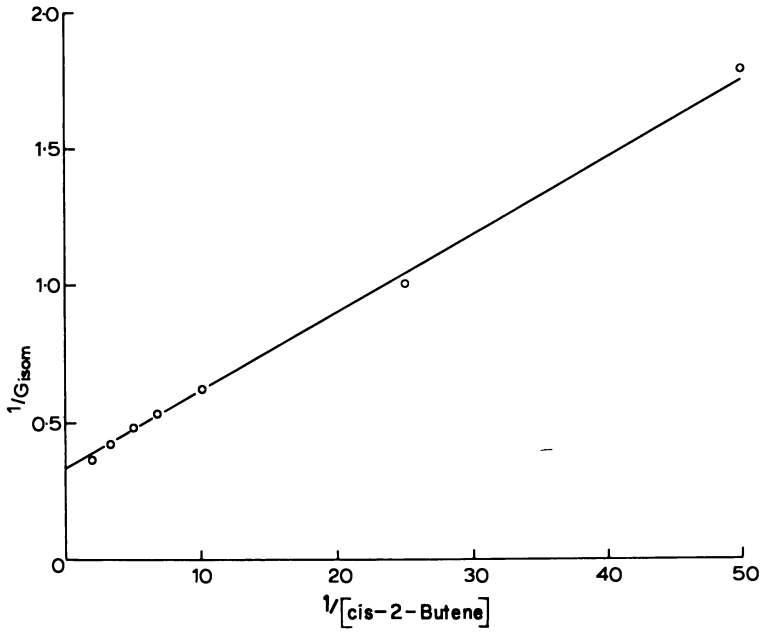

Figure 6. $1/G_{isom}$ vs. $[\text{cis-2-butene}]^{-1}$ *for* cis-2-*butene in toluene*

Electron Scavenging by Nitrous Oxide. Nitrous oxide is an effective electron scavenger in hydrocarbons (*44*), producing high yields of nitrogen. The possible reactions involved are

$$N_2O + e^- \rightarrow N_2 + O^- \quad (7)$$

$$O^- + S^+ \rightarrow OH + S'\cdot \quad (8)$$

or

$$O^- + S \rightarrow OH^- + S'\cdot \quad (9)$$

The electrons not captured by nitrous oxide may undergo capture

$$e^- + S^+ \rightarrow S^* \quad (10)$$

$$e^- + S \rightarrow S^- \quad (11)$$

followed by

$$S^+ + S^- \rightarrow 2S \text{ (or } 2S^*, S_2^*, S^* + S) \quad (12)$$

The yield of nitrogen may be increased at higher nitrous oxide concentrations by (*39*):

$$O^- + N_2O \rightarrow O_2^- + N_2 \quad (13a)$$

or

$$N_2O^- + N_2O \rightarrow O_2^- + 2N_2 \quad (13b)$$

Publication Date: January 1, 1968 | doi: 10.1021/ba-1968-0082.ch026

The reaction

$$N_2O + e^* \rightarrow N_2 + O(^3P) + e \qquad (14)$$

could be brought about by electrons with sufficient kinetic energy, as suggested by Dainton (*18*) [$\Delta H°$ for $N_2O \rightarrow N_2 + O(^3P)$ is 1.73 e.v. (*9*)].

The observations can qualitatively, at least, be understood in terms of these processes. The sharp fall in the isomerization (and excited state) yields up to 0.2*M* N_2O is caused by Reaction 7's competing with 10 or less probably the combination of Reaction 11 followed by 12. The yield of excited states of benzene produced by Reaction 10 is therefore about 2 per 100 e.v. The slight decrease in isomerization yield with increasing nitrous oxide concentration above 0.2*M* must be caused by the interaction of nitrous oxide with more energetic electrons or electrons which would otherwise undergo geminate recombination with positive ions and form excited states of benzene. The steady increase in the nitrogen yield is caused by the increasing role of Reactions 13a or b and 14. Most of the electrons involved in Reaction 14 have lower energy than needed to excite aromatic solvent molecules. The nitrous oxide concentration dependence indicates an average lifetime for free electrons of about 10^{-10} sec. Photochemical experiments in which benzene solutions of nitrous oxide were irradiated with 2537 A. light showed that neither the $^1B_{2u}$ nor $^3B_{1u}$ states sensitize the decomposition of N_2O. This is surprising, since the process

$$C_6H_6(^3B_{1u}) + N_2O \rightarrow C_6H_6(^1A_{1u}) + N_2 + O(^3P) \qquad (15)$$

is exothermic and should occur through the nitrous oxide triplet state (*28*). Triplet-triplet transfer may occur only if some kind of chemical complex is formed, and this may not be possible with nitrous oxide.

Effect of Inert Gases. These experiments are part of an attempt to specify the separate roles of $^1B_{2u}$ and $^3B_{1u}$ excited states of benzene in radiolysis. Higher excited states of aromatic solvents do not form these states by either internal conversion or intersystem crossing (*4*), owing in part at least to decomposition or the formation of valence isomers such as fulvene (*49*). Accepting the fact that excited states are formed by electron-ion recombination or electron impact, it is of considerable importance to determine the ratios of singlet and triplet states directly formed before intersystem crossing.

The effect of spin-orbit coupling in enhancing intersystem crossing is well established (*26, 29, 38, 42*) and offers the possibility of measuring the yield of excited singlet states which do not undergo intersystem crossing or fluorescence, and are internally converted or externally quenched. The presence of xenon increases the isomerization yield, and the usual kinetic analysis of the data for the solutions containing 0.25*M*

Publication Date: January 1, 1968 | doi: 10.1021/ba-1968-0082.ch026

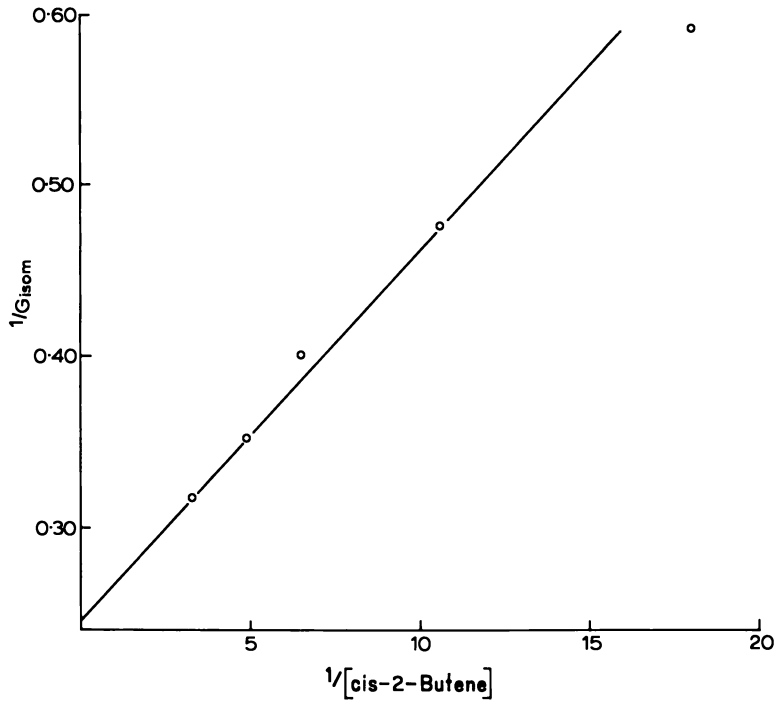

Figure 7. $1/G_{isom}$ vs. $[\text{cis-2-}butene]^{-1}$ *for* cis-2-*butene in benzene and 0.25*M *xenon*

xenon shown in Figure 1 yields $k_2/k_4 = 11.4$ (Figure 7), and the excited state yield increases to 6.0. It is expected that xenon will quench the triplet state of benzene, and it is about 1/10 as efficient as 2-butene in this respect. Photochemical experiments (to be reported elsewhere) have shown that the quantum yield for the triplet state benzene (in the liquid state) is about 0.61. Xenon is able to promote intersystem crossing of excited singlet states which would otherwise undergo fluorescence or internal conversion. We shall assume that the enhancement of 1.3 molecules per 100 e.v. for the cis-trans isomerization corresponds to the fraction 0.4 of benzene singlet excited states, which in the absence of xenon do not undergo intersystem crossing to the triplet state. This allows an estimate of 3.5–4.0 molecules per 100 e.v. for the excited singlet yield in the irradiated system. The effect of krypton is less marked at lower concentrations and argon has no effect, as expected. Complications arising from ion-molecule reactions probably occur, and transfer of excitation energy from excited states of the inert gases is possible (*3, 19, 32, 33, 34*). At the higher concentrations an appreciable fraction of the energy is

deposited by initial interaction with the inert gas, particularly for xenon, and the subsequent physiochemical processes in benzene–inert gas mixtures are matters of conjecture. The excited states of xenon are lower in energy than the corresponding states of krypton—*e.g.*, the $^3P_2$ states are 8.31 and 9.91 e.v., respectively, and electronic energy transfer without decomposition is more likely with the former. Ausloos *et al.* (*1*) find that the importance of ionic reactions increases in the order Ar > Kr > Xe.

It appears that at lower concentrations ($< 0.3M$) inert gas induces intersystem crossing; other ill-defined processes occur at the higher concentrations.

Effect of Additives and Excited State Formation. Both carbon dioxide and sulfur hexafluoride are about as effective as nitrous oxide in reducing hydrogen yields in cyclohexane by electron scavenging (*44*). Any electron scavenging effect is obscured by isomerization catalysis by free radicals or radical ions. Carbon tetrachloride acts similarly. Saturation with water has a negligible effect, and this argues against a significant role of positive ions or carbanions derived from the olefin. It shows also that ionic forms of the solvent involved in excited state production are too short lived to react with the low concentrations of water. A similar comment applies to the experiments with ethyl alcohol. It is an effective positive ion scavenger in cyclohexane (*5*), but the $C_6H_6^+$ must be neutralized too quickly for any effect to be observable.

The earlier experiments (*14*) showed that the effect of piperidine arises from its function as a positive ion or proton scavenger. It is, however, an effective quencher of excited singlet states of benzene ($k_Q \approx 10^{10}$ mole^{-1} sec.$^{-1}$) (*12*), and the decrease in isomerization is most probably caused by this. The isomerization yield in the presence of both N_2O and piperidine is much the same as for each additive separately. If the singlet-quenching hypothesis is correct, the results imply that electron scavenging by nitrous oxide prevents the formation of singlet benzene. Pyridine is also an efficient deactivator of the $^1B_{2u}$ state of benzene (*12*), and the small reduction in isomerization may be caused by this. Nitromethane is an effective electron scavenger (*17*), but it readily quenches benzene fluorescence and can probably deactivate both the $^1B_{2u}$ and $^3B_{1u}$ states by energy transfer.

Conclusions

Triplet excited states of benzene, toluene, and possibly pyridine are formed by irradiation. These states are short lived in all the solvents, and interactions associated with the liquid state may be responsible. The excitation of olefin by sub-excitation electrons is a possibility which

Publication Date: January 1, 1968 | doi: 10.1021/ba-1968-0082.ch026

cannot be excluded. The triplet levels of olefins and aromatic solvents are probably separated by only 0.5 e.v., and consequently direct interaction of sub-excitation electrons with the olefin must be of limited importance. In solvents without low energy states, such as cyclohexane, direct action could be more effective. Only about a third of the excited states in benzene are produced by electron-ion recombination; the remainder must arise from electron impact excitation. The assumption that the isomerization of 2-butene is caused by triplet-triplet excitation energy transfer is essentially correct.

Previous evidence that about 60% of the excited states formed (*16*) are initially singlet is consistent with the present result using the spin-orbit coupling effect of xenon.

A 3:1 ratio of triplet:singlet yields is to be expected only if the spurs contain a sufficient number of recombining ions and any exciting electrons remain close to positive ions (*37*). A serious problem which remains is the reason for higher triplet yields measured by isomerization methods compared with pulse radiolysis—*e.g.*, 2.8 is the estimated yield in benzene–biacetyl solution (*13*). The difference could arise from quenching of excited states during the pulse, preventing their observation. Nanosecond pulse experiments may resolve the discrepancy.

The participation of excited states higher than the lowest singlet and triplet cannot be excluded, and tests directed towards this possibility need to be applied.

Publication Date: January 1, 1968 | doi: 10.1021/ba-1968-0082.ch026

Acknowledgments

The authors are grateful to ICI (Fibres) Ltd. for a maintenance grant for W. T.

Literature Cited

(1) Ausloos, P., Rebbert, R. E., Lias, S. G., *J. Chem. Phys.* **42,** 540 (1965).
(2) Birks, J. B., *Phys. Letters* **24A,** 479 (1967).
(3) Bone, L. I., Sieck, L. W., Futrell, J. H., *J. Chem. Phys.* **44,** 3667 (1966).
(4) Braun, C. L., Kato, S., Lipsky, S., *J. Chem. Phys.* **39,** 1645 (1963).
(5) Buchanan, J. W., Williams, F., *J. Chem. Phys.* **44,** 4377 (1966).
(6) Burns, W. G., Cundall, R. B., Griffiths, P. A., Marsh, W. R., *Trans. Faraday Soc.* **64,** 129 (1968).
(7) Caldwell, R. A., Whitten, D. G., Hammond, G. S., *J. Am. Chem. Soc.* **88,** 2659 (1966).
(8) Clever, H. L., Battino, R., Taylor, J. H., Gross, P. M., *J. Phys. Chem.* **61,** 1078 (1967).
(9) Collin, J., Lossing, F. P., *J. Chem. Phys.* **28,** 900 (1958).
(10) Cramer, W. A., Piet, G. J., *Trans. Faraday Soc.* **63,** 1402 (1967).
(11) Cullis, C. F., Francis, J. M., Swallow, A. J., *Proc. Roy. Soc.* **A287,** 15 (1965).
(12) Cundall, R. B., Evans, G. B., to be published.

(13) Cundall, R. B., Evans, G. B., Land, E. J., to be published.
(14) Cundall, R. B., Griffiths, P. A., *Discussions Faraday Soc.* **36,** 111 (1963).
(15) Cundall, R. B., Griffiths, P. A., *Trans. Faraday Soc.* **61,** 1968 (1965).
(16) Cundall, R. B., Griffiths, P. A., *Chem. Commun.* **1966,** 194.
(17) Cundall, R. B., Street, G. C., to be published.
(18) Dainton, F. S., "The Chemistry of Ionization and Excitation," G. R. A. Johnson, G. Scholes, eds., p. 3, Taylor & Francis, London, 1967.
(19) Davis, D. R., Libby, W. F., Kevan, L., *J. Am. Chem. Soc.* **87,** 2766 (1965).
(20) Dubois, J. T., van L. Sels, J. W., *Symp. Luminescence, Munich, 1965,* p. 109.
(21) Field, F. H., Franklin, J. L., "Electron Impact Phenomena," Academic Press, New York, 1957.
(22) Fischer, E., Lehmann, H. P., Stein, G., *J. Chem. Phys.* **45,** 3905 (1966).
(23) Golub, M. A., *J. Am. Chem. Soc.* **82,** 5093 (1960).
(24) Golub, M. A., Stephens, C. L., Brasch, J. L., *J. Chem. Phys.* **45,** 1503 (1966).
(25) Golub, M. A., Stephens, G. L., *J. Phys. Chem.* **70,** 3576 (1966).
(26) Grabowska, A., *Spectrochem. Acta.* **19,** 307 (1963).
(27) Hentz, R. R., Peterson, D. B., Srivastava, S. B., Barzynski, H. F., Burton, M., *J. Phys. Chem.* **70,** 2362 (1966).
(28) Herzberg, G., *Z. Physik. Chem.* **B17,** 68 (1932).
(29) Horrocks, A., Keavell, A., Tickle, K., Wilkinson, F., *Trans. Faraday Soc.* **62,** 3393 (1966).
(30) Kallmann, H., Furst, M., *Phys. Rev.* **79,** 859 (1950).
(31) Kemp, J. T., Salmon, G. A., Land, E. J., Nosworthy, J. M., "Energy Transfer in Radiation Processes," G. O. Phillips, ed., p. 72, Elsevier, Amsterdam, 1966.
(32) Kevan, L., *J. Chem. Phys.* **44,** 683 (1966).
(33) Klassen, N. V., *J. Chem. Phys.* **71,** 2409 (1967).
(34) Koob, R., Kevan, L., *J. Phys. Chem.* **70,** 1336 (1966).
(35) Land, E. J., "Pulse Radiolysis," M. Ebert, J. P. Keene, A. J. Swallow, J. H. Baxendale, eds., p. 294, Academic Press, New York, 1965.
(36) Lehmann, H. P., Stein, G., Fischer, E., *Chem. Commun.* **1965,** 583.
(37) Magee, J. L., "Comparative Effects of Radiation," M. Burton *et al.*, eds., p. 130, Wiley, New York, 1960.
(38) McClure, D. S., *J. Chem. Phys.* **17,** 905 (1949).
(39) Munday, C. S., Richards, J. T., Scholes, G., Simic, M., "The Chemistry of Ionization and Excitation," G. R. A. Johnson, G. Scholes, eds., p. 151, Taylor & Francis, London, 1967.
(40) Nosworthy, J. M., *Trans. Faraday Soc.* **61,** 1138 (1965).
(41) Platzman, R. L., *Radiation Res.* **2,** 1 (1955).
(42) Robinson, G. W., *J. Mol. Spec.* **6,** 58 (1961).
(43) Sato, S., Yugeta, R., Shinsaka, K., Terao, T., *Bull. Chem. Soc., Japan* **39,** 156 (1966).
(44) Scholes, G., Simic, M., *Nature* **202,** 895 (1964).
Scholes, G., Simic, M., Adams, G. E., Boag, J. W., Michael, B. D., *Nature* **204,** 1187 (1964).
(45) Schulte-Frohlinde, D., Gusten, H., *Z. Physik. Chem., N.F.,* **29,** 281 (1961).
(46) van L. Sels, J. W., Dubois, J. T., *J. Chem. Phys.* **45,** 1522 (1966).
(47) Shida, T., Hamill, W. H., *J. Am. Chem. Soc.* **88,** 5371 (1966).
(48) Smith, D. R., Pieroni, J. J., *Can. J. Chem.* **45,** 2723 (1967).
(49) Ward, H. R., Wishnok, J. S., Sherman, P. D., *J. Am. Chem. Soc.* **89,** 162 (1967).
(50) Wilzbach, K. E., Kaplan, L., *J. Am. Chem. Soc.* **88,** 2066 (1966).

RECEIVED February 12, 1968.

Mechanisms of Deferred Luminescence in Organic Solids after γ-Irradiation at 77°K.

A. DEROULEDE, F. KIEFFER, and M. MAGAT

Laboratoire de Physico-Chimie des Rayonnements, Orsay, France

Publication Date: January 1, 1968 | doi: 10.1021/ba-1968-0082.ch027

The technique of radiophotoluminescence excitation spectra is used to study the displacement of electrons from physical traps to solute molecules and vice-versa in solutions of biphenyl in methylcyclohexane. Bleaching in the infrared leads to the disappearance of trapped electrons and of the first peak of radiothermoluminescence. If a bleached sample is illuminated in one of the two biphenyl anion absorption bands, both infrared-stimulated RPL and a weak first glow peak reappear. It is concluded that of the two RTL peaks observed at 90° and 95°K. in methylcyclohexane glass, the first is caused by recombination of electrons with solute cations and the second by diffusion and recombination of solute anions and cations.

Recent investigations on the radiothermoluminescence (RTL) of organic substances have led to the conclusion that the emission of light is caused by the recombination of charged species trapped during γ-irradiation and liberated when the substance is subsequently warmed (*1, 5, 10, 15, 21, 37*). The photothermoluminescence (PTL)—*i.e.*, thermoluminescence (PTL)—*i.e.*, thermoluminescence observed after ultraviolet irradiation, has been shown similarly to be caused by the recombination of charged species produced in the process of photoionization (*3, 23, 25, 28, 44, 45*). Optical detrapping of electrons by light of suitable wavelengths also leads to recombination of charged species and emission of light: both radiophotoluminescence (RPL) (*6, 9, 16, 32, 41, 42*) and photophotoluminescence (PPL) (*17, 24, 30, 31, 44, 45*) have been observed upon optical stimulation of γ-irradiated organic solids and ultraviolet-photoionized organic solids, respectively.

An important common feature of these four types of deferred luminescence lies in its spectral composition. In the presence of a luminescent

In Radiation Chemistry; Hart, E.;
Advances in Chemistry; American Chemical Society: Washington, DC, 1968.

solute (or impurity) the emission consists of the fluorescence and phosphorescence of this solute, the ratio of phosphorescence to fluorescence being considerably enhanced compared with the ratio observed in the photoluminescence (*2, 4, 6, 7, 9, 17, 30*) of identical solutions. This common feature suggests that a common mechanism might be responsible: the recombination of charged species.

Charge recombination can occur in two ways: (1) diffusion of electrons or holes released from physical or molecular traps and their reaction with trapped charges of the opposite sign, and (2) diffusion and mutual neutralization of molecular or radical ions. In rigid glasses or crystalline solids, the former alone is likely to happen at temperatures near 77°K. Thus, the RPL emitted upon illumination at 77°K. in the absorption bands of the trapped electron or the trapped anion can be attributed only to the first type of process. Glow peaks occurring at higher temperatures have been shown to coincide in many substances with temperatures at which molecular mobility in the solid increases, such as phase transitions (*29, 35*), and can therefore be ascribed to the second process. The origin of glow peaks occurring at lower temperatures, such as the first two peaks observed in crystalline cyclohexane, is still uncertain (*8*).

Much information about the migrations of charged species in irradiated organic solids at 77°K. or higher has been gathered by studying conductivity (*19, 20, 40, 43*).

Methylcyclohexane (MCH) appeared to be a particularly suitable matrix for studying the mechanisms of deferred luminescence. As reported earlier (*12*), the RTL of glassy MCH containing durene, biphenyl, or naphthalene consists of two glow peaks, at 90° and 95°K. Only the first can be completely bleached out by illumination with light of wavelength greater than 1.1 μ. Another difference between these two peaks is that, under the operating conditions used (which did not, in fact, exclude oxygen), the emission spectrum in the first peak consisted of both fluorescence and phosphorescence of the solutes, while phosphorescence only was observed in the second peak. We therefore postulated different mechanisms, attributing the first peak to a recombination of detrapped electrons with solute cations, and the second one to a recombination of some ionic species of molecular dimensions. Diffusion of the latter is possible indeed at 95°K. since Roncin (*34*) has shown by ESR spectroscopy that the diffusion of trapped solvent radicals in this matrix sets in precisely at this temperature.

Caperan (*11*) has shown that in non-deaerated solutions of durene in MCH glass the light sum emitted in the second peak increases linearly with durene concentration, whereas that of the first peak increases less steeply (Figure 1). If the first peak is caused by the reaction

$$e^- + Ar^+ \rightarrow Ar^*$$

Publication Date: January 1, 1968 | doi: 10.1021/ba-1968-0082.ch027

(where Ar^+ and Ar^* represent the solute cation and excited molecule, respectively), its increase with increasing concentration is at first surprising since several investigations have shown a competition between physical traps and solute molecules for electrons released during irradiation. Both absorption spectroscopy (*18, 22, 26*) and ESR spectroscopy (*38, 39*) have shown that such a competition leads to a decrease in the number of trapped electrons with increasing solute concentration. However, we must remember that the luminescence emitted is proportional to the product $(e^-)(Ar^+)$, and that (Ar^+) increases with increasing solute concentration. Therefore, the mechanism proposed for the first peak is not incompatible with the increase of this peak observed with increasing solute concentration. Caperan attributes the second peak to the reaction:

$$Ar^+ + Ar^- \rightarrow Ar^*.$$

A quantitative treatment of RTL is extremely difficult owing to a possible participation of solvent ions with subsequent transfer of excitation to the solute.

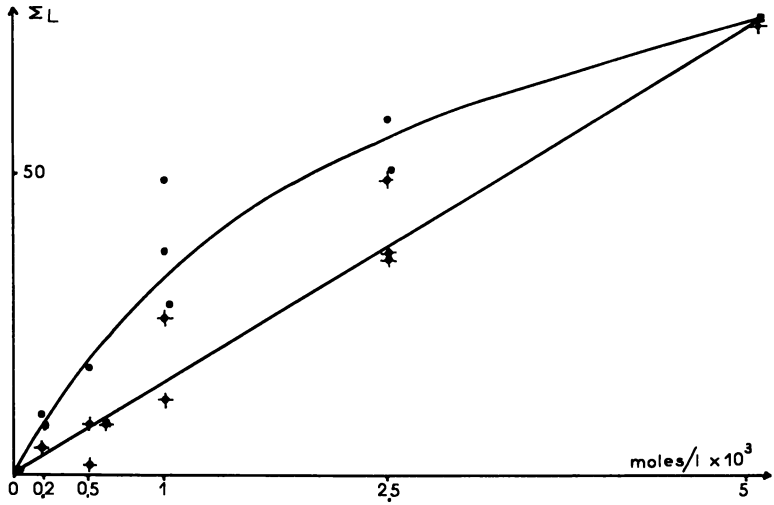

Figure 1. RTL of durene in MCH glass

Dose: 600 rads
●: *Light sum of first peak*
✦: *Light sum of second peak*

For PTL, however, where solvent molecules are not ionized, a quantitative treatment has been carried out by Gauthier-Bodard and Bullot (*23*). For deaerated solutions of durene in MCH glass, they found

that the PTL emitted after irradiation with light of wavelength 275 mμ can be fully explained by the recombination of durene cations with electrons in the first peak and with durene anions in the second peak.

We have recently applied the technique of excitation spectra to the study of the RPL of MCH glasses containing biphenyl (*16*). By plotting the intensity of the light burst emitted *vs.* the wavenumber of the exciting light, we obtained excitation spectra which, for $10^{-2}M$ biphenyl solution, were identical with the absorption spectrum of biphenyl anion (*33*). For a $10^{-4}M$ solution, the excitation spectrum was situated in the same region as the absorption spectrum of trapped electrons in 3-methylpentane (3-MP) (*22*), and in a $10^{-3}M$ solution, both trapped electron and anion spectra appeared. We thus had a means of following the appearance or disappearance of both negative species after various treatments: illumination in the trapped electron band or in the anion band, and heating above the glow peak, or any combination of these. In the present work we shall show the correlation of the first peak with the presence of trapped electrons and of the second peak with trapped anions.

Experimental

After bubbling helium through the solution to remove possible traces of CO_2, 0·5-ml. samples in shallow copper containers are linked to a vacuum line and degassed by the freeze-pump-thaw technique. They are then irradiated at 77°K. with a cobalt-60 source to a dose of usually about 60 krad, at a dose rate of about 80 rads/min. The container is opened under liquid nitrogen and transferred to a liquid nitrogen cryostat, where it is positioned at an angle of 45° with respect to two silica light guides set at right angles to each other in the wall of the cryostat (Figure 2). The sample is illuminated with light from a xenon arc (or a tungsten filament lamp in the infrared region), through a monochromator and one of the light guides.

A photomultiplier tube is placed at the end of the other light guide. Two synchronized electromechanical shutters placed between the light source and the monochromator and in front of the photomultiplier, protect the latter while the exciting light is on. Excitation lasted for 0.25 sec., and the photomultiplier was uncovered 0.25 sec. after excitation. Thus, we can study only solutes whose phosphorescence lifetimes are longer than about 0.2 sec. To obtain a constant flux of photons at different wavenumbers, we adjust the monochromator slit widths according to a calibration with a thermopile. The photomultiplier output was displayed on an oscilloscope and photographed. The plot of the photoresponse against wavenumber of the exciting light constitutes the RPL excitation spectrum.

Prolonged photobleaching in the infrared is carried out through the monochromator plus a silicon filter which eliminates any stray light of wavenumber greater than about 9000 $cm.^{-1}$.

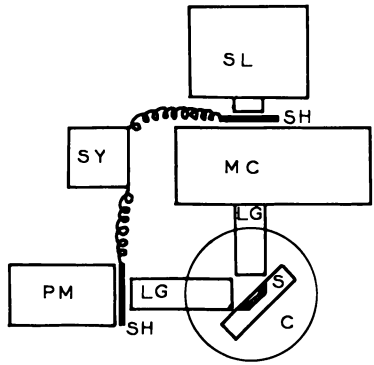

Figure 2. Block diagram of experimental setup

Legend:
SL, light source
SH, shutter
SY, synchronizer "Comobelmec"
MC, monochromator
LG, light guide
PM, photomultiplier
C, cryostat
S, sample

Results

Excitation Spectrum in MCH. (1) Figure 3A shows the RPL excitation spectrum of biphenyl in MCH glass, and a fine structure appears in the infrared part of the excitation spectrum. We have observed analogous fine structures also in 3-MP glass and in polycrystalline cyclohexane containing biphenyl. Such a structure has not been observed in absorption spectroscopy (*22*). Its significance is not clear, but it does not correspond to discrete trapping levels since illumination in the lowest energy band (6300 $cm.^{-1}$) bleaches the whole of the infrared spectrum. [As A. C. Albrecht has suggested to us, these fine structures are in fact caused by the infrared absorption bands of the solvents. This can be seen in Figures 3A and 3D.]

(2) The infrared part of the excitation spectrum can be observed some 24 hours after the end of irradiation. Thus, the trapped electrons seem to be very stable in MCH at 77°K., although Chachaty (*13*), who observed both trapped electrons and biphenyl anions in MCH glass by ESR spectroscopy, states that the half-life of trapped electrons is only about 30 min. [However, he does not exclude entirely that some bleaching by day light may have occurred in his case (*14*).]

(3) After prolonged bleaching at 6300 or 7300 cm.$^{-1}$, the sample no longer responds to infrared light (Figure 3B). Response in anion bands is diminished only slightly, and more in the 15,500 cm.$^{-1}$ band than in the 24,500 cm.$^{-1}$ band; this may be caused by some overlapping of the trapped electron absorption with the 15,500 cm.$^{-1}$ band.

(4) After thermal bleaching of the first RTL peak (*i.e.*, heating at a rate of about 2°C./min. until the first glow peak has passed and the light intensity just begins to increase again owing to the second peak) and rapid cooling to 77°K., the excitation spectrum is modified exactly as above.

(5) The glow curve of a sample which no longer responds to infrared light (owing to photobleaching or thermal bleaching) consists of the second peak only.

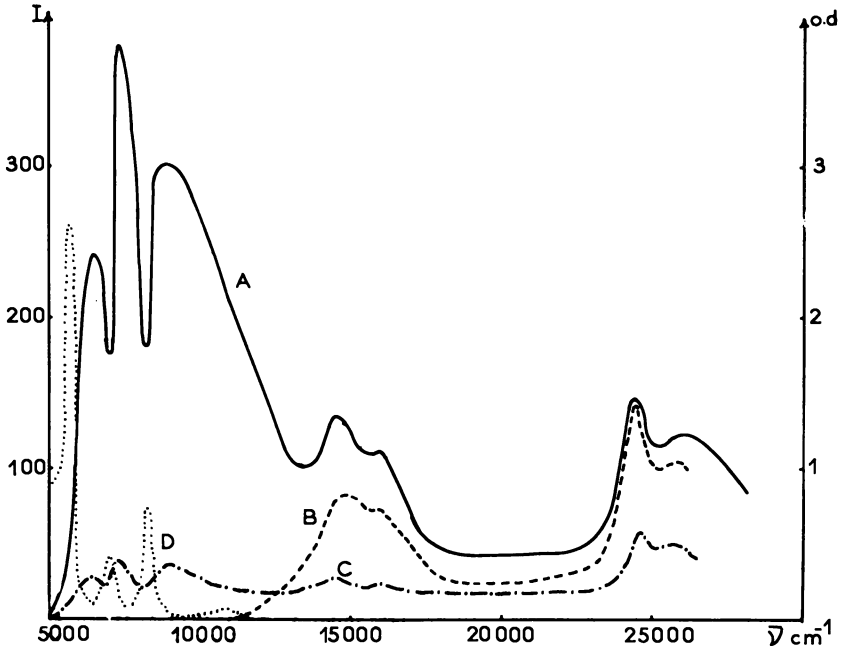

Figure 3. RPL excitation spectra of 5 × 10^{-4}M biphenyl in MCH glass

(A): After γ-irradiation
(B): After bleaching at 7300 cm.$^{-1}$
(C): After photodetachment at 25,000 cm.$^{-1}$
(D): Absorption spectrum of MCH at room temperature

(6) After Treatment 3 or 4, illumination in the 15,500 or 24,500 cm.$^{-1}$ regions restores a considerable response in the infrared (Figure 3C). This is shown also by Tables I and II. The restored photoresponse at 7300

cm.$^{-1}$ passes through a maximum and decreases with further illumination in the anion bands.

(7) In a sample with a restored infrared response, the first glow peak reappears but seems weaker than would be expected from the photoresponse.

(8) In a sample with a decreased response in the anion absorption bands, the second glow peak also is reduced.

Table I. Evolution of the Photoresponse of a 5 × 10^{-4}M Solution of Biphenyl in MCH Glass after Thermal Bleaching of the First Peak and Illumination in the 15,500 cm.$^{-1}$ Band

Successive Treatments of Sample	*Photoresponse (in relative units) at ν cm.$^{-1}$*		
	7300	*15,500*	*25,000*
γ-Irradiation (180 krads)	4.6	2.2	2.7
Thermal bleaching of first peak	0.006	1.2	2.5
Illumination at 15,500 cm.$^{-1}$ for 3 min.	0.3	0.6	0.8
Illumination at 15,500 cm.$^{-1}$ for 11 min.	0.2	0.3	0.4

Table II. Evolution of the Photoresponse of a 5 × 10^{-4}M Solution of Biphenyl in MCH Glass after Optical Bleaching at 7300 cm.$^{-1}$ and Illumination in the 24,500 cm.$^{-1}$ Band

Successive Treatments of Sample	*Photoresponse (in relative units) at ν cm.$^{-1}$*		
	7300	*14,500*	*24,500*
γ-Irradiation (60 krads)	3	1.35	1.5
Illumination at 7300 cm.$^{-1}$ for 75 min.	0.003	0.8	1.5
Illumination at 24,500 cm.$^{-1}$ for 10 sec.	0.17	0.7	1.3
Illumination at 24,500 cm.$^{-1}$ for 30 sec.	0.18	0.5	1.1
Illumination at 24,500 cm.$^{-1}$ for 3 min.	0.4	0.3	0.5
Illumination at 24,500 cm.$^{-1}$ for 10 min.	0.3	0.15	0.25

Other Solvents. Similar spectra to those of biphenyl in MCH glass are obtained in 3-MP glass, but in this case the response in the infrared disappears rapidly at 77°K. At the low dose rate employed (80 rads/min.), the infrared response is hardly measurable 20 min. after irradiation ends but can be increased considerably by illumination in the 15,500 cm.$^{-1}$ anion band (Figure 4).

In polycrystalline solutions of biphenyl in cyclohexane, excitation spectra similar to those observed in MCH are obtained, but the response in the trapped electron band is weaker than in MCH at the same concentrations of biphenyl. Hence, trapping of electrons by the matrix occurs in doped crystals but is less efficient than in glasses.

Publication Date: January 1, 1968 | doi: 10.1021/ba-1968-0082.ch027

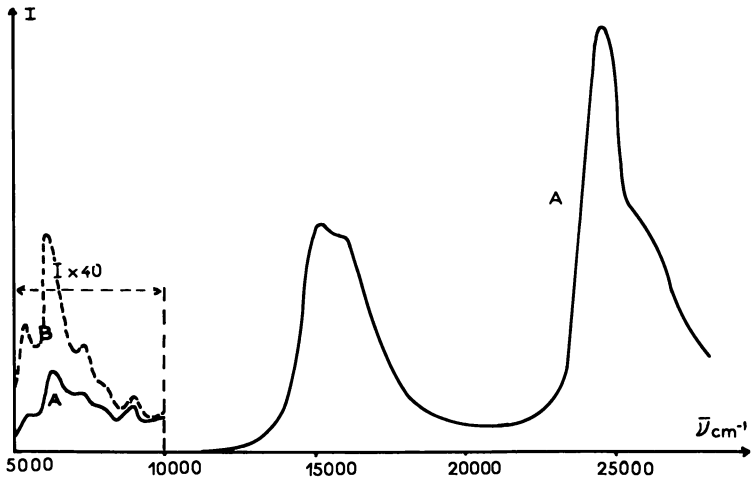

Figure 4. RPL excitation spectra of 10^{-3}M biphenyl in 3-MP glass
(A): After γ-irradiation
(B): After photodetachment at 15,500 cm.$^{-1}$

In polycrystalline carbon tetrachloride, no response is obtained in either the biphenyl anion band or in the infrared. This was to be expected for Shida and Hamill (*36*) found that owing to dissociative electron capture by the solvent, only cations of biphenyl are formed in CCl_4, the corresponding anion being probably Cl^-.

Discussion

All our observations can be interpreted in terms of electron detrapping. If electrons are trapped during irradiation either in "physical defects" in the solvent or by attachment to biphenyl molecules, they can be liberated by illumination in the corresponding absorption bands:

$$e^-_{tr} \xrightarrow[\text{infrared}]{h\nu} e^-_{mobile} \quad (1)$$

$$Ar^- \xrightarrow[\nu = 15000 \text{ or } 25000 \text{ cm.}^{-1}]{h\nu} Ar + e^-_{mobile} \quad (2)$$

The mobile electrons can either neutralize biphenyl cations, giving rise to the RPL which we observe:

$$e^- + Ar^+ \rightarrow Ar^* \rightarrow Ar + h\nu \quad (3)$$

or be captured by (a) biphenyl molecules to give biphenyl anions

$$e^- + Ar \rightarrow Ar^- \quad (4)$$

Publication Date: January 1, 1968 | doi: 10.1021/ba-1968-0082.ch027

or by (b) physical defects to give trapped electrons. Such displacements of electrons have been observed in 3-MP glass by Wiseall and Willard (*43*), who showed by conductivity measurements that electrons are freed from traps by light of 7300 $cm.^{-1}$ and detached from biphenyl anions by light of 24,400 $cm.^{-1}$.

We observe, though much less perfectly, the reversible passage of electrons from traps to biphenyl molecules which has been so strikingly described by Gallivan and Hamill (*22*) and by Dyne and Miller (*18*). This is because we do not measure directly the concentrations of anions or of trapped electrons but a phenomenon proportional to the product of these concentrations with the concentration of biphenyl cations remaining in the glass at the time of each measurement. It is therefore normal that after prolonged bleaching in one band, entailing a considerable decrease in cation concentration, owing to Reaction 3, excitation in the absorption band of the other negative species should produce a lower response than could be expected from the displacement of electrons from one sort of traps to the other.

Buben and co-workers (*32, 41, 42*) investigated RPL excitation spectra, and they observed in aromatic matrices a similar concomitant decrease of two types of bands (*42*). They attributed one of these to anions and the other to trapped holes. In our case at least, this hypothesis does not apply because it would be incompatible with the observed restoration of the infrared response and of the first glow peak which can be fully explained by the photodetachment of electrons from biphenyl anions and their retrapping in the matrix.

The observed link between infrared response of a sample and the first glow peak proves conclusively that electrons liberated from the matrix are responsible for the first peak.

The second glow peak is reduced when the number of trapped anions is reduced. Therefore, the second glow peak must be ascribed at least partially to the diffusion of biphenyl cations and anions and their mutual neutralization:

$$Ar^+ + Ar^- \rightarrow Ar + Ar^* \rightarrow Ar + h\nu \qquad (5)$$

It is in principle impossible to bleach out the second peak completely by illumination in the anion bands, for at the temperature of the first peak a proportion of the electrons liberated from their matrix traps is captured by biphenyl molecules (Reaction 4), so that anions become available again for diffusion and recombination at 95°K.

It is probable that at doses sufficient to produce a fair number of solvent radicals (*e.g.*, about 1 Mrad), these also act as traps for the electrons and holes, as suggested by Buben and co-workers (*32, 41, 42*), and thus contribute to the second glow peak.

Publication Date: January 1, 1968 | doi: 10.1021/ba-1968-0082.ch027

In conclusion, the first glow peak (90°K.) in MCH glass containing biphenyl can be described by Reactions 1 and 3 and the second peak (95°K.) by Reaction 5. We cannot exclude at present a participation of solvent cations, as follows:

In the first peak:

$$e^- + S^+ \rightarrow S^*, \text{ followed by excitation transfer:}$$

$$S^* + Ar \rightarrow S + Ar^* \rightarrow Ar + h\nu$$

In the second peak:

$$Ar^- + S^+ \rightarrow S^* + Ar \rightarrow S + Ar^* \rightarrow Ar + h\nu$$

The excitation transfer involved in these reactions would be more likely in the second peak where the solute molecule is necessarily close to the excited solvent molecule.

The great advantage of using RPL excitation spectra is that it constitutes a method of determining selectively the absorption spectra of negative ions alone without any overlapping with the absorption bands of the corresponding cations which, generally, are present at the same time and often lie in the same spectral region. It makes it possible, therefore, to estimate the relative amounts of trapped electrons and solute anions formed in the radiolysis of glassy or crystalline organic solutions of different concentrations. From this the distance to which electrons can migrate during irradiation can be evaluated (*16*).

Our work is thus far qualitative, but we hope to have quantitative results which will give information about the possible contribution of other species, such as solvent cations and radical ions to the RTL of MCH.

Publication Date: January 1, 1968 | doi: 10.1021/ba-1968-0082.ch027

Literature Cited

(1) Alfimov, M. V., Nikol'skii, V. G., Buben, N. Ya., *Kinetika i Kataliz* **5**, 268 (1964).
(2) Bagdasaryan, Kh. S., Milyutinskaya, R. I., Kovalev, Yu. V., *Khim. Vysok. Energ.* **1**, 127 (1967).
(3) Brocklehurst, B., Gibbons, W. A., Lang, F. T., Porter, G., Savadatti, M. I., *Trans. Faraday Soc.* **62**, 1793 (1966).
(4) Brocklehurst, B., Porter, G., Yates, J. M., *J. Phys. Chem.* **68**, 203 (1964).
(5) Brocklehurst, B., Russell, R. D., *Nature* **213**, 65 (1967).
(6) Brocklehurst, B., Russell, R. D., Savadatti, M. I., *Trans. Faraday Soc.* **62**, 1129 (1966).
(7) Bullot, J., Deroulede, A., Kieffer, F., *Intern. Lumineszenz-Symp., Munich, 1965*, p. 173.
(8) Bullot, J., Deroulede, A., Kieffer, F., *J. Chim. Phys.*, 150 (1966).
(9) Bullot, J., Deroulede, A., Kieffer, F., unpublished results.
(10) Burton, M., Dillon, M., Rein, R., *J. Chem. Phys.* **41**, 2228 (1964).
(11) Caperan, M. J., Ph.D. Thesis, Faculté des Sciences, Orsay (1967).

(12) Caperan, M. J., Bullot, J., Deroulede, A., Kieffer, F., *C.R. Acad. Sci. Paris* **264,** 1013 (1967).
(13) Chachaty, C., *J. Chim. Phys.*, 614 (1967).
(14) Chachaty, C., private communication.
(15) Deroulede, A., Kieffer, F., Magat, M., *Israël J. Chem.* **1,** 509 (1963).
(16) Deroulede, A., Kieffer, F., *Nature* **215,** 1475 (1967).
(17) Dolan, E., Albrecht, A. C., *J. Chem. Phys.* **37,** 1149 (1962).
(18) Dyne, P. J., Miller, O. A., *Can. J. Chem.* **43,** 2696 (1965).
(19) Frankevich, E. L., *Usp. Khim.* **35,** 1161 (1966).
(20) Frankevich, E. L., Yakovlev, B. S., *Izv. Akad. Nauk S.S.S.R., Ser. Khim. Nauk*, 1358 (1964).
(21) Funabashi, K., Herley, P. J., Burton, M., *J. Chem. Phys.* **43,** 3939 (1965).
(22) Gallivan, J. B., Hamill, W. H., *J. Chem. Phys.* **44,** 1279 (1966).
(23) Gauthier-Bodard, M., Bullot, J., *Intern. Conf. Luminescence, Munich* (1967).
(24) Gauthier-Bodard, M., Bullot, J., unpublished results.
(25) Gibbons, W. A., Porter, G., Savadatti, M. I., *Nature* **206,** 1355 (1965).
(26) Guarino, J. P., Hamill, W. H., *J. Am. Chem. Soc.* **86,** 777 (1964).
(27) Johnson, G. E., Albrecht, A. C., *J. Chem. Phys.* **44,** 3162, 3179 (1966).
(28) Linschitz, H., Berry, M. G., Schweitzer, D., *J. Am. Chem. Soc.* **76,** 5833 (1954).
(29) Magat, M., *J. Chim. Phys.*, 142 (1966).
(30) McClain, W. M., Albrecht, A. C., *J. Chem. Phys.* **43,** 465 (1965).
(31) McClain, W. M., Albrecht, A. C., *J. Chem. Phys.* **44,** 1594 (1966).
(32) Nikol'skii, V. G., Tochin, V. A., Buben, N. Ya., *Fiz. Tverd. Tela* **5,** 2248 (1963).
(33) Ronayne, M. R., Guarino, J. P., Hamill, W. H., *J. Am. Chem. Soc.* **84,** 4230 (1962).
(34) Roncin, J., private communication.
(35) Semenov, N. N., I.U.P.A.C. Congress, Montréal, 1961, p. 353.
(36) Shida, T., Hamill, W. H., *J. Chem. Phys.* **44,** 2375 (1966).
(37) Skelly, D. W., Hamill, W. H., *J. Chem. Phys.* **43,** 3497 (1965); **44,** 2891 (1966).
(38) Smith, D. R., Pieroni, J. J., *Can. J. Chem.* **43,** 2141 (1965).
(39) Smith, D. R., Pieroni, J. J., *J. Phys. Chem.* **70,** 2379 (1966).
(40) Tochin, V. A., *Fiz. Tverd. Tela* **7,** 293 (1964).
(41) Tochin, V. A., Buben, N. Ya., *Khim. Vysok. Energ.* **1,** 78 (1967).
(42) Tochin, V. A., Nikol'skii, V. G., Buben, N. Ya., *Khim. Vysok. Energ.* **1,** 71 (1967).
(43) Wiseall, B., Willard, J. E., *J. Chem. Phys.* **46,** 4387 (1967).
(44) Yamamoto, N., Nakato, Y., Tsubomura, H., *Bull. Chem. Soc. Japan* **39,** 2603 (1966).
(45) *Ibid.*, **40,** 461 (1967).

RECEIVED January 2, 1968.

28

Ionic Reactions in Ethyl Chloride

THOMAS O. TIERNAN and B. MASON HUGHES

Aerospace Research Laboratories, Wright-Patterson Air Force Base, Ohio 45433

Publication Date: January 1, 1968 | doi: 10.1021/ba-1968-0082.ch028

Ion-molecule reactions in gaseous ethyl chloride are identified by detailed mass spectrometric investigation. The majority of these reactions lead ultimately to a single unreactive ionic product, $C_4H_{10}Cl^+$, which constitutes about 70% of the total ionic yield at a system pressure of 1000 μ. From the radiolysis products of ethyl chloride and of ethyl chloride with various additives, the ionic fragmentation scheme is deduced at the higher pressures used. Ion-scavenging techniques are used to characterize unreactive ions in the radiolysis system. The product distribution resulting from excited ethyl chloride molecule decomposition is derived from related photolysis studies and is used in conjunction with data obtained for the other reaction processes to construct a complete mechanism for the radiolytic decomposition.

The revival of interest in ionic processes during the last decade precipitated the examination of such reactions in many chemical systems, chiefly by mass spectrometric techniques which were developed independently in several laboratories (*10, 36, 40*). Among the earlier investigations of this type were studies of certain alkyl halides (*14, 31, 32*), which are of particular interest because they provided the first reported examples of reactions in which collision complexes formed from ion-neutral interactions were directly observed. Such intermediates are not generally detected because of their very short lifetimes. Since the initial observation, however, "stable" reaction complexes have been reported in a variety of other compounds including acrylonitrile, benzene, and cyanogen (*17, 18, 41*). Recent experiments in this laboratory (*3, 12, 28, 43*) have been concerned with the formation of intermediate complexes in ion-molecule reactions in hydrocarbons. These studies have shown clearly that collisional stabilization of such intermediates is possible, and in some cases lifetimes have been estimated. These findings

In Radiation Chemistry; Hart, E.;
Advances in Chemistry; American Chemical Society: Washington, DC, 1968.

are significant in applying data derived by mass spectrometric methods to radiation chemistry, where the pressure range used is frequently several orders of magnitude higher than that realized in the mass spectrometer and where stabilization of intermediate ionic species may be expected to occur readily, thereby altering radically the ionic reaction mechanisms which the spectrometric studies suggest.

Several recent publications indicate that the role of intermediate complexes in ionic reactions is still controversial (*21, 24, 25*). Our interest in this and earlier observations of persistent complexes in alkyl halides already mentioned prompted us to study ionic reactions in ethyl chloride. The previously noted mass spectrometric investigations of alkyl halides did not include the chlorides, and radiolytic studies of these compounds have been limited to the propyl and butyl chlorides which apparently isomerize (*39*). The present investigation consists of two phases. In the initial phase, the ion-molecule reactions for ethyl chloride were probed by the sensitive mass spectrometric methods which we have applied in recent studies of a similar nature (*3, 12, 28, 43*). In the latter part of this study, the gas-phase radiolysis and vacuum-ultraviolet photolysis of ethyl chloride have been studied to identify those products which arise from ionic precursors. More specifically, we wished to define the behavior under radiolytic conditions of those intermediate ionic species which the spectrometric studies suggested were important, and we hoped to arrive at a reasonable conciliation of the ionic reaction information derived from these different but complementary techniques.

Publication Date: January 1, 1968 | doi: 10.1021/ba-1968-0082.ch028

Experimental

Mass Spectrometric Methods. The mass spectrometric techniques used have been described (*12, 28 43*). Mass spectra at elevated pressures were determined using a Bendix Time-of-Flight mass spectrometer with a specially designed ion-molecule reaction source, developed in this laboratory. This instrument, which can be operated at source pressures up to about 1 torr, has been described (*42*). It is equipped with a high capacity pumping system which provides a pressure differential from source to surrounding vacuum envelope of about 1000:1, and the analyzer region is evacuated by a separate pump so that the pressure in the flight tube does not exceed 10^{-6} torr when the source pressure is 1 torr. The source dimensions are such that the distance from the collimated electron beam to the exit aperture is 0.28 cm. Throughout the experiments, the repeller potential was adjusted to give a source field strength of 10.6 volts/cm., and the source temperature was maintained at 250°C. For a given experiment the source pressure was maintained constant, within about 1%, by a Granville-Phillips series 312 automatic pressure controller, activated by an MKS Baratron model 77H-1 pressure transducer.

In addition to the studies at elevated pressures which allow us to observe higher order ion-molecule processes and to determine the over-all

condensation sequence, individual ionic reaction steps were identified by a dual stage mass spectrometer. The ARL tandem mass spectrometer used has been described (*11*). Briefly, it consists of two double-focusing mass spectrometers in tandem separated by an intermediate collision chamber with a separate gas inlet. The first-stage spectrometer yields a mass- and energy-resolved ion beam which is impacted on the target gas in the collision chamber. The ionic products of this interaction are analyzed in the second-stage spectrometer. The two stages are in an in-line configuration to maximize collection of momentum transfer products, as from ion-molecule reactions. For all experiments reported, the energy of the impacting ionic species was maintained at an indicated 0.3 e.v. The energy spread of the ion beam is also estimated to be 0.3 e.v.

The instrument was used to study individual ionic reactions which were suggested by the condensation sequence for the ethyl chloride system. Obviously, first-order reactions observed in the high pressure investigation are readily examined in the tandem by introducing the system gas into the first stage and selecting the desired reactant ion. The study of higher order processes for such a system, however, would require elevating the pressure sufficiently in the first stage to produce these higher order ions. In fact, pressure limitations prohibit the use of the first stage of the tandem as a source for such higher order ions; therefore, such reactions are studied by introducing into the first stage a source gas which will yield by unimolecular fragmentation an ion of the same empirical formula as that involved in the high pressure reaction sequence. Certainly, this method must be used with caution since there may well be unknown differences in the reactant ion energy or structure in the two cases, but prior experience indicates that reliable reaction data can usually be obtained this way.

Radiolysis and Photolysis Techniques. The source of ionizing radiation was a 50-Kev. x-ray unit, operated at peak energy and 50-ma. current. The radiolysis vessels were spherical borosilicate glass flasks (1000 cc.) into which thin bubble windows were blown of thickness on the order of 20 mg./sq. cm. These vessels were fitted with calibrated volumes to facilitate determination of absolute yields. The majority of irradiations were conducted at a gas pressure of 357 mm. Hg, although several experiments at a pressure of 40 mm. Hg are also reported. Using a nitrous oxide dosimeter (*15, 38*) the dose rate for ethyl chloride at 357 mm. Hg pressure was determined to be 1.2×10^{18} e.v./min.

The vacuum ultraviolet photolysis source was a krypton resonance lamp, constructed with some modifications according to the design of workers at the National Bureau of Standards (*22, 29*). This lamp, fitted with lithium fluoride windows, was sealed directly to the reaction vessel whose volume was *ca.* 50 cc. The spectral emission of the lamp was examined with a scanning monochromator of the Seya-Namioka type. Some 75% of the emission in the region 1000–1600 A. was found to consist of the 1236-A. line. All photolysis experiments were carried out with a sample pressure of 40 mm. Hg. In addition to the 1236-A. line,

Publication Date: January 1, 1968 | doi: 10.1021/ba-1968-0082.ch028

the emission spectrum exhibited a peak at 1165 A. which was about 20% as intense as the former line. Much smaller peaks were detected at 1550 and 1600 A., which may be attributed to water impurities. Since the impurity lines taken together were only about 5% of the intensity of the 1236-A. line, apparently these are a negligible component of the lamp emission. In any case, the reported absorption spectrum of ethyl chloride (*33*) shows that the B and C bands which fall in the 1540–1610-A. region are extremely diffuse and much weaker than observed for the major absorption region from 1350 A. and below.

Radiolysis and photolysis products were analyzed by injecting samples into an F & M gas chromatograph provided with a flame ionization detector. A 1/4-inch o.d. Teflon column 2 ft. long, packed with Porapak Q, was used to separate the components from the column in a reasonably short time. In some cases fractions were trapped out from the helium stream at the column outlet and analyzed on a C.E.C. 21-103C mass spectrometer. Conventional high vacuum techniques were used in handling all gaseous samples and products.

Materials. Ethyl chloride and other gases were obtained from the Matheson Co. All samples were degassed and vacuum purified. Deuterated compounds were obtained from Merck Sharp and Dohme, Ltd. and were used as received except for removing noncondensible gas at liquid nitrogen temperature.

Publication Date: January 1, 1968 | doi: 10.1021/ba-1968-0082.ch028

Results and Discussion

Ionic Reactions. The unimolecular ionic dissociation of ethyl chloride, which is exhibited by the low pressure ($\sim 10^{-6}$ mm. Hg) mass spectrum, yields the following major ions in the indicated relative abundances: $C_2H_2^+$, 0.069; $C_2H_3^+$, 0.18; $C_2H_5^+$, 0.17; $CH_2{}^{35}Cl^+$, 0.043; $CH_2{}^{37}Cl^+$, 0.017; $C_2H_5{}^{35}Cl^+$, 0.15; $C_2H_5{}^{37}Cl^+$, 0.046. Although the exact nature of the fragmentation processes which lead to these ions is not known, these are the primary species which will interact further with ethyl chloride as the pressure is elevated sufficiently to effect reactive collisions. Consequently, the reactions of each of these species with ethyl chloride has been examined in the tandem mass spectrometer, using ethyl chloride as the source of the mass and energy selected impacting ion which was generated in the first stage of the instrument. The reactions observed when a pressure of 5 μ of gas were introduced into the collision chamber are listed below with the relative rate constants. CH_2Cl^+ ion was produced in such small yield that the rate data obtained for it was unreliable and therefore is not reported.

$$C_2H_2^+ + C_2H_5Cl \xrightarrow{k_{1a}} C_2H_5^+ + C_2H_2Cl \qquad k_{1a}/k_{1b} = 2.8/1 \qquad (1a)$$

$$\xrightarrow{k_{1b}} C_2H_4^+ + C_2H_3Cl \qquad (1b)$$

$$C_2H_3^+ + C_2H_5Cl \xrightarrow{k_{2a}} C_2H_5^+ + C_2H_3Cl \qquad k_{2a}/k_{2b} = 2/1 \qquad (2a)$$

$$\xrightarrow{k_{2b}} C_2H_6Cl^+ + C_2H_2 \qquad (2b)$$

$$C_2H_4^+ + C_2H_5Cl \xrightarrow{k_{3a}} C_2H_3Cl^+ + C_2H_6 \qquad (3a)$$

$$\xrightarrow{k_{3b}} C_2H_5^+ + C_2H_4Cl \qquad k_{3a}/k_{3b}/k_{3c}/k_{3d} = \qquad (3b)$$

$$\xrightarrow{k_{3c}} C_2H_4Cl^+ + C_2H_5 \qquad 2.3/1.7/1.7/1 \qquad (3c)$$

$$\xrightarrow{k_{3d}} C_4H_8^+ + HCl \qquad (3d)$$

$$C_2H_5^+ + C_2H_5Cl \xrightarrow{k_{4a}} C_2H_6Cl^+ + C_2H_4 \qquad k_{4a}/k_{4b} = 13/1 \qquad (4a)$$

$$\xrightarrow{k_{4b}} C_3H_5^+ + (CH_4 + HCl) \qquad (4b)$$

$$C_2H_5Cl^+ + C_2H_5Cl \xrightarrow{k_{5a}} C_2H_6Cl^+ + C_2H_4Cl \qquad k_{5a}/k_{5b} = 4.6/1 \qquad (5a)$$

$$\xrightarrow{k_{5b}} C_2H_3Cl^+ + (C_2H_5Cl + H_2) \qquad (5b)$$

It is also of interest to consider possible further reactions with ethyl chloride of the secondary ionic products from these processes. For $C_2H_6Cl^+$, the cross section for Reaction 5a is large enough to permit production of this ion in reasonable abundance even at the comparatively low pressures possible in the first stage of the tandem spectrometer; hence, it was possible to observe the reaction of this ion directly. As Reaction 6 shows, this leads to a condensation product which loses a molecule of HCl:

$$C_2H_6Cl^+ + C_2H_5Cl \rightarrow C_4H_{10}Cl^+ + HCl \qquad (6)$$

Small abundances of proton transfer and charge transfer products were also observed from the reaction of this ion but were negligible by comparison with Reaction 6. The only other secondary ion of appreciable abundance (Reactions 1 through 6) and which might conceivably contribute to higher order ionic products not already identified, is $C_2H_3Cl^+$. Therefore, its reaction with ethyl chloride was investigated by using vinyl chloride as a source molecule in the first stage. Essentially no reaction was observed.

Publication Date: January 1, 1968 | doi: 10.1021/ba-1968-0082.ch028

A striking feature of the ionic reaction scheme for ethyl chloride which is evident from examining the reactions above is the fact that virtually all of these processes lead either to the protonated molecule ion or to other precursors of this product. In addition, the protonated species is efficiently converted to the $C_4H_{10}Cl^+$ ion; hence, one expects that at higher pressures there will be essentially only this one ionic species present in any appreciable quantity. This conclusion is also supported by the high pressure mass spectrometer data discussed below.

In another series of experiments, isotopically labelled reactants were used to establish mechanistic details of the various reactions. For one group of these studies, appropriate deuterated reactants were obtained by introducing either ethylene-d_4 or ethane-d_6 into the first stage of the machine. Reactions 7–10a′ show the results of these experiments. In cases where a given ion was observed with more than one isotopic composition, the relative yields are noted.

$$C_2D_2^+ + C_2H_5Cl \rightarrow C_2H_5^+ + C_2D_2Cl \quad (7)$$

$$C_2D_3^+ + C_2H_5Cl \rightarrow C_2H_5^+ + C_2D_3Cl \quad (8a)$$

$$\rightarrow C_2H_5DCl^+ + C_2D_2 \quad (8b)$$

$$C_2D_4^+ + C_2H_5Cl \rightarrow C_2H_3Cl^+ + C_2D_4H_2 \quad (9a)$$

$$\rightarrow C_2H_5^+ + C_2D_4Cl \quad (9b)$$

$$\rightarrow C_2H_4Cl^+ + C_2D_4H \quad (9c)$$

$$\xrightarrow{0.53} C_4H_4D_4^+ + HCl \quad (9d)$$

$$\xrightarrow{0.47} C_4H_5D_3^+ + DCl \quad (9d')$$

$$C_2D_5^+ + C_2H_5Cl \xrightarrow{0.30} C_2D_5HCl^+ + C_2H_4 \quad (10a)$$

$$\xrightarrow{0.70} C_2H_5DCl^+ + C_2D_4 \quad (10a')$$

In Reaction 7 the $C_2H_4^+$ product (produced in Reaction 1b) could not be observed since it has the same mass as that of the primary beam which, of course, obscures the much smaller secondary product if it is present. To study effectively the parent ion reaction in this manner, it was necessary to introduce ethyl chloride-d_5 into the collision chamber of the tandem instrument and impact it with $C_2H_5Cl^+$ ions. Table I illustrates the results for this reaction, using both $C_2H_5{}^{35}Cl^+$ and $C_2H_5{}^{37}Cl^+$ as impacting species. The slight differences observed in the two cases reflect in part the fact that for $C_2H_5{}^{37}Cl^+$ it was necessary to use a much smaller primary ion signal since its intensity as a primary fragment is only about one-third that of the $C_2H_5{}^{35}Cl^+$ ion.

Publication Date: January 1, 1968 | doi: 10.1021/ba-1968-0082.ch028

Table I. Ionic Products from the Reaction of $C_2H_5Cl^+$ with C_2D_5Cl at a Collision Chamber Pressure of 5 μ in the Tandem Mass Spectrometer

	Relative Yield of Reactant Ion	
Product Ion	$C_2H_5{}^{35}Cl^+$	$C_2H_5{}^{37}Cl^+$
$C_2H_3Cl^+$	0.054	0.079
$C_2D_3Cl^+$	0.075	0.11
$C_2H_5DCl^+$	0.24	0.21
$C_2D_5Cl^+$	0.058	0.066
$C_2D_5HCl^+$	0.57	0.54

It is apparent, by considering Reactions 1 through 6, that there is a remarkable diversity of ionic reactions in this chlorocarbon system. This may be contrasted with hydrocarbon systems such as propane in which a single ion-molecule reaction type, in this case, hydride-ion transfer, is predominant (*4*). In reaction behavior, the ethyl chloride is more similar to other polar compounds such as ethanol, which also exhibit a broad spectrum of ion-molecule reaction types. The isotopic studies indicate that even some of the apparently simple reactions, such as 4a, which would normally be regarded as proton transfer, are actually more complicated in their mechanisms. Thus, for the particular case just cited, the analogous reaction with $C_2D_5^+$ ions does, in fact, yield a product corresponding to that which would result from a discrete deuteron transfer (Reaction 10a′), but there is also a reaction product which appears to require the formation of an intermediate collision complex (Reaction 10a) since the alternative explanation involving transfer of an HCl entity does not seem likely. However, since the products of this reaction do not indicate that complete mixing of hydrogen isotopes occurs in the intermediate, as observed in unsaturated hydrocarbons in which complex formation seems to be well established (*12, 28, 43*), it may be concluded that Reaction 10 involves a different type of complex than that formed in hydrocarbon systems. The observed isotopic product distribution in Reaction 10 can be explained if one assumes that both products result from decomposition of a complex intermediate ion, whose formation does not entail carbon-carbon bonding but involves a structure of the form C—Cl—C, or what might be termed a "dialkyl chloronium" type structure. Such an intermediate structure with an angular geometry would facilitate transfer of an H or D species to either of the opposite alkyl segments, followed by elimination of the remaining olefinic fragment. Such a mechanism, however, would lead one to expect approximately equal amounts of the two possible products, and this is obviously not the case. It is also conceivable though that Reaction 10a′ may proceed by more than one path, involving a longer-range transfer process which does not require an intimate collision. More

Publication Date: January 1, 1968 | doi: 10.1021/ba-1968-0082.ch028

convincing support for the concept of a "dialkyl chloronium" intermediate is provided by a study of the corresponding reaction in methyl chloride. Thus, CD_3^+ ions reacting with methyl chloride give products analogous to those observed in Reaction 10, and more importantly, these products are formed in about equal abundance.

$$CD_3^+ + CH_3Cl \xrightarrow{0.55} CH_2Cl^+ + CD_3H \qquad (11a)$$

$$\xrightarrow{0.45} CD_2Cl^+ + CH_3D \qquad (11a')$$

A more detailed account of the methyl chloride system will be presented elsewhere.

From the above discussion, it is reasonable to suppose that the $C_4H_{10}Cl^+$ ion produced in Reaction 6 may also have the dialkyl chloronium ion type structure. Such a process would be somewhat analogous to the formation of what are apparently protonated ethers in the reactions of protonated alcohol ions with alcohols (*27*, *37*). The most recently published study of ion-molecule reactions in alcohols (*19*), however, indicates that the latter reaction in methanol actually occurs without loss of a water molecule and hence is different from Reaction 6, where HCl is split off from the product ion.

In considering the other reactions with isotopically labelled ions, ethyl ion is produced by three different reactants (Reactions 7, 8a, and 9b), but since the neutral products can only be inferred, the mechanisms of these processes are not entirely clear. While all three reactions might be considered to involve Cl^- transfer from the neutral reactant (as implied by the reactions as written), the same ionic product could also be formed by dissociative charge transfer (Reaction 12).

$$C_2D_2^+ + C_2H_5Cl \rightarrow C_2H_5Cl^+ + C_2D_2 \qquad (12a)$$

$$\rightarrow C_2H_5^+ + Cl \qquad (12b)$$

Energetic calculations for the alternative reaction paths are of some value in deciding which is the more feasible. For $C_2D_2^+$, charge transfer to C_2H_5Cl is exothermic by some 12 kcal./mole, while the alternative chloride ion transfer reaction is endothermic by approximately 5 kcal./mole (*9*), suggesting that the former process is favored. For the $C_2D_3^+$ reactant, however, charge transfer is essentially ruled out since it would be endothermic by more than 50 kcal./mole. Chloride ion transfer on the other hand is exothermic by about 18 kcal./mole in this case. With the $C_2D_4^+$ reactant, the choice between reactions on an energetic basis is less clear since both processes in question here seem to be endothermic for ground state ions. Chloride transfer is more energetically feasible, however. Such estimates of reaction energetics, which do not account

Publication Date: January 1, 1968 | doi: 10.1021/ba-1968-0082.ch028

for the possible participation of excited ions, will not always provide reliable guidelines.

Reaction 9 shows that the major portion of the reacting ethylene ions interact with ethyl chloride by discrete transfer steps including H^- transfer, H_2^- transfer, and possibly Cl^- transfer. Also, as discussed later, the total cross section for reaction of ethylene ions in this system is quite large ($>$ 100 sq. A.). This may be compared with the corresponding reaction of ethylene ions with ethane, for which extremely small cross-sections have been found (*44*). In the latter case, however, the H^- transfer reaction is endothermic, and the H_2^- transfer process would not have been detected in the previous experiments. These facts may explain the low reactivity reported. With ethyl chloride, H^- transfer to ethylene ions is also indicated to be endothermic by the usual calculations. This suggests that the reactant ethylene ions in this system may well be vibrationally excited. It would also account for the chloride ion transfer to this ion, mentioned above. The ratio of rate constants observed for $C_2H_4^+$ reaction with ethyl chloride is $k_{H_2^-}/k_{H^-} = 1.4$. In addition to the reactions just discussed, part of the ethylene ion reactant forms a complex intermediate with C_2H_5Cl, and elimination of HCl and DCl from this intermediate occurs with about equal probability.

For the parent ion reactions shown in Table I, the observed products appear to be formed entirely by specific transfer processes, and there is no evidence of the extensive isotopic mixing characteristic of reactions in which long-lived collision complexes are formed. It is also notable that no ion corresponding to such a complex—*i.e.*, the dimer ion—was observed. This is quite different from the ethyl bromide and ethyl iodide systems where such "persistent" collision complexes have actually been observed (*32*).

The data in Table I illustrate other interesting features of the parent ion reactions in this chlorocarbon. The major ionic product, corresponding to the hydronated molecule ion, is actually formed by two processes —a proton transfer reaction and a deuterium abstraction from the neutral. The results indicate that these processes compete in the ratio, $k_D/k_{H^+} = 0.41$. In addition, the minor ionic species $C_2H_3Cl^+$ and $C_2D_3Cl^+$ are produced by two competing reactions, one of which is an H_2 transfer process. The latter reaction type has also been observed in hydrocarbon systems, but in these cases the neutral reactants were unsaturated species (*1, 2, 6, 7*). The other competing process is apparently a D_2^- transfer reaction, and again, previous reports of such reactions in hydrocarbons were observed with unsaturated acceptor molecules (*5, 8*). Our data show that the relative rates of the two processes are in the ratio, $k_{H_2}/k_{D_2^-} = 0.73$ for the ethyl chloride system. Of the remaining products in Table I, $C_2D_5Cl^+$ is obviously a charge transfer product. Moreover, if

Publication Date: January 1, 1968 | doi: 10.1021/ba-1968-0082.ch028

some of the reacting parent molecule ions were excited, a dissociative charge transfer process yielding some of the observed $C_2D_3Cl^+$ would be possible. This, then, is an alternative pathway to this product, which may be considered in addition to that suggested above.

Compare the reaction above for the chlorocarbon under consideration with the corresponding reactions in the analogous systems. For ethane (*28*), the analogous hydrocarbon, the reaction of $C_2H_6^+$ ions shows a much smaller cross section than we observed for the $C_2H_5Cl^+$ ion in ethyl chloride (*see* Table II). In other respects, though, the two cases are considerably similar. Thus, in the hydrocarbon system, the protonated molecule ion, $C_2H_7^+$, has been observed as a product of the parent ion reaction. Since such a reaction would be endothermic, Munson *et al.* (*28*) were forced to postulate that excited reactant ions were involved. The parent ion reaction in ethyl chloride shows a closer similarity, however, to the corresponding reaction in ethyl alcohol. In the latter case, the protonated molecule ion is the only product observed from the parent reaction (*37*), and the cross section for this process is quite large. The high degree of reactivity for these polar compounds is considered further below.

Table II. Total Cross Sections for Reactions of Ions with Ethyl Chloride at a Source Field Strength of 10 volts/cm.[a]

Ion	σ_r(*sq. cm.* $\times 10^{16}$)
$C_2H_2^+$	198
$C_2H_3^+$	102
$C_2H_4^+$	105
$C_2H_5^+$	91
CH_2Cl^+	86
$C_2H_5Cl^+$	175
$C_2H_6Cl^+$	82

[a] Cross section of an ion containing Cl is given for both isotopes.

Condensation Sequence at Elevated Pressures. To examine the ionic reaction trends suggested by our experiments at pressures which closely approximate typical radiolysis conditions, ethyl chloride has been studied in the high pressure single-stage Bendix instrument already described. Figures 1 and 2 show the pressure dependence of ions in this system at pressures up to 200 μ. The relative intensity data for the various ions are also shown on a reduced scale at pressures up to 1000 μ in Figure 3. The trends exhibited by these results are in excellent agreement with the conclusions drawn from the tandem experiments which have already been discussed. As predicted, the $C_4H_{10}Cl^+$ species becomes the major ionic product at higher pressures, accounting for some 70% of the total

Publication Date: January 1, 1968 | doi: 10.1021/ba-1968-0082.ch028

ionization at the highest pressure indicated. These higher pressure results also confirm previous indications that the $C_2H_3Cl^+$, $C_2H_4Cl^+$, and other minor ions shown are essentially unreactive with ethyl chloride.

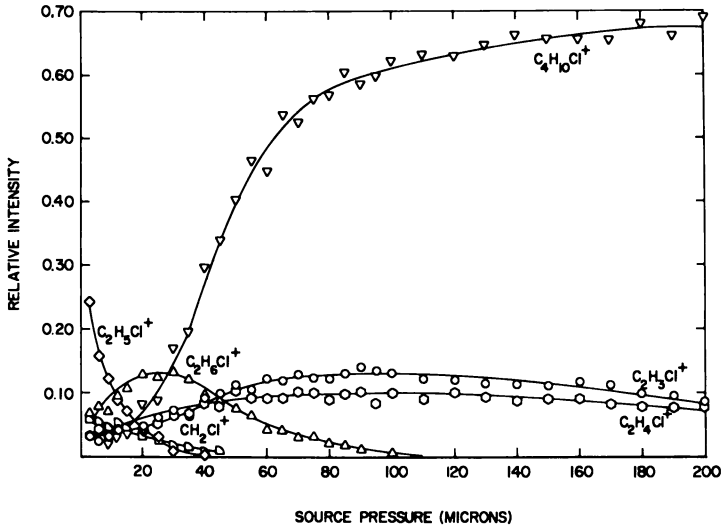

Figure 1. Dependence of the relative intensities of the parent ion and its higher order ionic products and other minor ions in ethyl chloride on the source chamber pressure in the mass spectrometer

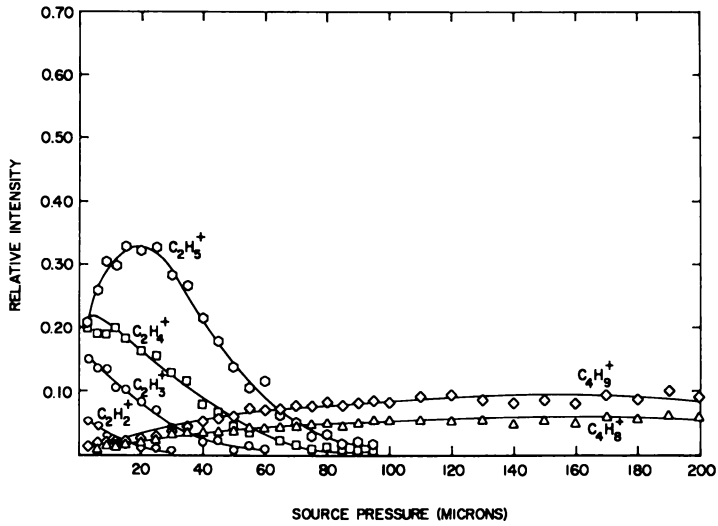

Figure 2. Dependence of the relative intensities of fragment ions and certain product ions in ethyl chloride on ion source pressure

Publication Date: January 1, 1968 | doi: 10.1021/ba-1968-0082.ch028

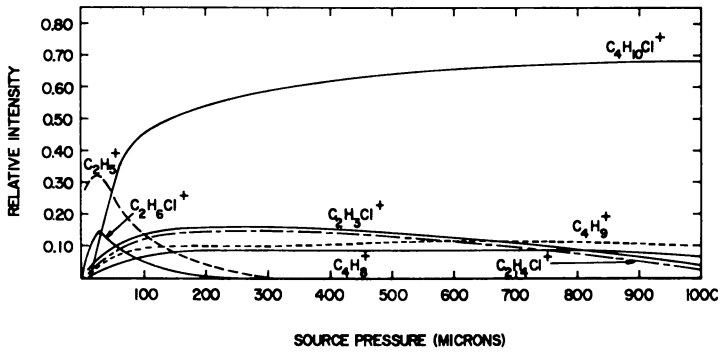

Figure 3. Relative ionic intensities in ethyl chloride at mass spectrometer source chamber pressures up to 1000μ

Even these ions begin to decrease in the region of 1000 μ pressure, however, and since no other ionic products are observed, this may reflect a change in the primary fragmentation spectrum which could occur with the increase in pressure.

The reactivity of the various ions in the ethyl chloride system can be compared on the basis of their reaction cross sections. Kinetic analysis leads to the usual exponential decay relationship for a reacting ion,

$$I_p = I_o \exp(-\sigma_r n) \tag{13}$$

where I_p is the reactant ion intensity at a given value of the number density, n, I_o is the corresponding initial intensity and σ_r is the phenomenological cross section. From this equation, the cross section for a particular reaction can be evaluated from the slope of a semilogarithmic plot of relative ion intensity *vs.* pressure. Such plots are shown in Figures 4 and 5 for the major reactant ions. The cross sections estimated from these plots are given in Table II; they are quite large, especially for the parent ion and acetylene ion, indicating a high degree of reactivity with ethyl chloride. By comparison, cross sections for reactions of $C_2H_6^+$ and $C_2H_2^+$ with ethane, have been reported as 3.3–8.9 sq. A. and 96 sq. A., respectively (*28*). On the other hand, other polar compounds, including the remaining alkyl halides, alcohols, etc., have also been observed to exhibit large reactive cross sections (*26, 41*). Since these compounds have sizable permanent dipoles, these larger cross sections might be interpreted in terms of an additive contribution to the ion-induced dipole interaction, as originally suggested by Hamill and co-workers (*41*). Such factors will be discussed in more detail for the entire alkyl halide series in future publications.

Publication Date: January 1, 1968 | doi: 10.1021/ba-1968-0082.ch028

Comparison with Other Alkyl Halides. Our mass spectrometric observations of ionic reactions in ethyl chloride can be compared with previously reported data on these reactions in other similar alkyl halides. The primary fragmentation patterns obtained for ethyl bromide (*41*) and ethyl iodide (*14, 31*) are similar to that for ethyl chloride. Each of these alkyl halides appears to exhibit a substantial parent ion abundance and each shows an ion-molecule reaction product corresponding to $C_4H_{10}X^+$ (X = Cl, Br, I). It is the major product for the chloride and bromide compounds and may be also for the iodide, although no abundances were indicated for the latter study. There is a distinct difference, however, between the present investigation and earlier studies with respect to the reaction postulated as the source of the $C_4H_{10}X^+$ product. The parent ion was identified as being the precursor of this product in both the ethyl bromide (*41*) and ethyl iodide (*14, 31*) systems, while the results obtained here for ethyl chloride indicate that the protonated parent ion is the species which yields the $C_4H_{10}Cl^+$ product.

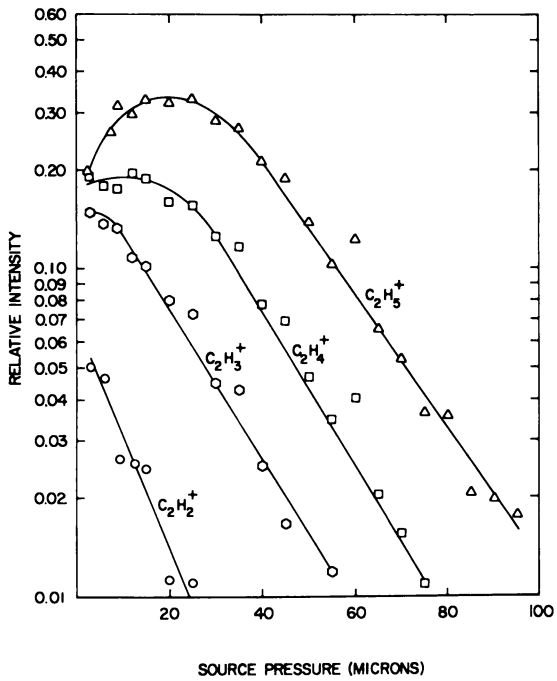

Figure 4. Semilogarithmic plots of the relative intensities of primary fragment ions as functions of the pressure of ethyl chloride

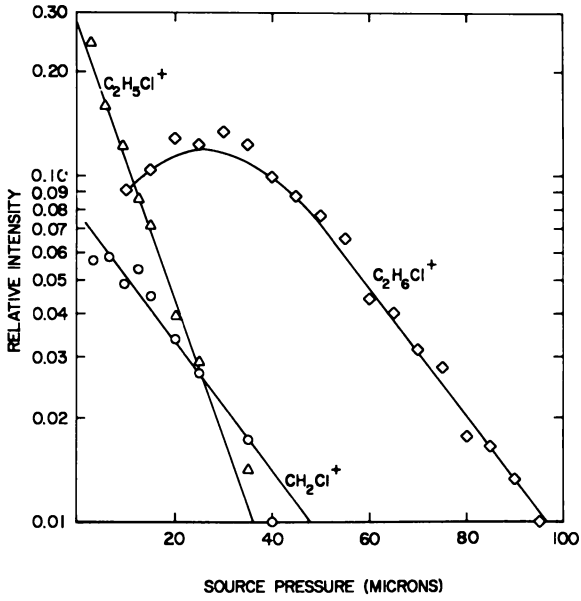

Figure 5. Semilogarithmic plots of the relative intensities of CH_2Cl^+, $C_2H_5Cl^+$, and $C_2H_6Cl^+$ as functions of ethyl chloride pressure

To substantiate further Reaction 6 for the high pressure system, the order of formation of the product ions was determined in the single source mass spectrometer for ethyl chloride. By definition, the intensity of a product ion of order, n, is proportional to the nth power of the pressure; hence, the reaction order of a given ion is obtained directly from the slope of a plot of the logarithmic value of the intensity as a function of the logarithm of the source pressure. In the experiments reported here, the relative intensity, $I_i/\Sigma I_i^+$, is used rather than the absolute ion intensity, I_i^+. The relative intensity is calculated on the assumption that each ion has the same sensitivity. In Figure 6, the logarithm of relative intensity is plotted *vs.* the logarithm of pressure for the $C_4H_{10}Cl^+$ ion. Since the relative intensity is used, the slope of the log-log plot will be $[n - 1]$ rather than n. Only the initial portion of such a plot is expected to be linear since at some point all the reactant ion will be consumed. From the initial slope it was determined that $C_4H_{10}Cl^+$ is a third-order product, just as expected if it is formed from the protonated parent ion. A portion of this product could also result from the collisional stabilization of the intermediate complex from the ethyl ion–ethyl chloride reaction as discussed earlier. $C_4H_{10}Cl^+$ ions formed by such a process would also show third-order pressure dependence. In similar measurements, the ionic

Publication Date: January 1, 1968 | doi: 10.1021/ba-1968-0082.ch028

products $C_2H_3Cl^+$, $C_2H_4Cl^+$, and $C_4H_9^+$, for which the order plots are not shown, exhibited second-order pressure dependence, again consistent with their formation by the mechanism discussed.

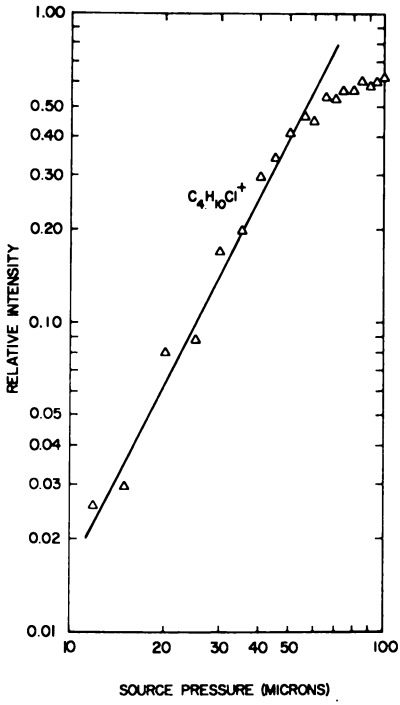

Figure 6. Logarithmic plot of relative intensity of $C_4H_{10}Cl^+$ as a function of ethyl chloride pressure

In investigating ethyl bromide, the parent-daughter relationships for the various ion-molecule reactions were established by appearance potential measurements, the customary method of identification for single-source experiments. This technique cannot necessarily distinguish reactants where consecutive processes occur. Since the protonated parent ion was also observed as a substantial product in ethyl bromide, with an appearance potential identical to that of both the parent ion and the $C_4H_{10}Br^+$ ion, it is possible that the reaction producing the latter ion in the bromide system is actually the same as that found in this study of the corresponding chloride. For ethyl iodide, however, no protonated product such as the $C_2H_6I^+$ was reported, and the difference in the reaction mechanism is not so readily explained. It would seem that these other

Publication Date: January 1, 1968 | doi: 10.1021/ba-1968-0082.ch028

alkyl halides could profitably be reinvestigated by the more definitive mass spectrometric methods now available.

The other significant difference between the ethyl chloride and the corresponding bromide and iodide has already been mentioned—*i.e.*, the failure to observe in the present work any "persistent" collision complex from the parent ion reaction with ethyl chloride, whereas such intermediates were detected for both ethyl bromide and ethyl iodide (*14, 31, 32*). The data obtained for the parent ion reaction in ethyl chloride suggest, in fact, that complex formation in the usual sense may not occur at all in this case. Evidence for this conclusion is provided by the isotopic product distribution indicated in Table I. All of the products observed may be attributed to specific transfer processes, and there is no ionic product which suggests the extensive isotopic mixing which would be characteristic of an intermediate complex in which C-C bonding occurs. Theard and Hamill (*41*) suggested that the collision complexes they observed in the alkyl bromides and iodides were three-electron bonded structures of the type, RX:XR. This is reasonable since this particular geometry permits the only possible molecular orbital arrangement in which all the atoms in the complex can be bonded. These authors also noted earlier studies supporting the interpretation that the vacancy created in RX^+ by the ionization process arises from a nonbonding electron with alkyl iodides or bromides but from a bonding electron with alkyl chlorides. Thus, such a complex intermediate would not be expected for this reaction in the alkyl chlorides and indeed, our results indicate that complex formation does not occur for the parent ion reaction in ethyl chloride. With the protonated parent ion reaction, on the other hand, the situation is quite different, and this ion must form some type of collision complex with this chloride. Since the structure of the protonated parent ion itself is far from evident, it is difficult to speculate with regard to the structure of the complex intermediate.

Implications of Mass Spectrometric Data for Radiation Chemistry. Apart from the positive identification of the ion-molecule reactions in ethyl chloride, the most significant observation from the mass spectrometric studies which has direct application to the radiolysis of this compound is the fact that at pressures greater than *ca.* 100 μ, essentially the only stable ion in this system is $C_4H_{10}Cl^+$. Therefore, the neutralization of ions as a potential contributor to radiolysis products will be important only for this ion. Moreover, this will hold true even if there are variations in the extent of primary fragmentation with increasing pressure. The radiolysis studies which will now be described assess the contribution of ionic processes to radiolytic yields and provide some indications as to the mode of neutralization of the stable ionic species in the ethyl chloride system.

Publication Date: January 1, 1968 | doi: 10.1021/ba-1968-0082.ch028

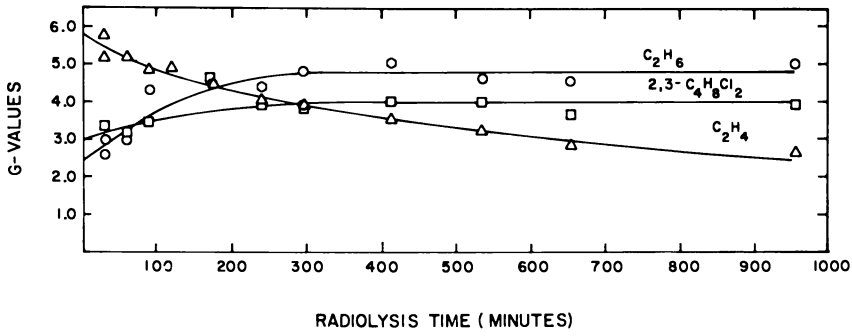

Figure 7. Major product yields as a function of irradiation time in the radiolysis of ethyl chloride

Publication Date: January 1, 1968 | doi: 10.1021/ba-1968-0082.ch028

Radiolysis and Photolysis of Ethyl Chloride. The major products from the radiolysis of ethyl chloride are hydrogen, methane, acetylene, ethylene, ethane, 2,3-dichlorobutane, and 2-chlorobutane. Smaller quantities of 1,3-dichlorobutane and 1-chlorobutane were also detected. The 1-chlorobutane product was too small to be estimated quantitatively with any accuracy. HCl must also be produced as a decomposition product (discussed below), but it could not be estimated by the analytical techniques used in this study. In Figure 7 the yields of the four largest organic radiolysis products are plotted as a function of the total radiation dose. From the latter plots and similar graphs for the other products, initial yields were extrapolated (Table III). In earlier experiments conducted in this study, ethylene and acetylene products were not clearly resolved in the gas chromatographic analysis. Therefore, the yields of these products are usually reported as a combined sum in Table III. In later experiments with improved analytical techniques ethylene and acetylene could be determined separately, and individual yields for these products were determined in some cases. Table III also shows the product yields from radiolysis of ethyl chloride with small amounts of various additives introduced to facilitate determination of the radiolysis mechanism. Those products not reported could not be estimated, owing to analytical complications. The extent of conversion in all experiments was of the order of 0.1% or less. Both NO and O_2 were added as radical scavengers, and the concentrations used were adequate to achieve maximum scavenging effect. The recombination energies of the primary ionic fragments expected in ethyl chloride are sufficiently large as compared with the ionization potential of NO to permit charge transfer to this additive if it is present in sufficient concentration. However, this is not true for oxygen scavenger which has a much higher ionization potential. Since both scavengers have substantially the same effect on the product yields,

exception for the ethylene product, the interception of primary ions by these additives is not a problem at the concentrations used. In the presence of radical scavenger, the chlorinated butanes, ethane, and methane are drastically affected. These results lead to the conclusion that the butane products are formed entirely by radical reactions, while methane and ethane are produced to the extent of some 90% by these processes. The remaining products, however, including almost all of the ethylene and acetylene, results from non-radical reactions.

Table III. Product Yields from Radiolysis of Ethyl Chloride at a Pressure of 357 mm.

	G (Product)						
Additive	H_2	CH_4	C_2H_2, C_2H_4	C_2H_6	2-C_4H_9Cl	2,3-$C_4H_8Cl_2$	1,3-$C_4H_8Cl_2$
None	4.41	1.09	5.80[a]	2.40	1.44	3.00	0.47
5% NO	2.17	0.12	5.37	0.17	0.00	0.00	0.00
5% O_2	—	—	4.14	0.17	0.00	0.00	0.00
0.5% C_6H_6	3.57	1.11	5.73	2.40	1.17	2.43	—
5% C_2H_3Cl	—	—	5.62	1.40	—	1.59	—

[a] $C_2H_2/C_2H_4 = 0.42$.

Table III also shows that hydrogen and the chlorinated butanes are reduced substantially when ethyl chloride is irradiated in the presence of benzene. The other products are essentially unaffected by this additive. In the radiolysis of certain alkanes (*4*), benzene, added in small amounts, does not interfere with the fast ion-molecule reactions of primary ionic fragments or with free radical processes, but it will efficiently condense unreactive or long-lived ions in the system. It is reasonable to assume that this is also true for alkyl halide systems and that the reduction in product yields compared with the pure compound upon adding benzene may be attributed to the interception of unreactive ions. Since the rate constants for reactions of the expected primary ions with ethyl chloride are very large (*see* Table II), the concentration of benzene used in our experiments should not interfere with the initial fast ion-molecule reactions. For ethyl chloride ion-molecule reactions, $C_4H_{10}Cl^+$ is the only unreactive ion of appreciable abundance which is expected in this system at the elevated pressures used in the radiolysis experiments. Thus, the reduced product yields in the presence of benzene additive can be identified tentatively with the removal of this stable ion and the elimination of its resultant neutralization products.

Vinyl chloride was added in one series of experiments (Table III). Since the ethyl chloride starting material contained a few hundredths of a percent of vinyl chloride impurity which could not be removed, this

Publication Date: January 1, 1968 | doi: 10.1021/ba-1968-0082.ch028

experiment was conducted to determine if this minor impurity could seriously affect the radiolytic product yields. The relatively large concentration of 5% of this additive substantially reduces products attributable to radical reactions but effectively leaves the C_2H_2–C_2H_4 yields unaltered. The most likely effect of the vinyl chloride impurity would therefore seem to be the scavenging of hydrogen and chlorine atoms. Nevertheless, the extremely small concentration of impurity present in pure ethyl chloride is probably negligible.

Table IV gives the relative product distribution from the vacuum ultraviolet photolysis of ethyl chloride at 40 mm. pressure using the 1236-A. krypton resonance line. Owing to the low intensity of emission from the resonance lamp, higher pressures were not used in the photolysis experiments in order to prevent the major portion of the reaction from occurring in the region of the window where surface interactions are likely. Therefore, to provide a basis for more direct comparison between the photolytic and radiolytic yields, the radiolysis of ethyl chloride was also examined at 40 mm. pressure. The relative yields from several experiments of the latter study are given in Table IV. The lowest conversion yields from the radiolysis at the lower pressure show a relative distribution which is in close agreement with the relative product distribution detected from the radiolysis at 357 mm. Therefore, there is no substantial pressure effect on the decomposition product yields in ethyl chloride over the range 40–357 mm.

Table IV. Relative Product Distribution from the Radiolysis and Photolysis of Ethyl Chloride at a Pressure of 40 mm.

Experiment	Irradiation Time, Min.	Relative Yields						
		H_2	CH_4	C_2H_2,	C_2H_6	2-C_4H_9Cl	2,3-$C_4H_8Cl_2$	1,3-$C_4H_8Cl_2$
Radiolysis	60	0.82[a]	0.2[a]	1.00	0.42	0.32	0.54	0.10
Radiolysis	120	—	—	1.00	0.58	0.26	0.63	0.18
Radiolysis	180	—	—	1.00	0.64	0.27	0.66	0.18
Photolysis	60	0.85	0.09	1.00[b]	0.22	0.17	0.35	0.11
Photolysis with 5% NO	60	0.44	0.04	1.00[c]	0.021	0	0	0

[a] Hydrogen and methane yields are assumed to be the same as those in Table III for radiolysis at higher pressure.
[b] $C_2H_2/C_2H_4 = 0.24$.
[c] $C_2H_2/C_2H_4 = 0.21$. The absolute yield of ethylene was the same as observed in the photolysis of pure ethyl chloride.

The photolysis data provide important information relative to the modes of decomposition of excited ethyl chloride molecules. The fact that the photolysis yields show a larger excess of ethylene–acetylene

Publication Date: January 1, 1968 | doi: 10.1021/ba-1968-0082.ch028

compared with most other products than for the radiolysis of ethyl chloride suggests that the major primary dissociation process in the photolysis is molecular elimination of HCl. The excess energy available from photolysis with the 1236-A. line for the process yielding ethylene is sufficient to permit further dissociation of the latter product to acetylene and hydrogen.

$$\begin{array}{l} C_2H_5Cl^* \rightarrow C_2H_4 + HCl \\ \qquad\qquad\quad \hookrightarrow C_2H_2 + H_2 \end{array} \qquad (14)$$

The occurrence of this reaction sequence is further substantiated by the observation that adding nitric oxide in the photolysis experiments does not change ethylene–acetylene yields (Table IV). Evidence for the analogous process in ethyl iodide involving elimination of HI has been presented in previous photolysis studies (*23, 34*). The ethane product observed in the present photolysis study must certainly be formed by the reaction of ethyl radicals which presumably result from another primary dissociation process,

$$C_2H_5Cl^* \rightarrow C_2H_5 + Cl \qquad (15)$$

Since no butane is observed as a photolysis product, and since the accepted value for the ratio of rate constants for disproportionation to combination reactions for ethyl radicals is 0.12 (*45*), ethyl radical interactions may be ruled out as a source of ethane. Therefore, the ethane probably arises from an abstraction reaction following the initial dissociation,

$$C_2H_5 + C_2H_5Cl \rightarrow C_2H_6 + C_2H_4Cl \qquad (16)$$

Simple energetic considerations indicate that this reaction should have an activation energy of about 11 kcal./mole and therefore would not be a likely process for thermal radicals. However, the ethyl radicals produced in Reaction 15 are almost certainly "hot" radicals. The energy available from the 1236-A. krypton resonance line is 231 kcal./mole. Taking the C_2H_5—Cl bond dissociation energy to be 83 ± 7 kcal./mole [from electron impact studies by Irsa (*20*)], the total excess energy of the products should be 148 ± 7 kcal./mole and of this, approximately 82 kcal./mole will be carried off by the ethyl radical. Further evidence for the participation of "hot" radicals in the reaction sequence is provided by the scavenged product yields reported in Table IV (discussed below). Previous workers have also obtained evidence for "hot" radicals in the photolysis of other alkyl halides and have presumed their participation in processes analogous to Reaction 16 (*23*).

The photolysis yields in the presence of radical scavenger, reported in Table IV, show clearly that the chlorobutanes, ethane, and methane,

Publication Date: January 1, 1968 | doi: 10.1021/ba-1968-0082.ch028

as well as a substantial portion of the hydrogen, are produced by radical reactions. These radical products suggest the occurrence of the following additional primary processes in the photolysis:

$$C_2H_5Cl^* \rightarrow C_2H_4Cl + H \quad (17)$$

$$\rightarrow CH_3 + CH_2Cl \quad (18)$$

Radicals formed by these primary fragmentations may then abstract hydrogen to yield the observed products.

$$H + C_2H_5Cl \rightarrow H_2 + C_2H_4Cl \quad (19)$$

$$CH_3 + C_2H_5Cl \rightarrow CH_4 + C_2H_4Cl \quad (20)$$

$$Cl + C_2H_5Cl \rightarrow HCl + C_2H_4Cl \quad (21)$$

The remaining photolysis products, the chlorobutane and dichlorobutanes, can be accounted for readily by appropriate radical combination reactions.

$$2\,C_2H_4Cl \rightarrow C_4H_8Cl_2 \quad (22)$$

$$C_2H_5 + C_2H_4Cl \rightarrow C_4H_9Cl \quad (23)$$

Disproportionation products are expected to be minor from Reaction 22 since the ratio, $k_{\text{disproportionation}}/k_{\text{combination}} \leqslant 0.01$ has been reported for C_2H_4Cl radical interactions (*45*). In fact, vinyl chloride was not detected as a product in this study. [The value of 0.01 is the lowest one given in Ref. *45*. The actual ratio for k_d/k_c depends on whether the entity transferred is considered to be a H or Cl atom and on the identity of the dichlorobutane isomer. Heicklen (*16*) has considered in detail all possible reaction paths. From his data it is possible to deduce an over-all disproportionation to combination ratio of 0.44 for C_2H_4Cl radicals.]

The photolysis data in Table IV show that ethane and methane yields are not entirely eliminated when NO is added to ethyl chloride. These residual yields may well represent the contributions to these products which result from "hot" radical reactions. We have already discussed the probable formation of "hot" ethyl radicals in the photolysis and the formation of other "hot" species such as methyl radicals, and hydrogen atoms also seems likely. The participation of "hot" H atoms is suggested by considering the nonscavengeable H_2 yield. According to the mechanism advanced, the nonradical H_2 yield should be equal to the acetylene yield. In fact, the former is somewhat higher (0.44 for H_2 compared with 0.21 for C_2H_2). This discrepancy can be explained if part of the nonscavengeable H_2 yield is formed by "hot" H atoms and is therefore not affected by nitric oxide. On the assumption that this is actually the case and that the nonradical yield of hydrogen is equivalent to the acetylene yield in the photolysis, applying the mechanism outlined and the

Publication Date: January 1, 1968 | doi: 10.1021/ba-1968-0082.ch028

yields reported in Table IV, we deduce the following scheme for excited neutral molecule decomposition in ethyl chloride:

$$C_2H_5Cl^* \xrightarrow{0.51} \begin{matrix} C_2H_4 + HCl \\ \hookrightarrow C_2H_2 + H_2 \end{matrix} \qquad (14)$$

$$C_2H_5Cl^* \xrightarrow{0.33} C_2H_4Cl + H \qquad (17)$$

$$\xrightarrow{0.11} C_2H_5 + Cl \qquad (15)$$

$$\xrightarrow{0.05} CH_3 + CH_2Cl \qquad (18)$$

The proposed mechanism for photolytic decomposition of ethyl chloride predicts the product relation, $2[C_4H_8Cl_2] + [C_4H_9Cl] = [H_2]_{radical} + [C_2H_6] + [CH_4] + [HCl]$. Inserting the indicated concentrations from Table V into this equation gives $1.09 = 0.72 + [HCl]$. Clearly, HCl must be a substantial product, even though we were unable to estimate its concentration in our experiments, and presumably it would account for the remainder of the material balance.

The photolysis data indicate the product ratio, 2,3-$C_4H_8Cl_2$/1,3-$C_4H_8Cl_2$ = 3.2. Since all of the chlorobutane products (including 2-C_4H_9Cl), are formed by appropriate combinations of $H_3C—CH—Cl$ and $H_2C—CH_2—Cl$ radicals, it can be deduced from this ratio, ignoring possible differences in steric factors, that abstraction of a H atom from the α-carbon of ethyl chloride is 7.4 times more probable than abstraction from the β-carbon. This comparatively low concentration of the β-radical accounts for the failure to observe 1,4-dichlorobutane as a product in these experiments since its concentration would be $(1/7.4)^2$ times the 2,3-dichlorobutane concentration and therefore too small to be observed by our analytical methods. The small quantity of 1-chlorobutane observed as a photolysis product can be explained similarly since it would also involve the β-chloroethyl radical.

The relative product distribution produced by photons of 10-e.v. energy in the krypton resonance radiation photolysis will also be taken as representative of excited neutral decomposition induced by electron impact at energies exceeding the ionization potential of ethyl chloride (10.9 e.v.). That is, the contribution to the radiolysis products from excited neutral molecule decomposition will be assumed to have the same relative distribution as that observed in the photolytic decomposition. While superexcited molecules will also be produced in the radiolysis, there is considerable evidence to support the view that their modes

Publication Date: January 1, 1968 | doi: 10.1021/ba-1968-0082.ch028

of decomposition do not differ appreciably from those of molecules excited to energies just below the ionization potential. Doepker and Ausloos (7), for example, have used applied field experiments to evaluate the neutral decomposition modes in the radiolysis of cyclobutane, and they find good agreement between this distribution and that produced by absorption of photons in the energy range 8.4–10 e.v. Thus, the approach outlined above is not entirely unwarranted in assessing the radiolysis mechanism.

Let us now consider in detail the radiolysis of ethyl chloride. Although it is well known that the relative intensities of ionic fragments observed in the low pressure mass spectrum of a compound do not necessarily represent the abundances of these ions in a radiolysis system at higher pressures (owing to a difference in the time scale of events), such a spectrum still provides a useful indication of possible primary ionic dissociation modes. The primary ions observed in the mass spectrum of ethyl chloride and their relative abundances are shown below.

$$[C_2H_5Cl^+]^* \rightarrow \underset{(0.20)}{C_2H_5Cl^+} \tag{24}$$

$$\rightarrow \underset{(0.06)}{CH_2Cl^+ + CH_3} \tag{25}$$

$$\rightarrow \underset{(0.17)}{C_2H_5^+ + Cl} \tag{26}$$

$$\rightarrow \underset{(0.18)}{C_2H_4^+ + HCl} \tag{27}$$

$$\rightarrow \underset{(0.17)}{C_2H_3^+ + (H_2 + Cl)} \tag{28}$$

$$\rightarrow \underset{(0.069)}{C_2H_2^+ + H_2 + HCl} \tag{29}$$

An examination of the ion-molecule reactions in which these fragments participate (Reactions 1–6), immediately permits one to exclude some of the suggested primary ions since the neutral products which would result are not observed in the radiolysis. Thus, neither vinyl chloride nor methyl chloride were detected as radiolysis products and so the primary fragments $C_2H_2^+$, $C_2H_3^+$, and CH_2Cl^+ must be formed in negligible amounts at the higher pressures at which these experiments were conducted. Therefore, these modes of fragmentation need not be considered in the radiolysis. The remaining primary species $C_2H_4^+$, $C_2H_5^+$, and the parent ion, $C_2H_5Cl^+$, are all conceivably involved to some extent in the ionic decomposition scheme. By considering the product yields, we can estimate the relative importance of these primary fragmentations in the

Publication Date: January 1, 1968 | doi: 10.1021/ba-1968-0082.ch028

radiolysis. The ethyl ion undergoes an ion-molecule reaction which produces methane as a neutral product. From the radiolysis data in Table III, a portion of the methane also results from reactions of radicals. Since the benzene scavenger has no effect on the methane yield, neutralization of stable ions does not contribute to formation of this product. Therefore, the nonscavengeable methane yield, $G = 0.12$, may be identified with the contribution from ion-molecule processes, but Reaction 4a shows that ethyl ions also produce ethylene as a product of interaction with ethyl chloride. Taking the ratio of k_{4a}/k_{4b} (given earlier) and the methane yield just noted, we calculate a yield of $G = 1.56$ for ethylene produced from ion-molecule reactions. From these yields a relative value of 1.68 can be assigned to the initial ionic fragmentation producing ethyl ions.

On the basis of previous discussion, the only additional source of ethylene in the radiolysis is the decomposition of excited neutral ethyl chloride molecules. If the ion-molecule contribution to this product is subtracted from the total yield reported in Table III, an ethylene–acetylene yield of $G = 4.24$ may be attributed to excited neutral decomposition. If we now assume that the photolysis experiments provide a direct measure of the neutral excited molecule decomposition to be expected in the radiolysis, this ethylene yield may be used as a basis for normalization to estimate the contributions from this source to the other products using the relative photolysis distributions from Table IV. In this way, the contributions from excited neutral decomposition reported in Table V were derived.

The radiolysis product yields in the presence of ion scavenger (Table III) also show that ethane is not formed from neutralization of stable ions. Therefore, the remainder of the ethane product (above that indicated to result from neutral decomposition) must be produced by an ion-molecule process—*i.e.*, a yield of $G = 1.47$. The ion-molecule reactions previously listed show that ethylene ions react with ethyl chloride to form ethane. From the relative rates indicated for Reactions 3a–3d and the ethane yield just derived, a relative yield of 2.46 may be deduced for the ionic fragmentation to ethylene ion in the radiolysis.

We turn now to the chlorobutane products, whose yields are reduced when benzene is added (Table III). This reduction may be considered to represent the contribution from neutralization processes—*i.e.*, a $G = 0.27$ for 2-C_4H_9Cl, and a $G = 0.57$ for 2,3-$C_4H_8Cl_2$ (Table V). The balance of the chlorobutane products, less the amounts arising from excited neutral decompositions, can be considered to result from ion-molecule reactions—*i.e.*, $G = 0.45$ for 2-C_4H_9Cl and $G = 0.95$ for 2,3-$C_4H_8Cl_2$. Considering the ion-molecule reactions which produce the precursor of these products—C_2H_4Cl radicals—both $C_2H_5Cl^+$ and $C_2H_4^+$

Publication Date: January 1, 1968 | doi: 10.1021/ba-1968-0082.ch028

reactant ions yield these radicals. The quantities of chlorobutane products require a total yield of $G = 2.35$ for C_2H_4Cl radicals, and using the same methods noted, we deduce that a yield of $G = 1.24$ may be assigned to the $C_2H_4^+$ reaction while a yield of $G = 1.11$ of these radicals is formed by the parent ion reaction (Reaction 5a). These observations lead to an estimate of $G = 1.35$ for the primary ionic fragmentation to $C_2H_5Cl^+$.

Table V. Contributions to Product Yields from Various Sources in the Radiolysis of Ethyl Chloride

Product	*Excited Neutral Decompositions*	*Ion-Molecule Reactions and Ionic Fragmentation*	*Neutralization*
H_2	3.60	0.24	0.57
CH_4	0.97	0.12	0
C_2H_4, C_2H_2	4.24	1.56	0
C_2H_6	0.93	1.47	0
2-C_4H_9Cl	0.72	0.45	0.27
2,3-$C_4H_8Cl_2$	1.48	0.95	0.57
1,3-$C_4H_8Cl_2$	0.47	—	0

Intensities have now been derived for each of the primary ionic dissociation modes. The complete ionic fragmentation scheme for excited ethyl chloride ions under radiolysis conditions is shown below.

$$[C_2H_5Cl^+]^* \xrightarrow{0.25} C_2H_5Cl^+ \tag{24}$$

$$\xrightarrow{0.31} C_2H_5^+ + Cl \tag{26}$$

$$\xrightarrow{0.45} C_2H_4^+ + HCl \tag{27}$$

It is appropriate to compare the intensities of the ionic dissociation modes deduced for the radiolysis with their corresponding intensities in the low pressure mass spectrum. The latter exhibits relative abundances of $C_2H_5Cl^+$, 0.20; $C_2H_5^+$, 0.17; and $C_2H_4^+$, 0.18 respectively. Thus, the parent molecule ion is being collisionally stabilized at the higher pressures characteristic of the radiolysis experiments, and the extent of fragmentation is consequently reduced. Similar conclusions have been drawn by others (*4*, *7*). The indicated ionic dissociation modes predict a total $G(\text{ions}) = 5.49$ for ethyl chloride which requires that W, the energy to form an ion pair, have a value of about 18 for this compound. Reported values are usually in the range 20–40 e.v. (*43*); hence, the value obtained is reasonable. This provides an additional measure of confidence in the fragmentation scheme which has been advanced.

Publication Date: January 1, 1968 | doi: 10.1021/ba-1968-0082.ch028

The only radiolysis product not accounted for completely is hydrogen. The ion-molecule reaction scheme shows that the parent ion reaction with ethyl chloride produces hydrogen. From the fragmentation yield already deduced for $C_2H_5Cl^+$, a yield of $G = 0.24$ for this ion-molecule contribution to hydrogen is obtained. The residual hydrogen product, less that assigned to excited neutral decomposition may therefore be considered to result from neutralization of stable ionic species—*i.e.*, a yield of $G = 0.57$. Consistency with our interpretation of the role of C_6H_6 as a scavenger of stable ions would require that this yield be 0.84 since this is the reduction in hydrogen observed on introducing this additive in the radiolysis. This may indicate that benzene, even at these low concentrations, is acting to some degree as a scavenger of H atoms. This is a known complication with some systems in using benzene as an ion scavenger.

A feature of the radiolysis experiments which requires some additional clarification concerns the ethylene product. One might object to the omission of any contribution from radical reactions to the ethylene product since radical scavengers affect the yield of this unsaturate. Thus, oxygen sharply reduces the ethylene product while nitric oxide has a less pronounced effect. However, since both scavengers have identical effects on all the rest of the products in the system, we are inclined to interpret the reduction of ethylene in the presence of these additives to quenching of the excited state of the ethyl chloride molecule which eliminates HCl. It has been supposed for some time that oxygen efficiently quenches certain excited states; hence, this suggestion does not seem unreasonable.

We have made no attempt to define the mode of neutralization of the stable ionic species, $C_4H_{10}Cl^+$, in the radiolysis of ethyl chloride. Since hydrogen and the chlorobutanes appear to be the only products, it may be supposed that the neutralization yields hydrogen and C_4H_8Cl radicals, the latter then abstracting a H atom to give the chlorobutane.

$$C_4H_{10}Cl^+ \xrightarrow{e^-} C_4H_8Cl + H_2 \quad (28)$$

$$C_4H_8Cl + C_2H_5Cl \rightarrow C_4H_9Cl + C_2H_4Cl \quad (29)$$

These radicals might also abstract chlorine from ethyl chloride

$$C_4H_8Cl + C_2H_5Cl \rightarrow C_4H_8Cl_2 + C_2H_5 \quad (30)$$

to give the dichlorobutane product. The ethyl radicals produced in such a process would probably not be "hot" radicals and hence would not abstract hydrogen from ethyl chloride. Thus, no reduction in ethane yields would be expected upon removal of the stable $C_4H_{10}Cl^+$ ion by benzene additive. Alternatively, a disproportionation reaction between the C_4H_8Cl and C_2H_4Cl radicals could produce the dichlorobutane.

Publication Date: January 1, 1968 | doi: 10.1021/ba-1968-0082.ch028

$$C_4H_8Cl + C_2H_4Cl \rightarrow C_2H_4 + C_4H_8Cl_2 \quad (31)$$

A ratio of $k_d/k_c = 4.0$ has been reported for this reaction (*45*).

As a final point, consider the observed behavior of the major product yields with increasing ethyl chloride decomposition (Figure 7). The dichlorobutane yield is essentially constant with an increase in the absorbed radiation dose, while the ethane yield rises sharply and the ethylene–acetylene product is substantially reduced. These observations suggest the occurrence of additional reaction processes other than those already suggested. Also, the fact that the ethane increase is not matched by the ethylene decrease indicates that these two phenomena are not necessarily coupled. The most likely explanation is that ethylene is attacked by Cl atoms,

$$Cl + C_2H_4 \rightarrow C_2H_4Cl \quad (32)$$

forming an addition product. This reaction is well-substantiated in several photochemical systems. Such an explanation is not entirely satisfactory, however, since the radicals formed here would be expected to result in an increased yield of dichlorobutane also. Our estimates of dichlorobutane at the higher conversions may be somewhat low since this product condensed on the walls of the reaction vessel when substantial concentrations developed. The increased ethane product could be explained readily by interception of ethyl radicals by some product other than the substrate itself. One product which seems to be a probable scavenger of these radicals is HCl, since the analogous reaction with HI has been proposed for the radiation decomposition of ethyl iodide (*26*).

$$C_2H_5 + HCl \rightarrow C_2H_6 + Cl \quad (33)$$

This reaction might also account for the difficulty in detecting even traces of HCl in the present investigation.

Publication Date: January 1, 1968 | doi: 10.1021/ba-1968-0082.ch028

Summary

Ionic reactions in ethyl chloride have been studied by both mass spectrometric and radiolysis techniques. The radiolysis mechanism advanced on the basis of our experimental observations indicates that the major radiolytic reaction mode in this system is excited neutral molecule decomposition. While the role of ionic reactions in the radiolysis therefore appears to be relatively minor, it was possible to establish a good correlation between the predictions of the mass spectrometric studies with respect to ionic intermediates and the participation of such ions in the radiolytic reaction scheme. These results emphasize the advantages of combining the techniques used here to obtain a complete description of the reactive system.

In Radiation Chemistry; Hart, E.;
Advances in Chemistry; American Chemical Society: Washington, DC, 1968.

Acknowledgment

The authors are grateful for the contribution of D. D. Davis of the National Bureau of Standards, who provided valuable assistance in the design and construction of the photolysis lamps used. The authors also thank A. K. Bhattacharya, who accomplished some of the experimental measurements reported here. This work was carried out during the tenure of a National Academy of Sciences–OAR Postdoctoral Research Associateship awarded to B. M. Hughes for 1967-68.

Literature Cited

(1) Abramson, F. P., Futrell, J. H., *J. Phys. Chem.* **71,** 1233 (1967).
(2) Ausloos, P., Lias, S. G., *J. Chem. Phys.* **43,** 127 (1965).
(3) Bone, L. I., Futrell, J. H., *J. Chem. Phys.* **46,** 4084 (1967).
(4) Bone, L. I., Sieck, L. W., Futrell, J. H., "The Chemistry of Ionization and Excitation," p. 223, Taylor and Francis, Ltd., London, 1967.
(5) Derwish, G. A. W., Galli, A., Giardini-Guidoni, A., Volpi, G., *J. Chem. Phys.* **41,** 2998 (1964).
(6) Doepker, R. D., Ausloos, P., *J. Chem. Phys.* **42,** 3746 (1965).
(7) *Ibid.*, **44,** 1641 (1966).
(8) *Ibid.*, p. 1951.
(9) Franklin, J. L., Field, F. H., "Electron Impact Phenomena," Academic Press, New York, 1956.
(10) Franklin, J. L., Field, F. H., Lampe, F. W., *J. Am. Chem. Soc.* **78,** 5697 (1956).
(11) Futrell, J. H., Miller, C. D., *Rev. Sci. Instr.* **37,** 1521 (1966).
(12) Futrell, J. H., Tiernan, T. O., *J. Phys. Chem.* **72,** 158 (1968).
(13) Gevantman, L. H., Williams, R. R., *J. Phys. Chem.* **56,** 569 (1952).
(14) Gillis, H. A., Williams, R. R., Hamill, W. H., *J. Am. Chem. Soc.* **83,** 17 (1961).
(15) Harteck, P., Dondes, S., *Nucleonics* **14,** 66 (March 1956).
(16) Heicklen, J., *J. Am. Chem. Soc.* **87,** 445 (1965).
(17) Henglein, A., Jacobs, G., Muccini, G. A., *Z. Naturforsch.* **18a,** 98 (1963).
(18) Henglein, A., *Z. Naturforsch.* **17a,** 44 (1962).
(19) Henis, J. M. S., *J. Am. Chem. Soc.* **90,** 844 (1968).
(20) Irsa, A. P., *J. Chem. Phys.* **26,** 18 (1957).
(21) Kebarle, P., Haynes, R. M., Searles, S., ADVAN. CHEM. SER. **58,** 210 (1966).
(22) Laufer, A. H., McNesby, J. R., *J. Chem. Phys.* **42,** 3329 (1965).
(23) Luebbe, Jr., R. H., Willard, J. E., *J. Am. Chem. Soc.* **81,** 761 (1959).
(24) Meisels, G. G., ADVAN. CHEM. SER. **58,** 243 (1966).
(25) Meisels, G. G., Tibbals, H. F., *Proc. Ann. Conf. Mass Spectrometry Allied Topics, 15th, Denver, Colo., 1967,* p. 11.
(26) Moran, T., Hamill, W. H., *J. Chem. Phys.* **39,** 1413 (1963).
(27) Munson, M. S. B., *J. Am. Chem. Soc.* **87,** 5313 (1965).
(28) Munson, M. S. B., Franklin, J. L., Field, F. H., *J. Phys. Chem.* **68,** 3098 (1964).
(29) Okabe, H., *J. Opt. Soc. Am.* **54,** 478 (1964).
(30) Platzman, R. L., *Intern. J. Appl. Radiation Isotopes* **10,** 116 (1961).
(31) Pottie, R. F., Barker, R., Hamill, W. H., *Radiation Res.* **10,** 644 (1959).
(32) Pottie, R. F., Hamill, W. H., *J. Phys. Chem.* **63,** 877 (1959).
(33) Price, W. C., *J. Chem. Phys.* **9,** 539 (1936).
(34) Schindler, R., Wijnen, M. H. J., *Z. Physik. Chem.* **34,** 109 (1962).

(35) Schindler, R. N., *Radiochim. Acta* **2,** 62 (1963).
(36) Schissler, D. O., Stevenson, D. P., *J. Chem. Phys.* **24,** 926 (1956).
(37) Sieck, L. W., Abramson, F. P., Futrell, J. H., *J. Chem. Phys.* **45,** 2859 (1966).
(38) Simpson, R. E., *Health Phys.* **8,** 143 (1962).
(39) Takehisa, M., Levey, G., Willard, J. E., *J. Am. Chem. Soc.* **88,** 5694 (1966).
(40) Tal'roze, V. L., Lyubimova, A. K., *Dokl. Akad. Nauk S.S.S.R.* **86,** 909 (1952).
(41) Theard, L. P., Hamill, W. H., *J. Am. Chem. Soc.* **84,** 1134 (1962).
(42) Tiernan, T. O., Futrell, J. H., Abramson, F. P., Miller, C. D., *Proc. Ann. Conf. Mass Spectrometry Allied Topics, 15th, Denver, Colo., 1967,* p. 79.
(43) Tiernan, T. O., unpublished data.
(44) Tiernan, T. O., Futrell, J. H., *J. Phys. Chem.*, in press.
(45) Trotman-Dickenson, A. F., Milne, G. S., *Natl. Bur. Std.* **NSRDS-NBS 9** (1967).

RECEIVED January 29, 1968.

The H/D Isotope Effect in the Radiolysis of Hexane

TINO GÄUMANN and BONZO REIPSO

Institut de chimie-physique de l'EPUL, CH-1007 Lausanne, Switzerland

Publication Date: January 1, 1968 | doi: 10.1021/ba-1968-0082.ch029

The radiolysis of the protiated and the deuterated form of n-hexane and mixtures thereof has been examined as a function of temperature and at one N_2O-concentration. A strong isotope effect can be observed for fragmentation giving hexene and hydrogen by a unimolecular process, whereas the other product-distribution is not much affected by deuteration. N_2O does not decrease the primary formation of C_6D_{13}-radicals in mixtures. A novel reaction type is proposed for these systems giving hexene and water in a unimolecular step.

Deuterated products find increasing use in radiolytical research because they permit one to probe into the system without the need of scavengers that are liable to change the reaction sequences. For aromatic compounds, it is generally accepted that deuterated molecules are more stable against radiation than their protiated counterpart (*6, 17, 19*). Little is known about the behavior of products other than hydrogen and radicals. In this publication we enlarge our examination of such systems that we have started elsewhere (*7*). The experimental details of the work will be published elsewhere (*8*).

Basic Processes

The main product of the hexane radiolysis is hydrogen. It can be formed in two ways: either by a unimolecular process directly yielding molecular hydrogen or by the intermediate of atomic hydrogen:

$$C_6H_{14} \rightsquigarrow \begin{cases} \rightarrow H_2 + \text{prod.} & (1) \\ \rightarrow H + \text{prod.} & (2) \end{cases}$$

In Radiation Chemistry; Hart, E.;
Advances in Chemistry; American Chemical Society: Washington, DC, 1968.

The latter can be hot by having additional kinetic energy, or it is already thermalized when it reacts according to Reaction 3:

$$H + C_6H_{14} \rightarrow H_2 + C_6H_{13}\cdot \quad (3)$$

Jenkinson and Dyne (*3*) used deuterated cyclohexane to differentiate between Reactions 1 and 2. From the formation of D_2 and HD in diluted hydrocarbon solution they concluded that the former reaction is much less important than the radical process. This is in net contradiction with the results obtained with scavengers that show about equal importance for both reactions (*7*, *16*). This work will show that the apparent difficulty is because of the isotopic effect.

The second product of Reaction 3 and possibly of Reaction 2 is a hexyl radical. Contrary to cyclohexane three isomers are possible with different heats of formation. This complicates the analytical problem, but it gives us the possibility to distinguish between the above mentioned reactions and the abstraction reactions of the following type:

$$R\cdot + C_6H_{14} \rightarrow RH + C_6H_{13}\cdot \quad (4)$$

where R is a primary alkyl radical with one to six carbon atoms (*7*, *34*). These radicals with up to five carbon atoms are formed in a fragmentation of the carbon–carbon bond. Since no evidence is known to us that in the liquid state such a fragmentation can be because of the (energetically feasible) displacement Reaction 5,

$$H + C_6H_{14} \rightarrow R'H + R\cdot \quad (5)$$

we assume that the alkyl radicals are formed in the primary step

$$C_6H_{14} \rightarrow R\cdot + R\cdot' \quad (6)$$

The alkyl radicals disappear by combination and disproportionation, but considerable confusion exists as to their basic yield. From experiments with scavengers results a value of about 2 for the *G*-value of primary formed hexyl radicals (*22*, *34*); the disproportionation/combination ratio of hexyl radicals has been determined as 0.7 (*1*). These two values are, however, not compatible with the measured product distribution as a function of temperature (*7*).

Reactions 1, 2, and 6 can have precursors that can be interfered with scavengers—*e.g.*, N_2O that reacts with electrons (*27*). It will be shown that this leads to new reactions that are not yet completely understood.

The so-called low-molecular-weight products with less than six carbon atoms (*33*) are formed in reactions that are not known in detail. The study of isotopic mixtures of hydrocarbons has not yielded much insight into these reactions, so they will be neglected in the further discussion.

Publication Date: January 1, 1968 | doi: 10.1021/ba-1968-0082.ch029

The Hydrogen Production

The hydrogen yield is smaller in the deuterated species as is shown in Table I. Such a decrease in the hydrogen production on deuteration is shown by all hydrocarbons tested so far, even in cases where this process is of minor importance (*cf.* $G(H_2) = 0.03$ in C_6H_6 and $G(D_2) = 0.015$ for C_6D_6 at 25°C.). Since hydrogen is presumably formed by different reaction paths in hexane and benzene, this could be taken as evidence that an increase in deuteration quite generally leads also to an increase in radiation stability. In mixtures of light and deuterated hydrocarbons, the distribution of the hydrogen isotopes is in no case statistical, as is shown by the following figures:

C_6H_6—C_6D_6 1:1 25°C. H_2:HD:D_2 = 54:32:14 (*3, 6, 9, 10*)
C_6H_{14}—C_6D_{14} 1:1 −70°C. H_2:HD:D_2 = 41:38:21

The yield of H_2 and D_2 is always too large compared with HD. This demonstrates the importance of Reaction 1.

Table I. G-values of Products in Hexane at −70°C.

	Without Scavenger			*With 0.06M N_2O added*		
	C_6H_{14}	*1:1*	C_6D_{14}	C_6H_{14}	*1:1*	C_6D_{14}
Hydrogen	3.8	3.0	2.1	3.0	2.3	1.7
$C_2H_4 + C_2H_6$	0.30	0.27	0.28	0.18	0.22	0.31
C_3H_6	0.11	0.11	0.08	0.08	0.08	0.05
C_3H_8	0.23	0.32	0.34	0.18	0.22	0.29
1-C_4H_8	0.12	0.12	0.08	0.08	0.10	0.05
n-C_4H_{10}	0.37	0.52	0.63	0.28	0.40	
C_6H_{12}	2.5	1.4	1.0	4.0	2.8	2.2
C_8H_{18}	0.23		0.40	0.11		0.21
C_9H_{20}	0.16		0.28	0.11		0.17
$C_{10}H_{22}$	0.17	0.26	0.28	0.11	0.16	0.18
$C_{11}H_{24}$	0.02		0.02	0.02		0.02
$C_{12}H_{26}$	0.75	0.71	0.53	1.2	1.2	1.3

Measurements of the hydrogen yield over the whole concentration range of C_6D_{14} (*see* Figure 1) seem to indicate that the light form is preferentially decomposed. The total hydrogen yield can be expressed as a linear function of the molar fraction y of the deuterated hexane. The pertinent figures are given in Table II for several temperatures and for N_2O added as electron scavenger. The difference for the hydrogen yield for light and heavy hexane is independent of temperature and N_2O added as electron scavenger. It amounts to an average value of ΔG(total hydrogen) = 1.5. In order to be able to distinguish between Reactions 1 and 2 for the deuterated species, Jenkinson and Dyne (*3*) proposed the

Publication Date: January 1, 1968 | doi: 10.1021/ba-1968-0082.ch029

plot of the fractional yield of D_2 as a function of the concentration y of the deuterated compound:

$$g(D_2) = G(D_2)/y = \alpha + \beta \cdot y \qquad (a)$$

In Table II, numbers are given for different temperatures and N_2O added as electron scavenger for this equation. According to Dyne, the coefficient α stands for deuterium formation by a unimolecular process. It is not very important for deuterium formation increases with temperature and

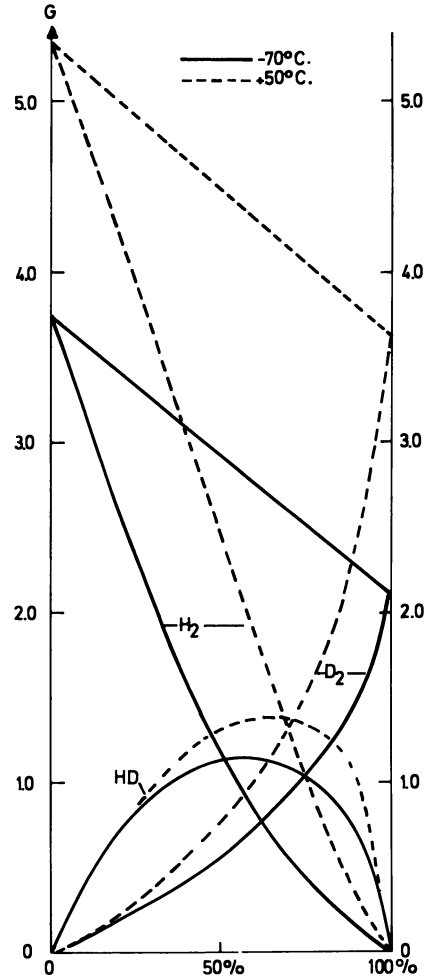

Figure 1. The hydrogen evolution as a function of the C_6D_{14}-concentration and temperature

is reduced by N_2O. The second term β in the equation gives the contribution by a bimolecular process—*e.g.*, the splitting off of a deuterium atom followed by a deuterium abstraction by this atom. We have shown elsewhere (7), that this deuterium atom cannot be a thermal one, since β is independent of temperature and N_2O added. It amounts to an average of $\beta = 1.5$. At $-70°C.$ the relationship (a) is linear over nearly the whole concentration range. This is no longer true at an irradiation temperature of $+50°C.$, where the extrapolated $G(D_2)$-value of 2.4 for pure deuterated hexane is much less than the measured value of 3.7.

Table II. Numbers for the Equation $x = \alpha + \beta y$ as a Function of Temperature and N_2O Added as Scavenger

x	T, °C.	α	$\alpha + \beta$	β	$\overline{\beta}$
G(Total hydrogen)	−70	3.8	2.1	−1.6 ± 0.1	−1.5 ± 0.1
	−70[b]	3.0	1.7	−1.3 ± 0.3	
	2	4.9	3.5	−1.4 ± 0.2	
	50	5.4	3.7	−1.7 ± 0.2	
$G(D_2)/y$[a]	−70	0.4	2.0	1.6 ± 0.2	1.5 ± 0.1
	−70[b]	0.2	1.6	1.4 ± 0.2	
	2	0.5	1.9	1.4 ± 0.1	
	50	0.8	2.4	1.6 ± 0.1	
$G(D_2) + G(HD)/2$	−70	0.08 ± 0.04	2.0	1.96 ± 0.07	
	−70[b]	0.01 ± 0.02	1.6	1.58 ± 0.04	
$G(C_6D_{13}\cdot)$	−70	0.02 ± 0.01	2.0	2.00 ± 0.03	
	−70[b]	0.02 ± 0.03	1.9	1.90 ± 0.09	

[a] y: molar fraction of C_6D_{14}.
[b] 0.06M N_2O added.

A relation similar to (a) can in principle also be written for $g(H_2)$ *vs.* $(1 - y)$ (*see* Figure 2). The experimental difficulty lies in the fact that whereas it is easy to prepare pure C_6H_{14} without deuterium in the molecule, the inverse is not true, since it is extremely difficult to prepare very pure C_6D_{14} with a deuteration better than 99.8%. An extrapolation to 100% C_6D_{14} is therefore not entirely free from an experimental bias. The relation is again linear at an irradiation temperature of $-70°C.$, but it is curved downwards at $+50°C.$ If one accepts the model of Dyne, one is forced to the conclusion that $G(H_2$ molecular) is much larger than $G(D_2$ molecular), Reaction 1 thus showing an isotope effect of 9:1 at $-70°C.$ and about 6:1 at $+50°C.$ in favor of the lighter compound.

This shows clearly that it can be very misleading to measure deuterated compounds in a nondeuterated solvent and to draw conclusions as to the behavior of nondeuterated compounds.

Publication Date: January 1, 1968 | doi: 10.1021/ba-1968-0082.ch029

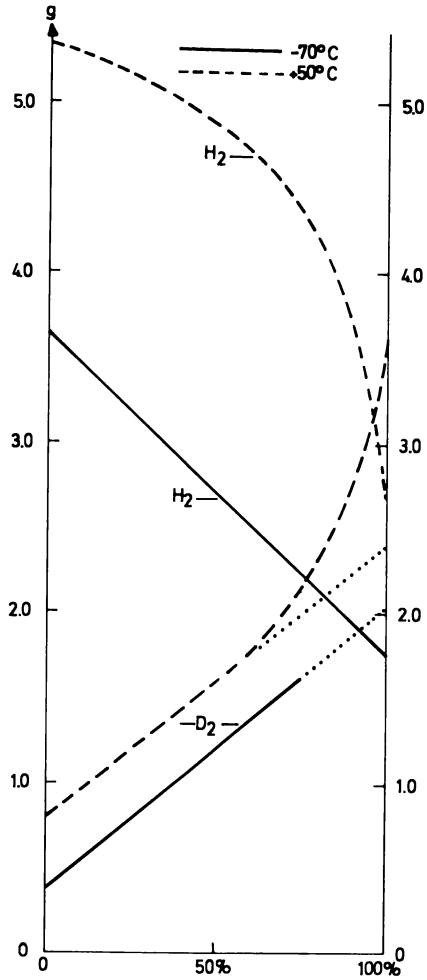

Figure 2. The partial g-value for D_2- and H_2-formation as a function of the C_6D_{14}-concentrations

The Hexene Production

The hexenes form besides hydrogen the largest product group in the radiolysis of the paraffins. They can be formed by Reaction 1 and by disproportionation of hexyl radicals. The decrease of their G-value on deuteration is 1.5, the corresponding decrease of G(molecular hydrogen) is 1.6. This is additional proof for an isotope effect for Reaction 1. This reaction explains also the observation that the isomeric distribution of

the hexenes does not correspond to the thermodynamic equilibrium at the irradiation temperature that one would expect if disproportionation of hexyl radicals would be the main reaction giving hexene (*see* Table III). The change in the isomeric distribution on deuteration goes in the direction expected for a larger percentage contribution of the disproportionation reaction—*i.e.*, increasing importance of the *cis*-form and a smaller percentage of 1-hexene.

Table III. Distributions of the Hexenes in G-values

					Total yield of	
	1-	*2-cis-*	*2-trans-*	*3-trans-*	C_6H_{12}	C_6D_{12}
C_6H_{14}	0.66	0.36	1.15	0.36	2.53	
1:1	0.28	0.20	0.69	0.26	1.08	0.35
C_6D_{14}	0.15	0.20	0.47	0.15		0.97
C_6H_{14}[a]	1.31	0.32	1.75	0.68	4.06	
1:1[a]	0.92	0.24	1.55	0.52	2.30	1.03
C_6D_{14}[a]	0.43	0.20	1.19	0.38		2.20

[a] 0.06*M* N_2O added.

The deuterated and nondeuterated hexenes overlap partially in the gas chromatogram. For N_2O added as scavenger at −70°C., a series of measurements have been done for different ratios of C_6H_{14} and C_6D_{14}. Under the condition that the distribution stays the same over the whole concentration range—a condition that could be checked for three isomers —a simple calculation allows the separation of light and heavy hexenes. Since only the range of low concentrations of C_6D_{14} has been studied, no deductions can be made concerning C_6D_{12}. The light hexenes are linear functions of the concentration of C_6D_{14} up to 50% and extrapolate to zero at 100%.

Products Formed by Radical Reactions

The existence of radicals in irradiated hexane has been demonstrated by EPR-methods (*5, 29*). Their reactions and yield have been reviewed by Holroyd (*18*) and Hardwick (*16*). By using mixtures of light and deuterated hexanes we were able to show that the products with seven to twelve carbon atoms are formed by statistical combination of alkyl radicals with one to six carbon atoms (*7*). The *G*-value of hexyl radicals has been estimated from the formation of iodides to be 1.8 at −80°C. and 2.0 at 0°C. (*34*). These are probably lower limits since iodine can also interfere with primary species. Perner and Schuler (*22*) arrived at a value of 2.0 for room temperature with TI as scavenger.

In Radiation Chemistry; Hart, E.; Advances in Chemistry; American Chemical Society: Washington, DC, 1968.

Publication Date: January 1, 1968 | doi: 10.1021/ba-1968-0082.ch029

If the hexyl concentration is calculated from the G-values of the intermediate and dimeric products, one arrives at a value of 2.1 for C_6H_{14} and 2.0 for C_6D_{14} in good agreement with the radical yield if disproportionation is neglected. Barker decomposed $(C_6H_{13})_2Hg$ by γ-irradiation and got for the hexyl radicals a disproportionation/combination ratio of 0.7 (*1*). Compared with values obtained for other alkyl radicals, this value seems to be rather high and completely uncompatible with the above mentioned results. We cannot see a simple explanation for this disagreement. If we concern ourselves for the moment with the radical yields calculated only from the dimer and intermediate-product concentration, thus neglecting disproportionation, we see that no isotope effect can be observed for the radical formation. If the disproportionation is as important as Barker assumes, this means that the figures we derive in the further discussion are lower limits. The data in Table IV show that not only the yield for hexyl radicals is the same for light and heavy hexane, but also the distribution for 3-:2-:1-hexyl is the same at −70°C., thus showing no isotope effect for primary hexyl formation. At higher temperature the hydrogen abstraction by primary radicals such as

$$C_2H_5\cdot + C_6H_{14} \rightarrow C_2H_6 + \text{s-}C_6H_{13}\cdot \qquad (7)$$

comes into play, increasing the yield of secondary hexyl radicals and decreasing the yield of products formed by combination with primary alkyl radicals, notably the paraffins with seven to eleven carbon atoms and the dimers formed with 1-hexyl.

At 50°C. the distribution for the hexyl radicals is 41:50:9 for C_6H_{14}. Because of the larger zero-point energy the abstraction at a given temperature competes less favorably with combination in the case of C_6D_{14}, the hexyl radical yield increases slower with increasing irradiation temperature, together with a smaller decrease of the 1-hexyl. We have shown in another publication that a probability can be calculated for the fragmentation of hexane into radicals that give dimers, intermediate-molecular-weight products and at higher temperatures also low-molecular-weight products (*34*). This probability is practically independent of temperature if one corrects for the abstraction Reaction 7.

Table IV. Temperature Dependence for Some Products

	C_6H_{14}		C_6D_{14}	
	−70°C.	*+50°C.*	*−70°C.*	*+50°C.*
hexyl yield[a]	2.1	3.5	2.0	2.6
3-:2-:1-hexyl	35:39:26	41:50:9	34:39:27	40:46:14
C_9H_{20} or C_9D_{20}	0.16	0.078	0.28	0.25

[a] Calculated from the dimers and the intermediate-molecular-weight products.

Publication Date: January 1, 1968 | doi: 10.1021/ba-1968-0082.ch029

Such a distribution is shown in Figure 3 for both hexanes. The figures give the approximate *G*-values for a particular bond, when the disproportionation is neglected. Under the condition that the disproportionation/combination ratio does not change on deuteration, they can be compared for a possible isotope effect of the fragmentation yielding radicals. The probability is the same for the split of a C–H bond—*e.g.*, 0.8 for the sum of the four C–H bonds in position 2 of hexane—but a small inverse isotope effect is observed for C–C scission. Because of the above mentioned assumptions we are unable to decide if this corresponds to reality, however such an effect would be predicted on the basis of quasi-equilibrium theory.

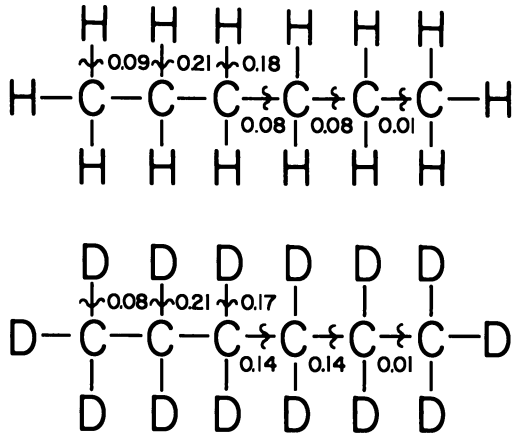

Figure 3. G-values for radical fragmentation of different bonds

Gas-chromatographic analysis allows us to distinguish between molecules of the same structure but with different deuterium content (7). Such measures showed that the alkyl radicals with one to five C-atoms as calculated from the intermediate-molecular-weight products are linear with the concentration of the hexane they are formed from. This is valid for the whole temperature range of hexane. It can be concluded that the process of C–C-fragmentation is independent of temperature and for this reaction no transfer of reactivity takes place from light to heavy hexane or vice versa.

The same linear dependence is true for C_6D_{13}-radicals at an irradiation temperature of −70°C. (*see* Figure 4) and +50°C. It is not true for the C_6H_{13}-radicals at higher irradiation temperatures than −20°C.

because the hydrogen abstraction Reaction 7 consumes mainly light hexane. Hardwick (*11, 12, 13, 14, 15*) proposed that the hydrogen atoms of Reaction 3 are mainly thermal atoms that can be scavenged by scavengers with double bonds. Widmer and Gäumann (*35*) showed that this cannot be true since the corresponding products of the hydrogen addition to an olefin are not formed in the necessary amount in contrast to the addition of the alkyl radicals to the double bond, where even the correct activation energy could be determined (*see* Ref. 7). Toma and Hamill (*30, 31*) proposed the existence of hot hydrogen atoms and set an upper limit of 0.5 for the *G*-value of thermal H-atoms in cyclohexane. Scavenger experiments with H_2S led Meissner and Henglein (*20*) to the conclusion that the *G*-value for hydrogen atoms is 3, with 50% of them as thermal H-atoms. For an irradiation temperature of 25°C., the *G*-value for hydrogen is 5.2. If we interpolate the aforementioned values of the molecular hydrogen, we arrive at $G(\text{molecular } H_2)$ of about 2.2. This leaves a value for $G(\text{H-atoms})$ of 3 in excellent agreement with Henglein's value. In this case, however, the second product of Reaction 2 can not be a hexyl radical since its total yield is 2 and it is also formed by Reaction 3. This gives an overall yield for hexyl radicals of 6. From the results with partially deuterated hexanes it follows that the Reaction 2 also yields two hydrogen atoms from the same hexane molecule, leaving a hexene or a disubstituted methylene as product (*7*). Its contribution to the *G*-value of the Reaction 2 is, however, not known. This diminishes the amount of hexenes that are formed by disproportionation, making the value of 0.7 for the disproportionation/combination ratio even less probable. Kaldor and Rajbenbach (*24*) used perfluorobutane and olefins as combined scavengers and arrived at $G(H_{mol}) = 2.6$, $G(H_{thermal}) = 1.4$, and $G(H_2) = 1.2$ at 25°C. If thermal D-atoms are important, they will preferentially abstract hydrogen from C_6H_{14} and at higher C_6D_{14}-concentrations the C_6D_{13}-radical concentration must derivate from linearity. Since this cannot be observed, either Reaction 2 does not take place for D-atoms or the latter are not thermal. In Figure 4 it is shown that at −70°C. the amount of deuterium formed calculated as $G(D_2) + G(HD)/2$ matches the yield of C_6D_{13}-radicals. The contribution from deuterium formed in a molecular process is relatively small and can be accommodated within the experimental error. If we do not want to replace the Reaction 2 by another reaction, we are forced to the conclusion that the D-atoms of this reaction are mainly hot. Since even in this case the yields for the different active species do not match, we have to accept that either of the two Reactions 2 or 3 has to be abandoned. A possibility would be to replace Reaction 3 by the combination of two hydrogen atoms or the reaction of an excited or charged species

Publication Date: January 1, 1968 | doi: 10.1021/ba-1968-0082.ch029

with hexane giving as final products hydrogen molecules and hexyl radicals, but from our results no definite proposal can be drawn.

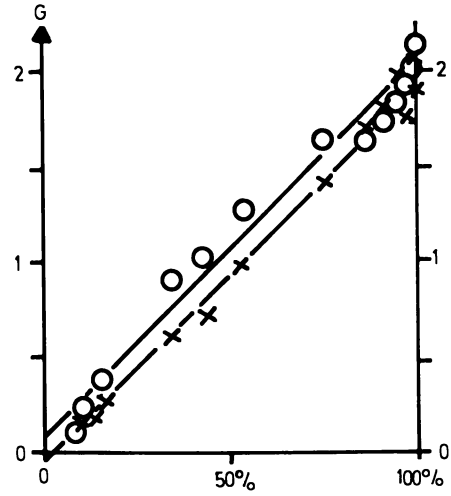

Figure 4. $C_6D_{13}\cdot$ formed and deuterium split off as a function of the C_6D_{14}-concentration at −70°C. (o) = $C_6D_{13}\cdot$, (x) = $G(D_2) + G(HD)/2$

N_2O as Scavenger

N_2O has been shown to reduce the hydrogen yield caused by electron scavenging (*27*). This means that the sequence

$$C_6H_{14} \longrightarrow C_6H_{14}^{+} + e^{-} \rightarrow H_2 + \text{prod.} \qquad (8)$$

is replaced by

$$C_6H_{14} + N_2O \longrightarrow C_6H_{14}^{+} + e^{-} + N_2O \rightarrow \text{not hydrogen} \qquad (9)$$

From Table I it can be seen that 0.06*M* N_2O diminishes $G(H_2)$ by 0.8 and $G(D_2)$ by 0.4. As has been shown in Table III, the hexenes increase strongly. The low-molecular-weight products are slightly decreased by equal amounts. The intermediate-molecular-weight products decrease by about 40%, whereas the dimers show a strong increase as has also been observed for cyclohexane (*2*). A strange feature is the distribution of the hexyl radicals at low irradiation temperature, *viz.* 3-:2-:1-hexyl equal to 42:37:21 for C_6H_{14} and 43:38:19 for C_6D_{14}, 3-hexyl being the main radical formed. The hydrogen abstraction by alkyl radicals at elevated temperatures yields more 2-hexyls than 3-hexyls. The

Publication Date: January 1, 1968 | doi: 10.1021/ba-1968-0082.ch029

same is observed with N_2O: 34:56:10 for C_6H_{14} and 43:43:14 for C_6H_{14} and 43:43:14 for C_6D_{14} for 50°C. Several authors proposed the following reaction sequence to explain the increased hexyl yield (*2*, *25*, *26*).

$$e^- + N_2O \rightarrow N_2 + O^- \quad (10)$$

$$O^- + C_6H_{14} \rightarrow OH^- + C_6H_{13}\cdot \quad (11)$$

$$OH^- + C_6H_{14} \rightarrow H_2O^- + C_6H_{13}\cdot \quad (12)$$

$$O^-, OH^-, H_2O^- + X^+ \rightarrow \text{charge neutralization} \quad (13)$$

The oxygen anion may be replaced by the other species O, OH, H_2O^-, according to where the charge neutralization comes in. In contrast to the results published on cyclohexane, we are unable to find hexyl alcohol. However, water can be found with a *G*-value that corresponds within the rather large limit of error (±25%) to a $G(N_2)$ of 3.2 for a N_2O concentration of 0.06*M*. This would correspond to an increase in hexyl radicals by more four units in *G*-value. At −70°C. this increase is less than 1.0 for C_6H_{14} and 1.2 for C_6D_{14}, compared with an increase of about 1.4 for the hexenes. The increase in hexene- and radical yields is too small to match the nitrogen production, even if one allows for rather large errors in the measurement and takes disproportionation into consideration. One explanation might be that nitrogen is also formed by secondary reaction of the N_2O^- with N_2O as has been proposed by Warman for the gas phase (*32*). This, however, does not explain the *G*-value of water. Another explanation is that the "original" hexyl- and hexene yield is somewhat decreased by N_2O, but not completely suppressed. Such a partial decrease is not unexpected, since the low-molecular-weight products show a similar behavior.

The hexenes increase more on N_2O-addition than the hexyl radicals. This cannot be explained by Reaction 11 and 12, since the disproportionation/combination ratio is certainly smaller than 1. Further, only the *trans*-hexenes and 1-hexene increase, the *G*-value of 2-*cis*-hexene remaining independent of the N_2O-concentration at −70°C. up to 0.4*M* (*21*). We have to assume a reaction that produces hexenes in a unimolecular step. That is why we propose the additional reactions:

$$C_6H_{14} + O\cdot \rightarrow C_6H_{12} + H_2O \quad (14a)$$

or

$$C_6H_{14}^+ + O^- \rightarrow C_6H_{12} + H_2O \quad (14b)$$

With the following heats of reaction: C_6H_{14}: −40 kcal./mole; O: +59 kcal./mole; 2-C_6H_{12}: −12 kcal./mole; H_2O: −68 kcal./mole; Reaction 14a is exothermic by 99 kcal./mole. Since hexane in the liquid state is mainly in the all-*trans* form (*23*, *28*), mainly *trans*-hexenes will be formed for the 2- and 3-hexene. It may be mentioned that the analogous abstrac-

Publication Date: January 1, 1968 | doi: 10.1021/ba-1968-0082.ch029

tion step (Reaction 11) is exothermal by only 9 kcal./mole ($C_6H_{13}\cdot$: 2 kcal./mole; $OH\cdot$: 8 kcal./mole).

The numbers of Table II indicate that the $C_6D_{13}\cdot$-yield in mixtures of light and heavy hexane is not changed upon N_2O-addition and is still linear up to high concentrations of C_6D_{14}. In pure C_6D_{14}, $G(C_6D_{13}\cdot)$ is equal to 3.2. The linear extrapolation leads to a value of 1.9. It can be concluded that the precursor yielding C_6D_{13}-radicals is not affected by N_2O-addition, that the Reactions 11 and 12 must show a strong isotope effect by abstracting mainly light hydrogen from C_6H_{14} and that the G value for these two reactions is of the order of 1.3. Reactions of a type such as Reaction 14 must accordingly have at least the same G-value. The bimolecular process that is represented by the coefficient β in Equation (a) is not affected by N_2O-addition, nor is the H_2:HD:D_2-distribution in mixtures of light and heavy hexane. The main effect of N_2O on the fragmentation of hexane consists at −70°C. apparently in a reduction of the yield of radicals with one to five carbon atoms.

Discussion

The main results can be summarized as follows:

(a) The total hydrogen production is diminished on deuteration by an amount that is independent of temperature.

(b) Although N_2O diminishes the hydrogen production, the isotopic composition does not change. The same is true when iodine is added (7).

(c) With the assumption of a uni- and a bimolecular process, the hydrogen production can be explained at −70°C. The bimolecular process is independent of scavenger and temperature for the deuterium production.

(d) The so-called unimolecular process becomes less important with deuteration. It is accompanied by a diminution of the hexene yield. All other products have approximately the same yield in both hexanes.

(e) The C_6D_{13}-yield and $[G(D_2) + G(HD)/2]$ show a 1:1 correspondence at −70°C. Except at very high C_6D_{14}-concentrations the $C_6D_{13}\cdot$-yield is not increased by N_2O.

From this it is apparent that there are at least two entirely different processes in hexane. One yields products in a unimolecular step:

$$C_6H_{14} \xrightarrow{\wedge\wedge\wedge} C_6H_{12} + H_2 \qquad (1)$$

The probability for this process is strongly decreased by deuteration, since the estimated yield of 1.7 for molecular hydrogen in C_6H_{14} is decreased to a value of 0.4 in C_6D_{14}. This already small yield in deuterated hexane is further decreased by an addition of an electron scavenger such as N_2O. It is accepted that N_2O captures electrons and thus interferes with the charge recombination process. Under the assumption that it has

no other effect, it seems logical to assume that the products of Reaction 1 are caused by charge recombination, that C_6D_{14} is more stable for this reaction and that its importance increases with temperature for C_6D_{14}. If these molecular contributions are substracted from the respective hydrogen yields, there results a distribution for the isotopic composition that could be explained by the following reaction sequence:

$$C_6H_{14},\ (C_6D_{14}) \longrightarrow H,\ (D) + C_6H_{13}\cdot,\ (C_6D_{13}\cdot)\ G \sim 1.7 \qquad (2')$$

$$H,\ (D) + C_6H_{14} \xrightarrow{k_H} H_2,\ (HD) + C_6H_{13}\cdot \qquad (3')$$

$$H,\ (D) + C_6D_{14} \xrightarrow{k_D} HD,\ (D_2) + C_6D_{13}\cdot \qquad (3'')$$

The asymmetric position of the maximum of the $G(HD)$ curve in Figure 1 could be explained with a value of 0.4 for the ratio k_D/k_H. This corresponds to an isotope effect expected for moderately hot hydrogen atoms. As we will show in a forthcoming publication (*8*), the $G(HD)$ curve is getting more asymmetric with increasing temperature. This would imply that the isotope effect increases with temperature. Because we are not yet able to explain the temperature dependence of radiolysis (*7*), this unexpected conclusion must not necessarily invalidate the explanation for −70°C.

Dyne (*4*) has proposed a simplified reaction scheme that generally explains most of the observed results. He admits that a common active precursor can be formed by different reaction paths—*e.g.*, by an ion pair formation and combination and by direct excitation. This common precursor can react by different decomposition paths, giving different "primary" products. Our results do not substantiate this view entirely, but since most of our (and his) conclusions are based on deuterated compounds, where Reaction Type 1 is much less important than Reaction 2′, it might well be that within the limits of error such a model is still acceptable. The results of Table II are not entirely compatible with Reactions 2 and 3, unless one accepts that Reaction 3″ is very unimportant. This would mean that the H-atoms formed are nearly thermal, contrary to the D-atoms that must possess kinetic energy. Furthermore, the yield for hexyl radicals does not match this simple reaction sequence. We feel, therefore, that one of these reactions has to be replaced by a so far unknown reaction path.

Acknowledgment

We would like to thank the Swiss National Foundation for the support of this work.

Literature Cited

(1) Barker, R., *Trans. Faraday Soc.* **63,** 2640 (1967).
(2) Blackburn, R., Charlesby, A., *Nature* **210,** 1036 (1966).
(3) Dyne, P. J., Jenkinson, W. M., *Can. J. Chem.* **40,** 1746 (1962).
(4) Dyne, P. J., *Can. J. Chem.* **43,** 1080 (1965).
(5) Fessenden, R. W., Schuler, R. H., *J. Chem. Phys.* **39,** 2147 (1963).
(6) Gäumann, T., *Helv. Chim. Acta* **46,** 2873 (1963).
(7) Gäumann, T., "Aspects of Hydrocarbon Radiolysis," p. 215, T. Gäumann, J. Hoigné, eds., Academic Press, London, 1968.
(8) Gäumann, T., Reipso, B., *Helv. Chim. Acta* **51** (1968) (in preparation).
(9) Gordon, S., Burton, M., *Science* **115,** 406 (1952).
(10) Gordon, S., Burton, M., *Discussions Faraday Soc.* **12,** 88 (1952).
(11) Hardwick, T. J., *J. Phys. Chem.* **64,** 1623 (1960).
(12) *Ibid.*, **65,** 101 (1965).
(13) *Ibid.*, **66,** 119 (1962).
(14) *Ibid.*, **66,** 291 (1962).
(15) *Ibid.*, **66,** 2246 (1962).
(16) Hardwick, T. J., "The Chemical and Biological Action of Radiations," Vol. X, p. 125, M. Haissinsky, ed., Academic Press, London, 1966.
(17) Hoigné, J., Gäumann, T., *Helv. Chim. Acta* **47,** 260 (1964).
(18) Holroyd, R. A., "Aspects of Hydrocarbon Radiolysis," p. 1, T. Gäumann, J. Hoigné, eds., Academic Press, London, 1968.
(19) Juppe, G., Rau, H., Doppema, F., Euratom Rept. **No. 3172.e** (1967).
(20) Meissner, G., Henglein, A., *Ber. Bunsenges. Phys. Chem.* **69,** 264 (1965).
(21) Menger, A., *Helv. Chim. Acta* (to be published).
(22) Perner, D., Schuler, R. H., *J. Phys. Chem.* **70,** 2224 (1966).
(23) Piercy, J. E., Seshagiri, Rao M. G., *J. Chem. Phys.* **46,** 3951 (1967).
(24) Rajbenbach, L. A., Kaldor, U., *J. Chem. Phys.* **46,** 242 (1967).
(25) Sagert, N. H., Blair, A. S., *Can. J. Chem.* **45,** 1351 (1967).
(26) Sato, S., Yugeta, R., Shinsaka, K., Terao, T., *Bull. Chem. Soc. Japan* **39,** 156 (1966).
(27) Scholes, G., Simic, M., *Nature* **202,** 895 (1964).
(28) Scott, R. A., Scheraga, H. A., *Biopolymers* **4,** 237 (1966).
(29) Thyrion, F., Dodelet, J. P., Fauquenoit, C., Claes, P., *J. Chim. Phys.* **65,** 227 (1968).
(30) Toma, S. Z., Hamill, W. H., *J. Am. Chem. Soc.* **86,** 1478 (1964).
(31) *Ibid.*, **86,** 4761 (1964).
(32) Warman, J. M., *Nature* **213,** 381 (1967).
(33) Widmer, H., Gäumann, T., *Helv. Chim. Acta* **46,** 944 (1963).
(34) *Ibid.*, **46,** 2766 (1963).
(35) *Ibid.*, **46,** 2780 (1963).

RECEIVED January 25, 1968.

30

Radiolysis of Cyclohexane at Very High Dose Rates

A. W. BOYD, C. WILLIS, O. A. MILLER, and A. E. ROTHWELL

Research Chemistry Branch, Chalk River Nuclear Laboratories, Atomic Energy of Canada Ltd., Chalk River, Ontario, Canada

Publication Date: January 1, 1968 | doi: 10.1021/ba-1968-0082.ch030

Cyclohexane was irradiated at 0.2–25 Mrads at dose rates from 5×10^{24} to 8×10^{27} e.v./gram sec. with 1.5 Mev. electrons and with ^{60}Co γ-rays at 1×10^{16} e.v./gram sec. Solutions of benzene, nitrous oxide, and sulfur hexafluoride in cyclohexane were irradiated at 6×10^{27} e.v./gram sec. In pure cyclohexane from 5×10^{26} to 8×10^{27} e.v./gram sec. $G(H_2) = 4.0 \pm 0.2$, $G(C_6H_{10}) = 2.6 \pm 0.3$, and $G(C_6H_{11})_2 = 1.1 \pm 0.2$ from 0.5 to 25 Mrads. At these dose rates $G(C_6H_{10})/G(C_6H_{11})_2$ is 2.6 ± 0.1, whereas it is 2.0 ± 0.1 at 10^{16} e.v./gram sec. At 5×10^{24} to 5×10^{25} e.v./gram sec. only product ratios were determined, but $G(C_6H_{10})/G(C_6H_{11})_2$ decreased significantly, suggesting that radical-radical reactions occur which are negligible at the low dose rates. Cyclohexene and bicyclohexyl product yields suggest that the additives used do not change the yield of thermal hydrogen atoms.

The effect of dose rate on product yields has been used extensively in radiation chemistry as an aid in determining mechanisms (*1*). Recently, pulsed electron sources giving doses of several megarads in 10^{-8}–10^{-7} sec. (which is equal to about 10^{28} e.v./gram sec.) have become available. Pulses from these sources give radical concentrations as high as 0.01*M*, and radical-radical reactions occur that are negligible at lower dose rates.

Using one of these sources we have determined product yields from the radiolysis of cyclohexane and the effects on these yields of adding nitrous oxide, benzene, and sulfur hexafluoride.

In Radiation Chemistry; Hart, E.;
Advances in Chemistry; American Chemical Society: Washington, DC, 1968.

Experimental

The high intensity pulsed electron source used was a Febetron 705 system (Field Emission Corp., McMinnville, Ore.). In this source the discharge from a stack of capacitor-inductance modules is applied to the field emission cathode of a vacuum tube to give an electron pulse through the tube window with energies from 0.5–1.6 Mev. at currents ~ 4000 amp. The current waveform is shown in Figure 1.

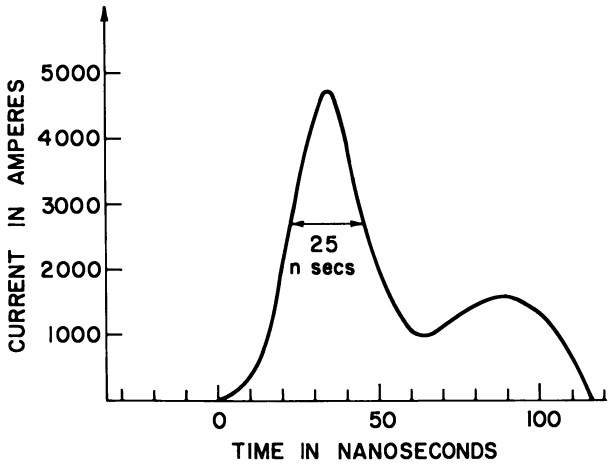

Figure 1. Current waveform of electron pulse from Febetron 705

The cyclohexane samples were irradiated in the stainless steel cells shown in Figure 2 and in glass cells 4 cm. in diameter and 0.3 cm. deep. The stainless steel cells were used for dose rates greater than 0.1 Mrad per pulse since glass cells shattered or cracked at these dose rates.

The absorbed dose in the sample in the stainless steel cells was determined by adiabatic calorimetry (*19*). Aluminum, nickel, and graphite calorimeters with the same diameter and thickness (160 mg./sq. cm.) as the liquid samples were put inside the cells behind the stainless steel window so that the geometry of the samples and the calorimeters was equivalent. The dose in the calorimeters was determined from temperature rise and their specific heat. This was corrected for relative stopping powers of the calorimeter material and cyclohexane to give the dose in cyclohexane. With the stainless steel cell window at 1.5–2 cm. from the Febetron tube window doses of 6–8 Mrads in cyclohexane were obtained. In this region aluminum and graphite calorimeters were used. The reproducibility per pulse is 1–2%, and the absorbed doses in the sample are believed to be accurate within ±3%. The variation in dose rate over the volume of the sample is less than a factor of 2 (*2*). To obtain doses of less than 1 Mrad, the electron beam was scattered by the arrangement

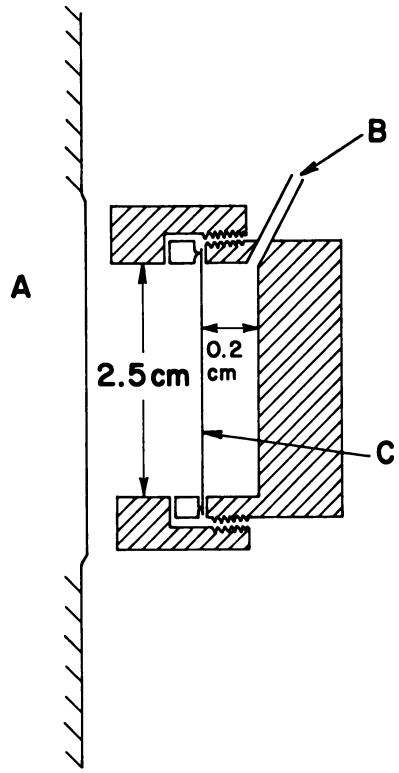

Figure 2. Stainless steel irradiation cell

A: Febetron tube window
B: Filling tube, connected to Hoke valve
C: Cell window, 0.0127-cm. stainless steel

shown in Figure 3. In this the beam is collimated to 1.3 cm. by holes in the two stainless steel plates and scattered by the 0.0026-cm. thick platinum foil. With the cell window 2 cm. from the foil the dose per pulse is $\sim$ 1 Mrad in cyclohexane. With this arrangement the dose decreases approximately as the square of the distance from the foil. Over the range 0.5–1 Mrad per pulse nickel calorimeters were used since these are more sensitive owing to the lower specific heat of nickel. The accuracy of the absorbed dose in this range is better than $\pm 5\%$. Variation of intensity over the sample with the scattering foil is less than that at 6–8 Mrads as was shown by a smaller deviation from the equilibrium cooling curve of the calorimeters at these lower dose rates. Below 0.5 Mrad calorimetry is not sensitive enough to give sufficient accuracy, and only relative product yields were obtained. The ^{60}Co γ-ray irradiations were done

Publication Date: January 1, 1968 | doi: 10.1021/ba-1968-0082.ch030

in a Gammacell 220 at a dose rate of 10^{16} e.v./gram sec. The dose rate was determined with the Fricke dosimeter.

Cyclohexane and benzene (Fisher "spectranalyzed" grade) and nitrous oxide and sulfur hexafluoride (Matheson) were used as supplied. The samples were thoroughly freed from dissolved air and frozen into the cells on a grease and mercury-free vacuum line. Hydrogen and nitrogen were measured using conventional vacuum line techniques and a mass spectrometer. Cyclohexene and bicyclohexyl were determined by gas liquid chromatography (*16*).

Results

Hydrogen, cyclohexene, and bicyclohexyl yields from the radiolysis of pure cyclohexane at different doses and dose rates are given in Table I. At dose rates from 5×10^{26} to 8×10^{27} e.v./gram sec. the yields are independent of dose from $\sim$ 0.5 to 25 Mrads and are 20–30% lower than those at 10^{16} e.v./gram sec. Also the ratio of cyclohexene to bicyclohexyl increases by about 30% at the higher dose rates. At dose rates of 10^{24}–10^{25} e.v./gram sec. the ratio of cyclohexene to bicyclohexyl appears to be intermediate between those at 10^{26}–10^{27} and at 10^{16} e.v./gram sec.

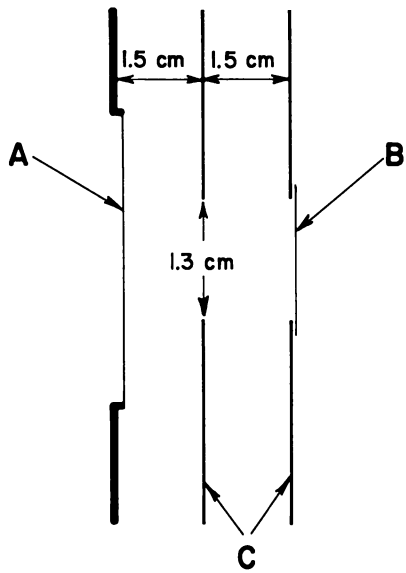

Figure 3. Aperture and scattering foil assembly

A: Febetron tube window
B: Platinum foil, 0.0025 cm. thick
C: Stainless steel plates, 0.15 cm. thick

Publication Date: January 1, 1968 | doi: 10.1021/ba-1968-0082.ch030

Table I. Radiolytic Yields of Hydrogen, Cyclohexene, and Bicyclohexyl from Cyclohexane

^{60}Co γ-Rays Dose Rate 1 × 10^{16} e.v./gram sec.

Dose, Mrads	$G(H_2)$	$G(C_6H_{10})$	$G(C_6H_{11})_2$	$\frac{G(C_6H_{10})}{G(C_6H_{11})_2}$
0.5	5.44	3.36	1.61	2.1
1	5.27	3.32	1.42	2.2
2	—	3.18	1.70	1.8
4	4.86	2.87	1.41	2.0
8	4.84	2.38	1.27	1.9

1.5 Mev. Electron Pulses

Dose Rate, e.v./gram sec.	*Dose, Mrads*	$G(H_2)$	$G(C_6H_{10})$	$G(C_6H_{11})_2$	$\frac{G(C_6H_{10})}{G(C_6H_{11})_2}$
~8 × 10^{27}	8	4.0	2.5	1	2.5
~8 × 10^{27}	24	4.2	2.6	0.9	2.8
~9 × 10^{26}	0.9	3.9	2.5	1.0	2.5
~9 × 10^{26}	1.8	4.0	2.3	0.9	2.5
~9 × 10^{26}	4.5	3.9	2.6	—	—
~4 × 10^{26}	0.4	4.2	—	1.2	—
~4 × 10^{26}	0.8	4.2	2.8	1.1	2.7
~4 × 10^{26}	1.6	4.2	—	—	—
~4 × 10^{25}	0.15	[a]	2.6	1.1	2.4
~5 × 10^{24}	0.1	[a]	2.6	1.2	2.2

[a] $G(H_2)$ assumed to be 4.0, and other values calculated from this.

The product yields from the radiolysis of cyclohexane containing benzene, nitrous oxide, and sulfur hexafluoride, with electron pulses at a dose rate of 6 × 10^{27} e.v./gram sec. and a dose of 7 Mrads, are shown in Figures 4, 5, 6, and 7. Also included in these figures are data of other workers (*12, 17*) at *ca.* 10^{16} e.v./gram sec. with ^{60}Co γ-rays. Comparison between the results at the two dose rates shows that the effect of the additives is qualitatively the same. However, there are some differences in the amounts by which the yields change.

Discussion

Pure Cyclohexane. The major products from the radiolysis of cyclohexane are hydrogen, cyclohexene, and bicyclohexyl. Dewhurst (*4*) proposed that these could be formed by the production of hydrogen atoms and cyclohexyl radicals, followed by abstraction by hydrogen atoms and recombination and disproportionation of the cyclohexyl radicals. Dyne and Jenkinson (*5*) showed that part of the hydrogen yield is unimolecularly formed. It was suggested that excited cyclohexane molecules give

Publication Date: January 1, 1968 | doi: 10.1021/ba-1968-0082.ch030

hydrogen and cyclohexene directly as well as radicals. Dyne (*8*) has also proposed that excited cyclohexane molecules may be formed directly by ionizing radiation or by ion pair recombination. These processes are described by Reactions 1 to 5.

$$C_6H_{12} \rightarrow C_6H_{12}^* \quad (1)$$

$$C_6H_{12} \rightarrow C_6H_{12}^+ + e \quad (1a)$$

$$C_6H_{12}^+ + e \rightarrow C_6H_{12}^* \quad (1b)$$

$$C_6H_{12}^* \rightarrow C_6H_{11} + H \quad (2)$$

$$C_6H_{12}^* \rightarrow C_6H_{10} + H_2 \quad (2a)$$

$$H + C_6H_{12} \rightarrow C_6H_{11} + H_2 \quad (3)$$

$$C_6H_{11} + C_6H_{11} \rightarrow (C_6H_{11})_2 \quad (4)$$

$$C_6H_{11} + C_6H_{11} \rightarrow C_6H_{10} + C_6H_{12} \quad (5)$$

The initial yields with ^{60}Co γ-rays at a dose rate of $\sim 1 \times 10^{16}$ e.v./gram sec. given by Dyne and Stone (*6*) are $G(H_2) = 5.55$, $G(C_6H_{10}) = 3.27$, and $G(C_6H_{11})_2 = 1.95$.

The yield from Reaction 2a as determined by the use of dilute solutions of C_6D_{12} in C_6H_{12} is uncertain owing to isotope effects and energy transfer (*8*). It cannot be much more than 1.1 since the ratio of Reaction 5 to Reaction 4 has been given as 1.3 (*10*) and 1.1 (*3*).

A more recent addition to the above reaction scheme is the distinction between thermal and hot hydrogen atoms. A yield of thermal hydrogen atoms of ~1.3 is obtained by McCrumb and Schuler (*11*). All these reactions and yields may be summarized as follows:

Observed $G(H_2) = 5.5$	
Yield from Reaction 2a	$= 0.8$
Yield from Reaction 3 thermal H atoms	$= 1.3$
Therefore,	
yield from Reaction 3 hot H atoms	$= 5.5 - (0.8 + 1.3) = 3.4$
Observed $G(C_6H_{10}) = 3.3$	
Yield from Reaction 2a	$= 0.8$
Therefore, yield from Reaction 5	$= 3.3 - 0.8 = 2.5$
Observed $G(C_6H_{11})_2 = 1.9$	
Yield from Reaction 4	$= 1.9$
Therefore,	
ratio of Reaction 5 to Reaction 4	$= 2.5/1.9 = 1.31$

The yields obtained at 10^{26}–10^{27} e.v./gram sec. are markedly lower than these values for $\sim 10^{16}$ e.v./gram sec. This reduction in yields may be caused by Reactions 6, 7, and 8.

$$H + H \rightarrow H_2 \quad (6)$$

Publication Date: January 1, 1968 | doi: 10.1021/ba-1968-0082.ch030

$$H + C_6H_{11} \rightarrow C_6H_{12} \quad (7)$$

$$H + C_6H_{11} \rightarrow H_2 + C_6H_{10} \quad (8)$$

If Reaction 6 or 7 occurs, the hydrogen yield is reduced, and if Reaction 8 occurs, the cyclohexene yield is increased relative to that of bicyclohexyl. Since hot hydrogen atoms are considered to abstract from cyclohexane much more readily than thermal hydrogen atoms, only thermal hydrogen atoms will be involved in Reactions 6 to 8.

The yields do not vary between 5×10^{26} and 8×10^{27} e.v./gram sec., suggesting that at these dose rates practically all the thermal hydrogen atoms are reacting with themselves or cyclohexyl radicals.

Accepting these conclusions, the yield of hydrogen at 10^{26}–10^{27} e.v./gram sec. can be derived from the values given above and the observed yields of cyclohexene and bicyclohexyl.

Observed $G(C_6H_{11})_2$	$= 1.1$
Yield from Reaction 4	$= 1.1$
Observed $G(C_6H_{10})$	$= 2.6$
Yield from Reaction 5	$= 1.4 = 1.3 \times 1.1$
Yield from Reaction 2a	$= 0.8$
Therefore, yield from Reaction 8	$= 0.4 = 2.6 - (1.4 + 0.8)$
$G(H_2)$	
Yield from hot H atoms	$= 3.4$
Yield from Reaction 2a	$= 0.8$
Yield from Reaction 8	$= 0.4$
Therefore, total yield	$= 4.6$
Observed $G(H_2)$	$= 4.0$

The difference between the calculated $G(H_2) = 4.6$ and the observed value $G(H_2) = 4.0$ implies that the effective yield of thermal H atoms in cyclohexane is higher than that proposed by McCrumb and Schuler (*11*).

The rate constant for Reaction 3 is given as 6.6×10^6 liter/mole-sec. (*9*), and a value of 1×10^6 liter/mole-sec. can be calculated from data in Ref. *11*. From the results presented it seems likely that

$$\frac{k_3(H)(C_6H_{12})}{k_3(H)(C_6H_{12}) + k_6(H)(H) + k_7(H)(C_6H_{11}) + k_8(H)(C_6H_{11})} < 0.1$$

at a dose rate of 5×10^{26} e.v./gram sec.

The rate constant for Reaction 6 is taken to be 1.5×10^{10} liter/mole-sec. Burns and Barker (*1*) calculated $(k_7 + k_8)$ to be $2(k_4k_6)^{1/2}$ and take $k_4 = 3.39 \times 10^9$ liter/mole-sec. From computer calculations the average concentrations of (H) and (C_6H_{11}) during the pulse at 5×10^{26} e.v./gram sec. are estimated to be 1.2×10^{-4} and $8 \times 10^{-5}M$, respectively. Using these values, the maximum value of k_3 is 2×10^5 liter/mole-sec.

Publication Date: January 1, 1968 | doi: 10.1021/ba-1968-0082.ch030

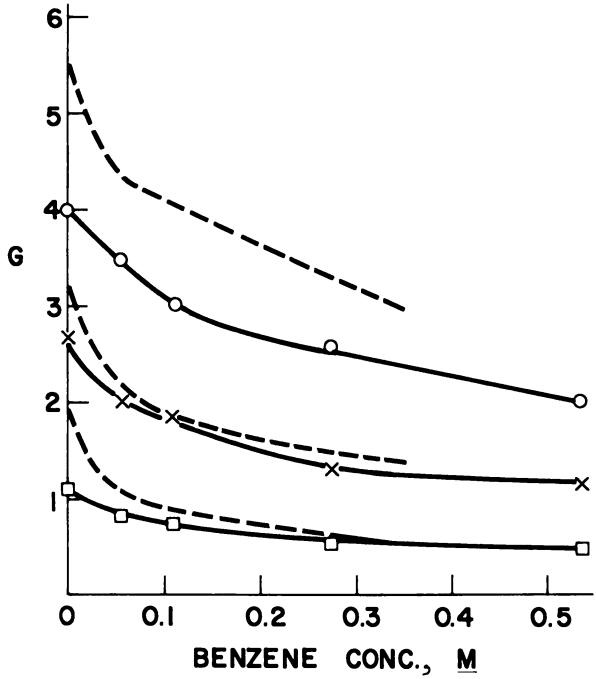

Figure 4. Hydrogen, cyclohexene, bicyclohexyl yields from molar solutions of benzene in cyclohexane

At ~ 10^{25} e.v./gram sec.
○: H_2
×: C_6H_{10}
□: $C_{12}H_{22}$
At ~ 10^{16} e.v./gram sec. (17)
--- H_2, C_6H_{10}, *and* $C_{12}H_{22}$

The results at the lower Febetron dose rates of 10^{24}–10^{25} e.v./gram sec. show a decrease in the ratio of cyclohexene to bicyclohexyl. This may be caused by a reduction in the reaction of thermal hydrogen atoms with radicals and indicate a return to the low dose rate (*i.e.*, 10^{16} e.v./gram sec.) mechanism. However, dosimetry at these dose rates at the present time is not sufficiently accurate to warrant further discussion.

It may be argued that the low yields obtained at 10^{26}–10^{27} e.v./gram sec. are caused by the relatively high doses used or uncertainties in the dosimetry. As Table I shows, the hydrogen yield decreases with dose at 10^{16} e.v./gram sec., but the decrease is not enough to account for the reduction at the higher dose rates. Moreover, the decrease in the hydrogen yield at 10^{16} e.v./gram sec. is accompanied by a small decrease in the cyclohexene to bicyclohexyl ratio. Thus, the high ratio we obtain is not a dose effect.

Publication Date: January 1, 1968 | doi: 10.1021/ba-1968-0082.ch030

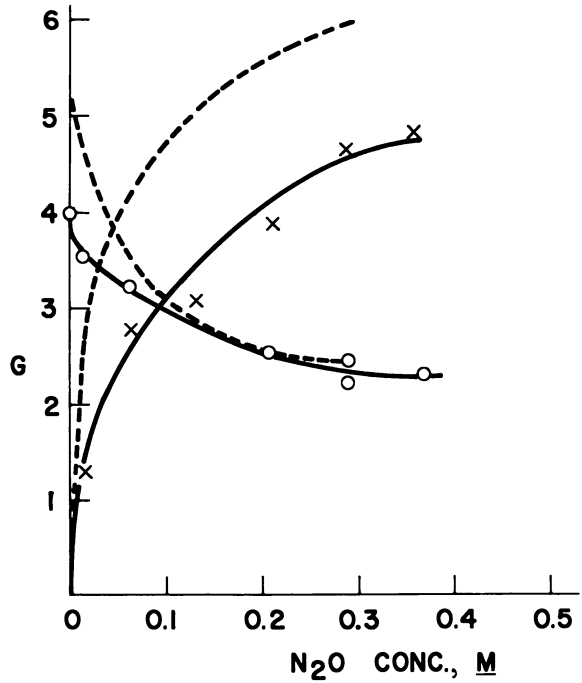

Figure 5. Hydrogen and nitrogen yields from molar solutions of nitrous oxide in cyclohexane

○: H_2 at $\sim 1 \times 10^{18}$ e.v./gram sec.
×: N_2 at $\sim 1 \times 10^{18}$ e.v./gram sec.
--- H_2 and N_2 at $\sim 10^{16}$ e.v./gram sec. (12)

There are uncertainties in the dosimetry we have used at the high dose rates, but as stated they are believed to be less 5%. Further the ratio of cyclohexene to bicyclohexyl does not depend on dosimetry. Another aspect of the comparison between low and high dose rates is the invariance of yields at the high dose rates up to 25 Mrads.

Cyclohexane and Benzene. At conventional dose rates the yields of the three major products decrease with increasing benzene concentration. At $\sim 0.35M$ benzene the hydrogen yield is $G(H_2) \sim 3.0$, a reduction of 2.5 G units (*17*). This is greater than the yield of thermal H atoms (*11*), and Stone and Dyne (*17*) have showed that the major part of this reduction is caused by some physical process such as energy transfer or charge transfer.

In the Febetron irradiations, the fractional lowering of the hydrogen yield by benzene is the same as at low dose rates, but there is less effect on the cyclohexene and bicyclohexyl yields, and the ratio of cyclohexene

Publication Date: January 1, 1968 | doi: 10.1021/ba-1968-0082.ch030

to bicyclohexyl is unaffected. If the reduction in the hydrogen yield were caused by Reaction 9,

$$H + C_6H_6 \rightarrow C_6H_7 \quad (9)$$

thermal H atoms would disappear in this way. The yield of cyclohexene from Reaction 8 would be reduced, and the ratio of cyclohexene to bicyclohexyl should decrease. Our results are thus consistent with energy or charge transfer to benzene.

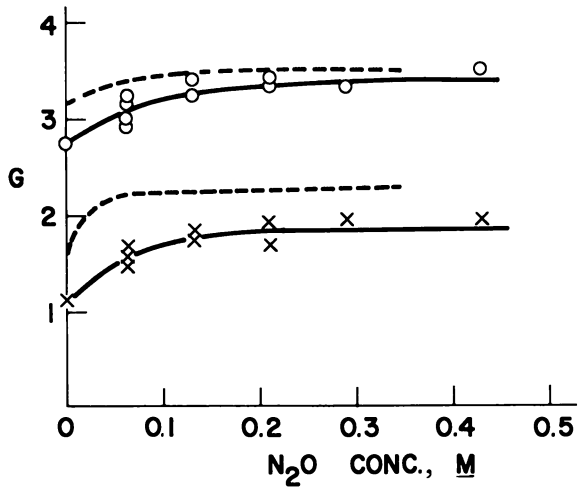

Figure 6. Cyclohexene and bicyclohexyl yields from molar solutions of nitrous oxide in cyclohexane

○: C_6H_{10} *at* $\sim 1 \times 10^{18}$ *e.v./gram sec.*
×: $C_{12}H_{22}$ *at* $\sim 1 \times 10^{18}$ *e.v./gram sec.*
--- C_6H_{12} *and* $C_{12}H_{22}$ *at* $\sim 10^{16}$ *e.v./gram sec.* (12)

Cyclohexane and Nitrous Oxide. The effect of nitrous oxide on the yields of hydrogen, cyclohexene, and bicyclohexyl at conventional dose rates has been studied by Sagert and Blair (*12*), and their results are included in Figures 7 and 8. These authors explain their results by the replacement of Reaction 1b, ($C_6H_{12}^+ + e^- \rightarrow C_6H_{12}^*$), by Reactions 10 to 12.

$$C_6H_{12} \rightarrow C_6H_{12}^+ + e^- \quad (1a)$$

$$e^- + N_2O \rightarrow N_2 + O^- \quad (10)$$

$$O^- + C_6H_{12}^+ \rightarrow C_6H_{11} + OH \quad (11)$$

$$OH + C_6H_{12} \rightarrow C_6H_{11} + H_2O \quad (12)$$

Publication Date: January 1, 1968 | doi: 10.1021/ba-1968-0082.ch030

These are consistent with the reduction of the hydrogen yield and increases in the cyclohexene and bicyclohexyl yields as well as for formation of nitrogen.

If these reactions occur in or near the spurs, they should not depend on dose rate, and the concentration dependence of the changes in the liquid products and hydrogen yields should be similar at both dose rates.

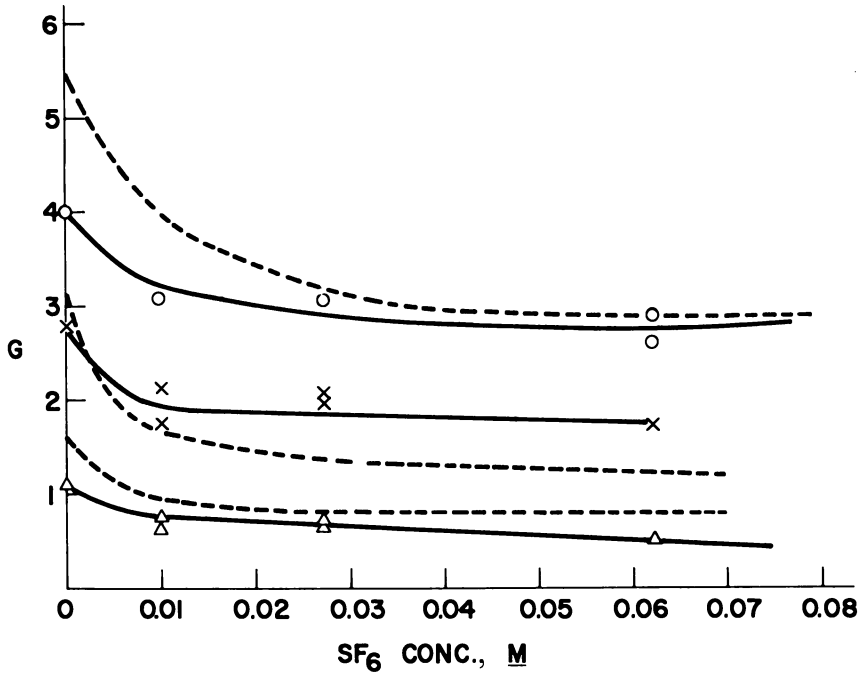

Figure 7. Hydrogen, cyclohexene, and bicyclohexyl yields from molar solutions of sulfur hexafluoride in cyclohexane

At ~ 10^{18} e.v./gram sec.
○: H_2
×: C_6H_{10}
△: $C_{12}H_{22}$
At ~ 10^{16} e.v./gram sec. (12)
- - - H_2, C_6H_{10}, and $C_{12}H_{22}$

In the irradiations at low and high dose rates both the cyclohexene and bicyclohexyl increase to constant values at a concentration of 0.1*M* N_2O. The concentration dependence of the nitrogen and hydrogen yields in both sets of irradiations is different from that of the liquid yields.

There is an initial rapid change, then a more gradual one, and a plot of the reciprocal of the nitrogen yield *vs.* the reciprocal of the N_2O concentration does not give a straight line. The first is almost certainly

Publication Date: January 1, 1968 | doi: 10.1021/ba-1968-0082.ch030

Reaction 10. Warman (*18*) has shown that Reaction 13 must be included to account for the yields observed in the gas-phase radiolysis of alkane–N_2O mixtures, but this would leave no O^- to give extra C_6H_{11} by Reactions 11 and 12.

$$O^- + N_2O \rightarrow N_2O + O_2^- \quad (13)$$

Although there is no obvious contender for the reaction that gives extra nitrogen and reduces the hydrogen yield further, such a reaction would reduce the electron yield in C_6H_{12} as measured by $G(N_2)$. Although from Figure 5 there appears to be a dose rate effect on the formation of nitrogen, the nitrogen yields obtained by other workers (*13*, *14*, *15*) are intermediate between those of Sagert and Blair (*12*) and the Febetron values.

The cyclohexene and bicyclohexyl yields in the Febetron irradiations at N_2O concentrations above 0.1*M* are $\sim$ 3.5 and $\sim$ 1.9, respectively. Since the unimolecular yield is decreased by N_2O, the extra yield of cyclohexene that must presumably come from Reaction 8 ($H + C_6H_{11} \rightarrow C_6H_{10} + H_2$), is $\sim$ 0.8. Since this is the same as the extra yield in pure cyclohexane it appears that the yield of thermal hydrogen atoms is not affected by adding N_2O.

Cyclohexane and SF_6. Sulfur hexafluoride reacts rapidly with electrons, and its effect on the hydrogen, cyclohexene, and bicyclohexyl yields has been explained (*12*) by the replacement of Reaction 1b by Reactions 14 and 15.

$$e^- + SF_6 \rightarrow SF_6^- \quad (14)$$

$$SF_6^- + C_6H_{12}^+ \rightarrow \text{not } C_6H_{12}^* \quad (15)$$

As with N_2O the shapes of yield *vs.* concentration curves show little or no dependence on dose rate. As stated this is to be expected if these reactions occur in or near spurs. Again the difference between the cyclohexene yield and the bicyclohexyl yields is greater than that caused by unimolecular dissociation, implying that SF_6 like N_2O does not affect the yield of thermal hydrogen atoms.

General Comments

An increase in the ratio of cyclohexene to bicyclohexyl, but no decrease in hydrogen yields, has been observed in the radiolysis of cyclohexane with high LET radiation (*1*). As our results imply that a reduction in the hydrogen yield should accompany an increase in this ratio, the constant value of the hydrogen yield is presumably caused by other reactions occurring in the tracks that produce hydrogen.

Publication Date: January 1, 1968 | doi: 10.1021/ba-1968-0082.ch030

The effect of benzene in the Febetron irradiations is markedly different from that of the electron scavengers. The difference between the cyclohexene and bicyclohexyl yields is much smaller and implies that benzene decreases the yield of thermal hydrogen atoms. Thus, benzene is not acting as an electron scavenger as has been suggested (*17*).

Acknowledgment

It is a pleasure to acknowledge the many helpful discussions we have had with N. H. Sagert.

Literature Cited

(1) Burns, W. G., Barker, R., *Progr. Reaction Kinetics* **3,** 303 (1965).
(2) Charbonnier, F. M., private communication.
(3) Cramer, W. A., *J. Phys. Chem.* **71,** 1171 (1967).
(4) Dewhurst, H. A., *J. Phys. Chem.* **63,** 813 (1959).
(5) Dyne, P. J., Jenkinson, W. M., *Can. J. Chem.* **38,** 539 (1960).
(6) Dyne, P. J., Stone, J. A., *Can. J. Chem.* **39,** 238 (1961).
(7) Dyne, P. J., Denhartog, J., Smith, D. R., *Discussions Faraday Soc.* **36,** 135 (1964).
(8) Dyne, P. J., *Can. J. Chem.* **43,** 1080 (1965).
(9) Hardwick, T. J., *J. Phys. Chem.* **65,** 101 (1961).
(10) Klots, C. E., Johnsen, R. H., *Can. J. Chem.* **41,** 2702 (1963).
(11) McCrumb, J. L., Schuler, R. H., *J. Phys. Chem.* **71,** 1953 (1967).
(12) Sagert, N. H., Blair, A. S., *Can. J. Chem.* **45,** 1351 (1967).
(13) Sato, S., Yugeta, R., Shinsaka, K., Terao, T., *Bull. Chem. Soc. Japan* **39,** 156 (1966).
(14) Scholes, G., Simic, M., *Nature* **202,** 895 (1964).
(15) Sherman, W. V., *J. Chem. Soc.* **1966,** A599.
(16) Stone, J. A., *Can. J. Chem.* **42,** 2872 (1964).
(17) Stone, J. A., Dyne, P. J., *Radiation Res.* **3,** 353 (1962).
(18) Warman, J. M., *Nature* **213,** 381 (1967).
(19) Willis, C., Miller, O. A., Rothwell, A. E., Boyd, A. W., *Radiation Res.*, in press.

RECEIVED January 2, 1968. Issued as AECL-3115.

Radiolysis of Fluorocarbons

Valence Tautomerization

J. FAJER and D. R. MACKENZIE

Brookhaven National Laboratory, Upton, N. Y. 11973

Publication Date: January 1, 1968 | doi: 10.1021/ba-1968-0082.ch031

Fluorocarbon compounds were radiolyzed to establish the existence and assess the role of valence tautomers in radiation chemistry. Dewar-octafluorotoluene and -decafluoroxylene have been isolated and identified as products of the photolysis and radiolysis of their respective aromatic parent in condensed phase. Dewar hexafluorobenzene was irradiated to 10 Mrad doses and found to revert to its Kekulé isomer with a G-value of ≈ 10, to polymerize with G ≈ 20, and, in addition, to give rise to a new isomer. The concept of an "energy sink" is introduced whereby part of the energy absorbed by an aromatic system is stored in the form of interconvertible valence isomers which react further to yield polymers or decay to the ground state.

Photochemical valence isomerization has, for some time now, been observed or inferred for benzene and many of its derivatives (*12*). The analogous radiolytic reaction was recently established when we isolated a Dewar isomer, hexafluorobicyclo [2.2.0] hexa-2,5-diene, as a product of the γ radiolysis of hexafluorobenzene (*4*).

The following structures are discussed in the text:

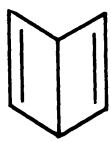

Dewar

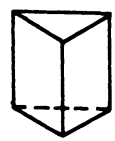

Prismane

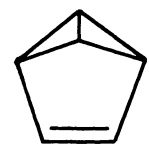

Benzvalene

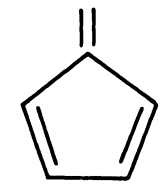

Fulvene

An increasing body of evidence suggests that many processes and intermediates observed in photochemistry are also detected, under appropriate conditions, in radiation chemistry (*6*, *7*). Our results with

In Radiation Chemistry; Hart, E.;
Advances in Chemistry; American Chemical Society: Washington, DC, 1968.

C_6F_6 combined with the many instances of valence photoisomerization led us to suggest that tautomerization may well occur frequently, and play a significant role in the radiolysis of aromatic compounds (*4*). We were particularly intrigued by the question of whether valence isomerization may not be considered an "energy sink," *i.e.*, a pathway for storing the energy from excited states and the recombinations of radicals and ions in the form of relatively long-lived species. The tautomers could in turn either revert back to the ground state, an explanation for the "protective effect" of aromatic systems, or undergo further reaction to yield, for example, the polymeric compounds reported in the radiolysis of benzene. We present here additional evidence of valence isomerization found in the γ radiolyses of octafluorotoluene and *o*-decafluoroxylene and report on the radiolytic behavior of Dewar hexafluorobenzene.

Publication Date: January 1, 1968 | doi: 10.1021/ba-1968-0082.ch031

Experimental

We define **D** as Dewar, **B** as hexafluorobenzene, **T** as octafluorotoluene, and **X** as *o*-decafluoroxylene.

B, T, and **X** were obtained from Imperial Smelting or Aldrich Chemical. The compounds were purified by preparative scale gas chromatography (GLC), after which they showed only a single peak on diisodecyl phthalate columns, and were stored *in vacuo* over molecular sieves. **B** was further purified by contact with a sodium mirror. Perfluorodimethyl cyclobutane, E. I. duPont, was used without further purification. **DB** was prepared photochemically and isolated immediately before use for γ irradiations.

Samples were handled on a mercury-free vacuum system and were degassed to better than 10^{-5} torr except as noted. Photolyses were carried out in quartz vessels with an unfiltered General Electric AH6 mercury arc. Radiolyses were performed in ^{60}Co sources at dose rates of 6 and 12×10^6 rads/hr. (Fricke dosimeter) in borosilicate ampoules. Small samples of **DB** ($\approx$ 30 μliters) were irradiated in thin-walled NMR tubes.

Products were analyzed by GLC on diisodecyl phthalate columns operated at 25°C. for 10 minutes, and programmed at 10°C./min. thereafter. Effluent fractions were trapped at 77°K. and characterized further by ultraviolet, infrared, and mass spectroscopy. Quantitative analyses of **B** and **DB,** after the radiolysis of **DB,** were based on calibrations with synthetic mixtures. Polymer yields (solids of molecular weight comparable to or greater than that of perfluorobiphenyl) were determined as previously described (*11*). ^{19}F NMR spectra were run in CCl_4 solution with CCl_3F as internal reference.

Results

Photolysis of liquid (or gaseous) **T** yields a product, isolated by chromatography, of molecular weight 236 (mass spectrum) and therefore isomeric with **T.** After heating to 100°C., this compound reverts back to **T** as established by infrared and mass spectra. The isomer shows

infrared absorption bands at 1762 and 1725 cm.$^{-1}$. These properties are consistent with those of the mixture of **DT** (methyl group at the bridgehead or on the double bond) obtained by gas phase photolysis of **T** at 2537 A. by Camaggi *et al.* (*3*).

Photolysis of liquid or gaseous **X** yields a product isolated as above. Mass spectrometry shows a parent peak of 286 (C_8F_{10}) and the infrared spectrum, bands at 1730 and 1770 cm.$^{-1}$ attributable (*3*) to —FC=C(CF_3)— and —FC=CF— respectively. When heated at 120°C. for several hours, this new isomer converts back to **X** as established by infrared and mass spectra of authentic *o*-perfluoroxylene. Some possible structures of this isomer can readily be excluded. Its GLC retention time is much shorter than any of the following aromatic compounds: perfluoroethylbenzene, perfluoro-*m*- or *p*-xylene. Prismanes would not show the infrared double bond absorption observed. The isomer does not absorb above 280 n.m. in the ultraviolet. A conjugated diene structure such as fulvene, therefore, appears unlikely. In addition, isomerization to fulvene and its derivatives is not reversible in the case of hydrocarbons (*1*). Benzvalene, Dewar, or some unknown isomer thus remain as the alternatives. The ^{19}F NMR spectrum of the tautomer shows absorption signals at 64.6(a), 67.6(b), 83.8(f), 117.9(c or d), 121.9(d or c), and 192.9(e) p.p.m. (The letters in parentheses are the assignments; the chemical shifts are referred to CCl_3F internal standard.) The resonances at 117.9 and 121.9 p.p.m. are close to those of the olefinic fluorines in **DB** reported by Camaggi (*3*) and Haller (*8*): 122.8 and 121.2 p.p.m., respectively; the 192.9 is close to their bridgehead fluorines, 191.0 or 190.1 p.p.m. The fluorine at 83.8 p.p.m. (f) is downfield from the other olefinic fluorines presumably because of the influence of the CF_3 adjacent to it. (Allylic coupling between (a) and (f) results in the splitting of the former and the broadening of the latter.) All the above data are consistent with the Dewar structure shown:

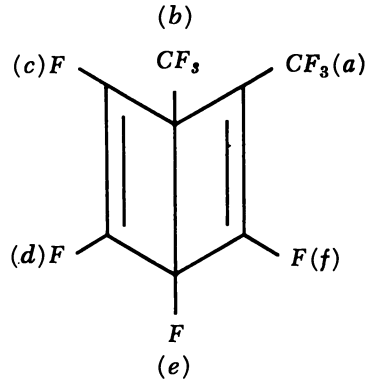

Publication Date: January 1, 1968 | doi: 10.1021/ba-1968-0082.ch031

Photolysis of 10% **B** in perfluorodimethylcyclobutane solution, or of neat **B**, yields a product identified on the basis of its physical properties as **DB**.

Radiolysis of liquid **T** and **X**, at total doses of 10^8 to 10^9 rads, yields **DT** and **DX**, respectively. (**DX** is also a detectable product of the irradiation of liquid **X** at a partial pressure of 100 mm. of O_2.) The isomers were positively identified by verification of their GLC retention times, infrared, and mass spectra.

Radiolysis of liquid **DB** results mainly in isomerization back to **B**, $G_B \approx 10$, and in polymerization, $G_{polymer} \approx 20$ at doses of 10^7 rads. These irradiations also give rise to a new GLC product, **PB**, of mass 186 which, when recycled through a GLC column, yields **DB** and **B**. This new compound is clearly isomeric with C_6F_6. We assume that **PB** is hexafluoroprismane by analogy with the behavior of hexamethylprismane (*10, 12*) which similarly converts to its Dewar and Kekulé isomers. At this writing, however, we have been unable to isolate **PB** without inducing decomposition. Other column packings are currently being attempted. (Warning: The mixture of **PB, DB,** and **B** is shock sensitive: degassed samples frequently exploded when suddenly vented.)

Publication Date: January 1, 1968 | doi: 10.1021/ba-1968-0082.ch031

Discussion

(a) **Photolysis.** The photosynthesis of **DT** and **DX** was, of course, a necessary prerequisite to identification of these compounds in radiolysis. We encountered no difficulties in the preparation of **DX, DT,** or **DB** in condensed phase, although Bryce-Smith *et al.* (*2*) did not find any isomers in the photolysis of neat **B**. Haller (*9*) and Bryce-Smith (*2*) were also unable to detect tautomers in the photolysis of **B** in hydrocarbon solution. They showed conclusively that the reactions in cyclohexane result in addition products of **B** with the solvent and proceed *via* a free radical mechanism. It is clear from the present work in perfluorodimethylcyclobutane, where **DB** is found, that, in fluorocarbon solution, the combination of strong C—F bond and weak F—F bond prevent the free radical reaction. For the systems considered here, Reaction 1

$$C_6F_5—F + C_6H_{11}—H \rightarrow C_6F_5—C_6H_{11} + HF \qquad (1)$$

is more exothermic than Reaction 2

$$C_6F_5—F + C_6F_{11}—F \rightarrow C_6F_5—C_6F_{11} + F_2 \qquad (2)$$

by over 100 kcal. and competes effectively with photoisomerization. In the photolysis of neat **B**, hydrogen containing impurities such as water, which are removed in our work by the sodium treatment, can similarly explain the discrepancy between our own and the previous results (*2*).

(b) **Radiolysis.** We have now established that valence isomerization occurs in the radiation chemistry not only of perfluorobenzene but of perfluoro-toluene and -xylene as well. These could be formed, as we suggested (*4*) for Dewar C_6F_6, by direct excitation, or ion-electron recombination followed by collisional deactivation, or even by radical-fluorine recombination. (Triplet state intermediates are not likely in view of the tautomers observed in the presence of oxygen both in photolysis (*9*) and radiolysis.) The question again arises whether similar tautomerization takes place in hydrocarbon radiolysis. Given the instability (*1*, *13*, *14*) of the isomers of C_6H_6 which are known, it appears unlikely that these would have been detected by the routine GLC methods used to analyze radiolysis products. We see no immediate reason, however, why radiation-induced isomerization should not occur in hydrocarbons. Radiolysis of alkyl-substituted benzenes, whose tautomers (*12*) are considerably more stable than those of C_6H_6, may prove more fruitful in the actual isolation of hydrocarbon isomers.

Finally, we consider the role of valence isomers when these do occur. The two oversimplified pathways we considered—*i.e.*, the isomer is very reactive and leads to other products and in addition stores energy until it decays back to the Kekulé ground state—clearly hold for **DB** in liquid phase. (This behavior is quite consistent with the high percentage of $C_6F_6^+$ parent ion found (*5*) in the 70-e.v. mass spectrum of **DB** on the one hand, and with the 1849 A. photopolymerization (*8*) of **DB** on the other.)

The concept of an energy sink is further reinforced by the additional isomer (**PB**) which we have detected. It means, in fact, that an aromatic compound, following excitation, can not only dissipate its acquired energy into the nonlocalized π system but in addition can decay into discrete, metastable isomeric states which are also interconvertible. These in turn can further react to form polymeric product or return to the ground state.

Acknowledgment

We are indebted to L. Kaplan and K. E. Wilzbach, Argonne National Laboratory, who kindly obtained and interpreted the ^{19}F NMR spectra. We also thank I. Haller, IBM, for communication of his results prior to publication and R. Smol for his assistance.

Literature Cited

(1) Angus, H. J. F., Blair, J. M., Bryce-Smith, D., *J. Chem. Soc.* **1960**, 2003.
(2) Bryce-Smith, D., Connett, B. E., Gilbert, A., *Chem. Ind. (London)* **1966**, 855.
(3) Camaggi, G., Gozzo, F., Cevidalli, G., *Chem. Commun.* **1966**, 313.

(4) Fajer, J., MacKenzie, D. R., *J. Phys. Chem.* **71,** 784 (1967).
(5) Fajer, J., Forrest, J., unpublished results.
(6) Fischer, E., Lehmann, H. P., Stein, G., *J. Chem. Phys.* **45,** 3905 (1966).
(7) Fischer, E., Fischer, G., Stein, G., *J. Chem. Phys.* **46,** 3680 (1967).
(8) Haller, I., *J. Am. Chem. Soc.* **88,** 2070 (1966).
(9) Haller, I., *J. Chem. Phys.* **47,** 1117 (1967).
(10) Lemal, D. M., Lokensgard, J. P., *J. Am. Chem. Soc.* **88,** 5934 (1966).
(11) MacKenzie, D. R., Bloch, F. W., Wiswall, R. H., *J. Phys. Chem.* **69,** 2526 (1965).
(12) Schäfer, W., Hellman, H., *Angew. Chem., Intern. Ed.*, **6,** 518 (1967).
(13) van Tamelen, E. E., Pappas, S. P., *J. Am. Chem. Soc.* **85,** 3297 (1963).
(14) Wilzbach, K. E., Ritscher, J. S., Kaplan, L., *J. Am. Chem. Soc.* **89,** 1031 (1967).

RECEIVED December 26, 1967. This work was performed under the auspices of the U. S. Atomic Energy Commission.

Publication Date: January 1, 1968 | doi: 10.1021/ba-1968-0082.ch031

A Review of Radiation-Chemical Synthetic Reactions with Alkyl Halides

I. V. VERESHCHINSKY, L. D. LEBEDEV, V. Y. MIRETSKY, and A. T. PODKHALYUZIN

Karpov Institute, Moscow, USSR

Publication Date: January 1, 1968 | doi: 10.1021/ba-1968-0082.ch032

The radiation-chemical synthesis of dibutyltin dibromide from n-butyl bromide and metallic tin is characterized by an induction period, a considerable radiation-chemical yield, a square-root dependence on the dose rate and is most likely a chain process. The radiation-chemical synthesis of decachloropentane from 1,1,1,5-tetrachloropentane and molecular chlorine is a multistage chain process. Optimum conditions prevail when chlorination is conducted at moderate temperatures and low dose rates. Cyanogen chloride, synthesized from tetrachloroethylene or carbon tetrachloride and free nitrogen, is a product of the radiation-chemical fixation of nitrogen.

No systematic study has been made thus far of the controlled radiation-chemical synthesis of organic compounds with the purpose of obtaining an appreciable radiation-chemical yield.

An attempt has been made here to investigate certain reactions of radiation-chemical syntheses in the condensed phase (*10*). One component in all our binary reaction systems was the RHal (alkyl halide), while the other was represented by a free element (tin, nitrogen, or chlorine) of the IVth, Vth or the VIIth group of the periodic chart. As expected, the nature of the latter component most strongly influenced the character and the parameters of the radiation processes examined.

RHal + Sn Reaction

Radiation-Chemical Synthesis of Dibutyltin dibromide. The pilot plant used for the radiation-chemical synthesis of dibutyltin dibromide (DBTDB) has been described (*7*). The materials used were *n*-butyl

In Radiation Chemistry; Hart, E.;
Advances in Chemistry; American Chemical Society: Washington, DC, 1968.

bromide (99% pure) and tin powder (99.5% tin) with a prevailing grain size ranging from 10 to 40 microns. After removing organic admixtures, tin was treated with diluted hydrochloric acid to dissolve the oxide surface film. As a result the tin powder surface area increased from 0.7 to 2.1 sq. meters/gram. The surface of tin which had not entered the reaction continued to increase and exceeded 20 sq. meters/gram as the reaction progressed.

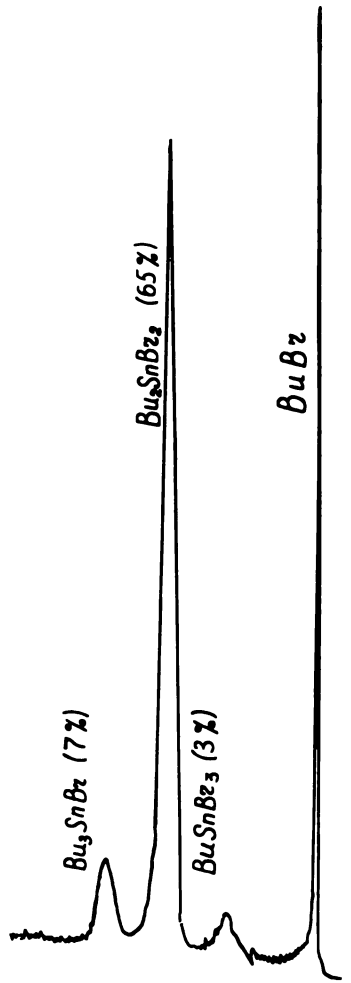

Figure 1. Chromatogram of reaction mixture after separating the solid phase. Conditions: column, 2 meters; 2% silicone oil on Chromosorb W, 40-60 mesh; hydrogen feed rate, 30 ml./min.; temperature, 180°C.; detector, katharometer

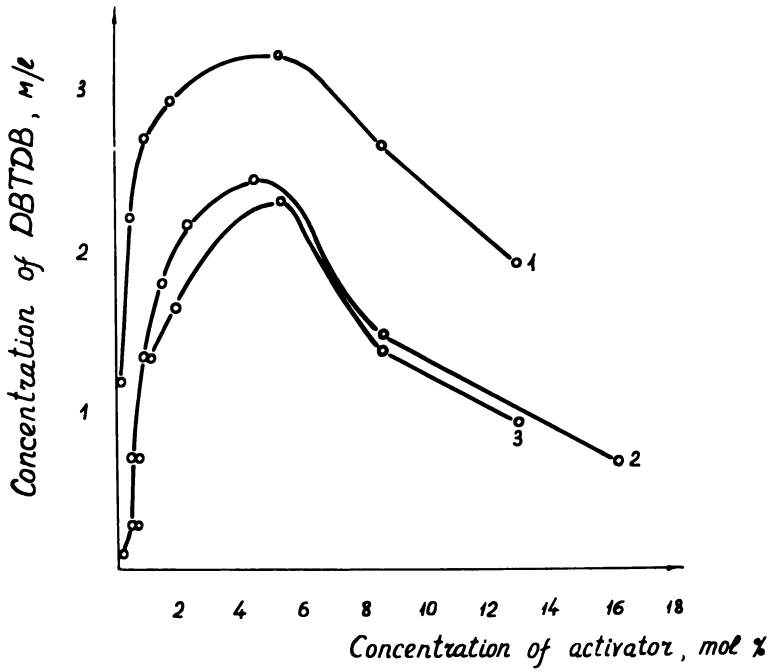

Figure 2. Influence of activator concentration on DBTDB yield

(1): n-C_4H_9OH; absorbed dose, 1.1 Mrads
(2): n-C_4H_9OH; absorbed dose, 0.55 Mrad
(3): H_2O; absorbed dose, 1.1 Mrads

Experiments were conducted at 85°–90°C., atmospheric pressure, and with intensive mechanical mixing. The average absorbed dose rate was 100 rads per second.

The *n*-butyl bromide–tin reaction under gamma radiation yields DBTDB as the main product.

$$2C_4H_9Br + Sn \rightarrow (C_4H_9)_2SnBr_2$$

Small amounts of tributyltin bromide and butyltin tribromide also form (Figure 1).

A characteristic peculiarity of the DBTDB radiation-chemical synthesis is the induction period (*1, 2, 3*). Many different methods have been used, and optimum conditions for the reaction have been found, which practically eliminates the induction period. One method was the above-mentioned treatment of tin powder. Another highly effective method was the introduction of diverse activators like water or *n*-butyl alcohol. Figure 2 shows the DBTDB content curves in relation to the amount of activator.

The action of water and alcohol is similar. While in the absence of activators, at a dose below 0.7 Mrad the reaction is very slow, the DBTDB content reaches 60%, at the same dose, when the activator is introduced.

The rate of DBTDB production depends on the ratio of the initial components of the reaction—*n*-butyl bromide and tin (Figure 3).

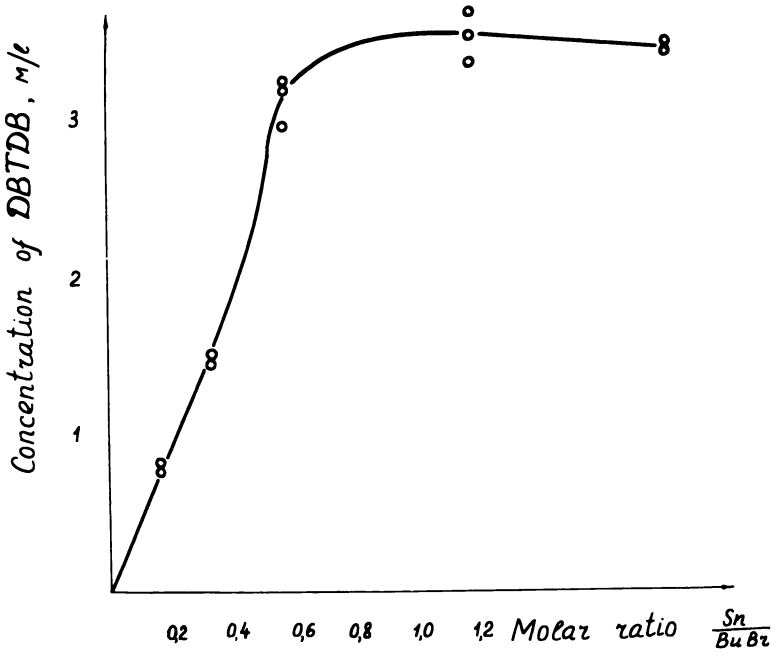

Figure 3. Influence of reaction components' ratio on DBTDB

The study of the parameters of the reaction, which proceeded practically without an induction period, revealed basic macrokinetic regularities. Temperature proved to be an important factor in the process. The effective activation energy was determined from the kinetic curves of DBTDB production in the temperature range 20°–95°C., shown in Figure 4. The activation energy is 6.2 kcal./mole and is noticeably less than the value of 30.8 kcal./mole given by Fentiman *et al.* (2) for the same reaction. This value, which is too high, in our opinion, possibly results from conducting the experiments in ampoules without effective mixing.

The dose rate directly affects the reaction between metallic tin and *n*-butyl bromide. Figure 5 shows the kinetic curves of DBTDB buildup

Publication Date: January 1, 1968 | doi: 10.1021/ba-1968-0082.ch032

at doses differing by half-order: 175, 16, and 2.5 rads/sec., and a high conversion of 90, 60, and 38%, respectively. Beyond the induction period, which occurs at a small dose, the DBTDB production rate is proportional to the square root of dose rate.

DBTDB production apparently proceeds by a chain mechanism. The following factors tend to confirm this:

(a) The radiation-chemical yield reaches 10^3–10^4 molecules/100 e.v. at a high conversion.

(b) The reaction system responds specifically to the introduction of activators.

(c) The reaction rate is related to the square root of the dose rate.

The reaction stops as soon as radiation is terminated and recommences at the previous rate when a radiation source is again introduced.

An additional argument in support of the chain mechanism is the influence of inhibitors upon the rate of DBTDB production. Specific

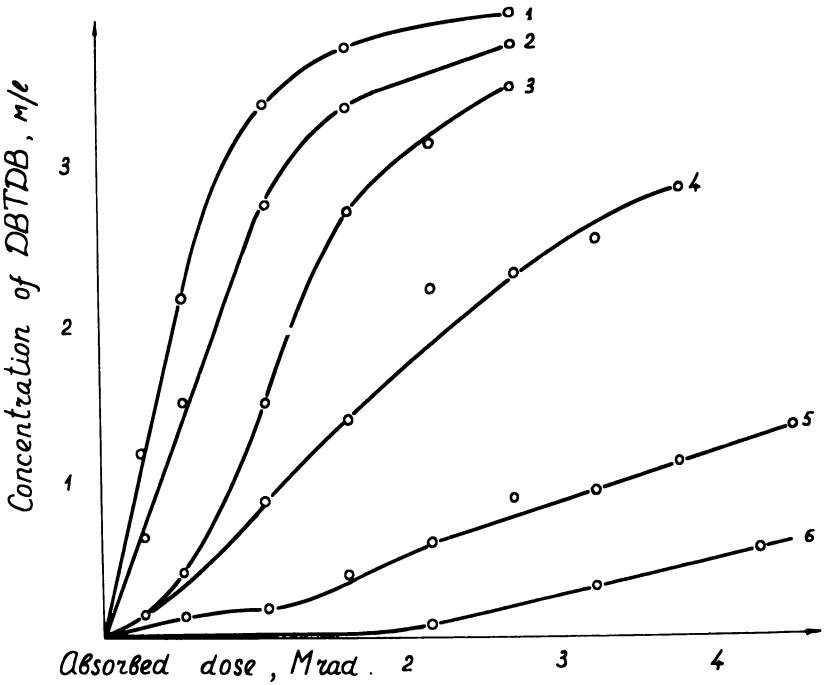

Figure 4. DBTDB production as a function of radiation dose and temperature

(1): 95°C.
(2): 85°C.
(3): 75°C.
(4): 60°C.
(5): 40°C.
(6): 20°C.

experiments have shown that the presence of oxygen in the reaction system or the introduction of such acceptors as benzoquinone, hydroquinone, or *m*-dinitrobenzene at concentrations of 10^{-4}–$10^{-2}M$ inhibit the reaction noticeably.

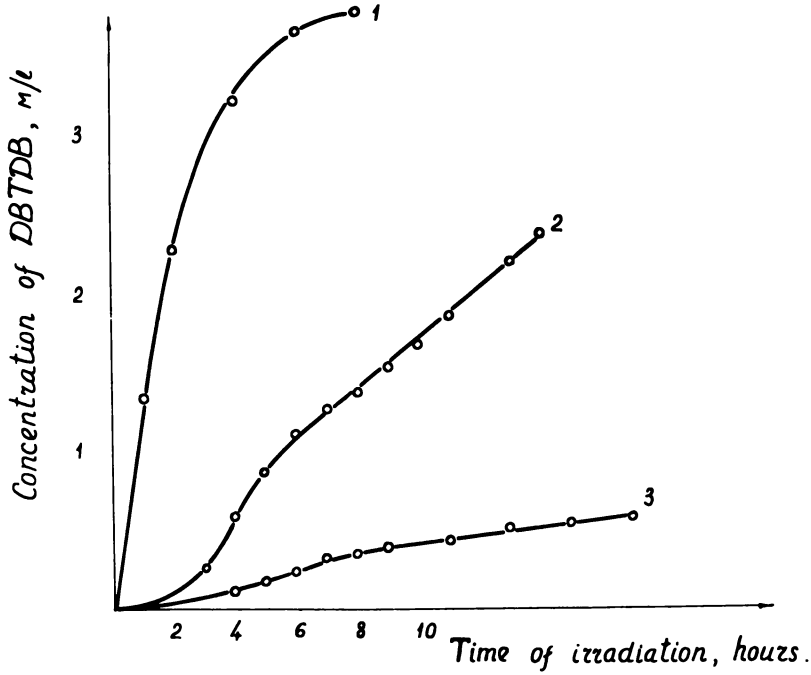

Figure 5. DBTDB production as a function of radiation dose and dose rate

(1): 75 rads/sec.
(2): 16
(3): 2.5

RHal + Cl_2 Reaction

Radiation-Chemical Synthesis of Decachloropentane. The installation used for the radiation-chemical synthesis of decachloropentane has been described (*4*). The initial substance was 1,1,1,5-tetrachloropentane (TClP) at least 99.5% pure, with the following constants:

$$d_4^{20} = 1.3585 \qquad {}^{20}n_D = 1.4880.$$

A 50-gram batch of TClP was placed in the reaction vessel. The chlorine discharge rate was 3.9–4.1 liters/hour. Samples were taken during chlorination for subsequent gas chromatographic and elemental

Publication Date: January 1, 1968 | doi: 10.1021/ba-1968-0082.ch032

analysis. A modification of Schoniger's method was used to determine the total chlorine content in the samples (5). Each sample was subjected to chromatography. The samples which differed from previous ones by the appearance of a new peak with a longer retention time were later analyzed by mass spectrometry. This method of gas chromatography and mass spectrometry for analyzing the reaction mixture has allowed us to determine the number of atoms of chlorine in a molecule of synthesized polychloropentane and to identify penta-, hexa-, hepta-, octa-, nona-, and decachloropentanes. The chlorination of TClP may be represented as a series of consecutive reactions of the following type.

$$C_5H_nCl_{12-n} + Cl_2 \rightarrow C_5H_{n-1}Cl_{12-n+1} + HCl$$

It should be noted that appreciable amounts of isomers are produced at every stage—*i.e.*, the process, strictly speaking, consists of a series of parallel-consecutive reactions, with differing production rates for each isomer. In determining the total rate of isomer production, we regard the process of decachloropentane production as consisting of six irreversible consecutive reactions.

$$C_5H_8Cl_4 \xrightarrow{k_4} C_5H_7Cl_5 \xrightarrow{k_5} C_5H_6Cl_6 \xrightarrow{k_6} C_5H_5Cl_7 \xrightarrow{k_7}$$

$$C_5H_4Cl_8 \xrightarrow{k_8} C_5H_3Cl_9 \xrightarrow{k_9} C_5H_2Cl_{10}$$

While the values of the rate constants of the radiation chlorination of tetra- and pentachloropentanes are comparable with those in thermal experiments, the rate constants of the radiation chlorination of hexa-, hepta-, octa- and nonachloropentanes are greater by one order of magnitude or more (Figure 6).

The introduction of two or three atoms of chlorine occurs in the diffusion region does not require radiation and proceeds with relative ease. When every atom of carbon in the molecule of polychloropentane is bound to at least one atom of chlorine, the induction effect in the molecule surpasses the effect of polarization, and further entry of chlorine atoms in the molecule is slowed; in addition, steric factors enter into play. The rate of chlorine solubility in the reaction mixture exceeds the rate of subsequent chlorination reactions, and the process enters the kinetic region.

The influence of temperature on the rate of TClP chlorination and on the composition of the reaction mixture is determined considerably by the decrease in chlorine solubility in polychloropentane mixtures which occurs with increased temperature. Thus, for the chlorination of hexa- and heptachloropentanes the relative changes in the rate constants and chlorine solubility practically coincide (Table I).

Publication Date: January 1, 1968 | doi: 10.1021/ba-1968-0082.ch032

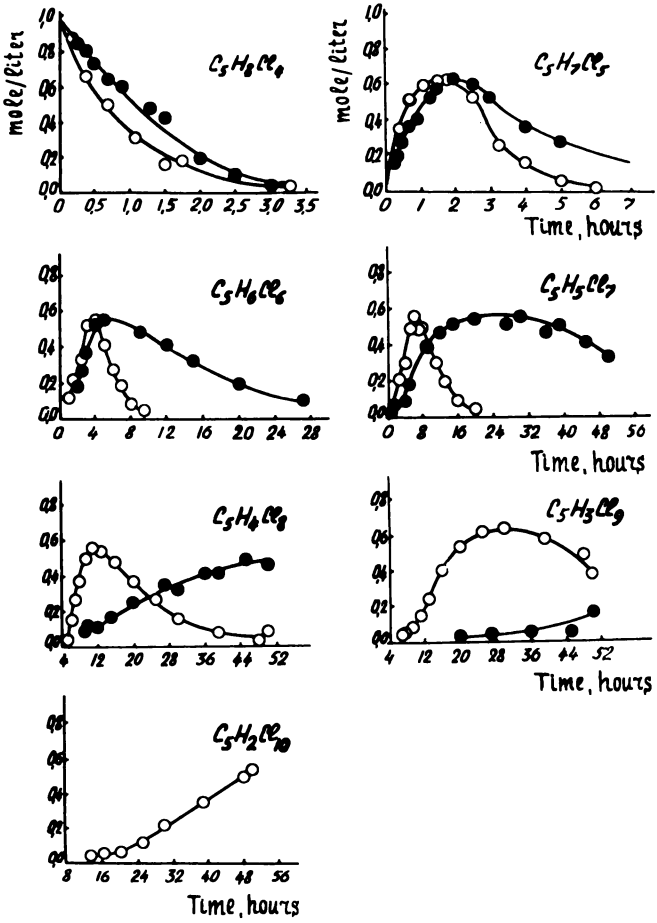

Figure 6. Dependence of polychloropentanes concentration on chlorination time at 120°C.

○ *Radiation experiments; dose rate, 33 Krads/hr.*
● *Thermal experiments without radiation*

Table I. Influence of Temperature on Chlorination

Chlorination Temperature, T, °C.	*Ratio of Chlorine Solubility at 120°C. to Solubility at T, °C.*	*Ratio of Chlorination Rate Constant at 120°C. to T, °C.*	
		Hexachloropentane	*Heptachloropentane*
160	1.9	1.9	2.0
180	2.5	2.4	2.4
200	3.3	3.0	3.5

Of particular interest is the influence of temperature on the radiation synthesis of highly chlorinated polychloropentanes—decachloropentane and nonachloropentane.

The decrease in chlorine concentration in the solution with an increase in temperature and the related transition of the reaction to the diffusion phase leads to a local deficiency in chlorine. As the temperature changes from 100° to 200°C., the content of decachloropentane drops greatly (Table II). With an increase in temperature, the content of the degradation and dehydrochlorination products continuously increase.

Table II. Dependence of Polychloropentane Content on Radiation Chlorination Temperature

Chlorination Temperature, °C.	100	120	160	180	200
Absorbed dose, Krad	16.5	16.5	16.5	13.2	0.92
$C_5H_2Cl_{10}$, %	70	56	24	7	3
$C_5H_3Cl_9$, %	25	42	53	59	58

The fact that we have for the first time synthesized and identified decachloropentane most likely results from conducting the radiation chlorination under mild conditions with a relatively low temperature (*6*).

The fact that the initial stages of chlorination occur in the diffusion region complicates the investigation of the dose rate dependence of the radiation chlorination rate (*7*). During the transition to subsequent stages of chlorination, which proceed to a considerable extent in the kinetic region, the dose rate dependence of the chlorination rate is nearly square root (Figure 7).

The radiation-chemical yield (G) at every stage of the process directly depends on the number of atoms of chlorine in a molecule of polychloropentane (Figure 8). Generally, the G value decreases with increasing dose rate and increasing chlorine content in a molecule.

RHal + N_2 Reaction

Radiation-Chemical Fixation of Molecular Nitrogen and Synthesis of Cyanogen Chloride. The radiation-chemical fixation of molecular nitrogen by hydrocarbons takes place in the liquid phase with relatively high radiation-chemical yields ($G \sim 1$), but it leads to the formation of a broad set of nitrogen containing products, which are difficult to identify (*8*, *10*). The transition to perchlorohydrocarbons considerably restricts the possible products of radiolytic transformations.

Experiments with solutions of molecular nitrogen in carbon tetrachloride or in tetrachlorethylene were conducted under static conditions with different nitrogen pressure above the solution. The dependence of

Publication Date: January 1, 1968 | doi: 10.1021/ba-1968-0082.ch032

the radiation-chemical yield of fixed nitrogen on pressure, at the same absorbed doses, was linear (Figure 9).

Cyanogen chloride was identified among the products of radiation synthesis. The quantitative determination of CN ions was made photocolorimetrically by the pyridine barbituate method. Chlorine concentration was determined in the same dose range.

The infrared spectra of the radiolysis products of the $C_2Cl_4 + N_2$ system showed a band at 2260 $cm.^{-1}$, characteristic of the CN group which disappeared when the radiolysis products were treated with hydrochloric acid. Most likely, ClCN condensed to cyanuric chloride $C_3N_3Cl_3$.

The concentration of ClCN increases with increasing temperature. The initial slope of the curves shown in Figure 10 allows one to estimate the values of the radiation-chemical yield of the radiation transformation products:

	G(ClCN)	$G(Cl_2)$
$C_2Cl_4 + N_2$	0.12	2.5
$CCl_4 + N_2$	0.12	2.5

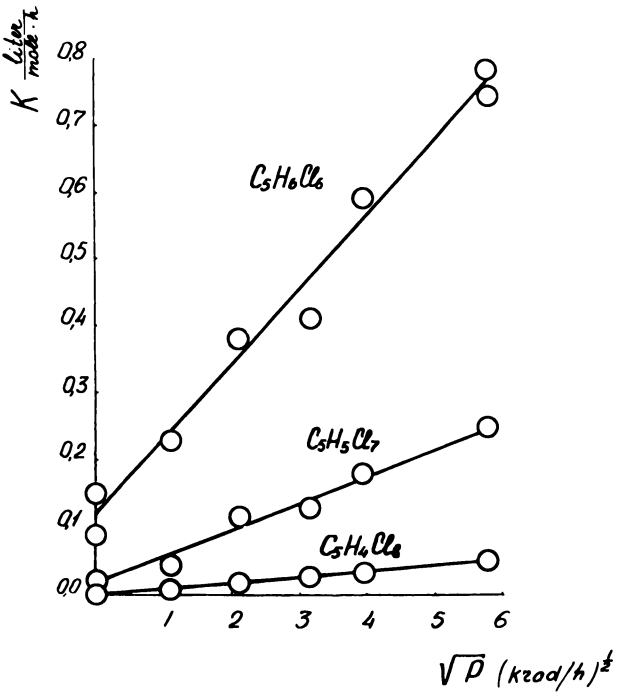

Figure 7. Dependence of polychloropentane chlorination rate constant on dose rate

Publication Date: January 1, 1968 | doi: 10.1021/ba-1968-0082.ch032

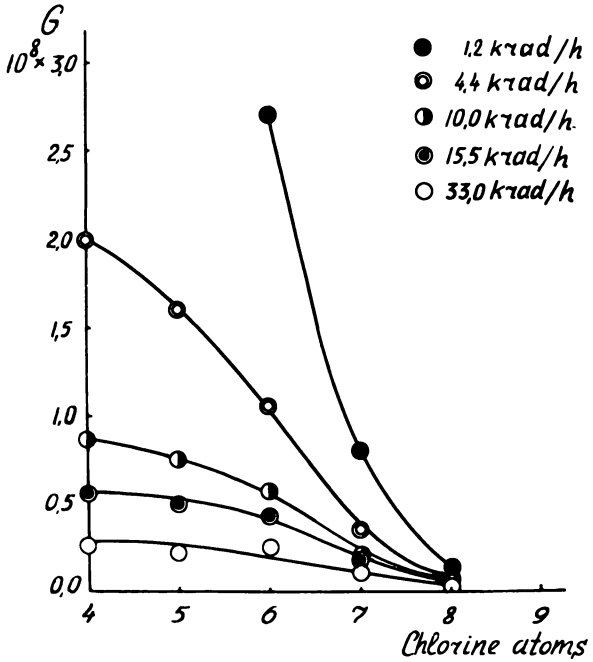

Figure 8. Dependence of radiation-chemical yield of chlorination on the number of chlorine atoms in a molecule of the initial polychloropentane at different dose rates

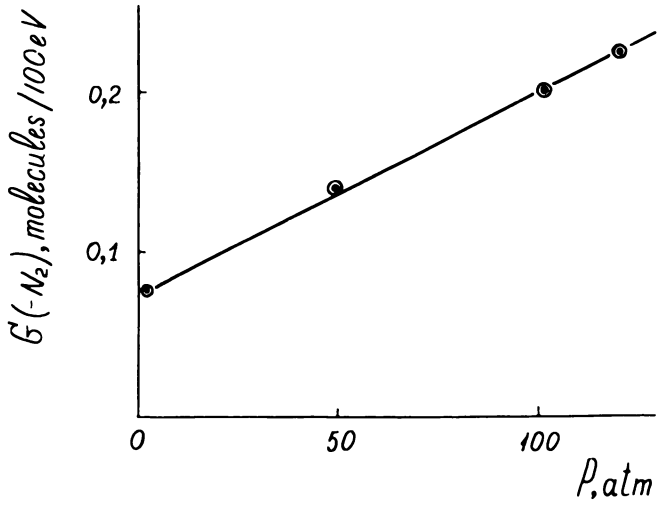

Figure 9. Dependence of radiation-chemical yield of nitrogen fixation in the N_2–C_2Cl_4 system on nitrogen pressure

Publication Date: January 1, 1968 | doi: 10.1021/ba-1968-0082.ch032

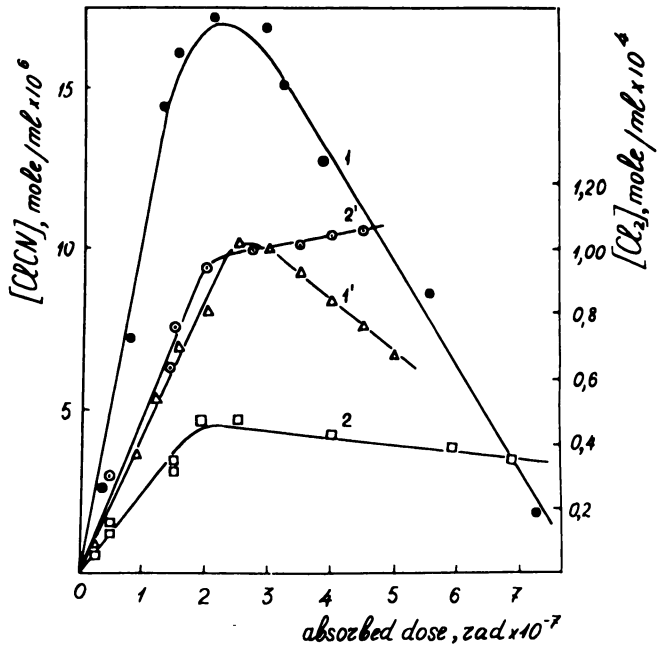

Figure 10. ClCN production (Curves 1 and 2) and chlorine production (Curves 1′ and 2′) as a function of absorbed dose during the γ-radiolysis of nitrogen solutions in tetrachloroethylene (Curves 1 and 1′) and in carbon tetrachloride (Curves 2 and 2′) at 30°C. Nitrogen pressure above solution was 120 atm.

When a dose of 25 Mrads is absorbed, the ClCN accumulation decreases. Further increase in the general concentration of fixed nitrogen proves the existence of reactions which lead to the formation of other nitrogen-containing compounds.

The similarity of the ClCN and Cl_2 production curves might be associated with the simultaneous formation from hydrocarbon chloride of atomic chlorine and radical products which interact with nitrogen.

Summary

The radiation-chemical syntheses described have been studied to the extent of determining the basic macrokinetic regularities. Therefore, it is impossible to offer argumented suppositions regarding the mechanism of the majority of elementary reactions underlying these processes.

A characteristic feature of the radiation-chemical synthesis is the decrease in the role of thermal reactions, which lead to the formation of several degradation products. This creates favorable conditions for using these processes to synthesize compounds.

Literature Cited

(1) Abramova, L. V., Vereshchinsky, I. D., Koshechkov, T. A., Miretsky, V. Y., Pozdeyev, V. V., Ryabukhin, I S., Sheverdina, N. I., "Industrial Uses of Large Radiation Sources," Vol. I, p. 83, International Atomic Energy Agency, Vienna, 1963.
(2) Fentiman, A. F., Wyant, R. E., Jeffrey, D. A., Kircher, J. E., *J. Organometal. Chem.* **4,** 302 (1965).
(3) Fentiman, A. P., Wyant, R. E., McFarling, J. L., Kircher, J. E., *J. Organometal. Chem.* **6,** 645 (1966).
(4) Lebedev, D. D., Vereshchinsky, I. V., *Proc. Tihany Symp. Radiat. Chem., 2nd, Tihany, Hung., 1966*, 365 (1967).
(5) Lebedev, D. D., Korobkina, T. V., Vereshchinsky, I. V., *Plant. Lab.* **32,** 530 (1966).
(6) Lebedev, D. D., Vereshchinsky, I. V., *Zh. Org. Khim.* **3,** 2247 (1967).
(7) Miretsky, V. Y., Vereshchinsky, I. V., Ivanov, A. Y., Kocheshkov, K. A., Pozdeyev, V. V., Sheverdina, N. I., *Khim. Prom.* **44,** 261 (1968).
(8) Podkhalyuzin, A. T., Vereshchinsky, I. V., Borisov, E. A., *Bull. Izobret.* **13,** 122410 (1965).
(9) Podkhalyuzin, A. T., Vereshchinsky, I. V., *Dokl. Akad. Nauk, SSSR* **178,** 1123 (1968).
(10) Vereshchinsky, I. V., *Proc. Intern. Congr. Pure Appl. Chem., 20th, Moscow, 1965*, B45.
(11) Vereshchinsky, I. V., Pozdeyev, V. V., Miretsky, V. Y., Ivanov, A. Y., *Bull. Izobret.* **9,** 181104 (1966).
(12) Vereshchinsky, I. V., Podkhalyuzin, A. T., *Dokl. Akad. Nauk, SSSR* **165,** 107 (1965).

RECEIVED May 23, 1968.

33

The Reaction of Nitrous Oxide with Excited Molecules in the Radiolysis and Photolysis of Liquid Alkanes

R. A. HOLROYD

Atomics International Division of North American Rockwell Corp., Canoga Park, Calif. 91304

Publication Date: January 1, 1968 | doi: 10.1021/ba-1968-0082.ch033

In the 1470-A. photolysis of cyclohexane–nitrous oxide solutions, nitrous oxide reacts with excited cyclohexane molecules to form nitrogen and oxygen atoms. The reaction of N_2O with photoexcited 2,2,4-trimethylpentane molecules is much less efficient than with cyclohexane. In the radiolysis of these solutions, $G(N_2)$ is the same for different alkanes at low ($\lesssim$ 5 mM) N_2O concentrations. At higher concentrations, $G(N_2)$ from the radiolysis of cyclohexane is greater than $G(N_2)$ from the radiolysis of 2,2,4-trimethylpentane solutions. The N_2 yields from 2,2,4-trimethylpentane are in excellent agreement with the theoretical yields of electrons expected to be scavenged by N_2O. The yield of N_2 in the radiolysis of cyclohexane which is in excess of that formed from electrons is attributed to energy transfer from excited cyclohexane molecules to nitrous oxide.

Nitrous oxide has been used extensively in radiation chemical studies (*1, 16, 17, 18, 19, 20, 21, 22, 23*) to assess the importance of ionic processes. The reaction of nitrous oxide with the electron results in the formation of nitrogen, Reaction 1.

$$e^- + N_2O \rightarrow N_2 + O^- \qquad (1)$$

Kinetic studies of the competitive reactions of other electron scavengers support this hypothesis (*18, 20*). In the radiolysis of solutions of nitrous oxide in alkanes, reactions with other intermediates must be considered. Radicals, hydrogen atoms, and positive ions can be eliminated (*5, 20*), but a reaction with excited molecules is possible. It has been reported

In Radiation Chemistry; Hart, E.;
Advances in Chemistry; American Chemical Society: Washington, DC, 1968.

recently that photoexcited cyclohexane molecules transfer energy to benzene and cyclohexane (*9, 25*). Therefore, it is reasonable to expect that dissociative energy transfer to nitrous oxide can also occur (*8*). To assess the importance of such energy transfer in the radiolysis, solutions of nitrous oxide in several alkanes were photolyzed at 1470 A., and the results were compared with the radiolysis of these solutions.

Experimental

The hydrocarbons (Phillips research grade) were passed through a dried silica gel column before use. Nitrous oxide (Matheson Co.) was used as received. Solutions were prepared by adding a known amount of nitrous oxide to a degassed sample of alkane.

For photolysis at 1470 A. a combination Xe arc and reaction cell (*15*) was used. The light flux through the sapphire exit window was about 8×10^{-9} Einsteins/sec. The actinometer used was the photolysis of cyclohexane for which $\phi(H_2)$ has been shown to be 1.0 (*25*). In the cell the solutions were in contact with the sapphire window. Solutions were photolyzed for $\sim$ 20 min., and the conversion was approximately 0.1%. The solutions were stirred during photolysis and cooled to 13 $\pm$ 2°C. to prevent evaporation. The concentration of nitrous oxide in the liquid phase was calculated from the Bunsen coefficients of 3.3 for cyclohexane and *n*-hexane and 3.8 for 2,2,4-trimethylpentane (*26*).

The radiation cells were made from 9-mm. o.d. borosilicate glass tubing. The concentration of nitrous oxide was calculated by assuming that the amount in the gas phase was negligible since the solutions filled approximately 90% of the cells. The samples were thermostatted at 35°C. and irradiated for one hour in a ^{60}Co γ-ray facility at a dose rate of approximately 1.3×10^{19} e.v. liter^{-1} sec.$^{-1}$. Ferrous sulfate dosimetry was used. Since we wished to compare different alkanes, samples were prepared in pairs; one sample of the pair always contained cyclohexane and the other some other alkane. Each sample of each pair contained the same amount of nitrous oxide.

After photolysis or radiolysis, products volatile at −196°C. were first transferred to a calibrated volume, and the pressure was recorded. This gaseous fraction was then analyzed by gas chromatography on a Linde 5A molecular sieve column. The liquid fraction was analyzed on a 2-meter Poropak Q column for cyclohexanol, on a 30% β,β'-oxydipropionitrile + 10% $AgNO_3$ column for cyclohexene, and on a Dow 11 silicone column for dicyclohexyl.

Results and Discussion

Photolysis. The principal products of the photolysis of pure liquid cyclohexane are hydrogen and cyclohexene; dicyclohexyl is a minor product (*9, 25*). If nitrous oxide is present, the yield of hydrogen is reduced (Table I), and nitrogen is formed (Figure 1). These effects are complimentary since $\phi(H_2) + \phi(N_2) \cong 1$. The nitrous oxide does not affect

Publication Date: January 1, 1968 | doi: 10.1021/ba-1968-0082.ch033

$\phi(C_{12}H_{22})$ but does reduce $\phi(C_6H_{10})$ although not by as much as $\phi(H_2)$. The major oxygenated product formed is cyclohexanol and $\phi(C_6H_{11}OH) \sim \phi(N_2)/2$.

Table I. Photolysis of Cyclohexane–Nitrous Oxide Solutions

	Quantum Yields				
$[N_2O]$ mM	H_2	N_2	C_6H_{10}	$C_{12}H_{22}$	$C_6H_{11}OH$
0	1.0	0	.86[a]	.06	0
16	.84	.18	.80	.06	—
28	.81	.22	.80	.06	.13
50	.78	.28	.73	.07	—
48 (+ 5% benzene)	.32	.04	.37	.013	—
71	.65	.40	—	—	.18
99	.67	.42	.68	.055	—
144	.57	.50	—	—	.26

[a] Cyclohexene yield decreases somewhat with conversion.

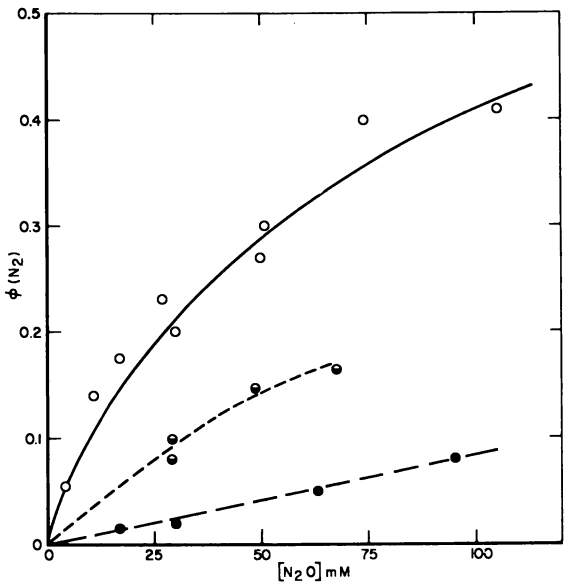

Figure 1. Quantum yield of nitrogen in the 1470-A. photolysis of alkane–nitrous oxide solutions at 13°C. Yields are relative to $\phi(H_2) = 1$ for liquid cyclohexane photolysis at 1470 A. Ordinate is concentration of N_2O in moles/liter

○ *Cyclohexane*
◒ n-*Hexane*
● *2,2,4-Trimethylpentane*

Table II. Photolysis of Alkane–Nitrous Oxide Solutions

Alkane	$[N_2O]$ mM	*Quantum Yields* N_2	H_2	CH_4
2,2,4-Trimethylpentane	0	0	.11	.21
	17	.015	.07	.21
	30	.02	.08	.19
	63	.05	.07	.19
	95	.08	.05	.20
2,2-Dimethylbutane	0	0	.07	.30
	68	.04	.08	.28
n-Hexane	29	.09	.93	—
	49	.14	.87	—
	68	.16	.81	—

Four other alkanes were photolyzed in the presence of nitrous oxide principally to determine the yield of N_2. In all four cases $\phi(N_2)$ was less than for cyclohexane solutions (Table II and Figure 1). For cyclopentane and 2,2-dimethylbutane $\phi(N_2)$ at 68 m*M* N_2O is only 0.04, which is 10% of the yield of N_2 for cyclohexane. For 2,2,4-trimethylpentane solutions $\phi(N_2)$ is also low, and $\phi(CH_4)$, a major product, is unaffected by N_2O. *n*-Hexane seems to be an intermediate case with respect to N_2 formation; like cyclohexane $\phi(N_2) + \phi(H_2) \cong 1$ here too.

There are several possible explanations which need to be considered for the formation of N_2 in the photolysis of cyclohexane–nitrous oxide solutions. These include direct absorption of vacuum ultraviolet light by nitrous oxide, photoionization of the solvent followed by electron attachment by nitrous oxide, and reaction of nitrous oxide with either excited cyclohexene or excited cyclohexane molecules. Of these possibilities only the last explanation—reaction of excited cyclohexane molecules with nitrous oxide—is important.

Photolysis of nitrous oxide at 1470 A. in these solutions can be discounted since the molar absorption coefficient for cyclohexane is 10,000 M^{-1} cm.$^{-1}$ (*10*) and that for nitrous oxide about 2500M^{-1} cm.$^{-1}$ (*13*). Preferential absorption by nitrous oxide would occur if nitrous oxide were adsorbed on the sapphire window, but this is discounted since the nitrogen yield is a function of the alkane present.

At longer wavelengths, near the absorption edge of cyclohexane (>1750 A.), the molar absorption coefficient of nitrous oxide is greater than that of cyclohexane. Nitrogen might be formed from the direct photolysis of nitrous oxide at these wavelengths, but the wavelength would have to be one at which cyclohexane also absorbs. This long wavelength photolysis cannot be an important source of N_2 for the following

Publication Date: January 1, 1968 | doi: 10.1021/ba-1968-0082.ch033

reasons. (1) If photolysis at a longer wavelength occurred, then all the photoproducts of cyclohexane would be reduced together by nitrous oxide. This is not the case, for while the yield of dicyclohexyl is unaffected by nitrous oxide, a 50% reduction in $\phi(H_2)$ is observed. (2) If long wavelength photolysis occurred, then N_2 formation should occur to a similar extent in all alkanes since the alkanes studied have grossly similar absorption spectra (*12*), yet the nitrogen yields vary from alkane to alkane. (3) The arc emits principally 1470 A. light.

Photoionization of the hydrocarbon followed by dissociative electron attachment (Reaction 1) should be considered since the ionization potential of a molecule is less in the liquid phase than it is in the gas phase. For hydrocarbons the ionization potential is 1 to 1.5 e.v. less in the liquid phase (*24*). The photon energy at 1470 A. is about 1.4 e.v. below the gas-phase ionization potentials of cyclohexane and 2,2,4-trimethylpentane (*14*). Some ionization may therefore occur, but the efficiency of this process is expected to be low. Photoionization is eliminated as a source of N_2 for the following reasons. (1) If photoionization occurred and the electron reacted with nitrous oxide, then O^- would be formed. It has been shown in the radiolysis of cyclohexane–nitrous oxide solutions that subsequent reactions of O^- result in the formation of cyclohexene and dicyclohexyl (*1, 16, 17*) and very little cyclohexanol (*16*, Table III). In the photolysis nitrous oxide reduces the yield of cyclohexene and does not affect the yield of dicyclohexyl. This indicates that O^- is not formed in the photolysis, and consequently N_2 does not result from electron capture. (2) A further argument against photoionization is that cyclohexane and 2,2,4-trimethylpentane have comparable gas-phase ionization potentials but exhibit quite different behavior with respect to N_2 formation.

The intermediates in the photolysis of cyclohexane which might react with nitrous oxide to form N_2 are hydrogen atoms, excited C_6H_{10}, and excited C_6H_{12}. Hydrogen atoms can be eliminated on the basis that $\phi(H)$ is only 0.14 (*25*) and that the rate of reaction of H atoms with nitrous oxide is too slow (*5*). The cyclohexene which is formed in the photolysis, Reaction 3, could initially have as much as 7 e.v. excess energy and could conceivably sensitize the decomposition of nitrous oxide. Such a reaction would produce N_2 but would not affect the yield of hydrogen. Since $\phi(H_2)$ is reduced by nitrous oxide, excited cyclohexene cannot be the main source of N_2.

Excited cyclohexane molecules are produced in the primary process, Reaction 2 (*9, 25*). If N_2 were formed by energy transfer from $C_6H_{12}^*$ to

$$C_6H_{12} + h\nu \rightarrow C_6H_{12}^* \quad (2)$$

$$C_6H_{12}^* \rightarrow H_2 + C_6H_{10} \quad (3)$$

Publication Date: January 1, 1968 | doi: 10.1021/ba-1968-0082.ch033

$$C_6H_{12}^* + N_2O \rightarrow N_2 + O + C_6H_{12} \quad (4)$$

nitrous oxide, Reaction 4, this would cause a reduction in $\phi(H_2)$ and $\phi(C_6H_{10})$ since Reaction 4 competes with Reaction 3. It is concluded that energy transfer to nitrous oxide is the principal source of N_2. If the oxygen atom generated by Reaction 4 is in an excited singlet state, it would be expected to react readily with cyclohexane by insertion into a carbon-hydrogen bond (*6*), Reaction 5. This is the case since cyclohexanol is formed but its yield is only 50% of (N_2). Apparently other

$$O + C_6H_{12} \rightarrow (C_6H_{11}\text{—}O\text{—}H)^* \begin{matrix} \xrightarrow{50\%} C_6H_{11}OH \\ \xrightarrow{50\%} \text{other products} \end{matrix} \quad (5)$$

products are also formed in this reaction. No other products which might result from Reaction 5 were found in this study. However, nitrous oxide does not reduce $\phi(C_6H_{10})$ quite as much as it does $\phi(H_2)$ (*see* Table I). Thus, a product of Reaction 5 may be cyclohexene, which is formed by elimination of H_2O from the intermediate.

Table III. Radiolysis of Alkane–Nitrous Oxide Solutions[a]

	2,2,4-Trimethylpentane			*Cyclohexane*			
$[N_2O]$, mM	$G(N_2)$	$G(H_2)$	$G(CH_4)$	$G(N_2)$	$G(H_2)$	$G(C_6H_{11}OH)$	G(excess N_2)
1.3	0.65	—	—	0.64	—	—	0.2
6	1.0	2.0	0.95	1.13	4.4	—	0.2
11	1.2	1.8	0.90	1.36	3.8	—	0.2
21	1.45	2.2	0.86	1.95	3.5	0.21	0.4
44	2.01	2.0	0.89	2.56	3.5	—	0.4
73	2.44	2.6	0.75	3.10	3.7	0.36	0.6
138	—	—	—	—	—	0.39	0.8
162	3.07	1.9	0.75	3.82	2.5	—	0.9
310	3.71	0.9	0.68	4.90	2.1	0.52	1.9

[a] Yield in molecules/100 e.v.

The mechanism consisting of Reactions 2, 3, and 4 requires that $[\phi(N_2)]^{-1}$ depend linearly on $[N_2O]^{-1}$, Equation I, where ϕ_2 is the quantum yield of excited molecules formed in Reaction 2.

$$1/\phi(N_2) = 1/\phi_2 + k_3/k_4\phi_2[N_2O] \quad (I)$$

The data are plotted in Figure 2. The ratio k_4/k_3 was evaluated from this plot to be $28 \pm 4M^{-1}$ at 10°C. Comparison of this value with the corresponding ratio for benzene (*25*) indicates nitrous oxide is a more effective quencher than benzene.

Publication Date: January 1, 1968 | doi: 10.1021/ba-1968-0082.ch033

In other alkanes the reaction of excited molecules with nitrous oxide is less important, and in some cases it may not occur at all. In *n*-hexane the N_2 yields are about one-half what they are in cyclohexane. In other alkanes such as 2,2,4-trimethylpentane the yields of N_2 were quite low. A small yield could be attributed to one of the other effects discussed, but if it is attributed to excited alkane molecules, then energy transfer to nitrous oxide is much less important in 2,2,4-trimethylpentane than in cyclohexane.

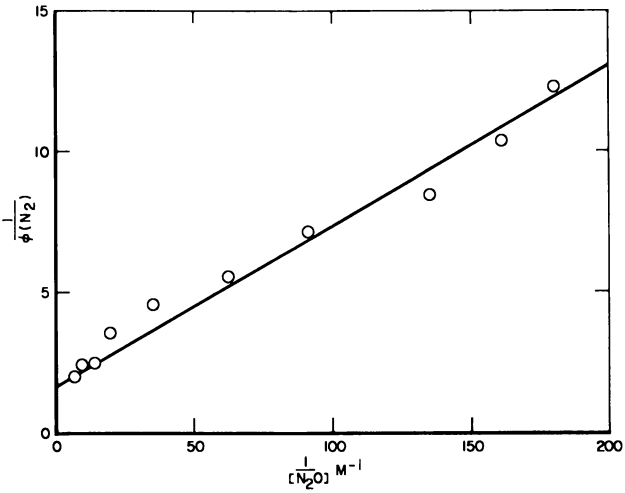

Figure 2. Kinetic plot of Equation I for the photolysis of cyclohexane–nitrous oxide solutions. Abscissa is $1/\phi(N_2)$; Ordinate is $1/[N_2O]$ in M^{-1}

Radiolysis. The photochemical experiments suggest that in the radiolysis a reaction of nitrous oxide with excited molecules would be expected in cyclohexane but should be less important in 2,2,4-trimethylpentane. The radiolysis results (Figure 3 and Table III) show that at nitrous concentrations less than 10 m*M*, where reactions of excited molecules are unimportant, $G(N_2)$ is the same for cyclohexane and 2,2,4-trimethylpentane solutions. At concentrations of nitrous oxide from 20 to 160 m*M*, $G(N_2)$ from cyclohexane solutions is greater than $G(N_2)$ from 2,2,4-trimethylpentane solutions, and the excess yield increases with the concentration of nitrous oxide. [The nitrogen yields reported here for the concentration range 5–200 m*M* are in good agreement with those reported by Sherman (*20*)] Nitrous oxide reduces $G(H_2)$ from cyclohexane (*16, 17, 18, 20,* and Table III), but it has little effect on $G(H_2)$ and $G(CH_4)$ from 2,2,4-trimethylpentane.

Publication Date: January 1, 1968 | doi: 10.1021/ba-1968-0082.ch033

To account for the N_2 yields, it is assumed that nitrous oxide scavenges electrons in both 2,2,4-trimethylpentane and cyclohexane but also scavenges excited molecules in cyclohexane. The electron is a precursor of much of the H_2 formed in the radiolysis of cyclohexane, but in 2,2,4-trimethylpentane most of the hydrogen is formed in processes which do not involve reactions of scavengeable electrons. Freeman (7) has calculated from theoretical considerations the yields of electrons expected to be scavenged by nitrous oxide as a function of concentration. The total yield of electrons is assumed to be 3 electrons/100 e.v. The number of electrons which react with nitrous oxide at each concentration is then calculated from the initial spatial separation of the charges and the probability of reaction of the electron with nitrous oxide for each separation. The calculated values for cyclohexane are shown as the solid line in Figure 3. Since the dielectric constants are similar, the theory would predict the same values for 2,2,4-trimethylpentane if the spatial distribution of charges were similar and the mobility and diffusion coefficient of the electron were the same in the two liquids. The yields of nitrogen for 2,2,4-trimethylpentane are in excellent agreement with the theoretical values, suggesting that the principal reaction of nitrous oxide in this case is electron scavenging. The divergence of $G(N_2)$ above 200 mM is caused partly by energy absorption in the nitrous oxide directly.

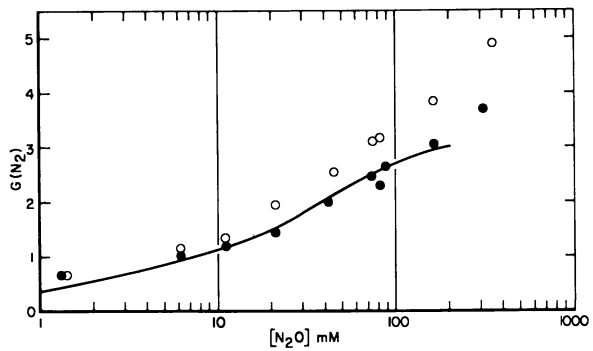

Figure 3. Yields of nitrogen in molecules/100 e.v. as a function of nitrous oxide concentration in cyclohexane, ○, and in 2,2,4-trimethylpentane ●. Solid line represents theoretical yields of electrons scavenged by nitrous oxide (7)

For cyclohexane solutions the yield of nitrogen exceeds that caused by electron scavenging (as given by theory or by the 2,2,4-trimethylpentane results). This excess yield can be reasonably accounted for if nitrous oxide reacts with some cyclohexane derived intermediate which

Publication Date: January 1, 1968 | doi: 10.1021/ba-1968-0082.ch033

is concluded to be excited molecules (Reaction 4). The reasons for this conclusion are given below.

(1) The excess N_2 is formed in the radiolysis in the concentration region where reactions of excited molecules occur. The excess nitrogen yields were treated like the photolysis results in order to calculate k_4/k_3. A plot of $1/G$ (excess N_2) *vs.* $[N_2O]^{-1}$ was found to be linear, and from the values of slope and intercept k_4/k_3 was found to be $14M^{-1}$ at 35°C. This value is in reasonable agreement with the photolysis results, considering that the rate of energy transfer may vary with temperature. Apparently the excited molecules formed in the radiolysis have properties similar to photoexcited molecules. The yield of these excited molecules, calculated from this plot is 1.2 ± 0.2 molecules/100 e.v. [This is a minimum value for the total number of excitations produced by the radiation. Additional excited molecules are expected from neutralization reactions, and it is not known how efficiently higher excited states are converted to this excited state.]

(2) The reaction of excited molecules with nitrous oxide provides an explanation for the formation of cyclohexanol in the radiolysis. The yields of cyclohexanol measured in this study are given in Table III. Somewhat lower yields were reported by others: Blackburn and Charlesby (*1*) report $G(C_6H_{11}OH) + G(C_6H_{10}O) < \sim 0.1$ at nitrous oxide concentrations between 15 and 130 m*M*, and Sagert and Blair (*16*) found $G(C_6H_{11}OH) = 0.25$ at nitrous oxide concentrations between 150 and 250 m*M*. As is shown in Table III, $G(C_6H_{11}OH)$ is approximately one-half the yield of excess nitrogen formed. In the photolysis the quantum yield of cyclohexanol is one-half $\phi(N_2)$. Thus, it is reasonable that in the radiolysis the cyclohexanol is formed by attack of singlet oxygen atoms on cyclohexane, Reaction 5.

(3) Benzene, a known quencher of excited molecules, reduces $G(N_2)$ in cyclohexane solutions but not significantly in 2,2,4-trimethylpentane solutions. In the photolysis of cyclohexane, benzene reduces the extent of decomposition as a result of energy transfer, Reaction 6 (*9*, *25*). Further, in the photolysis of cyclohexane–nitrous oxide solutions,

$$C_6H_{12}^* + C_6H_6 \rightarrow C_6H_{12} + C_6H_6 \qquad (6)$$

benzene reduces the yield of N_2 formed (Table I) because benzene competes with nitrous oxide for the excited cyclohexane molecules. In the radiolysis of 88 m*M* nitrous oxide in cyclohexane, adding 5% benzene reduces $G(N_2)$ by 0.5 molecules/100 e.v. or 70% of the excess yield at this concentration of nitrous oxide. In the radiolysis of 88 m*M* nitrous oxide in 2,2,4-trimethylpentane, addition of 5% benzene reduces $G(N_2)$ only 5%. The reduction of $G(N_2)$ in cyclohexane by benezene can be

Publication Date: January 1, 1968 | doi: 10.1021/ba-1968-0082.ch033

explained by energy transfer from excited cyclohexane molecules to benzene which competes with transfer to nitrous oxide.

Conclusions

Evidence has been presented for the formation of excited cyclohexane molecules which survive long enough to transfer energy to nitrous oxide. The observed lifetime is $14/k_4$ sec., which corresponds to $\sim 10^{-9}$ sec. if Reaction 4 is diffusion controlled. However, energy transfer may occur faster than the diffusion rate since in this case a solvent molecule is excited. For example, photochemical studies have shown that for quenching of an excited benzene molecule in liquid benzene the quenching rate constant can be as large as $10^{11}M^{-1}$ sec.$^{-1}$ (*11*). If k_4 were of this magnitude, then the lifetime of C_6H_{12}* would need to be only $\sim 10^{-10}$ sec. to account for the results.

On the other hand, it has been argued by Burton *et al.* (*2, 3, 4*) that the lifetime of singlet excited cyclohexane molecules is too short ($\sim 10^{-13}$ sec.) to be observed. This conclusion is based largely on the behavior of scintillators containing fluorescent solutes dissolved in cyclohexane. It is important at this point to emphasize that at solute concentrations close to millimolar (which are usually employed in scintillator studies) excited cyclohexane molecules cannot be detected by nitrous oxide. Higher concentrations of both nitrous oxide and benzene (*25*) are required to observe energy transfer. This study confirms that in the radiolysis of cyclohexane, solutes at millimolar concentrations interact mainly with the electron and not with excited molecules.

Acknowledgments

I am indebted to W. M. Bowe, Jr. for his experimental assistance and to J. M. Warman for several stimulating discussions.

Literature Cited

(1) Blackburn, R., Charlesby, A., *Nature* **210,** 1036 (1966).
(2) Burton, M., Ghosh, A., Yguerabide, J., *Rad. Res. Suppl.* **2,** 462 (1960).
(3) Burton, M., *Z. Electrochem.* **64,** 975 (1960).
(4) Burton, M., *Mol. Cryst.*, in press.
(5) Dainton, F. S., Sills, S. A., *Proc. Chem. Soc.* **1962,** 223.
(6) DeMore, W., Raper, O. F., *J. Chem. Phys.* **46,** 2500 (1967).
(7) Freeman, G. R., *J. Chem. Phys.* **46,** 2822 (1967).
(8) Holroyd, R. A., *J. Phys. Chem.* **72,** 759 (1968).
(9) Holroyd, R. A., Yang, J. Y., Servedio, F. M., *J. Chem. Phys.* **46,** 4540 (1967).
(10) Lipsky, S., private communication.
(11) Lipsky, S., "Physical Processes in Radiation Biology," L. Augenstein, ed., p. 215, Academic Press, New York, 1964.

(12) Lombos, B. A., Sanvageau, P., Sandorfy, C., *Chem. Phys. Letters* **1,** 42 (1967).
(13) McNesby, J. R., Okabe, H., *Advan. Photochem.* **1,** 184 (1964).
(14) Price, W. C., Bralsford, R., Harris, P. V., Ridley, R. G., *Spectrochem. Acta* **14,** 45 (1959).
(15) Radnoti, D., Eisel, E., Yang, J. Y., *Rev. Sci. Instr.* **37,** 970 (1966).
(16) Sagert, N. H., Blair, A. S., *Can. J. Chem.* **45,** 1351 (1967).
(17) Sato, S., Yugeta, R., Shinsaka, K., Tereo, T., *Bull. Chem. Soc. Japan* **39,** 156 (1966).
(18) Scholes, G., Simic, M., *Nature* **202,** 895 (1964).
(19) Seki, H., Imamura, M., *Bull. Chem. Soc. Japan* **38,** 1229 (1965).
(20) Sherman, W. V., *J. Chem. Soc.* **1966 A,** 599.
(21) Sherman, W. V., *J. Am. Chem. Soc.* **88,** 1567 (1966).
(22) Sherman, W. V., *J. Phys. Chem.* **70,** 2872 (1966).
(23) *Ibid.*, p. 667.
(24) Vermeil, C., Matheson, M., Leach, S., Muller, F., *J. Chim. Phys.* **61,** 598 (1964).
(25) Yang, J. Y., Servedio, F. M., Holroyd, R. A., *J. Chem. Phys.* **48,** 1331 (1968).
(26) Yen, L. C., McKetta, Jr., J. J., *J. Chem. Eng. Data* **7,** 288 (1962).

RECEIVED December 29, 1967. Work supported by Research Division of U. S. Atomic Energy Commission.

Pulse Radiolysis of Monomers and Polymers

A. J. SWALLOW

Paterson Laboratories, Christie Hospital and Holt Radium Institute, Manchester, 20, England

Publication Date: January 1, 1968 | doi: 10.1021/ba-1968-0082.ch034

In aqueous solution the primary radiolysis products react rapidly at the vinyl group of monomers, giving ions or radicals. For styrene and α-methylstyrene, appreciable ring addition occurs also. Rate constants for reactions of the radicals formed are tabulated. Styrene and α-methylstyrene in the pure state give rise to short-lived anions and long-lived radicals on irradiation, and the results are correlated with those obtained from measurements on the polymer which is formed. Ionic reactions are important in the irradiation of styrene and α-methylstyrene in organic solvents. Studies are reported on the mechanism of protection of polymers by sulfur-containing compounds. When irradiated in the solid state, poly(methyl methacrylate) gives some radicals which disappear over tens or hundreds of microseconds, leaving behind further radicals which remain trapped.

The study of radiation-induced polymerization is one of the most successful in radiation chemistry but is still incomplete. For example, little is known about the initiation stages, and many aspects of the mechanisms are still in dispute. Pulse radiolysis offers a means of studying monomers and polymers in a new way and provides certain advantages over flash photolysis, which has hardly been applied to monomers or polymers. Apart from the relevance to the chemistry of synthetic polymers, such studies should help in understanding the effect of radiation on macromolecules of biological significance. For these and other reasons, several groups of workers have pulsed polymeric systems, and, as so often in pulse radiolysis, have often worked along similar lines, thus providing an opportunity to compare results. This paper attempts to review the work which has been published in the pulse radiolysis of synthetic polymeric systems.

In Radiation Chemistry; Hart, E.;
Advances in Chemistry; American Chemical Society: Washington, DC, 1968.

Monomers in Dilute Aqueous Solution

Reactions with the Primary Species. In aqueous solution the monomers are exposed to the action of the species formed from the water in the primary act. The rate constants published for the reactions of the hydroxyl radicals and hydrated electrons are included in Table I. Most of the hydroxyl rate constants were measured using thiocyanate and are therefore subject to the usual uncertainties of this method (*5*). No rate constants appear to have been published for the reactions of the hydrogen atoms.

Table I. Rate Constants for Formation of Monomer Radicals or Ions in Aqueous Solution

Reaction	*Rate Constant,* M^{-1} *sec.*$^{-1}$	*Reference*
$OH + CH_2{=}CH_2$	1×10^9	(*13*)
$OH + CH_2{=}CHCONH_2$	2.9×10^9	(*25*)
	2.0×10^9	(*9*)
$SO_4^- + CH_2{=}CHCN$	1.7×10^8	(*19*)
$SO_4^- + CH_2{=}CHOCOCH_3$	1.1×10^9	(*19*)
$(H_2O)_n^- + CH_2{=}CH_2$	$<2.5 \times 10^6$	(*14*)
$(H_2O)_n^- + CH_2{=}CH{-}CH{=}CH_2$	8×10^9	(*18*)
$(H_2O)_n^- + CH_2{=}CHCONH_2$	1.8×10^{10}	(*18*)
	2.1×10^{10}	(*9*)
	3.3×10^{10}	(*8*)
$(H_2O)_n^- + CH_2{=}C(CH_3)COO^-$	8×10^9	(*18*)
$(H_2O)_n^- + CH_2{=}CHC_6H_5$	1.1×10^{10}	(*18*)
	1.5×10^{10}	(*18*)
$(H_2O)_n^- + CH_2{=}CHC_6H_4N$	1.4×10^{10}	(*8*)
$(H_2O)_n^- + CH_2{=}CHC_6H_4NH^+$	3×10^{10}	(*8*)

Table I shows that hydroxyl radicals react rapidly with both monomers examined. High rate constants would also be expected for other monomers. Hydrated electrons do not react rapidly with ethylene, but a slow reaction cannot be excluded. Hydrated electrons react with other monomers with rate constants around $1–2 \times 10^{10} M^{-1}$ sec.$^{-1}$. A similar high reactivity would be expected for unexamined vinyl monomers. There is no reason to suppose that the hydration of the electron plays an important part in the reaction; hence, electrons generated by radiation in other media should also react with vinyl monomers. For vinylpyridine, comparison of the neutral form with the protonated form shows a significantly higher rate constant for reaction with the protonated form, but other such comparisons (where possible) have not yet been made.

Table I also shows rate constants for reactions of the sulfate radical ion. By preparing suitable aqueous solutions, it may also be possible to measure reaction rates of radicals like $\cdot CH_2OH$, CO_2^-, etc.

Publication Date: January 1, 1968 | doi: 10.1021/ba-1968-0082.ch034

Products Formed by Hydroxyl Radicals. It is generally assumed that OH radicals add to the vinyl double bond, for example with ethylene:

$$OH + CH_2{=}CH_2 \rightarrow CH_2OH{-}CH_2\cdot \qquad (1)$$

It has been found that the radicals formed by reaction of OH radicals with ethylene do not react with ferric ions to produce acetaldehyde in the yield which would be expected if the only reactions occurring were Reaction 1 followed by Reaction 2.

$$CH_2OH{-}CH_2\cdot + Fe^{3+} \rightarrow CH_3CHO + Fe^{2+} + H^+ \qquad (2)$$

It was originally thought that some OH radicals must abstract hydrogen atoms from ethylene to form C_2H_3 radicals (*14*), but it is now concluded that all OH radicals add to ethylene (Reaction 1) and that the β-hydroxyethyl radicals enter into reactions, not all of which give rise to acetaldehyde (*13*). Other recent evidence also supports this view (*4*). The absorption spectrum of the β-hydroxyethyl radicals is similar to that of the α-hydroxyethyl radicals which can be prepared from ethyl alcohol (*13*).

In the pulse radiolysis of acrylamide, methacrylamide, and some other monomers, Chambers *et al.* have observed broad absorption bands with peaks near 370 mμ (*9*), which can plausibly be attributed to OH adducts at the β position—*e.g.*,

$$OH + CH_2{=}CHCONH_2 \rightarrow CH_2OH{-}\dot{C}HCONH_2 \qquad (3)$$

With styrene and α-methylstyrene, nitrous oxide-saturated solutions exhibit several sharp peaks after a 5000-rad pulse (*30*). One sharp peak is seen with a maximum at 345 mμ for styrene (optical density in 1.6-cm. cell = 0.14) and 350 mμ for α-methylstyrene (optical density = 0.1). The position of the absorption maximum is consistent with that expected for an adduct of the hydroxyl radical at the benzene ring (*7*). For many aromatic compounds, the extinction coefficient of such adducts at the maximum is about $3700M^{-1}$ cm.$^{-1}$ (*8*). Using this figure we can calculate that 90% of the OH radicals add to the ring for styrene and 60% for α-methylstyrene. These high percentages are consistent with the high rate constants ($2\text{–}5 \times 10^9 M^{-1}$ sec.$^{-1}$) for reaction of OH radicals with benzene and other aromatic compounds (*3*).

Nitrous oxide-saturated solutions of styrene and α-methylstyrene also give sharp peaks at about 305 and 320 mμ, after pulse radiolysis. These resemble the characteristic double peaks of benzyl at 306 and 317 mμ (*16*). The peaks are therefore attributed mainly to adducts of OH radicals at the β-position in the vinyl group, to give radicals resembling benzyl—*e.g.*,

$$OH + CH_2{=}CHC_6H_5 \rightarrow CH_2OH{-}\dot{C}HC_6H_5 \qquad (4)$$

Publication Date: January 1, 1968 | doi: 10.1021/ba-1968-0082.ch034

The most recent value for the extinction coefficient of the benzyl radical (in cyclohexane solution) is $1.2 \times 10^4\ M^{-1}$ cm.$^{-1}$ at 317 mμ and $6 \times 10^3 M^{-1}$ cm.$^{-1}$ at 360 mμ (*16*). Other recent values are $1.9 \times 10^4 M^{-1}$ cm.$^{-1}$ at 318 mμ (*20*) and $1.8 \times 10^4 M^{-1}$ cm.$^{-1}$ at 320 mμ (*17*). If we assume that similar extinction coefficients apply in aqueous solution, that the hydroxyl adducts of styrene and α-methylstyrene have the same extinction coefficient as benzyl, and that no other species absorb at these wavelengths, we would estimate that about 20–40% of the OH radicals add to the β-position of the vinyl group for styrene and 15–30% for α-methylstyrene.

Products Formed by Hydrated Electrons and Hydrogen Atoms. When hydrated electrons react with uncharged vinyl monomers, they may in principle give rise directly to hydrogen atom adducts:

$$(H_2O)_n^- + M \rightarrow MH + OH^- + (H_2O)_{n-1} \qquad (5)$$

Alternatively, anions may be formed in the first case, which might or might not be protonated by reaction with water or hydrogen ions. Chambers *et al.* find that pulse radiolysis of neutral aqueous acrylamide ($10^{-2}M$) gives rise to absorptions with peaks at 275 and 370 mμ (*9*). The peak at 275 mμ does not appear when an excess of N_2O is present, whereas the peak at 370 mμ is almost unaffected by N_2O. It may be therefore that the absorption at 275 mμ and half the absorption at 370 mμ are caused by an anion formed by reaction of the hydrated electron with acrylamide (*9*) or else by a hydrogen atom adduct formed directly as in Reaction 5 or by protonation of an anion. The peak at 275 mμ is absent in a solution which is sufficiently acid for all hydrated electrons to give hydrogen atoms, so that the species responsible for the peak could not be a hydrogen atom adduct, unless hydrogen atoms react with acrylamide to give a radical with a structure different from the hydrogen adduct formed from hydrated electrons. [In a recent communication (K. Chambers, E. Collinson, F. S. Dainton, Joint Annual Meetings of Chemical Society, Institute of Chemistry of Ireland and Royal Institute of Chemistry, Dublin, April 1968) it is concluded that the species absorbing at 275 and 370 mμ in the pulse radiolysis of aqueous acrylamide is in fact formed by protonation of the anion, and is $\dot{C}H_2$—CH=C(OH)NH_2, whereas the species absorbing at 370 mμ only, formed by hydrogen atom attack, is CH_3—$\dot{C}$HCONH_2. Although the absorption at 275 mμ is no longer attributed to the anion, an absorption at 290 mμ can be seen at pH 11–12, and this is attributed to the anion. This work does not necessitate a revision of Table II of this paper, but it contains useful additional

Publication Date: January 1, 1968 | doi: 10.1021/ba-1968-0082.ch034

information, including valuable new rate constants.] Methacrylamide and *N-tert*-butylacrylamide behave like acrylamide, but acrylonitrile and acrylic acid show some differences. It would be interesting to establish the reactions of anionic species in such cases by using electrical conductivity in conjunction with pulse radiolysis. Among other experiments, it would be interesting to see whether the rate of protonation of the anion could be observed.

Styrene ($5 \times 10^{-3}M$) has been given 2-μsec. pulses in neutral solution (*30*), and after reaction with the hydrated electron it shows no sign of an absorption which could be attributed to the styrene anion. This could be because reaction with hydrated electrons occurs according to Reaction 5. If the anion is an intermediate, its reaction with hydrogen ions would be too slow to account for the absence of the anion absorption; hence, perhaps the anion is formed in the first case and then reacts with water. If we assume that this reaction occurs within a microsecond, the rate constant would be $> 10^4 M^{-1}$ sec.$^{-1}$. An absorption with a peak at $\sim$ 400 mμ is seen in the pulse radiolysis of styrene dissolved in cyclohexane (*24*, and *see below*), but is not seen when water is added before irradiation. The absence of the anion is attributed to rapid protonation by the water, and the rate constant for the reaction may be estimated at greater than about $10^9 M^{-1}$ sec.$^{-1}$. Further experiments could give a better value. α-Methylstyrene behaves similarly to styrene.

Styrene (or α-methylstyrene) could accept a hydrogen atom at the α- or β-position in the side chain or at several positions in the benzene ring. However, the α-position in the side chain is energetically unlikely. Incorporation of a hydrogen atom at the β-position in the side chain would give a methyl-substituted benzyl radical, $CH_3—\dot{C}HC_6H_5$ (or $CH_3—\dot{C}(CH_3)C_6H_5$), which might be expected to have a spectrum like that of benzyl itself, which has characteristic peaks at 306 and 317 mμ (*16*). Aqueous solutions of styrene (or α-methylstyrene) exhibit peaks at about 305 and 320 mμ after the hydrated electrons have reacted (*31*), but the intensity is only about one-seventh of that expected if all hydrated electrons (and hydrogen atoms) gave the substituted benzyl radical and if its extinction coefficient in aqueous solution were the same as for benzyl in cyclohexane solution. Hence, it may be that 15% of the hydrogen atoms appear at the β-position in the side chain with the remainder appearing at some position in the benzene ring. It might have been expected that the hydrogen atom ring adduct would exhibit a similar absorption to the OH radical ring adduct. Yet for both styrene and α-methylstyrene, the optical density at $\sim$ 350 mμ in the presence of nitrous oxide is twice that in the absence of nitrous oxide—not the same,

Publication Date: January 1, 1968 | doi: 10.1021/ba-1968-0082.ch034

Table II. Products Formed by Reaction *OH*

$CH_2{=}CH_2$	$CH_2OH{-}CH_2\cdot$
$CH_2{=}CHCONH_2$	$CH_2OH{-}\dot{C}HCONH_2$
$CH_2{=}C(CH_3)CONH_2$	$CH_2OH{-}\dot{C}(CH_3)CONH_2$
$CH_2{=}CHCONH$-*tert*-Bu	$CH_2OH{-}\dot{C}HCONH$-*tert*-Bu
$CH_2{=}CHC_6H_5$	80% $CH_2{=}CHC_6H_5OH$ 20% $CH_2OH{-}\dot{C}HC_6H_5$
$CH_2{=}C(CH_3)C_6H_5$	70% $CH_2{=}C(CH_3)C_6H_5OH$ 30% $CH_2OH{-}\dot{C}(CH_3)C_6H_5$

as would be expected from this view. Perhaps the discrepancy is connected with the fact that various sites in the ring are available for addition.

In acid solutions, the spectrum after the pulse of both styrene and α-methylstyrene is the same as in neutral solution. This contrasts with acrylamide and related compounds whose spectrum in acid solutions resembles that in nitrous oxide-saturated solutions. These effects are consistent with the view that the reaction of the electron with styrene and α-methylstyrene gives a hydrogen atom adduct which is the same as that formed by hydrogen atom attack, whereas with acrylamide and related compounds the anion is formed and is stable enough to be seen. In the experiments reported by Chambers *et al.* (*9*) the disappearance of the anion by reaction with water might have been expected as a first-order reaction if the rate constant were greater than about $10^2 M^{-1}$ sec.$^{-1}$. Hence, this figure may be regarded as an upper limit for the reaction (surprisingly low) (*see* bracketed note above).

Tentative identification of the products of the reaction of hydroxyl radicals, hydrated electrons, and hydrogen atoms with monomers on the basis of the discussion given here is summarized in Table II. Many of the products can exist in various mesomeric forms. For styrene and α-methylstyrene the percentages discussed in the text have been adjusted to make the totals add to 100%. The identification seems reasonably sound for the OH radical products but less so for the others. Apart from the need to identify the products from other monomers, more work is needed on the monomers already studied to test the speculations made and to quantify any conclusions.

Reactions of the Monomer Ions and Radicals. The rate constants for the reactions of monomer radicals (or ions) in aqueous solution are given in Tables III and IV. Mutual interactions of radicals (Table III) all

of Primary Species with Monomers

$(H_2O)_n^-$	H
No reaction so far detected	$CH_3—CH_2\cdot$
$CH_2^-—\dot{C}HCONH_2$	$CH_3—\dot{C}HCONH_2$
$CH_2^-—\dot{C}(CH_3)CONH_2$	$CH_3—\dot{C}(CH_2)CONH_2$
$CH_2^-—\dot{C}HCONH$-*tert*-Bu	$CH_3—\dot{C}HCONH$-*tert*-Bu
85% $CH_2=CHC_6H_6$	85% $CH_2=CHC_6H_6$
15% $CH_3—\dot{C}HC_6H_5$	15% $CH_3—\dot{C}HC_6H_5$
85% $CH_2=C(CH_3)C_6H_6$	85% $CH_2=C(CH_3)C_6H_6$
15% $CH_3—\dot{C}(CH_3)C_6H_5$	15% $CH_3—\dot{C}(CH_3)C_6H_5$

proceed with a rate constant of about $10^9 M^{-1}$ sec.$^{-1}$ (to within a factor of about 2), and this value is substantially above the usual rate constant for termination, as might be expected. There is little indication of appreciable difference between the reaction rates for different species. Reaction of monomer radicals with oxygen also proceeds rapidly, as expected (Table IV). The peroxy radicals formed from ethylene react more rapidly with each other than either HO_2 radicals or O_2^- radicals do (*15*). Their reaction with ferrous ions also seems to be somewhat faster than the latest value for the corresponding reaction of HO_2 (*21*). The reaction of the acrylamide radicals with ferricyanide is about eight times faster than the reaction of polyacrylamide radicals with ferricyanide (*12*).

Monomers in the Pure State and in Organic Solution

Pure Monomers. The first pulse radiolysis study of a polymerizing system was with isobutylene, which gave an absorption with a peak at 297 mμ, which disappeared in a fast first-order reaction (*6*). The absorption may be attributed to the trimethylcarbonium ion, which, from independent work, appears to have an absorption maximum at 292 mμ and an extinction coefficient close to $6.3 \times 10^3 M^{-1}$ cm.$^{-1}$ (*28*).

Most of the work with pure monomers has been with styrene and α-methylstyrene, which have been investigated separately by different groups. These two monomers appear to behave similarly. Katayama and colleagues were the first to study one of these monomers (*23*). They found that α-methylstyrene gave rise to a broad absorption with an apparent peak at 350 mμ and a shoulder at about 420 mμ. In the presence of water or DPPH the absorptions were substantially diminished. They attributed the absorption to the anion of α-methylstyrene, which can be produced independently of radiation by the action of sodium metal on

Publication Date: January 1, 1968 | doi: 10.1021/ba-1968-0082.ch034

α-methylstyrene. Later additional absorption was seen at 546.1 mμ, decaying at the same rapid rate as the other, and equally affected by DPPH or water (*22*). This result fully substantiated the earlier conclusion. Schneider and Swallow saw a similar rapidly decaying absorption in both styrene (half-life quoted as about 5 μsec.) (*29*) and α-methylstyrene (*31*). The absorption tailed off beyond about 550 mμ, but a larger absorption was seen in addition, with a peak at 315 mμ for styrene and 320 mμ for α-methylstyrene. The absorption at this wavelength was much longer lived, and in fact, part of it persisted for seconds at least (*29*). Metz, Thomas, and Potter worked with styrene and analyzed their data in terms of three species: (1) a rapidly decaying species (half-life 4 μsec.) with a broad absorption centering at about 370 mμ; this species was removed by water; (2) a more intensely absorbing longer-lived species with a peak at about 320 mμ; (3) a stable species with a peak in a similar region. This stable species could also be observed in styrene after γ-irradiation. It was very sensitive to photolysis (*27*).

Table III. Rate Constants for Mutual Interaction of Monomer Radicals or Ions in Aqueous Solution

Reaction (R = H or OH)	*Rate Constant* 2k, M^{-1} *sec.*$^{-1}$	*Reference*
2 $CH_2OH—CH_2\cdot$	6.3×10^8	(*13*)
2 $CH_2R—CH_2\cdot$	7×10^8	(*13*)
2 $CH_2R—\dot{C}HCONH_2$	1.3×10^9	(*9*)
2 $CH_2R—\dot{C}HCONH_2$[a]	1.8×10^9	(*9*)
	4.2×10^9	(*9*)
2 $CH_2R—\dot{C}(CH_3)CONH_2$	1.1×10^9	(*9*)
2 $CH_2R—\dot{C}(CH_3)CONH_2$[a]	1.6×10^9	(*9*)
	4.5×10^9	(*9*)
2 $CH_2R—\dot{C}HCONH$-*tert*-Bu	6×10^8	(*9*)
2 $CH_2R—\dot{C}HCONH$-*tert*-Bu[a]	7×10^8	(*9*)
	1.1×10^9	(*9*)
2 $HO(CH_2{=}CHC_6H_5)$	7.6×10^8	(*31*)
2 $HO(CH_2{=}C(CH_3)C_6H_5)$	8×10^8	(*31*)

[a] $R = e^-$ or OH.

Comparison of the data obtained by the three groups reveals many points of agreement. All three agree about the existence of the short-lived species, and above about 350 mμ the shapes of the spectra observed immediately after the pulse are consistent with each other, especially since the absorption "peaks" are broad ones and the absorptions obtained are not large. The tentative attribution of this species to an anion is now (*31*) agreed on by all. Below 350 mμ it is tempting to suppose that

Publication Date: January 1, 1968 | doi: 10.1021/ba-1968-0082.ch034

the difference between the Japanese work on the one hand and the American and European work on the other might be caused by instrumental factors, especially in view of the difficulties often encountered with spectral inhomogeneity in pulse radiolysis and the sensitivity of the "stable" species to light. The long-lived transient with the peak near 320 mμ (seen by Katayama and colleagues as a long-lived component of the absorption at higher wavelengths) is attributed for the main part to a radical with a benzyl-type structure (*31*). It is noted that such radicals would retain their structure if they add to monomer—*e.g.*, for styrene

$$RCH_2—\dot{C}HC_6H_5 + CH_2{=}CHC_6H_5 \rightarrow RCH_2—CH(C_6H_5)—CH_2—\dot{C}HC_6H_5 \quad (6)$$

Investigations are still being done on the "permanent" absorption(s) with peak(s) near 320 mμ (*27*).

Table IV. Rate Constants for Reactions of Monomer Radicals or Ions in Aqueous Solution

Reaction (R = H or OH)	*Rate Constant,* M^{-1} *sec.*$^{-1}$	*Reference*
$CH_2R—CH_2\cdot + O_2$	6.0×10^9	(*13*)
$CH_2R—\dot{C}HCONH_2 + O_2$[a]	1.9×10^9	(*9*)
$2\ CH_2R—CH_2O_2\cdot$	1.4×10^8	(*13*)
$CH_2R—CH_2O_2\cdot + Fe^{2+}$	2.4×10^6	(*13*)
$CH_2R—\dot{C}HCONH_2 + Fe(CN)_6^{3-}$	6.8×10^6	(*9*)

[a] $R = e^-$ or OH.

The kinetics and effect of additions on the absorptions are not yet clear. According to Katayama and colleagues the most rapidly decaying species disappears in a first-order reaction with a half-life of 25 μsec. (*22*). Metz *et al.* find a first-order reaction with a half-life of 4 μsec. (*27*). Schneider and Swallow, however, assert that the species disappears in a second-order reaction (*31*). Perhaps the variability is connected with the effect of traces of impurities, especially water. The Japanese and American groups had used elaborately dried styrene, whereas the European group had not. However, on this basis, we might expect the Japanese and American results to agree. Also the European styrene could not have contained much water; otherwise the short-lived absorption would not have been seen at all. Similarly, the kinetics of the decay of the long-lived transient are not easily understood. Water does not seem to affect this species (*27*). Oxygen affected it in the work of Schneider and Swallow (*31*) but not in that of Metz, Potter, and Thomas (*27*).

Attempts have been made to study the formation of polymer under pulse radiolysis conditions. Metz *et al.* have examined the ionic polymerization which should predominate with their very dry styrene (*26*).

Publication Date: January 1, 1968 | doi: 10.1021/ba-1968-0082.ch034

Schneider and Swallow have produced evidence to show that with their styrene the polymerization was free radical in nature (*29*). This is consistent with the likely presence of traces of water, and it would be expected that much less water would suffice to prevent ionic polymerization than would be needed to interfere with the reactions of the "primary" species. It can be deduced from Schneider and Swallow's polymer measurements that the termination rate constant is about $10^6 M^{-1}$ sec.$^{-1}$ (*31*), which is lower than the values which may be deduced from experiments at low dose rates (*10*) (around $2 \times 10^7 M^{-1}$ sec.$^{-1}$). However, all experiments may perhaps require some reinterpretation in view of the stable product absorbing at 320 mμ. The value of $10^6 M^{-1}$ sec.$^{-1}$ is consistent with literature values and is not inconsistent with the rate of disappearance of the transient absorption at 320 mμ, especially since termination rate constants must be average values, and in pulse radiolysis many rates should be observable (depending on the length of the polymerizing radical) and should vary downward from the rate of mutual reaction of the monomer radicals. In the absence of measured values, this latter rate may be taken to be $k = 2 \times 10^9 M^{-1}$ sec.$^{-1}$ as for benzyl (*16*), a value close to those given in Table III for monomeric radicals in aqueous solution. According to Schneider and Swallow's calculations polymerization had occurred with an initiation rate corresponding to $G = 0.95$ (*31*). Hence, most of the benzyl-type radicals had initiated polymerization rather than reacted with each other. From the conditions used in the experiments this means that the rate constant for addition of monomeric radicals to monomer must be greater than about $10^2 M^{-1}$ sec.$^{-1}$, probably much greater, and this is entirely reasonable.

Styrene and α-Methylstyrene in Organic Solvents. Pulse radiolysis studies have been made on styrene and α-methylstyrene dissolved in methanol, benzene, carbon tetrachloride, dioxane, tetrahydrofuran, hexane, and cyclohexane (*9, 24, 29, 30, 31*). The results are easiest to understand for the aliphatic hydrocarbons and especially for the styrene in cyclohexane, which has been studied the most (*31*). For such solutions, two absorption bands were seen after the pulse by Keene, Land, and Swallow (*24*) and Schneider and Swallow (*30*) with peaks at 320 and 390 mμ. The absorption at 320 mμ disappeared slowly by complex kinetics, and the 390-mμ absorption was very short lived, decaying by second-order kinetics with $k/\epsilon = 4\text{–}7 \times 10^6$ cm. sec.$^{-1}$. The relative intensities of the two peaks were quite variable. Chambers *et al.* saw the long lived absorption at 320 mμ but did not see a separate peak at 390 mμ, although it was observed that the absorption at 375 mμ decayed rapidly with $k/\epsilon = 2.6 \times 10^6$ cm. sec.$^{-1}$.

It seems likely that the absorption at 320 mμ is caused largely by the substituted benzyl radical. Since the species is too long lived to be

Publication Date: January 1, 1968 | doi: 10.1021/ba-1968-0082.ch034

the monomeric radical, it seems to be the growing polymer radical. The species at 390 mμ may be the anion as seen with the pure monomer. Adding traces of impurities (including water) markedly lowered the absorption at 390 mμ, which may explain the irreproducibility at this wavelength.

The yield of the absorption at 320 mμ was found to rise with concentration in a way suggesting that it is formed by anionic process—*e.g.*, by protonation of a styrene anion by its geminate partner (*31*). If it is a polymerizing radical, then the rate constant for addition of the benzyl-type radical to styrene must be at least 10^5–$10^6 M^{-1}$ sec.$^{-1}$. The yield of the observable anion seemed much less dependent on concentration, which is consistent with the view that it is formed by those electrons ($G \sim 0.2$) which escape from the spur. Absorptions with peaks close to 320 mμ are seen for all the other solvents above, but the component at the longer wavelength is seen only with the aliphatic hydrocarbons. For methanol solutions this may be because of rapid protonation.

Publication Date: January 1, 1968 | doi: 10.1021/ba-1968-0082.ch034

Polymers

A pulse radiolysis study has been reported on the mechanism of "protection" of a polymer in aqueous solution by sulfur compounds (*11*). Hydrated electrons did not react with polyethylene oxide (PEO), but it was presumed that OH radicals must react. When thiourea is present in an aqueous solution containing PEO, the transient thiourea absorption peak at 400 mμ does not appear, presumably because the OH radicals responsible for it are now reacting with PEO instead. By analogy with the work on sulfur compounds reported by Adams *et al.* (*2*) the peak at 400 mμ in the absence of PEO would now be attributed to a product formed by addition of the oxidized thiourea radical to thiourea. Various second-order reactions occur after a pulse has been delivered to the system containing thiourea, and the reaction of PEO radicals with reduced thiourea radicals could lead to "protection" of the polymer from radiation damage. Under low dose rate conditions the more likely protection mechanism would be reaction of PEO radicals with thiourea to abstract a hydrogen atom, but this reaction could not be demonstrated in the earlier work (*11*). Work using cysteamine (*1*) which is now better understood than thiourea, has succeeded in establishing Reaction 7.

$$P\cdot + NH_2CH_2CH_2SH \rightarrow PH + NH_2CH_2CH_2S\cdot \qquad (7)$$

At pH 7.5 the rate constant is *ca.* $5 \times 10^6 M^{-1}$ sec.$^{-1}$, which is about one-tenth that for the corresponding reaction of $\cdot CH_2OH$ radicals with cysteamine (*1*).

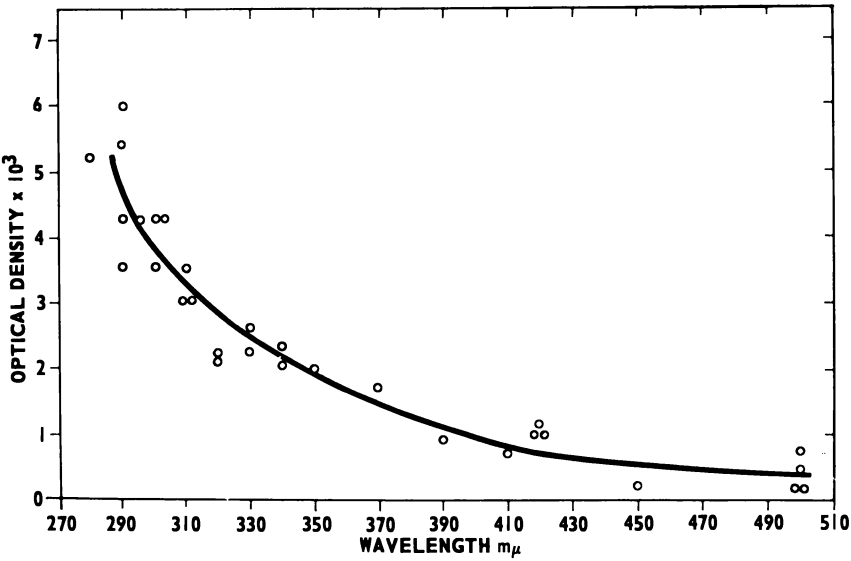

Figure 1. Spectrum after the pulse (~ 5000 rads) for poly(methyl methacrylate) containing unchanged monomer. Optical path length, 0.1 cm.

Pulse radiolysis experiments have been done with solid poly(methyl methacrylate) (32). The material had been prepared in blocks (3 × 1 × 1 cm. or 3 × 1 × 0.1 cm.) by γ-irradiation of methyl methacrylate and contained unchanged monomer at unknown concentration. Marked transient absorptions were seen after 5000-rad pulses, which decayed over a few tens or hundreds of microseconds to give a permanent species, stable for hours and which had a spectrum resembling that of the transient. A solution of methyl methacrylate in cyclohexane gave a similar broad absorption spectrum. The absorption spectrum immediately after the pulse for a block with a light path of 0.1 cm. is shown in Figure 1. Within experimental error there was no change in transient intensity between the first and 31st pulse. The decay kinetics were complex, varied from sample to sample, and were not the same at high wavelengths (*e.g.*, 600 mμ) as at low wavelengths (*e.g.*, 340 mμ).

The permanent absorption exhibited by the irradiated polymer is quite different from that shown by the polymer itself, which absorbs only weakly at 300–350 mμ. Absorptions below 300 mμ are difficult to interpret because of the monomer absorption. It is suggested that for the most part both transient absorption and permanent absorption are caused by the radical:

$$R—CH_2—\dot{C}(CH_3)—COOH$$

Publication Date: January 1, 1968 | doi: 10.1021/ba-1968-0082.ch034

which is probably also responsible for the ESR spectrum of irradiated poly(methyl methacrylate) containing traces of monomer. Some such radicals may be formed during the pulse by fission of the polymer chain, and more would be formed by reaction of radiation-produced radicals with unchanged monomer. Where the radicals are in favorable positions in the polymer matrix they recombine after the pulse, but a certain fraction (perhaps 25–50%) remain for hours after the pulse as trapped radicals. The difference between the kinetics at 600 and 340 mμ shows that other species are present at certain stages in addition to the one discussed.

Acknowledgments

The author thanks his colleagues, especially B. Cercek, M. Ebert, E. J. Land, and Christel Schneider for helpful discussions. He also thanks those who have sent private communications about their work, especially M. Katayama and D. J. Metz.

Literature Cited

(1) Adams, G. E., Armstrong, R. C., Charlesby, A., Michael, B. D., private communication.
(2) Adams, G. E., McNaughton, G. S., Michael, B. D., "The Chemistry of Ionization and Excitation," G. R. A. Johnson, G. Scholes, eds., p. 281, Taylor and Francis, London, 1967.
(3) Anbar, M., Neta, P., *Intern. J. Appl. Radiation Isotopes* **18**, 493 (1967).
(4) Basson, R. A., du Plessis, T. A., *Chem. Commun.* **1967**, 775.
(5) Baxendale, J. H., Stott, D. A., *Chem. Commun.* **1967**, 699.
(6) Burrell, E. J., *J. Phys. Chem.* **68**, 3885 (1964).
(7) Cercek, B., *J. Phys. Chem.* **71**, 2354 (1967).
(8) Cercek, B., private communication.
(9) Chambers, K. W., Collinson, E., Dainton, F. S., Seddon, W. A., Wilkinson, F., *Trans. Faraday Soc.* **63**, 1699 (1967).
(10) Chapiro, A., "Radiation Chemistry of Polymeric Systems," Interscience, New York, 1962.
(11) Charlesby, A., Fydelor, P. J., Kopp, P. M., Keene, J. P., Swallow, A. J., "Pulse Radiolysis," p. 193, Academic Press, London, 1965.
(12) Collinson, E., Dainton, F. S., Miles, B., Tazuke, S., Smith, D. R., *Nature* **198**, 26 (1963).
(13) Cullis, C. F., Francis, J. M., Raef, Y., Swallow, A. J., *Proc. Roy. Soc. (London)* **A300**, 443 (1967).
(14) Cullis, C. F., Francis, J. M., Swallow, A. J., *Proc. Roy. Soc. (London)* **A287**, 15 (1965).
(15) Czapski, G., Dorfman, L. M., *J. Phys. Chem.* **68**, 1169 (1964).
(16) Hagemann, R. J., Schwarz, H. A., *J. Phys. Chem.* **71**, 2694 (1967).
(17) Hamill, W. H., Guarino, J. P., Ronayne, M. R., Ward, J. A., *Discussions Faraday Soc.* **36**, 169 (1963).
(18) Hart, E. J., Gordon, S., Thomas, J. K., *J. Phys. Chem.* **68**, 1271 (1964).
(19) Henglein, A., private communication.
(20) Hodgkins, J. E., Megarity, E. D., *J. Am. Chem. Soc.* **87**, 5322 (1965).
(21) Jayson, G. G., Stirling, D. A., Swallow, A. J., *Chem. Commun.* **1967**, 931.

(22) Katayama, M., *Bull. Chem. Soc. Japan* **38**, 2208 (1965).
(23) Katayama, M., Hatada, M., Hirota, K., Yamazaki, H., Ozawa, Y., *Bull. Chem. Soc. Japan* **38**, 851 (1965).
(24) Keene, J. P., Land, E. J., Swallow, A. J., *J. Am. Chem. Soc.* **87**, 5284 (1965).
(25) Matthews, R. W., Sangster, D. F., *J. Phys. Chem.* **69**, 1938 (1965).
(26) Metz, D. J., private communication.
(27) Metz, D. J., Potter, R. C., Thomas, J. K., *J. Polymer Sci.* **A(1)5**, 877 (1967).
(28) Rosenbaum, J., Symons, M. C. R., *Mol. Phys.* **3**, 205 (1960).
(29) Schneider, C., Swallow, A. J., *J. Polymer Sci.* **B4**, 277 (1966).
(30) Schneider, C., Swallow, A. J., *Proc. Tihany Symp. Radiation Chem., 2nd* 471 (1967).
(31) Schneider, C., Swallow, A. J., *Makromol. Chem.* in press.
(32) Swallow, A. J., unpublished work.

RECEIVED January 2, 1968.

Ionic Polymerization in Irradiated Glasses

A. CHAPIRO, A. M. JENDRYCHOWSKA-BONAMOUR and L. PEREC

Laboratoire de Chimie des Radiations du C.N.R.S., 92-Bellevue, France

Publication Date: January 1, 1968 | doi: 10.1021/ba-1968-0082.ch035

Anionic polymerizations were observed on irradiating vitreous mixtures of acrylonitrile with N,N-*dimethylformamide, triethylamine, and isopropylamine. The reaction rate was highest in mixtures which form an optically clear glass at low temperatures. Irradiation at different temperatures showed that the rate exhibited a sharp maximum a few degrees above the glass transition point,* T_g. *Below this temperature no chain propagation occurred during irradiation, but an ionic postpolymerization was found after irradiation, while the mixture was warmed to room temperature. Cationic polymerizations were observed in vitreous solutions of styrene in hexachlorobutadiene and methylene chloride. Again the rate was highest near* T_g. *Poly(vinyl chloride) films were swollen at room temperature in mixtures of isobutylene and chloroform and irradiated at* $-78°$ *and* $-196°C$. *A cationic graft copolymerization was observed under such conditions.*

Although most radiation-induced polymerizations proceed by free radical mechanisms, evidence has accumulated in the last decade that ionic polymerizations occur under certain conditions. This has created considerable interest among radiation chemists since it provided unambiguous proof for the initiation of ionic processes by radiations. Experiments have shown that cationic polymerization is favored at low temperatures and that the yields are highest if the monomer is dissolved in halogenated solvents (*16*). Anionic polymerization is observed when acrylonitrile or methyl methacrylate is irradiated at low temperatures in amines or amides (*13, 14, 16*). It is believed that chlorinated substances "stabilize" the negative charge by converting electrons into Cl^- ions, whereas amines or amides "stabilize" the positive charge as quaternary ammonium-type ions.

In Radiation Chemistry; Hart, E.;
Advances in Chemistry; American Chemical Society: Washington, DC, 1968.

Radiation polymerization in glasses at low temperatures has been reported in the last few years. Vinyl acetate was found to polymerize much faster when irradiated in a quenched vitreous state below −130°C. than in the normal crystalline state (*2*). Several monomers were dissolved in mineral oil or other oily substances and irradiated at −78°C. and below. A rapid reaction was observed in diluted monomer solutions. The following monomers were examined: methyl methacrylate (*1, 5, 6, 7*), lauryl methacrylate (*8*), methyl acrylate (*5*), vinyl acetate (*5*), styrene (*5, 7*), vinyl chloride (*7*), and acrylonitrile (*7*). In all systems the reaction rates and molecular weights of the polymers exhibited a sharp maximum at very low monomer contents (5–15%). Copolymerization studies under the same conditions showed that the reaction proceeded by a free radical mechanism (*6, 9*). The structure of the solid mixtures of methyl methacrylate and styrene with mineral oil was examined using x-ray diffraction, polarized light, and electron microscopy (*17, 18*). Phase separation occurred when the liquid mixtures were cooled, the monomer being dispersed in small droplets in the vitreous oil. These droplets remained in a supercooled state down to very low temperatures and eventually settled into a glass. The polymerization kinetics could be interpreted, taking into account the heterogeneous nature of the reaction medium (*6, 7*).

More recently, acrylonitrile dissolved in vitreous methyltetrahydrofuran was irradiated at −196°C. and found to polymerize by an anionic mechanism (*3, 4*). Here again the rates exhibited a maximum at low monomer concentrations.

The present report is devoted to recent studies on anionic and cationic polymerizations in various glasses. The new results give better insight into the mechanism of these processes.

Publication Date: January 1, 1968 | doi: 10.1021/ba-1968-0082.ch035

Experimental

Acrylonitrile, styrene, and isobutylene were irradiated at low temperatures in binary mixtures with either low molecular weight compounds or polymers. The reagents were mixed at room temperature, sealed under vacuum, and the resulting liquid or swollen polymer was rapidly cooled to the irradiation temperature. Irradiations were carried out with cobalt-60 gamma-rays at a dose rate of 2000 rads/min. After irradiation the samples were warmed to room temperature under two different standard conditions. The sealed ampoules were either immersed in a water bath at 25°C. immediately after irradiation or first opened at −196°C. and then stirred in a large excess of warm acetone. The polymer was separated and dried to constant weight.

Results

Anionic Polymerizations (*15*). These experiments were performed with acrylonitrile. To favor the anionic polymerization, *N,N*-dimethylformamide (DMF), triethylamine (TEA), and isopropylamine (IPA) were selected as solvents. Acrylonitrile, *N,N*-dimethylformamide, and isopropylamine easily crystallize on cooling. Triethylamine, on the other hand, forms a glass below −170°C. Some of the binary mixtures investigated were partially crystalline at −196°C., but optically clear glasses were found over limited ranges of concentrations. Glass transition temperatures (T_g) were determined by differential thermal analysis (DTA). Some of the data are listed in Table I. No phase separation could be detected in any of the vitreous mixtures.

Table I. Structure of Solid Mixtures of Acrylonitrile (AN) with Dimethylformamide (DMF), Triethylamine (TEA), and Isopropylamine (IPA)

Composition	*Structure*	T_g, °C.
More than 75% DMF	Crystalline	−156
30% AN + 70% DMF	Glass	—
50% AN + 50% DMF		−160
60% AN + 40% DMF		−163
More than 60% AN	Crystalline	—
Pure TEA	Glass	−170
10% AN + 90% TEA		−160
15% AN + 85% TEA		−157
20% AN + 80% TEA		−160
More than 20% AN	Crystalline	—
More than 80% IPA	Crystalline	—
20% AN + 80% IPA	Glass	−139
30% AN + 70% IPA		−133
50% AN + 50% IPA		−138
60% AN + 40% IPA		−160
More than 70% AN	Crystalline	—

The polymerization was studied at different temperatures. Figure 1 shows the conversion curves obtained with a 30% solution of acrylonitrile in DMF at −196°, −155° and −150°C. It appears that at −196°C. the conversion reaches a limiting value, whereas above the glass transition temperature (−156°C.) the polymerization proceeds with a constant rate up to high conversions. This observation is discussed below. Figure 2 shows the relation between the composition of the binary mixtures and the rate of conversion at −196°C. In all cases, the rate is highest in

those mixtures which are vitreous at −196°C. The reaction is strongly retarded by moisture and inhibited by acetone; moreover, copolymerization studies with methyl methacrylate demonstrated that the reaction proceeds by an anionic mechanism.

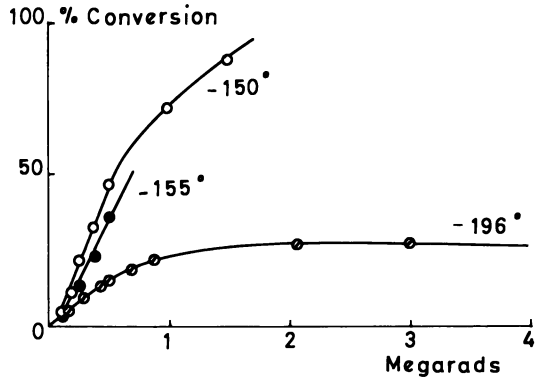

Figure 1. Conversion curves of a 30% solution of acrylonitrile in DMF at −196°, −155°, and −150°C. Dose rate, 2000 rads/min.

In all the above-described experiments the irradiated mixtures were allowed to warm to room temperature under vacuum. In one series of experiments, the ampoules were opened at −196°C., and their contents melted in the presence of acetone (an inhibitor of ionic polymerizations) according to the procedure described above. Under such conditions no polymer was obtained after irradiation at −196°C. Hence, the conversion curve for −196°C. in Figure 1 and the rate curves in Figure 2 pertain to polymer formed as a result of an anionic "after-effect" which occurs during the warming of the irradiated mixture under vacuum.

Trapped ionic species are created during irradiation at −196°C., as suggested by the bright green color of the irradiated glass. The shape of the conversion curve for the after-effect, obtained at −196°C. (Figure 1), indicates that the population of trapped ions reaches a limit for a certain dose, beyond which the average distance between ion pairs presumably precludes further trapping.

To gain more information on the reaction, irradiations were performed at different temperatures, and the reaction mixture was submitted to the two different treatments described above. The results obtained with a 30% solution of acrylonitrile in dimethylformamide and a 15% solution in triethylamine are shown in Figures 3 and 4, respectively. It appears that a very fast polymerization occurs in a narrow temperature

Publication Date: January 1, 1968 | doi: 10.1021/ba-1968-0082.ch035

range, a few degrees above the glass transition point. Below this temperature an after-effect occurs, while the mixture is warmed under vacuum. This after-effect is completely inhibited by acetone. Under irradiation near T_g, the trapping of ionic species is much less pronounced or even nil; most ions initiate chain propagation during irradiation. The resulting conversion curves do not reach a limiting plateau (Figure 1), and the after-effects on warming are small (Figure 3). At higher temperatures no polymer is formed in the range of doses used. It is believed that the ionic species produced by the radiation recombine rapidly in the liquid, thereby preventing long kinetic chains from developing.

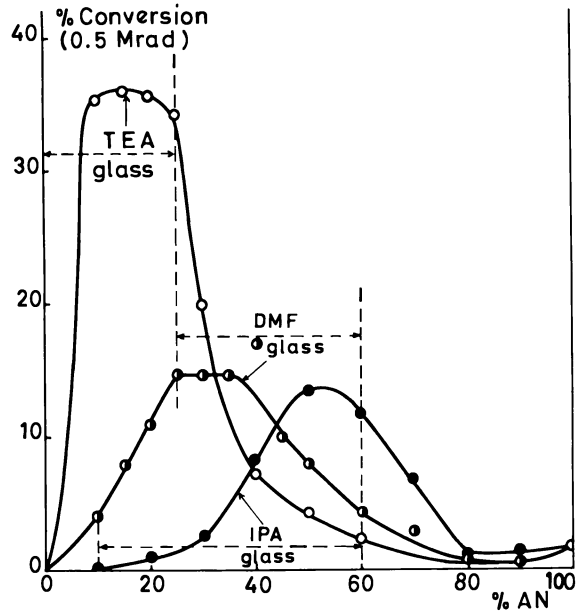

Figure 2. Conversion rates as a function of monomer content in mixtures of acrylonitrile with DMF, TEA, and IPA. Irradiation temperature, −196°C.

These results demonstrate that in a narrow temperature range, a few degrees above T_g, the reaction medium is particularly suitable for chain propagation. This medium is a highly viscous liquid in which molecular diffusion seems to be limited but sufficient to ensure chain propagation.

The results further indicate that no chain propagation occurs below T_g. Recombination of ion pairs occurs, however, in the glass, even at

very low temperatures as shown (a) by the shape of the conversion curve at −196°C., involving an after-effect (Figure 1), and (b) by the drop in the amount of polymer formed in the after-effect as the irradiation temperature rises from −196°C. to T_g (Figures 3 and 4).

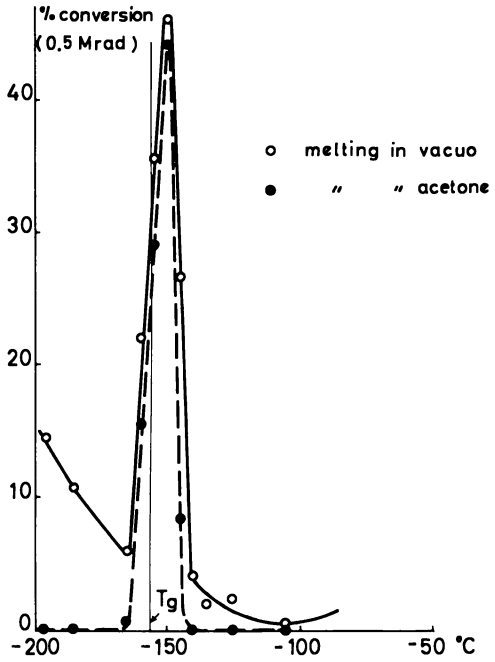

Figure 3. Conversion rates as a function of irradiation temperature for 30% solutions of acrylonitrile in DMF. Open circles and solid curve, for melting in vacuo; *solid circles and broken curve, for melting in acetone*

Moreover, if a vitreous mixture, irradiated at −196°C., was very slowly warmed to room temperature, much less polymer formed than when it was warmed rapidly. Hence, there must be a temperature range below T_g where ion pairs recombine without initiating polymerization.

The above data show that ions are trapped in vitreous mixtures irradiated below T_g. They slowly recombine, a process which requires a certain mobility in the glass. The rate of recombination (and hence mobility) increases as the temperature rises and approaches T_g. Chain propagation, however, only sets in at T_g, and its rate increases rapidly a few degrees above this temperature.

The G value of chain initiation derived from [weight of polymer]/[molecular weight] exhibits a maximum in the same temperature range

as the rate. Figure 5 shows the data for a 30% solution of acrylonitrile in DMF. G (initiation) seems to be higher than 4 at the maximum. In the temperature range where polymerization occurs during irradiation, the G value is higher for the mixtures allowed to warm under vacuum (Curve 1). This suggests that some active centers (perhaps radicals) are still trapped at these temperatures. At −196°C. the G value of trapped initiating centers is 2.6.

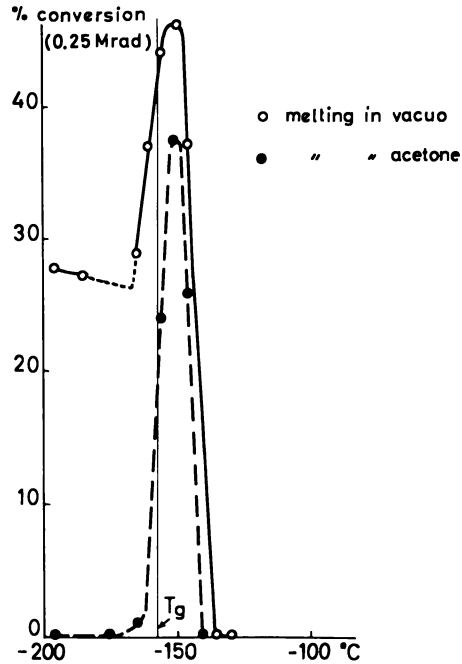

Figure 4. Conversion rates as a function of irradiation temperature for 15% solutions of acrylonitrile in TEA. Open circles and solid curve, for melting in vacuo; *solid circles and broken curve, for melting in acetone*

Cationic Polymerization (*15*). Styrene was used as the monomer, and hexachlorobutadiene (HCBu) and methylene chloride ($MeCl_2$) were selected as admixtures to favor the cationic reaction. The binary mixtures are vitreous over limited concentration ranges (*see* Table II).

The polymerization rate exhibits a maximum in those mixtures which form optically clear glasses. The reaction is sensitive to moisture and strongly inhibited by acetone. Vitreous mixtures irradiated below T_g turn reddish-brown, indicating the presence of trapped ionic species.

Publication Date: January 1, 1968 | doi: 10.1021/ba-1968-0082.ch035

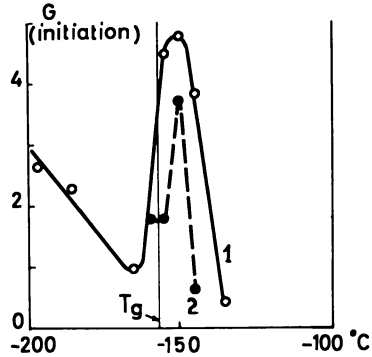

Figure 5. Influence of irradiation temperature on G *values of chain initiation for 30% solutions of acrylonitrile in DMF derived from the ratio [yield of polymer] / [molecular weight]*

Curve 1: melting in vacuo
Curve 2: melting in acetone

Table II. Structure of Solid Mixtures of Styrene (St) with Hexachlorobutadiene (HCBu) and Methylene Chloride ($MeCl_2$)

Composition	*Structure*	T_g, °C.
Pure HCBu	Glass	−106
20% St + 80% HCBu		−113
40% St + 60% HCBu		−120
More than 60% St	Crystalline	—
More than 80% $MeCl_2$	Crystalline	—
20% St + 80% $MeCl_2$	Glass	−162
40% St + 60% $MeCl_2$		−160
More than 40% St	Crystalline	—

Under comparable conditions and for the same dose, the amount of polymer formed is one order of magnitude smaller than in the anionic reaction with acrylonitrile.

The influence of irradiation temperature on the conversion in a 35% solution of styrene in hexachlorobutadiene is shown in Figure 6. The reaction mixtures were allowed to warm to room temperature under vacuum. Here again, the plot exhibits a sharp maximum for irradiations near T_g. An interesting feature of this system is that the monomer polymerizes in the liquid phase at temperatures greatly above T_g. The reaction rate is, however, much lower than that near T_g. This clearly demonstrates that favorable reaction conditions arise in the system in a narrow temperature range around T_g.

Publication Date: January 1, 1968 | doi: 10.1021/ba-1968-0082.ch035

In a recent publication Okamura *et al.* (*12*) describe similar results in a different system. It is believed that the unusual rate increase observed in these various systems which are chemically so different is caused by the physical state of the reaction medium at temperatures a few degrees above T_g. The high viscosity of this gel-like medium presumably favors chain propagation in its competition with termination. This effect, which is kinetically similar to the "gel-effect" in free radical polymerizations, can only arise if the termination step (charge recombination) becomes diffusion controlled. The latter process would arise if both ionic species involved in the reaction were of macromolecular size. This is undoubtedly true for the growing chain, but the mobility of the counter ion should only be significantly reduced in such a medium if it is of a polymolecular structure, involving perhaps a voluminous solvation cluster.

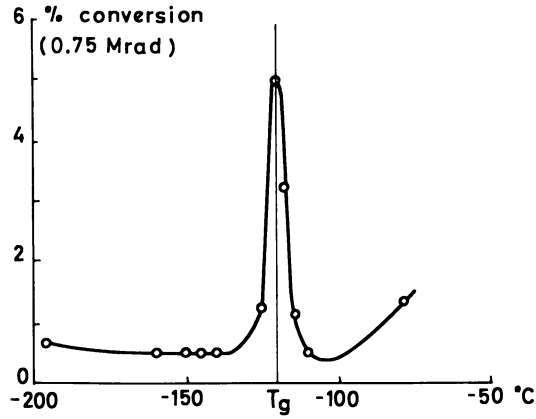

Figure 6. Rates of conversion as a function of irradiation temperature for 35% solutions of styrene in hexachlorobutadiene

Polymerization in Polymeric Glasses (*10, 11*). Poly(vinyl chloride) (PVC) films 0.35 mm. thick were used as a matrix. The pure polymer has a glass transition point at *ca.* +80°C. When soaked in a monomer at room temperature PVC swells slightly and softens. This plasticized polymer vitrifies again at low temperature.

The polymer films were immersed at 25°C. and under vacuum in various monomers until equilibrium swelling was reached. The samples were cooled to −78° or −196°C. and irradiated at these temperatures. Various additives were used to determine reaction mechanisms. Copolymerization studies were also conducted under the same reaction conditions.

It was found (*11*) that while acrylonitrile and methyl methacrylate polymerized by a free radical mechanism, styrene led to both cationic and free radical intermediates. Graft copolymers were formed in the process.

To establish a purely ionic reaction, experiments were conducted with isobutylene, a monomer known to react exclusively with cationic initiators. Chloroform was added to the systems to ensure better polymer swelling. Under these conditions polymerization occurred, the monomer being grafted onto the PVC films. Conversion curves are shown in Figure 7. A limiting conversion is reached after a dose of *ca.* 8 Mrad, corresponding to a grafting ratio of 22%.

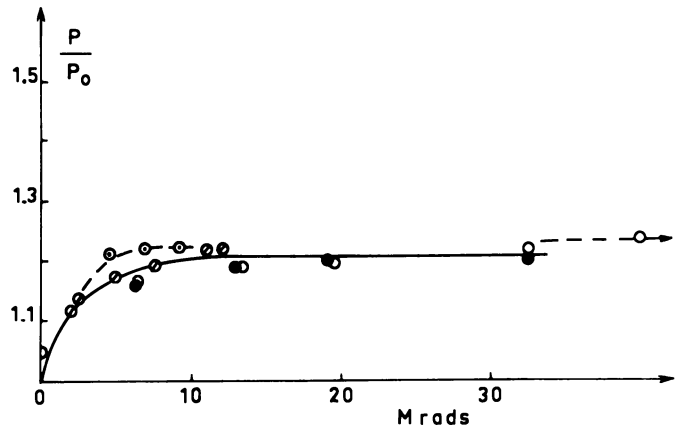

Figure 7. Grafting ratios of PVC films swollen at 25°C. in a 25% solution of isobutylene in chloroform and subjected to cobalt-60 gamma-rays or 7 Mev. electrons at −78°C. Broken curve corresponds to intermittent irradiation

The results show that polymerizations in polymeric glasses follow kinetics comparable with those observed in the low molecular, vitreous mixtures described above. In the present system PVC acts like many other chlorinated compounds and favors a cationic polymerization of those monomers which polymerize by this mechanism. It is most likely that here again propagation does not occur in the glass but at a temperature close to T_g.

An interesting conclusion can be derived from the fact that radiation initiates cationic grafting of isobutylene. Since chain transfer is usually small in such systems, it seems pertinent to assume that the reaction is initiated by a polymeric ion and moreover that this ion attaches itself

to the olefin with which it reacts. The following sequence of reactions could account for the observation.

Ionization

(1)

Chain Initiation

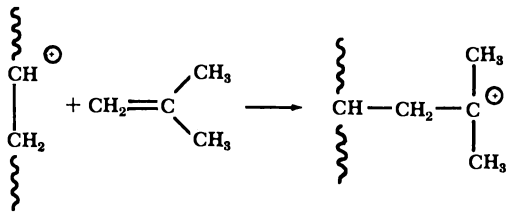

(2)

Propagation

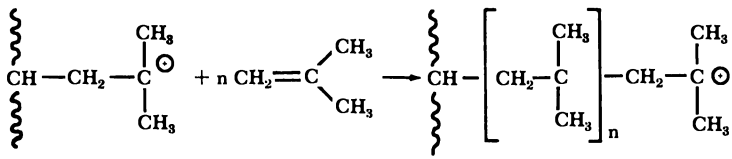

(3)

Termination presumably results from the interaction of a growing chain end with a chloride ion. Step 2 is an ion-molecule reaction in which molecular attachment occurs *via* electron transfer. The proposed reaction mechanism accounts for the rate increase of radiation-initiated cationic polymerizations observed in the presence of chlorinated compounds. It suggests further that an initial ion derived from the chlorinated compound becomes chemically bonded to the polymeric chain.

Conclusion

Our results throw some light on the behavior of ions in irradiated glasses. The polymerization data show that both cations and anions may become trapped at low temperatures. These ions undergo charge recombination while still entrapped in the vitreous phase, but ionic chains only develop at, or above, the glass transition temperature. The grafting data further suggest that positive ions, resulting from the radiolysis of chlorinated substances, can react with olefins by attaching themselves to the olefin molecule *via* an electron transfer process.

Publication Date: January 1, 1968 | doi: 10.1021/ba-1968-0082.ch035

Literature Cited

(1) Amagi, Y., Chapiro, A., *J. Chim. Phys.* **59,** 537 (1962).
(2) Barkalov, I., Goldanskii, V. I., Enikolopian, N. S., Terekhova, S. F., Trofimova, G. M., *Dokl. Akad. Nauk. SSSR* **147,** 395 (1962); *J. Polymer Sci. Ser. C* **4,** 909 (1964).
(3) Bodard, M., Ph.D. Thesis, University of Paris, 1967.
(4) Bodard, M., Marx, R., *Intern. Symp. Macromol. Chem., Prague, 1965,* "Preprint," p. 452.
(5) Chapiro, A., Pertessis, M., *J. Chim. Phys.* **61,** 991 (1964).
(6) Chapiro, A., Nakashio, S., *J. Chim. Phys.* **63,** 1031 (1966).
(7) Chapiro, A., Roussel, D., *J. Polymer Sci. Ser. C* **16,** 3011 (1967).
(8) Chapiro, A., Perec, L., *J. Chim. Phys.* **63,** 842 (1966).
(9) Chapiro, A., Jendrychowska-Bonamour, A. M., Roussel, D., *Compt. Rend. Acad. Sci.* **258,** 914 (1964).
(10) Chapiro, A., Jendrychowska-Bonamour, A. M., *Compt. Rend. Acad. Sci.* **265,** 484 (1967).
(11) Jendrychowska-Bonamour, A. M., *European Polym. J.,* in press.
(12) Katsu, I., Tsuji, K., Hayashi, K., Okamura, S., *J. Polymer Sci. Ser. A-1,* **5,** 1899 (1967).
(13) Mezhirova, L. P., Sheinker, A. P., Abkin, A. D., *Vysokomol. Soed.* **3,** 99 (1961).
(14) *Ibid.,* **5,** 473 (1963).
(15) Perec, L., Ph.D. Thesis, University of Paris, 1968.
(16) Pinner, S. H., "The Chemistry of Cationic Polymerization," P. H. Plesch, ed., pp. 611-671, Pergamon Press, London, 1963.
(17) Spritzer, C., Sella, C., Chapiro, A., *Compt. Rend. Acad. Sci.* **260,** 2789 (1965).
(18) *Ibid.,* **261,** 1275 (1965).

RECEIVED January 19, 1968.

The Ultraviolet and Infrared Spectra of Free Radicals in Irradiated Polyethylene

MALCOLM DOLE

Department of Chemistry and Materials Research Center, Northwestern University, Evanston, Ill. 60201

G. G. A. BÖHM

Radiation Processing Research, Long Island, N. Y. 11590

Publication Date: January 1, 1968 | doi: 10.1021/ba-1968-0082.ch036

Transient as well as stable ultraviolet absorption bands are produced during the γ-ray or electron beam irradiation of polyethylene. These bands have been observed subsequent to the irradiation at temperatures varying from 77°K. to 120°C., and from the variation in their intensities conclusions concerning the mechanism of their formation and decay can be postulated. The assignment of the bands to specific ultraviolet absorbing groups has been aided by theoretical predictions and by the work of others on low molecular weight compounds studied either in the gas phase or in frozen matrices. Ultraviolet spectroscopy is a valuable complement to ESR techniques in studying transient free radicals in irradiated polyethylene.

The ultraviolet absorption spectra of allyl type free radicals have been studied by a number of workers. One of the earliest investigations was that of Porter and Strachan (*16*) who photolyzed toluene, ethylbenzene, isopropylbenzene, and *tert*-butylbenzene and obtained the wavelengths of the maximum of the most intense absorption bands given in Table I. The medium for the production of their free radicals was 10^{-2} molar solutions of benzene or toluene in a frozen glass composed of three parts of isopentane and two parts of methylcyclohexane at liquid nitrogen temperature. Very recently Sauer and Ward (*17*) produced the cyclohexadienyl and methylcyclohexadienyl free radicals by pulse radiolysis of a gaseous mixture of 50 atm. of argon and 5 atm. of hydrogen containing a few cm. pressure of benzene or toluene. The free radicals were

In Radiation Chemistry; Hart, E.;
Advances in Chemistry; American Chemical Society: Washington, DC, 1968.

formed on the addition of hydrogen atoms to the aromatic ring. They could also make the same free radicals by pulse radiolysis of a mixture made by dissolving a solution of the hydrocarbon in methanol in triply distilled water. The λ_{max} values of the absorption bands observed by them, Table I, were smaller than those of the benzyl or substituted benzyl free radicals given by Porter and Strachan as would be expected because of (1) the difference in the medium, and (2) the fewer number of double bonds in resonance with the unpaired electron.

Hamill, Guarino, and Ronayne (*11*) gamma irradiated 0.18 mole % benzyl chloride in glassy 2-methyltetrahydrofuran (MTHF) at liquid nitrogen temperature and obtained a maximum ultraviolet absorption band at 320 mμ in agreement with Porter and Strachan, *see* Table I. They also irradiated 1.0 mole % allyl chloride, allyl bromide and allyl alcohol in 3-methylpentane (3-MP) and in all cases observed a maximum absorption band at 228 mμ which they attributed to the allyl free radical. They also irradiated 3-chloro-1-butene and 3-chlorocyclohexene in 3-MP and determined the wavelengths of the absorption band maxima of the 1-methyl allyl and 2-cyclohexen-1-yl free radicals given in Table I.

Currie and Ramsay (*8*) discovered a diffuse system of absorption bands between 370 and 410 mμ during the gas phase photolysis of a number of allyl compounds. This absorption probably represents the weak absorption predicted by Longuet-Higgins and Pople (*12*) on the basis of their quantum mechanical calculations. Longuet-Higgins and Pople had also predicted a strong absorption band of the allyl free radical at 234 mμ. This last value is very close to the observations of Hamill *et al.* for the unsubstituted allyl free radical given in Table I.

Recently Burrell and Bhattacharyya (*4*) pulse radiolyzed a solution of allyl bromide in cyclohexane and observed a transient ultraviolet absorption band at 310 mμ which they attributed to the allyl free radical. Their optical technique did not permit them to study the absorption bands below 290 mμ. Another recent investigation was that of Callear and Lee (*5*) who flash-photolyzed gas mixtures of 1-butene with argon and isobutylene with argon. The most intense band observed by them in the case of 1-butene was at 225 mμ which they attributed to the allyl free radical in essential agreement with the work of Hamill *et al.* (*11*) mentioned above. For the isobutylene photolysis, the most intense observed band was at 238 mμ and this was assigned to the β-methallyl radical, *see* Table I.

When polyethylene is irradiated at room temperature, allyl and polyenyl type free radicals are formed (*2*) and are much more stable than alkyl type free radicals (*7, 13*). Electron spin resonance (ESR) experiments have demonstrated that the allyl or polyenyl free radicals are quite stable, persisting for relatively long periods (hours or days)

Publication Date: January 1, 1968 | doi: 10.1021/ba-1968-0082.ch036

in vacuo at room temperature. Thus, irradiated polyethylene serves as an excellent medium for the observation of the ultraviolet spectra of the different polyenyl type free radicals. Because the wavelengths of the absorption maxima of the different polyenyl species of the type $—\dot{C}H(CH{=}CH—)_nCH_2—$ are displaced from each other by about 40 mμ for each unit increase in n (except for the interval $n = 1$ to $n = 2$) (2), the separate polyenyl species are readily identified and studied. Inasmuch as their ESR spectra tend to overlap each other, ultraviolet spectroscopy in this case serves as a valuable complement to ESR spectroscopy.

Table I. Ultraviolet Absorption Spectra of Allyl Type Free Radicals

Parent Molecule[a]	*Medium*	*Free Radical*	*Wavelength of Absorption Maximum, mμ*	*Ref.*
$CH_3CH_2CH{=}CH_2$	4 mm. 1-butene + 100 mm. Ar	$CH_2{=}CH—CH_2\cdot$	225	*5*
$CH_2{=}CH—CH_2Cl$	3 MP[b]	$CH_2{=}CH—CH_2\cdot$	228	*11*
$CH_2{=}CH—CH_2Br$	3 MP[b]	$CH_2{=}CH—CH_2\cdot$	228	*11*
$CH_2{=}CH—CH_2OH$	3 MP[b]	$CH_2{=}CH—CH_2\cdot$	228	*11*
$(CH_3)_2C{=}CH_2$	0.5 mm. isobutylene + 100 mm. Ar	$\cdot CH_2—\overset{CH_3}{\overset{\vert}{C}}{=}CH_2$	238	*5*
$CH_3CHClCH{=}CH_2$	3 MP	$CH_3\dot{C}HCH{=}CH_2$	246	*11*
3-Chloro-cyclohexene-1	3 MP	c-$C_6H_9\cdot$	253	*11*
$CH_2BrCH{=}CH_2$	liquid c-C_6H_{12}	$CH_2{=}CH—CH_2\cdot$ (?)	310	*4*
ϕH	50 atm. Ar[c]	c—C_6H_7	302	*17*
ϕH	liq. H_2O	c—C_6H_7	311	*17*
ϕCH_3	50 atm. Ar	c—$C_6H_6CH_3$	307	*17*
ϕCH_3	liq. H_2O	c—$C_6H_6CH_3$	315	*17*
ϕCH_3	MP[d]	$\phi CH_2\cdot$	318.7	*16*
ϕCH_2Cl	MTHF[e]	$\phi CH_2\cdot$	320	*11*
ϕCH_2CH_3	MP	$\phi\dot{C}HCH_3$	322.2	*16*
$\phi CH(CH_3)_2$	MP	$\phi\dot{C}(CH_3)_2$	324.2	*16*
$\phi C(CH_3)_3$	MP	$\phi\dot{C}(CH_3)_2$	324.2	*16*

[a] ϕ represents C_6H_5.
[b] 3 MP represents 3-methylpentane.
[c] The 50 atm. Ar also contained 5 atm. H_2.
[d] MP represents a solution consisting of three parts of isopentane and two parts of methylcyclohexane.
[e] MTHF represents 2-methyltetrahydrofuran.

Irradiated polyethylene can also be used for the study of the infrared absorption bands of allyl type free radicals. Slovokhotova, Koritskii, and Buben (*18*) irradiated a low density polyethylene to 206 Mrads at −100°C. and observed, among other bands, a band at 944 cm.$^{-1}$ which disappeared on heating. They assigned this band to the chain (disubstituted) allyl group, —CH=CH—CH—. This band corresponds to the 968 cm.$^{-1}$ band of the vinylene group, —CH=CH—, which is attributed to out of plane deformations of the C—H bond. In the case of the conjugated polyenes, —(CH=CH—)$_n$, the extinction coefficient increases linearly with n, and we can expect the same for the polyenyl free radicals. Furthermore, the conjugated polyene infrared absorption bands equivalent to the 986 band of the vinylene group absorb very near to 986 cm.$^{-1}$. We could also expect the polyenyl free radicals similarly to absorb close to 944 cm.$^{-1}$, the absorption band in the infrared of the allyl group, but the extinction coefficient should increase linearly with the number of C—H bonds in the absorbing group. Infrared studies should not, however, be as useful in following the separate polyenyl species as ultraviolet spectroscopy.

Publication Date: January 1, 1968 | doi: 10.1021/ba-1968-0082.ch036

Experimental

For our ultraviolet and infrared studies we have used the combined irradiation and spectroscopic cell illustrated in Figure 1. In this cell the reservoir *A* is for liquid nitrogen, and the compartment in which the thin film (~20 μ thick for the ultraviolet measurements and ~150 μ for the infrared) is held at *L*. The thin strips, *J*, conduct heat away from the sample block, and they also can be heated electrically to raise the temperature of the film. During the irradiation the windows *M* are not in place, but the irradiation occurs through an inner window at *L* which is held in place by the pressure of the ambient atmosphere inasmuch as the sample compartment is evacuated through *B*. After the irradiation with the film still at liquid nitrogen temperature and in vacuo, the windows at *M* can be attached and the space between *L* and *M* evacuated. With reduction of pressure on the outside of *L*, the windows at *L* fall off, and can be rolled aside; at the same time the windows at *M* are held firmly in place. In this way the windows through which the high energy radiation (γ-rays or electron beam) passes do not have to be the same as the windows through which the ultraviolet or infrared spectra are taken. Furthermore, during this entire window changing procedure, the irradiated film is held *in vacuo* and at liquid nitrogen temperature. The cell illustrated in Figure 1 is a modification of that previously described by Dole and Böhm (*9*). The reader is referred to the latter paper for additional details.

In studying the polyenyl free radical decay at temperatures above room temperature by ultraviolet spectroscopy, the polyethylene was melted onto a quartz disc *in vacuo*, and, after cooling, irradiated, and subsequently annealed while firmly stuck to the quartz disc. This was

done to avoid temperature build up in the film, either during the irradiation or the annealing experiments.

The polyethylene used for the experiments was antioxidant-free Marlex-6009 and Marlex-6002 (not antioxidant-free) linear polyethylene. The dose rate of the electron beam irradiation was about 40 Mrads per hour. Most of the data were taken on Marlex-6009 polyethylene, but no difference could be detected in the behavior of the two samples as far as the spectroscopic studies are concerned.

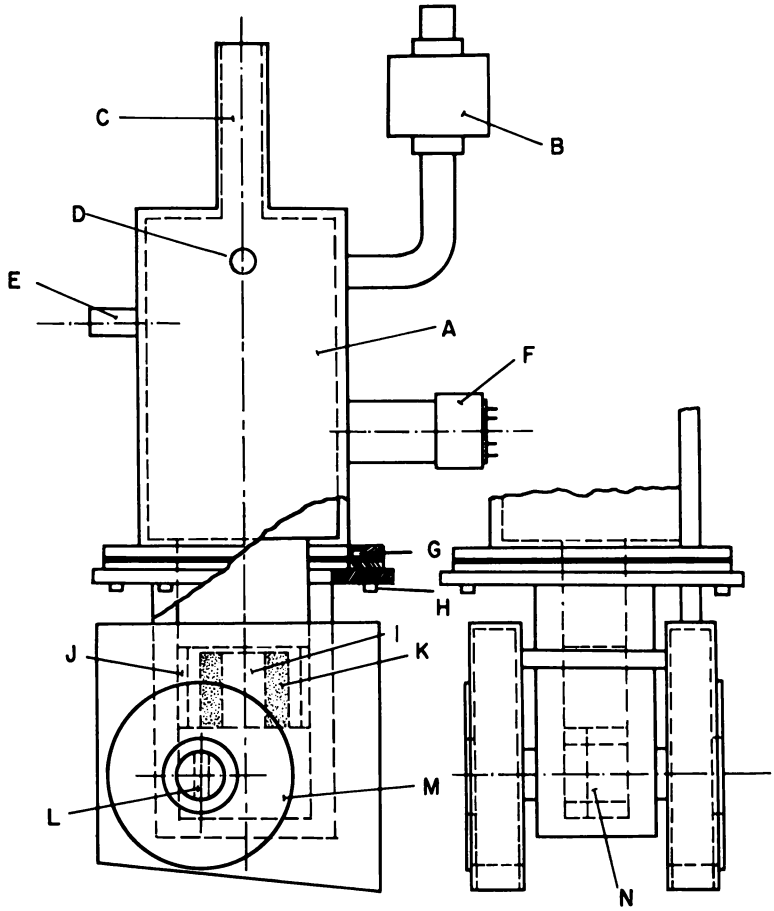

Figure 1. Combined ultraviolet and infrared spectroscopic cell and irradiation cell

Ultraviolet Spectra

Typical ultraviolet spectra are illustrated in Figure 2 in which the absorbance is plotted as a function of the wavelength for Marlex-6009

Publication Date: January 1, 1968 | doi: 10.1021/ba-1968-0082.ch036

polyethylene irradiated at liquid nitrogen temperature in vacuum to about 40 Mrads with the electron beam. Curve 1 immediately after the irradiation; curve 2 after annealing at 150°K. for about an hour; Curve 3, after annealing at room temperature *in vacuo* for three hours and curve 4, after exposure to air at room temperature for four days. All the curves of Figure 2 were taken at 77°K.

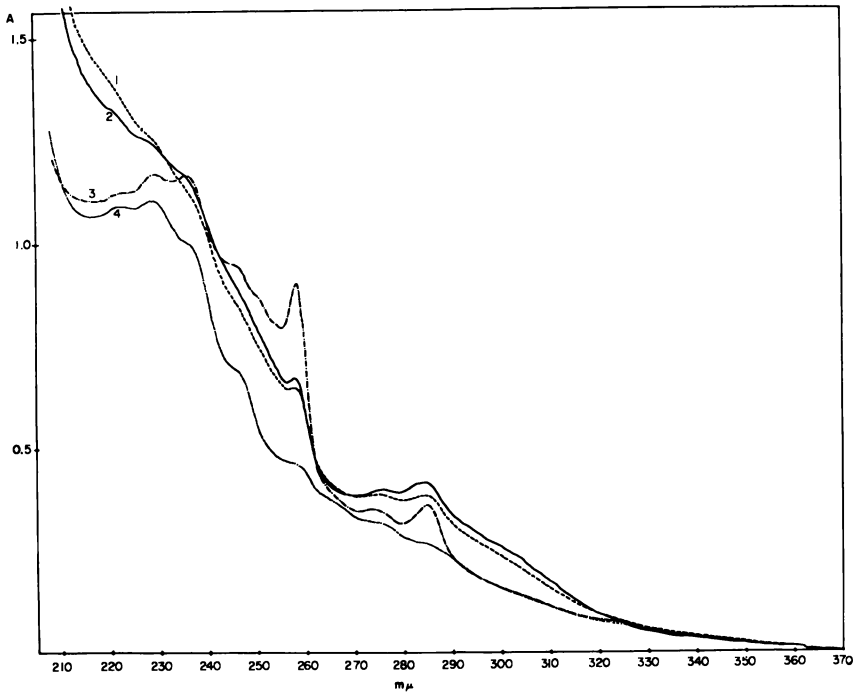

Figure 2. Ultraviolet absorbance as a function of wavelength. All spectra taken at liquid nitrogen temperature. Marlex-6002 linear polyethylene irradiated in vacuum at liquid nitrogen temperature to 40 Mrads. Curve 1, immediately after the irradiation; curve 2, after annealing at 150°K. in vacuum for one hour; curve 3, after annealing at room temperature in vacuum for three hours; Curve 4, after exposure to air at room temperature for four days

There are several interesting phenomena to be noted in studying these curves. First, annealing at 150°K. decreases the absorption at 215 mμ, but increases it slightly at 258, 285 and in the 300 to 315 mμ region. Heating to room temperature essentially causes the complete disappearance of the 215 mμ absorption band, while at the same time the 258 band is considerably enhanced. The general absorption in the 300 mμ region has also completely disappeared. When the latter is allowed for, the peak at 285 mμ can be shown to have been slightly

Publication Date: January 1, 1968 | doi: 10.1021/ba-1968-0082.ch036

enhanced by heating to room temperature. On exposure to air, the absorption owing to all of the reactive species has disappeared, leaving behind that caused by the stable diene at 236 mμ and triene at 275; these last two absorptions consist of three bands each, *see* Bodily and Dole (*2*).

Inasmuch as ESR studies of Cracco, Arvia, and Dole (*7*) showed that the alkyl type free radicals began to decay at 150°K. and were largely annealed out on heating at room temperature for three hours (although not completely), we suggest that the ultraviolet absorption in the 210 mμ region is to be assigned to the secondary alkyl free radical, $—CH_2\dot{C}HCH_2—$. At the time of writing we have under way experiments designed to test this hypothesis by a careful comparison of the rate of decrease of the ultraviolet band at 210 mμ with the rate of decrease of the alkyl free radical ESR signal, $CH_3\cdot$. It should be noted that Callear and Lee (*5*) observed that the methyl free radical, $CH_3\cdot$, absorbed at 216 mμ.

We believe that the absorption band at 258 mμ is to be attributed to the allyl free radical in irradiated polyethylene because of the following reasons: (1) the band wavelength is close to that observed by Hamill *et al.* (*11*) for the $CH_3\dot{C}HCH{=}CH_2$ free radical, 246 mμ, and for the c-C_6H_9. (2-cyclohexene-1-yl) free radical, 253 mμ. The wavelength is higher than that of the unsubstituted allyl free radical, 228 (*see* Table I), but this would be expected. (2) The 258 mμ peak disappears on irradiation with ultraviolet light at liquid nitrogen temperature and reappears on subsequent annealing at room temperature as noted by Bodily and Dole (*3*) following earlier work of Ohnishi *et al.* (*14*) and others who used ESR detection techniques.

In the pulse radiolysis of solutions of allyl bromide in cyclohexane Burrell and Bhattacharyya (*4*) observed a transient ultraviolet absorption band at 310 mμ which they attributed to the allyl free radical. In light of the other values of the allyl free radical given in Table I it is doubtful that the 310 mμ band can be attributed to the simple, unsubstituted allyl free radical. The band was not observed after a pulse radiolysis of the pure cyclohexane solvent. There are several other species which it might be, but the problem has not been resolved as yet.

In the ultraviolet spectrum of polyethylene taken at 77°K. after an irradiation to a dose of 40 Mrads there is also a broad absorption band in the region of 310 mμ to be seen. This is shown more clearly in Figure 3 in terms of a plot of the difference in the absorbance between Curve 1 of Figure 2 and curve 2. Actually the ΔA values of Figure 3 were not calculated from curves 1 and 2 of Figure 2, but from similar curves observed in another experiment. It is unlikely that the 310 mμ band can be attributed to trapped electrons because the energy of this band, 4.0 e.v., is much greater than the depth of electron traps in polyethylene,

Publication Date: January 1, 1968 | doi: 10.1021/ba-1968-0082.ch036

which are 0.027, 0.21 and 0.44 e.v., *see* Charlesby and Partridge (*6*) and Partridge (*15*), and greater than the electron affinity of free radicals, probably about 1 e.v. Longuet-Higgins and Pople (*12*) have estimated that the energy of the lowest singlet state in the radical cation and anion is about 0.35 e.v. below that of the allyl free radical. This difference amounts to 17 mμ which is much less than the difference between 310 and 258 mμ. Thus, the problem of the assignment of the transient 310 mμ absorption band has yet to be resolved.

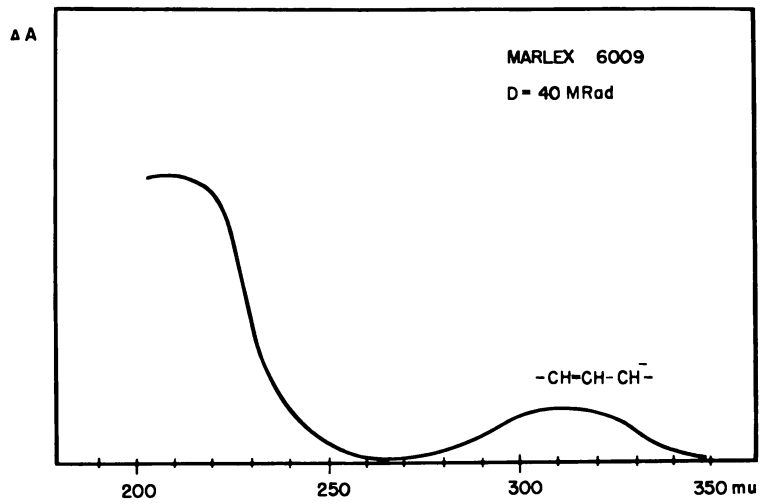

Figure 3. Absorbance of ultraviolet bands that anneal out at 150°K.

Another unresolved problem has to do with the type or types of allyl free radicals that we may be dealing with. In other words does the 258 mμ peak represent the terminal allyl free radical —ĊHCH=CH_2, or the chain, disubstituted allyl free radical, —CH_2ĊHCH=CHCH_2— ? Auerbach (*1*) believes that vinyl decay during the irradiation of Marlex-polyethylene leads to the formation of the allyl free radical. Indirect evidence for this mechanism of allyl free radical formation can be seen in some early results of Dole, Milner, and Williams (*10*) who demonstrated by means of infrared spectral measurements that vinyl decay occurred during the heating to room temperature after an irradiation at liquid nitrogen temperature. A similar increase in the allyl free radical concentration also occurs on heating to room temperature after a low temperature irradiation. Although vinyl decay may contribute to allyl free radical formation, it is not the only mechanism as is shown in the next section.

Publication Date: January 1, 1968 | doi: 10.1021/ba-1968-0082.ch036

Sauer and Ward (*17*), Table I, observed that the cyclodienyl free radical gave absorption maxima at 302 and 311 mμ, depending on the medium. These values are somewhat higher than the 285 mμ peak which we attribute to the linear dienyl free radical in irradiated polyethylene. On the other hand the benzyl free radicals observed by Porter and Strachan (*16*) all have absorption maxima in the range of the bands at 323 mμ in irradiated polyethylene which we attribute to the linear trienyl free radical. (The band at 323 mμ is clearly seen after the broad 310 peak has disappeared on warming to room temperature (2).)

Infrared Spectra

Another approach to the problem of the identification of transient species in irradiated polyethylene is through the use of infrared spectroscopy. Figure 4 illustrates some of the infrared absorption bands pertinent to this work. The spectra illustrated in Figure 4 were taken of polyethylene irradiated at 77°K., dotted line, and then after heating to

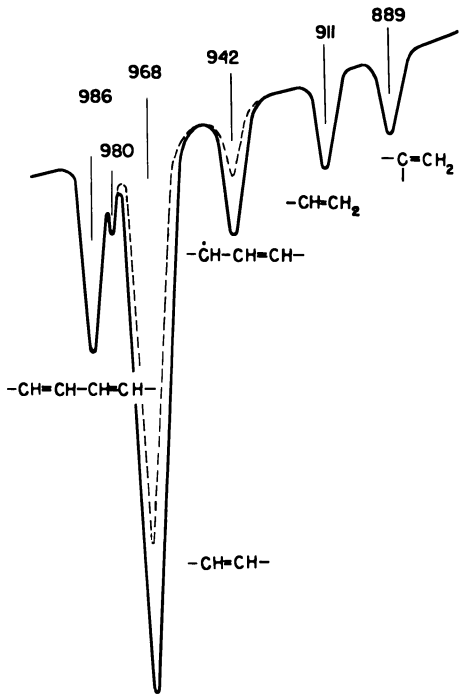

Figure 4. Infrared spectra of irradiated polyethylene. Dotted line, before annealing at room temperature. Solid line, after a room temperature annealing

Publication Date: January 1, 1968 | doi: 10.1021/ba-1968-0082.ch036

room temperature and recooling to liquid nitrogen temperature. Note the increase in the 968 cm.$^{-1}$ band owing to the vinylene group on annealing, as well as the increase in the 942 cm.$^{-1}$ band, that owing to the allyl free radical. In this experiment the vinyl band at 911 cm.$^{-1}$ showed no change on annealing. We interpret the changes in the 942 and 968 bands as resulting from decay reactions of the alkyl free radicals. The vinylene group would result from the recombination of alkyl free radicals on adjacent carbon atoms on the same chain after migration of either or both of the free radical centers to neighboring carbon atoms, while the allyl free radical would be formed by the migration of a free radical to a carbon atom next to a vinylene or vinyl double bond. Inasmuch as no change in the vinyl absorbance on annealing could be detected in this experiment, the increase in the allyl free radical abundance must have come to some extent, at least, from other processes than the decay of vinyl groups.

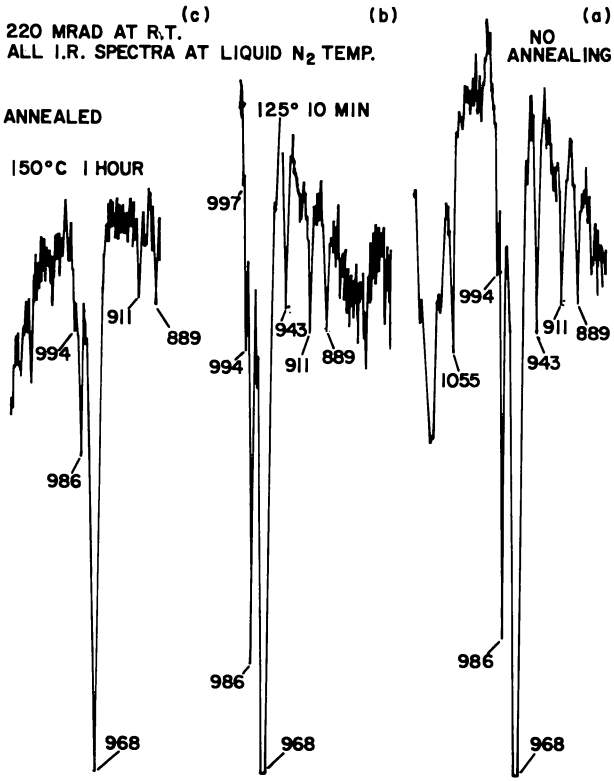

Figure 5. Infrared spectra taken at liquid nitrogen temperature of Marlex-6009 polyethylene irradiated to 220 Mrads at room temperature. Different spectra after different annealing times and temperatures

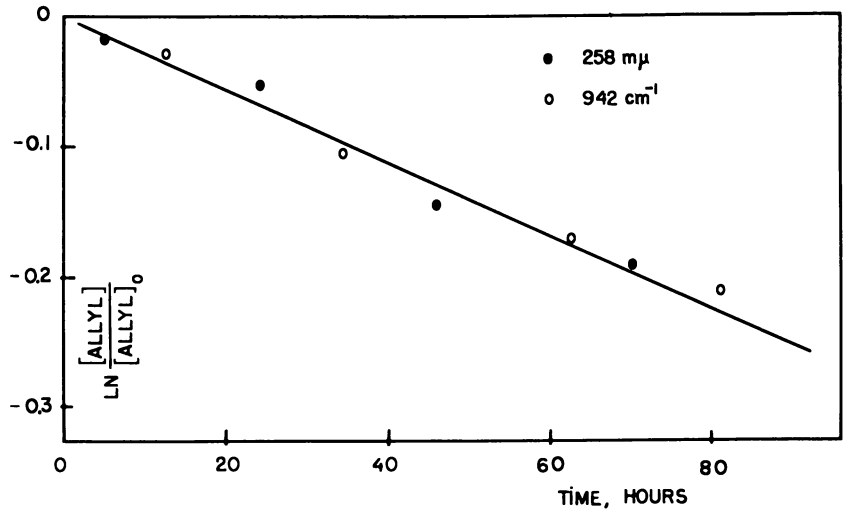

Figure 6. Comparison of the decay rates at room temperature of the absorption bands at 285 mμ and 942 cm.$^{-1}$

Figure 4 represents infrared spectra redrawn for clarity; in Figure 5 the actually observed curves are given. Observation of the infrared spectra at liquid nitrogen temperature sharpens the bands considerably over those observed at room temperature. In Figure 5, all of the spectra were taken at liquid nitrogen temperature. The most prominent band after the relatively heavy dose of 220 Mrads at room temperature is the 968 cm.$^{-1}$ band caused by the vinylene group, —CH=CH—. The band at 911 cm.$^{-1}$ is the vinyl group band and the bands at 986 and 994 cm.$^{-1}$ are probably caused by the conjugated diene and triene double bond groups or to cyclic structures or both. Of especial interest here is the 943 cm.$^{-1}$ band which is seen to be a transient, disappearing completely after annealing at 150°C. for one hour. Ultraviolet studies (to be published) have shown that the 258, 285 and 323 mμ bands assigned to the allyl, dienyl and trienyl free radicals all disappear on complete melting of the polyethylene. Thus, the 943 infrared band is to be assigned to these transient species, probaby to the allyl free radical. One way to test both this assignment and that of the 258 mμ band to the allyl free radical is to compare the rate of decay of these two bands on standing at room temperature. The result of this comparison is shown in Figure 6 where the very good correspondence of the decay rates of both can be seen. This agreement strengthens our assignment of the ultraviolet peak at 258 mμ to the allyl free radical in irradiated polyethylene.

Publication Date: January 1, 1968 | doi: 10.1021/ba-1968-0082.ch036

Acknowledgments

This reasearch was supported by the U. S. Atomic Energy Commission, Document No. AEC COO-1088-29, and by the Advanced Research Projects Agency of the Department of Defense through the Northwestern University Materials Research Center. We wish to thank Lloyd Cooke of the Union Carbide Corp. and James Reid of the Phillips Petroleum Co. for the gift of polyethylene samples.

Literature Cited

(1) Auerbach, I., *Polymer* **8,** 63 (1967).
(2) Bodily, D. M., Dole, M., *J. Chem. Phys.* **45,** 1428 (1966).
(3) *Ibid.*, **45,** 1433 (1966).
(4) Burrell, E. L., Jr., Bhattacharyya, P. K., *J. Phys. Chem.* **71,** 774 (1967).
(5) Callear, A. B., Lee, H. K., *Nature* **213,** 693 (1967).
(6) Charlesby, A., Partridge, R. H., *Proc. Roy. Soc. (London)* **271A,** 170 (1963).
(7) Cracco, F., Arvia, A. J., Dole, M., *J. Chem. Phys.* **37,** 2449 (1962).
(8) Currie, C. L., Ramsay, D. A., *J. Chem. Phys.* **45,** 488 (1966).
(9) Dole, M., Böhm, G. G. A., "Radiation Research," p. 274, North Holland Publishing Co., Amsterdam, 1967.
(10) Dole, M., Milner, D. C., Williams, T. F., *J. Am. Chem. Soc.* **80,** 1580 (1958).
(11) Hamill, W. H., Guarino, J. P., Ronayne, M. R., Ward, J. A., *Discussions Faraday Soc.* **36,** 169 (1963).
(12) Longuet-Higgins, H. C., Pople, J. A., *Proc. Phys. Soc. (London)* **A68,** 591 (1955).
(13) Ohnishi, S., Sugimoto, S., Nitta, I., *J. Chem. Phys.* **37,** 1283 (1962).
(14) *Ibid.*, **39,** 2647 (1963).
(15) Partridge, R. H., *J. Polymer Sci.* **3A,** 2817 (1965).
(16) Porter, G., Strachan, E., *Spectrochim. Acta* **12,** 299 (1958).
(17) Sauer, M. C., Jr., Ward, B., *J. Phys. Chem.* **71,** 3971 (1967).
(18) Slovokhotova, N. A., Koritskii, A. T., Buben, N. Ya., *Dokl. Akad. Nauk. Phys. Chem. Sect.* **129,** 1347 (1959); English Translation, *Consultant's Bureau*, p. 1145.

RECEIVED January 22, 1968.

GASES

Transition Yields in Irradiated Gases

CORNELIUS E. KLOTS, Health Physics Division, Oak Ridge National Laboratory, Oak Ridge, Tenn.

Yields are computed for a number of electronic transitions in gases under alpha-particle irradiation. The results are found to be usefully insensitive to approximations in the computational procedure. Comparison with experiment permits commentary on the latter. Deviations from the predictions of the optical approximation are interpreted as departures from high-energy equivalence.

Research sponsored by the U. S. Atomic Energy Commission under contract with Union Carbide Corp.

Publication Date: January 1, 1968 | doi: 10.1021/ba-1968-0082.ch037

A Microwave Cavity Method of Studying Recombination Following Pulse Radiolysis

M. S. ZUCKER and L. A. FERRARI, Brookhaven National Laboratory, Upton, Long Island, N. Y.

Microwave transmission through a cylindrical resonant cavity is used to study high density ($\sim 10^{13}$ e cm.$^{-3}$) low temperature (0.025 e.v. $\leqslant T \leqslant$ 0.050 e.v.) plasmas formed at high neutral pressures ($\sim$1 atmosphere) of various gases. A plasma column is formed by passing a pulsed beam of high energy electrons from a Van de Graaff accelerator along the axis of the cavity. The plasma starts to decay immediately after the pulse passes causing the resonant frequency of the cavity to shift with time. Since the resonant frequency can be correlated with plasma density, the latter can thus be followed as a function of time. Slater's perturbation theory can be relied upon to supply the relation between frequency shift and plasma density only when $(\omega_p/\omega) << 1$, where ω_p is the plasma, and $f = (\omega/2\pi)$ the microwave frequency. For $(\omega_p/\omega) \gtrsim 1$, and particularly when $(\nu/\omega) \ll 1$ (where ν is the collision frequency) it is necessary to solve exactly the field equations for a cavity with ionization present in it. The conditions $(\omega_p/\omega) \gtrsim 1$ and $(\nu/\omega) \gtrsim 1$ correspond precisely to that situation where a method utilizing an accelerator beam to produce uniform ionization is most appropriate, namely, for "dense" media with a high degree of ionization. The exact solution is known, and though complicated has been reduced to a computer code. The method is demonstrated for a situation where Slater's theory is valid. Choices of cavity dimension, microwave modes, etc., are discussed.

Gas-Phase Pulse Radiolysis of Oxygen and the Benzene-Argon-Hydrogen Systems

J. F. RILEY and R. W. CAHILL, Lockheed Palo Alto Research Laboratory, Palo Alto, Calif.

Lockheed Missiles & Space Co. (LMSC) has a gas-phase pulse radiolysis program funded by LMSC as an independent research project. The program began in 1967 although LMSC has operated a 2 Mev. Febetron since 1965. Our first pulse radiolysis experiments were to measure the rate of formation of ozone from oxygen at 200–800 torr. Ozone formation was pseudo-first order with a half-time of about 10 microseconds. The reaction was complete in 60 microseconds; ozone formation was followed by monitoring the optical absorption in the ultraviolet region on a microsecond time scale. A 9558Q EMI photomultiplier, 0.5 meter Ebert spectrometer, and Hg-Xe arc were used, together with a Tektronix 555 scope. The same apparatus was used to study two ternary systems: benzene-argon-hydrogen and benzene-argon-helium. In the region from 265 to 325 nanometers transient absorption spectra were recorded in both systems. The system containing hydrogen produced a spectrum characteristic of the cyclohexadienyl radical. We are making a detailed comparison of spectral differences and relative yields in the two systems.

Publication Date: January 1, 1968 | doi: 10.1021/ba-1968-0082.ch037

Solids

Growth and Decay Kinetics of Reaction Intermediates Formed in the Radiolysis of Organic Solids

JOHN E. WILLARD, University of Wisconsin, Madison, Wis.

This paper will discuss initial growth rates, steady-state plateau concentrations, and decay rates of trapped free radicals and other reaction intermediates produced by radiolysis of: (a) glassy and polycrystalline alkyl halides at 77°K.; (b) glassy hydrocarbon matrices containing dissolved alkyl halides at 77°K.; and (c) polycrystalline C_2Br_6. Evidence will be presented: (a) that most radicals combine with other radicals within the parent spur; (b) that in some systems combination is exclusively with the sibling partner; and (c) that the rate of decay of trapped radicals is "radiation catalyzed"—*i.e.*, is faster during exposure to ionizing radiation than in its absence. Effects of temperature, type of matrix, viscosity of the matrix, and isotopic substitution in the matrix and in the decaying radicals have been investigated. Methods of producing radicals have included irradiation with ^{60}Co γ-rays, with tritium beta rays and with ultraviolet light. Photoionization of tetramethyl-*p*-phenylenediamine

to produce electrons which cause dissociative electron capture of alkyl halides has also been used.

Change of Electric Conductivity of Organics by Gamma Irradiation

A. BRECCIA,[1] S. DELLONTE, F. FUOCHI, and J. NUCIFORA, Centro di Chimice delle radiasioni del C.N.R., Bologna, Italy

Studies have been carried out on the conductivity in d.c. on the following dried or melted compounds:

(1) Polyamides at M_n = 2,000; 10,000; 16,000; 40,000; 60,000.

(2) Urea, thiourea, selenium urea; xanthene, thioxanthene, Se-xanthene; and selenium-chromone-4-olo.

(3) Linear hydrocarbons and their keto and acid derivatives with C numbers in the range of 24 to 32.

The gamma doses varied in the range of 0.2 to 4 Mrads with a 4×10^4 rads/min. dose rate. An increase in conductivity in all the compounds and other findings were noted:

(1) Before the irradiation polyamides showed a decrease of conductivity at the increasing M_n except at M_n 60,000. After radiolysis the conductivity was higher but with the same value at different M_n, except at M_n 2000.

(2) For selenium derivatives and homologues the increasing conductivity was correlated with the distribution of the new traps and with the induced stable radicals.

(3) For hydrocarbons and derivatives, the increase of conductivity varied widely as a function of physical phase (melted or powdered) in a range 10^2 to 10^6 higher. A decrease of energy activation with increasing molecular weight (2.2–1.2 e.v.) was noted.

[1] Present address: University of Manchester, England.

Publication Date: January 1, 1968 | doi: 10.1021/ba-1968-0082.ch037

Organic Liquids

The Lifetime of Charged Species in Irradiated Dielectric Liquids

ANDRIES HUMMEL, Reactor Institute, Delft, Netherlands

The distribution of lifetimes of the charged species, formed in cyclohexane by high energy radiation, is calculated, using the experimental results on the number of these species reacting with solute molecules as a function of the concentration of the solute. The time in which half of the ions recombine, when no reaction with a solute takes place, is $6 \times$

10^{-10} seconds. Because of the fact that the diffusion coefficient of the negative entity in cyclohexane at room temperature is very large (2.5×10^{-4} sq. cm. sec.$^{-1}$), scavenging of this entity increases the lifetime of the ions considerably. The effect of scavenging of the negative entity on the lifetime distribution is calculated. Absolute rate constants for reactions of the charged species with solutes are also calculated.

Luminescence Studies as a Device for Investigation of Early Processes in Radiation Chemistry

PETER K. LUDWIG and MILTON BURTON, Radiation Laboratory, University of Notre Dame, Notre Dame, Ind. 46556

Publication Date: January 1, 1968 | doi: 10.1021/ba-1968-0082.ch037

Details of the neutralization process following radiation-induced primary charge separation may be examined *via* the medium of ultrafast techniques now employed in studies of luminescence decay processes. As an example, the form of luminescence decay curves of dilute organic scintillator in aliphatic hydrocarbon solution excited by x-ray pulses of about 0.5–1.0 nsec. duration is attributed (in previous papers) to neutralization processes involving ions. The relation, $t \propto r^3$, for the time required for neutralization of an ion pair of initial separation r, when applied to such curves, leads to a distribution function of ion-pair separations. A more appropriate and desirable approach involves solution of a diffusion equation (which includes a Coulomb interaction term) for various initial conditions. Such solutions are obtained by computer techniques employed in analogy to corresponding electrical networks. The results indicate that the $t \propto r^3$ law affords a fair description of the decay if the initial distribution can be assumed to be broad.

The Radiation Laboratory is operated by the University of Notre Dame under contract with the U.S. Atomic Energy Commission. This is AEC document number COO-38-606.

Negative Ion Formation in the Radiolysis of Perfluorocarbon Solutions in *n*-Hexane

L. A. RAJBENBACH, Soreq Nuclear Research Centre, Yavne, Israel

The radiolytic yields of hydrogen, hexenes, dedecanes, and hydrogen fluoride in solutions of perfluorocarbons in *n*-hexane were determined. Perfluoroalkanes from C_4F_{10} upward were found to depress the radiolytic hydrogen yield. The reduction in hydrogen was accompanied by formation of hydrogen fluoride. Perfluorocyclocarbons were found to

have the most pronounced effect on the hydrogen yield. The ability of perfluoroalkanes to reduce the hydrogen yield is correlated with the capacity of these solutes to attach thermal electrons in a resonant process, as measured in the gas phase by mass spectrometric and microwave cavity resonance techniques. The fact that the decrease in radiolytic hydrogen yield in solutions of perfluoro unsaturates is accompanied by the formation of hydrogen fluoride is attributed to the, as yet otherwise unestablished, ability of perfluoro olefins to undergo resonant electron attachment. The constancy of the radiolytic yields of hexane in solutions of perfluoroalkanes in *n*-hexane is interpreted as confirming our previous assumptions that the neutralization reaction between solvent molecular cation and an electron does not lead to the formation of molecular hydrogen and that the decomposition paths of the excited states formed by direct action of energy and those resulting from charge recombination reaction are not identical. Our results suggest also that the autoionization lifetime of the solute anions may be a more important factor affecting the radiolytic decomposition of solvent than the solute's cross section for electron capture.

Publication Date: January 1, 1968 | doi: 10.1021/ba-1968-0082.ch037

Gas-Phase Photolysis of Cyclohexane in the Photoionization Region

P. AUSLOOS, R. E. REBBERT, and S. G. LIAS, National Bureau of Standards, Washington, D. C. 20234

Cyclohexane (ionization energy, 9.88 e.v.) has been photolyzed at 1236 A. (10.0 e.v.) and 1048–1067 A. (11.6–11.8 e.v.). All major products have been determined in the absence of free radical scavengers and in the presence of added NO and O_2. In addition, cyclo-C_6D_{12}–H_2S mixtures were irradiated to determine the free radicals formed in the decomposition of the superexcited cyclohexane molecule. Accurate quantum yield determinations have been made, both by use of saturation current measurements during photolysis and by chemical actinometry. It is seen that an increase in photon energy results in an increase in the relative importance of processes producing H atoms or alkyl radicals while the yields of products attributed to "molecular elimination" processes, such as the formation of molecular hydrogen, diminish. Similar trends are seen in the solid-phase photolysis. The relative importances of the various primary processes are derived. The application of this information to the interpretation of the radiolysis of cyclohexane is discussed.

Kinetics of the Radiation Induced Isotopic Exchange between Iodobenzene and Iodine

H. ELIAS and R. RIESS, Lehrstuhl für Kernchemie, Technische Hochschule Darmstadt, Germany

In literature the radiation induced isotopic exchange reaction between iodobenzene and labelled iodine

$$\text{Ph-I} + \tfrac{1}{2}{}^*\text{I}_2 \xrightarrow{\wedge\wedge\wedge} \text{Ph-}{}^*\text{I} + \tfrac{1}{2}\text{I}_2 \qquad (1)$$

is discussed on the basis of the following steps:

$$\text{Ph-I} \xrightarrow{\wedge\wedge\wedge} \text{Ph}\cdot + \text{I}\cdot \qquad (2)$$

$$\text{Ph}\cdot + {}^*\text{I}_2 \rightarrow \text{Ph-}{}^*\text{I} + {}^*\text{I}\cdot \qquad (3)$$

In this paper the kinetics of Reaction 1 were studied in benzene as solvent at 30°C. in the presence and absence of oxygen (^{60}Co-radiation). For R, the rate of exchange, the following relationship was obtained:

$$R = \frac{a[\text{I}_2]^{1/2}}{1 + b[\text{I}_2]^{1/2}/[\text{Ph-I}]} \qquad (4)$$

This rate law cannot be explained on the basis of Reactions 2 and 3. It is instead compatible with the following steps:

$${}^*\text{I}_2 \xrightarrow{\wedge\wedge\wedge} 2\ {}^*\text{I}\cdot \qquad (5)$$

$${}^*\text{I}\cdot + \text{Ph-I} \rightarrow \text{Ph-}{}^*\text{I} + \text{I}\cdot \qquad (6)$$

$${}^*\text{I}\cdot + \text{I}_2 \rightarrow \text{I-}{}^*\text{I} + \text{I}\cdot \qquad (7)$$

Phenyl radicals seem to be involved only in the formation of radiolysis products, like diphenyliodonium iodide and tri-iodide, respectively. The detailed mechanism of Reaction 1, the results of scavenger experiments, and the influence of radiolysis products on the isotopic exchange are discussed.

Publication Date: January 1, 1968 | doi: 10.1021/ba-1968-0082.ch037

Excitation and Ionization Yields in Cyclohexane

F. S. DAINTON, E. C. FRANKEVICH,[1] T. MORROW, G. A. SALMON, and G. F. THOMPSON, The University of Leeds, Cookridge High Energy Radiation Research Centre

For solutions of naphthalene in cyclohexane the yield of triplet states of naphthalene, the intensity of monomer and excimer fluorescence, and the yield of singlet state naphthalene have been measured as a function of naphthalene concentration by pulse radiolysis methods. The influence of a number of electron scavengers on these yields has been determined

and also the influence of xenon which is known to quench singlet states by enhancing the rate of intersystem crossing. The electron scavenger nitromethane was found to be of particular interest since in addition to scavenging electrons it was found to be an efficient singlet state quencher, and these effects were observable in distinct concentration regions. The participation of charge neutralization processes in the production of excited states has been clearly demonstrated by observations of the influence of electrical fields on the radiation induced fluorescence from naphthalene solutions.

[1] Present address: Institute of Chemical Physics, Moscow.

Publication Date: January 1, 1968 | doi: 10.1021/ba-1968-0082.ch037

Olefin Formation in the Radiolysis of *n*-Hexadecane

L. G. WALKER, W. A. SUNDER, and W. E. FALCONER, Bell Telephone Laboratories, Inc., Murray Hill, N. J.

Prior studies of the condensed phase radiolysis of *n*-hexadecane (*1*, *2*) have not included data on olefin formation. Consequently, the products could not be correlated with a complete material balance. We have now developed a method of coulometric titration to an amperometric endpoint which gives total olefin content at low concentrations in high molecular weight paraffins. This technique, together with gas chromatography on polar columns stable at high temperatures, provides a quantitative measure of the yields of both congruent olefins (hexadecenes) and of the scission or fragmentation olefins (ethylene through the pentadecenes). The radiolysis of *n*-hexadecane close to its melting point in both solid and liquid phases has been examined using these techniques with the objectives of extending the material balance data, of understanding specifically the mechanisms whereby olefins are formed, and of distinguishing generally between ionic and radical precursors to the radiolytic end products. The fragmentation olefins are, within the experimental error, all linear and terminal. At least those from 1-hexene to 1-tetradecene have similar yields. A striking feature both in liquid and solid state radiolyses is that for the low molecular weight products, G(olefin) is only 0.1–0.2 G(paraffin). This low yield ratio of olefins to paraffins is incompatible with radical processes' being the sole mode of formation of the low molecular weight products.

Although the congruent olefins were not resolved individually, nevertheless it could be shown by gas chromatography that 1-hexadecene is only a small contributor to the C_{61} olefin fraction. The mechanisms

whereby congruent olefins are formed both in the liquid and solid phases are considered, and the yields of olefins are correlated with those of other major radiolytic products.

(1) Falconer, W. E., Salovey, R., *J. Chem. Phys.* **44**, 3151 (1966).
(2) Salovey, R., Falconer, W. E., *J. Phys. Chem.* **69**, 2345 (1965).

Excitation in Some Irradiated Organic Liquid Systems

GABRIEL STEIN, Hebrew University, Jerusalem, Israel

Publication Date: January 1, 1968 | doi: 10.1021/ba-1968-0082.ch037

The yield of excited states in organic liquids, and in particular in benzene solutions, is critically compared using results from light emission measurements, light absorption in pulse radiolysis studies, and total chemical yields, in particular as determined by isomerization methods. It is shown that the total yield of excited states originating from solvent excited states and from solute excited states formed without previous solvent excitation is not less than $G = 5$. Quantitative data are obtained for the yields of the different precursors including singlet and triplet states.

Radiolysis of Perfluorobicyclohexyl at Elevated Temperatures

F. W. BLOCH, D. R. MACKENZIE, and V. H. WILSON, Brookhaven National Laboratory, Upton, N. Y. 11973

Perfluorobicyclohexyl is conspicuously less stable thermally than most other fluorocarbons. At temperatures up to 350°C. we have found that its radiolytic decomposition rate is moderate and similar to that of other alicyclic fluorocarbons. However, in the temperature region above 385°C. and at pressures above 100 atm. G-values for its radiolytic decomposition increase drastically. At 385°C., $G_{\text{-}C_{12}F_{22}}$ is only 50, indicating that a chain mechanism is just becoming effective. At 450°C., $G_{\text{-}C_{12}F_{22}}$ is approximately 10^5, so that a chain of great length is operating. The apparent activation energy for the radiolytic decomposition at high pressure is 110 ± 10 kcal./mole. At pressures of 1–2 atm., thermal decomposition rates are much higher than at 100 atm., but radiolytic decomposition rates are low. In fact at 415°C. and 1.6 atm. radiolysis does not appear to contribute to the over-all decomposition rate. Reasons for the behavior are discussed in the light of the reactions known to occur in the complex system.

Radiolysis of Liquid Formamide: Gaseous Products and Pulse Data

A. MATSUMOTO and N. N. LICHTIN, Boston University, Boston, Mass. 02215

Steady ^{60}Co-gamma radiolysis at a dose rate of approximately 10^{17} e.v. ml.$^{-1}$ min.$^{-1}$ of dried, extensively purified, deaerated formamide gives four principal gaseous products with the following dose-independent yields per 100 e.v.: $G(H_2) = 0.9$, $G(CO) = 0.6$, $G(CO_2) = 0.2$, $G(NH_3) = 0.3$. N_2O, equilibrated at pressures of 5–500 torr, has little if any effect on $G(H_2)$ or $G(CO)$ but gives yields of N_2 per 100 e.v. which increase from 0.2 to 1.9 over this range. Added water, 10^{-2} to $10^{-1}M$, has little if any effect on $G(H_2)$, $G(CO)$, or $G(CO_2)$ but increases $G(NH_3)$ by an amount which decreases with increasing dose. (Correction of radiolytic yields for concurrent hydrolysis is necessary only for NH_3.) Pulsing with 1.15 Mev. electrons (work done at Brookhaven National Laboratory) results in a transient absorption spectrum characterized by an intense maximum at 400 n.m. and a shoulder centering around 500 n.m. Decay of absorption at 400 n.m. follows second-order kinetics ($k/\epsilon l = 1.6 \times 10^5$ sec.$^{-1}$) and is slower than the apparently first-order decay observed at 500 n.m., for which the specific rate is 3×10^5 sec.$^{-1}$. Mechanistic speculations will be offered.

Publication Date: January 1, 1968 | doi: 10.1021/ba-1968-0082.ch037

The Gamma Irradiation of Isoprene in the Presence of Vermiculite

CYRIL PONNAMPERUMA and COLIN S. MUNDAY,[1] Exobiology Division, National Aeronautics and Space Administration, Ames Research Center, Moffett Field, Calif.

The irradiation of isoprene, either by ultraviolet photolysis (Liu and Hammond, *J. Am. Chem. Soc.* **85**, 477, 1963) or by cobalt-60 rays, normally leads to the production of cyclic polymerization products. However, γ-irradiation of isoprene absorbed in clay minerals of known catalytic action, produced substantial yields of acyclic polymers containing discrete multiples of the basic 5-carbon skeleton. Analysis of these hydrogenated acyclic polymeric products, by gas chromatography and mass spectrometry, indicated that the C_{15} isoprenoid farnesane and the C_{20} compound phytane were present. Since importance is attached to the presence of pristane C_{19} and phytane in distinguishing hydrocarbons of biogenic origin from those of abiogenic origin in ancient sediments, the results may lead to a reappraisal of the established criteria on such questions as the origin of hydrocarbons in sedimentary rocks.

[1] National Academy of Sciences postdoctoral research associate.

Initiation Mechanism of Radiation Induced Polymerization

H. YOSHIDA, H. KAMIYAMA,[1] KA. HAYASHI,[1] H. YAMAOKA,
K. HAYASHI, and S. OKAMURA, Kyoto University, Kyoto, Japan

The rigid glass matrix method is useful to study intermediate species such as trapped electrons and ions formed by ionizing radiations because different species are selectively formed in proper matrices and trapped stably. In this investigation, ion radicals of solute monomers (nitroethylene, isobutylene, and styrene) in the irradiated glass matrices (2-methyltetrahydrofuran, *n*-butyl chloride, and 3-methylpentane) were studied mainly by ESR and electronic spectrum measurements. The formation mechanism of the ion radicals and their contribution to the initiation process of polymerizations (anionic polymerization for nitroethylene, and cationic one for isobutylene and styrene) are discussed. In any case where the polymerization occurred in the glass, the corresponding anion or cation radicals were observed from the glass containing monomer irradiated at 77°K. This suggests the ion radicals play an important role in the initiation process of radiation induced ionic polymerization.

[1] Address: Osaka Lab. JAERI., Osaka, Japan.

Publication Date: January 1, 1968 | doi: 10.1021/ba-1968-0082.ch037

INDEX

Publication Date: January 1, 1968 | doi: 10.1021/ba-1968-0082.ix001

In Radiation Chemistry; Hart, E.;
Advances in Chemistry; American Chemical Society: Washington, DC, 1968.

C

D

E

Publication Date: January 1, 1968 | doi: 10.1021/ba-1968-0082.ix001

F

Publication Date: January 1, 1968 | doi: 10.1021/ba-1968-0082.ix001

Publication Date: January 1, 1968 | doi: 10.1021/ba-1968-0082.ix001

J

K

L

Publication Date: January 1, 1968 | doi: 10.1021/ba-1968-0082.ix001

Publication Date: January 1, 1968 | doi: 10.1021/ba-1968-0082.ix001

Publication Date: January 1, 1968 | doi: 10.1021/ba-1968-0082.ix001

R

S

Publication Date: January 1, 1968 | doi: 10.1021/ba-1968-0082.ix001

T

U

V

W

X

Publication Date: January 1, 1968 | doi: 10.1021/ba-1968-0082.ix001